THERAPEUTIC DRUG MONITORING (TDM): A USEFUL TOOL FOR PEDIATRIC PHARMACOLOGY APPLIED TO ROUTINE CLINICAL PRACTICE

EDITED BY: Raffaele Simeoli, Erwin Dreesen, Thomas Dorlo, L. M. Hanff and Alwin Huitema

PUBLISHED IN: Frontiers in Pharmacology and Frontiers in Pediatrics

frontiers Research Topics

ISSN 1664-8714
ISBN 978-2-88976-355-9
DOI 10.3389/978-2-88976-355-9

About Frontiers

Frontiers is more than just an open-access publisher of scholarly articles: it is a pioneering approach to the world of academia, radically improving the way scholarly research is managed. The grand vision of Frontiers is a world where all people have an equal opportunity to seek, share and generate knowledge. Frontiers provides immediate and permanent online open access to all its publications, but this alone is not enough to realize our grand goals.

Frontiers Journal Series

The Frontiers Journal Series is a multi-tier and interdisciplinary set of open-access, online journals, promising a paradigm shift from the current review, selection and dissemination processes in academic publishing. All Frontiers journals are driven by researchers for researchers; therefore, they constitute a service to the scholarly community. At the same time, the Frontiers Journal Series operates on a revolutionary invention, the tiered publishing system, initially addressing specific communities of scholars, and gradually climbing up to broader public understanding, thus serving the interests of the lay society, too.

Dedication to Quality

Each Frontiers article is a landmark of the highest quality, thanks to genuinely collaborative interactions between authors and review editors, who include some of the world's best academicians. Research must be certified by peers before entering a stream of knowledge that may eventually reach the public - and shape society; therefore, Frontiers only applies the most rigorous and unbiased reviews.
Frontiers revolutionizes research publishing by freely delivering the most outstanding research, evaluated with no bias from both the academic and social point of view. By applying the most advanced information technologies, Frontiers is catapulting scholarly publishing into a new generation.

What are Frontiers Research Topics?

Frontiers Research Topics are very popular trademarks of the Frontiers Journals Series: they are collections of at least ten articles, all centered on a particular subject. With their unique mix of varied contributions from Original Research to Review Articles, Frontiers Research Topics unify the most influential researchers, the latest key findings and historical advances in a hot research area! Find out more on how to host your own Frontiers Research Topic or contribute to one as an author by contacting the Frontiers Editorial Office: frontiersin.org/about/contact

THERAPEUTIC DRUG MONITORING (TDM): A USEFUL TOOL FOR PEDIATRIC PHARMACOLOGY APPLIED TO ROUTINE CLINICAL PRACTICE

Topic Editors:
Raffaele Simeoli, Department of Pediatric Specialities, Division of Metabolic Biochemistry, Bambino Gesù Children's Hospital (IRCCS), Italy
Erwin Dreesen, KU Leuven, Belgium
Thomas Dorlo, The Netherlands Cancer Institute (NKI), Netherlands
L. M. Hanff, Princess Maxima Center for Pediatric Oncology, Netherlands
Alwin Huitema, The Netherlands Cancer Institute (NKI), Netherlands

Citation: Simeoli, R., Dreesen, E., Dorlo, T., Hanff, L. M., Huitema, A., eds. (2022). Therapeutic Drug Monitoring (TDM): A Useful Tool for Pediatric Pharmacology Applied to Routine Clinical Practice. Lausanne: Frontiers Media SA. doi: 10.3389/978-2-88976-355-9

Table of Contents

frontiers | Frontiers in Pharmacology

EDITORIAL
published: 24 May 2022
doi: 10.3389/fphar.2022.931843

Editorial: Therapeutic Drug Monitoring (TDM): A Useful Tool for Pediatric Pharmacology Applied to Routine Clinical Practice

Raffaele Simeoli[1]*, *Thomas P. C. Dorlo*[2], *Lidwien M. Hanff*[3], *Alwin D. R. Huitema*[2,3,4] and *Erwin Dreesen*[5]

[1]Division of Metabolic Diseases and Drug Biology, Bambino Gesù Children's Hospital, IRCCS, Rome, Italy, [2]Department of Pharmacy and Pharmacology, Netherlands Cancer Institute, Amsterdam, Netherlands, [3]Department of Pharmacology, Princess Máxima Center for Pediatric Oncology, Utrecht, Netherlands, [4]Department of Clinical Pharmacy, University Medical Center Utrecht, Utrecht University, Utrecht, Netherlands, [5]Clinical Pharmacology and Pharmacotherapy Unit, Department of Pharmaceutical and Pharmacological Sciences, KU Leuven, Leuven, Belgium

Keywords: therapeutic drug monitoring, pediatrics, pharmacokinetic/pharmacodynamics, antimicrobials, personalized therapy

Editorial on the Research Topic

Therapeutic Drug Monitoring (TDM): A Useful Tool for Pediatric Pharmacology Applied to Routine Clinical Practice

OPEN ACCESS

Edited and reviewed by:
Jeffrey Scott Barrett,
Critical Path Institute, United States

***Correspondence:**
Raffaele Simeoli
raffaele.simeoli@opbg.net

Specialty section:
This article was submitted to Obstetric and Pediatric Pharmacology, a section of the journal Frontiers in Pharmacology

Received: *29 April 2022*
Accepted: *04 May 2022*
Published: *24 May 2022*

Citation:
Simeoli R, Dorlo TPC, Hanff LM, Huitema ADR and Dreesen E (2022) Editorial: Therapeutic Drug Monitoring (TDM): A Useful Tool for Pediatric Pharmacology Applied to Routine Clinical Practice. Front. Pharmacol. 13:931843. doi: 10.3389/fphar.2022.931843

1 BACKGROUND

For many therapeutic areas in modern medicine, precision medicine is the current treatment paradigm. Interestingly, or probably disappointingly, the concept of precision medicine often only encompasses selecting the right drug for the right patient. Subsequent selection of the right dose for the right patient is at least equally important and is only scarcely considered. Therapeutic Drug Monitoring (TDM) can be defined as assessing the adequacy of the drug plasma concentrations in relation to a target concentration or concentration window at a specific time in a dosing interval. This evaluation, following appropriate clinical interpretation and according to the drug pharmacokinetic/pharmacodynamic (PK/PD) properties, can guide dosing. However, finding the optimal dosing in order to guarantee a therapeutic exposure remains complicated. Sources of PK variability, including age, genetic heritage, and disease conditions, all influence the chances of achieving therapeutic outcomes. This aspect is particularly evident in children and neonates where physiological changes, associated with growth and maturation, dramatically influence drug PK properties. Similarly, pediatric patients subjected to medical procedures, including dialysis or extracorporeal membrane oxygenation (ECMO), may require special dose considerations since these procedures could significantly affect PK parameters. In pediatrics, drug-administration issues are more prominent than in adults. To adjust the dose and to secure intake in pediatrics, adult formulations may need to be crushed, dissolved, or extemporaneously prepared as liquid. In the absence of reliable data on these manipulations, TDM may contribute to safe and effective therapy in pediatric practice.

The utility of TDM is often underestimated or exclusively applied to molecules where monitoring of drug concentrations is mandatory due to safety concerns. However, TDM is less commonly used for optimization towards effective drug exposure. Although the multiple benefits of TDM are well

known and recognized by clinicians, this knowledge seems to be only theoretical and its introduction into clinical practice remains far away from the application. TDM should rely on analytical methods such as high-performance liquid chromatography coupled to UV (HPLC-UV) or to mass spectrometry (LC-MS/MS) characterized by fast detection, and high accuracy and precision. These instruments are not always available for every drug and in every analytical laboratory, making TDM often unfeasible. Another issue that limits the application of TDM in pediatric patients is the invasiveness of blood sampling. The impact of blood sampling in children should not be underestimated. Even with professional psychological support, many children describe blood sampling as a dismal experience, and -naturally- TDM should therefore only be applied if clinically relevant. Low sampling volume limits in neonates and children make the bioanalytical procedures not always applicable, thereby limiting the use of TDM. To overcome this issue, several microsampling methods have been proposed including volumetric absorptive microsampling (VAMS) and dried blood spots (DBS) sampling. However, exhaustive analytical and clinical validation of these methods for conducting PK studies and TDM interventions is still rather limited.

2 SCOPE

The aim of this Research Topic was to show the utility of TDM applied to the routine clinical practice in pediatric patients. To this scope, we have collected reviews, research articles, case reports, and both pre-clinical and clinical study protocols that investigate the utility and the application of TDM in different pediatric settings and disease conditions. Moreover, an important contribution has been provided by population pharmacokinetic (popPK) studies that demonstrate how modelling and simulation approaches could provide important dosing guidance for drugs used *off-label* in neonates and children. These studies could be particularly useful to overcome the physiological and ethical issues connected to the realization of PK clinical studies on these subjects.

3 OVERVIEW OF CONTRIBUTIONS

3.1 Antimicrobial Therapy

Infections represent one of the main complications among hospitalized neonatal and pediatric patients, especially during long-standing periods in intensive care units (ICUs) where the presence of central catheters for parental nutrition and ventilators for respiratory support are often sources of bacterial colonization and require an appropriate shunt lock therapy to avoid systemic infections (Auriti et al., 2016; Ramasethu, 2017). Therefore, antimicrobial therapies are often introduced not only as therapeutic but also as prophylactic treatments. A further complication is represented by invasive procedures to which patients are often subjected. These include, for example, continuous renal replacement therapy (CRRT) and the ECMO. In these critical situations, drug administration (including antimicrobial agents) needs to consider the changes in PK parameters taking place in these patients. An increase in the distribution volume (Vd) or an augmented clearance of administered drugs can affect therapy effectiveness, exposing patients to a higher risk of therapeutic failures. An example of this important aspect has been described by Xu et al. These authors report two cases of critically ill pediatric patients with acute kidney injury requiring CRRT and receiving polymyxin B treatment due to carbapenem-resistant organism bloodstream infections. TDM of polymyxin B revealed an increased clearance of polymyxin B through CRRT that required supplanted dosing of the drug Xu et al. Similarly, a popPK analysis, aimed at describing primary PK/PD parameters of vancomycin and meropenem in pediatric patients undergoing ECMO, showed that the PK/PD target for vancomycin was achieved partially with conventional doses meanwhile higher dosing with extended infusion was needed in the case of meropenem Zylbersztajn et al. Even pathological conditions including hematological malignancies can affect PK properties of many administered drugs. An augmented renal clearance (ARC) is increasingly recognized in pediatric oncologic patients. In these immunocompromised subjects, broad-spectrum beta-lactams are commonly prescribed for empirical or selective treatment of bacterial infections. André et al. compared trough concentrations of meropenem and piperacillin in a cohort of unselected pediatric hematology-oncology patients stratified according to their estimated renal function as decreased, normal or with ARC, and to their neutrophil count. The results obtained by this retrospective evaluation showed that intermittent administration of meropenem and piperacillin often fails to ensure sufficient exposure in treated patients even at maximal recommended daily dosage, perhaps due to an increased drug clearance. Therefore, the authors suggest systematic TDM alongside assessment of renal function, as valid support for dosage adjustment in order to guarantee an appropriate antibiotic therapy in pediatric patients affected by malignancies André et al. These articles confirm that TDM may represent a valuable tool for assisting clinicians in optimizing antimicrobial exposure. A proof of concept in this direction has been provided by Gatti et al. The authors report their experience as clinical pharmacological advice (CPA) and conclude that a TDM-based real-time CPA may be particularly useful to optimize antimicrobial therapies in different challenging pediatric settings Gatti et al. The prospective EXPAT Kids study aims to evaluate PK/PD target attainment within the first 36 h after initiation of beta-lactam dosing in critically ill children. Schouwenburg et al. will also investigate the association between PK/PD target attainment and patient characteristics and clinical outcomes. Aiming to reduce the workload for medical staff, they will validate the use of residual material from heparinized astrup syringes for TDM. The results of the EXPAT Kids study are eagerly awaited and are expected to provide important new insights to improve clinical outcomes through better beta-lactam dosing.

3.2 Immunosuppressant Therapy

Hematopoietic stem cell transplantation (HSCT) remains the only curative treatment in several pediatric hematological

pathologies. Although this therapeutic approach has significantly improved clinical outcomes of pediatric patients with malignant and non-malignant disorders, graft-versus-host disease (GVHD) is an important cause of morbidity and mortality in patients receiving HSCT (Ferrara et al., 2009). One of the most difficult challenges to further improving HSCT outcomes is reducing toxicity while maintaining efficacy of conditioning regimens that include combinations of chemo- and serotherapy prior to HSCT. In this context, the use of TDM represents a valid support for personalized dosing of various conditioning agents and could be particularly useful, especially in children for whom pathological conditions lead to a greater PK variability. Recently, van der Stoep et al. provided an overview of the possible relationships between PK parameters and clinical outcomes or toxicities for the most commonly used conditioning agents in pediatric HSCT van der Stoep et al. Brooks et al. developed a popPK model for tacrolimus intravenous continuous infusion in pediatric and young adult HCT patients Brooks et al. The model was implemented in a Bayesian dosing tool, thereby making it available at the point-of-care and allowing a clinical impact.

High-dose methotrexate (HD-MTX) is widely used in pediatric acute lymphoblastic leukemia (ALL) treatment regimens. A popPK model of HD-MTX has been developed by Gao et al. in Chinese pediatric patients with ALL with the noteworthy aim to establish a personalized dosage regimen. In particular, potential covariates such as age, body weight, and biochemical measurements (renal and liver function) on MTX PK disposition were investigated. The results obtained from this study revealed that body weight and serum creatinine levels (SCr) were significant covariates on the disposition of MTX. Therefore, this popPK model combined with an *a posteriori* Bayesian approach can be used to estimate individual PK parameters and optimize personalized MTX therapy for pediatric patients with ALL Gao et al.

3.3 Bioanalytical Techniques Applied to TDM

Different types of bioanalytical techniques are commonlyused in clinical laboratories for TDM. Historically, gas chromatography (GC), HPLC-UV, and LC-MS/MS are the most frequently used technologies to measure drug concentrations in different biological matrices. Immunoassays, including the enzyme-linked immunosorbent assay (ELISA), are also used for the quantification of several drugs. Usually, these assays are easily accessible for many laboratories and do not require highly specialized personnel. However, immunoassays are not available for all drugs monitored in clinical laboratories and their sensitivity, specificity, and accuracy toward the target compound is lower than GC, HPLC-UV, or LC-MS/MS. Therefore, the latter techniques are usually preferred to perform TDM although not always accessible to all laboratories. In a recent study, Xia et al. have analyzed plasma valproic acid (VPA) concentrations in 711 pediatric patients with epilepsy and compared a routine Enzyme Multiplied Immunoassay Technique (EMIT) with a validated in-house LC-ESI-MS/MS method on the same samples. Consistency between the two assays was evaluated using linear regression and Bland-Altman analysis. Results revealed that both methods were closely correlated although EMIT assay overestimated VPA levels in human plasma compared with LC-ESI-MS/MS method. Therefore, the authors conclude that switching from immunoassays to LC-based techniques for TDM of VPA deserves close attention and a therapeutic range of 35.0–75.0 μg/ml could be more feasible. However, further studies are required to evaluate the eligibility of this alternative range in clinical practice Xia et al.

Similarly, a novel peptide biosensor (P_{ABL})-ELISA assay has been developed and validated by Montecchini et al. to investigate ABL1 *in vitro* activity in four immortalized leukemic cell lines. The assay was further validated on blasts derived from an adult affected by chronic myeloid leukemia (*BCR-ABL1* positive) and a child affected by ALL (*BCR-ABL1* negative). Phosphorylation of P_{ABL} was inhibited after incubating *BCR-ABL1* positive cell lysates with imatinib, but not with ruxolitinib. In conclusion, the authors suggest that the P_{ABL}-based ELISA assay provides a novel *in vitro* tool for screening both the aberrant ABL1 activity in *BCR-ABL1* like ALL leukemic cells and their potential response to tyrosine kinase (TK) inhibitors Montecchini et al.

3.4 Neonatal TDM

Neonatal pharmacology deserves particular attention due to the complexity of maturational and physiological changes that not only characterize neonates but also affect the response of these patients to pharmacological treatments. Although pre-terms are generally considered part of the neonatal population, they are physiologically and pharmacologically different from full-term neonates and, therefore, require specific considerations (Allegaert et al., 2007; Somani et al., 2016). For example, caffeine citrate is widely used to treat apnea of prematurity. However, maturation and genetic variation are responsible for high inter-individual variability in the clinical response to caffeine in preterm infants, making the optimal dose administered controversial. In a recent review of literature, Long et al. have evaluated the PK profile of caffeine in preterm infants alongside the safety and efficacy of different doses of caffeine, therapeutic concentration ranges, and the impact of genetic variability on caffeine therapy. Although safety and efficacy of standard-dose caffeine have been already assessed, evidence for the safety of higher administered doses is not yet explored. Therefore, the authors suggest the utility of TDM when dose optimization is required for preterm infants who lack clinical response to standard-dose caffeine. In fact, even polymorphisms in PD-related genes have a significant impact on the inter-individual variability in pharmacological response to caffeine, therefore an individualized therapy based on TDM data could be particularly useful during routine clinical practice Long et al.

4 CONCLUSION

In conclusion, TDM in pediatrics represents, similarly to adults, a useful tool that allows a more tailored drug administration and, therefore, the individualization of therapy to avoid risks of

therapeutic failures or drug toxicity. The contributions to this issue of Frontiers in Pediatrics clearly demonstrate the value of TDM for tailoring the administration of various drugs in pediatric patients, mainly during antimicrobial and immunosuppressive therapies. However, various challenges remain, preventing a wide uptake in routine clinical care. Overcoming the bioanalytical issues and providing a software tool for model-informed dosing support may be key for TDM to grow into a user-friendly and reliable tool for improving treatments in children and neonates.

AUTHOR CONTRIBUTIONS

All authors listed have made a substantial, direct, and intellectual contribution to the work and approved it for publication.

ACKNOWLEDGMENTS

The authors would like to thank all the reviewers who have revised the articles published within this Editorial Topic.

REFERENCES

Allegaert, K., Peeters, M. Y., Verbesselt, R., Tibboel, D., Naulaers, G., de Hoon, J. N., et al. (2007) Inter-individual Variability in Propofol Pharmacokinetics in Preterm and Term Neonates. *Br. J. Anaesth.*;99(6):864–870. doi:10.1093/bja/aem294

Auriti, C., Piersigilli, F., Ronchetti, M. P., Campi, F., Amante, P. G., Falcone, M., et al. (2016) Shunt Lock Therapy with Micafungin to Treat Shunt-Associated Candida Albicans Meningitis in an Infant. *J. Antimicrob. Chemother.*;71(7):2060–2061. doi:10.1093/jac/dkw072

Ferrara, J. L., Levine, J. E., Reddy, P., and Holler, E. (2009) Graft-versus-host Disease. *Lancet.* ;373(9674):1550–1561. doi:10.1016/S0140-6736(09)60237-3

Ramasethu, J. (2017) Prevention and Treatment of Neonatal Nosocomial Infections. *Matern. Health Neonatol. Perinatol.*, 3:5. doi:10.1186/s40748-017-0043-3

Somani, A. A., Thelen, K., Zheng, S., Trame, M. N., Coboeken, K., Meyer, M., et al. (2016) Evaluation of Changes in Oral Drug Absorption in Preterm and Term Neonates for Biopharmaceutics Classification System (BCS) Class I and II Compounds. *Br. J. Clin. Pharmacol.*;81(1):137–147. doi:10.1111/bcp.12752

Conflict of Interest: The authors declare that the research was conducted in the absence of any commercial or financial relationships that could be construed as a potential conflict of interest.

frontiers in Pharmacology

ORIGINAL RESEARCH
published: 13 July 2021
doi: 10.3389/fphar.2021.701452

Population Pharmacokinetics of High-Dose Methotrexate in Chinese Pediatric Patients With Acute Lymphoblastic Leukemia

Xuan Gao[1], Xiao-Wen Qian[2], Xiao-Hua Zhu[2], Yi Yu[2], Hui Miao[2], Jian-Hua Meng[2], Jun-Ye Jiang[2], Hong-Sheng Wang[2] and Xiao-Wen Zhai[2]**

[1]Outpatient and Emergency Management Office, National Children's Medical Center, Children's Hospital of Fudan University, Shanghai, China, [2]Department of Hematology and Oncology, National Children's Medical Center, Children's Hospital of Fudan University, Shanghai, China

OPEN ACCESS

Edited by:
Raffaele Simeoli, Bambino Gesù Children Hospital (IRCCS), Italy

Reviewed by:
Barbara Faganel Kotnik, University Children's Hospital, Slovenia
Laura B Ramsey, Cincinnati Children's Hospital Medical Center, United States

***Correspondence:**
Hong-Sheng Wang
honswang@hotmail.com
Xiao-Wen Zhai
xwzhai@fudan.edu.cn

Specialty section:
This article was submitted to Obstetric and Pediatric Pharmacology, a section of the journal Frontiers in Pharmacology

Received: *28 April 2021*
Accepted: *30 June 2021*
Published: *13 July 2021*

Citation:
Gao X, Qian X-W, Zhu X-H, Yu Y, Miao H, Meng J-H, Jiang J-Y, Wang H-S and Zhai X-W (2021) Population Pharmacokinetics of High-Dose Methotrexate in Chinese Pediatric Patients With Acute Lymphoblastic Leukemia. Front. Pharmacol. 12:701452. doi: 10.3389/fphar.2021.701452

High-dose methotrexate (HD-MTX) is widely used in pediatric acute lymphoblastic leukemia (ALL) treatment regimens. In this study, we aimed to develop a population pharmacokinetic (PK) model of HD-MTX in Chinese pediatric patients with ALL for designing personalized dosage regimens. In total, 4,517 MTX serum concentration data for 311 pediatric patients with ALL, aged 0.75–15.2 years and under HD-MTX treatment, were retrospectively collected at a tertiary Children's Hospital in China. The non-linear mixed-effect model was used to establish the population PK model, using NONMEM software. The potential covariate effects of age, body weight, and biochemical measurements (renal and liver function) on MTX PK disposition were investigated. The model was then evaluated using goodness-of-fit, visual predictive check. MTX PK disposition was described using a three-compartment model reasonable well. Body weight, implemented as a fixed allometric function on all clearance and volume of distribution parameters, showed a substantial improvement in model fit. The final population model demonstrated that the MTX clearance estimate in a typical child with body weight of 19 kg was 6.9 L/h and the central distribution of volume estimate was 20.7 L. The serum creatinine significantly affected the MTX clearance, with a 0.97% decrease in clearance per 1 μmol/L of serum creatinine. Other covariates (e.g., age, sex, bilirubin, albumin, aspartate transaminase, concomitant medication) did not significantly affect PK properties of MTX. The proposed population PK model could describe the MTX concentration data in Chinese pediatric patients with ALL. This population PK model combined with a maximum a *posteriori Bayesian* approach could be used to estimate individual PK parameters, and optimize personalized MTX therapy in target patients, thus aiming to reduce toxicity and improve treatment outcomes.

Keywords: methotrexate, population pharmacokinetics, NONMEM, acute lymphoblastic leukemia, pediatric patients

INTRODUCTION

Acute lymphoblastic leukemia (ALL) is the most common pediatric hematological cancer, accounting for 26–30% of all cancers diagnosed in children up to 14 years of age and contributing to approximately 80% of all childhood leukemia cases (Desantis et al., 2014; Pavlovic et al., 2019). Methotrexate (MTX) is a folate analog widely used as the first-line chemotherapy in high-dose (HD) consolidation and low-dose maintenance therapy for childhood ALL. The antileukemic effect of MTX is attributed to its competitive inhibition of dihydrofolate reductase (Galivan, 1980; Schmiegelow, 2009). HD-MTX is defined as a dose higher than 500 mg/m^2, which could elicit a broad range of antitumor activities (Evans et al., 1986; Howard et al., 2016; Kawakatsu et al., 2019; Shi et al., 2020). It has been reported that HD-MTX can reduce the relapse rate, increase the event-free survival rate, and suppress the development of central nervous system (CNS) leukemia in childhood ALL (Balis et al., 1985; Evans et al., 1986).

However, approximately 75% of the pediatric patients with ALL experienced therapy-related adverse effects (Gervasini and Vagace, 2012; Kawakatsu et al., 2019; Panetta et al., 2020), among them, 1–2% of the patients died from chemotherapy-associated toxicities (Hunger and Mullighan, 2015). Although the patients were provided aggressive folate supplementation, intravenous fluid hydration, and urine alkalinization during the course of HD-MTX therapy, the renal toxicity (i.e., renal dysfunction), at an approximate frequency of 1.8%, was observed often (Widemann et al., 2004). Renal toxicity leads to impaired MTX clearance and prolonged exposure to toxic concentrations, which can further deteriorate renal function and cause non-renal adverse events (AEs). Exposure to HD-MTX is highly associated with toxicity, including neurotoxicity (Bhojwani et al., 2014), hepatotoxicity (Cheng, 2008; Hegyi et al., 2012), mucositis (Cheng, 2008; Johansson et al., 2011), myelosuppression (Comandone et al., 2005; Joerger et al., 2010), and nephrotoxicity (Comandone et al., 2005; Yarlagadda and Perazella, 2008; Howard et al., 2016). These AEs often result in interruption or discontinuation of chemotherapy and increase relapse risks (Schmiegelow et al., 1989; Schmiegelow and Pulczynska, 1990; Schmiegelow, 2009).

MTX is primarily eliminated through the kidneys (up to 90% of the intravenous dose within 24 h) (Bleyer, 1978). It is metabolized to 7-hydroxy-MTX in the liver, which contributes to MTX activity (Csordas et al., 2013), and a small part of MTX is excreted in the bile with partial intestinal reabsorption. Several efflux and uptake transporters (e.g., BCRP, MRP2, MRP3, MRP4, OAT1, and OAT3) are involved in the pharmacokinetic (PK) disposition process of MTX, which could lead to substantial variability in PK exposure (Treviño et al., 2009; Leveque et al., 2011; Ramsey et al., 2013; Schulte et al., 2021). Recent studies suggested that MTX elimination varied significantly between HD-MTX courses, and extremely delayed MTX elimination was observed in approximately 0.5% of pediatric patients with ALL (Svahn et al., 2017). The routine therapeutic drug monitoring for MTX has been strongly recommended to reduce the incidence of AEs in the target patient population, as suggested by several clinical guidelines and drug labeling.

In general, conventional PK studies require the collection of a series of PK blood samples to compute the PK exposure parameters (i.e., Cmax, AUC) using a non-compartmental analysis approach. However, this approach is inapplicable for routine clinical therapeutic drug monitoring, especially in the pediatric population, since only sparse PK concentrations is available. The population PK approach has advantages such as unitizing sparse PK data in addition to quantifying and analyzing the covariate effect, and therefore is widely used in individual therapy. Although a number of population PK models of MTX have been established previously in various clinical settings, the extrapolation of the previous population PK models to a new clinical setting remains highly uncertain (as shown in the cases of vancomycin and ciclosporin) (Deng et al., 2013; Mao et al., 2018). Additionally, previous PK studies on MTX have suggested that more population PK studies are still needed due to the variation in patient demographic data and dosage regimens.

Considering these factors, the main objective of this study is to develop a population PK model of HD-MTX infusion in Chinese pediatric patients with ALL and to explore the potential effect of covariates that could affect MTX PK profiles.

MATERIALS AND METHODS

Study Population

The study protocol and collection of retrospective clinical data were approved by the Research Ethics Committee of Children's Hospital of Fudan University [No (2020) 444]. The study population identified was Chinese pediatric patients (≤ 18 years old) diagnosed with ALL who received HD-MTX at the Children's Hospital of Fudan University, Shanghai, from January 2014 to December 2019.

ALL Treatment Regimen

The pediatric patients with ALL were diagnosed and treated in accordance to the guidelines outlined in the China Children's Leukemia Group (CCLG) ALL-2008 protocol (Cui et al., 2018) and China Children's Cancer Group (CCCG) ALL-2015 protocol (Zhu et al., 2020). Children diagnosed with ALL were classified into the low-risk (LR), intermediate-risk (IR), and high-risk (HR) groups. MTX was administered as intravenous (IV) infusion over 24 h at a dosage regimen of 3 g/m^2 in the LR group and 5 g/m^2 for both IR and HR groups, respectively. Ten percent of the total dose was administered as a loading dose (0.5 h), followed by infusion of the remaining 90% of the dose over 23.5 h. In addition, after 1–2 h of starting MTX infusion, 6–12.5 mg dose (according to the patients' age) of MTX was administered via intrathecal injection to prevent CNS ALL. The patients were also orally administered 6-mercaptopurine 25 mg/m^2 daily for 14 days. The MTX dose for pediatric patients was reduced to a lower level in case of substantial delay in elimination in previous MTX chemotherapy. Biochemical tests (e.g., liver and renal function) were routinely conducted before (baseline), 48 h after, and at the end of MTX chemotherapy. According to clinical practice, findings of the renal and liver function tests for pediatric

patients must be roughly normal (e.g., SCr) before MTX chemotherapy.

Pharmacokinetic Sampling Collection

Routine samples for MTX concentration measurement for therapeutic drug monitoring were collected from the patients according to the clinical practice in hospital. As per clinical guidelines, delayed serum excretion was defined as an MTX concentration greater than 1.0 μmol/L at 42 h after the initiation of MTX infusion. Standard leucovorin rescue was administered at 15 mg/m^2/dose (intravenous) starting at 42 h and administered every 6 h, and was modified according to MTX serum concentrations until the MTX concentration at 48 h was less than 0.25 μmol/L. If MTX serum concentrations were higher than 0.4 μmol/L, leucovorin rescue was continued every 6 h until the MTX concentration was less than 0.25 μmol/L. Therefore, the PK blood samples were routinely collected at 24, 42, and 48 h after the treatment, and additional PK samples were collected every 24 h afterward if clinically indicated. The majority of patients received multiple cycles of HD-MTX therapy and multiple MTX concentrations were measured in each cycle.

Demographic data, including age at treatment, sex, body weight, body surface area (BSA), body mass index, time-varying laboratory tests, including data on serum creatinine levels (SCr), alanine transaminase (ALT), aspartate transaminase (AST), alkaline phosphatase (ALP), total bilirubin (TBIL), direct bilirubin, and albumin, were collected. PK data, including the date and time of dosage administration and PK collection, as well as MTX concentrations were collected and appended to the demographic data of each patient. MTX serum concentrations were measured by fluorescence polarization immunoassay. The concomitant medication during the MTX chemotherapy was recorded in the medical record of the hospital's HIS system. Medications known to alter MTX PK behaviors (e.g., dasatinib, imatinib, penicillin, omeprazole, and non-steroidal anti-inflammatory drug (NSAIDs)) during the MTX chemotherapy were selected for covariate analysis.

Population Pharmacokinetic Analysis

A total of 311 children were enrolled in this population PK modeling analysis. A total of 4,517 blood samples were collected for MTX concentration measurements. Population PK analysis was performed using non-linear mixed-effects model in the NONMEM® software (version 7.4, ICON Development Solutions, Ellicott City, MD, United States) and data were compiled using gFortran (version 4.60). Perl-speaks-NONMEM (PsN; version 4.6.0) and R language (version 3.4.0, http://www.r-project.org/) were used to visualize the outputs. The first-order conditional estimation algorithm with η-ε interaction (FOCE-I) was used throughout the model-building procedure. Discrimination between models during the model-building process was based on standard visual diagnostics and the objective function value (OFV), which were calculated to be proportional to twice the log-likelihood (−2LL). A decrease in OFV (ΔOFV) of 6.64 was considered a significant improvement of model fit ($p < 0.01$) between the two hierarchical models after inclusion of one additional parameter (one degree of freedom difference).

MTX concentrations were logarithmically converted. A base model without incorporating any covariates and capable of describing the data appropriately was selected. During this step of analysis, all possible structural compartments were investigated, i.e., one-, two-, and three-compartment disposition models.

Inter-individual variability (IIV) was added exponentially to all PK parameters (**Eq. 1**).

$$\theta_i = \theta \cdot \exp\left(\eta_{i,\theta}\right) \tag{1}$$

where θ_i is the individual parameter estimate for the ith individual, θ is the population estimate of the investigated PK parameter, and $\eta_{i,\theta}$ is the IIV of the investigated PK parameter, assumed to be normally distributed with a zero mean and variance ω^2. The residual unexplained variability, assumed to be normally distributed with a zero mean and variance σ^2, was modeled with an additive error on the natural log-transformed concentrations, which was approximately equivalent to an exponential residual error on an arithmetic scale.

Covariate Modeling

Demographic data on body weight were added in the model as a simultaneous incorporation of an allometric function on all clearance and distribution volume parameters (**Eq 2**, **3**, respectively).

$$CL_i = CL_{typical} \cdot \left(\frac{BW_i}{BW_{median}}\right)^{0.75} \cdot \exp\left(\eta_{i,CL}\right), \tag{2}$$

$$V_i = V_{typical} \cdot \left(\frac{BW_i}{BW_{median}}\right) \cdot \exp\left(\eta_{i,V}\right), \tag{3}$$

where BW_i is the individual body weight and BW_{median} is the median body weight of the patients (i.e., 19 kg) in this study CL_i and V_i are the individually predicted clearance and distribution of volume, respectively. $CL_{typical}$ and $V_{typical}$ are the typical clearance and distribution of volume value of the population, respectively.

The effect of age-related maturation on clearance was then evaluated using a saturation-type E_{max} function (**Eq. 4**).

$$CL_i = CL_{typical} \cdot \frac{Age}{Age_{50} + Age} \cdot \left(\frac{BW_i}{BW_{median}}\right)^{0.75} \cdot \exp\left(\eta_{i,CL}\right), \tag{4}$$

where Age_{50} is the age associated with reaching 50% of the clearance maturation.

Other covariates (e.g., sex, liver function, renal function, and concomitant drugs) were investigated for all model parameters using a forward selection ($p = 0.01$) and backward elimination ($p = 0.001$) procedure. The concomitant drugs used in ≥5% of patients were evaluated for covariate effects.

In addition to statistical significance, the explanation of the variability by inclusion of a covariate was considered. A covariate was excluded from the model if the reduction in variability was <5%.

Model Evaluation

Basic goodness-of-fit diagnostic plots were used to evaluate systematic errors and model misspecifications. The sampling

TABLE 1 | | Demographic characteristics of 311 pediatric patients with ALL.

Characteristics	Median (range)
Demographics	
Male (*n*, %)	197 (63.3)
Age, years	5.0 (0.75–15.2)
Height, cm	112 (67–175)
Body weight, kg	19.0 (4.5–113.0)
Biochemical test	
Albumin, g/L	43.4 (23.8–56.5)
Total protein, g/L	63.4 (17.4–78.6)
Total bilirubin, μmol/L	5.9 (1.5–114.0)
Direct bilirubin, μmol/L	1.9 (0.1–45.0)
AST, U/L	22.6 (7.0–319.0)
ALT, U/L	16.0 (2.0–390)
Serum creatinine, μmol/L	26.0 (8.0–135.0)
MTX dosage regimen [n (course)]	
5 g/m^2	142 (464)
4 g/m^2	47 (84)
3 g/m^2	154 (524)
2 g/m^2	42 (107)
1 g/m^2	28 (71)
Concomitant medication [*n* (course)]	
Dasatinib	13 (48)
Imatinib	4 (14)
Omeprazole	59 (142)
Sulphonamides	14 (15)
NSAIDs	24 (25)
Penicillin	6 (6)

Notes: The demographic data were summarized from 1,250 cycles of MTX chemotherapy. ALT: alanine transaminase, AST: aspartate transaminase.

importance resampling (SIR) was used to calculate parameter uncertainty in the final population PK model (samples = 2,000, resamples = 1,000). The overall predictive performance of the final model was evaluated using simulation-based diagnostics (i.e., using prediction-corrected visual predictive checks (Bergstrand et al., 2011), n = 1,000 simulations).

RESULTS

The PK data of 311 pediatric patients were included in the population PK modeling analysis. All patients received a total of 1,250 cycles of MTX chemotherapy. Demographic characteristics of the patients are shown in **Table 1**.

An OFV of 7,229.251 was yielded when one disposition compartment model was used to fit MTX concentration-time data. By employing a two-compartment model, the model fit was improved significantly (ΔOFV = −5,912.277), and the three-compartment model further improved the model fit substantially (ΔOFV = −274.754).

Body weight, implemented as a fixed allometric function on all clearance and volume of distribution parameters, showed a substantial improvement in model fit (ΔOFV = −268.666). Inclusion of age-related maturation effect on CL did not show a significant improvement in model fit further.

Inclusion of SCr in a linear function on clearance significantly improved model fit (ΔOFV = −284.008), with slope estimates of −0.0097, and reduced the variability of Q_1 by 29.2% (CV% of IIV from 37.7 to 26.7%). Adding TBIL on clearance (ΔOFV = −30.975) and albumin in the central volume of distribution (ΔOFV = −36.722) using linear function improved model fit significantly, with slope estimates of −0.0044 and −0.070, respectively. However, these two covariates did not substantially reduce either the inter-individual or residual variability further (i.e., <5%), as defined above and, therefore, were not included in the model. Other covariates (e.g., sex, AST, and ALT) did not significantly affect MTX PK properties.

The covariate effects of omeprazole (co-medicated in 19.0% of patients and 11.4% of total chemotherapy courses) and NSAIDs concomitant medication (co-medicated in 7.7% of patients and 2.0% of total chemotherapy courses) were investigated. Their inclusion on clearance improved model fit significantly (ΔOFV = −64.331 and −42.874, respectively); however, the reduction in either inter-individual or residual variability was minimal (<1.1%). Therefore, these two co-medications were not retained in the final model. Only 13 (4.2%) and 4 (1.3%) pediatric patients with BCR-ABL1-positivity received treatment with dasatinib and imatinib, respectively, and six pediatric patients received penicillin, which are known to delay MTX elimination. However, the effect of this concomitant therapy was not investigated in the covariate analysis due to the small number of patients (<4.2%) receiving these medications.

The final parameter estimates showed good precision with relatively small standard errors (<15%), confirming the stability of the model (**Table 2**). The final parameter estimates described the expected distribution and elimination processes, as well as the associated unexplained variability in the study population. Goodness-of-fit diagnostic plots (**Figure 1**) and visual predictive checks (**Figure 2**) demonstrated a good description of the observed data and adequate predictive performance of the final model. Only 7 (0.15%) predictions lied outside the 5 to −5 CWRES for both the population predictions and time graphs. The R^2 values for OBS vs. PRED and IPRED were 0.882 and 0.925, respectively.

DISCUSSION

The dataset used herein is one of the largest pediatric ALL datasets for Chinese patients receiving HD-MTX chemotherapy, has a good depth of data collected at or beyond 96 h after the start of MTX infusion, and is suitable for determining whether there is an association between AEs and therapeutic outcomes.

HD-MTX remains an important chemotherapy regime for the treatment of patients with ALL. HD-MTX with leucovorin rescue regimen aims to increase MTX concentrations in specific pharmacological sanctuaries (e.g., CNS and testes), results in subsequently increase in cellular MTX uptake in resistant tumor cells, and to overcome intracellular resistance mechanisms (Ackland and Schilsky, 1987). It is a well-established fact that efficacy and toxicity are highly related to drug exposure in a list of chemotherapies. Seidel et al. (1997) found that higher MTX clearance was associated with poorer

TABLE 2 | | Final population PK parameter estimates of methotrexate in children with ALL.

Parameters	NONMEM estimates	SIR median (95%CI)	CV for IIV	SIR median (95%CI)
CL (L/h)	6.9 (2.5)	6.9 (6.62–7.19)	17.5 (5.8)	17.6 (16.0–19.7)
V_C (L)	20.7 (4.9)	20.5 (18.5–22.4)	—	—
Q_1 (L/h)	0.255 (7.4)	0.258 (0.232–0.285)	26.2 (17.2)	26.2 (18.4–33.6)
V_{P1} (L)	41.0 (11.4)	42.1 (34.4–51.3)	—	—
Q_2 (L/h)	0.217 (8.7)	0.224 (0.193–0.260)	—	—
V_{P2} (L)	3.17 (9.8)	3.28 (2.75–3.88)	—	—
SCr on CL (%)	−0.97 (4.7)	−0.96 (−0.91 to −1.00)	—	—
σ	0.354 (4.3)	0.350 (0.336–0.366)	—	—

CL is elimination clearance. V_C is the central volume of distribution. Q is the inter-compartmental clearance. V_P is the peripheral volume of distribution. σ is the additive residue error on the log scale.

*Population estimates in **Table 2** are given for a "typical" child with body weight of 19 kg. Body weight, was implemented as a fixed allometric function on all clearance and volume of distribution parameters using exponent of 0.75 and 1.0, respectively.*

The coefficients of variation for inter-individual variability (IIV) were calculated as $100 \times (e^{variance})^{1/2}$. The relative standard errors (%RSE) were calculated as 100 × (standard deviation/mean).

The SCr was implemented on CL as a linear function [$CL = CL_{typical} \times ((SCr-26) \times 0.0097)$].

SIR: Sampling importance resampling approach. The uncertainty was derived from the SIR, with options of 2,000 samples and 1,000 resamples.

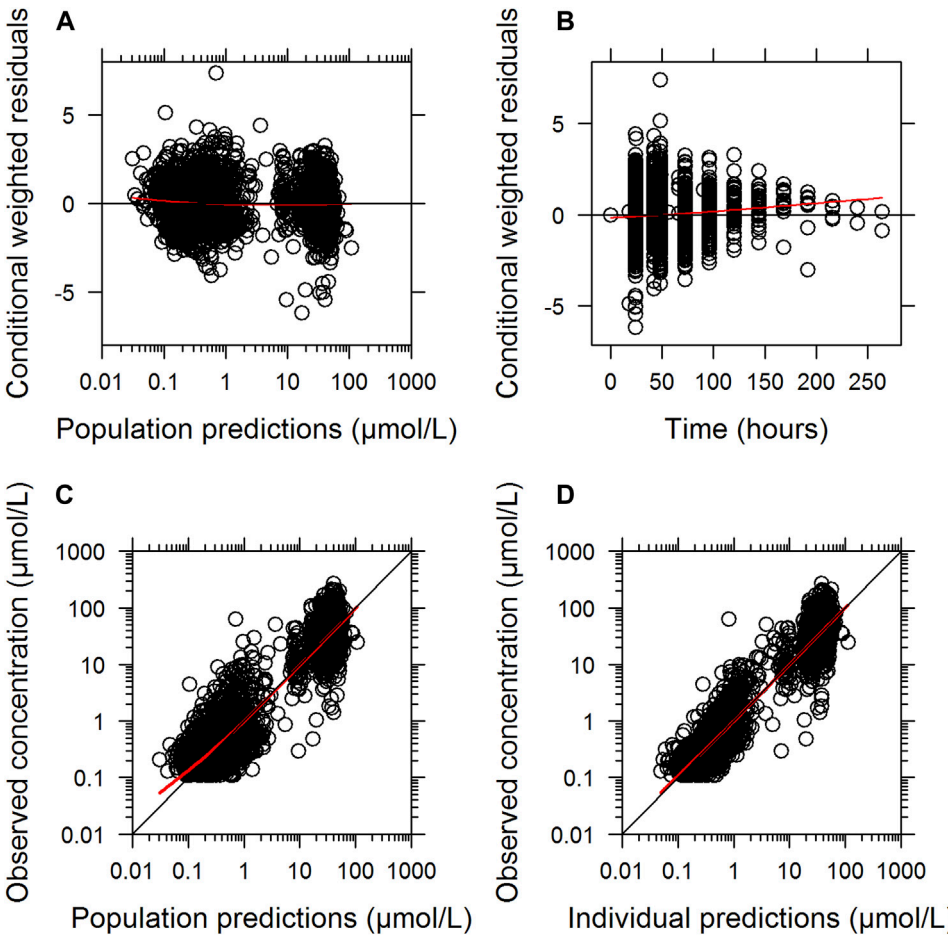

FIGURE 1 | Goodness-of-fit of the final population pharmacokinetic model describing MTX. Conditionally weighted residuals *vs.* population predicted concentrations **(A)**; conditionally weighted residuals *vs.* time **(B)**. Observed plasma concentrations *vs.* population predicted concentrations **(C)**; Observed plasma concentrations *vs.* individually predicted concentrations **(D)**; Solid red lines represent locally weighted least squares regressions.

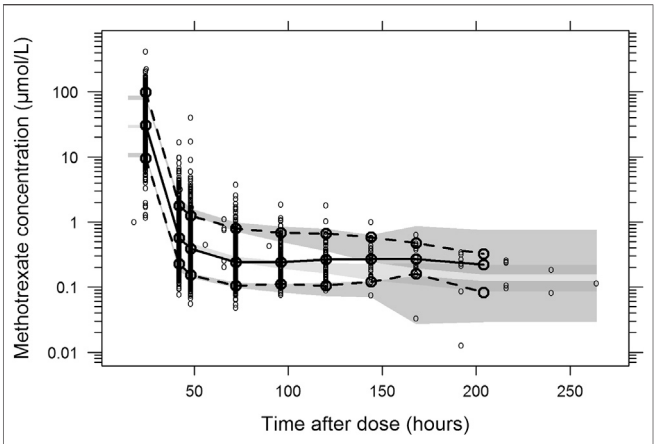

FIGURE 2 | Prediction- and variability-corrected visual predictive check of the final population pharmacokinetic model for methotrexate. Based on 1,000 stochastic simulations. Open circles represent the observations, and solid lines represent the 5th, 50th, and 95th percentiles of the observed data. The shaded areas represent the 95% confidence intervals around the simulated 5th, 50th, and 95th percentiles.

treatment outcomes in patients with childhood ALL. MTX mainly underwent renal elimination and displayed a high IIV in PK exposure (Evans et al., 1986; Evans et al., 1997; Evans et al., 1998; Schmiegelow, 2009). The population PK model allows the determination of the PK parameters as well as identification of the source of variability. The previous population PK models suggested that a list of covariates [e.g., age (Aumente et al., 2006; Thompson et al., 2007; Colom et al., 2009), body weight (Aumente et al., 2006; Colom et al., 2009), renal function (Dupuis et al., 2008; Fukuhara et al., 2008; Mao et al., 2014), and polymorphisms of transporters (Kim et al., 2012; Liu et al., 2017)] were related to MTX PK exposure.

Unlike the previously published population PK models using the two-compartment disposition model (Wall et al., 2000; Aumente et al., 2006; Faltaos et al., 2006; Piard et al., 2007; Min et al., 2009; Buitenkamp et al., 2010; Jönsson et al., 2011; Watanabe et al., 2014; Beechinor et al., 2019), the current study based on 311 pediatric patients enabled to fit the MTX concentration-time data by using a three-compartment disposition model. The final model demonstrated that the MTX clearance estimate in a typical child with a body weight of 19 kg was 6.9 L/h. This value was similar to those reported previously: 8.8 L/h in 79 ALL pediatric patients with an average body weight of 25.3 kg by Piard et al. (Piard et al., 2007), 7.87 L/h in 64 ALL pediatric patients with an average body weight of 25 kg (Faganel et al., 2011), and 7.73 L/h in 36 ALL pediatric patients with an average body weight of 23.4 kg (Hui et al., 2019). The central distribution of volume estimate in current study was 20.7 L, which was similar to that reported by a previous study (16.7 L) involving 64 pediatric patients with ALL/ML (Faganel et al., 2011) and somewhat higher than that reported by another pediatric study (9.3 L for a typical child with body weight of 20 kg) (Aumente et al., 2006).

Previous MTX population PK studies showed that body weight was more frequently included in the model, even though BSA has been reported as a significant covariate in some studies (Ruhs et al., 2012). Aumente et al. (2006) showed that the body weight was proportional to the MTX clearance with the slope estimate of 0.15, in pediatric patients aged more than 10 years, while in an over proportional manner using an allometric power function with an exponent estimate of 0.876 in those aged less than 10 years. Colom et al. (2009) indicated that the clearance was proportional to the body weight, with 0.55 L/h increase per 1 kg increase in body weight. In current study, body weight was allometrically implemented on all clearance and volume parameters using a fixed exponent of 0.75 and 1.0, respectively, as proposed previously (Holford et al., 2013). This could have significantly improved the model fit.

Since MTX was mainly eliminated through the kidneys, renal impairment could affect the elimination and increase the systemic PK exposure of MTX sequentially. Previous population PK studies on MTX chemotherapy in patients with cancer have reported significant effects of creatinine clearance (CRCL) or SCr on MTX clearance (Fukuhara et al., 2008; Ruhs et al., 2012; Mao et al., 2014). A study on pediatric lymphoblastic malignancies indicated that plasma MTX concentration at 48 h was positively correlated with 24 and 48 h SCr levels, but negatively correlated with 24 and 48 h CRCL (Mao et al., 2014). By using a power function in population PK modeling analysis, Fukuhara et al. found that CRCL was positively correlated with MTX clearance (Fukuhara et al., 2008), with the exponent estimate of 0.112. In current study, SCr was identified as a statistically significant covariate on clearance of MTX, which corresponded with above studies. Moreover, a recent population PK model utilizing approximately 32,000 MTX concentration data from a large-scale pediatric patient population receiving MTX chemotherapy (Taylor et al., 2020) found a non-linear relationship between time-varying SCr and clearance. In the current study, we were unable to find a non-linear relationship between time-varying SCr and clearance; this might be due to the narrow distribution of SCr and the small sample size compared to those of the previous study. Moreover, we predicted the effect of SCr on clearance based on the SCr distribution in our study using the equation used by Taylor et al. The predicted SCr effect on clearance was around ±20%, which was consistent with findings from current modeling analysis.

A few reports indicated that concomitant medication, such as penicillin and NSAIDs, could decrease MTX clearance by 61% and 16%, respectively (Kim et al., 2012). It has been reported that omeprazole could decrease MTX clearance by 27% (Joerger et al., 2006). In the current study, the inclusion of omeprazole and NSAIDs concomitant medication resulted in a statistically significant improvement in model fit. However, the effect of these drugs on MTX PK parameters was not retained in the final model due to a minimal reduction in either the inter-individual or residual variability.

This study had some limitations. 1) The MTX concentration data were obtained retrospectively from a single center, while the data from a multi-center clinical study would be considered to improve the accuracy of population PK modeling analysis. 2) Polymorphisms of transporters (e.g., SLC19A1, SLCO1B1,

ABCB1, and ABCG2) have been demonstrated to play a role in MTX PK disposition and could improve the model prediction. However, these polymorphisms were not detected in the current retrospective study and need to be investigated in the future.

CONCLUSION

In this study, MTX PK profiles were accurately captured using the proposed population PK model. The body weight and SCr were significant covariates on the PK disposition of MTX. The proposed model combined with the maximum *a posteriori* Bayesian approach could estimate individual PK parameters and optimize personalized MTX therapy for pediatric patients with ALL.

DATA AVAILABILITY STATEMENT

The original contributions presented in the study are included in the article/supplementary material, further inquiries can be directed to the corresponding author.

ETHICS STATEMENT

The studies involving human participants were reviewed and approved by Research Ethics Committee of Children's Hospital of Fudan University. Written informed consent to participate in this study was provided by the participants' legal guardian/next of kin.

AUTHOR CONTRIBUTIONS

X-WZ conceived and designed the study. H-SW, X-WQ, X-HZ, YY, HM, J-HM and J-YJ collected the data, H-SW and X-WQ evaluated the data. XG and H-SW built the model, drafted the article and wrote the article. X-WZ reviewed and edited the article. All authors read and approved the final article.

FUNDING

The work was supported by the Health and Family Planning Commission of Shanghai Municipality (201740011) and the Cyrus Tang Foundation.

ACKNOWLEDGMENTS

We would like to pay our best sincere and kind respect to pediatric patients for their participation, to the doctors and nurses at the Children's Hospital of Fudan University for caring for the patients, as well as the department of pharmacy for MTX concentration measurements.

REFERENCES

Ackland, S. P., and Schilsky, R. L. (1987). High-dose Methotrexate: a Critical Reappraisal. *Jco* 5, 2017–2031. doi:10.1200/JCO.1987.5.12.2017

Aumente, D., Santos Buelga, D., Lukas, J. C., Gomez, P., Torres, A., and Garcia, M. J. (2006). Population Pharmacokinetics of High-Dose Methotrexate in Children with Acute Lymphoblastic Leukaemia. *Clin. Pharmacokinet.* 45, 1227–1238. doi:10.2165/00003088-200645120-00007

Balis, F. M., Savitch, J. L., Bleyer, W. A., Reaman, G. H., and Poplack, D. G. (1985). Remission Induction of Meningeal Leukemia with High-Dose Intravenous Methotrexate. *Jco* 3, 485–489. doi:10.1200/jco.1985.3.4.485

Beechinor, R. J., Thompson, P. A., Hwang, M. F., Vargo, R. C., Bomgaars, L. R., Gerhart, J. G., et al. (2019). The Population Pharmacokinetics of High-Dose Methotrexate in Infants with Acute Lymphoblastic Leukemia Highlight the Need for Bedside Individualized Dose Adjustment: A Report from the Children's Oncology Group. *Clin. Pharmacokinet.* 58, 899–910. doi:10.1007/s40262-018-00734-0

Bergstrand, M., Hooker, A. C., Wallin, J. E., and Karlsson, M. O. (2011). Prediction-corrected Visual Predictive Checks for Diagnosing Nonlinear Mixed-Effects Models. *AAPS J.* 13, 143–151. doi:10.1208/s12248-011-9255-z

Bhojwani, D., Sabin, N. D., Pei, D., Yang, J. J., Khan, R. B., Panetta, J. C., et al. (2014). Methotrexate-induced Neurotoxicity and Leukoencephalopathy in Childhood Acute Lymphoblastic Leukemia. *Jco* 32, 949–959. doi:10.1200/JCO.2013.53.0808

Bleyer, W. A. (1978). The Clinical Pharmacology of methotrexate.New Applications of an Old Drug. *Cancer* 41, 36–51. doi:10.1002/1097-0142(197801)41:1<36::aid-cncr2820410108>3.0.co;2-i

Buitenkamp, T. D., Mathot, R. A. A., de Haas, V., Pieters, R., and Zwaan, C. M. (2010). Methotrexate-induced Side Effects Are Not Due to Differences in Pharmacokinetics in Children with Down Syndrome and Acute Lymphoblastic Leukemia. *Haematologica* 95, 1106–1113. doi:10.3324/haematol.2009.019778

Cheng, K. K.-F. (2008). Association of Plasma Methotrexate, Neutropenia, Hepatic Dysfunction, Nausea/vomiting and Oral Mucositis in Children with Cancer. *Eur. J. Cancer Care* 17, 306–311. doi:10.1111/j.1365-2354.2007.00843.x

Colom, H., Farré, R., Soy, D., Peraire, C., Cendros, J.-M., Pardo, N., et al. (2009). Population Pharmacokinetics of High-Dose Methotrexate after Intravenous Administration in Pediatric Patients with Osteosarcoma. *Ther. Drug Monit.* 31, 76–85. doi:10.1097/ftd.0b013e3181945624

Comandone, A., Passera, R., Boglione, A., Tagini, V., Ferrari, S., and Cattel, L. (2005). High Dose Methotrexate in Adult Patients with Osteosarcoma: Clinical and Pharmacokinetic Results. *Acta Oncologica* 44, 406–411. doi:10.1080/02841860510029770

Csordas, K., Hegyi, M., Eipel, O. T., Muller, J., Erdelyi, D. J., and Kovacs, G. T. (2013). Comparison of Pharmacokinetics and Toxicity after High-Dose Methotrexate Treatments in Children with Acute Lymphoblastic Leukemia. *Anticancer Drugs* 24, 189–197. doi:10.1097/CAD.0b013e32835b8662

Cui, L., Li, Z.-G., Chai, Y.-H., Yu, J., Gao, J., Zhu, X.-F., et al. (2018). Outcome of Children with Newly Diagnosed Acute Lymphoblastic Leukemia Treated with CCLG-ALL 2008: The First Nation-wide Prospective Multicenter Study in China. *Am. J. Hematol.* 93, 913–920. doi:10.1002/ajh.25124

Deng, C., Liu, T., Wu, K., Wang, S., Li, L., Lu, H., et al. (2013). Predictive Performance of Reported Population Pharmacokinetic Models of Vancomycin in Chinese Adult Patients. *J. Clin. Pharm. Ther.* 38, 480–489. doi:10.1111/jcpt.12092

Desantis, C. E., Lin, C. C., Mariotto, A. B., Siegel, R. L., Stein, K. D., Kramer, J. L., et al. (2014). Cancer Treatment and Survivorship Statistics, 2014. *CA A Cancer J. Clinicians* 64, 252–271. doi:10.3322/caac.21235

Dupuis, C., Mercier, C., Yang, C., Monjanel-Mouterde, S., Ciccolini, J., Fanciullino, R., et al. (2008). High-dose Methotrexate in Adults with Osteosarcoma: a Population Pharmacokinetics Study and Validation of a New Limited Sampling Strategy. *Anti-Cancer Drug* 19, 267–273. doi:10.1097/cad.0b013e3282f21376

Evans, W. E., Crom, W. R., Abromowitch, M., Dodge, R., Look, A. T., Bowman, W. P., et al. (1986). Clinical Pharmacodynamics of High-Dose Methotrexate in Acute Lymphocytic Leukemia. *N. Engl. J. Med.* 314, 471–477. doi:10.1056/NEJM198602203140803

Evans, W. E., Relling, M. V., Boyett, J. M., and Pui, C.-H. (1997). Does Pharmacokinetic Variability Influence the Efficacy of High-Dose Methotrexate for the Treatment of Children with Acute Lymphoblastic Leukemia: what Can We Learn from Small Studies?. *Leuk. Res.* 21, 435–437. doi:10.1016/s0145-2126(96)00128-2

Evans, W. E., Relling, M. V., Rodman, J. H., Crom, W. R., Boyett, J. M., and Pui, C.-H. (1998). Conventional Compared with Individualized Chemotherapy for Childhood Acute Lymphoblastic Leukemia. *N. Engl. J. Med.* 338, 499–505. doi:10.1056/NEJM199802193380803

Faganel, K. B., Grabnar, I., Bohanec, Gr. P., Dolžan, V., and Jazbec, J. (2011). Association of Genetic Polymorphism in the Folate Metabolic Pathway with Methotrexate Pharmacokinetics and Toxicity in Childhood Acute Lymphoblastic Leukaemia and Malignant Lymphoma. *Eur. J. Clin. Pharmacol.* 67, 993–1006. doi:10.1007/s00228-011-1046-z

Faltaos, D. W., Hulot, J. S., Urien, S., Morel, V., Kaloshi, G., Fernandez, C., et al. (2006). Population Pharmacokinetic Study of Methotrexate in Patients with Lymphoid Malignancy. *Cancer Chemother. Pharmacol.* 58, 626–633. doi:10.1007/s00280-006-0202-0

Fukuhara, K., Ikawa, K., Morikawa, N., and Kumagai, K. (2008). Population Pharmacokinetics of High-Dose Methotrexate in Japanese Adult Patients with Malignancies: a Concurrent Analysis of the Serum and Urine Concentration Data. *J. Clin. Pharm. Ther.* 33, 677–684. doi:10.1111/j.1365-2710.2008.00966.x

Galivan, J. (1980). Evidence for the Cytotoxic Activity of Polyglutamate Derivatives of Methotrexate. *Mol. Pharmacol.* 17, 105–110.

Gervasini, G., and Vagace, J. M. (2012). Impact of Genetic Polymorphisms on Chemotherapy Toxicity in Childhood Acute Lymphoblastic Leukemia. *Front. Gene* 3, 249. doi:10.3389/fgene.2012.00249

Hegyi, M., Gulácsi, Á., Cságoly, E., Csordás, K., Eipel, O. T., Erdélyi, D. J., et al. (2012). Clinical Relations of Methotrexate Pharmacokinetics in the Treatment for Pediatric Osteosarcoma. *J. Cancer Res. Clin. Oncol.* 138, 1697–1702. doi:10.1007/s00432-012-1214-2

Holford, N., Heo, Y.-A., and Anderson, B. (2013). A Pharmacokinetic Standard for Babies and Adults. *J. Pharm. Sci.* 102, 2941–2952. doi:10.1002/jps.23574

Howard, S. C., Mccormick, J., Pui, C. H., Buddington, R. K., and Harvey, R. D. (2016). Preventing and Managing Toxicities of High-Dose Methotrexate. *The Oncologist* 21, 1471–1482. doi:10.1634/theoncologist.2015-0164

Hui, K. H., Chu, H. M., Fong, P. S., Cheng, W. T. F., and Lam, T. N. (2019). Population Pharmacokinetic Study and Individual Dose Adjustments of High-Dose Methotrexate in Chinese Pediatric Patients with Acute Lymphoblastic Leukemia or Osteosarcoma. *J. Clin. Pharmacol.* 59, 566–577. doi:10.1002/jcph.1349

Hunger, S. P., and Mullighan, C. G. (2015). Acute Lymphoblastic Leukemia in Children. *N. Engl. J. Med.* 373, 1541–1552. doi:10.1056/NEJMra1400972

Joerger, M., Huitema, A. D. R., Krähenbühl, S., Schellens, J. H. M., Cerny, T., Reni, M., et al. (2010). Methotrexate Area under the Curve Is an Important Outcome Predictor in Patients with Primary CNS Lymphoma: A Pharmacokinetic-Pharmacodynamic Analysis from the IELSG No. 20 Trial. *Br. J. Cancer* 102, 673–677. doi:10.1038/sj.bjc.6605559

Joerger, M., Huitema, A. D. R., van den Bongard, H. J. G. D., Baas, P., Schornagel, J. H., Schellens, J. H. M., et al. (2006). Determinants of the Elimination of Methotrexate and 7-Hydroxy-Methotrexate Following High-Dose Infusional Therapy to Cancer Patients. *Br. J. Clin. Pharmacol.* 62, 71–80. doi:10.1111/j.1365-2125.2005.02513.x

Johansson, Å. M., Hill, N., Perisoglou, M., Whelan, J., Karlsson, M. O., and Standing, J. F. (2011). A Population Pharmacokinetic/pharmacodynamic Model of Methotrexate and Mucositis Scores in Osteosarcoma. *Ther. Drug Monit.* 33, 711–718. doi:10.1097/FTD.0b013e31823615e1

Jönsson, P., Skärby, T., Heldrup, J., Schrøder, H., and Höglund, P. (2011). High Dose Methotrexate Treatment in Children with Acute Lymphoblastic Leukaemia May Be Optimised by a Weight-Based Dose Calculation. *Pediatr. Blood Cancer* 57, 41–46. doi:10.1002/pbc.22999

Kawakatsu, S., Nikanjam, M., Lin, M., Le, S., Saunders, I., Kuo, D. J., et al. (2019). Population Pharmacokinetic Analysis of High-Dose Methotrexate in Pediatric and Adult Oncology Patients. *Cancer Chemother. Pharmacol.* 84, 1339–1348. doi:10.1007/s00280-019-03966-4

Kim, I.-W., Yun, H.-y., Choi, B., Han, N., Park, S.-Y., Lee, E. S., et al. (2012). ABCB1 C3435T Genetic Polymorphism on Population Pharmacokinetics of Methotrexate after Hematopoietic Stem Cell Transplantation in Korean Patients: A Prospective Analysis. *Clin. Ther.* 34, 1816–1826. doi:10.1016/j.clinthera.2012.06.022

Levêque, D., Santucci, R., Gourieux, B., and Herbrecht, R. (2011). Pharmacokinetic Drug-Drug Interactions with Methotrexate in Oncology. *Expert Rev. Clin. Pharmacol.* 4, 743–750. doi:10.1586/ecp.11.57

Liu, S.-G., Gao, C., Zhang, R.-D., Zhao, X.-X., Cui, L., Li, W.-J., et al. (2017). Polymorphisms in Methotrexate Transporters and Their Relationship to Plasma Methotrexate Levels, Toxicity of High-Dose Methotrexate, and Outcome of Pediatric Acute Lymphoblastic Leukemia. *Oncotarget* 8, 37761–37772. doi:10.18632/oncotarget.17781

Mao, J.-J., Jiao, Z., Yun, H.-Y., Zhao, C.-Y., Chen, H.-C., Qiu, X.-Y., et al. (2018). External Evaluation of Population Pharmacokinetic Models for Ciclosporin in Adult Renal Transplant Recipients. *Br. J. Clin. Pharmacol.* 84, 153–171. doi:10.1111/bcp.13431

Mao, J., Zhang, L., Shen, H., Tang, Y., Song, H., Zhao, F., et al. (2014). Creatinine Clearance Rate and Serum Creatinine Concentration Are Related to Delayed Methotrexate Elimination in Children with Lymphoblastic Malignancies. *neo* 61, 77–82. doi:10.4149/neo_2014_011

Min, Y., Qiang, F., Peng, L., and Zhu, Z. (2009). High Dose Methotrexate Population Pharmacokinetics and Bayesian Estimation in Patients with Lymphoid Malignancy. *Biopharm. Drug Dispos.* 30, 437–447. doi:10.1002/bdd.678

Panetta, J. C., Roberts, J. K., Huang, J., Lin, T., Daryani, V. M., Harstead, K. E., et al. (2020). Pharmacokinetic Basis for Dosing High-dose Methotrexate in Infants and Young Children with Malignant Brain Tumours. *Br. J. Clin. Pharmacol.* 86, 362–371. doi:10.1111/bcp.14160

Pavlovic, S., Kotur, N., Stankovic, B., Zukic, B., Gasic, V., and Dokmanovic, L. (2019). Pharmacogenomic and Pharmacotranscriptomic Profiling of Childhood Acute Lymphoblastic Leukemia: Paving the Way to Personalized Treatment. *Genes* 10, 191. doi:10.3390/genes10030191

Piard, C., Bressolle, F., Fakhoury, M., Zhang, D., Yacouben, K., Rieutord, A., et al. (2007). A Limited Sampling Strategy to Estimate Individual Pharmacokinetic Parameters of Methotrexate in Children with Acute Lymphoblastic Leukemia. *Cancer Chemother. Pharmacol.* 60, 609–620. doi:10.1007/s00280-006-0394-3

Ramsey, L. B., Panetta, J. C., Smith, C., Yang, W., Fan, Y., Winick, N. J., et al. (2013). Genome-wide Study of Methotrexate Clearance Replicates SLCO1B1. *Blood* 121, 898–904. doi:10.1182/blood-2012-08-452839

Rühs, H., Becker, A., Drescher, A., Panetta, J. C., Pui, C.-H., Relling, M. V., et al. (2012). Population PK/PD Model of Homocysteine Concentrations after High-Dose Methotrexate Treatment in Patients with Acute Lymphoblastic Leukemia. *PLoS One* 7, e46015. doi:10.1371/journal.pone.0046015

Schmiegelow, K. (2009). Advances in Individual Prediction of Methotrexate Toxicity: a Review. *Br. J. Haematol.* 146, 489–503. doi:10.1111/j.1365-2141.2009.07765.x

Schmiegelow, K., and Pulczynska, M. (1990). Prognostic Significance of Hepatotoxicity during Maintenance Chemotherapy for Childhood Acute Lymphoblastic Leukaemia. *Br. J. Cancer* 61, 767–772. doi:10.1038/bjc.1990.172

Schmiegelow, K., Schrøder, H., Pulczynska, M. K., and Hejl, M. (1989). Maintenance Chemotherapy for Childhood Acute Lymphoblastic Leukemia: Relation of Bone-Marrow and Hepatotoxicity to the Concentration of Methotrexate in Erythrocytes. *Cancer Chemother. Pharmacol.* 25, 65–69. doi:10.1007/BF00694341

Schulte, R. R., Choi, L., Utreja, N., Van Driest, S. L., Stein, C. M., and Ho, R. H. (2021). Effect of SLCO1B1 Polymorphisms on High-Dose Methotrexate Clearance in Children and Young Adults with Leukemia and Lymphoblastic Lymphoma. *Clin. Transl. Sci.* 14, 343–353. doi:10.1111/cts.12879

Seidel, H., Nygaard, R., Moe, P. J., Jacobsen, G., Lindqvist, B., and Slørdal, L. (1997). On the Prognostic Value of Systemic Methotrexate Clearance in Childhood Acute Lymphocytic Leukemia. *Leuk. Res.* 21, 429–434. doi:10.1016/s0145-2126(96)00127-0

Shi, Z. Y., Liu, Y. O., Gu, H. Y., Xu, X. Q., Yan, C., Yang, X. Y., et al. (2020). Population Pharmacokinetics of High-dose Methotrexate in Chinese Pediatric Patients with Medulloblastoma. *Biopharm. Drug Dispos.* 41, 101–110. doi:10.1002/bdd.2221

Svahn, T., Mellgren, K., Harila-Saari, A., Åsberg, A., Kanerva, J., Jónsson, Ó., et al. (2017). Delayed Elimination of High-Dose Methotrexate and Use of Carboxypeptidase G2 in Pediatric Patients during Treatment for Acute Lymphoblastic Leukemia. *Pediatr. Blood Cancer* 64, e26395, doi:10.1002/pbc.26395

Taylor, Z. L., Mizuno, T., Punt, N. C., Baskaran, B., Navarro Sainz, A., Shuman, W., et al. (2020). MTXPK.org: A Clinical Decision Support Tool Evaluating High-Dose Methotrexate Pharmacokinetics to Inform Post-Infusion Care and Use of Glucarpidase. *Clin. Pharmacol. Ther.* 108, 635, 643. doi: doi: doi:10.1002/cpt.1957

Thompson, P. A., Murry, D. J., Rosner, G. L., Lunagomez, S., Blaney, S. M., Berg, S. L., et al. (2007). Methotrexate Pharmacokinetics in Infants with Acute Lymphoblastic Leukemia. *Cancer Chemother. Pharmacol.* 59, 847–853. doi:10.1007/s00280-006-0388-1

Treviño, L. R., Shimasaki, N., Yang, W., Panetta, J. C., Cheng, C., Pei, D., et al. (2009). Germline Genetic Variation in an Organic Anion Transporter Polypeptide Associated with Methotrexate Pharmacokinetics and Clinical Effects. *Jco* 27, 5972–5978. doi:10.1200/JCO.2008.20.4156

Wall, A., Gajjar, A., Link, A., Mahmoud, H., Pui, C.-H., and Relling, M. (2000). Individualized Methotrexate Dosing in Children with Relapsed Acute Lymphoblastic Leukemia. *Leukemia* 14, 221–225. doi:10.1038/sj.leu.2401673

Watanabe, M., Fukuoka, N., Takeuchi, T., Yamaguchi, K., Motoki, T., Tanaka, H., et al. (2014). Developing Population Pharmacokinetic Parameters for High-Dose Methotrexate Therapy: Implication of Correlations Among Developed Parameters for Individual Parameter Estimation Using the Bayesian Least-Squares Method. *Biol. Pharm. Bull.* 37, 916–921. doi:10.1248/bpb.b13-00672

Widemann, B. C., Balis, F. M., Kempf-Bielack, B., Bielack, S., Pratt, C. B., Ferrari, S., et al. (2004). High-dose Methotrexate-Induced Nephrotoxicity in Patients with Osteosarcoma. *Cancer* 100, 2222–2232. doi:10.1002/cncr.20255

Yarlagadda, S. G., and Perazella, M. A. (2008). Drug-induced crystal Nephropathy: an Update. *Expert Opin. Drug Saf.* 7, 147–158. doi:10.1517/14740338.7.2.147

Zhu, Y., Yang, R., Cai, J., Yu, J., Tang, Y., Chen, Y., et al. (2020). Septicemia after Chemotherapy for Childhood Acute Lymphoblastic Leukemia in China: A Multicenter Study CCCG-ALL-2015. *Cancer Med.* 9, 2113–2121. doi:10.1002/cam4.2889

Conflict of Interest: The authors declare that the research was conducted in the absence of any commercial or financial relationships that could be construed as a potential conflict of interest.

frontiers in Pharmacology

CASE REPORT
published: 20 July 2021
doi: 10.3389/fphar.2021.706329

Case Report: Predicting the Range of Lamotrigine Concentration Using Pharmacokinetic Models Based on Monte Carlo Simulation: A Case Study of Antiepileptic Drug-Related Leukopenia

Xiuqing Zhu[1,2], *Tao Xiao*[1], *Shanqing Huang*[1], *Shujing Liu*[1], *Xiaolin Li*[1], *Dewei Shang*[1,2]* *and Yuguan Wen*[1,2]*

[1]Department of Pharmacy, The Affiliated Brain Hospital of Guangzhou Medical University (Guangzhou Huiai Hospital), Guangzhou, China, [2]Guangdong Engineering Technology Research Center for Translational Medicine of Mental Disorders, Guangzhou, China

OPEN ACCESS

Edited by:
Erwin Dreesen,
KU Leuven, Belgium

Reviewed by:
Robin Michelet,
Freie Universität Berlin, Germany
Caren Lee Hughes,
Mayo Clinic Florida, United States

***Correspondence:**
Dewei Shang
shang_dewei@163.com
Yuguan Wen
wenyuguandede@163.com

Specialty section:
This article was submitted to Obstetric and Pediatric Pharmacology, a section of the journal Frontiers in Pharmacology

Received: 07 May 2021
Accepted: 08 July 2021
Published: 20 July 2021

Citation:
Zhu X, Xiao T, Huang S, Liu S, Li X, Shang D and Wen Y (2021) Case Report: Predicting the Range of Lamotrigine Concentration Using Pharmacokinetic Models Based on Monte Carlo Simulation: A Case Study of Antiepileptic Drug-Related Leukopenia. Front. Pharmacol. 12:706329. doi: 10.3389/fphar.2021.706329

Lamotrigine (LTG), a wide-spectrum antiepileptic drug, is frequently associated with cutaneous side-effects, whereas hematological side-effects such as leukopenia have rarely been reported for it. We report the case of a 15-year-old Chinese female epileptic patient weighing 60 kg who developed combined asymptomatic leukopenia after receiving concomitant therapy with LTG and valproate acid (VPA). In this case report, antiepileptic drug-related leukopenia may have occurred in definite relation to an increase in LTG concentration and reversed with the discontinuation of VPA. Monte Carlo (MC) simulations were performed to estimate the steady-state serum concentrations (C_{ss}) of LTG for different dosing regimens in adolescent Chinese epileptic patients weighing the same as the patient considered in the case study, based on pharmacokinetic (PK) models published in past research. Adjustments to the dosage of LTG for the patient were analyzed to illustrate the application of MC simulations and verify the results. The predicted LTG concentrations within a prediction interval between the 10th and 90th percentiles that represented 80% of the simulated populations, could adequately capture the measured LTG concentrations of the patient, indicating that MC simulations are a useful tool for estimating drug concentrations. Clinicians may benefit from the timely probabilistic predictions of the range of drug concentration based on an MC simulation that considers a large sample of virtual patients. The case considered here highlights the importance of therapeutic drug monitoring (TDM) and implementing model-informed precision dosing in the course of a patient's individualized treatment to minimize adverse reactions.

Keywords: lamotrigine, pharmacokinetic models, Monte Carlo simulation, case report, adolescence, steady-state serum concentrations, antiepileptic drug, leukopenia

INTRODUCTION

Lamotrigine (LTG) is a new-generation antiepileptic drug, the pharmacokinetic (PK) variability of which plays a key role in dosing requirements for it (Johannessen and Tomson, 2006). Multiple factors, such as the co-medication, concurrent diseases, age, body weight, pregnancy, and genetic polymorphisms, have been shown to affect its PK variability (Wang et al., 2019; Methaneethorn and Leelakanok, 2020; Zhu et al., 2021). An increase in toxicity has been noted in definite relation to an increase in LTG concentration (Hirsch et al., 2004), and the prevalence of toxicity increases significantly with LTG serum concentrations >15 mg/L (Søndergaard Khinchi et al., 2008; Jacob and Nair, 2016). Severe toxicity, such as cardiovascular toxicity, may occur in adults with LTG serum concentrations >25 mg/L (Alyahya et al., 2018). LTG is a good candidate for therapeutic drug monitoring (TDM). Thus, there is a need to monitor LTG concentrations, especially among pediatric patients, and when other co-administered antiepileptics are prescribed or discontinued in treatment regimens.

Model-informed precision dosing (MIPD) is a promising concept that can be used to characterize or quantify the variability in therapeutic outcomes and support the choice of optimal dosing regimens for individualized therapy, thereby increasing the rate of success of the treatment (Darwich et al., 2017; Kluwe et al., 2021). MIPD tools can offer support for making decisions about individualized treatment by clinicians (Kluwe et al., 2021). The Monte Carlo (MC) simulation, which is commonly used in medicine to optimize antimicrobial therapy, is a valuable tool for statistically modeling and predicting the likely results of different treatment regimens or the achievement of therapeutic targets by expanding the sample size, in light of variations in the relevant parameters with respect to the estimation of the targets of analysis (Roberts et al., 2011). It can incorporate the influence of different therapy scenarios and PK data derived from specific populations (Jang et al., 2018), and is useful for estimating the range of drug concentration of the usual empirical dosing regimens (Baek et al., 2015). In this study, MC simulations were performed to estimate the steady-state serum concentrations (C_{ss}) of LTG for different dosing regimens in adolescent Chinese epileptic patients weighing the same as the patient considered in the case study, based on PK models published in past research. A clinical case of the adjustments of dosage of LTG for a 15-year-old Chinese female epileptic patient weighing 60 kg, who had developed combined leukopenia 11 days after starting LTG, was analyzed to illustrate the application of MC simulations and verify the results. Given the possible, delayed return of TDM measurements (Leung et al., 2019), clinicians may only need to input the dose and the body weight (BW) of the patient to obtain timely probabilistic predictions of the range of LTG concentration based on an MC simulation that considers a large sample of virtual patients.

MONTE CARLO SIMULATION AND RESULTS

A flowchart of the MC simulation based on the Crystal Ball software (Fusion Version 11.1.1.3.00, Oracle Corporation, the United States) is shown in **Figure 1**. The simulation on Excel spreadsheets in general requires the definitions of certain inputs as assumptions and certain outputs as forecasts, and generates random numbers for the assumptions defined in the input cells. These are then fed into formulae defined in the forecast cells. The MC simulation can reflect a complex real-world scenario by using a large sample of trials. For each trial of an MC simulation, the above process is repeated. Finally, a forecast chart can be used to explore ranges of forecasts and the corresponding probabilities of the given goals. Therefore, the MC simulation can yield descriptive statistics concerning the assumption and forecasted values, and can provide the probability of target attainment (PTA) with forecasts within a defined range. In this study, C_{ss} was considered to be the set of forecasts in the output cells.

A previously described one-compartment model with first-order absorption and elimination was implemented to determine the time profiles of LTG concentration (Hussein and Posner, 1997). The values of C_{ss} were modeled for dosing regimens by using the following equation:

$$C_{ss} = \frac{k_a * F * X_0}{V_d * k_a - CL}\left(\frac{e^{-\frac{CL}{V_d}*t}}{1-e^{-\frac{CL}{V_d}*\tau}} - \frac{e^{-k_a*t}}{1-e^{-k_a*\tau}}\right)$$

where k_a is the rate of absorption (h^{-1}), F is the absolute bioavailability of the form of oral dosage (%), X_0 is a single dose (mg), V_d is the apparent volume of distribution (L), CL is total serum clearance (L/h), t is the time of blood sampling (h), and τ is the dosing interval (h). All the above parameters in the equation were used as modeling inputs for virtual populations, and were taken from the assumed dosing regimens and published PK models without being re-estimated (see **Figure 1**).

The PK parameters considered in the simulated model were t, k_a, F, V_d, and CL. t was presumed to have a uniform distribution of values ranging from 0 to τ h. Inter-subject variability [expressed as standard deviation (SD)] was included for k_a and F by using the log-normal distribution during the simulations (Doan et al., 2014). Given that the trough C_{ss} of LTG collected by Zhang et al. (2017) did not involve information on the rate and extent of the absorption processes, the data on k_a and F were obtained from published PK studies, and yielded values of (1.30 ± 0.22) h^{-1} and (97.60 ± 4.80)% (Garnett, 1997; Grasela et al., 1999), respectively, while the values of V_d and CL of LTG were obtained from a population pharmacokinetic (PPK) study by Zhang et al. (2017) on Chinese children aged >12 years who had been suffering from epilepsy. The value of V_d used in the simulated model was fixed at 23.10 L because no inter-individual variability was reported by Zhang et al. (2017). The BW is an informative covariate for the CL of adolescent patients in modeling, as shown by Zhang et al. (2017), and was assumed to be 60 kg. This corresponded to the BW value of the case below. The population mean CL_{pop} (L/h) was calculated as $CL_{pop} = 1.49 \times (BW/51.5)^{0.509} \times 0.498^{VPA} \times 1.7^{IND}$, where BW was set to 60 kg and VPA/IND denotes combination with valproate acid (VPA) or an enzyme inducer (IND) (yes = 1, no = 0) (Zhang et al., 2017). Based on the final PPK model of adolescents developed by Zhang et al. (2017), CL_j (L/h) was derived for different scenarios, and was calculated as $CL_j = 1.610 \times e^{\eta j}$ for LTG monotherapy, $CL_j = 0.802 \times$

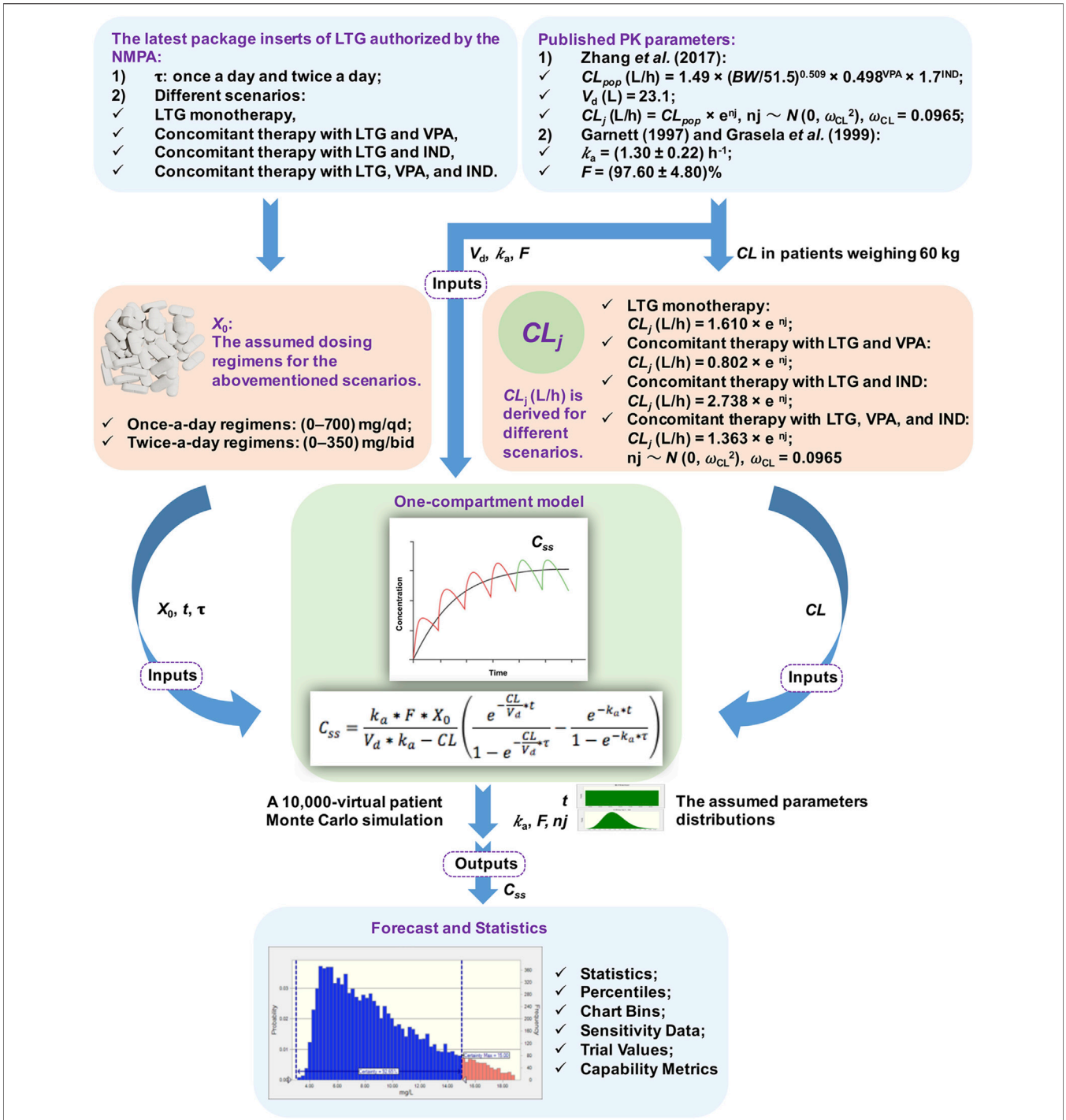

FIGURE 1 | Flowchart of the Monte Carlo (MC) simulation. Note. NMPA: The National Medical Products Administration, τ: the dosing interval, LTG: lamotrigine, VPA: valproate acid, IND: enzyme inducer, PK: pharmacokinetic, *CL*: total serum clearance, *BW*: total body weight, V_d: the apparent volume of distribution, k_a: the rate of absorption, *F*: the absolute bioavailability of the form of oral dosage, X_0: a single dose, *t*: the time of blood sampling, C_{ss}: steady-state serum concentrations, ω_{CL}: the inter-individual random error on *CL*, nj: the inter-individual variability in *CL*, CL_{pop}: the population mean *CL*, CL_j: the *CL* of the *j*th virtual patient.

e^{nj} for concomitant therapy with LTG and VPA, $CL_j = 2.738 \times e^{nj}$ for concomitant therapy with LTG and IND, and $CL_j = 1.363 \times e^{nj}$ for concomitant therapy with LTG, VPA, and IND. CL_j denotes the *CL* of the *j*th virtual patient and nj denotes the inter-individual variability in *CL*, following a normal distribution with zero mean and a variance of ω_{CL}^2. An MC simulation on data from 10,000 virtual patients was performed to calculate estimates of C_{ss} of LTG for once-a-day regimens between 0 and 700 mg/qd,

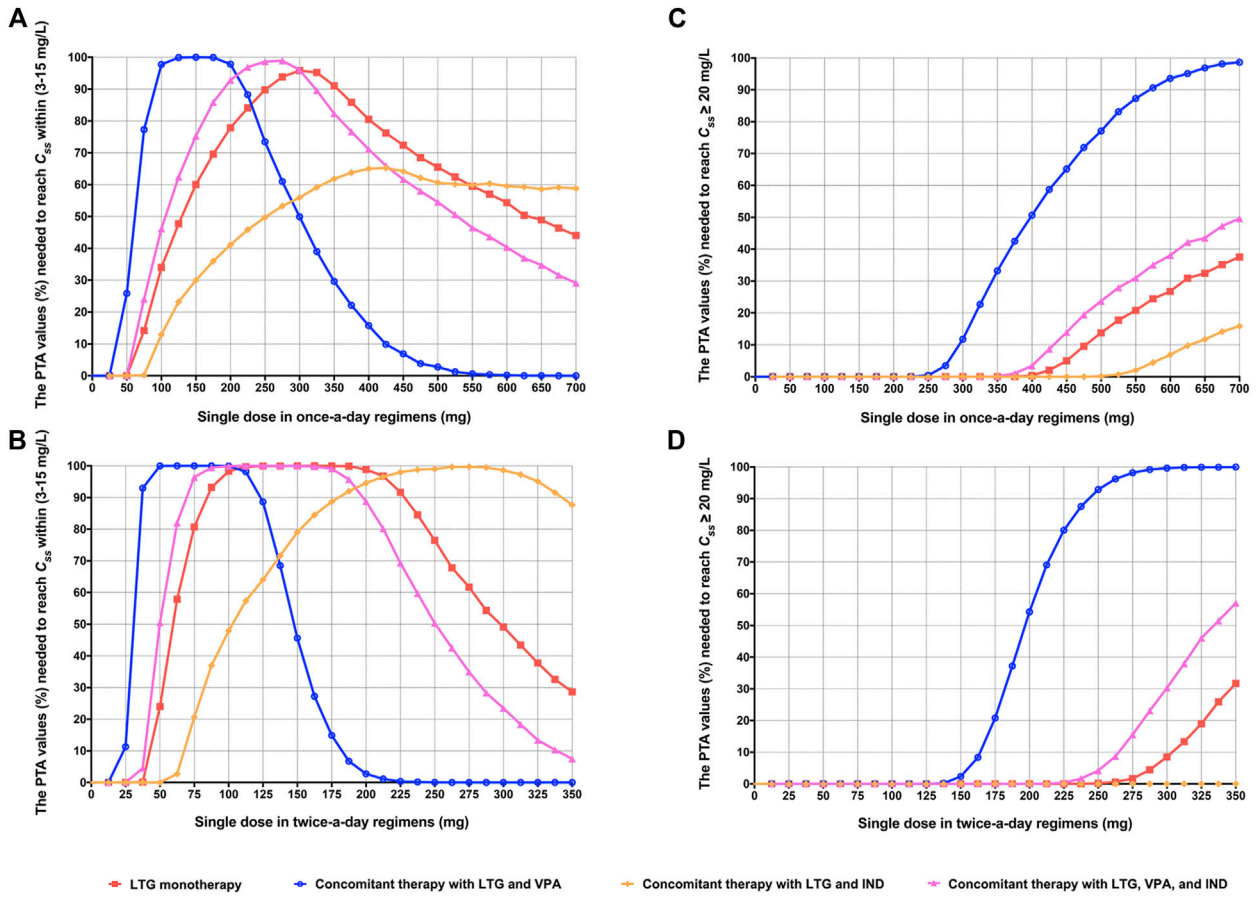

FIGURE 2 | The evolution of the probability of target attainment (PTA) values (%) needed to reach steady-state serum concentrations (C_{ss}) within the target range (3–15 mg/L) and ≥20 mg/L for different once-daily regimens **(A,C)** and twice-daily regimens **(B,D)** in different scenarios of concomitant therapy in adolescent Chinese epileptic patients weighing 60 kg, obtained by using Monte Carlo (MC) simulations. The solid node in the curve represents the result of a kind of assumed dosing regimen.

and twice-a-day regimens between 0 and 350 mg/bid in the context of the abovementioned scenarios.

Finally, the MC simulation resulted in 10,000 individual values of C_{ss} for each regimen along with the PTA values to reach C_{ss} within the range of 3–15 mg/L and ≥20 mg/L, the recommended ranges of the therapeutic reference and the laboratory alert, respectively, for LTG as an anticonvulsant drug according to the latest *Arbeitsgemeinschaft für Neuropsychopharmakologie und Pharmakopsychiatrie* (AGNP) guidelines for TDM in neuropsychopharmacology (Hiemke et al., 2018). The predicted mean values of C_{ss} and calculated PTA values for each of the above dosing regimens of LTG in different scenarios are shown in **Supplementary Tables S1–S4**. Accordingly, the evolution of the PTA values (%) needed to reach C_{ss} within the target range of 3–15 mg/L and ≥20 mg/L, respectively, for different regimens obtained by the MC simulations is presented in **Figure 2**. As is shown there, the dosing regimens (87.5–225 mg/bid) had higher than 90% of the PTA values to reach C_{ss} within the range of 3–15 mg/L for LTG monotherapy, which means that these dosing regimens could achieve the range of target concentration with a risk of below 10% to reach a concentration of under 3 mg/L or above 15 mg/L; however, dosing regimens greater than 125 mg/bid showed rapid downward trends in PTA values (lower than 90%) in the context of concomitant therapy with LTG and VPA, thus increasing the risk of a concentration above 20 mg/L (see **Figures 2B,D**) (Chhun et al., 2009). Therefore, clinicians may benefit from the timely estimations of the range of LTG concentration by quickly searching for its probabilistic predictions in various dosing regimens from **Figure 2**. The clinical case below was analyzed to verify the results of the MC simulation and illustrate the application of the setup in **Figure 2**.

CLINICAL CASE

A clinical case provided by us was used to verify the performance of the MC simulations. A patient, weighing 60 kg, with a four-year history of seizures, was admitted to the Affiliated Brain Hospital of Guangzhou Medical University due to recurrent seizures. Her antiepileptic drug history included LTG. Her dosing titration regimens of LTG after admission were 25 mg/bid (days 1–5), 50 mg/bid (days 6–9), 75 mg/bid (days 10–12), 100 mg/bid (days 13–20), and 125 mg/bid (days 21–38). Her

TABLE 1 | | Adverse drug reaction probability scale (Naranjo) in antiepileptic drug-related leukopenia.

Items	Yes	No	Do not know	Score
1. Are there previous conclusive reports on this reaction?	+1	0	0	+1
2. Did the adverse event appear after the suspected drug was administered?	+2	−1	0	+2
3. Did the adverse reaction improve when the drug was discontinued or a specific antagonist was administered?	+1	0	0	+1
4. Did the adverse reaction reappear when the drug was re-administered?	+2	−1	0	0
5. Are there alternative causes (other than the drug) that could on their own have caused the reaction?	−1	+2	0	0
6. Did the reaction reappear when a placebo was given?	−1	+1	0	0
7. Was the drug detected in blood (or other fluids) in concentrations known to be toxic?	+1	0	0	0
8. Was the reaction more severe when the dose was increased or less severe when the dose was decreased?	+1	0	0	+1
9. Did the patient have a similar reaction to the same or similar drugs in any previous exposure?	+1	0	0	0
10. Was the adverse event confirmed by any objective evidence?	+1	0	0	+1
Total scores				6

Definite: Score ≥ 9; Probable: 5–8; Possible: 1–4; Doubtful: ≤0.

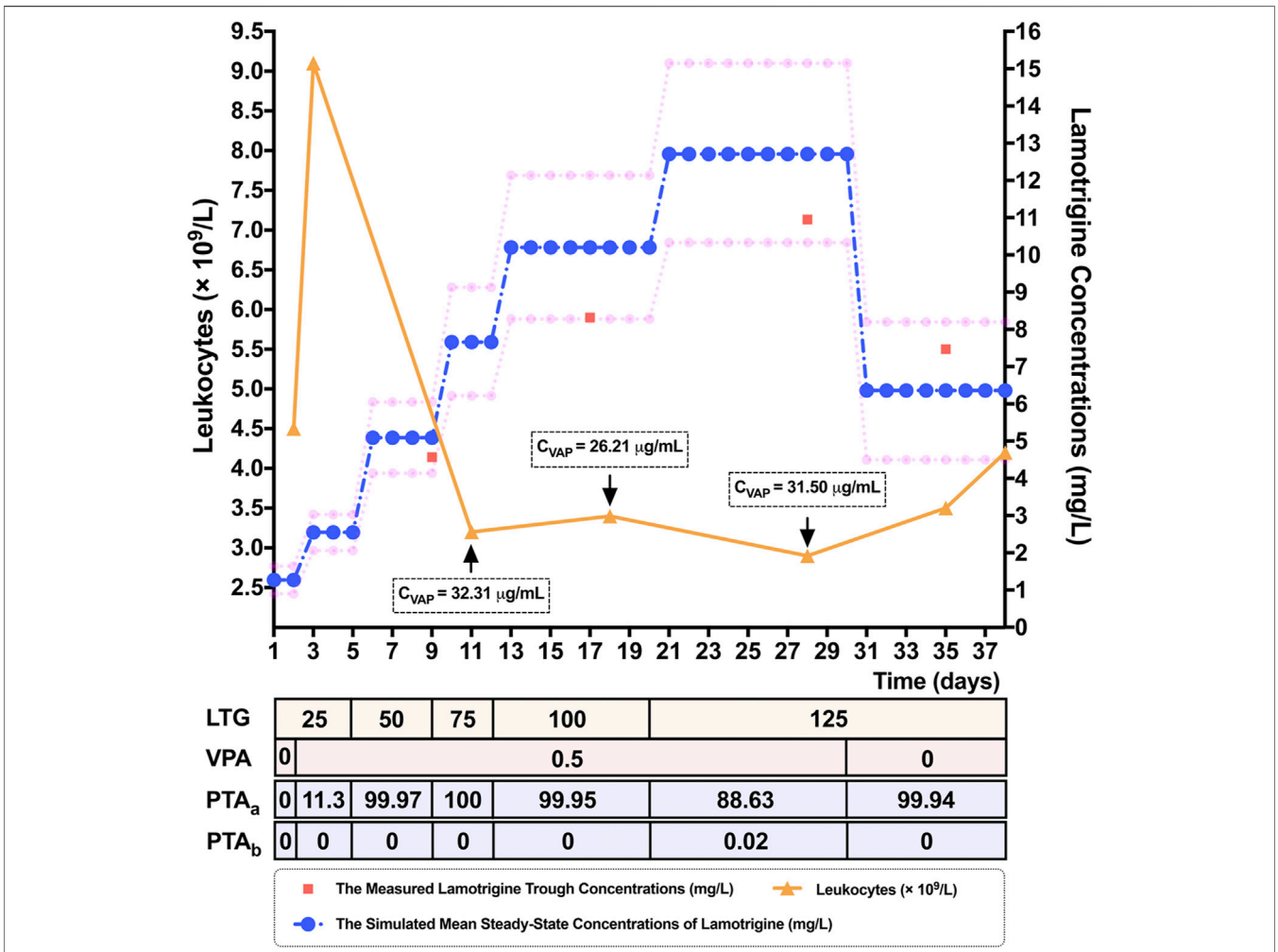

FIGURE 3 | Simulated mean steady-state concentrations (C_{ss}) (represented by blue dots) and the corresponding 10th and 90th percentiles (represented by pink dots), of the response to lamotrigine (LTG) for dosing regimens of 25 mg/bid to 125 mg/bid by adolescent Chinese patients with epilepsy weighing 60 kg in a 10,000-virtual patient Monte Carlo (MC) simulation. The 80% prediction interval, encompassing 80% of the simulated sample, adequately captured the measured LTG concentrations (represented by red squares) of a 15-year-old female epileptic Chinese patient weighing 60 kg. The patient's leukocytes (represented by orange triangles) decreased when the LTG concentration was increased, and had normalized when she was discharged. Note. LTG: the dosing titration regimens of LTG (mg/bid), VPA: the dosing titration regimens of the co-administered valproate acid (VPA) (g/qd), C_{VPA}: the measured trough concentrations of VPA, PTA_a: the probability of target attainment values (%) needed to reach C_{ss} within the range of 3–15 mg/L, PTA_b: the probability of target attainment values (%) needed to reach C_{ss} ≥ 20 mg/L.

leukocytes were 4.5×10^9/L (normal, 4–10×10^9/L) on day 2. On day 3, VPA (0.5 g/qd) was co-administered. With regard to the target concentrations and dose adaptations, the patient was informed that LTG was considered as the main antiepileptic drug in her maintenance-phase treatment, owing to the endocrinal side effects of VPA that are likely to affect the fertility of young females (Svalheim et al., 2015). Thus, the escalation in LTG dosage needed to continue until the target range of C_{ss} of 3–15 mg/L for LTG was obtained based on her clinical response. The LTG dosage still needed to be increased to up to 125 mg/bid rather than reduced when co-administered with VPA because the desired clinical effect had not been achieved on day 21. Unexpectedly, her leukocytes gradually decreased to 3.2×10^9/L on day 11, and continued to decrease to 2.9×10^9/L by day 28. Her seizures were well controlled until day 24; however, considering that her recent asymptomatic leukopenia was probably associated with the concomitant use of LTG and VPA (Naranjo score = 6, see **Table 1**) (Naranjo et al., 1981), the clinicians discontinued VPA on day 31, while the LTG dosage was continued. Her leukocytes increased after this and continued to normalize when she was discharged.

To verify the results of the MC simulation in **Figure 2**, MC simulations of the 10,000 virtual patients weighing the same as the patient considered in the case study were conducted to calculate the estimates of C_{ss} of LTG for each of the regimens, corresponding to the patient's dosing titration regimens. All the parameters used as modeling inputs for the virtual populations as well as their assumed distributions were identical to those reported in **Figure 1**. The predicted mean values of C_{ss} and the calculated PTA values for each of the above dosing regimens of LTG in this clinical case study are shown in **Supplementary Table S5**. The predicted mean LTG concentrations (10th–90th percentile range), at dosing regimens of LTG of 125 mg/bid as monotherapy, and LTG 125 mg/bid as concomitant therapy with VPA, obtained using the MC simulations were 6.36 (4.50–8.20) mg/L and 12.71 (10.33–15.15) mg/L, respectively. As is shown in **Figure 3**, the prediction interval between the 10th and 90th percentiles, encompassing 80% of the simulated sample (i.e., an 80% chance that the predicted value fell within this range), captured the patient's TDM data well, with all points lying between the upper and lower bounds of the prediction interval, indicating that the forecasted result was reliable (Prasad et al., 2018). By referring to **Figure 2B**, we see that the PTA values reached C_{ss} within 3–15 mg/L for LTG dosing regimens of 125 mg/bid and 250 mg/bid as monotherapy were close to 100% and below 80%, respectively. Finally, the empirical LTG dosing regimen of 125 mg/bid was chosen by clinicians as the patient's maintenance doses after considering the efficacy, safety, and cost effectiveness. A clinical follow-up revealed that the patient's seizures had been controlled well, and she had tolerated this dose.

DISCUSSION

Uridine glucuronosyltransferases (UGTs) play essential roles in the metabolism of LTG. The LTG dosage in adjunctive therapy is usually dependent on its interactions with other co-administered antiepileptic drugs. VPA can inhibit the metabolic activities of many hepatic drug-metabolizing enzymes to varying extents (Riva et al., 1996). Thus, a lower dose may be recommended in cases of drastically increased LTG concentrations owing to co-administered enzyme inhibitors (e.g., VPA) (Zaccara and Perucca, 2014). However, according to the latest package inserts of LTG authorized by the National Medical Products Administration (NMPA), the recommended maintenance doses for LTG in adolescent Chinese epileptic patients older than 12 years of age are 100–200 mg/day for LTG monotherapy, the same as those for concomitant therapy with LTG and VPA. In this case, the choice that clinicians are likely to face is one of whether to maintain the LTG dosing regimen of 125 mg/bid as monotherapy or increase it (e.g., double dosing). Finally, the clinicians chose the former after comprehensively considering clinical efficacy and safety.

LTG is frequently associated with rashes, whereas its hematological side-effects have rarely been noted (Bachmann et al., 2011; Okur et al., 2012). Some cases of antiepileptic drug-related leukopenia have been reported (Acharya and Bussel, 2000; Kilbas, 2006; Okur et al., 2012). The underlying mechanisms of antiepileptic drug-related leukopenia are unknown. The direct bone-marrow suppression of VPA, and the concentration-dependent and idiosyncratic toxicity associated with LTG may in part explain their common hematological toxicities (Acharya and Bussel, 2000; Okur et al., 2012). However, the continuation of antiepileptic drug therapy is probably safe despite the asymptomatic leukopenia (O'Connor et al., 1994). The risk factors associated with LTG-induced hematologic toxicities include concomitant therapy with other antiepileptic drugs such as VPA as well as exceeding the recommended starting dosage of LTG and subsequent escalation in dose (Mackay et al., 1997; Okur et al., 2012). In this case, the patient's laboratory tests were unremarkable except for leukopenia, which was more severe when the LTG concentration was increased or less severe when it was reduced, indicating that LTG was suspected as the probable cause of leukopenia. This could be potentiated by the co-administrated VPA. Furthermore, the recommended initial dosage of LTG was not exceeded, but the recommended rate of dose escalation (commonly, increasing the LTG dosage by 25–50 mg/day every one to two weeks for adolescent Chinese epileptic patients taking VPA) was exceeded to control the seizures as soon as possible in the context of the history of LTG as medication. Thus, LTG concentrations need to be closely monitored, especially when VPA is co-administered or discontinued and the recommended escalation in the LTG dose is exceeded.

The results of the MC simulation in this study show the advantages of predicting the ranges of drug concentrations based on the patient's weight and concomitant therapy scenarios owing to an expanded sample size. Such outcomes make it possible to determine the empirical dosing regimens that most frequently obtain the desired concentrations in the context of a delayed return of the results of TDM. If the probability was above *N*%, this meant that more than *N*% of the predicted C_{ss} in the simulated populations were in the target interval; in other words, the dosage

regimens were considered recommendable when the highest probabilities of the range of the target C_{ss} in the simulated populations were achieved. This technique has been used to determine remedial regimens for non-adherent epileptic patients (Yu et al., 2019; Wang et al., 2020), and to estimate the ranges of concentration and frequency of antiepileptic drugs with the assumed dosage regimens (Chhun et al., 2009; Bouillon-Pichault et al., 2011; Van Matre and Cook, 2016). The results of our simulations are shown in **Figure 2**, and this simulation method may help clinicians choose suitable empirical dosage regimens based on the weight of the adolescent epileptic patient by estimating the probability of the range of concentration of LTG.

Notably, two key points in the MC simulation highlighted the limitations of this study. The first one is the question of the validity of the target interval (Chhun et al., 2009). The target ranges of C_{ss} of 3–15 mg/L and ≥20 mg/L were defined based on the AGNP guidelines, owing to a lack of validation of the target values of C_{ss} on the large population of adolescent Chinese epileptic patients. The patient exhibited leukopenia at LTG concentrations within the range of the therapeutic reference, indicating that children might be more susceptible to the adverse effects of LTG such as hematological toxicities (Alyahya et al., 2018). Thus, it is important to evaluate the differences in the target values of C_{ss} between adults and children in future studies (Chhun et al., 2009). Related is the question of appropriateness of the distributions of the assumptions. The best way to describe the distributions of parameters in this population might be grounded in further epidemiological investigation. The second limitation is that the verification of the predicted range of concentrations for adolescent epileptic patients might have been restricted owing to the limited sample size for TDM. In this case, however, an 80% prediction interval (the 10th–90th percentiles) that represents 80% of the simulated populations adequately covered the measured LTG concentrations of the patient, indicating that MC simulations are a useful tool for estimating drug concentrations. The double dosing of LTG as monotherapy was not chosen owing to its high predicted concentrations that could have increased the risk of toxicity. However, the primary goal of epilepsy therapy in clinical practice is to control seizures with minimal adverse effects. Individualized treatment should be based on the TDM while monitoring its clinical efficacy and safety.

CONCLUSION

In summary, antiepileptic drug-related leukopenia may be a dilemma in the context of effective antiepileptic drug therapy. However, it is likely related to an increase in antiepileptic drug concentration that is reversed with the discontinuation of the drug or a reduction in dosage. Close monitoring of antiepileptic drug-related hematological side-effects is advisable in epileptic patients when administering antiepileptics. The case considered here highlighted the importance of performing TDM in the course of a patient's individualized treatment to minimize adverse reactions. The MC simulation is a useful tool for routine clinical practices such as the TDM for adolescent epileptic patients.

DATA AVAILABILITY STATEMENT

The raw data supporting the conclusions of this article will be made available by the authors, without undue reservation.

ETHICS STATEMENT

The studies involving human participants were reviewed and approved by the ethical committee of the Affiliated Brain Hospital of Guangzhou Medical University. Written informed consent from the participants' legal guardian/next of kin was not required to participate in this study in accordance with the national legislation and the institutional requirements.

AUTHOR CONTRIBUTIONS

DS and YW together conceived and designed the study. XZ wrote the original draft preparation. TX and SH performed the data analyses. SL provided the figures. XL reviewed and edited the manuscript.

FUNDING

The authors received the grants from the National Natural Science Foundation of China (grant number 81403016), Science and Technology Plan Project of Guangdong Province (grant number 2019B030316001), Guangzhou municipal key discipline in medicine (2021–2023), and Guangzhou Municipal Science and Technology Project for Medicine and Healthcare (grant numbers 20201A011047 and 20202A011016).

ACKNOWLEDGMENTS

We thank International Science Editing (http://www.internationalscienceediting.com) for editing this manuscript.

SUPPLEMENTARY MATERIAL

The Supplementary Material for this article can be found online at: https://www.frontiersin.org/articles/10.3389/fphar.2021.706329/full#supplementary-material

REFERENCES

Acharya, S., and Bussel, J. B. (2000). Hematologic Toxicity of Sodium Valproate. *J. Pediatr. Hematology/Oncology* 22 (1), 62–65. doi:10.1097/00043426-200001000-00012

Alyahya, B., Friesen, M., Nauche, B., and Laliberté, M. (2018). Acute Lamotrigine Overdose: a Systematic Review of Published Adult and Pediatric Cases. *Clin. Toxicol.* 56 (2), 81–89. doi:10.1080/15563650.2017.1370096

Bachmann, T., Bertheussen, K. H., Svalheim, S., Rauchenzauner, M., Luef, G., Gjerstad, L., et al. (2011). Haematological Side Effects of Antiepileptic Drug Treatment in Patients with Epilepsy. *Acta Neurol. Scand.* 124 (Suppl. 191), 23–27. doi:10.1111/j.1600-0404.2011.01539.x

Baek, I.-H., Lee, B.-Y., Kang, J., and Kwon, K.-I. (2015). Pharmacokinetic Modeling and Monte Carlo Simulation of Ondansetron Following Oral Administration in Dogs. *J. Vet. Pharmacol. Therap.* 38 (2), 199–202. doi:10.1111/jvp.12147

Bouillon-Pichault, M., Nabbout, R., Chhun, S., Rey, E., Chiron, C., Dulac, O., et al. (2011). Topiramate Pharmacokinetics in Infants and Young Children: Contribution of Population Analysis. *Epilepsy Res.* 93 (2-3), 208–211. doi:10.1016/j.eplepsyres.2010.12.004

Chhun, S., Jullien, V., Rey, E., Dulac, O., Chiron, C., and Pons, G. (2009). Population Pharmacokinetics of Levetiracetam and Dosing Recommendation in Children with Epilepsy. *Epilepsia* 50 (5), 1150–1157. doi:10.1111/j.1528-1167.2008.01974.x

Darwich, A. S., Ogungbenro, K., Vinks, A. A., Powell, J. R., Reny, J.-L., Marsousi, N., et al. (2017). Why Has Model-Informed Precision Dosing Not yet Become Common Clinical Reality? Lessons from the Past and a Roadmap for the Future. *Clin. Pharmacol. Ther.* 101 (5), 646–656. doi:10.1002/cpt.659

Doan, T. N., Kong, D. C. M., Patel, K., Walker, P., Spencer, A., and Kirkpatrick, C. M. J. (2014). Comparison of the Probability of Target Attainment of Anidulafungin against Candida Spp. in Patients with Acute Leukaemia. *Int. J. Antimicrob. Agents* 44 (5), 450–457. doi:10.1016/j.ijantimicag.2014.07.019

Garnett, W. R. (1997). Lamotrigine: Pharmacokinetics. *J. Child. Neurol.* 12 (Suppl. 1), S10–S15. doi:10.1177/088307389701200104l

Grasela, T. H., Fiedler-Kelly, J., Cox, E., Womble, G. P., Risner, M. E., and Chen, C. (1999). Population Pharmacokinetics of Lamotrigine Adjunctive Therapy in Adults with Epilepsy. *J. Clin. Pharmacol.* 39 (4), 373–384. doi:10.1177/00912709922007949

Hiemke, C., Bergemann, N., Clement, H., Conca, A., Deckert, J., Domschke, K., et al. (2018). Consensus Guidelines for Therapeutic Drug Monitoring in Neuropsychopharmacology: Update 2017. *Pharmacopsychiatry* 51 (1-02), 9–62. doi:10.1055/s-0043-116492

Hirsch, L. J., Weintraub, D., Du, Y., Buchsbaum, R., Spencer, H. T., Hager, M., et al. (2004). Correlating Lamotrigine Serum Concentrations with Tolerability in Patients with Epilepsy. *Neurology* 63 (6), 1022–1026. doi:10.1212/01.wnl.0000138424.33979.0c

Hussein, Z., and Posner, J. (1997). Population Pharmacokinetics of Lamotrigine Monotherapy in Patients with Epilepsy: Retrospective Analysis of Routine Monitoring Data. *Br. J. Clin. Pharmacol.* 43 (5), 457–465. doi:10.1046/j.1365-2125.1997.00594.x

Jacob, S., and Nair, A. B. (2016). An Updated Overview on Therapeutic Drug Monitoring of Recent Antiepileptic Drugs. *Drugs R. D.* 16 (4), 303–316. doi:10.1007/s40268-016-0148-6

Jang, S. M., Gharibian, K. N., Lewis, S. J., Fissell, W. H., Tolwani, A. J., and Mueller, B. A. (2018). A Monte Carlo Simulation Approach for Beta-Lactam Dosing in Critically Ill Patients Receiving Prolonged Intermittent Renal Replacement Therapy. *J. Clin. Pharmacol.* 58 (10), 1254–1265. doi:10.1002/jcph.1137

Johannessen, S. I., and Tomson, T. (2006). Pharmacokinetic Variability of Newer Antiepileptic Drugs. *Clin. Pharmacokinet.* 45 (11), 1061–1075. doi:10.2165/00003088-200645110-00002

Kilbas, S. (2006). Lamotrigine-induced Leucopenia. *Epileptic Disord.* 8 (4), 317. doi:10.1684/epd.2006.0039

Kluwe, F., Michelet, R., Mueller-Schoell, A., Maier, C., Klopp-Schulze, L., van Dyk, M., et al. (2021). Perspectives on Model-Informed Precision Dosing in the Digital Health Era: Challenges, Opportunities, and Recommendations. *Clin. Pharmacol. Ther.* 109 (1), 29–36. doi:10.1002/cpt.2049

Leung, D., Ensom, M. H. H., and Carr, R. (2019). Survey of Therapeutic Drug Monitoring Practices in Pediatric Health Care Programs across Canada. *Can. J. Hosp. Pharm.* 72 (2), 126–132. doi:10.4212/cjhp.v72i2.2882

Mackay, F. J., Wilton, L. V., Peace, G. L., Freemantle, S. N., and Mann, R. D. (1997). Safety of Long-Term Lamotrigine in Epilepsy. *Epilepsia* 38 (8), 881–886. doi:10.1111/j.1528-1157.1997.tb01252.x

Methaneethorn, J., and Leelakanok, N. (2020). Sources of Lamotrigine Pharmacokinetic Variability: A Systematic Review of Population Pharmacokinetic Analyses. *Seizure* 82, 133–147. doi:10.1016/j.seizure.2020.07.014

Naranjo, C. A., Busto, U., Sellers, E. M., Sandor, P., Ruiz, I., Roberts, E. A., et al. (1981). A Method for Estimating the Probability of Adverse Drug Reactions. *Clin. Pharmacol. Ther.* 30 (2), 239–245. doi:10.1038/clpt.1981.154

O'Connor, C. R., Schraeder, P. L., Kurland, A. H., and O'Connor, W. H. (1994). Evaluation of the Mechanisms of Antiepileptic Drug-Related Chronic Leukopenia. *Epilepsia* 35 (1), 149–154. doi:10.1111/j.1528-1157.1994.tb02925.x

Okur, M., Kaya, A., Çaksen, H., and Taşkın, G. (2012). Lamotrigine-associated Thrombocytopenia and Leukopenia. *J. Emerg. Med.* 42 (5), 584–585. doi:10.1016/j.jemermed.2010.05.060

Prasad, B., Bhatt, D. K., Johnson, K., Chapa, R., Chu, X., Salphati, L., et al. (2018). Abundance of Phase 1 and 2 Drug-Metabolizing Enzymes in Alcoholic and Hepatitis C Cirrhotic Livers: a Quantitative Targeted Proteomics Study. *Drug Metab. Dispos.* 46 (7), 943–952. doi:10.1124/dmd.118.080523

Riva, R., Albani, F., Contin, M., and Baruzzi, A. (1996). Pharmacokinetic Interactions between Antiepileptic Drugs. *Clin. Pharmacokinet.* 31 (6), 470–493. doi:10.2165/00003088-199631060-00005

Roberts, J. A., Kirkpatrick, C. M. J., and Lipman, J. (2011). Monte Carlo Simulations: Maximizing Antibiotic Pharmacokinetic Data to Optimize Clinical Practice for Critically Ill Patients. *J. Antimicrob. Chemother.* 66 (2), 227–231. doi:10.1093/jac/dkq449

Søndergaard Khinchi, M., Nielsen, K. A., Dahl, M., and Wolf, P. (2008). Lamotrigine Therapeutic Thresholds. *Seizure* 17 (5), 391–395. doi:10.1016/j.seizure.2007.11.023

Svalheim, S., Sveberg, L., Mochol, M., and Taubøll, E. (2015). Interactions between Antiepileptic Drugs and Hormones. *Seizure* 28, 12–17. doi:10.1016/j.seizure.2015.02.022

Van Matre, E. T., and Cook, A. M. (2016). Steady-state Pharmacokinetic Simulation of Intermittent vs. Continuous Infusion Valproic Acid Therapy in Non-critically Ill and Critically Ill Patients. *Neurol. Res.* 38 (9), 786–791. doi:10.1080/01616412.2016.1206164

Wang, C.-Y., Jiao, Z., Ding, J.-J., Yu, E.-Q., and Zhu, G.-X. (2020). Remedial Dosing Recommendations for Delayed or Missed Doses of Valproic Acid in Patients with Epilepsy Based on Monte Carlo Simulations. *Epilepsy Behav.* 111, 107265. doi:10.1016/j.yebeh.2020.107265

Wang, Z.-Z., Zhang, Y.-F., Huang, W.-C., Wang, X.-P., Ni, X.-J., Lu, H.-Y., et al. (2019). Effects of Comedication and Genetic Factors on the Population Pharmacokinetics of Lamotrigine: A Prospective Analysis in Chinese Patients with Epilepsy. *Front. Pharmacol.* 10, 832. doi:10.3389/fphar.2019.00832

Yu, E.-Q., Jiao, Z., Wang, C.-Y., Ding, J.-J., and Zhang, X.-H. (2019). Remedial Dosing Recommendations for Delayed or Missed Doses of Lamotrigine in Pediatric Patients with Epilepsy Using Monte Carlo Simulations. *Epilepsy Behav.* 96, 132–140. doi:10.1016/j.yebeh.2019.04.007

Zaccara, G., and Perucca, E. (2014). Interactions between Antiepileptic Drugs, and between Antiepileptic Drugs and Other Drugs. *Epileptic Disord.* 16 (4), 409–431. doi:10.1684/epd.2014.0714

Zhang, Z.-B., Ji, S.-M., Han, Y., Zang, L.-L., Wang, Y.-H., Lu, W., et al. (2017). Population Pharmacokinetic Models of Lamotrigine in Different Age Groups of Chinese Children with Epilepsy. *Eur. J. Clin. Pharmacol.* 73 (4), 445–453. doi:10.1007/s00228-016-2190-2

Zhu, X., Huang, W., Lu, H., Wang, Z., Ni, X., Hu, J., et al. (2021). A Machine Learning Approach to Personalized Dose Adjustment of Lamotrigine Using Noninvasive Clinical Parameters. *Sci. Rep.* 11 (1), 5568. doi:10.1038/s41598-021-85157-x

Conflict of Interest: The authors declare that the research was conducted in the absence of any commercial or financial relationships that could be construed as a potential conflict of interest.

frontiers in Pharmacology

REVIEW
published: 26 July 2021
doi: 10.3389/fphar.2021.681842

Caffeine for the Pharmacological Treatment of Apnea of Prematurity in the NICU: Dose Selection Conundrum, Therapeutic Drug Monitoring and Genetic Factors

Jia-Yi Long[1,2†‡], Hong-Li Guo[1†], Xin He[1], Ya-Hui Hu[1], Ying Xia[1], Rui Cheng[3], Xuan-Sheng Ding[2], Feng Chen[1] and Jing Xu[1]**

[1]Pharmaceutical Sciences Research Center, Department of Pharmacy, Children's Hospital of Nanjing Medical University, Nanjing, China, [2]School of Basic Medical Sciences and Clinical Pharmacy, China Pharmaceutical University, Nanjing, China, [3]Neonatal Intensive Care Unit, Children's Hospital of Nanjing Medical University, Nanjing, China

Caffeine citrate is the drug of choice for the pharmacological treatment of apnea of prematurity. Factors such as maturity and genetic variation contribute to the interindividual variability in the clinical response to caffeine therapy in preterm infants, making the optimal dose administered controversial. Moreover, the necessity for therapeutic drug monitoring (TDM) of caffeine is still worth discussing due to the need to achieve the desired target concentrations as well as concerns about the safety of higher doses. Therefore, we reviewed the pharmacokinetic profile of caffeine in preterm infants, evidence of the safety and efficacy of different doses of caffeine, therapeutic concentration ranges of caffeine and impact of genetic variability on caffeine therapy. Whereas the safety and efficacy of standard-dose caffeine have been demonstrated, evidence for the safety of higher administered doses is insufficient. Thus, preterm infants who lack clinical response to standard-dose caffeine therapy are of interest for TDM when dose optimization is performed. Polymorphisms in pharmacodynamics-related genes, but not in pharmacokinetics-related genes, have a significant impact on the interindividual variability in clinical response to caffeine therapy. For preterm infants lacking clinical response, how to develop individualized medication regimens for caffeine remains to be explored.

Keywords: preterm infant, apnea of prematurity, caffeine, pharmacokinetics, therapeutic drug monitoring, polymorphism

OPEN ACCESS

Edited by:
Raffaele Simeoli, Bambino Gesù Children Hospital (IRCCS), Italy

Reviewed by:
Carl Hunt, Uniformed Services University of the Health Sciences, United States
Sinno Simons, Erasmus Medical Center, Netherlands

***Correspondence:**
Feng Chen
cy.chen508@gmail.com
Jing Xu
njxujing@163.com

‡Visiting graduate student from China Pharmaceutical University.

†These authors have contributed equally to this work.

Specialty section:
This article was submitted to Obstetric and Pediatric Pharmacology, a section of the journal Frontiers in Pharmacology

Received: *17 March 2021*
Accepted: *12 July 2021*
Published: *26 July 2021*

Citation:
Long J-Y, Guo H-L, He X, Hu Y-H, Xia Y, Cheng R, Ding X-S, Chen F and Xu J (2021) Caffeine for the Pharmacological Treatment of Apnea of Prematurity in the NICU: Dose Selection Conundrum, Therapeutic Drug Monitoring and Genetic Factors. Front. Pharmacol. 12:681842. doi: 10.3389/fphar.2021.681842

Abbreviations: ADA, adenosine dehydrogenase; AHR, aryl hydrocarbon receptor; AOP, apnea of prematurity; AR, adenosine receptor; BPD, bronchopulmonary dysplasia; CAP, Caffeine for Apnea of Prematurity; CBH, cerebellar hemorrhage; NONMEM, nonlinear mixed effects models; PBPK, physiologic based pharmacokinetics; PD, pharmacodynamics; PDA, patent ductus arteriosus; PDE, phosphodiesterase; PK, pharmacokinetics; PPK, population pharmacokinetics; RCT, randomized controlled trial; ROP, retinopathy of prematurity; TDM, therapeutic drug monitoring; VLBW, very low birth weight.

INTRODUCTION

Apnea of prematurity (AOP), classified as central, obstructive, or mixed, is usually defined as a cessation of breathing in a premature infant for 20 s or longer, or a shorter pause accompanied by bradycardia (<100 bpm), cyanosis, or pallor (Eichenwald, 2016). It is a common problem among preterm infants, particularly extremely preterm infants (Saroha and Patel, 2020). The reported incidence of AOP varies, but it is clearly inversely related to gestational age. Its incidence is 10% in neonates born beyond 34 weeks gestation. However, in newborns who are at 30–34 weeks gestation at birth, the incidence ranges from 20 to 85%. Ninety percent of the extremely low birth weight (less than 1,000 g) newborn population are reported to have AOP (Eichenwald, 2016; Erickson et al., 2021). Observational studies have demonstrated associations between apneic events and deficits in cerebral oxygenation (Schmid et al., 2015; Horne et al., 2017), increased risk for retinopathy of prematurity (ROP) (Di Fiore et al., 2010), neurodevelopmental impairment (Janvier et al., 2004; Martin et al., 2011), and even death or disability (Lodha et al., 2015).

Several interventions decrease apneic event frequency and duration. These include respiratory interventions including continuous positive airway pressure and pharmacologic therapies, such as methylxanthines, which have been used for over 40 years (Gentle et al., 2018). Caffeine is the first choice among all methylxanthines because of its efficacy, better tolerability and wider therapeutic index as well as longer half-life (Dobson and Hunt, 2013). Researchers of the international Caffeine for Apnea of Prematurity (CAP) trial confirmed the short- and long-term benefits and safety of neonatal caffeine therapy, including reduced rates of bronchopulmonary dysplasia (BPD), patent ductus arteriosus (PDA), and of severe ROP (Schmidt et al., 2006), and improved survival rates without neurodevelopmental disability at 18–21 months of age (Schmidt et al., 2007). Five- and 11 years follow-up studies confirmed that neonatal caffeine therapy appeared to have lasting beneficial effects on motor function and is effective and safe even into middle school age (Schmidt et al., 2012; Schmidt et al., 2017; Murner-Lavanchy et al., 2018). Therefore, caffeine has now become one of the most preferred drugs worldwide for AOP treatment and has been named the "silver" or "magic" bullet (Aranda et al., 2010; Bancalari, 2014).

Despite caffeine's frequent use in routine neonatal practice, there are controversies surrounding this medicine, which future researches may resolve, including the optimal dose of caffeine administration (Moschino et al., 2020) and therapeutic drug monitoring (TDM) (Shrestha and Jawa, 2017; Saroha and Patel, 2020). Of note, neonatal caffeine therapy results in significant intersubject variability, and it remains unclear why apneic episodes persist in some preterm infants but not in others (He et al., 2020). Therefore, we summarize pharmacokinetic studies of caffeine in a population of preterm infants, as well as evidence of the safety, efficacy and therapeutic concentration ranges at different doses. We also discuss the dose optimization and the necessity for TDM of caffeine, and provide the first review of the impact of genetic variability on the clinical response to caffeine therapy.

PHARMACOKINETICS OF CAFFEINE IN PRETERM INFANTS

Most of the pharmacokinetic (PK) studies for caffeine were performed in premature neonates (**Table 1** and **Table 2**). Due to the difficulty of adequate sampling in preterm babies, most studies have been population pharmacokinetic (PPK) studies using nonlinear mixed effects models (NONMEM) or P-pharm approaches (**Table 2**). The pharmacokinetics of caffeine is largely independent of the route of administration. Oral caffeine is almost completely bioavailable and is rapidly and completely absorbed from the gastrointestinal tract, reaching peak plasma concentrations in 30 min to 2 h after administration (Aranda et al., 1979a; Bonati et al., 1982; Blanchard and Sawers, 1983). Caffeine is hydrophilic and distributed evenly in all body fluids without tissue accumulation (Arnaud, 1976; Arnaud, 2011). It is also highly lipid-soluble to cross all biological membranes, including the blood-brain barrier, leading to a similar caffeine concentration between the plasma and cerebrospinal fluid of neonates (Turmen et al., 1979; Tanaka et al., 1984; Arnaud, 1987). The volume of distribution in preterm infants is mainly affected by the current body weight and gestational age, and its value is slightly greater than that in healthy adults, possibly due to the increased residence time of caffeine in the extracellular fluid (Aranda et al., 1979a; Bonati et al., 1982; Gorodischer and Karplus, 1982; Lelo et al., 1986; Thomson et al., 1996; Falcão et al., 1997; Lee et al., 1997; Lee et al., 2002; Kearns et al., 2003; Charles et al., 2008; Gao et al., 2020; Guo et al., 2020).

The metabolism of caffeine occurs primarily in the liver. In adults, with the catalysis by CYP2A1 and CYP2E1, caffeine undergoes 1-, 3-, and 7-demethylation to generate the biologically active metabolites theophylline, theobromine, and paraxanthine, which can then be further demethylated to monomethylxanthine (Gu et al., 1992; Thorn et al., 2012). Dimethylxanthine or monomethylxanthine is converted to methyluric acid by xanthine oxidase, whereas paraxanthine can also undergo 8-hydroxylation or generate 5-acetylamino-6-formylamino-3-methyluracil catalyzed by CYP2A6 or N-acetyltransferase-2, respectively (Begas et al., 2007; Thorn et al., 2012). However, in neonates, approximately 85% of caffeine is excreted unchanged in the urine, whereas this proportion in adults is less than 2% (Arnaud, 2011; Aldridge et al., 1979). CYP1A2 is the cytochrome P450 enzyme responsible for more than 90% of caffeine metabolism, studies have shown that CYP1A2 expression is not evident within the first 30 days of newborns' life due to delayed ontogeny, and CYP1A2 content in liver microsomes of infants aged 1–3 months is only 10–15% of that in adults (Arnaud, 2011; Song et al., 2017; Sonnier and Cresteil, 1998). Correspondingly, the main metabolite in newborns during the first trimester of life is caffeine, whereas 8-hydroxylation appears early and matures approximately 1 month after birth, demethylation metabolism gradually

TABLE 1 | Pharmacokinetics of caffeine in healthy adults and preterm infants.

First author, year[ref]	Number of cases	GA (weeks)	PNA (days)	BW (g)	CW (kg)	Route of administration	Dose of caffeine base (mg/kg)			T_{max} (minutes)	C_{max} (μg/ml)	CL (ml/kg/h)	V (L/kg)	$t_{1/2}$
							S	L	M					
Healthy Adults														
Bonati et al. (1982)	4	NR	26–36[a,b]	NR	70	po	5.0			47	8.3	60.9	0.56	6.3
Lelo et al. (1986)	6	NR	19–21[a,b]	NR	62–104[a]	po	270[c]			NR	NR	124.2	0.63–0.71[a]	4.1
Preterm Infants														
Aranda et al. (1979a)	12	28.5	11.5	1,114.7	NR	iv	10.2	NR	11.2/day	30–120[a]	6–10	8.9	0.916	102.9
	3	30.0	19.7	1,334.3		po	10.0	NR	2.5/day					
	7	27.4	29.4	1,099.3		NR								
	10	27.7	35.2	1,041.5		NR								
Gorodischer and Karplus (1982)	13	30.6	1–42[a]	1,399	NR	iv	15 (1–7 doses)			NR	NR	8.5	0.781	65.0
Pearlman et al. (1989)	17	29.7	20.7	1,270	1.36	iv, po[d]		10	2.5–5 (1–2 doses/day)	NR	17.83	NR	NR	52.03
De Carolis et al. (1991)	5	30	0	1,670	NR	iv	5			NR	NR	NR	NR	72
	10	29.2	15	1,140		iv	5							
			NR			iv, po[e]		5	1.25/day					

Data are expressed as the mean, unless otherwise specified. NR, not reported; GA, gestational age; PNA, postnatal age; BW, birth weight; CW, current weight; T_{max}, time to peak; C_{max}, peak plasma concentration of caffeine; CL, clearance; V, volume of distribution; $t_{1/2}$, elimination half-life; po, oral administration; iv, intravenous injection; S, single dose; L, loading dose; M, maintenance dose.

[a]*Data are expressed as the range.*

[b]*Units are years.*

[c]*Unit is mg.*

[d]*16 cases were administered orally and 1 case was administered intravenously.*

[e]*The loading dose was administered intravenously and the maintenance dose was administered orally.*

TABLE 2 | Population pharmacokinetics of caffeine in preterm infants.

First author, year[ref]	Number of cases	GA (weeks)	PNA (days)	BW (g)	CW (kg)	Dose of caffeine citrate		C_p (μg/ml)	CL (ml/kg/h)	V (L/kg)	$t_{1/2}$	Modeling program	Pharmacokinetic parameters
						L (mg/kg)	M (mg/kg/day)						
Thomson et al. (1996)	80	25–41[a]	1–100[a]	600–2900[a]	NR	20	5	NR	7.9	0.64	NR	NONMEM	CL (L/day) = 0.14 × WT (kg) + 0.0024 × PNA (days) V (L) = 0.82
Lee et al. (1997)	38	28.2	4	1,167	NR	6	3	60.7	4.9	0.97	144	NONMEM	CL (L/h) = 0.00399 × CW (kg) + 0.000128 × PNA (days)
	39					30	15	31.1					V (L)[c] = θ_1 × CW (kg) + (θ_2 × PNA (days)
	42					60	30	6.8					
Falcão et al. (1997)	75	23–35[a]	1–78[a]	600–2000[a]	NR	17.4–21.3[a]	2.1–9.5[a]	11.8	7.6	0.911	NR	NONMEM	CL (ml/h)[d] = (5.81 × CW [kg] + 1.22 × PNA [weeks]) × θ_1 × θ_2 V (ml) = 911× CW (kg)
Lee et al. (2002)	18	28.9	NR	1,115.6	NR	20	5	3.6–28.4[a]	6.28	0.96	106	P-Pharm	CL (L/h) = 0.004248 × WT (kg) + 0.00154; r = 0.8, $p < 0.01$ V (L) = 0.6299 × WT (kg) + 0.259; r = 0.67, $p < 0.01$
Charles et al. (2008)	59	27.6	12	1,009	0.992	80	20	47.4	7.0[b]	0.851[b]	101	NONMEM	CL (L/h) = 0.167 × (CW [kg]/70)$^{0.75}$ × (PNA [days]/12)$^{0.358}$
	51					20	5	14.7					V (L) = 58.7 × (CW [kg]/70)$^{0.75}$ K_a (h^{-1}) = 1.48; F = 1.0
Guo et al. (2020)	46	28.97	21.22	1,240	1.39	20	8–10[a]	9.16–42.4[a]	10.2	2.494	NR	NONMEM	CL (L/h) = 0.268 × (CW [kg]/70)$^{0.75}$ V (L) = 109 × (CW [kg]/70) × e $^{0.471\times PNA\ (days)/19.5}$
Gao et al. (2020)	99	28.51	24.87	1,129	1.306	20	5–10[a]	6.5–44.4[a]	12[b]	1.175[b]	NR	NONMEM	CL (L/h) = 0.0167 × (CW [g]/1,280)$^{0.75}$ × (PMA [weeks]/31.1)$^{0.564}$ × (CREA [μmol/L]/68)$^{-0.162}$ V (L) = 1.43 × (CW [g]/1,280)

Data are expressed as the mean, unless otherwise specified. NR, not reported; GA, gestational age; PNA, postnatal age; PMA, postmenstrual age; BW, birth weight; NONMEM, nonlinear mixed effects models; CW, current weight; WT, weight; L, loading dose; M, maintenance dose; C_P, plasma concentration of caffeine; CL, clearance; V, volume of distribution; $t_{1/2}$, elimination half-life; CREA, serum creatinine concentration.

[a]*Data are expressed as the range.*

[b]*Data are expressed as the median.*

[c]*For GA > 28 weeks, $\theta_1 = 0.764$, $\theta_2 = 0.0468$; for GA ≤ 28 weeks, $\theta_1 = 0.755$, $\theta_2 = 0.0224$.*

[d]*If GA ≤ 28 weeks, $\theta_1 = 0.757$, otherwise = 1; if the current primary source of the patients' nutrition is parenteral nutrition, $\theta_2 = 0.836$, otherwise = 1.*

matures with postnatal age, and acetylation is immature until at least 1 year of age (Aldridge et al., 1979; Carrier et al., 1988; Pons et al., 1989; Cazeneuve et al., 1994; al-Alaiyan et al., 2001; Blake et al., 2006). In addition, theophylline can be converted back to caffeine in premature infants by active methylation (Bory et al., 1978; Bory et al., 1979).

The serum half-life of caffeine in preterm infants is prolonged more than ten times that of adults because of immature hepatic metabolism and renal excretion (Aranda et al., 1979b; Bonati et al., 1982; Gorodischer and Karplus, 1982; Lelo et al., 1986; Pearlman et al., 1989; De Carolis et al., 1991). Caffeine's clearance in preterm infants is influenced by various factors such as the current weight, postnatal age, gestational age, parenteral nutrition, and serum creatinine concentration, with values of approximately one-tenth of those in adults (Bonati et al., 1984; Lelo et al., 1986; Thomson et al., 1996; Falcão et al., 1997; Lee et al., 1997; Lee et al., 2002; Charles et al., 2008; Gao et al., 2020; Guo et al., 2020). For example, caffeine clearance shows a rapid maturation with postnatal age in a very recent study (Engbers et al., 2021). Earlier studies found that the elimination half-life and clearance of caffeine can reach adult levels at approximately 5–6 months after birth (Aranda et al., 1979b; Pons et al., 1988). However, a re-evaluation and validation of ontogeny functions for CYP1A2 describes an increase in relative intrisic metabolic clearance from birth to 3 years followed by a decrease to adult values (Salem et al., 2014). Therefore, the PK process of caffeine in neonates is variable and continues to mature with development, which needs to be taken into consideration when administered.

DOSAGE OF CAFFEINE IN PRETERM INFANTS

Standard Dose of Caffeine and Its History

Caffeine is often available as caffeine citrate, which comes in both oral and injectable formulations, and the dose of caffeine base is half that of caffeine citrate (Shrestha and Jawa, 2017). As early as in 1977, Aranda et al. published the first study of caffeine used to treat AOP (Aranda et al., 1977). In that study, 18 preterm infants received an intravenous loading dose of 20 mg/kg caffeine citrate followed by a maintenance dose of 5–10 mg/kg once or twice daily for 2–3 days, and a marked reduction in apnea spells was observed. In the next 10 years, the same dose regimen was tested in several studies with small sample sizes (n = 16 to n = 23), and the therapeutic effect of caffeine on AOP was observed by comparison with placebo or theophylline (Murat et al., 1981; Brouard et al., 1985; Anwar et al., 1986; Bairam et al., 1987). In 1999, a multicenter, double-blind, randomized trial of caffeine citrate was performed using the above dose regimen. In this trial, eighty-five infants who were 28–32 weeks post-conception and 24 h or more after birth were randomized to caffeine or placebo for up to 10 days, and the results showed that this dose regimen was safe and effective for those recruited neonates (Erenberg et al., 2000). Based partly on such data, the U.S. Food and Drug Administration approved the dose regimen of caffeine citrate as a loading dose of 20 mg/kg followed by an intravenous or oral maintenance dose of 5 mg/kg/day, which is similar to what was approved by the European Medicines Agency (Erenberg et al., 2000; NDA 20-793/S-001, 2000; European Medicines Agency, 2009). Therefore, in this review, we refer to this as the "standard dose" regimen for caffeine.

In 2006, a large, multicenter, randomized, placebo-controlled trial, called the CAP trial, revealed the short- and long-term efficacy and safety of the standard dose regimen of caffeine (Schmidt et al., 2006; Schmidt et al., 2007). In the CAP trial, preterm infants with very low birth weight (VLBW, 500–1,250 g) were randomized to placebo or caffeine citrate at a loading dose of 20 mg/kg, followed by a maintenance dose of 5 mg/kg/24 h, which could be increased to 10 mg/kg/24 h for persistent apnea. This trial demonstrated several well-known beneficial short-terms effects of caffeine (Schmidt et al., 2006). Regarding the long-term effects, preterm infants had a higher rate of survival without neurodevelopmental disability and a lower incidence of severe ROP, cerebral palsy and cognitive delay at a corrected age of 18–21 months (Schmidt et al., 2007), with an improvement in gross motor function at 5 years (Schmidt et al., 2012). In addition, they also revealed that neonatal caffeine therapy at the doses used in CAP trial is effective and safe into miiddle school age (Doyle et al., 2017; Schmidt et al., 2017; Murner-Lavanchy et al., 2018; Schmidt et al., 2019). Due to the CAP trial, the standard-dose caffeine regimen has been widely used (**Table 3**). However, variable clinical outcomes do exist after standard-dose caffeine treatment.

Higher Doses of Caffeine

Many studies have shown higher doses of caffeine to be more effective with negligible adverse effects (**Table 4**). Multiple studies have reported that higher doses of caffeine are more effective in reducing episodes of apnea and reducing extubation failure rates (Scanlon et al., 1992; Mohammed et al., 2015; Zhao et al., 2016; Wan et al., 2020). Among them, Mohammad et al. compared a higher dose (loading 40 mg/kg and maintenance of 20 mg/kg/day) with standard-dose caffeine citrate in 120 preterm infants < 32 weeks gestation with AOP within the first 10 days of life (Mohammed et al., 2015). In this trial, the higher dose of caffeine, in addition to being observed to have a better therapeutic effect, was also associated with a significant increase in tachycardia episodes. However, the clinical findings in this trial had no significant impact on physicians' decision to withhold caffeine.

Other RCTs examined different dosing regimens of caffeine citrate for periextubation management of ventilated preterm infants. In 2003, Steer et al. compared three dose regimens of caffeine citrate (3, 15 and 30 mg/kg) for periextubation management of 127 preterm infants < 32 weeks gestation who were ventilated for > 48 h and found that there was no statistically significant difference in the incidence of extubation failure between different dosing groups (Steer et al., 2003). However, in a subsequent multicenter, double-blind RCT, the same authors found that a dose of 20 mg/kg was given 24 h before a planned extubation or within 6 h of an unplanned extubation reduced the rate of extubation failure within 48 h compared to a lower dose of 5 mg/kg, without evidence of harm in the first year of life (Steer et al., 2004).

TABLE 3 | Main efficacy and safety results in standard dose caffeine treatment studies.

First author, year[ref.]	Study characteristics	Number of cases	Groups	Mean GA (weeks)	Mean PNA (days)	Dose of caffeine citrate		Main efficacy and safety results for caffeine treatment
						L (mg/kg)	M (mg/kg/day)	
Aranda et al. (1977)	noncontrolled	18	Caffeine	27.5	18.2	20[a]	5–10 (2–3 days after L)	↓frequency of apnea ($p < 0.001$) ↓blood hydrogen ion concentration ($p < 0.001$) ↓capillary carbon dioxide tension ($p < 0.01$) no significant change in heart rate
Murat et al. (1981)	randomized, controlled	18	Caffeine	30.1	13.2	20	5	↓apnea index[b] on day 1 and 5 ($p < 0.01$)
			Control	29.8	16.1			↓apnea index[b] from days 0–1 and from days 0–5 ($p < 0.01$) no adverse side effects
Brouard et al. (1985)	randomized	16	Caffeine	30.5	11.7	20	5	↓apnea frequency from days 0–1 ($p < 0.001$) and from days 0–5 ($p < 0.001$) in both groups no adverse effects
			Theophylline	30.5	11.6			
Anwar et al. (1986)	controlled	38[c]	Caffeine	32.0	35.0	20	5	↓apnea duration ($p < 0.05$) ↓percent periodic breathing ($p < 0.05$) ↓apnea density ($p < 0.05$) 4 infants were more irritable and restless
			Control	32.2	39.9			
Bairam et al. (1987)	randomized, double-blind	20	Caffeine	30.3	6.2	20	2.5[d]	↑respiratory rates ($p < 0.001$) in both groups lower mean heart rate, smaller daily variations of mean plasma levels compared to theophylline group significant sodium loss no significant gastrointestinal side effects
			Theophylline	30.0	5.5			
Erenberg et al. (2000)	multicenter, randomized, double-blind, placebo-controlled	85	Caffeine	29.8	5.6	20	5	↓number of apnea episodes by ≥ 50% in 6 days ($p < 0.05$) eliminating apnea better in 5 days ($p < 0.05$) no significant differences in number and percentage of adverse events caffeine citrate-related NEC in 1 infant
			Placebo	29.9	4.9			
Schmidt et al. (2006)	multicenter, randomized, placebo-controlled (the CAP trial)	2,006	Caffeine	27	3[e]	20	5 (to 10 if apnea persisted)	↓duration of respiratory support ($p < 0.01$) ↓cointerventions of doxapram, postnatal corticosteroids, and red-cell transfusions ($p < 0.001$) ↓incidence of BPD ($p < 0.001$) ↓PDA treatment ($p < 0.001$) ↓weight gain temporarily ($p < 0.05$)
			Placebo	27	3[e]			
Schmidt et al. (2007)	follow-up reports of the CAP trial	1,869	Caffeine	18.8 months[e,f]				↓rate of death or disability ($p = 0.008$) ↓incidence of cerebral palsy ($p = 0.009$) ↓incidence of cognitive delay ($p = 0.04$) ↓incidence of ROP > stage 3 ($p = 0.01$)
			Placebo	18.7 months[e,f]				
Schmidt et al. (2012)		1,640	Caffeine	5.2 years[e,f]				↑gross motor function ($p = 0.006$) no significant difference in death or disability ($p = 0.09$)
			Placebo	5.1 years[e,f]				
Schmidt et al. (2017)		920	Caffeine	11.4 years[e,f]				↓risk of motor impairment ($p = 0.009$) no significant differences in combined rate of academic, motor, and behavioral impairments ($p = 0.07$)
			Placebo	11.4 years[e,f]				
		870	Caffeine	11.4 years[e,f]				↑motor coordination ($p = 0.01$)

(Continued on following page)

TABLE 3 | (*Continued*) Main efficacy and safety results in standard dose caffeine treatment studies.

First author, year[ref.]	Study characteristics	Number of cases	Groups	Mean GA (weeks)	Mean PNA (days)	Dose of caffeine citrate		Main efficacy and safety results for caffeine treatment
						L (mg/kg)	M (mg/kg/day)	
Murner-Lavanchy et al. (2018)			Placebo	11.4 years[e,f]				↑visuomotor integration ($p < 0.05$) ↑visual perception ($p = 0.02$) ↑visuospatial organization ($p = 0.03$) no significant differences in general intelligence, attention, executive function, and behavior
Doyle et al. (2017))		142	Caffeine	11.4 years[e,f]				↑expiratory flow rates in mid-childhood ($p = 0.008$)
			Placebo	11.4 years[e,f]				
Schmidt et al. (2019)		821	Caffeine	11.4 years[e,f]				↓social support and peer scores (50.8 vs. 52.6, $p = 0.01$) no significant differences in scores on other 9 dimensions of health-related quality of life
			Placebo	11.4 years[e,f]				

NR, not reported; GA, gestational age; PNA, postnatal age; L, loading dose; M, maintenance dose; NEC, necrotizing enterocolitis; BPD, bronchopulmonary dysplasia; PDA, patent ductus arteriosus; ROP, retinopathy of prematurity

[a]*The initial dose was 20 mg/kg orally once or twice a day, and it was changed due to the accumulation of caffeine in the blood in preterm infants.*

[b]*Refers to the average number of apnea episodes per 100 min calculated from the recording within 24 h.*

[c]*The caffeine group additionally included four 14 day-old term infants with apnea.*

[d]*Dose regimen was 1.25 mg/kg every 12 h.*

[e]*Data are expressed as the median.*

[f]*Data are expressed as the corrected age.*

With the inclusion of additional subjects in the above-mentioned study, Gray compared the long-term effects of the two dose regimens used in Steer's study (Gray et al., 2011). In this trial, 20 mg/kg/day caffeine citrate resulted in neither adverse outcomes in cognitive development, temperament, morbidity, mortality or disability at 1 year nor in behavior at 2 years.

Several findings also revealed the benefits of higher doses of caffeine for VLBW preterm infants. A retrospective analysis suggested that a higher average daily dose of caffeine citrate was associated with better neurodevelopmental outcomes in VLBW infants (Ravichandran et al., 2019). Another RCT trial found that a maintenance dose as high as 10 mg/kg better reduced the duration of apnea and caffeine treatment in this population (Zhang et al., 2019).

Four meta-analyses also synthesized the findings from the trials comparing higher and lower doses of caffeine citrate (**Table 5**). Among of them, three papers reported that higher caffeine dosage regimens might be better in reducing the risk of BPD and extubation failure (Chen et al., 2018; Pakvasa et al., 2018; Vliegenthart et al., 2018; Brattström et al., 2019), two reported a decrease in apnea frequency (Chen et al., 2018; Brattström et al., 2019) and one reported a shortened duration of mechanical ventilation (Brattström et al., 2019). Regarding safety concerns, three meta-analyses concluded a higher risk of tachycardia with higher dose of caffeine (Chen et al., 2018; Pakvasa et al., 2018), but no other adverse outcomes were increased.

However, a pilot RCT found an increased incidence of cerebellar hemorrhage (CBH) in infants < 31 weeks' gestation who were randomized to a higher-dose caffeine citrate (loading 80 mg/kg) (McPherson et al., 2015). Further analysis of this trial demonstrated that early high-dose caffeine therapy was associated with a trend toward an increase in seizure incidence (40 vs 58%, $p = 0.1$) and burden (48.9 vs 170.9, $p = 0.1$) (Vesoulis et al., 2016). These results discouraged a larger RCT. More recently, a retrospective study of 218 preterm infants < 28 weeks' gestation who received a loading dose of caffeine citrate within the first 36 h of life was conducted (Firman et al., 2019). The use of early high loading dose caffeine citrate (a median dose of 80 mg/kg) was not shown to be associated with CBH. Although the two studies obtained different short-term outcomes, they both found that at 2 years of age, the Bayley-III scores used to assess neurodevelopment were not significantly different between the two dose groups.

Collectively, most previous RCTs had small sample sizes, and only two of them have reported 2 years clincal outcomes, which, although positive, need to be treated with caution. Thus, whether to use higher caffeine dosage regimens and how to optimize the caffeine dose are still questionable.

THERAPEUTIC DRUG MONITORING OF CAFFEINE

Therapeutic Concentration of Standard Dose of Caffeine

The role of TDM for the control of therapeutic ranges of caffeine has often been challenged due to its benign safety profile when standard dosing is used. As early as in 1977, Aranda et al. revealed that the plasma concentration of standard dose caffeine needed to be monitored and the effective therapeutic concentration was established at 5–20 mg/L by referring to the use of theophylline (Aranda et al., 1977). Subsequently, the same authors also noted that the minimum effective plasma concentration of caffeine was

TABLE 4 | Advantageous and Disadvantageous Results for Higher vs. Lower Doses of Caffeine in Randomized Controlled Trials.

First author, Year[ref.]	Type of study	Number of cases	GA, Other characteristics	Dose of caffeine citrate				Advantageous results for higher dose	Disadvantageous results for higher dose
				Higher dose		Lower dose			
				L	M	L	M		
Romagnoli et al. (1992)	Single center RCT	37[a]	<32	10	2.5	10	5		↑frequency of tachycardia and gastrointestinal intolerance (compared to other groups, $p < 0.001$)
Scanlon et al. (1992)	Single center RCT	44[b]	<31	50	12	25	6	↓more apnea episodes within 24 h (> 1/2 vs. 1/3)	
Steer et al. (2003)	Single center RCT	127	<32, ventilated for > 48 h	30 60	15 30	6	3	↓more documented apnea within 1 week after extubation ($p = 0.01$)	
				24 h before planned extubation, or within 6 h after unplanned extubation					
Steer et al. (2004)	Multicenter RCT	234	<30, ventilated for > 48 h	80	20	20	5	↓extubation failure ($p < 0.01$) ↓duration of mechanical ventilation in infants GA < 28 weeks ($p = 0.01$) ↓documented apnea ($p < 0.01$)	
				24 h before planned extubation, or within 6 h after unplanned extubation					
Gray et al. (2011)	Multicenter RCT	246	<30	80	20	20	5	↑mean general quotient ($p = 0.048$, after excluding two disabled children who could not be assessed, $p = 0.075$)	
Mohammed et al. (2015)	Single center RCT	120	<32	40	20	20	10	↓extubation failure ($p = 0.02$) ↓frequency and days of documented apnea ($p < 0.001$) ↓duration of oxygen therapy ($p = 0.04$)	↑episodes of tachycardia ($p = 0.04$)
McPherson et al. (2015)	Single center RCT	74	≤30	80 total over 36 h	10	30 total over 36 h	10		↑incidence of cerebellar hemorrhage ($p = 0.03$) ↑hypertonicity ($p = 0.02$) and deviant neurologic signs ($p = 0.04$) at term equivalent age
Zhao et al. (2016)	Single center RCT	164	<32	20	15	20	5	↓frequency of apnea ($p < 0.009$) ↑success rate of removal of the ventilator ($p = 0.015$) ↑effective rate of caffeine treatment ($p = 0.003$)	
Zhang et al. (2019)	Single center RCT	78	28–32, born weight < 1,500 g	20	10	20	5	↑response rate of caffeine treatment ($p = 0.035$) ↓duration of apnea ($p = 0.01$) and time of caffeine treatment ($p = 0.035$)	
Wan et al. (2020)	Single center RCT	97	<30, ventilated for > 48 h	20	10	20	5	↓extubation failure ($p = 0.017$), age of extubation ($p = 0.000$), duration of invasive ventilation ($p = 0.003$), duration of ventilation before extubation ($p = 0.000$), and number of days of apnea ($p = 0.001$)	

GA, gestational age (weeks); L, loading dose (mg/kg); M, maintenance dose (mg/kg/day).
[a]*A control group of 14 cases was included in the trial.*
[b]*An aminophylline group of 14 cases was included in the trial.*

3–4 mg/L, but an optimal ventilatory response was observed at greater than 8 mg/L, and slight toxicity manifesting as temporary jitteriness was not detected until 50–84 mg/L (Aranda et al., 1979a; Aranda and Turmen, 1979). Therefore, Aranda et al. concluded that the optimal therapeutic concentration of caffeine is 8–20 mg/L, which both produces an adequate response to control apnea and avoids the risk of toxic effects (Aranda and Turmen, 1979).

Blood caffeine levels in preterm infants were almost within this conventional target range in other studies using similar standard dose regimens. In an RCT, 37 preterm infants rapidly achieved the therapeutic concentration within 24 h after starting treatment

TABLE 5 | Results for Higher vs. Lower Doses of Caffeine in Meta-analyses.

First author, year[ref.]	Number of trials (patients)	Significant results (RR [95% CI][a], Number of patients)	Nonsignificant results ($p > 0.05$)
Vliegenthart et al. (2018)	6 RCTs ($n = 620$)	extubation failure (0.51 [0.37; 0.70], 463) tachycardia (3.39 [1.50; 7.64], 528)	BPD, BPD combined mortality, hospital mortality, NEC ≥ grade 2, SIP, ROP ≥ grade 3, IVH > grade 2, hyperglycemia, mortality < 1year, major disability at 1 year, death or disability at 1 year, general quotient at 1 year
Brattström et al. (2019)	6 RCTs ($n = 816$)	BPD (0.76 [0.60; 0.96], 645) extubation failure (0.51 [0.36;0.71], 489) apnea frequency (−5.68 [−6.15; −5.22][b], 571) tachycardia (2.56 [1.45; 4.50][b], 653) MV duration (−1.69 [−2.13; −1.25][b], 727)	hospital mortality, NEC, ROP ≥ grade 3, IVH ≥ grade 3, IVH, PVL, CBH, lesions indicative of brain injury, PDA treatment, major disabilities, seizure, somatic growth
Chen et al. (2018)	13 RCTs ($n = 1,515$)	BPD (0.79 [0.68; 0.91], 1,084) extubation failure (0.50 [0.35;0.71], 372) apnea frequency (−1.55 [−2.72; −0.39][b], 168) apnea duration (−4.85 [−8.29; −1.40][b], 150) tachycardia (2.02 [1.30; 3.12], 880)	hospital mortality, NEC, ROP, IVH, PVL, hyperglycemia, electrolyte disturbance, hypertension, feed intolerance, restlessness,
Pakvasa et al. (2018)	3 RCTs ($n = 432$)	BPD (0.65 [0.65;0.97][c], 432)	

RCT, randomized controlled trial; BPD, bronchopulmonary dysplasia; MV, mechanical ventilation; NEC, necrotizing enterocolitis; SIP, spontaneous intestinal perforation; ROP, retinopathy of prematurity; IVH, intraventricular hemorrhage; PVL, periventricular leukomalacia; CBH, cerebellar hemorrhage; PDA, patent ductus arteriosus.

[a]*Results are expressed as the relative ratio [95% confidence intervals], unless otherwise specified.*

[b]*Results are expressed as the mean differences [95% confidence intervals].*

[c]*Results are expressed as odds ratios [95% confidence intervals].*

with a significant reduction in apneic episodes (Romagnoli et al., 1992). A study of 18 Asian preterm infants reported mean serum caffeine concentrations of 10–20 mg/L, and concluded that conventional caffeine therapeutic concentrations should be adhered to in order to ensure safety and efficacy (Lee et al., 2002). Leon et al. found that when the maintenance dose was 6 mg/kg, the 25th to 75th percentile range of mean serum caffeine concentrations in 108 preterm infants was comparable between two different loading dose groups (20 or 25 mg/kg), ranging from 18 to 23 mg/L (Leon et al., 2007). Another study found that the majority of preterm infants achieved target plasma caffeine levels of 5–20 mg/L when treated with a median dose of 5.0 mg/kg (range 2.5–10.9 mg/kg), with 95% of measures within this range in a cohort of 101 preterm infants with 23–32 weeks gestation, including those with renal or hepatic dysfunction (Natarajan et al., 2007a).

Therefore, blood caffeine concentrations of 5–20 or 8–20 mg/L have been commonly recognized as effective therapeutic concentrations for AOP treatment. Routine monitoring of caffeine levels is not recommended by the American Academy of Pediatrics Committee on Fetus and Newborn in their statement on AOP (Eichenwald, 2016). However, when we traced back to the origin, we recognized that the study by Aranda et al. was the fisrt study to determine the therapeutic concentration range of caffeine only based on 18 premature infants' data (Aranda et al., 1977). Surprisingly, the blood caffeine concentrations were not measured in the well-known CAP trial and the drug was monitored according to its clinical effect only (Schmidt et al., 2006). Of note, the study by Natarajan et al. included a group of preterm neonates ($n = 94$) who lacked clinical response and had median to 75th quartile of plasma caffeine concentrations of 10.2–14.1 mg/L, suggesting that some neonates may need higher targets of caffeine to control apnea (Natarajan et al., 2007a). Collectively, whether to monitor the level of caffeine in preterm neonates using standard doses still needs to be explored.

Therapeutic Concentration of Higher Dose of Caffeine

Many studies have shown that using higher dose of caffeine was more effective with negligible adverse effects than the standard-dose regimen and explored different effective therapeutic ranges of caffeine. A caffeine PK study including 13 premature infants found that the blood caffeine level varied widely from 12 to 36 mg/L when the single dose regimen of 15 mg/kg was used (Gorodischer and Karplus, 1982). Another RCT reported that 73% of the plasma caffeine concentration measurements in the high-dose group ranged from 26 to 40 mg/L, and apnea episodes were reduced more rapidly within 8 and 24 h without serious adverse effects compared to the standard-dose group (Scanlon et al., 1992). In a PK study conducted by Lee et al., in which no undesired consequences occurred when the mean serum caffeine concentrations were 35.8 or 69.0 mg/L (Lee et al., 1997), a therapeutic concentration > 35 mg/L was proposed to effectively prevent apnea after extubation. Similarly, Steer et al. reported that two higher dose groups with mean serum caffeine concentrations of 31.4 and 59.9 mg/L had short-term benefits and safety during peri-extubation among 127 infants < 32 weeks gestation (Steer et al., 2003). Subsequently, a commentary by Dr. Gal in 2007 questioned the traditional therapeutic concentration (Gal, 2007). According to his findings, higher serum caffeine concentrations produced more significant clinical responses including the reduced incidence of apnea, bradycardia, and of oxygen desaturation, which affirmed a target range of 8–40 mg/L, proposed by Natarajan et al. in another review (Natarajan et al., 2007b). In addition, a retrospective chart review of 198 infants born ≤

29 weeks gestation showed that serum concentrations of caffeine > 14.5 mg/L were correlated with a reduction in the incidence of chronic lung disease (Chavez Valdez et al., 2011).

However, a small observational prospective study found that serum caffeine levels ≥ 20 mg/L were associated with increased proinflammatory cytokines in preterm infants during the first week of life (Alur et al., 2015). In another study of 115 preterm infants, there was no association between episodes of apnea and serum caffeine concentrations, although there was a significant but weak correlation between caffeine concentration and heart rate (Yu et al., 2016). Meanwhile, some cases reported acute intoxication due to overdose. A case report in 1980 presented two full-term infants with acute caffeine overdose who still had seizure activity when caffeine levels decreased to 31.9 mg/L and 10 mg/L, respectively, although the effect of perinatal asphyxia could not be ruled out (Banner and Czajka, 1980). Another 31 weeks gestational neonate experienced toxic reactions, including hypertonia, sweating, tachycardia, heart failure, pulmonary edema, metabolic disturbances and gastric dilatation, due to the blood caffeine level's reaching 217.5 mg/L at 36.5 h after dosing, but these symptoms disappeared on day 7 at plasma concentrations of 60–70 mg/L (Anderson et al., 1999). Neurological symptoms, such as uninterrupted tremors, hypertonia, persistent reflex posture, crying, and digestive disorders were reported in a 33 weeks preterm newborn with a serum caffeine level of 160 mg/L at 66 h after administration, whereas his psychomotor development returned to normal after 3 months of age (Perrin et al., 1987). In addition, it is unfortunate that blood caffeine concentrations of subjects were not provided in most RCTs investigating doses of caffeine for AOP (Gray et al., 2011; McPherson et al., 2015; Mohammed et al., 2015; Zhao et al., 2016; Zhang et al., 2019; Wan et al., 2020). Due to lack of high-quality evidence for the long-term safety of high levels of caffeine, further determination of the therapeutic concentration range is difficult.

Therapeutic Drug Monitoring and Dose Optimization of Caffeine

In the aforementioned studies, thetherapeutic concentration of caffeine was commonly recognized as 5–20 or 8–20 mg/L when using the standard dose regimen. However, some preterm neonates lacked a positive clinical response, although their caffeine levels were within the therapeutic concentration range, suggesting that these neonates may need to use higher doses to control apnea episodes. But using high doses may induce adverse reactions, and how to determine therapeutic doses for neonates who lack a clinical response still needs to be investigated. Therefore, is it feasible to guide dose optimization based on the monitoring caffeine levels?

Refer to *Therapeutic Concentration of Standard Dose of Caffeine*, routine monitoring of blood caffeine levels is generally not recommended. Leon et al. found that when a caffeine dose regimen close to standard (loading 20 or 25 mg/kg and maintenance of 6 mg/kg/day) was used, the serum drug concentrations were maintained in a safe therapeutic range and were independent of corrected gestational age, weight, and postnatal age within the first 2 weeks of life (Leon et al., 2007). Nevertheless, a PPK study found that the day-to-day variability in caffeine clearance of preterm neonates was twice the interindividual variability, implying that adjusting maintenance doses in light of previous serum concentrations is futile (Charles et al., 2008). However, some studies reported that higher levels of caffeine resulted in a greater response, and caffeine concentration monitoring was essential to ensure reaching the expected drug levels (Gal, 2007; Kahn and Godin, 2016). The 2019 guidelines of the National Institute for Health and Care Excellence recommend that caffeine levels should be monitored using reference ranges from the local laboratories to ensure safety when the daily maintenance dose is higher than 20 mg/kg (NICE, 2019). Combined with clinical practice, a growing body of research has endorsed the view that therapeutic monitoring of caffeine is of interest when therapeutic response is lacking or toxicity is suspected (Natarajan et al., 2007a; Gal, 2007; Leon et al., 2007; Gal, 2009; Kahn and Godin, 2016; Yu et al., 2016).

Naturally, the dose optimization of caffeine cannot be generalized. On the one hand, the change in caffeine clearance in preterm infants is a postnatal maturational progression (Aranda and Beharry, 2020). For routine use of caffeine, Koch et al. developed a simulated PK model and proposed an adjustment strategy based on postnatal age to maintain stable caffeine concentrations, with steps of increasing the caffeine maintenance daily dose by 1 mg/kg every 1 to 2 postnatal weeks, 6 mg/kg in the second week, 7 mg/kg in the third to fourth weeks, and 8 mg/kg in the fifth to eighth weeks (Koch et al., 2017). Recently, it has also been proposed that individualized caffeine medication can be administered with the help of a physiologic based pharmacokinetics (PBPK) model (Abduljalil et al., 2020; Aranda and Beharry, 2020; Verscheijden et al., 2020). On the other hand, the clinical response is specific to each individual and influenced by many factors such as gestational age, birth weight and genetic variability (Gal, 2007; Bloch-Salisbury et al., 2010; Francart et al., 2013; Ravichandran et al., 2019; He et al., 2020). Although increasing evidence has proven that the higher dose of caffeine is beneficial for newborns, there are also potential toxic risks and unknown long-term safety problems. In addition, the reported therapeutic concentration ranges of caffeine may not be simply combined together because of the differences such as the population, sample size, biological matrix, as well as assay methods in each study. This highlights the need to tailor the most appropriate range of individual therapeutic concentration according to blood caffeine levels, and the development of minimally invasive sampling techniques and noninvasive sampling of caffeine may contribute to achieving this requirement (Patel et al., 2013; Bruschettini et al., 2016; Chaabane et al., 2017).

IMPACT OF GENETIC VARIABILITY ON THE CLINICAL RESPONSE TO CAFFEINE THERAPY

Earlier studies have found that heritability impacts the incidence of AOP, which raised interest in elucidating the effects of genetic factors on AOP as well as caffeine therapy (Tamim et al., 2003; Bloch-Salisbury et al., 2010). The therapeutic effect of caffeine depends on the disposition process of caffeine *in vivo*, that is, PK, and the interaction with target receptors, that is, pharmacodynamics (PD). Researches to date are precisely based on these two aspects.

In terms of PK, a recent retrospective study found that there were no significant differences in caffeine systemic exposure levels between apneic and apnea-free groups, as well as no significant association between the C_0/D ratio and genetic variations in *CYP1A2* genes (rs2472299 and rs762551) (He et al., 2020). Correspondingly, in another PPK study of Chinese preterm neonates, the investigators found no significant association between several genetic variants in *CYP1A2* (rs2069514, rs2069521, rs2069526, rs2470890, rs35694136, rs3743484, rs56107638 and rs762551) and PK parameters (Gao et al., 2020). These findings echo delayed CYP1A2 ontogenesis and immature metabolism in premature infants, indicating that the contribution of genetic polymorphisms in caffeine-metabolizing enzymes to the variability in treatment response is limited. Notably, however, it has also been reported that the distribution of the aryl hydrocarbon receptor (*AHR*) CC genotype (rs4410790) differed significantly between the two groups with different responses to caffeine treatment in Chinese preterm neonates (He et al., 2020). Although AHR is normally a transcription factor that can regulate CYP1A2 expression, the authors stated that this finding may not be explained by the AHR-CYP1A2 metabolic pathway mechanisms.

In contrast, several studies have reported the effect of genetic polymorphisms associated with caffeine PD on treatment response. Adenosine receptor (AR) gene polymorphisms are the most described genetic factors in those current studies. AR is a class of G protein-coupled receptors with four known subtypes, A_1, A_{2A}, A_{2B} and A_3, which is encoded by the *ADORA1*, *ADORA2A*, *ADORA2B*, and *ADORA3* genes, respectively (Chen et al., 2013; Borea et al., 2018). With a molecular structure similar to that of adenosine, caffeine acts as a nonspecific antagonist of A_1AR and A_{2A}AR to exert pharmacological effects at physiological concentrations (McLellan et al., 2016; Kumar and Lipshultz, 2019). In some studies, AR gene polymorphisms have already been found to be associated with intersubject variability in sensitivity to caffeine-induced anxiety (Childs et al., 2008; Rogers et al., 2010). Referring to these findings, Kumral et al. conducted a retrospective case-control study and found that *ADORA1* (rs16851030) CC genotype carriers had better responsiveness to caffeine than CT or TT genotype carriers.They also revealed that the correlation between *ADORA2A* (rs35320474, rs5751876, rs3761422) CT or TT genotypes and vulnerability to AOP as well as the correlation between *ADORA2A* (rs35320474) CT or TT genotypes and greater risk of BPD (Kumral et al., 2012). A significantly increased frequency of *ADORA2A* (rs5751876) CT, TT genotypes and T allele in caffeine nonresponders compared to caffeine responders was also reported in another prospective case-control study of Egyptian preterm neonates (Mokhtar et al., 2018). Moreover, a most recent retrospective study of Chinese preterm infants found that carriers of *ADORA1* T > G (rs10920568), G > T (rs12744240) and *ADORA3* C > A (rs10776727) as well as T > C (rs2298191) mutant genotypes did not respond to caffeine treatment, whereas *ADORA2A* T > A (rs34923252) and A > C (rs5996696) mutation genotype carriers responded better (He et al., 2020). In addition, this study also showed that a variant (rs521704, C > A) in the coding gene of adenosine dehydrogenase (ADA), which catalyzes adenosine metabolism, was associated with the response of premature infants to caffeine therapy (He et al., 2020). Phosphodiesterase (PDE), one of the targets of caffeine at nonphysiological concentrations, was also correlated, as carriers of the homozygous mutant genotype of *PDE4D* (rs10075508, C > T) responded poorly to standard-dose caffeine treatment (McLellan et al., 2016; Kumar and Lipshultz, 2019; He et al., 2020).

Collectively, although the sample size number of these studies is small, several genetic polymorphisms have been revealed to be associated with individual variances in response to caffeine therapy. Therefore, studies with larger sample sizes are needed to confirm these findings and further researches are warranted to explain how genetic variants play a critical role in the response to caffeine therapy in premature infants.

CONCLUSION

Caffeine is effective in reducing apnea frequency in preterm neonates. The available evidence has confirmed the efficacy and safety of standard doses of caffeine, and routine TDM seems unnecessary in neonates who respond positively to caffeine treatment. However, the well-known CAP trial only started caffeine treatment when apnea occurred, and when to start standard-dose caffeine therapy is also a quite controversial issue that requires long-term safety studies. For developmental premature infants, a dosing adjustment strategy based on postnatal age was proposed to maintain stable caffeine concentrations, and individualized caffeine medication may be administered with the help of PPK and PBPK models. For neonates lacking a positive clinical response, as the evidence for the use of higher doses of caffeine is insufficient, and TDM should be performed to achieve the desired blood caffeine level and ensure safety. The long-term results of larger trials of higher doses of caffeine are expected and would be more reasonable if corresponding blood caffeine concentrations could be provided. In addition, the study of genetic factors has preliminarily revealed the association between genetic polymorphisms and clinical response to caffeine therapy. Further studies are required to explain how genetic variants play a role in the response to caffeine therapy in premature infants. And how to establish an approach to individualize medication regimens for infants with poor clinical response by integrating tools such as TDM, genetic testing, PPK and PBPK models is also a direction for future exploration.

AUTHOR CONTRIBUTIONS

JL, HG, FC, JX: Wrote the manuscript and prepared the tables. XH, YH, YX: Revised the manuscript. RC, XD: Contributed to the language polish. HG, FC: Provided financial support. All the authors reviewed and agreed the final manuscript.

FUNDING

This research was supported by the Specially Appointed Medical Expert Project of the Jiangsu Commission of Health (2019) and Special Fund for Clinical Research of the Wu Jieping Medical Foundation (320.6750.2020-04-07). This study was also supported by the Scientific Research Support Foundation for Top Young Scholars at the Children's Hospital of Nanjing Medical University (2020).

REFERENCES

Abduljalil, K., Pan, X., Pansari, A., Jamei, M., and Johnson, T. N. (2020). Preterm Physiologically Based Pharmacokinetic Model. Part II: Applications of the Model to Predict Drug Pharmacokinetics in the Preterm Population. *Clin. Pharmacokinet.* 59 (4), 501–518. doi:10.1007/s40262-019-00827-4

al-Alaiyan, S., al-Rawithi, S., and Raines, D. (2001). Caffeine Metabolism in Premature Infants. *J. Clin. Pharmacol.* 41 (6), 620–627. doi:10.1177/00912700122010500

Aldridge, A., Aranda, J. V., and Neims, A. H. (1979). Caffeine Metabolism in the Newborn. *Clin. Pharmacol. Ther.* 25 (4), 447–453. doi:10.1002/cpt1979254447

Alur, P., Bollampalli, V., Bell, T., Hussain, N., and Liss, J. (2015). Serum Caffeine Concentrations and Short-Term Outcomes in Premature Infants of ⩽29 Weeks of Gestation. *J. Perinatol* 35 (6), 434–438. doi:10.1038/jp.2014.226

Anderson, B. J., Gunn, T. R., Holford, N. H. G., and Johnson, R. (1999). Caffeine Overdose in a Premature Infant: Clinical Course and Pharmacokinetics. *Anaesth. Intensive Care* 27 (3), 307–311. doi:10.1177/0310057x9902700316

Anwar, M., Mondestin, H., Mojica, N., Novo, R., Graff, M., Hiatt, M., et al. (1986). Effect of Caffeine on Pneumogram and Apnoea of Infancy. *Arch. Dis. Child.* 61 (9), 891–895. doi:10.1136/adc.61.9.891

Aranda, J. V., and Beharry, K. D. (2020). Pharmacokinetics, Pharmacodynamics and Metabolism of Caffeine in Newborns. *Semin. Fetal Neonatal Med.* 25 (6), 101183. doi:10.1016/j.siny.2020.101183

Aranda, J. V., and Turmen, T. (1979). Methylxanthines in Apnea of Prematurity. *Clin. Perinatol.* 6 (1), 87–108. doi:10.1016/s0095-5108(18)31165-5

Aranda, J. V., Gorman, W., Bergsteinsson, H., and Gunn, T. (1977). Efficacy of caffeine in treatment of apnea in the low-birth-weight infant. *J. Pediatr.* 90 (3), 467–472. doi:10.1016/s0022-3476(77)80718-x

Aranda, J. V., Cook, C. E., Gorman, W., Collinge, J. M., Loughnan, P. M., Outerbridge, E. W., Aldridge, A., and Neims, A. H. (1979). Pharmacokinetic Profile of Caffeine in the Premature Newborn Infant With Apnea. *J. Pediatr.* 94 (4), 663–668. doi:10.1016/s0022-3476(79)80047-5

Aranda, J. V., Collinge, J. M., Zinman, R., and Watters, G. (1979). Maturation of Caffeine Elimination in Infancy. *Arch. Dis. Child.* 54 (12), 946–949. doi:10.1136/adc.54.12.946

Aranda, J. V., Beharry, K., Valencia, G. B., Natarajan, G., and Davis, J. (2010). Caffeine Impact on Neonatal Morbidities. *J. Matern. Fetal. Neonatal Med.* 23 (Suppl 3), 20–23. doi:10.3109/14767058.2010.517704

Arnaud, M. J. (1976). Identification, Kinetic and Quantitative Study of [2-14C] and [1-Me-14C]Caffeine Metabolites in Rat's Urine by Chromatographic Separations. *Biochemical Medicine* 16 (1), 67–76. doi:10.1016/0006-2944(76)90010-7

Arnaud, M. J. (1987). The Pharmacology of Caffeine. *Prog Drug Res* 31, 273–313. doi:10.1007/978-3-0348-9289-6_9

Arnaud, MJ (2011). Pharmacokinetics and Metabolism of Natural Methylxanthines in Animal and Man. *Handb Exp Pharmacol* 2011, 33–91. doi:10.1007/978-3-642-13443-2_3

Bairam, A., Boutroy, M.-J., Badonnel, Y., and Vert, P. (1987). Theophylline Versus caffeine: Comparative Effects in Treatment of Idiopathic Apnea in the Preterm Infant. *J. Pediatr.* 110 (4), 636–639. doi:10.1016/s0022-3476(87)80569-3

Bancalari, E. (2014). Current Management of Apnea in Premature Infants: Is Caffeine the Magic Bullet? *Early Hum. Develop.* 90, S1–S2. doi:10.1016/s0378-3782(14)50001-1

Banner, W., Jr., and Czajka, P. A. (1980). Acute Caffeine Overdose in the Neonate. *Arch. Pediatr. Adolesc. Med.* 134 (5), 495–498. doi:10.1001/archpedi.1980.02130170045015

Begas, E., Kouvaras, E., Tsakalof, A., Papakosta, S., and Asprodini, E. K. (2007). *In Vivo* evaluation of CYP1A2, CYP2A6, NAT-2 and Xanthine Oxidase Activities in a Greek Population Sample by the RP-HPLC Monitoring of Caffeine Metabolic Ratios. *Biomed. Chromatogr.* 21 (2), 190–200. doi:10.1002/bmc.736

Blake, M. J., Abdel-Rahman, S. M., Pearce, R. E., Leeder, J. S., and Kearns, G. L. (2006). Effect of Diet on the Development of Drug Metabolism by Cytochrome P-450 Enzymes in Healthy Infants. *Pediatr. Res.* 60 (6), 717–723. doi:10.1203/01.pdr.0000245909.74166.00

Blanchard, J., and Sawers, S. J. A. (1983). The Absolute Bioavailability of Caffeine in Man. *Eur. J. Clin. Pharmacol.* 24 (1), 93–98. doi:10.1007/bf00613933

Bloch-Salisbury, E., Hall, M. H., Sharma, P., Boyd, T., Bednarek, F., and Paydarfar, D. (2010). Heritability of Apnea of Prematurity: a Retrospective Twin Study. *Pediatrics* 126 (4), e779–e787. doi:10.1542/peds.2010-0084

Bonati, M., Latini, R., Galletti, F., Young, J. F., Tognoni, G., and Garattini, S. (1982). Caffeine Disposition After Oral Doses. *Clin. Pharmacol. Ther.* 32 (1), 98–106. doi:10.1038/clpt.1982.132

Bonati, M., Latini, R., Tognoni, G., Young, J. F., and Garattini, S. (1984). Interspecies Comparison of *In Vivo* Caffeine Pharmacokinetics in Man, Monkey, Rabbit, Rat and Mouse. *Drug Metab. Rev.* 15 (7), 1355–1383. doi:10.3109/03602538409029964

Borea, P. A., Gessi, S., Merighi, S., Vincenzi, F., and Varani, K. (2018). Pharmacology of Adenosine Receptors: The State of the Art. *Physiol. Rev.* 98 (3), 1591–1625. doi:10.1152/physrev.00049.2017

Bory, C., Baltassat, P., Porthault, M., Bethenod, M., Frederich, A., and Aranda, J. (1978). Biotransformation of Theophylline to Caffeine in Premature Newborn. *Lancet* 312 (8101), 1204–1205. doi:10.1016/s0140-6736(78)92188-8

Bory, C., Baltassat, P., Porthault, M., Bethenod, M., Frederich, A., and Aranda, J. V. (1979). Metabolism of Theophylline to Caffeine in Premature Newborn Infants. *J. Pediatr.* 94 (6), 988–993. doi:10.1016/s0022-3476(79)80246-2

Brattström, P., Russo, C., Ley, D., and Bruschettini, M. (2019). High-versus Low-Dose Caffeine in Preterm Infants: a Systematic Review and Meta-Analysis. *Acta Paediatr.* 108 (3), 401–410. doi:10.1111/apa.14586

Brouard, C., Moriette, G., Murat, I., Flouvat, B., Pajot, N., Walti, H., et al. (1985). Comparative Efficacy of Theophylline and Caffeine in the Treatment of Idiopathic Apnea in Premature Infants. *Arch. Pediatr. Adolesc. Med.* 139 (7), 698–700. doi:10.1001/archpedi.1985.02140090060028

Bruschettini, M., Barco, S., Romantsik, O., Risso, F., Gennai, I., Chinea, B., et al. (2016). DBS-LC-MS/MS Assay for Caffeine: Validation and Neonatal Application. *Bioanalysis* 8 (18), 1893–1902. doi:10.4155/bio-2016-0127

Carrier, O., Pons, G., Rey, E., Richard, M.-O., Moran, C., Badoual, J., et al. (1988). Maturation of Caffeine Metabolic Pathways in Infancy. *Clin. Pharmacol. Ther.* 44 (2), 145–151. doi:10.1038/clpt.1988.129

Cazeneuve, C., Pons, G., Rey, E., Treluyer, J., Cresteil, T., Thiroux, G., et al. (1994). Biotransformation of Caffeine in Human Liver Microsomes from Foetuses, Neonates, Infants and Adults. *Br. J. Clin. Pharmacol.* 37 (5), 405–412. doi:10.1111/j.1365-2125.1994.tb05706.x

Chaabane, A., Chioukh, F. Z., Chadli, Z., Ben Fredj, N., Ben Ameur, K., Ben Hmida, H., et al. (2017). Therapeutic Drug Monitoring of Caffeine in Preterm Infants: Could Saliva Be an Alternative to Serum? *Therapies* 72 (6), 685–689. doi:10.1016/j.therap.2017.06.004

Charles, B. G., Townsend, S. R., Steer, P. A., Flenady, V. J., Gray, P. H., and Shearman, A. (2008). Caffeine Citrate Treatment for Extremely Premature Infants with Apnea: Population Pharmacokinetics, Absolute Bioavailability, and Implications for Therapeutic Drug Monitoring. *Ther. Drug Monit.* 30 (6), 709–716. doi:10.1097/ftd.0b013e3181898b6f

Chavez Valdez, R., Ahlawat, R., Wills-Karp, M., Nathan, A., Ezell, T., and Gauda, E. B. (2011). Correlation Between Serum Caffeine Levels and Changes in Cytokine Profile in a Cohort of Preterm Infants. *J. Pediatr.* 158 (1), 57–64.e1. doi:10.1016/j.jpeds.2010.06.051

Chen, J.-F., Eltzschig, H. K., and Fredholm, B. B. (2013). Adenosine Receptors as Drug Targets - What Are the Challenges? *Nat. Rev. Drug Discov.* 12 (4), 265–286. doi:10.1038/nrd3955

Chen, J., Jin, L., and Chen, X. (2018). Efficacy and Safety of Different Maintenance Doses of Caffeine Citrate for Treatment of Apnea in Premature Infants: A Systematic Review and Meta-Analysis. *Biomed. Res. Int.* 2018, 9061234. doi:10.1155/2018/9061234

Childs, E., Hohoff, C., Deckert, J., Xu, K., Badner, J., and de Wit, H. (2008). Association between ADORA2A and DRD2 Polymorphisms and Caffeine-Induced Anxiety. *Neuropsychopharmacol* 33 (12), 2791–2800. doi:10.1038/npp.2008.17

De Carolis, M. P., Romagnoli, C., Muzii, U., Tortorolo, G., Chiarotti, M., De Giovanni, N., et al. (1991). Pharmacokinetic Aspects of Caffeine in Premature Infants. *Dev. Pharmacol. Ther.* 16 (3), 117–122. doi:10.1159/000480570

Di Fiore, J. M., Bloom, J. N., Orge, F., Schutt, A., Schluchter, M., Cheruvu, V. K., et al. (2010). A Higher Incidence of Intermittent Hypoxemic Episodes Is Associated with Severe Retinopathy of Prematurity. *J. Pediatr.* 157 (1), 69–73. doi:10.1016/j.jpeds.2010.01.046

Dobson, N. R., and Hunt, C. E. (2013). Pharmacology Review: Caffeine Use in Neonates: Indications, Pharmacokinetics, Clinical Effects, Outcomes. *NeoReviews* 14 (11), e540–e550. doi:10.1542/neo.14-11-e540

Doyle, L. W., Ranganathan, S., and Cheong, J. L. Y. (2017). Neonatal Caffeine Treatment and Respiratory Function at 11 Years in Children Under 1,251 G at

Birth. *Am. J. Respir. Crit. Care Med.* 196 (10), 1318–1324. doi:10.1164/rccm.201704-0767oc

Eichenwald, E. C. (2016). Committee on Fetus and Newborn, American Academy of Pediatrics. Apnea of Prematurity. *Pediatrics* 137 (1), e20153757. doi:10.1542/peds.2015-3757

Engbers, A. G. J., Völler, S., Poets, C. F., Knibbe, C. A. J., Reiss, I. K. M., Koch, B. C. P., et al. (2021). The Pharmacokinetics of Caffeine in Preterm Newborns: No Influence of Doxapram but Important Maturation With Age. *Neonatology* 118 (1), 106–113. doi:10.1159/000513413

Erenberg, A., Leff, R. D., Haack, D. G., Mosdell, K. W., Hicks, G. M., Wynne, B. A., et al. (2000). Caffeine Citrate for the Treatment of Apnea of Prematurity: a Double-Blind, Placebo-Controlled Study. *Pharmacotherapy* 20 (6), 644–652. doi:10.1592/phco.20.7.644.35167

Erickson, G., Dobson, N. R., and Hunt, C. E. (2021). Immature Control of Breathing and Apnea of Prematurity: the Known and Unknown. *J. Perinatol*. doi:10.1038/s41372-021-01010-z

European Medicines Agency (2009). *Peyona (previously Nymusa)*. Available at: https://www.ema.europa.eu/en/medicines/human/EPAR/peyona-previously-nymusa (Accessed January 10, 2021)

Falcão, A. C., de Gatta, M. M. F., Iribarnegaray, M. F. D., Buelga, D. S., García, M. J., Dominguez-Gil, A., et al. (1997). Population Pharmacokinetics of Caffeine in Premature Neonates. *Eur. J. Clin. Pharmacol.* 52 (3), 211–217. doi:10.1007/s002280050276

Firman, B., Molnar, A., and Gray, P. H. (2019). Early High-dose Caffeine Citrate for Extremely Preterm Infants: Neonatal and Neurodevelopmental Outcomes. *J. Paediatr. Child. Health* 55 (12), 1451–1457. doi:10.1111/jpc.14446

Francart, S. J., Allen, M. K., and Stegall-Zanation, J. (2013). Apnea of Prematurity: Caffeine Dose Optimization. *J. Pediatr. Pharmacol. Ther.* 18 (1), 45–52. doi:10.5863/1551-6776-18.1.45

Gal, P. (2007). Caffeine Therapeutic Drug Monitoring Is Necessary and Cost-Effective. *J. Pediatr. Pharmacol. Ther.* 12 (4), 212–215. doi:10.5863/1551-6776-12.4.212

Gal, P. (2009). Optimum Use of Therapeutic Drug Monitoring and Pharmacokinetics-Pharmacodynamics in the NICU. *J. Pediatr. Pharmacol. Ther.* 14 (2), 66–74. doi:10.5863/1551-6776-14.2.66

Gao, X. B., Zheng, Y., Yang, F., Wang, C. H., Jiang, Z. H., Wu, Y. E., Jacqz-Aigrain, E., et al. (2020). Developmental Population Pharmacokinetics of Caffeine in Chinese Premature Infants With Apnoea of Prematurity: A post-marketing Study to Support Paediatric Labelling in China. *Br. J. Clin. Pharmacol.*

Gentle, S. J., Travers, C. P., and Carlo, W. A. (2018). Caffeine Controversies. *Curr. Opin. Pediatr.* 30 (2), 177–181. doi:10.1097/mop.0000000000000588

Gorodischer, R., and Karplus, M. (1982). Pharmacokinetic Aspects of Caffeine in Premature Infants With Apnoea. *Eur. J. Clin. Pharmacol.* 22 (1), 47–52. doi:10.1007/bf00606424

Gray, P. H., Flenady, V. J., Charles, B. G., Steer, P. A., and Caffeine Collaborative Study, G. (2011). Caffeine Citrate for Very Preterm Infants: Effects on Development, Temperament and Behaviour. *J. Paediatr. Child. Health* 47 (4), 167–172. doi:10.1111/j.1440-1754.2010.01943.x

Gu, L., Gonzalez, F. J., Kalow, W., and Tang, B. K. (1992). Biotransformation of Caffeine, Paraxanthine, Theobromine and Theophylline by cDNA-Expressed Human CYP1A2 and CYP2E1. *Pharmacogenetics* 2 (2), 73–77. doi:10.1097/00008571-199204000-00004

Guo, A., Zhu, Z., Xue, J., Di, X., Fan, J., Huang, L., et al. (2020). Population Pharmacokinetic Study of Caffeine Citrate in Chinese Premature Infants With Apnea. *J. Clin. Pharm. Ther.* 45 (6), 1414–1421. doi:10.1111/jcpt.13240

He, X., Qiu, J. C., Lu, K. Y., Guo, H. L., Li, L., Jia, W. W., et al. (2020). Therapy for Apnoea of Prematurity: A Retrospective Study on Effects of Standard Dose and Genetic Variability on Clinical Response to Caffeine Citrate in Chinese Preterm Infants. *Adv. Ther.* 38 (1), 607–626. doi:10.1007/s12325-020-01544-2

Horne, R. S. C., Fung, A. C. H., NcNeil, S., Fyfe, K. L., Odoi, A., and Wong, F. Y. (2017). The Longitudinal Effects of Persistent Apnea on Cerebral Oxygenation in Infants Born Preterm. *J. Pediatr.* 182, 79–84. doi:10.1016/j.jpeds.2016.11.081

Janvier, A., Khairy, M., Kokkotis, A., Cormier, C., Messmer, D., and Barrington, K. J. (2004). Apnea Is Associated with Neurodevelopmental Impairment in Very Low Birth Weight Infants. *J. Perinatol* 24 (12), 763–768. doi:10.1038/sj.jp.7211182

Kahn, D. J., and Godin, R. (2016). Is it Time to Embrace the Caffeine Level? *Pediatrics* 137 (5), e20160403A. doi:10.1542/peds.2016-0403a

Kearns, G. L., Abdel-Rahman, S. M., Alander, S. W., Blowey, D. L., Leeder, J. S., and Kauffman, R. E. (2003). Developmental Pharmacology - Drug Disposition, Action, and Therapy in Infants and Children. *N. Engl. J. Med.* 349 (12), 1157–1167. doi:10.1056/nejmra035092

Koch, G., Datta, A. N., Jost, K., Schulzke, S. M., van den Anker, J., and Pfister, M. (2017). Caffeine Citrate Dosing Adjustments to Assure Stable Caffeine Concentrations in Preterm Neonates. *J. Pediatr.* 191, 50–56. doi:10.1016/j.jpeds.2017.08.064

Kumar, V. H. S., and Lipshultz, S. E. (2019). Caffeine and Clinical Outcomes in Premature Neonates. *Children (Basel)* 6 (11), 118. doi:10.3390/children6110118

Kumral, A., Tuzun, F., Yesilirmak, D. C., Duman, N., and Ozkan, H. (2012). Genetic Basis of Apnoea of Prematurity and Caffeine Treatment Response: Role of Adenosine Receptor Polymorphisms. *Acta Paediatr.* 101 (7), e299–e303. doi:10.1111/j.1651-2227.2012.02664.x

Lee, T. C., Charles, B., Steer, P., Flenady, V., and Shearman, A. (1997). Population Pharmacokinetics of Intravenous Caffeine in Neonates with Apnea of Prematurity*. *Clin. Pharmacol. Ther.* 61 (6), 628–640. doi:10.1016/s0009-9236(97)90097-7

Lee, H. S., Khoo, Y. M., Chirino-Barcelo, Y., Tan, K. L., and Ong, D. (2002). Caffeine in Apnoeic Asian Neonates: a Sparse Data Analysis. *Br. J. Clin. Pharmacol.* 54 (1), 31–37. doi:10.1046/j.1365-2125.2002.01589.x

Lelo, A., Birkett, D., Robson, R., and Miners, J. (1986). Comparative Pharmacokinetics of Caffeine and its Primary Demethylated Metabolites Paraxanthine, Theobromine and Theophylline in Man. *Br. J. Clin. Pharmacol.* 22 (2), 177–182. doi:10.1111/j.1365-2125.1986.tb05246.x

Leon, A. E., Michienzi, K., Ma, C. X., and Hutchison, A. A. (2007). Serum Caffeine Concentrations in Preterm Neonates. *Am. J. Perinatol* 24 (1), 39–47. doi:10.1055/s-2006-958163

Lodha, A., Seshia, M., McMillan, D. D., Barrington, K., Yang, J., Lee, S. K., et al. (2015). Association of Early Caffeine Administration and Neonatal Outcomes in Very Preterm Neonates. *JAMA Pediatr.* 169 (1), 33–38. doi:10.1001/jamapediatrics.2014.2223

Martin, R. J., Wang, K., Köroğlu, Ö., Di Fiore, J., and Kc, P. (2011). Intermittent Hypoxic Episodes in Preterm Infants: Do They Matter? *Neonatology* 100 (3), 303–310. doi:10.1159/000329922

McLellan, T. M., Caldwell, J. A., and Lieberman, H. R. (2016). A Review of Caffeine's Effects on Cognitive, Physical and Occupational Performance. *Neurosci. Biobehav. Rev.* 71, 294–312. doi:10.1016/j.neubiorev.2016.09.001

McPherson, C., Neil, J. J., Tjoeng, T. H., Pineda, R., and Inder, T. E. (2015). A Pilot Randomized Trial of High-Dose Caffeine Therapy in Preterm Infants. *Pediatr. Res.* 78 (2), 198–204. doi:10.1038/pr.2015.72

Mohammed, S., Nour, I., Shabaan, A. E., Shouman, B., Abdel-Hady, H., and Nasef, N. (2015). High versus Low-Dose Caffeine for Apnea of Prematurity: a Randomized Controlled Trial. *Eur. J. Pediatr.* 174 (7), 949–956. doi:10.1007/s00431-015-2494-8

Mokhtar, W. A., Fawzy, A., Allam, R. M., Zidan, N., and Hamed, M. S. (2018). Association between Adenosine Receptor Gene Polymorphism and Response to Caffeine Citrate Treatment in Apnea of Prematurity; an Egyptian Single-Center Study. *Egypt. Pediatr. Assoc. Gaz.* 66 (4), 115–120. doi:10.1016/j.epag.2018.09.001

Moschino, L., Zivanovic, S., Hartley, C., Trevisanuto, D., Baraldi, E., and Roehr, C. C. (2020). Caffeine in Preterm Infants: Where Are We in 2020? *ERJ Open Res.* 6 (1), 00330–2019. doi:10.1183/23120541.00330-2019

Murat, I., Moriette, G., Blin, M. C., Couchard, M., Flouvat, B., De Gamarra, E., et al. (1981). The Efficacy of Caffeine in the Treatment of Recurrent Idiopathic Apnea in Premature Infants. *J. Pediatr.* 99 (6), 984–989. doi:10.1016/s0022-3476(81)80038-8

Murner-Lavanchy, I. M., Doyle, L. W., Schmidt, B., Roberts, R. S., Asztalos, E. V., Costantini, B., et al. (2018). Neurobehavioral Outcomes 11 Years after Neonatal Caffeine Therapy for Apnea of Prematurity. *Pediatrics* 141 (5), e20174047. doi:10.1542/peds.2017-4047

Natarajan, G., Botica, M.-L., Thomas, R., and Aranda, J. V. (2007). Therapeutic Drug Monitoring for Caffeine in Preterm Neonates: an Unnecessary Exercise? *Pediatrics* 119 (5), 936–940. doi:10.1542/peds.2006-2986

Natarajan, G., Lulic-Botica, M., and Aranda, J. V. (2007). Pharmacology Review: Clinical Pharmacology of Caffeine in the Newborn. *NeoReviews* 8 (5), e214–e221. doi:10.1542/neo.8-5-e214

NDA 20-793/S-001 (2000). *NDA 20-793/S-001*. Available at: https://www.accessdata.fda.gov/drugsatfda_docs/label/2000/20793s1lbl.pdf (Accessed January 10, 2021).

NICE (2019). Specialist Neonatal Respiratory Care for Babies Born Preterm. Available at: https://www.nice.org.uk/guidance/ng124/chapter/Recommendations (Accessed December 20, 2020).

Pakvasa, M. A., Saroha, V., and Patel, R. M. (2018). Optimizing Caffeine Use and Risk of Bronchopulmonary Dysplasia in Preterm Infants. *Clin. Perinatology* 45 (2), 273–291. doi:10.1016/j.clp.2018.01.012

Patel, P., Mulla, H., Kairamkonda, V., Spooner, N., Gade, S., Della Pasqua, O., et al. (2013). Dried Blood Spots and Sparse Sampling: a Practical Approach to Estimating Pharmacokinetic Parameters of Caffeine in Preterm Infants. *Br. J. Clin. Pharmacol.* 75 (3), 805–813. doi:10.1111/j.1365-2125.2012.04392.x

Pearlman, S. A., Duran S., C., Wood, M. A., Maisels, M. J., and Berlin, Jr., C. M., Jr (1989). Caffeine Pharmacokinetics in Preterm Infants Older Than 2 Weeks. *Dev. Pharmacol. Ther.* 12 (2), 65–69. doi:10.1159/000480966

Perrin, C., Debruyne, D., Lacotte, J., Laloum, D., Bonte, J.-B., and Moulin, M. (1987). Treatment of Caffeine Intoxication by Exchange Transfusion in a Newborn. *Acta Paediatr.* 76 (4), 679–681. doi:10.1111/j.1651-2227.1987.tb10546.x

Pons, G., Carrier, O., Richard, M.-O., Rey, E., d'Athis, P., Moran, C., et al. (1988). Developmental Changes of Caffeine Elimination in Infancy. *Dev. Pharmacol. Ther.* 11 (5), 258–264. doi:10.1159/000457700

Pons, G., Rey, E., Carrier, O., Richard, M. O., Moran, C., Badoual, J., et al. (1989). Maturation of AFMU Excretion in Infants. *Fundam. Clin. Pharmacol.* 3 (6), 589–595. doi:10.1111/j.1472-8206.1989.tb00461.x

Ravichandran, S., Chouthai, N. S., Patel, B., Sharma, A., Gupte, A., Ma, M. M., et al. (2019). Higher Daily Doses of Caffeine Lowered the Incidence of Moderate to Severe Neurodevelopmental Disabilities in Very Low Birth Weight Infants. *Acta Paediatr.* 108 (3), 430–435. doi:10.1111/apa.14465

Rogers, P. J., Hohoff, C., Heatherley, S. V., Mullings, E. L., Maxfield, P. J., Evershed, R. P., et al. (2010). Association of the Anxiogenic and Alerting Effects of Caffeine with ADORA2A and ADORA1 Polymorphisms and Habitual Level of Caffeine Consumption. *Neuropsychopharmacol* 35 (9), 1973–1983. doi:10.1038/npp.2010.71

Romagnoli, C., De Carolis, M. P., Muzii, U., Zecca, E., Tortorolo, G., Chiarotti, M., et al. (1992). Effectiveness and Side Effects of Two Different Doses of Caffeine in Preventing Apnea in Premature Infants. *Ther. Drug Monit.* 14 (1), 14–19. doi:10.1097/00007691-199202000-00003

Salem, F., Johnson, T. N., Abduljalil, K., Tucker, G. T., and Rostami-Hodjegan, A. (2014). A Re-evaluation and Validation of Ontogeny Functions for Cytochrome P450 1A2 and 3A4 Based on *In Vivo* Data. *Clin. Pharmacokinet.* 53 (7), 625–636. doi:10.1007/s40262-014-0140-7

Saroha, V., and Patel, R. M. (2020). Caffeine for Preterm Infants: Fixed Standard Dose, Adjustments for Age or High Dose? *Semin. Fetal Neonatal Med.* 25, 101178. doi:10.1016/j.siny.2020.101178

Scanlon, J. E., Chin, K. C., Morgan, M. E., Durbin, G. M., Hale, K. A., and Brown, S. S. (1992). Caffeine or Theophylline for Neonatal Apnoea? *Arch. Dis. Child.* 67 (4 Spec No), 425–428. doi:10.1136/adc.67.4_spec_no.425

Schmid, M. B., Hopfner, R. J., Lenhof, S., Hummler, H. D., and Fuchs, H. (2015). Cerebral Oxygenation during Intermittent Hypoxemia and Bradycardia in Preterm Infants. *Neonatology* 107 (2), 137–146. doi:10.1159/000368294

Schmidt, B., Roberts, R. S., Davis, P., Doyle, L. W., Barrington, K. J., Ohlsson, A., et al. (2006). Caffeine Therapy for Apnea of Prematurity. *N. Engl. J. Med.* 354 (20), 2112–2121. doi:10.1056/nejmoa054065

Schmidt, B., Roberts, R. S., Davis, P., Doyle, L. W., Barrington, K. J., Ohlsson, A., et al. (2007). Long-term Effects of Caffeine Therapy for Apnea of Prematurity. *N. Engl. J. Med.* 357 (19), 1893–1902. doi:10.1056/nejmoa073679

Schmidt, B., Anderson, P. J., Doyle, L. W., Dewey, D., Grunau, R. E., Asztalos, E. V., et al. (2012). Survival without Disability to Age 5 Years after Neonatal Caffeine Therapy for Apnea of Prematurity. *JAMA* 307 (3), 275–282. doi:10.1001/jama.2011.2024

Schmidt, B., Roberts, R. S., Anderson, P. J., Asztalos, E. V., Costantini, L., Davis, P. G., et al. (2017). Academic Performance, Motor Function, and Behavior 11 Years after Neonatal Caffeine Citrate Therapy for Apnea of Prematurity. *JAMA Pediatr.* 171 (6), 564–572. doi:10.1001/jamapediatrics.2017.0238

Schmidt, B., Anderson, P. J., Asztalos, E. V., Doyle, L. W., Grunau, R. E., Moddemann, D., et al. (2019). Self-reported Quality of Life at Middle School Age in Survivors of Very Preterm Birth. *JAMA Pediatr.* 173 (5), 487–489. doi:10.1001/jamapediatrics.2018.4853

Shrestha, B., and Jawa, G. (2017). Caffeine Citrate - Is it a Silver Bullet in Neonatology? *Pediatr. Neonatal.* 58 (5), 391–397. doi:10.1016/j.pedneo.2016.10.003

Song, G., Sun, X., Hines, R. N., McCarver, D. G., Lake, B. G., Osimitz, T. G., et al. (2017). Determination of Human Hepatic CYP2C8 and CYP1A2 Age-dependent Expression to Support Human Health Risk Assessment for Early Ages. *Drug Metab. Dispos* 45 (5), 468–475. doi:10.1124/dmd.116.074583

Sonnier, M., and Cresteil, T. (1998). Delayed Ontogenesis of CYP1A2 in the Human Liver. *Eur. J. Biochem.* 251 (3), 893–898. doi:10.1046/j.1432-1327.1998.2510893.x

Steer, P., Flenady, V., Shearman, A., Lee, T., Tudehope, D., and Charles, B. (2003). Periextubation Caffeine in Preterm Neonates: a Randomized Dose Response Trial. *J. Paediatr. Child. Health* 39 (7), 511–515. doi:10.1046/j.1440-1754.2003.00207.x

Steer, P., Flenady, V., Shearman, A., Charles, B., Gray, P. H., Henderson-Smart, D., et al. (2004). High Dose Caffeine Citrate for Extubation of Preterm Infants: a Randomised Controlled Trial. *Arch. Dis. Child. - Fetal Neonatal Ed.* 89 (6), F499–F503. doi:10.1136/adc.2002.023432

Tamim, H., Khogali, M., Beydoun, H., Melki, I., Yunis, K., and National Collaborative Perinatal Neonatal, N. (2003). Consanguinity and Apnea of Prematurity. *Am. J. Epidemiol.* 158 (10), 942–946. doi:10.1093/aje/kwg226

Tanaka, H., Nakazawa, K., Arima, M., and Iwasaki, S. (1984). Caffeine and its Dimethylxanthines and Fetal Cerebral Development in Rat. *Brain Develop.* 6 (4), 355–361. doi:10.1016/s0387-7604(84)80111-4

Thomson, A. H., Kerr, S., and Wright, S. (1996). Population Pharmacokinetics of Caffeine in Neonates and Young Infants. *Ther. Drug Monit.* 18 (3), 245–253. doi:10.1097/00007691-199606000-00005

Thorn, C. F., Aklillu, E., McDonagh, E. M., Klein, T. E., and Altman, R. B. (2012). PharmGKB Summary. *Pharmacogenet Genomics* 22 (5), 389–395. doi:10.1097/fpc.0b013e3283505d5e

Turmen, T., Louridas, T. A., and Aranda, J. V. (1979). Relationship of Plasma and CSF Concentrations of Caffeine in Neonates With Apnea. *J. Pediatr.* 95 (4), 644–646. doi:10.1016/s0022-3476(79)80788-x

Verscheijden, L. F. M., Koenderink, J. B., Johnson, T. N., de Wildt, S. N., and Russel, F. G. M. (2020). Physiologically-based Pharmacokinetic Models for Children: Starting to Reach Maturation? *Pharmacol. Ther.* 211, 107541. doi:10.1016/j.pharmthera.2020.107541

Vesoulis, Z. A., McPherson, C., Neil, J. J., Mathur, A. M., and Inder, T. E. (2016). Early High-Dose Caffeine Increases Seizure Burden in Extremely Preterm Neonates: A Preliminary Study. *J. Caffeine Res.* 6 (3), 101–107. doi:10.1089/jcr.2016.0012

Vliegenthart, R., Miedema, M., Hutten, G. J., van Kaam, A. H., and Onland, W. (2018). High versus standard dose caffeine for apnoea: a systematic review. *Arch Dis Child. Fetal Neonatal Ed* 103 (6), F523–F529. doi:10.1136/archdischild-2017-313556

Wan, L, Huang, L, and Chen, P (2020). Caffeine Citrate Maintenance Doses Effect on Extubation and Apnea Postventilation in Preterm Infants. *Pediatr Pulmonol.* 55, 2635–2640. doi:10.1002/ppul.24948

Yu, T, Balch, AH, Ward, RM, Korgenski, EK, and Sherwin, CM (2016). Incorporating Pharmacodynamic Considerations into Caffeine Therapeutic Drug Monitoring in Preterm Neonates. *BMC Pharmacol Toxicol* 17 (1), 22. doi:10.1186/s40360-016-0065-x

Zhang, X, Zhang, HT, Lyu, Y, Wang, LF, and Yang, ZY (2019). [Clinical effect and safety of different maintenance doses of caffeine citrate in treatment of apnea in Very Low Birth Weight Preterm Infants: a Prospective Randomized Controlled Trial]. *Zhongguo Dang Dai Er Ke Za Zhi* 21 (6), 558–561.

Zhao, Y., Tian, X., and Liu, G. (2016). [Clinical Effectiveness of Different Doses of Caffeine for Primary Apnea in Preterm Infants]. *Zhonghua Er Ke Za Zhi* 54 (1), 33–36. doi:10.3760/cma.j.issn.0578-1310.2016.01.008

Conflict of Interest: The authors declare that the research was conducted in the absence of any commercial or financial relationships that could be construed as a potential conflict of interest.

Publisher's Note: All claims expressed in this article are solely those of the authors and do not necessarily represent those of their affiliated organizations, or those of the publisher, the editors and the reviewers. Any product that may be evaluated in this article, or claim that may be made by its manufacturer, is not guaranteed or endorsed by the publisher.

frontiers in Pharmacology

ORIGINAL RESEARCH
published: 13 August 2021
doi: 10.3389/fphar.2021.709332

Population Pharmacokinetics of Vancomycin and Meropenem in Pediatric Extracorporeal Membrane Oxygenation Support

Brenda Zylbersztajn[1], Suzanne Parker[2], Daniel Navea[3], Giannina Izquierdo[4], Paula Ortiz[5], Juan Pablo Torres[4], Cristian Fajardo[6], Rodrigo Diaz[6], Cristian Valverde[1] and Jason Roberts[2,7,8,9]*

[1]Pediatric Intensive Care Unit, Clinica Las Condes, Santiago, Chile, [2]UQ Centre for Clinical Research, The University of Queensland, Brisbane, QLD, Australia, [3]Laboratory, Clinica Las Condes, Santiago, Chile, [4]Department of Infectious Disease, Clinica Las Condes, Santiago, Chile, [5]Pediatric Intensive Care Unit, Roberto Del Rio Hospital, Santiago Chile, [6]Intensive Care Unit, Clinica Las Condes, Santiago, Chile, [7]Department of Intensive Care Medicine, Royal Brisbane & Women's Hospital, Brisbane, QLD, Australia, [8]Division of Anaesthesiology Critical Care Emergency and Pain Medicine, Nîmes University Hospital, University of Montpellier, Nîmes, France, [9]Department of Pharmacy, Royal Brisbane & Women's Hospital, Brisbane, QLD, Australia

OPEN ACCESS

Edited by:
Raffaele Simeoli,
Bambino Gesù Children's Hospital (IRCCS), Italy

Reviewed by:
Gail Mary Annich,
Hospital for Sick Children, Canada
Georg Hempel,
University of Münster, Germany

***Correspondence:**
Brenda Zylbersztajn
bzylbersztajn@clc.cl

Specialty section:
This article was submitted to Obstetric and Pediatric Pharmacology, a section of the journal Frontiers in Pharmacology

Received: 13 May 2021
Accepted: 04 August 2021
Published: 13 August 2021

Citation:
Zylbersztajn B, Parker S, Navea D, Izquierdo G, Ortiz P, Torres JP, Fajardo C, Diaz R, Valverde C and Roberts J (2021) Population Pharmacokinetics of Vancomycin and Meropenem in Pediatric Extracorporeal Membrane Oxygenation Support. Front. Pharmacol. 12:709332. doi: 10.3389/fphar.2021.709332

Objective: Describe primary pharmacokinetic/pharmacodynamic (PK/PD) parameters of vancomycin and meropenem in pediatric patients undergoing ECMO and analyze utilized dosing to reach PK/PD target.

Design: Prospective, multicentric, population PK analysis.

Setting: Two hospitals with pediatric intensive care unit.

Patients: Pediatric patients (1 month - 15 years old) receiving vancomycin and meropenem for empiric or definitive infection treatment while ECMO support.

Measurements and Main Results: Four serum concentration were obtained for patients receiving vancomycin (n = 9) and three for meropenem (n = 9). The PK/PD target for vancomycin was a ratio of the area under the curve to the minimal inhibitory concentration (AUC/MIC) of >400, and for meropenem was 4 times above MIC for 50% of the dosing interval ($fT_{50\%}$ > 4xMIC). Pharmacokinetic modeling was performed using PMetrics 1.5.0. We included nine patients, with 11 PK profiles for each antimicrobial. The median age of patients was 4 years old (2 months - 13 years) and 45% were male. Creatinine clearance (CL) was 183 (30–550) ml/min/1.73 m^2. The median dose was 13.6 (range 10–15) mg/kg every 6–12 h and 40 mg/kg every 8–12 h for vancomycin and meropenem, respectively. Two compartment models were fitted. Weight was included as a covariate on volume of the central compartment (Vc) for meropenem. Weight was included as a covariate on both Vc and clearance (CL) and serum creatinine was also included as a covariate on CL for vancomycin. The pharmacokinetic parameters CL and Vc were 0.139 ± 0.102 L/h/kg and 0.289 ± 0.295 L/kg for meropenem and 0.060 ± 0.055 L/h/kg and 0.419 ± 0.280 L/kg for vancomycin, respectively. Across each dosing interval 91% of patients achieved the PK/PD targets for adequate exposure for meropenem and 63.6% for vancomycin.

Conclusion: Pharmacokinetic/pharmacodynamic objectives for vancomycin were achieved partially with conventional doses and higher dosing with extended infusion were needed in the case of meropenem.

Keywords: vancomycin, meropenem, pediatric, extracorporeal membrane oxygenation, pharmacokinetic, pharmacodynamic

INTRODUCTION

Extracorporeal membrane oxygenation (ECMO) allows respiratory or cardiac support for critically ill patients (Fraser et al., 2012). ECMO is not considered a treatment cure, although it sustains life while the underlying pathology is being managed. It also provides a bridge to heart or lung transplantation or full organ recovery (Abdul-Aziz et al., 2019).

Patients on ECMO are critically ill and receive multiple drugs; therefore, understanding the pharmacokinetic (PK) alterations that occur on ECMO is crucial. Different anti-infective drugs are frequently used in patients on ECMO because multiple intravenous devices and long intensive care unit (ICU) stay (Sherwin et al., 2016).

Vancomycin is a frequently used first-line antibiotic for treating infections caused by methicillin-resistant *Staphylococcus aureus* or other Gram-positive suceptible bacteria (Rybak et al., 2009). The pharmacokinetic/pharmacodynamic (PK/PD) target that best predicts the efficacy of vancomycin is the ratio of the area under the curve to the minimal inhibitory concentration (AUC/MIC) (Liu et al., 2011). Previous vancomycin PK reported data in newborn on ECMO have shown an increased volume of distribution (Vd) and decreased clearance (CL) (Buck, 1998), but conclusions could not be extrapolated to pediatric patients because organ development and physiological factors affects drug's PK in newborns (Lu and Rosenbaum, 2014).

Meropenem is a carbapenem antibiotic widely used as first-line therapy for infections caused by nosocomial Gram-negative bacilli such as extended-spectrum β-lactamase (ESBL) - producing Enterobacteriaceae. Meropenem is a time-dependent antibiotic and there PK/PD target is the time that free drug concentrations remain above the minimum inhibitory concentration (MIC) at the site of infection (fT % >MIC). To ensure a bactericidal effect, free drug concentration should be about 4 to 6 times the MIC, at least 40% of the dosing interval (Cies et al., 2015). Recent data showed that prolonged or continuous infusion of meropenem can achieve a higher fT > MIC and might be associated with improved microbiological outcomes (Drusano, 2003; Tam et al., 2003; Drusano, 2004; Lodise et al., 2006; Cies et al., 2015; Kongthavonsakul et al., 2016; Rapp et al., 2020).

Most of the meropenem PK data from children are limited to healthy volunteers or non ICU patients. The available pharmacokinetic data for pediatric ICU patients demonstrates greater CL and Vd (Cies et al., 2017). There are scarce data describing the impact of ECMO on the pharmacokinetics and dosing requirements of meropenem in critically ill pediatric patients, and most of this data is derived from case reports (Cies et al., 2014; Cies et al., 2016; Saito et al., 2020).

Currently, there are no guidelines on antimicrobial dosing for pediatric patients undergoing ECMO. Dosing regimens are based on recommendations for critically ill pediatric patients, data from adults or newborns and considerations of physicochemical characteristics, plasma concentrations of different drugs and clinical outcomes (Zylbersztajn et al., 2018). The aim of this study was to describe the population pharmacokinetics of vancomycin and meropenem in pediatric patients undergoing ECMO, as well as the achievement of therapeutic exposures with currently used dosing regimens.

MATERIALS AND METHODS

This study was a prospective, multicentric, PK/PD study. It included pediatric patients who were admitted to the pediatric ICU between July 2017 and November 2019 at two hospitals in Santiago, Chile. The Ethical Committee for Research of Clinica Las Condes approved this prospective study (approval number: M012017) and required signed written informed consent from each patient's parents. Patients younger than 15 years of age requiring ECMO and antimicrobial treatment with vancomycin and or meropenem for suspected or confirmed infection were included. Neonates were excluded.

Meropenem was administered as a 3-h infusion with intravenous doses of 20–40 mg/kg every 8 or 12 h. Vancomycin was administered as a 2-h infusion at 10–15 mg/kg intravenously every 6 or 12 h. Both antibiotics' doses were adjusted according to renal function. Blood samples were collected at 1 and 3 h post-infusion and before

TABLE 1 | Patient characteristics.

	Vancomycin	Meropenem
Female (n)	6	5
Male (n)	3	4
ECMO PK profiles (n)	11	11
ECMO VA (n)	5	5
ECMO VV (n)	4	4
Oxygenator	polymethylpentene, phosphorylcholine coating	
CRRT (n)	2	4
Empiric treatment	8	6
Pneumonia	7	6
Endocarditis	1	1
Refractory septic shock	1	2

Number (n); extracorporeal membrane oxygenation (ECMO); pharmacokinetic (PK); veno-venous (VV); veno-arterial (VA); continuous renal replacement therapy (CRRT).

TABLE 2 | Patient characteristics.

	Vancomycin			Meropenem		
Characteristic	**Mean**	**Median**	**Range**	**Mean**	**Median**	**Range**
Age (months)	50.4	24	2–132	68.3	48	2–165
Weight (kg)	15.5	10	3.5–37	20.4	16	3.5–45
Height (cm)	92.7	82	50–140	103	100	50–155
Serum creatinine (mg/dl)	0.34	0.22	0.08–1.23	0.41	0.3	0.08–1.27
Serum albumin (g/L)	3.8	3.55	2.8–5.4	3.6	3.5	2.6–5.4
Total bilirubin (mg/dl)	3.5	0.86	0.31–30.1	3.7	0.95	0.41–30.1
C-reactive protein (mg/L)	60.1	47	1.2–248	90.4	57.5	1.2–423
24 h hydric fluid balance (ml)	56.4	37.5	-1,203 – 1,220	-79.2	4.5	-2,615 – 1,170

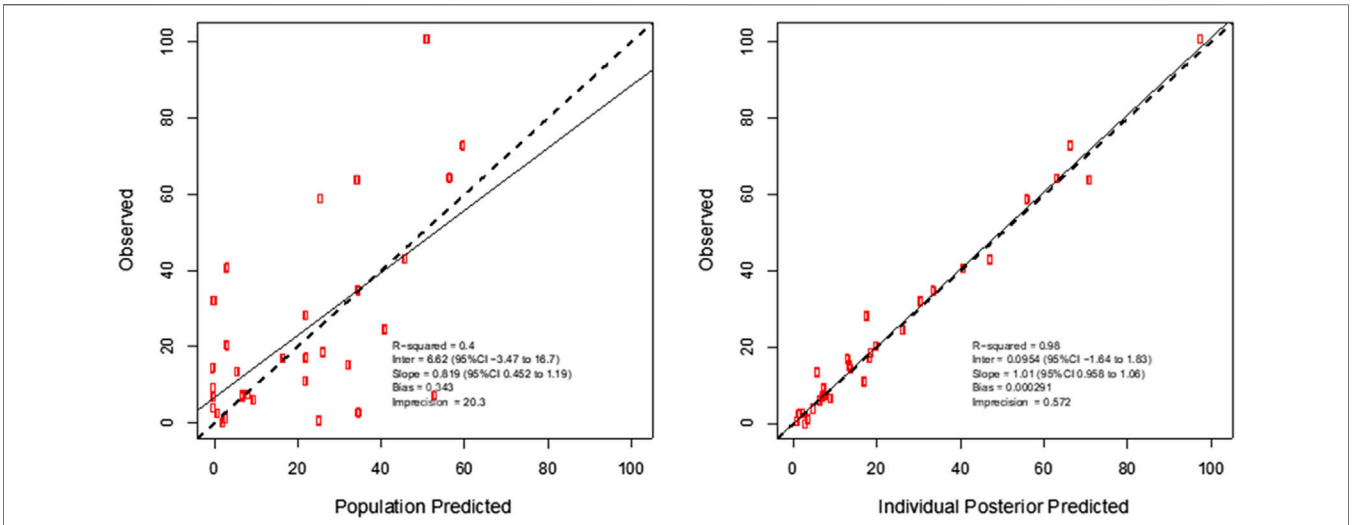

FIGURE 1 | Individual predicted concentration diagnostic plots for the final covariate model for plasma meropenem concentrations. Data are presented in mg/L.

the following dose for meropenem. For vancomycin, blood samples were collected at 0.5, 1, and 2 h post-infusion and before the following dose. Samples were collected under steady state conditions: 24 h for meropenem and 48 h for vancomycin from the beginning of the treatment.

Unbound vancomycin plasma concentration were determined by an immunoenzymatic assay (Cobas c 311, Roche, Japan) with a precision of 2.4%, accuracy of 1.8% and lower limit of quantification (LLOQD) of 1.7 mcg/mL. Unbound meropenem plasma concentrations were determined by high-performance liquid chromatography (Agilent Infinity 1,260, Santa Clara, United States) with a UV detector. The methodology was adapted to the equipment conditions from available publications (Elkhaïli et al., 1996; McWhinney et al., 2010; Wolff et al., 2013) and validated according to the recommendations of the Bioanalytical Method Validation Guidance for Industry (U.S. Department of Health and Human Services, 2018). The stationary phase was a Zorbax Eclipse Plus C18 column (3.5 µm, 75 × 4.6 mm) and the mobile phase was acetonitrile with 10 mM ammonium acetate (pH 4.0) (5:95, organic solvent:buffer initiallity) in gradient to minute 7(50:50, organic solvent:buffer). Meropenem was detected by UV detection at 298 nm. The flow rate was 1.0 ml/min. The retention time of meropenem was 3.5 min. Standard curves were prepared in blank human plasma. The standard curve was linear between 0.2 ug/mL and 100 ug/mL. Meropenem in plasma samples was quantified using the peak area of standard samples for calibrations. The precision of the methodology was 0.6% and accuracy was 0.5%. The lower limit of quantification (LLOQD) for meropenem was determined by replicate of 10 matrix blank samples, determining the standard deviation (SD) of the response obtained, the result was expressed as 10 times the SD obtained, reported as 0.16 ug/mL.

For both analytes, the measurement was performed on the free-drug, non-protein bound fraction. In the case of vancomycin through a specific colorimetric reaction and meropenem through the extraction of the free-drug fraction by organic solvent and subsequent purification of the sample.

Model Development

Pharmacokinetic modelling was performed using PMetrics 1.5.0 with RStudio 0.99.902 and digital compiler Gfortran 5.2. We

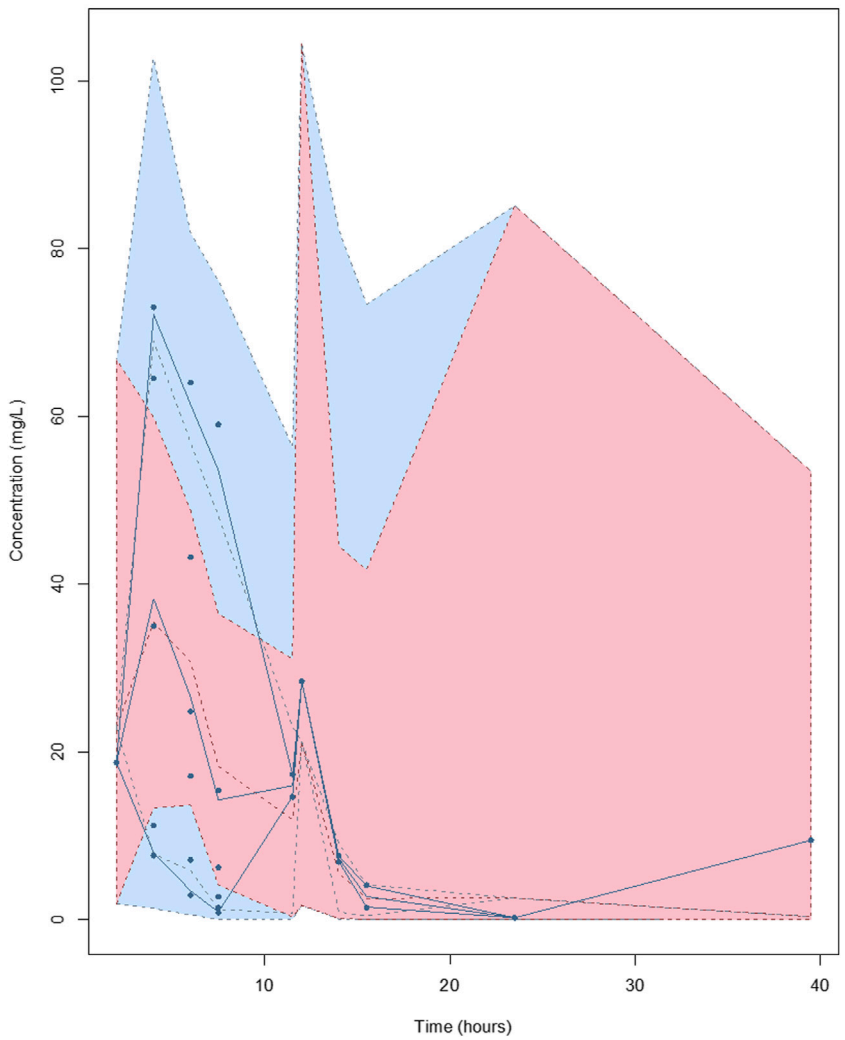

FIGURE 2 | Visual predictive checks of the final covariate model for meropenem. The lines represent the percentiles of 1,000 simulated meropenem concentration-time profiles superimposed with observed meropenem concentrations (circles). The blue shading around the lines represents the 95% CI around each percentile. The distribution of the simulated concentration profiles is similar to that of the observed concentrations, with all of observed concentrations between 5th and 95th simulated percentiles, respectively, suggesting that the model describes the data adequately.

considered 33 plasma samples for meropenem and 44 plasma samples for vancomycin. For the population pharmacokinetic analysis, one-, two- and three-compartment models were fitted using plasma meropenem and vancomycin concentration data, using non-parametric adaptive grid subroutines from the PMetrics package for R (Los Angeles CA, United States). Primary pharmacokinetic parameters of CL and Vd for the central compartment were calculated. Elimination from the central compartment and inter-compartmental distribution were modelled as first-order processes. Inter-compartmental distribution was described as rate of transfer from the unbound compartment to a peripheral compartment (Kcp) and rate of transfer from a peripheral compartment to the unbound compartment (Kpc). Additive (lambda) and multiplicative (gamma) error models were tested using a polynomial equation for standard deviation as a function of observed concentration, Y. ($SD = C_0 + C_1.Y$), with observation weighting performed as error = SD. gamma or error = $(SD^2+lambda^2)^{0.5}$. Volume of the peripheral compartment (Vp) was calculated as (Vc*Kcp)/Kpc, where Vc is the volume of the central compartment. Total Vd was calculated as the sum of Vc and Vp.

Model Diagnostics

We selected the final model on the basis of minimizing the Akaike Information Criterion (AIC) and likelihood of the nested models (-2*Log-likelihood, -2*LL), with both criteria penalized by the number of parameters in the model. A reduction of -2*LL as

TABLE 3 | Pmetrics model for the final covariate model for meropenem.

```
#Primary variables
CL,0.1.7
V,2,3.5
KCP,0.1.2.8
KPC,0,2.8
#Covariates
WGT
#Secondary variables
Vw = V*(WGT/20.4)
Ke = CL/Vw
#Output equations
Y (1) = X (1)/Vw
#Error model
G = 1
0.2.0.1,0,0
```

*CL, clearance from the central compartment; V, volume of the central compartment (L); Kcp, first-order rate constant for distribution from central to peripheral compartment (h^{-1}); Kpc, first-order rate constant for distribution from peripheral to central compartment (h^{-1}); WGT, total body weight; Vw, typical estimate of volume of the central compartment for a total body weight of 20.4 kg; Ke, first-order elimination rate constant (h^{-1}); Y (1), concentration of drug in the central compartment; Error, each observation is weighted by 1/(Error)^2 using a multiplicative error model (Error = SD*gamma), where SD is the standard deviation of each observation which is modelled by a polynomial equation with coefficients of the assay error specified in the bottom rows for unbound meropenem concentrations and G (gamma) is a value relating to extra process noise related to the observation, such as mis-specified dosing and observation times.*

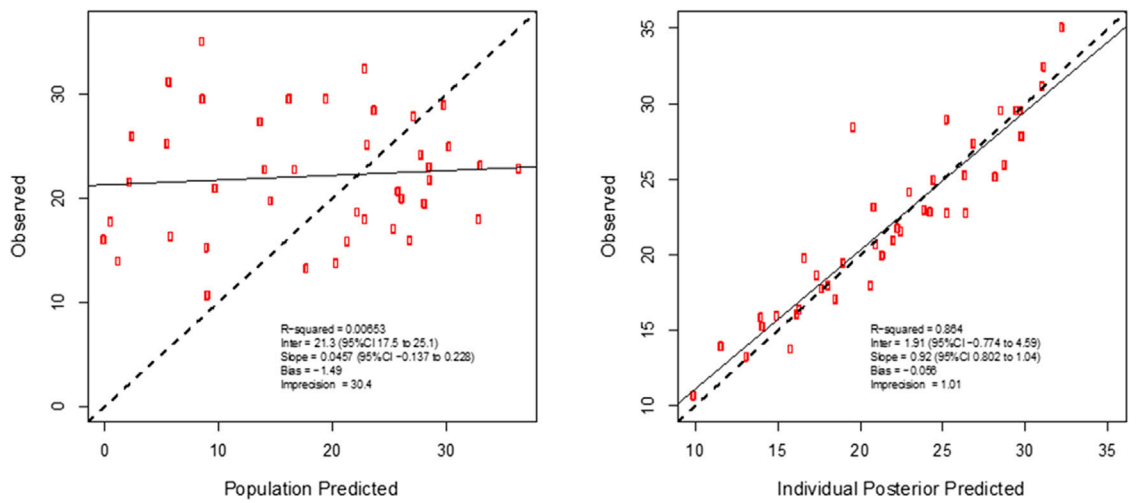

FIGURE 3 | Individual predicted concentration diagnostic plots for the final covariate model for plasma vancomycin concentrations. Data are presented in mg/L.

calculated within Pmetrics was used for statistical comparison of nested models. We also factored bias (mean weighted predicted-observed error) and imprecision (bias-adjusted, mean weighted squared predicted-observed error) and correlation co-efficient into the selection of the final model. Shrinkage was calculated as the percentage of total variance in each model probability distribution.

Covariate Screening

Covariate model building was performed using sequential assessment of biologically plausible clinical characteristics. Continuous data was used for all covariates tested, with the exception of gender, which was male/female. The association of the covariates versus parameters was assessed by regression with linear or non-linear associations able to be used in the covariate model testing with inclusion based upon biological plausibility and a statistically significant improvement in log-likelihood. Inclusion age (months), weight (kg), height (cm), gender, C-reactive protein (mg/L), albumin (g/L), total bilirubin (mg/dl), serum creatinine (mg/dl), 24-h hydric balance (ml).

For the PK/PD target attainment assessment, AUC of vancomycin was calculated using Pmetrics. For meropenem analysis, we used the plasma concentration at 1 h after the end of a 3-h infusion of the drug corresponding to a dosing interval of 50%. The target exposure for vancomycin was an AUC/MIC ratio >400 using the MIC of *Staphylococcus aureus* of 1 mcg/mL, and that for meropenem was plasma concentrations > 4xMIC for at

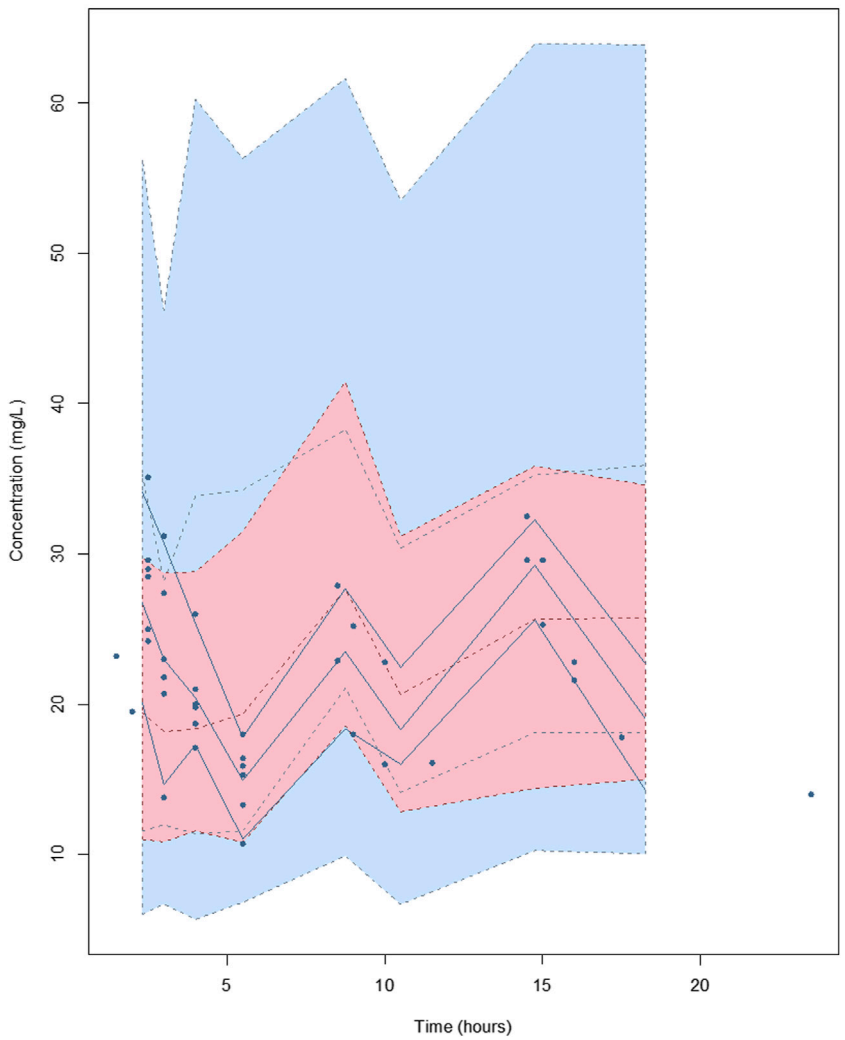

FIGURE 4 | Visual predictive checks of the final covariate model for vancomycin. The lines represent the percentiles of 1,000 simulated vancomycin concentration-time profiles superimposed with observed vancomycin concentrations (circles). The blue shading around the lines represents the 95% CI around each percentile. The distribution of the simulated concentration profiles is similar to that of the observed concentrations, with all of observed concentrations between 5th and 95th simulated percentiles, respectively, suggesting that the model describes the data adequately.

least 50% of the dosing interval, using the MIC of *Pseudomonas aeruginosa* of 2 mcg/mL.

RESULTS

Nine patients were included in the pharmacokinetic modelling. The median age was 4 years old (2 months - 13 years) and 45% of patients were male. The median estimated creatinine clearance was 178 (30–239) ml/min/1.73 m^2. The median doses was 54 (20–60) mg/kg/day in 2–4 divided doses for vancomycin and 120 (60–120) mg/kg/day in 2-3 divided doses for meropenem. Two patients received only vancomycin and two patients received only meropenem. Six patients completed one treatment of meropenem and vancomycin. One patient received meropenem and vancomycin in three different occasions. We performed a total of 11 PK profiles for each antimicrobial. Demographic and clinical characteristics of patients are reported in **Tables 1** and **2**.

For meropenem the inclusion of a second compartment was accepted on the basis of a decrease in the log-likelihood of 10.1. The inclusion of total body weight as a covariate on central volume (Vw; $r^2 = 0.17$) was accepted on the basis of a decrease in log-likelihood of 44.6, as well as improvements to the slope and bias on the observed vs predicted plots. The diagnostic plots to confirm the goodness-of-fit of the final covariate model were considered acceptable and are shown in **Figure 1**. The visual

TABLE 4 | Pmetrics model for the final covariate model for vancomycin.

```
#Primary variables
CL,0.3.0.7
V,2.4.6
Kcp,0.12.1
Kpc,0.01.0.7
#Covariates
WGT
CREA
#Secondary variables
CLw = CL*(wgt/15.5)*(0.56*(0.34/crea))
Vw = V*(wgt/15.5)
Ke = CLw/Vw
#Output equations
Y (1) = X (1)/Vw
#Error model
G = 3
2,1,0,0
```

*CL, clearance from the central compartment; V, volume of the central compartment (L); Kcp, first-order rate constant for distribution from central to peripheral compartment (h^{-1}); Kpc, first-order rate constant for distribution from peripheral to central compartment (h^{-1}); WGT, total body weight; CREA, serum creatine concentration (mg/dl); CLw, typical estimate of clearance from the central compartment for a total body weight of 15.5 kg and serum creatinine of 0.34 mg/dl; Vw, typical estimate of volume of the central compartment for a total body weight of 15.5 kg; Ke, first-order elimination rate constant (h^{-1}); Y (1), concentration of drug in the central compartment; Error, each observation is weighted by 1/(Error)^2 using a multiplicative error model (Error = SD*gamma), where SD is the standard deviation of each observation which is modelled by a polynomial equation with coefficients of the assay error specified in the bottom rows for vancomycin concentrations and G (gamma) is a value relating to extra process noise related to the observation, such as mis-specified dosing and observation times.*

TABLE 5 | Population pharmacokinetic model data of meropenem concentrations of paediatric patients undergoing extracorporeal membrane oxygenation.

PK parameter	Units	Mean	SD	Median	CV%	Shrink%
CL	$L.h^{-1}.\ kg^{-1}$	0.139	0.102	0.144	73.3	2.2
Vc	$L.\ kg^{-1}$	0.289	0.295	0.289	72.0	4.8
Kcp	h^{-1}	1.37	0.992	1.30	72.6	25.2
Kpc	h^{-1}	1.25	0.984	1.34	79.0	20.6
Vp (Vc*kcp/kpc)	$L.\ kg^{-1}$	0.317	0.297			
Vd (vc + vp)	$L.kg^{-1}$	0.606	0.592			

Pharmacokinetic (PK); clearance of meropenem (CL); central volume of distribution of meropenem (Vc); rate of transfer from the central compartment to a peripheral compartment (Kcp); rate of transfer from a peripheral compartment to the central compartment (Kpc); volume of distribution of meropenem (Vd); standard deviation (SD); coefficient of variation (CV%); model shrinkage (Shrink%).

TABLE 6 | Population pharmacokinetic model data of vancomycin concentrations of paediatric patients undergoing extracorporeal membrane oxygenation.

PK parameter	Units	Mean	SD	Median	CV%	Shrink%
CL	$L.h^{-1}.kg^{-1}$	0.060	0.055	0.061	92.2	8.1
Vc	$L.kg^{-1}$	0.419	0.280	0.397	61.0	8.7
Kcp	h^{-1}	0.483	0.304	0.481	63.0	7.0
Kpc	h^{-1}	0.248	0.114	0.286	45.8	13.9
Vp (Vc*kcp/kpc)	$L.h^{-1}$	0.816	0.747			
Vd (vc + vp)	$L.kg^{-1}$	1.235	1.027			

Pharmacokinetic (PK); clearance of vancomycin (CL); central volume of distribution of vancomycin (Vc); rate of transfer from the central compartment to a peripheral compartment (Kcp); rate of transfer from a peripheral compartment to the central compartment (Kpc); volume of distribution of vancomycin (Vd); standard deviation (SD); model shrinkage (Shrink%).

predictive check plot is provided in **Figure 2**. The final model is reported in **Table 3**.

For vancomycin the inclusion of a second compartment was accepted on the basis of a decrease in log-likelihood of 31.0. The inclusion of total body weight as a covariate on central volume (Vw; r^2 = 0.71) was accepted on the basis of a decrease in log-likelihood of 21.3. The inclusion of total body weight and serum creatinine as covariates on clearance (CLw; r^2 = 0.71 and 0.29, respectively) was accepted on the basis of a decrease in log-likelihood of 78.9 and 17.9. The diagnostic plots to confirm the goodness-of-fit of the final covariate model were considered acceptable and are shown in **Figure 3**. The visual predictive check plot is provided in **Figure 4**. The final model is reported in **Table 4**.

There were no plasma concentration below the LLOQD for either antimicrobial. The primary pharmacokinetic parameters are summarized in **Table 5** for meropenem and **Table 6** for vancomycin.

For meropenem, 91% of PK profiles achieved therapeutic exposures based on the PK/PD targets of $fT_{\ 50\%}$ > 4 x MIC and for vancomycin only 63.6% of PK profiles reached AUC/MIC>400. The PK/PD target attainment results are summarized in **Table 7**.

DISCUSSION

To the best of our knowledge, this study is the first to perform pharmacokinetic modelling of meropenem concentrations for paediatric patients receiving ECMO. This study also builds on the current, yet limited knowledge, of vancomycin pharmacokinetics in paediatric patients receiving ECMO.

The main findings of this study are that the meropenem clearance was lower than most reported studies, range ($0.13–1.053\ L.h^{-1}.kg^{-1}$). There is little information available describing the Vd of meropenem in pediatric critically ill patients on ECMO, with meropenem PK data limited to case reports (Cies et al., 2014; Cies et al., 2016; Saito et al., 2020) and

TABLE 7 | Pharmacokinetic/pharmacodynamic results for vancomycin and meropenem.

PK profile	Trough vancomycin (mg/ml)	AUC/MIC vancomycin	Achieved PK/PD target	Cp t50 meropenem	Achieved PK/PD target
1	17.8	558.3	Yes	20.56	Yes
2	12.7	306.8	No	35.00	Yes
3	18.0	543.0	Yes	64.50	Yes
4	16.1	492.8	Yes	40.90	Yes
5	10.7	239.1	No	18.70	Yes
6	13.3	339.6	No	101.00	Yes
7	16.4	547.4	Yes	73.00	Yes
8	15.3	419.7	Yes	11.20	Yes
9	23.6	599.2	Yes	28.40	Yes
10	14.0	394.0	No	43.20	Yes
11	15.9	440.9	Yes	7.30	No

Area under curve/minimum inhibitory concentration (AUC/MIC); pharmacokinetic/pharmacodynamic (PK/PD); plasma concentration at half a dosing interval (Cp t50).

one prospective study with larger Vd than our results (Wang et al., 2021). Most of them administered the antibiotic by continuous or prolonged infusion and higher than conventional dosing were used to achieve target PK/PD or a successfull clinical outcome.

Previous studies about PK of meropenem in pediatric critically ill patients without ECMO support shows great dispersion of results (Kongthavonsakul et al., 2016; Cies et al., 2017; Rapp et al., 2020); scientific evidence to establish the influence of ECMO on meropenem PK in this group of patients is missing.

Several publications about pharmacokinetics of vancomycin and pediatric patients on ECMO support, with different designs and conclusions are available. In a retrospective study, Lonabaugh et al. proposed lower dosing than our results, 30 mg/kg/day every 12 h for patients with normal renal function (Lonabaugh et al., 2017). We found similar results for both PK parameters than a retrospective study by Moffett et al., nevertheless **we better** characterized the drug distribution phase, but they proposed lower doses than ours (Moffett et al., 2018).

In a population pharmacokinetic study, Mulla et al. found PK parameters similar than ours and they recommended vancomycin dosing between 15 mg/kg every 8 h and 20 mg/kg every 6 h. However, they included only seven pediatric prospective patients (Mulla and Pooboni, 2005).

Our previous retrospective pharmacokinetic study of vancomycin in pediatric patients on ECMO, reported similar PK parameters to the current study (Zylbersztajn et al., 2018). All studies, including this one, identify a relationship between vancomycin clearance and serum creatinine concentrations and this result is expected as vancomycin is nearly completely renally eliminated (Rybak, 2006).

In our actual study, four PK profile of vancomycin achieved lower PK/PD target, three of them corresponded to a dosing of 15 mg/kg every 6 h. Besides, there was a relationship between trough plasma concentration lower than 15 mcg/mL and AUC/MIC lower than 400. Although no dose modifications were made for the present study, it would be appropriate to consider higher doses in specific patients. PK/PD target of AUC/MIC greater than 400 is the preferred target for treatment of *Staphylococcus aureus* infections in the adult population (Liu et al., 2011), the extrapolation to pediatric population is not clear yet (Le et al., 2013), then, we continue recommending therapeutic drug monitoring for the individualization of dosing in critically ill patients on ECMO.

No other studies have reported population PK data from South American paediatric patients.

Limitations of this study include that a subgroup analysis was not performed to assess the impact of continuous renal replacement therapy (CRRT) on meropenem or vancomycin PK, due to a low number of patients under this technique. Furthermore, in this study there was a limited number of patients or PK profiles, however, we reached a sample size of connections to achieve adequate results (U.S. Department of Health and Human Services, 2019). Another limitation was the lack of clinical outcome evaluation due to the study.

This research contributes to increase the knowledge of the impact of ECMO on pharmacokinetics of vancomycin and meropenem in pediatric patients.

Based on previous studies and the results of this prospective pharmacokinetic study, maximal dosing of meropenem using an extended infusion and at least current dosing of vancomycin with therapeutic drug monitoring are necessary to achieve adequated PK/PD targets in this patient cohort. Nevertheless, larger and prospective studies are needed for robust dosing recommendations.

DATA AVAILABILITY STATEMENT

The raw data supporting the conclusions of this article will be made available by the authors, without undue reservation.

ETHICS STATEMENT

The studies involving human participants were reviewed and approved by Comite de Etica de la Investigación de Clinica Las Condes. Written informed consent to participate in this study was provided by the participants' legal guardian/next of kin.

AUTHOR CONTRIBUTIONS

BZ: first authorship, data collection, data analysis, writing manuscript SP: data analysis, writing manuscript DN: data collection, data analysis, writing manuscript GI: writing manuscript PO: data collection JT: writing manuscript CF: data collection RD: data collection CV: data collection, data analysis, writing manuscript JR: last authorship, data analysis, writing manuscript.

FUNDING

Research Project Academic Direction (PIDA) 2016 Academic Direction, Clínica Las Condes. SP is a recipient of National Health and Medical Research Council-funded Fellowships (APP1142757), JR is a recipient of a National Health and Medical Research Council-funded Centre for Research Excellence Research Excellence (APP1044941), Project Grant (1062040) and Fellowship (APP1048652).

ACKNOWLEDGMENTS

The authors would like to thank Jaime Cordero MD, Roberto Dalmazzo MD, Jorge Morales PharmD and the Pediatric Intensive Care Unit medical residents and nurses for their support and colaboration.

REFERENCES

Abdul-Aziz, M. H., Shekar, K., and Roberts, J. A. (2019). Antimicrobial Therapy during ECMO - Customised Dosing with Therapeutic Drug Monitoring: The Way to Go? *Anaesth. Crit. Care Pain Med.* 38 (5), 451–453. doi:10.1016/j.accpm.2019.07.005

Buck, M. L. (1998). Vancomycin Pharmacokinetics in Neonates Receiving Extracorporeal Membrane Oxygenation. *Pharmacotherapy* 18 (5), 1082–1086.

Cies, J. J., Moore, W. S., 2nd, Enache, A., and Chopra, A. (2017). Population Pharmacokinetics and Pharmacodynamic Target Attainment of Meropenem in Critically Ill Young Children. *J. Pediatr. Pharmacol. Ther.* 22, 276–285. doi:10.5863/1551-6776-22.4.276

Cies, J. J., Moore, W. S., Conley, S. B., Dickerman, M. J., Small, C., Carella, D., et al. (2016). Pharmacokinetics of Continuous Infusion Meropenem with Concurrent Extracorporeal Life Support and Continuous Renal Replacement Therapy: A Case Report. *J. Pediatr. Pharmacol. Ther.* 21 (1), 92–97. doi:10.5863/1551-6776-21.1.92

Cies, J. J., Moore, W. S., Dickerman, M. J., Small, C., Carella, D., Chopra, A., et al. (2014). Pharmacokinetics of Continuous-Infusion Meropenem in a Pediatric Patient Receiving Extracorporeal Life Support. *Pharmacotherapy* 34, E175–E179. doi:10.1002/phar.1476

Cies, J. J., Moore, W. S., Jr, Calaman, S., Brown, M., Narayan, P., Parker, J., et al. (2015). Pharmacokinetics of Continuous-Infusion Meropenem for the Treatment of *Serratia marcescens* Ventriculitis in a Pediatric Patient. *Pharmacotherapy* 35, e32–6. doi:10.1002/phar.1567

Drusano, G. L. (2004). Antimicrobial Pharmacodynamics: Critical Interactions of 'bug and Drug'. *Nat. Rev. Microbiol.* 2, 289–300. doi:10.1038/nrmicro862

Drusano, G. L. (2003). Prevention of Resistance: a Goal for Dose Selection for Antimicrobial Agents. *Clin. Infect. Dis.* 36, S42–S50. doi:10.1086/344653

Elkhaïli, H., Niedergang, S., Pompei, D., Linger, L., Leveque, D., and Jehl, F. (1996). High-performance Liquid Chromatographic Assay for Meropenem in Serum. *J. Chromatogr. B Biomed. Appl.* 686, 19–26. doi:10.1016/s0378-4347(96)00205-8

Fraser, J. F., Shekar, K., Diab, S., Dunster, K., Foley, S. R., McDonald, C. I., et al. (2012). ECMO - the Clinician's View. *ISBT Sci. Ser.* 7 (1), 82–88. doi:10.1111/j.1751-2824.2012.01560.x

Kongthavonsakul, K., Lucksiri, A., Eakanunkul, S., Roongjang, S., Issaranggoon Na Ayuthaya, S., and Oberdorfer, P. (2016). Pharmacokinetics and Pharmacodynamics of Meropenem in Children with Severe Infection. *Int. J. Antimicrob. Agents* 48 (2), 151–157. doi:10.1016/j.ijantimicag.2016.04.025

Le, J., Bradley, J. S., Murray, W., Romanowski, G. L., Tran, T. T., Nguyen, N., et al. (2013). Improved Vancomycin Dosing in Children Using Area under the Curve Exposure. *Pediatr. Infect. Dis. J.* 32 (4), e155–63. doi:10.1097/INF.0b013e318286378e

Liu, C., Bayer, A., Cosgrove, S. E., Daum, R. S., Fridkin, S. K., Gorwitz, R. J., et al. (2011). Clinical Practice Guidelines by the Infectious Diseases Society of America for the Treatment of Methicillin-Resistant *Staphylococcus aureus* Infections in Adults and Children. *Clin. Infect. Dis.* 52 (3), e18–55. doi:10.1093/cid/ciq146

Lodise, T. P., Lomaestro, B. M., and Drusano, G. L. (2006). Application of Antimicrobial Pharmacodynamic Concepts into Clinical Practice: Focus on Beta-Lactam Antibiotics: Insights from the Society of Infectious Diseases Pharmacists. *Pharmacotherapy* 26, 1320–1332. doi:10.1592/phco.26.9.1320

Lonabaugh, K. P., Lunsford, K. J., Fang, G. Y., Kaufman, D. A., Addison, S. D., and Buck, M. L. (2017). Vancomycin Dosing in Pediatric Extracorporeal Membrane Oxygenation: Potential Impacts of New Technologies. *J. Pediatr. Pharmacol. Ther.* 22 (5), 358–363. doi:10.5863/1551-6776-22.5.358

Lu, H., and Rosenbaum, S. (2014). Developmental Pharmacokinetics in Pediatric Populations. *J. Pediatr. Pharmacol. Ther.* 19 (4), 262–276. doi:10.5863/1551-6776-19.4.262

McWhinney, B. C., Wallis, S. C., Hillister, T., Roberts, J. A., Lipman, J., and Ungerer, J. P. (2010). Analysis of 12 Beta-Lactam Antibiotics in Human Plasma by HPLC with Ultraviolet Detection. *J. Chromatogr. B Analyt Technol. Biomed. Life Sci.* 878, 2039–2043. doi:10.1016/j.jchromb.2010.05.027

Moffett, B. S., Morris, J., Galati, M., Munoz, F., and Arikan, A. A. (2018). Population Pharmacokinetics of Vancomycin in Pediatric Extracorporeal Membrane Oxygenation. *Pediatr. Crit. Care Med.* 19, 973–980. doi:10.1097/PCC.0000000000001682

Mulla, H., and Pooboni, S. (2005). Population Pharmacokinetics of Vancomycin in Patients Receiving Extracorporeal Membrane Oxygenation. *Br. J. Clin. Pharmacol.* 60 (3), 265–275. doi:10.1111/j.1365-2125.2005.02432.x

Rapp, M., Urien, S., Foissac, F., Béranger, A., Bouazza, N., Benaboud, S., et al. (2020). Population Pharmacokinetics of Meropenem in Critically Ill Children with Different Renal Functions. *Eur. J. Clin. Pharmacol.* 76 (1), 61–71. doi:10.1007/s00228-019-02761-7

Rybak, M. J., Lomaestro, B. M., Rotschafer, J. C., Moellering, R. C., Craig, W. A., Billeter, M., et al. (2009). Vancomycin Therapeutic Guidelines: a Summary of Consensus Recommendations from the Infectious Diseases Society of America, the American Society of Health-System Pharmacists, and the Society of Infectious Diseases Pharmacists. *Clin. Infect. Dis.* 49 (3), 325–327. doi:10.1086/600877

Rybak, M. J. (2006). The Pharmacokinetic and Pharmacodynamic Properties of Vancomycin. *Clin. Infect. Dis.* 42 (Suppl. 1), S35–S39. doi:10.1086/491712

Saito, J., Shoji, K., Oho, Y., Aoki, S., Matsumoto, S., Yoshida, M., et al. (2020). Meropenem Pharmacokinetics during Extracorporeal Membrane Oxygenation and Continuous Haemodialysis: a Case Report. *J. Glob. Antimicrob. Resist.* 22, 651–655. doi:10.1016/j.jgar.2020.04.029

Sherwin, J., Heath, T., and Watt, K. (2016). Pharmacokinetics and Dosing of Anti-infective Drugs in Patients on Extracorporeal Membrane Oxygenation: A Review of the Current Literature. *Clin. Ther.* 38 (9), 1976–1994. doi:10.1016/j.clinthera.2016.07.169

Tam, V. H., Louie, A., Lomaestro, B. M., and Drusano, G. L. (2003). Integration of Population Pharmacokinetics, a Pharmacodynamic Target, and Microbiologic Surveillance Data to Generate a Rational Empiric Dosing Strategy for Cefepime against *Pseudomonas aeruginosa*. *Pharmacotherapy* 23, 291–295. doi:10.1592/phco.23.3.291.32110

U.S. Department of Health and Human Services (2019). Food and Drug Administration, Center for Drug Evaluation and Research (CDER), Center for Biologics Evaluation and Research (CBER) Population Pharmacokinetics

Guidance for Industry. Available at: https://www.fda.gov/Drugs/GuidanceComplianceRegulatoryInformation/Guidances/default.htm July 2019.
U.S. Department of Health and Human Services (2018). Food and Drug Administration, Center for Drug Evaluation and Research (CDER), Center for Veterinary Medicine (CVM). Available at: http://www.fda.gov/Drugs/GuidanceComplianceRegulatoryInformation/Guidances/default.htm May 2018.
Wang, Y., Li, Z., Chen, W., Yan, G., Wang, G., Lu, G., et al. (2021). Pharmacokinetics of Meropenem in Children with Sepsis Undergoing Extracorporeal Life Support: A Prospective Observational Study. *J. Clin. Pharm. Ther.* 1, 1–8. doi:10.1111/jcpt.13344
Wolff, F., Deprez, G., Seyler, L., Taccone, F., Hites, M., Gulbis, B., et al. (2013). Rapid Quantification of Six β-lactams to Optimize Dosage Regimens in Severely Septic Patients. *Talanta* 103, 153–160. doi:10.1016/j.talanta.2012.10.024
Zylbersztajn, B. L., Izquierdo, G., Santana, R. C., Fajardo, C., Torres, J. P., Cordero, J., et al. (2018). Therapeutic Drug Monitoring of Vancomycin in Pediatric Patients with Extracorporeal Membrane Oxygenation Support. *J. Pediatr. Pharmacol. Ther.* 23 (4), 305–310. doi:10.5863/1551-6776-23.4.305

Conflict of Interest: The authors declare that the research was conducted in the absence of any commercial or financial relationships that could be construed as a potential conflict of interest.

Publisher's Note: All claims expressed in this article are solely those of the authors and do not necessarily represent those of their affiliated organizations, or those of the publisher, the editors and the reviewers. Any product that may be evaluated in this article, or claim that may be made by its manufacturer, is not guaranteed or endorsed by the publisher.

frontiers in Pharmacology

CASE REPORT
published: 16 August 2021
doi: 10.3389/fphar.2021.717148

Case Report: Low Hematocrit Leading to Tacrolimus Toxicity

Alexandre Piletta-Zanin[1,2]*, *Aurélie De Mul*[2,3], *Nathalie Rock*[2,4], *Pierre Lescuyer*[5], *Caroline F. Samer*[1,6] and *Frédérique Rodieux*[1]

[1]Division of Clinical Pharmacology and Toxicology, Department of Anesthesiology, Pharmacology, Intensive Care and Emergency Medicine, Geneva University Hospitals, Geneva, Switzerland, [2]Division of Pediatric Specialties, Department of Women, Children and Adolescents, Geneva University Hospitals, Geneva, Switzerland, [3]Pediatric Nephrology Unit, Department of Women, Children and Adolescents, Geneva University Hospitals, Geneva, Switzerland, [4]Swiss Pediatric Liver Center, Department of Women, Children and Adolescents, Geneva University Hospitals, Geneva, Switzerland, [5]Division of Laboratory Medicine, Department of Diagnostic, Geneva University Hospitals, Geneva, Switzerland, [6]Faculty of Medicine, University of Geneva, Geneva, Switzerland

Tacrolimus is a calcineurin inhibitor characterized by a narrow therapeutic index and high intra- and inter-individual pharmacokinetic variability. Therapeutic drug monitoring in whole-blood is the standard monitoring procedure. However, tacrolimus extensively binds to erythrocytes, and tacrolimus whole-blood distribution and whole-blood trough concentrations are strongly affected by hematocrit. High whole-blood tacrolimus concentrations at low hematocrit may result in high unbound plasma concentrations and increased toxicity. We present the case of a 16-year-old girl with kidney and liver transplant in whom low concentrations of tacrolimus in the context of low hematocrit led to significant increase in the dosage of tacrolimus and participate, along with a genetic polymorphism of *ABCB1*, in nephrotoxicity.

Keywords: tacrolimus, monitoring, hematocrit, toxicity, subtherapeutic, pharmacokinetic, ABCB1, pharmacogenetic

OPEN ACCESS

Edited by:
Erwin Dreesen,
KU Leuven, Belgium

Reviewed by:
Jiao Zheng,
Shanghai Jiaotong University, China
Niccolò Lombardi,
University of Florence, Italy

***Correspondence:**
Alexandre Piletta-Zanin
alexandre.piletta-zanin@hcuge.ch

Specialty section:
This article was submitted to Obstetric and Pediatric Pharmacology, a section of the journal Frontiers in Pharmacology

Received: *30 May 2021*
Accepted: *04 August 2021*
Published: *16 August 2021*

Citation:
Piletta-Zanin A, De Mul A, Rock N, Lescuyer P, Samer CF and Rodieux Fé (2021) Case Report: Low Hematocrit Leading to Tacrolimus Toxicity. Front. Pharmacol. 12:717148. doi: 10.3389/fphar.2021.717148

INTRODUCTION

Tacrolimus is one of the most frequently prescribed immunosuppressant after solid organ transplant. Because of its narrow therapeutic index, tacrolimus concentrations have to be maintained within the therapeutic margin to achieve therapeutic immunosuppression and minimize toxicity (Böttiger et al., 1999; Astellas Pharma US, 2012). Therapeutic drug monitoring (TDM) of tacrolimus trough concentrations (C_t) performed in whole-blood is the standard procedure (Böttiger et al., 1999; Astellas Pharma US, 2012).

High inter-individual variability in tacrolimus pharmacokinetic (PK) parameters and C_t is observed after administration of a fixed dose of tacrolimus. Several clinical factors may influence the PK of tacrolimus, such as type of organ transplanted, time since transplantation, age, sex, food intake, concomitant treatments, liver and kidney dysfunction, as well as genetic factors such as polymorphisms of the cytochromes P450 (CYP) 3A4/5 and drug transporter P-glycoprotein (P-gp). As tacrolimus extensively binds to erythrocytes, tacrolimus whole-blood distribution and tacrolimus whole blood concentration (TWBC) are strongly affected by hematocrit (Hct) (Staatz et al., 2010).

Abbreviations: CNI, calcineurin inhibitors; CYP, Cytochrome P450; Ct, trough concentration; ECLIA, Electro-chemiluminescence Immunoassay; Hct, hematocrit; IV, intravenous; KDIGO, kidney disease improving global outcome; LC/MS, Liquid chromatography-mass spectrometry; P-gp, P-glycoprotein; PK, pharmacokinetic; TDM, Therapeutic drug monitoring; TWBC, Tacrolimus whole blood concentration.

TABLE 1 | Patient's laboratory values and relevant clinical evolution.

Post-operative day	Clinical evolution		Tacrolimus dose	Plasma creatinine	GFR (modified Schwartz)	Hct	TWBC (ECLIA)	Predicted TWBC for 40% Hct
		Units	mg/d	44–80 µmol/l	ml/min/1.73m2	%	µg/l	µg/l
		Target/ref ranges				36–46	7–12	
d 0	*Liver and kidney transplant*							
d 11			4.4	114	52	24.6	6.1	10.5
d 12			5.4	91	65	25.2	6.4	10.8
d 13			6	84	71	24.1	7.9	12.5
d 14			8	77	77	24.2	5.4	8.5
d 15			12	67	89	25.4	2.8	5
d 16			10	61	98	24.4	7.1	11.2
d 17			9	64	93	24	8.4	**15**
d 18	*Acute kidney injury (stage 1)*		10	92	65	23.4	8.4	**15**
d 19	*Suspicion of graft rejection*		12	108	55	24.2	5.8	9.8
d 20	*No signs of graft rejection (renal biopsy)*		14	110	54	23.5	3.9	7.3
d 22			14	114	52	21.5	5.7	11.5
d 23	*Tremor, hypertension, hyperglycemia*		10	116	52	19.6	5.8	11.5
d 24			10	115	52	24.6	5.4	8.7
d 25			10	103	58	24.9	4.6	7.3
d 26			9	97	61	24.6	6.4	11.5
d 27			8	88	68	25.3	4.9	8
d 30	*Kidney recovery*							

Bold values indicates the highly supratherapeutic concentrations.

We report, for the first time, the case of a pediatric patient who developed severe tacrolimus toxicity despite subtherapeutic TWBC, due to low Hct levels.

CASE

A 16-year-old girl known to have autosomal recessive polycystic kidney disease with end-stage renal disease and liver fibrosis received liver and kidney transplant, from the same deceased donor. The postoperative immunosuppressive regimen consisted of intravenous (IV) basiliximab (Simulect®), corticosteroids (methylprednisone, prednisone), IV mycophenolate mofetil (Cellcept®) and oral immediate-release tacrolimus (Modigraf®). From the day following transplantation (day 1), tacrolimus was given through a nasogastric tube as granules for oral suspension at the initial dosing regimen of 5 mg/d (0.1 mg/kg/d) in two daily doses, followed by dose adjustments to reach the target TWBC of 7–12 µg/l (Roche Elecsys® electrochemiluminescence immunoassay–ECLIA), as recommended in our institution. Mycophenolate mofetil was given at a dose of 2 g/d. Steroids were given as follows: IV methylprednisone 500 mg during surgery, 250 mg on the first postoperative day and 125 mg on day 2, followed by oral prednisone with a reduction regimen starting on day 3 at a dose of 80 mg/d as standard protocol for liver and renal transplantation in our institution. Other standard transplantation treatment consisted of IV piperacilline-tazobactam followed by oral trimethoprim/sulfamethoxazole, IV ganciclovir, oral omeprazole, oral labetalol, and IV acetaminophen. A nasogastric tube was used to administer oral drugs.

The post-operative period was complicated by significant anemia due to hemorrhage during hepatectomy, requiring blood transfusions at day 3 and intracerebral hemorrhage with intracranial hypertension requiring sedation with IV propofol, IV midazolam, IV morphine, IV rocuronium from day 8 to day 19, as well as oral levetiracetam. An infected biloma was diagnosed on day 15 by computed tomography with intravenous contrast and treated by IV meropenem.

TWBC were highly variable during the first 10 postoperative days; concentrations ranged from 6.1 to 24 µg/l with a dose of 2.4–5 mg/d. From day 11 to day 16, TWBC remained subtherapeutic despite the increase in dose up to 12 mg/d (see **Table 1**). On day 17 and 18, a therapeutic TWBC of 8.4 µg/l was finally achieved with a dose of 10 mg/d. On day 18, the patient developed a Stage 1 acute kidney injury based on Kidney Disease Improving Global Outcome (KDIGO) consensus [Kidney Disease: Improving Global Outcomes (KDIGO) Transplant Work Group, 2012; Levey et al., 2020]. From day 19, due to a suspicion of graft rejection, the dose was increased to 14 mg/d; on day 20 methylprednisone 600 mg/d was introduced and TWBC remained subtherapeutic. Renal biopsy on day 20 showed no sign of graft rejection (including negative CD4 staining), but confirmed severe acute tubular necrosis. On day 23, the patient had other signs consistent with tacrolimus toxicity such as hyperglycemia requiring insulin treatment, resistant hypertension treated with oral labetolol and oral minoxidil, and tremors. On day 23, despite the persistence of

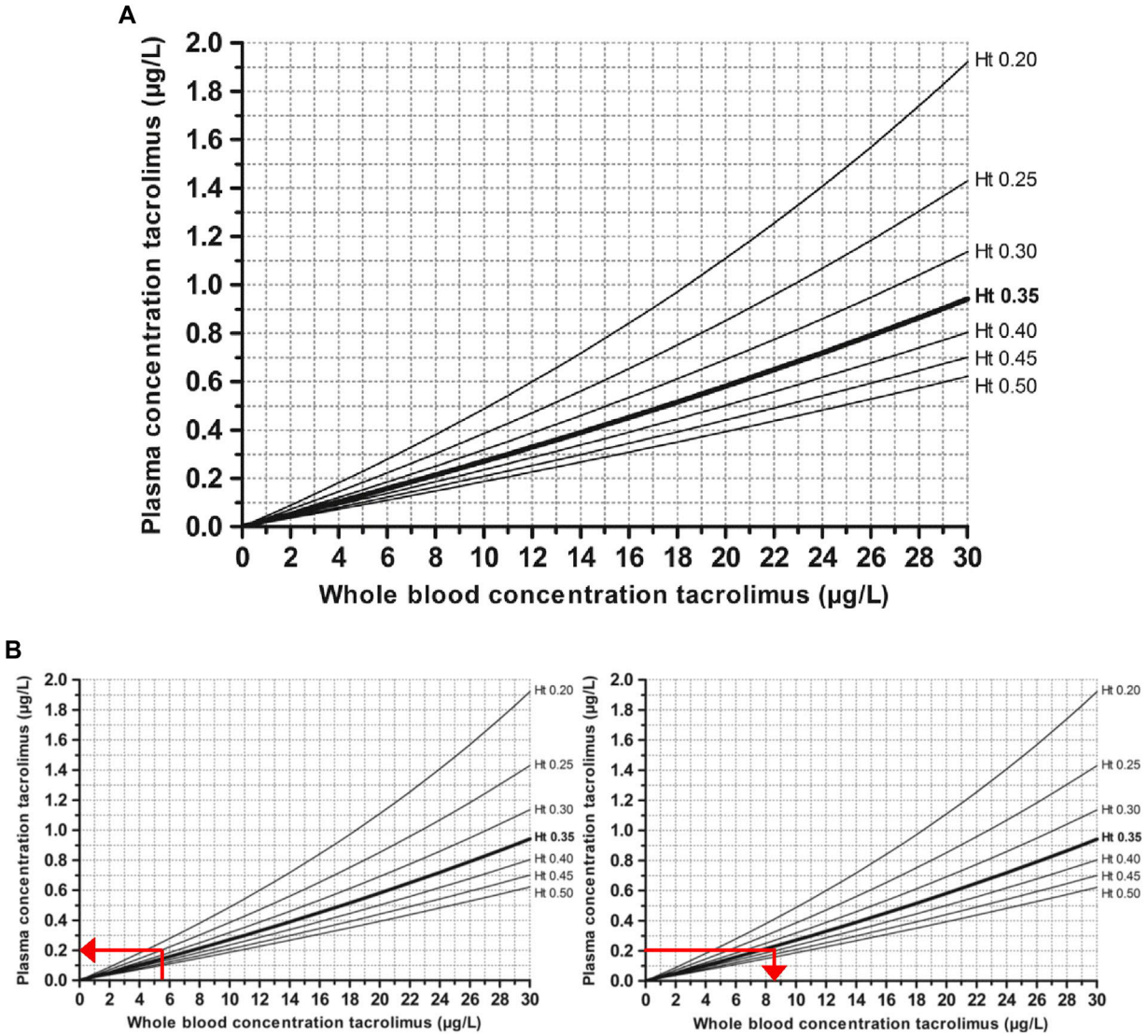

FIGURE 1 | Nomograph of predicted tacrolimus plasma concentrations corrected for hematocrit. **(A)** Schijvens' nomograph **(B)** Use of the Schijvens' nomograph to convert the measured TWBC (5.4 µg/l with 24.6% Hct) on day 24 to **[B(i)]** predicted tacrolimus plasma concentration and **[B(ii)]** predicted TWBC for 40% Hc.

subtherapeutic TWBC, in order to limit nephrotoxicity, tacrolimus dosage was decreased to 10 mg/d.

Investigations were conducted to assess the causes of tacrolimus toxicity despite a subtherapeutic TWBC. Patient's medical compliance was adequate and she was not taking any over-the-counter medications. No PK interactions or the presence of the biloma could explain the decreased TWBC concentrations and signs of toxicity. TWBC measured by ECLIA were confirmed using a liquid chromatography-mass spectrometry (LC/MS) method to exclude an analytical interference. The potential inducing effect of methylprednisolone and prednisone on CYP3A (Anglicheau et al., 2003) was not correlated with the sudden drop in TWBC. *CYP3A4, CYP3A5* and *ABCB1* genotyping (c. 3435T>C and c.2677T>G/A) were performed on the DNA of the donor and recipient. CYP3A phenotyping was performed on the recipient with midazolam as a probe drug and measurement of the OH-midazolam/midazolam metabolic ratio. The donor and the recipient had CYP3A4 normal activity and were CYP3A5 non expressors. Genotyping of the *ABCB1* gene encoding P-glycoprotein (P-gp) revealed that the donor was a heterozygous carrier of the c. 3435T>C polymorphism. Although this genetic polymorphism is associated with a decrease in P-gp activity of the transplanted organ, no study has shown an impact of this genotype on tacrolimus concentrations (Yan et al., 2016).

Because of a persistent anemia with an Hct value of less than 25%, the nomograph of "predicted tacrolimus plasma concentrations corrected for Hct" published by Schijvens et al. (2019), which described the relationship between TWBC and

plasma tacrolimus concentrations for different Hct levels, was used to correct the TWBC (see **Figure 1A**). Predicted TWBC for 40% Hct revealed supratherapeutic concentrations (15 μg/l) on day 17 and 18 as well as high concentrations (11.5 μg/l) on day 22 and 23. Tacrolimus plasma concentrations were measured on day 24 by LC/MS and compared to the tacrolimus plasma concentrations predicted by the nomograph to assess the method's accuracy (**Figure 1B**).

Based on the biopsy, clinical and laboratory findings, and retrospective determination of the predicted TWBC based on Hct values, we concluded that despite low tacrolimus TWBC, tacrolimus toxicity with nephrotoxicity, hyperglycemia and tremor were explained by a higher unbound fraction of tacrolimus.

After the tacrolimus dosage was adjusted on the basis of the predicted Hct-corrected TWBC, renal function began to recover and tremors decreased. Normal renal function was restored by day 30; insulin was progressively decreased and discontinued by day 41.

DISCUSSION

Oral absorption of tacrolimus is incomplete and influenced by food intake (Astellas Pharma US, 2012). Once absorbed, tacrolimus is primarily metabolized by CYP3A4/5 and distributed mainly into erythrocytes (Astellas Pharma US, 2012).

Tacrolimus is 85–98% bound to erythrocytes (Beysens et al., 1991; Trull, 1998; Steven, 2001). In plasma, tacrolimus is 99% bound, mainly to albumin and α-1-glycoprotein acid. This results in a free/unbound fraction in blood of less than 1% (Zahir et al., 2004). In addition to the type of transplanted organ, time since transplantation, age and sex, concomitant food consumption, changes in CYP3A4/5 activity, due to genetic polymorphisms or drug-drug interactions, as well as Hct levels have been shown to influence the PK of tacrolimus (Undre and Schäfer, 1998; Zhao et al., 2009; Staatz et al., 2010; Astellas Pharma US, 2012).

Tacrolimus is substrate of the P-gp, a multidrug efflux carrier expressed in many tissues, including the kidney, liver and intestine (Sikma et al., 2015). Intestinal P-gp has been shown to influence tacrolimus absorption (Masuda et al., 2005) while renal P-gp is not affecting tacrolimus blood concentrations but is rather linked to intracellular concentrations (Yan et al., 2016).

Tacrolimus metabolites are excreted 95% in the bile and only 2% in the urine (Möller et al., 1999). Although biliary obstruction or biloma could hypothetically impair biliary excretion of tacrolimus, reports in the literature are scarce and biliary flow has shown little effect on the PK of oral tacrolimus (Böttiger et al., 2002).

Tacrolimus TDM has been shown to be effective in reducing toxicity as well as preventing graft rejection (Staatz et al., 2001). Therapeutic tacrolimus target concentrations are based on empirical observations in adult transplant recipients. Because the concentration of the unbound fraction of tacrolimus represents the pharmacologically active drug and the fraction in equilibrium with the tissue concentration, unbound tacrolimus plasma concentrations would be the adequate surrogate for predicting clinical outcomes and dose adjustment. Measurement of total tacrolimus in plasma would be another possible alternative, as studies have shown a linear relationship between total and unbound tacrolimus plasma concentrations (Sikma et al., 2020). However, TWBC measurement is the gold-standard for tacrolimus TDM. The reasons for this are mainly technical: 1) The higher drug concentrations in whole blood than in plasma allows for easier quantification; 2) whole blood/plasma distribution ratio is affected by temperature; 3) plasma tacrolimus concentrations are vulnerable to hemolysis (Størset et al., 2014). In addition, to date, there are no validated methods or target concentrations for unbound or total tacrolimus in plasma (Machida et al., 1991; Sikma et al., 2020).

Numerous studies have previously identified Hct as a key factor in the interpretation of TWBC (Jusko et al., 1995; Størset et al., 2014; Sikma et al., 2020). As tacrolimus is a drug with a low hepatic extraction coefficient, when Hct increases, whole blood concentrations are expected to increase, with unbound concentrations remaining unchanged. With high Hct, downward adjustment of the dosage may result in decreased unbound concentrations and graft rejection (Zahir et al., 2004; Zahir et al., 2004). Conversely, low Hct levels may result in decreased whole blood concentrations without affecting the unbound plasma concentration (Undre and Schäfer, 1998; Zheng et al., 2012; Hebert et al., 2013; Størset et al., 2014; Sikma et al., 2020). The risk in this low Hct situation, is misinterpretation of subtherapeutic TWBC leading to an unnecessary or even dangerous increase in dose and toxicity (Sikma et al., 2020).

A few studies have developed PK models, equations and/or nomographs to integrate Hct in the interpretation of TWBC measurements (Størset et al., 2014; Sikma et al., 2020).

Storset et al. (2014) developed a population PK model and an equation to 'normalize' the TWBC to 45% Hct. In a paediatric study including 36 children (255 samples), Schijvens et al. (2019) developed an equation that integrates TWBC and Hct values, and transformed the usual whole blood target concentrations into *predicted target concentrations according to Hct*. They also developed a nomograph that defines the relationship between TWBC and plasma tacrolimus concentrations for different Hct and predicts the plasma tacrolimus concentration for different Hct.

Nephrotoxicity is a very common adverse effect of tacrolimus (Randhawa et al., 1997). It has been shown to correlate with the administered dose of tacrolimus, tacrolimus plasma concentrations above the TWBC and local renal exposure to tacrolimus (Bentata, 2020; Sikma et al., 2020). Tacrolimus overexposure also increases the risk of neurotoxicity, post-transplant diabetes, gastrointestinal complaints and hypertension (Zahir et al., 2004; Yuan et al., 2009; Stienstra et al., 2016).

The deterioration of renal function frequently observed in patients after transplantation is most often multifactorial, favored by sepsis, hypovolemia, inflammatory phenomena and the administration of nephrotoxic agents such as tacrolimus (Sharma et al., 2009; Leroy et al., 2010); this is most likely the case in our patient who was hypovolemic and had received a

contrast agent. Furthermore, with regard to tacrolimus, in addition to the high doses she had received, *ABCB1* genetics of the donor may have affected the risk of nephrotoxicity. The *ABCB1* CT c.3435 predicts reduced P-gp functionality at the graft level and thus could theoretically have participated in the intraparenchymal accumulation of tacrolimus (Hauser et al., 2005). Although still controversial in the literature, this variant has been associated with decreased renal function at 1, 3 and 6 months and 1 year after transplantation ($p < 0.01$) when the graft carries the CT or TT genotypes compared with CC (Tavira et al., 2015; Sallustio et al., 2021).

Determination of tacrolimus plasma concentrations in our patient could have prevented dose increase and involvement in acute nephrotoxicity, as well as the development of hypertension, hyperglycemia and neurotoxicity.

CONCLUSION

Our case report illustrates how low Hct can lead to misinterpretation of subtherapeutic tacrolimus concentrations, subsequently leading to a dangerous dose increase and risk of toxicity.

Due to the absence of analytical methods to measure unbound tacrolimus, as well as validated methods to determine the Hct-corrected whole blood concentration, the gold standard for TDM remains the measurement of TWBC. In practice, when prescribing tacrolimus, the risk of toxicity in case of low Hct should be kept in mind, even when TWBC are within target concentrations. In situations of low Hct, we recommend aiming for the lower therapeutic level.

DATA AVAILABILITY STATEMENT

The original contributions presented in the study are included in the article/supplementary material, further inquiries can be directed to the corresponding author.

ETHICS STATEMENT

Written informed consent was obtained from the individual(s), and minor(s)' legal guardian/next of kin, for the publication of any potentially identifiable images or data included in this article.

AUTHOR CONTRIBUTIONS

AP-Z and FR contributed to conception and design, collection of clinical data, writing and editing the manuscript. CS, AD, and NR critically reviewed the manuscript for important intellectual content and suggested valuable comments, which improved the quality of the manuscript. PL was responsible for the laboratory analyses and critically revised the manuscript. All authors read and approved the final manuscript.

REFERENCES

Anglicheau, D., Flamant, M., Schlageter, M. H., Martinez, F., Cassinat, B., Beaune, P., et al. (2003). Pharmacokinetic Interaction between Corticosteroids and Tacrolimus after Renal Transplantation. *Nephrol. Dial. Transplant.* 18 (11), 2409–2414. doi:10.1093/ndt/gfg381

Astellas Pharma US (2012). *Prograf (Tacrolimus) Prescribing Information*. Illinois, US: Astellas Pharma US. Available at: https://www.accessdata.fda.gov/drugsatfda_docs/label/2012/050709s031lbl.pdf

Bentata, Y. (2020). Tacrolimus: 20 Years of Use in Adult Kidney Transplantation. What We Should Know about its Nephrotoxicity. *Artif. Organs* 44 (2), 140–152. doi:10.1111/aor.13551

Beysens, A. J., Wijnen, R. M., Beuman, G. H., van der Heyden, J., Kootstra, G., and van As, H. (1991). FK 506: Monitoring in Plasma or in Whole Blood? *Transpl. Proc* 23 (6), 2745–2747.

Böttiger, Y., Brattström, C., Tydén, G., Säwe, J., and Groth, C. G. (1999). Tacrolimus Whole Blood Concentrations Correlate Closely to Side-Effects in Renal Transplant Recipients. *Br. J. Clin. Pharmacol.* 48 (3), 445–448. doi:10.1046/j.1365-2125.1999.00007.x

Böttiger, Y., Undre, N. A., Säwe, J., Stevenson, P. J., and Ericzon, B. G. (2002). Effect of Bile Flow on the Absorption of Tacrolimus in Liver Allograft Transplantation. *Transplant. Proc.* 34 (5), 1544–1545. doi:10.1016/s0041-1345(02)03013-0

Hauser, I. A., Schaeffeler, E., Gauer, S., Scheuermann, E. H., Wegner, B., Gossmann, J., et al. (2005). ABCB1 Genotype of the Donor but Not of the Recipient Is a Major Risk Factor for Cyclosporine-Related Nephrotoxicity after Renal Transplantation. *JASN* 16 (5), 1501–1511. doi:10.1681/asn.2004100882

Hebert, M. F., Zheng, S., Hays, K., Shen, D. D., Davis, C. L., Umans, J. G., et al. (2013). Interpreting Tacrolimus Concentrations during Pregnancy and Postpartum. *Transplantation* 95 (7), 908–915. doi:10.1097/tp.0b013e318278d367

Jusko, W. J., Piekoszewski, W., Klintmalm, G. B., Shaefer, M. S., Hebert, M. F., Piergies, A. A., et al. (1995). Pharmacokinetics of Tacrolimus in Liver Transplant Patients*. *Clin. Pharmacol. Ther.* 57 (3), 281–290. doi:10.1016/0009-9236(95)90153-1

Kidney Disease: Improving Global Outcomes (KDIGO) Transplant Work Group (2012). KDIGO Clinical Practice Guideline for Acute Kidney Injury. *Kidney Int. Suppl.* 2, 1. doi:10.1038/kisup.2012.1

Leroy, S., Isapof, A., Fargue, S., Fakhoury, M., Bensman, A., Deschênes, G., et al. (2010). Tacrolimus Nephrotoxicity: Beware of the Association of Diarrhea, Drug Interaction and Pharmacogenetics. *Pediatr. Nephrol.* 25 (5), 965–969. doi:10.1007/s00467-009-1402-8

Levey, A. S., Eckardt, K. U., Dorman, N. M., Christiansen, S. L., Hoorn, E. J., Ingelfinger, J. R., et al. (2020). Nomenclature for Kidney Function and Disease: Report of a Kidney Disease: Improving Global Outcomes (KDIGO) Consensus Conference. *Kidney Int.* 97 (6), 1117–1129. doi:10.1016/j.kint.2020.02.010

Machida, M., Takahara, S., Ishibashi, M., Hayashi, M., Sekihara, T., and Yamanaka, H. (1991). Effect of Temperature and Hematocrit on Plasma Concentration of FK 506. *Transpl. Proc* 23 (6), 2753–2754.

Masuda, S., Goto, M., Okuda, M., Ogura, Y., Oike, F., Kiuchi, T., et al. (2005). Initial Dosage Adjustment for Oral Administration of Tacrolimus Using the Intestinal MDR1 Level in Living-Donor Liver Transplant Recipients. *Transplant. Proc.* 37 (4), 1728–1729. doi:10.1016/j.transproceed.2005.02.081

Möller, A., Iwasaki, K., Kawamura, A., Teramura, Y., Shiraga, T., Hata, T., et al. (1999). The Disposition of 14C-Labeled Tacrolimus after Intravenous and Oral Administration in Healthy Human Subjects. *Drug Metab. Dispos* 27 (6), 633–636.

Randhawa, P. S., Starzl, T. E., and Demetris, A. J. (1997). Tacrolimus (FK506)-Associated Renal Pathology. *Adv. Anat. Pathol.* 4 (4), 265–276. doi:10.1097/00125480-199707000-00032

Sallustio, B. C., Noll, B. D., Hu, R., Barratt, D. T., Tuke, J., Coller, J. K., et al. (2021). Tacrolimus Dose, Blood Concentrations and Acute Nephrotoxicity, but Not CYP3A5/ABCB1 Genetics, Are Associated with Allograft Tacrolimus

Concentrations in Renal Transplant Recipients. *Br. J. Clin. Pharmacol.* doi:10.1111/bcp.14806

Schijvens, A. M., van Hesteren, F. H. S., Cornelissen, E. A. M., Bootsma-Robroeks, C. M. H. H. T., Brüggemann, R. J. M., Burger, D. M., et al. (2019). The Potential Impact of Hematocrit Correction on Evaluation of Tacrolimus Target Exposure in Pediatric Kidney Transplant Patients. *Pediatr. Nephrol.* 34 (3), 507–515. doi:10.1007/s00467-018-4117-x

Sharma, P., Welch, K., Eikstadt, R., Marrero, J. A., Fontana, R. J., and Lok, A. S. (2009). Renal Outcomes after Liver Transplantation in the Model for End-Stage Liver Disease Era. *Liver Transpl.* 15 (9), 1142–1148. doi:10.1002/lt.21821

Sikma, M. A., Hunault, C. C., Huitema, A. D. R., De Lange, D. W., and Van Maarseveen, E. M. (2020). Clinical Pharmacokinetics and Impact of Hematocrit on Monitoring and Dosing of Tacrolimus Early after Heart and Lung Transplantation. *Clin. Pharmacokinet.* 59 (4), 403–408. doi:10.1007/s40262-019-00846-1

Sikma, M. A., Van Maarseveen, E. M., Hunault, C. C., Moreno, J. M., Van de Graaf, E. A., Kirkels, J. H., et al. (2020). Unbound Plasma, Total Plasma, and Whole-Blood Tacrolimus Pharmacokinetics Early after Thoracic Organ Transplantation. *Clin. Pharmacokinet.* 59 (6), 771–780. doi:10.1007/s40262-019-00854-1

Sikma, M. A., van Maarseveen, E. M., van de Graaf, E. A., Kirkels, J. H., Verhaar, M. C., Donker, D. W., et al. (2015). Pharmacokinetics and Toxicity of Tacrolimus Early after Heart and Lung Transplantation. *Am. J. Transplant.* 15 (9), 2301–2313. doi:10.1111/ajt.13309

Staatz, C. E., Goodman, L. K., and Tett, S. E. (2010). Effect of CYP3A and ABCB1 Single Nucleotide Polymorphisms on the Pharmacokinetics and Pharmacodynamics of Calcineurin Inhibitors: Part I. *Clin. Pharmacokinet.* 49 (4), 207–221. doi:10.2165/11317350-000000000-00000

Staatz, C., Taylor, P., and Tett, S. (2001). Low Tacrolimus Concentrations and Increased Risk of Early Acute Rejection in Adult Renal Transplantation. *Nephrol. Dial. Transpl.* 16 (9), 1905–1909. doi:10.1093/ndt/16.9.1905

Steven, H. Y. W. (2001). Therapeutic Drug Monitoring for Immunosuppressants. Clinica Chimica Acta. *Int. J. Clin. Chem.* 23 (6), 2745–2747. doi:10.1016/s0009-8981(01)00678-7

Stienstra, N. A., Sikma, M. A., van Dapperen, A. L., de Lange, D. W., and van Maarseveen, E. M. (2016). Development of a Simple and Rapid Method to Measure the Free Fraction of Tacrolimus in Plasma Using Ultrafiltration and LC-MS/MS. *Ther. Drug Monit.* 38 (6), 722–727. doi:10.1097/ftd.0000000000000351

Størset, E., Holford, N., Midtvedt, K., Bremer, S., Bergan, S., and Åsberg, A. (2014). Importance of Hematocrit for a Tacrolimus Target Concentration Strategy. *Eur. J. Clin. Pharmacol.* 70 (1), 65–77. doi:10.1007/s00228-013-1584-7

Tavira, B., Gómez, J., Díaz-Corte, C., Coronel, D., Lopez-Larrea, C., Suarez, B., et al. (2015). The Donor ABCB1 (MDR-1) C3435T Polymorphism Is a Determinant of the Graft Glomerular Filtration Rate Among Tacrolimus Treated Kidney Transplanted Patients. *J. Hum. Genet.* 60 (5), 273–276. doi:10.1038/jhg.2015.12

Trull, A. K. (1998). Therapeutic Monitoring of Tacrolimus. *Ann. Clin. Biochem.* 35 (2), 167–180. doi:10.1177/000456329803500201

Undre, N. A., and Schäfer, A. (1998). Factors Affecting the Pharmacokinetics of Tacrolimus in the First Year after Renal Transplantation. *Transplant. Proc.* 30 (4), 1261–1263. doi:10.1016/s0041-1345(98)00234-6

Yan, L., Li, Y., Tang, J.-T., An, Y.-F., Wang, L.-L., and Shi, Y.-Y. (2016). Donor ABCB1 3435 C>T Genetic Polymorphisms Influence Early Renal Function in Kidney Transplant Recipients Treated with Tacrolimus. *Pharmacogenomics* 17 (3), 249–257. doi:10.2217/pgs.15.165

Yuan, H., Xi, L. Y., Zhu, L. J., Huang, Z. J., and Yang, G. P. (2009). Relation between Blood Pressure and Dose, Plasma Concentration of Tacrolimus in Patients with Renal Transplantation. *Int. J. Cardiol.* 137 (S95), 321. doi:10.1016/j.ijcard.2009.09.321

Zahir, H., McCaughan, G., Gleeson, M., Nand, R. A., and McLachlan, A. J. (2004). Factors Affecting Variability in Distribution of Tacrolimus in Liver Transplant Recipients. *Br. J. Clin. Pharmacol.* 57 (3), 298–309. doi:10.1046/j.1365-2125.2003.02008.x

Zahir, H., McCaughan, G., Gleeson, M., Nand, R. A., and McLachlan, A. J. (2004). Changes in Tacrolimus Distribution in Blood and Plasma Protein Binding Following Liver Transplantation. *Ther. Drug Monit.* 26 (5), 506–515. doi:10.1097/00007691-200410000-00008

Zhao, W., Elie, V., Roussey, G., Brochard, K., Niaudet, P., Leroy, V., et al. (2009). Population Pharmacokinetics and Pharmacogenetics of Tacrolimus in De Novo Pediatric Kidney Transplant Recipients. *Clin. Pharmacol. Ther.* 86 (6), 609–618. doi:10.1038/clpt.2009.210

Zheng, S., Easterling, T. R., Umans, J. G., Miodovnik, M., Calamia, J. C., Thummel, K. E., et al. (2012). Pharmacokinetics of Tacrolimus during Pregnancy. *Ther. Drug Monit.* 34 (6), 660–670. doi:10.1097/ftd.0b013e3182708edf

Conflict of Interest: The authors declare that the research was conducted in the absence of any commercial or financial relationships that could be construed as a potential conflict of interest.

Publisher's Note: All claims expressed in this article are solely those of the authors and do not necessarily represent those of their affiliated organizations, or those of the publisher, the editors and the reviewers. Any product that may be evaluated in this article, or claim that may be made by its manufacturer, is not guaranteed or endorsed by the publisher.

frontiers in Pharmacology

ORIGINAL RESEARCH
published: 27 September 2021
doi: 10.3389/fphar.2021.755075

A Proof of Concept of the Role of TDM-Based Clinical Pharmacological Advices in Optimizing Antimicrobial Therapy on Real-Time in Different Paediatric Settings

Milo Gatti[1,2], *Pier Giorgio Cojutti*[2], *Caterina Campoli*[3], *Fabio Caramelli*[4], *Luigi Tommaso Corvaglia*[1,5], *Marcello Lanari*[1,6], *Andrea Pession*[1,7], *Stefania Ramirez*[8], *Pierluigi Viale*[1,3] *and Federico Pea*[1,2]*

[1]Department of Medical and Surgical Sciences, Alma Mater Studiorum University of Bologna, Bologna, Italy, [2]SSD Clinical Pharmacology, IRCCS Azienda Ospedaliero-Universitaria di Bologna, Bologna, Italy, [3]Infectious Diseases Unit, IRCCS Azienda Ospedaliero-Universitaria di Bologna, Bologna, Italy, [4]Pediatric Intensive Care Unit, IRCCS Azienda Ospedaliero-Universitaria di Bologna, Bologna, Italy, [5]Neonatal Intensive Care Unit, IRCCS Azienda Ospedaliero-Universitaria di Bologna, Bologna, Italy, [6]Pediatric Emergency Unit, IRCCS Azienda Ospedaliero-Universitaria di Bologna, Bologna, Italy, [7]Pediatric Oncology & Hematology Unit 'Lalla Seràgnoli', IRCCS Azienda Ospedaliero-Universitaria di Bologna, Bologna, Italy, [8]LUM Metropolitan Laboratory, AUSL Bologna, Bologna, Italy

OPEN ACCESS

Edited by:
Raffaele Simeoli,
Bambino Gesù Children's Hospital (IRCCS), Italy

Reviewed by:
Giacomo Luci,
University of Pisa, Italy
Jiao Zheng,
Shanghai Jiaotong University, China

***Correspondence:**
Federico Pea
federico.pea@unibo.it

Specialty section:
This article was submitted to Obstetric and Pediatric Pharmacology, a section of the journal Frontiers in Pharmacology

Received: *07 August 2021*
Accepted: *13 September 2021*
Published: *27 September 2021*

Citation:
Gatti M, Cojutti PG, Campoli C, Caramelli F, Corvaglia LT, Lanari M, Pession A, Ramirez S, Viale P and Pea F (2021) A Proof of Concept of the Role of TDM-Based Clinical Pharmacological Advices in Optimizing Antimicrobial Therapy on Real-Time in Different Paediatric Settings. Front. Pharmacol. 12:755075. doi: 10.3389/fphar.2021.755075

Introduction: Antimicrobial treatment is quite common among hospitalized children. The dynamic age-associated physiological variations coupled with the pathophysiological alterations caused by underlying illness and potential drug-drug interactions makes the implementation of appropriate antimicrobial dosing extremely challenging among paediatrics. Therapeutic drug monitoring (TDM) may represent a valuable tool for assisting clinicians in optimizing antimicrobial exposure. Clinical pharmacological advice (CPA) is an approach based on the correct interpretation of the TDM result by the MD Clinical Pharmacologist in relation to specific underlying conditions, namely the antimicrobial susceptibility of the clinical isolate, the site of infection, the pathophysiological characteristics of the patient and/or the drug-drug interactions of cotreatments. The aim of this study was to assess the role of TDM-based CPAs in providing useful recommendations for the real-time personalization of antimicrobial dosing regimens in various paediatric settings.

Materials and methods: Paediatric patients who were admitted to different settings of the IRCCS Azienda Ospedaliero-Universitaria of Bologna, Italy (paediatric intensive care unit [ICU], paediatric onco-haematology, neonatology, and emergency paediatric ward), between January 2021 and June 2021 and who received TDM-based CPAs on real-time for personalization of antimicrobial therapy were retrospectively assessed. Demographic and clinical features, CPAs delivered in relation to different settings and antimicrobials, and type of dosing adjustments were extracted. Two indicators of performance were identified. The number of dosing adjustments provided over the total number of delivered CPAs. The turnaround time (TAT) of CPAs according to a predefined scale (optimal, <12 h; quasi-optimal, between 12–24 h; acceptable, between 24–48 h; suboptimal, >48 h).

Results: Overall, 247 CPAs were delivered to 53 paediatric patients (mean 4.7 ± 3.7 CPAs/patient). Most were delivered to onco-haematological patients (39.6%) and to ICU patients (35.8%), and concerned mainly isavuconazole (19.0%) and voriconazole (17.8%). Overall, CPAs suggested dosing adjustments in 37.7% of cases (24.3% increases and 13.4% decreases). Median TAT was 7.5 h (IQR 6.1–8.8 h). Overall, CPAs TAT was optimal in 91.5% of cases, and suboptimal in only 0.8% of cases.

Discussion: Our study provides a proof of concept of the helpful role that TDM-based real-time CPAs may have in optimizing antimicrobial exposure in different challenging paediatric scenarios.

Keywords: clinical pharmacology advice, personalized antimicrobial therapy, neonatology, paediatric intensive care unit, paediatric emergency, paediatric onco-haematology

INTRODUCTION

Severe bacterial infections are a growing problem in the pediatric population and the rise of multidrug-resistant (MDR) pathogens may seriously challenge optimal treatment (Hsu and Tamma, 2014). Antimicrobial use is quite common among hospitalized children, possibly exceeding 50% in different paediatric settings, but unfortunately most antimicrobials do not have specific paediatric posology based on pharmacokinetic and/or pharmacokinetic/pharmacodynamic studies that were carried out in this patient population (Korth-Bradley, 2018). Although the paradigm shift that states "children are not small adults" is widely accepted nowadays (Moore, 1998), in most cases dose scaling in pediatrics is still based on allometric scaling (Le and Bradley, 2018). This approach selects drug dosage on the basis of the non-proportional relationship that exists between the pharmacokinetic (PK) parameters, such as drug clearance and/or volume of distribution, and the body size descriptors, such as body surface area and/or lean body weight (Le and Bradley, 2018). Unfortunately, allometric scaling is far from being optimal, as it has some intrinsic limitations. Importantly, it does not take into account the process of organ maturation that occurs in the first years of life. It should not be overlooked that drug disposition in newborns, infants and toddlers may be affected by age-related factors both concerning organ development and maturation, and body composition, thus potentially rendering drug exposure unpredictable (Kearns et al., 2003). Renal function normalized to body weight (in terms of creatinine clearance in mL/min/kg) may be 2-3 fold higher during the first year of life than in adults (Hayton, 2000), and in the subsequent years progressively decreases reaching values similar to those of adults within 10 years of age (Funk et al., 2012). Additionally, allometric scaling does not consider the influence that some pathophysiological conditions may have in altering the pharmacokinetic behavior of some drugs. Interindividual pharmacokinetic variability, namely a well-known issue that may affect drug exposure and treatment outcomes (Collins and Varmus, 2015), may be especially relevant in the case of the critically ill and/or of the onco-hematological pediatric patients. The underlying presence of sepsis and/or septic shock, and/or of hematological malignancies like acute myeloid leukemia and/or acute lymphoblastic leukemia may frequently lead to the so-called augmented renal clearance, namely a pathophysiological condition that may significantly increase the renal clearance of hydrophilic drugs, as for example beta-lactams and/or aminoglycosides. Last, but not least, drug-drug interactions may furtherly make the implementation of appropriate antimicrobial dosing extremely challenging, as in the case of antifungal triazoles.

Therapeutic drug monitoring (TDM) may represent a valuable tool for assisting clinicians in optimizing antimicrobial dosing. However, for providing clinicians with optimal TDM-based dosing adjustments in each single patient, it is necessary that the results could be provided on real-time and that they are interpreted correctly. The clinical pharmacological advice (CPA) is an advice for optimizing drug exposure in each single patient that is delivered by the MD Clinical Pharmacologist who interprets on real-time the TDM results of antimicrobials in relation to some specific underlying conditions, namely the antimicrobial susceptibility of the clinical isolate, the site of infection, the pathophysiological characteristics of the patient and/or the potential drug-drug interactions of co-treatments.

The aim of this study was to provide a proof of concept of the role that TDM-based CPAs may have for real-time personalization of antimicrobial exposure in different paediatric settings.

MATERIALS AND METHODS

Study Design

This is a proof-of-concept study that has the purposes of describing the organizational procedures of a newly established Clinical Pharmacology Unit focused at providing real-time CPAs for individualizing antimicrobial exposure in different specific paediatric settings, and of assessing the clinical impact of the CPAs in the first 6 months of activity.

Organizational Procedures of the Clinical Pharmacology Unit

The IRCCS Azienda Ospedaliero-Universitaria of Bologna, Italy is a 1362-bed tertiary care teaching hospital which is currently organized in nine integrated activity Departments including 87 different operating units. The Clinical Pharmacology Unit was activated on November 2020, and since December 2020 started in

TABLE 1 | Scheduled timing, expected PK/PD target, and TDM-guided dosage adjustments of antimicrobials for which clinical pharmacological advice is available five-times weekly.

5 times weekly			
Antimicrobial	**Timing to CPA**	**Expected target**	**Dosage adjustment**
Piperacillin-Tazobactam	4–6 h for TDM result[c] CPA within 2–4 h[d]	C_{min} or C_{ss} > 4xMIC	Reduction 50% if C_{min} or C_{ss} > 10xMIC Increase 50% if C_{min} or C_{ss} < 2xMIC
Meropenem	4–6 h for TDM result[c] CPA within 2–4 h[d]	C_{min} or C_{ss} > 4xMIC	Reduction 50% if C_{min} or C_{ss} > 10xMIC Increase 50% if C_{min} or C_{ss} < 2xMIC
Ceftazidime	4–6 h for TDM result[c] CPA within 2–4 h[d]	C_{min} or C_{ss} > 4xMIC	Reduction 50% if C_{min} or C_{ss} > 10xMIC Increase 50% if C_{min} or C_{ss} < 2xMIC
Ampicillin-Sulbactam[b]	4–6 h for TDM result[c] CPA within 2–4 h[d]	C_{min} or C_{ss} > 4xMIC	Reduction 50% if C_{min} or C_{ss} > 10xMIC Increase 50% if C_{min} or C_{ss} < 2xMIC
Cefepime[b]	4–6 h for TDM result[c] CPA within 2–4 h[d]	C_{min} or C_{ss} > 4xMIC	Reduction 50% if C_{min} or C_{ss} > 10xMIC Increase 50% if C_{min} or C_{ss} < 2xMIC
Linezolid	4–6 h for TDM result[c] CPA within 2–4 h[d]	C_{min} 2–8 mg/L	Reduction 50% if C_{min} > 10 mg/L Increase 25–50% if C_{min} < 2 mg/L
Vancomycin[e]	4–6 h for TDM result[c] CPA within 2–4 h[d]	C_{ss} 18–20 mg/L	Prefer CI and calculate correct dosing in order to achieve an AUC/MIC >400 according to C_{ss} and MIC
Teicoplanin[e]	4–6 h for TDM result[c] CPA within 2–4 h[d]	C_{ss} 20–30 mg/L	Reduction 25–50% if C_{min} > 35 mg/L Increase 50% if C_{min} < 10 mg/L
Amikacin[e]	4–6 h for TDM result[c] CPA within 2–4 h[d]	C_{max} 8-10xMIC C_{min} < 1 mg/L	Reduction every 36–48 h if C_{min} > 1.5 mg/L Increase 25% if C_{max} < 8xMIC
Gentamicin[e]	4–6 h for TDM result[c] CPA within 2–4 h[d]	C_{max} 8-10xMIC C_{min} < 1 mg/L	Reduction every 36–48 h if C_{min} > 0.5 mg/L Increase 25% if C_{max} < 8xMIC
Rifampicin	4–6 h for TDM result[c] CPA within 2–4 h[d]	C_{max} 8–22 mg/L	Reduction 25–50% if C_{max} > 22 mg/L Increase 50% if C_{max} < 4 mg/L
Levofloxacin	4–6 h for TDM result[c] CPA within 2–4 h[d]	C_{max} 10xMIC C_{min} < 2 mg/L	Reduction every 36–48 h if C_{min} > 2 mg/L Increase 25% if C_{max} < 10xMIC
Ciprofloxacin	4–6 h for TDM result[c] CPA within 2–4 h[d]	C_{max} 10xMIC C_{min} < 2 mg/L	Reduction 25% if C_{min} > 2 mg/L Increase 25% if C_{max} < 10xMIC

(Continued on following page)

TABLE 1 | (*Continued*) Scheduled timing, expected PK/PD target, and TDM-guided dosage adjustments of antimicrobials for which clinical pharmacological advice is available five-times weekly.

5 times weekly			
Antimicrobial	**Timing to CPA**	**Expected target**	**Dosage adjustment**
Fluconazole	4–6 h for TDM result[c] CPA within 2–4 h[d]	C_{min} 10–20 mg/L	Reduction: 50% if C_{min} > 50 mg/L 25% if C_{min} 30–50 mg/L Increase: 25% if C_{min} < 10 mg/L
Voriconazole	4–6 h for TDM result[c] CPA within 2–4 h[d]	C_{min} 1–3 mg/L	Reduction stop if C_{min} > 8–10 mg/L 25-50% if C_{min} 3.5–8 mg/L Increase every 6–8 h if C_{min} < 1 mg/L
Posaconazole	4–6 h for TDM result[c] CPA within 2–4 h[d]	C_{min} 1–3 mg/L	Reduction 25–50% if C_{min} > 4 mg/L Increase every 12 h if C_{min} < 1 mg/L
Isavuconazole	4–6 h for TDM result[c] CPA within 2–4 h[d]	C_{min} 1–7 mg/L	Reduction 25–50% if C_{min} >8 mg/L Increase 25–50% if C_{min} < 1 mg/L
Ganciclovir/valganciclovir	4–6 h for TDM result[c] CPA within 2–4 h[d]	C_{min} 0.7–2 mg/L	Reduction stop if C_{min} > 5 mg/L 25-50% if C_{min} 2–5 mg/L Increase every 6–8 h if C_{min} < 0.5 mg/L

[a]*available from April 01, 2021.*
[b]*available from May 27, 2021.*
[c]*if sanding samples occurs within 2.00 pm; 24 h for samples sent after 2.00 pm.*
[d]*after TDM results communication.*
[e]*fully automated analytic procedure.*
[f]*experimental analytic methods.*
AUC, area under concentration-time curve; C_{max}, peak concentration; C_{min}, trough concentration; C_{ss}, steady-state concentration; CI, continuous infusion; CPA, clinical pharmacology advice; MIC, minimum inhibitory concentration; PK/PD, pharmacokinetic/pharmacodynamic; TDM, therapeutic drug monitoring.

providing educational webinars concerning the role of CPAs for real-time personalization of antimicrobial exposure that are based on TDM samples that are analyzed at the Unique Metropolitan Laboratory (LUM).

The CPA is an approach based on the correct interpretation of the TDM result by the MD Clinical Pharmacologist in relation to specific underlying conditions, namely the antimicrobial susceptibility of the clinical isolate according to the MIC provided by the Clinical Microbiologist, the site of infection, the pathophysiological characteristics of the patient (e.g., body mass index, renal function, sepsis, requirement for continuous renal replacement therapy or intermittent haemodialysis) and/or the influence of concomitant therapies. Clinical features of each patient (i.e., weight, height, diagnosis, concomitant therapies, date of starting antimicrobial therapy, drug dose and frequency of administration, time of blood sample collection) were supplied by the physician who requested the CPA and had the patient in charge. This approach allowed to provide dosing adjustment recommendations useful at optimizing drug exposure in each single patient.

The CPAs were provided five times weekly (from Monday to Friday) for 18 different antimicrobials: 13 antibiotics (piperacillin-tazobactam, ampicillin, meropenem, ceftazidime, cefepime, vancomycin, teicoplanin, amikacin, gentamicin, linezolid, levofloxacin, ciprofloxacin, and rifampicin), four antifungals (fluconazole, voriconazole, posaconazole, and isavuconazole), and one antiviral (ganciclovir) as detailed in **Table 1**. Optimal pharmacodynamic targets both for maximizing clinical efficacy and for minimizing resistance occurrence were considered a plasma steady-state concentration 4-fold above the minimum inhibitory concentration (MIC) (Css/MIC >4) for time-dependent antimicrobials, and a peak concentration to MIC ratio (Cmax/MIC) ≥ 8–12 for concentration-dependent antimicrobials (Abdul-Aziz et al., 2020) (**Table 1**). Blood samples for first TDM assessment were routinely collected at 48- and 72-h after the start of the treatment for beta-lactams and for other agents (e.g., linezolid, azoles), respectively, in order to ensure that steady state concentrations have been achieved. Re-assessments were commonly performed at least after 48-h the implementation of dosing adjustments recommended in CPAs.

The CPAs were provided usually within 4 h after that the TDM results were made available in the hospital intranet system by the LUM. Blood samples for TDM were processed by the LUM in the same day if they were delivered within 2.00 p.m., otherwise they were processed in the subsequent day.

The CPAs had been adopted by four specific paediatric settings, namely paediatric intensive care unit [ICU], paediatric onco-haematology/transplant unit, neonatology, and emergency paediatric ward. Antimicrobial treatment and relative

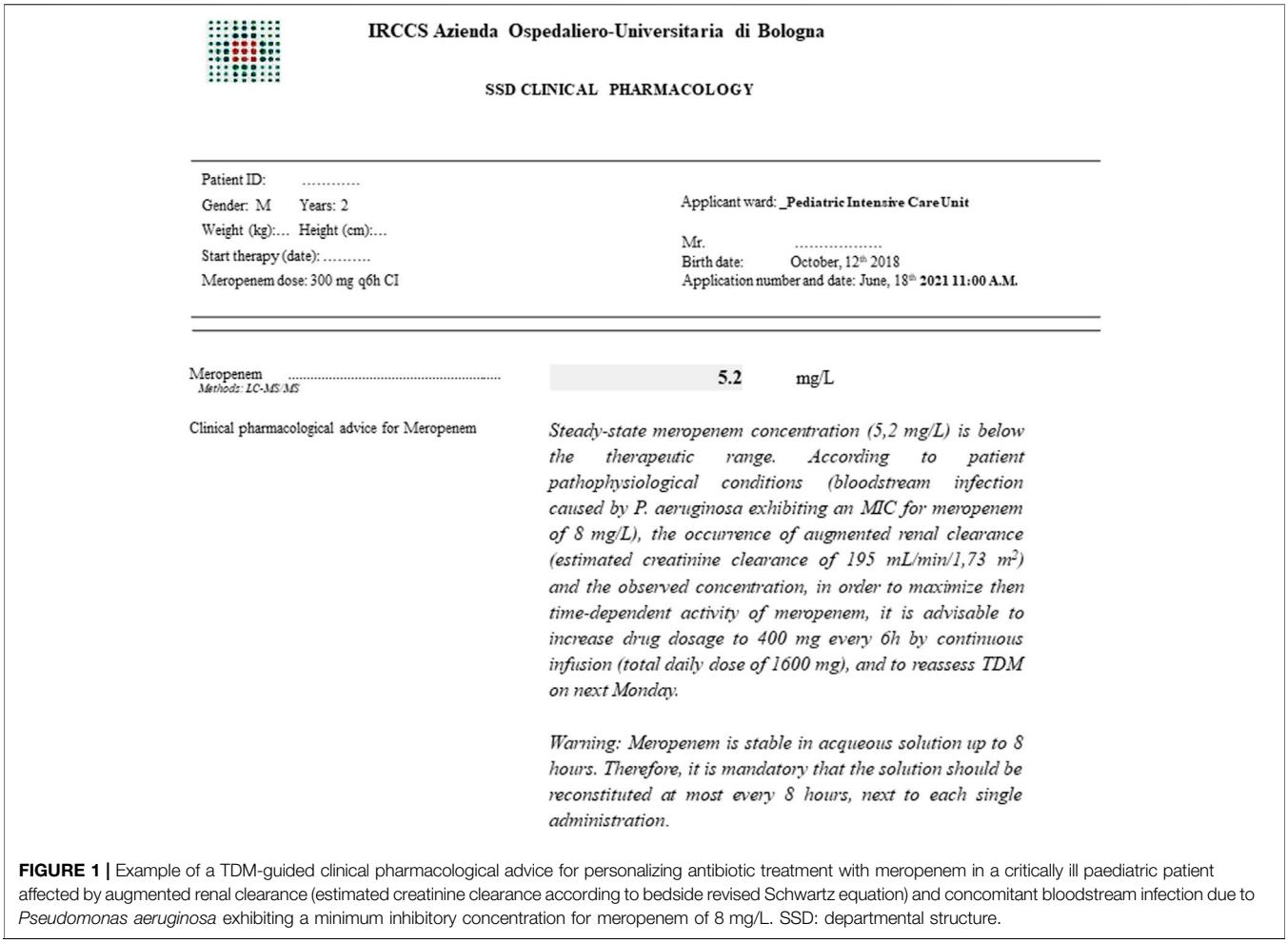

IRCCS Azienda Ospedaliero-Universitaria di Bologna

SSD CLINICAL PHARMACOLOGY

Patient ID: .....
Gender: M Years: 2
Weight (kg):... Height (cm):...
Start therapy (date): .....
Meropenem dose: 300 mg q6h CI

Applicant ward: **_Pediatric Intensive Care Unit**
Mr. .....
Birth date: October, 12th 2018
Application number and date: June, 18th **2021 11:00 A.M.**

Meropenem ..... **5.2** mg/L
Methods: LC-MS/MS

Clinical pharmacological advice for Meropenem

Steady-state meropenem concentration (5,2 mg/L) is below the therapeutic range. According to patient pathophysiological conditions (bloodstream infection caused by P. aeruginosa exhibiting an MIC for meropenem of 8 mg/L), the occurrence of augmented renal clearance (estimated creatinine clearance of 195 mL/min/1,73 m²) and the observed concentration, in order to maximize then time-dependent activity of meropenem, it is advisable to increase drug dosage to 400 mg every 6h by continuous infusion (total daily dose of 1600 mg), and to reassess TDM on next Monday.

Warning: Meropenem is stable in acqueous solution up to 8 hours. Therefore, it is mandatory that the solution should be reconstituted at most every 8 hours, next to each single administration.

FIGURE 1 | Example of a TDM-guided clinical pharmacological advice for personalizing antibiotic treatment with meropenem in a critically ill paediatric patient affected by augmented renal clearance (estimated creatinine clearance according to bedside revised Schwartz equation) and concomitant bloodstream infection due to *Pseudomonas aeruginosa* exhibiting a minimum inhibitory concentration for meropenem of 8 mg/L. SSD: departmental structure.

dosage were initially selected on the basis of dedicated national and local guidelines with the support of the infectious disease consultant, and successively adjusted according to the TDM-based CPAs. The relationship between antimicrobial exposure and clinical outcome in terms of efficacy and safety was regularly assessed during the delivery of CPAs.

Data Analysis of CPAs Provided in the First Six Months of Activity

Paediatric patients who were admitted to the four different specific paediatric settings of the IRCCS Azienda Ospedaliero-Universitaria of Bologna, Italy and who required TDM-based CPAs for real-time personalization of antimicrobials between January 2021 and June 2021 were retrospectively assessed. Demographic and clinical features (age, gender, diagnosis), and CPAs were retrieved for each patient.

Two indicators of performance were defined in order to assess the usefulness of the CPAs for real-time optimization of antimicrobial dosing in the paediatric settings. First, the proportion of dosing adjustments (increase or reduction) recommended in the CPAs and applied by the attending clinicians over the total number of delivered CPAs in relation to the different settings and antimicrobials. Second, the turnaround time (TAT) of the antimicrobial CPA, defined as the timeframe elapsing between the delivery of the TDM sample to the LUM and the publication in the hospital intranet of the definitive TDM-guided CPA. The TAT of the antimicrobial CPA was defined as optimal, if < 12 h; quasi-optimal, if between 12–24 h; acceptable, if between 24–48 h and suboptimal, if > 48 h. The scale was predefined according to the feasibility in promptly providing paediatricians a real-time CPA, so that the recommended dosing adjustments could be implemented as quickly as possible after the delivery of TDM sample to the laboratory.

Data were expressed as mean ± standard deviation (SD) or median and interquartile range (IQR) according to data distribution, while categorical variables were expressed as count and percentage.

The study was approved by the local Ethic Committee (No. 443/2021/Oss/AOUBo).

RESULTS

Organizational Aspects of the Clinical Pharmacology Unit

The Clinical Pharmacology Unit is included in the Department for the Integrated Management of Infective Risk of the IRCCS

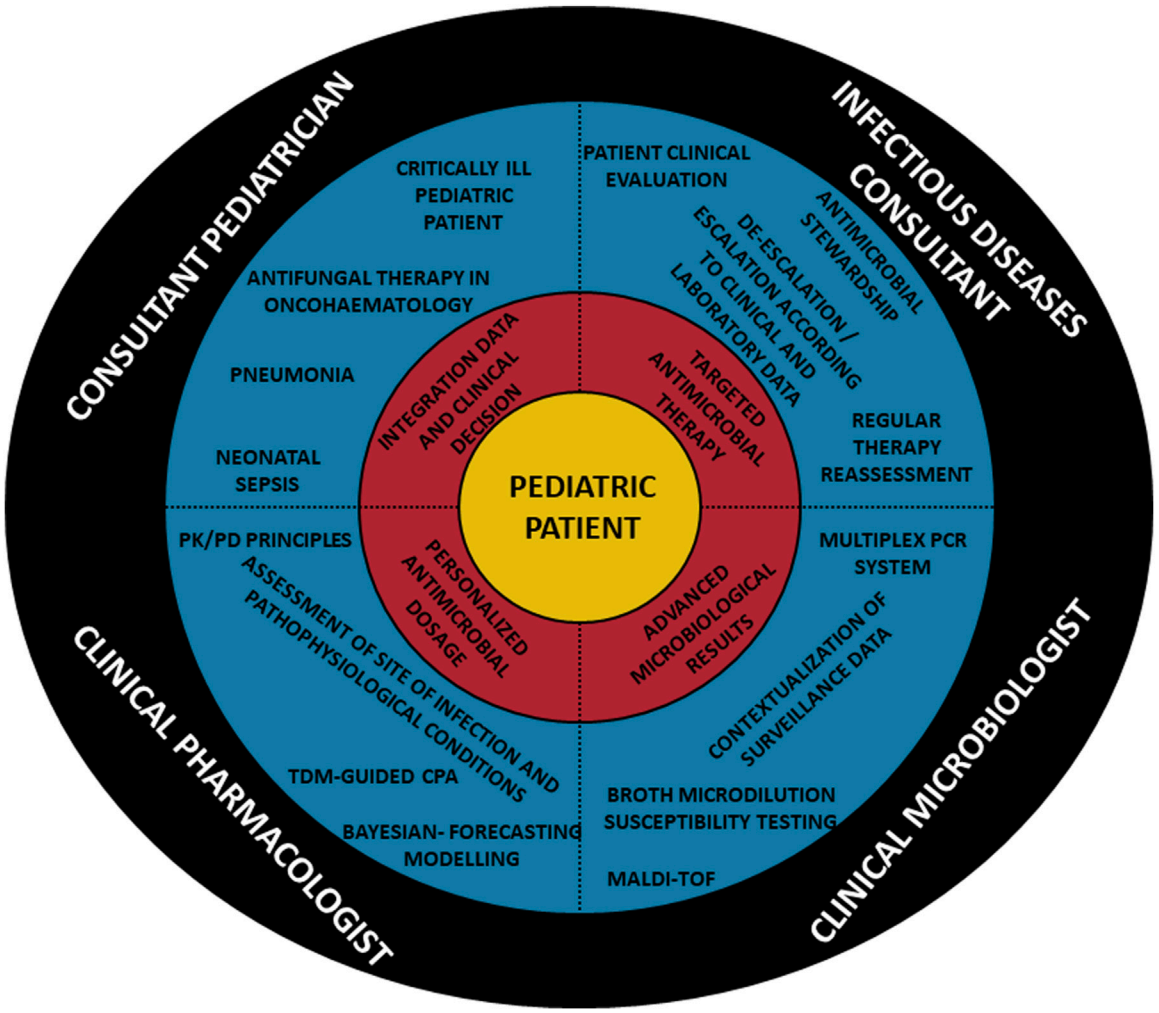

FIGURE 2 | Features of multidisciplinary taskforce involved in the management of empirical and targeted antimicrobial therapy in paediatric patients. CPA, clinical pharmacological advice; MALDI-TOF, Matrix Assisted Laser Desorption Ionization–Time of Flight; PK/PD, pharmacokinetic/pharmacodynamic; TDM, therapeutic drug monitoring.

Azienda Ospedaliero-Universitaria of Bologna. The priority goal consists in providing personalized CPAs for both inpatients and outpatients. An example of CPA performed in a specific paediatric scenario is shown in **Figure 1**. In the early period (Jan-Mar 2021), the main activity was to provide educational interventions in order to increase the awareness of clinicians regarding the importance that a real-time and integrated personalization of antimicrobial therapy may have in challenging paediatric scenarios. These interventions were based on dedicated webinars and on a specific on field work at the bedside aimed to identify which paediatric patients could have benefit more by a personalized CPAs, and to stress the importance of correct timing for TDM blood sampling in relation to the time of drug administration. The individualization of antimicrobial therapy in the paediatric population was made possible thanks to the implementation of a multidisciplinary taskforce composed by the pediatrician, the infectious disease consultant, the clinical microbiologist and the MD clinical pharmacologist. The main features of members involved in the multidisciplinary team and their coordinated and synergistic activities is shown in **Figure 2**.

Evaluation of the Impact of the CPAs in Different Hospital Paediatric Settings

Overall, during the 6-month period study, 247 CPAs were delivered to 53 paediatric patients (mean 4.7 ± 3.7 CPAs per patient). Median age of patients was 6 years (IQR 1–16 years), with no gender preponderance (male 49.1%). Leukemia and pneumonia were the most frequent underlying diseases, accounting for 39.6 and 20.8% of paediatric patients having CPAs, respectively (**Table 2**).

Most of the patients who received the CPAs were admitted to the paediatric onco-haematology/transplant unit (21;

TABLE 2 | Clinical and demographics features of paediatric patients in which at least one CPA for antimicrobial dosing adjustment was performed.

Demographics and clinical features	No. (%)
Age	
Median (years; IQR)	6 (1–16)
<1 year	9 (17.0%)
1–5 years	13 (24.5%)
5–12 years	15 (28.3%)
12–17 years	16 (30.2%)
Sex	
Male	26 (49.1%)
Female	27 (50.9%)
Weight	
Median (kg; IQR)	20 (11.1–31.8)
Height	
Median (cm; IQR)	120 (75.3–147)
Setting	
Neonatology	5 (9.4%)
Paediatric ICU	19 (35.9%)
Paediatric onco-haematology/Transplant Unit	21 (39.6%)
Emergency paediatric ward	8 (15.1%)
Underlying disease	
AML	12 (22.6%)
ALL	9 (17.0%)
HAP	9 (17.0%)
Solid neoplasms	4 (7.5%)
Meningo-ventriculitis	3 (5.7%)
Abdominal perforation	3 (5.7%)
Encephalopathy	3 (5.7%)
Neonatal sepsis	2 (3.8%)
CAP	2 (3.8%)
Necrotizing enterocolitis	2 (3.8%)
Others	4 (7.5%)

ALL, acute lymphatic leukaemia; AML, acute myeloid leukaemia; CAP, community-acquired pneumonia; HAP, hospital-acquired pneumonia; ICU, intensive care unit; IQR, interquartile range.

39.6%) and to the paediatric ICU (19; 35.8%), and overall received more than 80% of the total CPAs. The mean (±SD) number of CPAs per patient was higher in the paediatric onco-haematology/transplant unit and in the emergency paediatric ward, and amounted respectively to 6.2 ± 4.2 and 4.4 ± 4.9 (**Table 3**).

The CPAs concerned 17 out of the 18 antimicrobials for which the TDM was available, and were provided mainly for antibiotics (121; 49.0%) and for antifungals (112; 45.3%). Overall, 84.0% of the CPAs delivered to the paediatric ICU concerned antibiotics, and 78.5% of those delivered to the paediatric onco-haematology/transplant unit regarded azole antifungals. The total number of CPAs requested for each antimicrobial were ≥10 for four antibiotics (piperacillin-tazobactam, meropenem, linezolid, and teicoplanin), four antifungals (isavuconazole, voriconazole, posaconazole, and fluconazole), and for the antiviral ganciclovir (**Table 4**). The most frequently requested CPAs concerned isavuconazole (47; 19.0%) and voriconazole (44; 17.8%).

Overall, the CPAs recommended dosing adjustments in 37.7% of cases, and suggested increases in 24.3% and decreases in the other 13.4% (**Figure 3**). Most of the dosing adjustments were needed in the paediatric ICU patients (48%), with increases and decreases almost equally distributed.

In regard to each single antimicrobial agent, dose adjustments were recommended in 70.5 and 50.0% of CPAs concerning voriconazole and piperacillin-tazobactam, respectively. Dose increases concerned mainly voriconazole (20 cases; 45.5%) and meropenem (12 cases; 35.3%), whereas dose reductions were needed mainly for piperacillin-tazobactam (12 cases; 33.3%) and voriconazole (11 cases; 25.0%). Conversely, dose adjustments were considered unnecessary in most of the CPAs delivered for isavuconazole (95.7%), fluconazole (90.0%), teicoplanin (85.7%), and posaconazole (80.0%).

Median CPA turnaround time (TAT) was 7.5 h (IQR 6.1–8.8 h). No significant differences in median TAT was observed among the different paediatric setting (ranging from 6.4 h for neonatology to 8.2 h for paediatric onco-haematology/transplant unit) (**Figure 4**). Overall, CAP TAT was optimal in 91.5% of cases, and quasi-optimal in 96.0% of cases. Among the antimicrobials accounting for most of the delivered CPAs, the median TAT ranged between 6.4 h (IQR 4.1–7.5 h) for teicoplanin and 8.8 h (IQR 8.7–16.3 h) for posaconazole.

DISCUSSION

Our study provides a proof of concept of the helpful role that the CPAs based on TDM may have in optimizing antimicrobial exposure on real time in different populations and setting of hospitalized paediatric patient.

TABLE 3 | Number of clinical pharmacological advice performed in different paediatric settings.

Paediatric setting	No. of patients	Median age (IQR; years)	Male proportion	No. of CPA	CPA/patient
Neonatology	5	0.08 (0.06–0.16)	4 (80.0%)	7	1.4 ± 0.9
Paediatric ICU	19	4 (1.5–15)	5 (26.3%)	75	3.9 ± 2.1
Oncohaematology/Transplant Unit	21	9 (6–18)	13 (61.9%)	130	6.2 ± 4.2
Emergency paediatric ward	8	12.5 (5–18)	4 (50.0%)	35	4.4 ± 4.9
Overall	53	6 (1–16)	26 (49.1%)	247	4.7 ± 3.7

CPA, clinical pharmacology advice; ICU, intensive care unit, IQR: interquartile range

TABLE 4 | Antimicrobials with ≥10 CPAs delivered in the study period and the proportion of recommended dosing adjustments.

Drug	No. of CPA	No. of patients	CPA/patient	Dosing adjustment		
				Increased	Decreased	None
Antibiotics						
Piperacillin-Tazobactam	36	9	4	6 (16.7%)	12 (33.3%)	18 (50.0%)
Meropenem	34	10	3.4	12 (35.3%)	2 (5.9%)	20 (58.8%)
Linezolid	21	6	3.5	3 (14.3%)	5 (23.8%)	13 (61.9%)
Teicoplanin	14	1	14	2 (14.3%)	0 (0.0%)	12 (85.7%)
Antifungals						
Isavuconazole	47	5	9.4	2 (4.3%)	0 (0.0%)	45 (95.7%)
Voriconazole	44	6	7.3	20 (45.5%)	11 (25.0%)	13 (29.5%)
Fluconazole	10	2	5	1 (10.0%)	0 (0.0%)	9 (90.0%)
Posaconazole	10	1	10	2 (20.0%)	0 (0.0%)	8 (80.0%)
Antivirals						
Ganciclovir	10	1	10	3 (30.0%)	1 (10.0%)	6 (60.0%)

CPA, clinical pharmacology advice.

Both the indicators of performance of the CPAs may support the clinical utility of this approach. Dosing adjustments were needed in more than one third of cases, and the TAT of the CPAs was optimal in the vast majority of cases. This allowed clinicians to promptly implement recommended antimicrobial dosing adjustments in different challenging scenarios, and involved agents characterized by wide inter- and intraindividual variability according to specific pharmacokinetic-pharmacogenetic issues (e.g., voriconazole) (Bartelink et al., 2013) or underlying conditions (e.g., beta-lactams in critically ill children) (Marsot, 2018; Dhont et al., 2020), as found in our analysis. The prompt dosing adaptation may minimize either the risk of antimicrobial underexposure potentially associated with therapeutic failure, or those of overexposure potentially associated with toxicity.

In the last 10 years, TDM emerged as a valuable tool for assisting clinicians in optimizing antimicrobial dosing in different paediatric settings (Jager et al., 2016; Pauwels and Allegaert, 2016; John et al., 2019; De Rose et al., 2020; Hartman et al., 2020). The real added value of the CPA consists in the possibility of personalizing drug exposure on real-time in each single patient according to the antimicrobial susceptibility of the clinical isolate, the site of infection, the pathophysiological underlying conditions, and/or the drug-drug interactions of cotreatments. The innovative feature of this approach represents a paradigm shift in the TDM era. It is based on a multidisciplinary taskforce that may optimally handle complex hospitalized paediatric patients affected by severe infections, similarly to what just retrieved in other challenging scenarios (Viale et al., 2017; Gatti et al., 2019).

Antimicrobial use is quite frequent among hospitalized children, possibly exceeding 50% of cases in some paediatric settings (van Houten et al., 1998). Unfortunately, for most antimicrobials well-defined paediatric posology based on specific pharmacokinetic and/or pharmacokinetic/pharmacodynamic studies carried out in this patient population are currently lacking (Korth-Bradley, 2018) (Kearns et al., 2003; Ferro, 2015; De Rose et al., 2020). Consequently, our approach may represent the best way for dealing with the issue of appropriate treatment of infections in the paediatric setting. In this regard, we are confident that the implementation of TDM-guided CPAs for personalizing antimicrobial treatment could be of benefit especially in four challenging paediatric scenarios of infection.

Sepsis and Septic Shock in Critically Ill Paediatric Patients

Sepsis and septic shock represent a major cause of ICU admission and mortality among critically ill paediatric patients (Garcia et al., 2020). The American College of Critical Medicine/Pediatric Advanced Life Support protocol recommends the administration of antibiotic therapy within the first hours of sepsis diagnosis (Davis et al., 2017). Although the adherence to this approach has been associated with improved patient care quality and reduced mortality (Weiss et al., 2014; Balamuth et al., 2016), the choice of appropriate antimicrobial dosing may result extremely challenging in this scenario. Consequently, the failure in achieving optimal PK/PD target may lead to an increased risk of antimicrobial inefficacy or toxicity.

Pathophysiological alterations in volume of distribution, plasma protein binding, and drug clearance, coupled with dynamic age-associated physiological variations in glomerular filtration rate and/or in drug metabolizing enzymes, may lead to non-attainment of the PK/PD targets of antimicrobials in the critically ill paediatric patients (Kearns et al., 2003; Marsot, 2018; Dhont et al., 2020; Hartman et al., 2020).

Our findings showing that dosing adjustments were needed in almost 50% of the CPAs delivered for ICU paediatric patients support this hypothesis. It has been shown that the prevalence of augmented renal clearance among critically ill children may be higher than 25% (Dhont et al., 2020). This means that the need for personalized TDM-guided CPAs could be remarkable especially for antimicrobials that are eliminated by the renal route, like beta-lactams, for which dosage increases are frequently required in this setting.

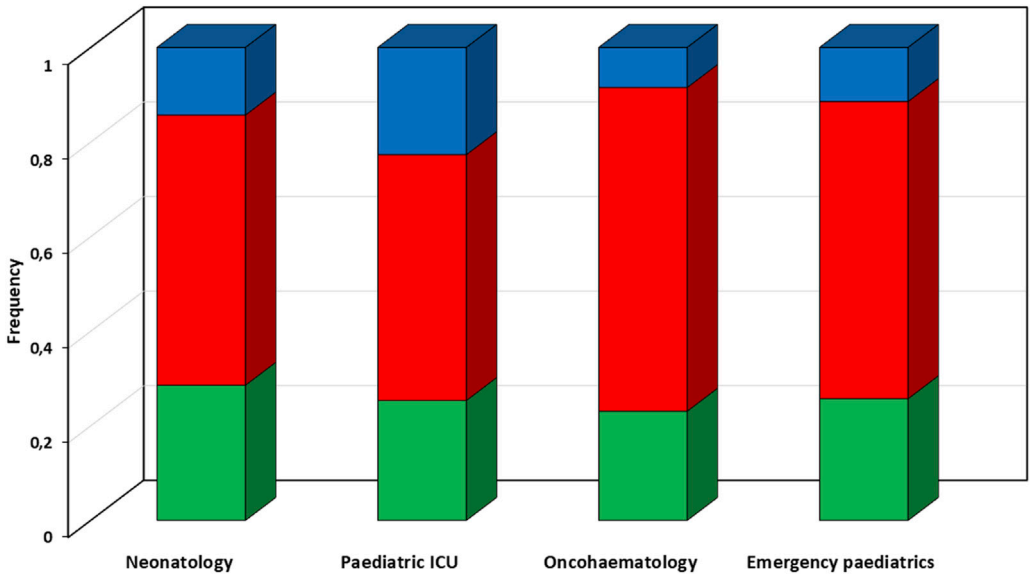

FIGURE 3 | Proportion of types of recommended dosing adjustments according to different paediatric settings. Red box, suggested dosing increase; green box, suggested dosing confirm; blue box, suggested dosing reduction. ICU, intensive care unit.

Neonatal Sepsis

Neonatal sepsis is a systemic condition of bacterial, viral, or fungal etiology associated with haemodynamic changes and other clinical manifestations that may result in remarkable morbidity and mortality (Shane et al., 2017). Different causative agents may be identified in early-compared to late-onset sepsis, leading to different therapeutic strategies (Shane et al., 2017). Empirical therapy of early-onset neonatal sepsis is based on the combination of ampicillin plus an aminoglycoside, whereas that of late-onset neonatal sepsis is based on the combination of vancomycin plus an aminoglycoside (Shane et al., 2017). Additionally, linezolid could represent a valuable alternative in neonatal ICUs with high prevalence of vancomycin-resistant Enterococci (Subramanya et al., 2019).

Antimicrobial TDM may be very helpful in this challenging scenario, considering that in the newborns the relationship between drug dose and exposure is quite unpredictable, especially in the pre-terms, due to the abrupt developmental physiological changes that occur in this age period (Pauwels and Allegaert, 2016; De Rose et al., 2020). In this regard, several evidences support the potential role of TDM in the management of neonatal sepsis (Hoff et al., 2009; Touw et al., 2009; Sicard et al., 2015; Sosnin et al., 2019; Tauzin et al., 2019).

In our study CPAs in neonatal septic patients were performed only in seven cases, but it is worth noting that dosing adjustments were need in almost half of these. This may support the need for implementing personalized TDM-guided CPAs in this challenging scenario. Indeed, the low number of CPAs delivered in this setting is justified strictly by ethical and clinical restrictions. Venipuncture is distressing and painful in this fragile population (although in unstable neonates the umbilical vein is commonly catheterized), and extensive sampling should be avoided because of the risk of iatrogenic anemia possibly resulting in requirement for blood transfusions (De Rose et al., 2020). We are now dealing with this issue by implementing a new rapid mass spectrometry method based on capillary microsampling (50 µL) that will make feasible to quantify 14 different antibiotics in each microsample, as showed previously by Bacco et al. (Barco et al., 2020). This would greatly contribute in increasing the feasibility of TDM-based CPAs in the neonatal setting.

Antifungal Prophylaxis or Treatment With Azoles in Onco-haematological Paediatric Patients

Invasive fungal infections represent a major cause of morbidity and mortality in children who are affected by onco-haematological malignancies or who need allogeneic haemopoietic stem-cell transplantation (Groll and Tragiannidis, 2010; Dvorak et al., 2012; Pana et al., 2017; Arad-Cohen et al., 2020; Groll et al., 2021). The breakdown in natural barriers due to mucositis and the need for indwelling catheters coupled with immunosuppression caused by underlying onco-haematological disease and/or myelosuppressive chemotherapy may represent major determinants of the increased risk of invasive fungal infections in this scenario (Dvorak et al., 2012).

Aspergillus spp are responsible for a large proportion of invasive fungal infections, followed by *Candida* species. Triazoles represent the most important class of antifungal agents for prophylaxis and treatment of invasive fungal infections (Groll and Tragiannidis, 2010). Unfortunately, the use of azoles is challenged by several pharmacokinetic and

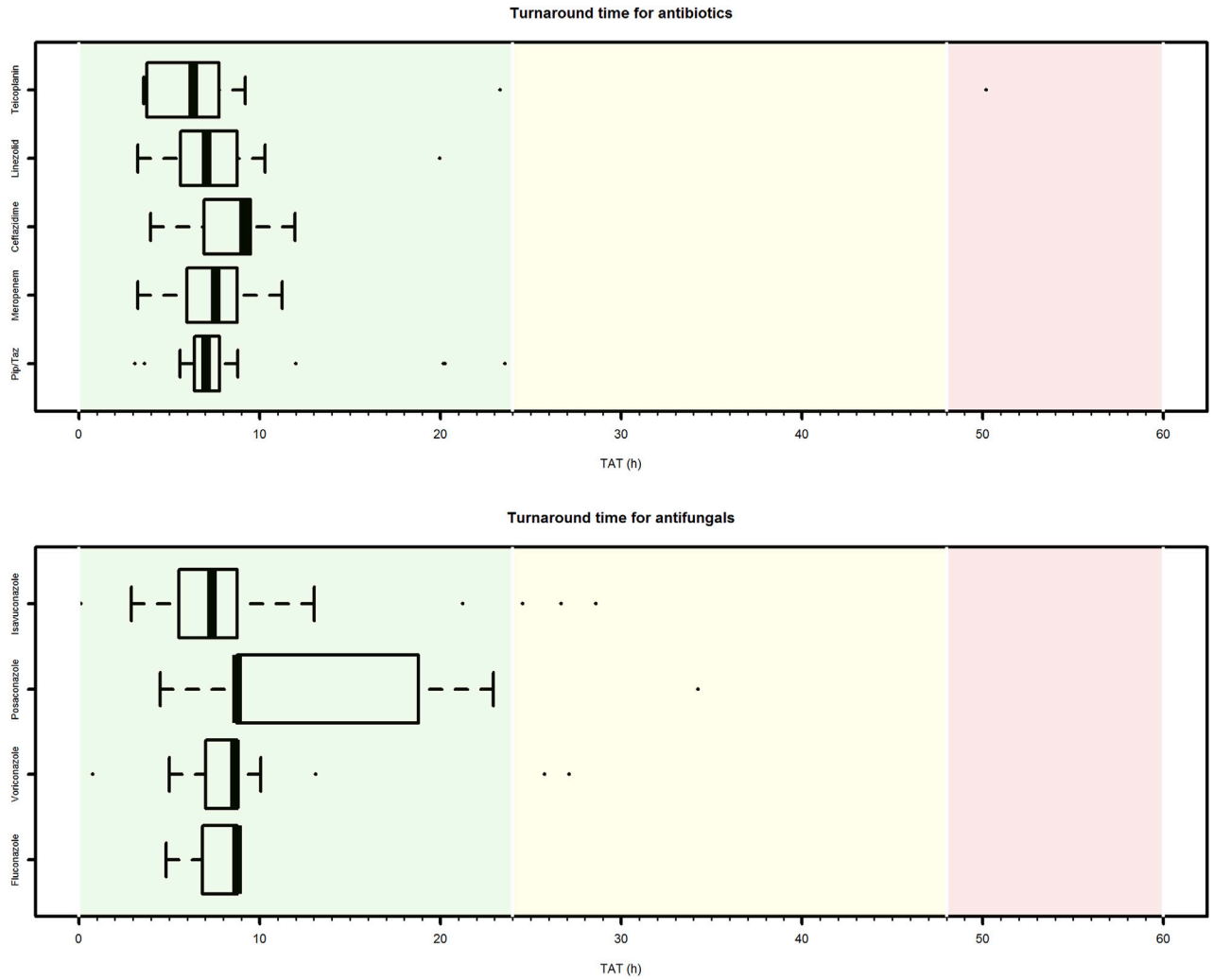

FIGURE 4 | Box plot of turnaround time of clinical pharmacological advices (CPAs) for antimicrobial dosing regimen individualization in paediatric settings. Only antibiotic or antifungal agents for which at least ten CPAs were delivered are showed. Pip/Taz, piperacillin/tazobactam.

pharmacogenetic issues in the paediatric scenario (Bury et al., 2021). Large interindividual and intraindividual variability in azole exposure is frequently present among oncohaematologic paediatric patients, especially for voriconazole. Additionally, the remarkable risk of clinically relevant drug-drug interactions with immunosuppressants and/or chemotherapeutic agents may make the achievement of therapeutic targets of exposure even more difficult. TDM-guided approach has just been considered to play a relevant role in the optimization of antifungal prophylaxis/treatment among onco-haematological paediatric patients (Groll et al., 2017; Allegra et al., 2018; Lempers et al., 2019).

Our data support this, as in almost 30% of the CPAs delivered in onco-haematological paediatric dosing adjustments of voriconazole were needed. This approach could minimize the risk of antifungal underexposure that may cause breakthrough invasive fungal infections, and/or that of overexposure, possibly causing toxicity (e.g., hepatotoxicity), in relation to drug-drug interactions, pharmacogenetic issues, or disease-related organ failure (Kyriakidis et al., 2017; Bury et al., 2021).

Community-Acquired Pneumonia (CAP) in Hospitalized Children

CAP is a common and potentially severe infection, with high incidence and relevant morbidity and mortality among children (McIntosh, 2002; Gupta et al., 2018), and is one of the major causes of admission to the emergency paediatric wards (Nascimento-Carvalho, 2020). Although respiratory viruses are the major causative pathogens in children under 5 years, also bacteria may play a relevant role. *Streptococcus pneumoniae*, *Haemophilus influenzae*, and *Mycoplasma pneumoniae* represent the most frequent bacterial pathogens (Gupta et al., 2018; Nascimento-Carvalho and Nascimento-Carvalho, 2019;

Nascimento-Carvalho, 2020). Ampicillin represents the first-line antibiotic therapy in hospitalized children with CAP. Vancomycin or linezolid should be considered in presence of CA-MRSA (Gupta et al., 2018; Nascimento-Carvalho, 2020).

TDM could be a valuable tool in optimizing antibiotic therapy in paediatric patients with severe CAP admitted in the emergency ward, as suggested by the fact that in our study approximately 20% of CPAs were performed in this setting. Both ampicillin and vancomycin are hydrophilic antimicrobials whose pharmacokinetic variability could be considered high and unpredictable in this scenario. In this regard, antibiotic dosing adjustments were recommended in more than 60% of cases, even if we recognize that the total number of delivered CPAs was quite low. These findings may justify the need for implementing personalized TDM-guided CPAs in paediatric patients affected by severe pneumonia, similarly to that has been suggested for adults (Pea and Viale, 2006).

Conclusion

In conclusion, our study provides a proof of concept of the helpful role that CPAs based on real-time TDM may have in optimizing antimicrobial exposure in different challenging paediatric scenarios. Although we recognize that the short duration of the study period and the limited sample size may be potential limitations, the non-negligible proportion of recommended dosing adjustments coupled with the optimal performance of TAT support the feasibility and usefulness of this approach. The forthcoming implementation of innovative methods based on capillary microsampling will make sample collection even more feasible in the paediatric setting, and this may hopefully lead to a relevant growth in the use of personalized TDM-guided CPAs for optimizing antimicrobial treatment.

DATA AVAILABILITY STATEMENT

The raw data supporting the conclusions of this article will be made available by the authors, without undue reservation.

ETHICS STATEMENT

The studies involving human participants were reviewed and approved by Azienda Ospedaliero Universitaria di Bologna Ethic Committee (No. 443/2021/Oss/AOUBo). Written informed consent from the participants' legal guardian/next of kin was not required to participate in this study in accordance with the national legislation and the institutional requirements.

AUTHOR CONTRIBUTIONS

MG, PC and FP made substantial contribution to study conception and design. MG and PC made substantial contribution to acquisition and analysis of data. MG, PC and FP made substantial contribution to interpretation of data. MG and PC were involved in drafting the article. All authors revised the article critically for important intellectual content. All authors approved the final version of the article.

REFERENCES

Abdul-Aziz, M. H., Alffenaar, J. C., Bassetti, M., Bracht, H., Dimopoulos, G., Marriott, D., et al. (2020). Antimicrobial Therapeutic Drug Monitoring in Critically Ill Adult Patients: a Position Paper. *Intensive Care Med.* 46, 1127–1153. doi:10.1007/s00134-020-06050-1

Allegra, S., Fatiguso, G., De Francia, S., Favata, F., Pirro, E., Carcieri, C., et al. (2018). Therapeutic Drug Monitoring of Voriconazole for Treatment and Prophylaxis of Invasive Fungal Infection in Children. *Br. J. Clin. Pharmacol.* 84, 197–203. doi:10.1111/bcp.13401

Arad-Cohen, N., Rowe, J. M., and Shachor-Meyouhas, Y. (2020). Pharmacological Prophylaxis of Infection in Pediatric Acute Myeloid Leukemia Patients. *Expert Opin. Pharmacother.* 21, 193–205. doi:10.1080/14656566.2019.1701654

Balamuth, F., Weiss, S. L., Fitzgerald, J. C., Hayes, K., Centkowski, S., Chilutti, M., et al. (2016). Protocolized Treatment Is Associated with Decreased Organ Dysfunction in Pediatric Severe Sepsis. *Pediatr. Crit. Care Med.* 17, 817–822. doi:10.1097/PCC.0000000000000858

Barco, S., Mesini, A., Barbagallo, L., Maffia, A., Tripodi, G., Pea, F., et al. (2020). A Liquid Chromatography-Tandem Mass Spectrometry Platform for the Routine Therapeutic Drug Monitoring of 14 Antibiotics: Application to Critically Ill Pediatric Patients. *J. Pharm. Biomed. Anal.* 186, 113273. doi:10.1016/j.jpba.2020.113273

Bartelink, I. H., Wolfs, T., Jonker, M., de Waal, M., Egberts, T. C., Ververs, T. T., et al. (2013). Highly Variable Plasma Concentrations of Voriconazole in Pediatric Hematopoietic Stem Cell Transplantation Patients. *Antimicrob. Agents Chemother.* 57, 235–240. doi:10.1128/AAC.01540-12

Bury, D., Tissing, W. J. E., Muilwijk, E. W., Wolfs, T. F. W., and Brüggemann, R. J. (2021). Clinical Pharmacokinetics of Triazoles in Pediatric Patients. *Clin. Pharmacokinet.* 60, 1103–1147. doi:10.1007/s40262-021-00994-3

Collins, F. S., and Varmus, H. (2015). A New Initiative on Precision Medicine. *N. Engl. J. Med.* 372, 793–795. doi:10.1056/NEJMp1500523

Davis, A. L., Carcillo, J. A., Aneja, R. K., Deymann, A. J., Lin, J. C., Nguyen, T. C., et al. (2017). American College of Critical Care Medicine Clinical Practice Parameters for Hemodynamic Support of Pediatric and Neonatal Septic Shock. *Crit. Care Med.* 45, 1061–1093. doi:10.1097/CCM.0000000000002425

De Rose, D. U., Cairoli, S., Dionisi, M., Santisi, A., Massenzi, L., Goffredo, B. M., et al. (2020). Therapeutic Drug Monitoring Is a Feasible Tool to Personalize Drug Administration in Neonates Using New Techniques: An Overview on the Pharmacokinetics and Pharmacodynamics in Neonatal Age. *Int. J. Mol. Sci.* 21, E5898. doi:10.3390/ijms21165898

Dhont, E., Van Der Heggen, T., De Jaeger, A., Vande Walle, J., De Paepe, P., and De Cock, P. A. (2020). Augmented Renal Clearance in Pediatric Intensive Care: Are We Undertreating Our Sickest Patients? *Pediatr. Nephrol.* 35, 25–39. doi:10.1007/s00467-018-4120-2

Dvorak, C. C., Fisher, B. T., Sung, L., Steinbach, W. J., Nieder, M., Alexander, S., et al. (2012). Antifungal Prophylaxis in Pediatric Hematology/oncology: New Choices & New Data. *Pediatr. Blood Cancer* 59, 21–26. doi:10.1002/pbc.23415

Ferro, A. (2015). Paediatric Prescribing: Why Children Are Not Small Adults. *Br. J. Clin. Pharmacol.* 79, 351–353. doi:10.1111/bcp.12540

Funk, R. S., Brown, J. T., and Abdel-Rahman, S. M. (2012). Pediatric Pharmacokinetics: Human Development and Drug Disposition. *Pediatr. Clin. North. Am.* 59, 1001–1016. doi:10.1016/j.pcl.2012.07.003

Garcia, P. C. R., Tonial, C. T., and Piva, J. P. (2020). Septic Shock in Pediatrics: the State-Of-The-Art. *J. Pediatr. (Rio J.* 96 Suppl 1 (Suppl. 1), 87–98. doi:10.1016/j.jped.2019.10.007

Gatti, M., Gasparini, L. E., Laratta, M., Sigurtà, A., Rossi, A., Brioschi, P., et al. (2019). Intensive Multidisciplinary Management in Critical Care Patients Affected by Severe Necrotizing Soft Tissue Infections: a Cooperative Method to Improve the Efficacy of Treatment. *Eur. J. Clin. Microbiol. Infect. Dis.* 38, 1153–1162. doi:10.1007/s10096-019-03521-2

Groll, A. H., Pana, D., Lanternier, F., Mesini, A., Ammann, R. A., Averbuch, D., et al. (2021). 8th European Conference on Infections in Leukaemia: 2020 Guidelines for the Diagnosis, Prevention, and Treatment of Invasive Fungal Diseases in Paediatric Patients with Cancer or post-haematopoietic Cell Transplantation. *Lancet Oncol.* 22, e254–e269. doi:10.1016/S1470-2045(20)30723-3

Groll, A. H., Townsend, R., Desai, A., Azie, N., Jones, M., Engelhardt, M., et al. (2017). Drug-drug Interactions between Triazole Antifungal Agents Used to Treat Invasive Aspergillosis and Immunosuppressants Metabolized by Cytochrome P450 3A4. *Transpl. Infect. Dis.* 19. doi:10.1111/tid.12751

Groll, A. H., and Tragiannidis, A. (2010). Update on Antifungal Agents for Paediatric Patients. *Clin. Microbiol. Infect.* 16, 1343–1353. doi:10.1111/j.1469-0691.2010.03334.x

Gupta, S., Lodha, R., and Kabra, S. K. (2018). Antimicrobial Therapy in Community-Acquired Pneumonia in Children. *Curr. Infect. Dis. Rep.* 20, 47. doi:10.1007/s11908-018-0653-6

Hartman, S. J. F., Brüggemann, R. J., Orriëns, L., Dia, N., Schreuder, M. F., and de Wildt, S. N. (2020). Pharmacokinetics and Target Attainment of Antibiotics in Critically Ill Children: A Systematic Review of Current Literature. *Clin. Pharmacokinet.* 59, 173–205. doi:10.1007/s40262-019-00813-w

Hayton, W. L. (2000). Maturation and Growth of Renal Function: Dosing Renally Cleared Drugs in Children. *AAPS PharmSci.* 2, E3. doi:10.1208/ps020103

Hoff, D. S., Wilcox, R. A., Tollefson, L. M., Lipnik, P. G., Commers, A. R., and Liu, M. (2009). Pharmacokinetic Outcomes of a Simplified, Weight-Based, Extended-Interval Gentamicin Dosing Protocol in Critically Ill Neonates. *Pharmacotherapy* 29, 1297–1305. doi:10.1592/phco.29.11.1297

Hsu, A. J., and Tamma, P. D. (2014). Treatment of Multidrug-Resistant Gram-Negative Infections in Children. *Clin. Infect. Dis.* 58, 1439–1448. doi:10.1093/cid/ciu069

Jager, N. G., van Hest, R. M., Lipman, J., Taccone, F. S., and Roberts, J. A. (2016). Therapeutic Drug Monitoring of Anti-infective Agents in Critically Ill Patients. *Expert Rev. Clin. Pharmacol.* 9, 961–979. doi:10.1586/17512433.2016.1172209

John, J., Loo, A., Mazur, S., and Walsh, T. J. (2019). Therapeutic Drug Monitoring of Systemic Antifungal Agents: a Pragmatic Approach for Adult and Pediatric Patients. *Expert Opin. Drug Metab. Toxicol.* 15, 881–895. doi:10.1080/17425255.2019.1671971

Kearns, G. L., Abdel-Rahman, S. M., Alander, S. W., Blowey, D. L., Leeder, J. S., and Kauffman, R. E. (2003). Developmental Pharmacology-Ddrug Disposition, Action, and Therapy in Infants and Children. *N. Engl. J. Med.* 349, 1157–1167. doi:10.1056/NEJMra035092

Korth-Bradley, J. M. (2018). The Path to Perfect Pediatric Posology - Drug Development in Pediatrics. *J. Clin. Pharmacol.* 58 Suppl 10 (Suppl. 10), S48–S57. doi:10.1002/jcph.1081

Kyriakidis, I., Tragiannidis, A., Munchen, S., and Groll, A. H. (2017). Clinical Hepatotoxicity Associated with Antifungal Agents. *Expert Opin. Drug Saf.* 16, 149–165. doi:10.1080/14740338.2017.1270264

Le, J., and Bradley, J. S. (2018). Optimizing Antibiotic Drug Therapy in Pediatrics: Current State and Future Needs. *J. Clin. Pharmacol.* 58 Suppl 10 (Suppl. 10), S108–S122. doi:10.1002/jcph.1128

Lempers, V. J., Meuwese, E., Mavinkurve-Groothuis, A. M., Henriet, S., van der Sluis, I. M., Hanff, L. M., et al. (2019). Impact of Dose Adaptations Following Voriconazole Therapeutic Drug Monitoring in Pediatric Patients. *Med. Mycol.* 57, 937–943. doi:10.1093/mmy/myz006

Marsot, A. (2018). Pharmacokinetic Variability in Pediatrics and Intensive Care: Toward a Personalized Dosing Approach. *J. Pharm. Pharm. Sci.* 21, 354–362. doi:10.18433/jpps30082

McIntosh, K. (2002). Community-acquired Pneumonia in Children. *N. Engl. J. Med.* 346, 429–437. doi:10.1056/NEJMra011994

Moore, P. (1998). Children Are Not Small Adults. *Lancet* 352, 630. doi:10.1016/S0140-6736(05)79591-X

Nascimento-Carvalho, A. C., and Nascimento-Carvalho, C. M. (2019). Clinical Management of Community-Acquired Pneumonia in Young Children. *Expert Opin. Pharmacother.* 20, 435–442. doi:10.1080/14656566.2018.1552257

Nascimento-Carvalho, C. M. (2020). Community-acquired Pneumonia Among Children: the Latest Evidence for an Updated Management. *J. Pediatr. (Rio J.* 96 Suppl 1 (Suppl. 1), 29–38. doi:10.1016/j.jped.2019.08.003

Pana, Z. D., Roilides, E., Warris, A., Groll, A. H., and Zaoutis, T. (2017). Epidemiology of Invasive Fungal Disease in Children. *J. Pediatr. Infect Dis Soc* 6 (S3), S3–S11. doi:10.1093/jpids/pix046

Pauwels, S., and Allegaert, K. (2016). Therapeutic Drug Monitoring in Neonates. *Arch. Dis. Child.* 101, 377–381. doi:10.1136/archdischild-2013-305309

Pea, F., and Viale, P. (2006). The Antimicrobial Therapy Puzzle: Could Pharmacokinetic-Pharmacodynamic Relationships Be Helpful in Addressing the Issue of Appropriate Pneumonia Treatment in Critically Ill Patients? *Clin. Infect. Dis.* 42, 1764–1771. doi:10.1086/504383

Shane, A. L., Sánchez, P. J., and Stoll, B. J. (2017). Neonatal Sepsis. *Lancet* 390, 1770–1780. doi:10.1016/S0140-6736(17)31002-4

Sicard, M., Launay, E., Caillon, J., Jacqueline, C., Legrand, A., Deslandes, G., et al. (2015). Pharmacokinetics of Linezolid Treatment Using Intravenous and Oral Administrations in Extremely Premature Infants. *Eur. J. Clin. Pharmacol.* 71, 611–615. doi:10.1007/s00228-015-1813-3

Sosnin, N., Curtis, N., Cranswick, N., Chiletti, R., and Gwee, A. (2019). Vancomycin Is Commonly Under-dosed in Critically Ill Children and Neonates. *Br. J. Clin. Pharmacol.* 85, 2591–2598. doi:10.1111/bcp.14084

Subramanya, S. H., Amberpet, R., Chaudhary, D., Nayak, N., Padukone, S., Bairy, I., et al. (2019). Neonatal Sepsis Due to Glycopeptide Resistant Enterococcus Faecium from Colonized Maternal Gut- Rare Case Evidence. *Antimicrob. Resist. Infect. Control.* 8, 29. doi:10.1186/s13756-019-0490-x

Tauzin, M., Cohen, R., Durrmeyer, X., Dassieu, G., Barre, J., and Caeymaex, L. (2019). Continuous-Infusion Vancomycin in Neonates: Assessment of a Dosing Regimen and Therapeutic Proposal. *Front. Pediatr.* 7, 188. doi:10.3389/fped.2019.00188

Touw, D. J., Westerman, E. M., and Sprij, A. J. (2009). Therapeutic Drug Monitoring of Aminoglycosides in Neonates. *Clin. Pharmacokinet.* 48, 71–88. doi:10.2165/00003088-200948020-00001

van Houten, M. A., Luinge, K., Laseur, M., and Kimpen, J. L. (1998). Antibiotic Utilisation for Hospitalised Paediatric Patients. *Int. J. Antimicrob. Agents* 10, 161–164. doi:10.1016/s0924-8579(98)00022-3

Viale, P., Tedeschi, S., Scudeller, L., Attard, L., Badia, L., Bartoletti, M., et al. (2017). Infectious Diseases Team for the Early Management of Severe Sepsis and Septic Shock in the Emergency Department. *Clin. Infect. Dis.* 65, 1253–1259. doi:10.1093/cid/cix548

Weiss, S. L., Fitzgerald, J. C., Balamuth, F., Alpern, E. R., Lavelle, J., Chilutti, M., et al. (2014). Delayed Antimicrobial Therapy Increases Mortality and Organ Dysfunction Duration in Pediatric Sepsis. *Crit. Care Med.* 42, 2409–2417. doi:10.1097/CCM.0000000000000509

Conflict of Interest: The authors declare that the research was conducted in the absence of any commercial or financial relationships that could be construed as a potential conflict of interest.

frontiers in Pharmacology

PERSPECTIVE
published: 01 October 2021
doi: 10.3389/fphar.2021.749692

Pediatric Therapeutic Drug Monitoring for Selective Serotonin Reuptake Inhibitors

Jeffrey R. Strawn[1,2,3]*, *Ethan A. Poweleit*[2,4,5,6], *Chakradhara Rao S. Uppugunduri*[7] and *Laura B. Ramsey*[2,4]

[1]Anxiety Disorders Research Program, Department of Psychiatry and Behavioral Neuroscience, University of Cincinnati, Cincinnati, OH, United States, [2]Division of Clinical Pharmacology, Cincinnati Children's Hospital Medical Center, Department of Pediatrics, University of Cincinnati College of Medicine, Cincinnati, OH, United States, [3]Division of Child and Adolescent Psychiatry, Department of Pediatrics, Cincinnati Children's Hospital Medical Center, Cincinnati, OH, United States, [4]Division of Research in Patient Services, Cincinnati Children's Hospital Medical Center, Department of Pediatrics, University of Cincinnati College of Medicine, Cincinnati, OH, United States, [5]Division of Biomedical Informatics, Cincinnati Children's Hospital Medical Center, Cincinnati, OH, United States, [6]Department of Biomedical Informatics, University of Cincinnati College of Medicine, Cincinnati, OH, United States, [7]CANSEARCH Research Platform in Pediatric Oncology and Hematology, Department of Pediatrics, Gynecology and Obstetrics, University of Geneva, Geneva, Switzerland

Therapeutic drug monitoring (TDM) is uncommon in child and adolescent psychiatry, particularly for selective serotonin reuptake inhibitors (SSRIs)—the first-line pharmacologic treatments for depressive and anxiety disorders. However, TDM in children and adolescents offers the opportunity to leverage individual variability of antidepressant pharmacokinetics to shed light on non-response and partial response, understand drug-drug interactions, evaluate adherence, and characterize the impact of genetic and developmental variation in pharmacokinetic genes. This perspective aims to educate clinicians about TDM principles and examines evolving uses of TDM in SSRI-treated youths and their early applications in clinical practice, as well as barriers to TDM in pediatric patients. First, the impact of pharmacokinetic genes on SSRI pharmacokinetics in youths could be used to predict tolerability and response for some SSRIs (*e.g.*, escitalopram). Second, plasma concentrations are significantly influenced by adherence, which may relate to decreased efficacy. Third, pharmacometric analyses reveal interactions with proton pump inhibitors, oral contraceptives, cannabinoids, and SSRIs in youths. Rapid developments in TDM and associated modeling have enhanced the understanding of variation in SSRI pharmacokinetics, although the treatment of anxiety and depressive disorders with SSRIs in youths often remains a trial-and-error process.

Keywords: therapeutic drug monitoring, selective serotonin reuptake inhibitor, depressive disorder, anxiety disorder, tolerability, pediatric, child and adolescent psychiatry

OPEN ACCESS

Edited by:
Erwin Dreesen,
KU Leuven, Belgium

Reviewed by:
Shirley Seo,
United States Food and Drug Administration, United States
Silvia M. Illamola,
University of Minnesota Twin Cities, United States

***Correspondence:**
Jeffrey R. Strawn
strawnjr@ucmail.uc.edu

Specialty section:
This article was submitted to Obstetric and Pediatric Pharmacology, a section of the journal Frontiers in Pharmacology

Received: *29 July 2021*
Accepted: *20 September 2021*
Published: *01 October 2021*

Citation:
Strawn JR, Poweleit EA, Uppugunduri CRS and Ramsey LB (2021) Pediatric Therapeutic Drug Monitoring for Selective Serotonin Reuptake Inhibitors. Front. Pharmacol. 12:749692. doi: 10.3389/fphar.2021.749692

INTRODUCTION

Therapeutic drug monitoring (TDM)—the determination of medication concentrations in patients with the goal of optimizing medication dosing—is uncommon in child and adolescent psychiatry, potentially owing to numerous barriers that have limited its adoption into clinical practice.

Selective serotonin reuptake inhibitors (SSRIs) are the mainstay of pharmacologic treatment for pediatric depressive (Goodyer and Wilkinson, 2019) and anxiety disorders (Strawn et al.,

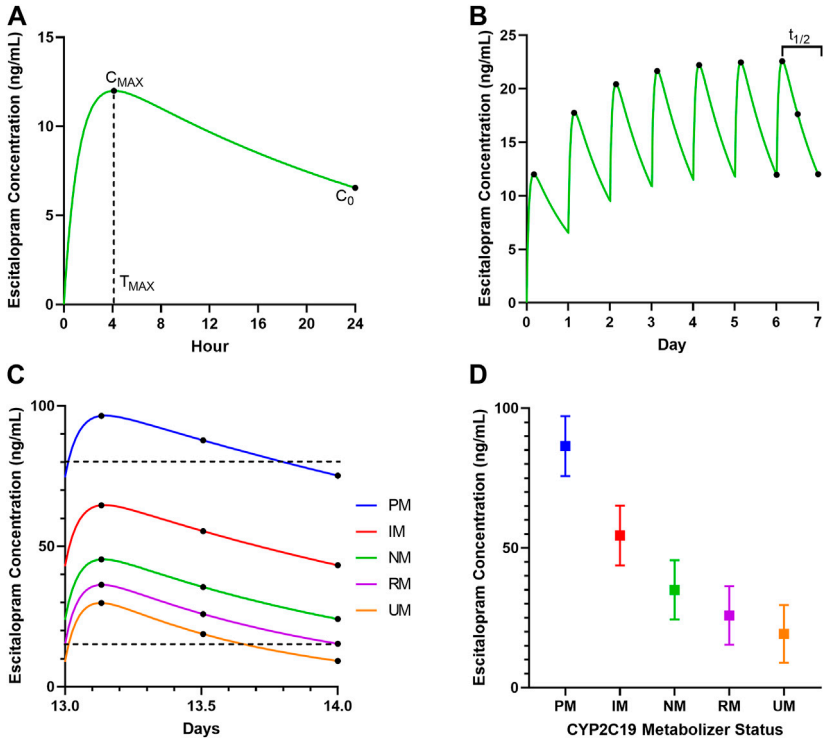

FIGURE 1 | The pharmacokinetics of escitalopram in a 14-year-old adolescent female. **(A)** Predicted concentration-time curve after a single 10 mg dose in a CYP2C19 normal metabolizer. The maximum concentration (C_{MAX}), trough concentration (C_0), and time to maximum concentration (T_{MAX}) are shown. **(B)** Concentration-time curve showing seven doses of 10 mg every 24 h in a CYP2C19 normal metabolizer. Dots indicate the C_{MAX} after each dose, the C_0 prior to the seventh dose and the concentrations at 12 and 24 h after the seventh dose. The half-life ($t_{1/2}$) is shown by the bracket above the curve for the seventh dose. **(C)** Escitalopram concentrations after the 14th dose of 20 mg/day are shown for a CYP2C19 poor metabolizer (blue, [PM]), intermediate metabolizer (red, [IM]), normal metabolizer (green, [NM]), rapid metabolizer (purple, [RM]) and ultrarapid metabolizer (orange, [UM]). Dots indicate the maximum concentration after the dose and the concentrations at 12 and 24 h after the 14th dose. Dotted lines indicate therapeutic window (Hiemke et al., 2018). **(D)** For each metabolizer phenotype, the squares indicate the concentration at 12 h after the 14th dose of 20 mg/day, with the whiskers indicating the maximum concentration (C_{MAX}) and the trough concentration (C_0).

2020b), as well as obsessive compulsive disorder (OCD) (Watson and Rees, 2008). SSRI dosing in children and adolescents generally relies on a 'one size fits all' approach. Clinicians often initiate antidepressants at low-doses and slowly titrate these medications until either encountering a side effect or response. If intolerable side effects occur, the SSRI dose is decreased, or the medication is discontinued. Moreover, the initial SSRI dose is often based on the dosages used in clinical trials and the clinician's comfort with titration. The dose a clinician targets for an individual patient is frequently the mean dose used in clinical trials and the adequacy of antidepressant treatment trials for individual patients is based on target doses (Brent et al., 2008; Strawn et al., 2020a), which fail to account for adherence and variation in drug exposure.

In contemporary clinical practice, factors that influence antidepressant exposure have not yet been incorporated into treatment guidelines for pediatric anxiety (Walter et al., 2020) and depressive disorders (Cheung et al., 2007). Moreover, many psychiatric clinicians contend that circulating antidepressant concentrations are unrelated to response (Ruhé et al., 2006). However, this conflicts with recommendations to titrate SSRI dose in patients with partial responses (Dwyer et al., 2020) and to consider lowering doses in patients with tolerability concerns (Wilens et al., 2003; Luft et al., 2018). Further, intrinsic factors that affect drug concentrations are rarely considered in clinical trials of antidepressants in youth.

Given the current approach to dosing SSRIs and increasing evidence linking variation in SSRI exposure and differences in efficacy and tolerability, TDM may have increasing utility in child and adolescent psychiatry. TDM offers the opportunity to leverage individual variability of antidepressant pharmacokinetics to: 1) shed light on non-response and partial response (Sakolsky et al., 2011); 2) understand drug-drug interactions (Vaughn et al., 2021); 3) evaluate adherence (Fekete et al., 2020); and 4) understand the impact of genetic and developmental variation in pharmacokinetic genes (Strawn et al., 2020c). With these considerations in mind, this Perspective introduces clinicians to TDM principles and illustrates TDM applications in child and adolescent psychiatry. In parallel, this Perspective introduces pharmacologists to the complexity of exposure-response and exposure-tolerability relationships in child and adolescent psychiatry and the unique factors that complicate these relationships.

SSRI Pharmacokinetics in Youths

SSRI exposure is affected by many individual factors (*e.g.*, age, concomitant medications, and cytochrome P450 (CYP) activity), as well as medication dose, amount, and frequency of doses. CYP activity is influenced by genetic polymorphisms affecting the amount and/or function of the protein, age-related changes in the maturation of the enzyme and altered enzyme activity due to specific diseases, as well as inflammation. Understanding the impact of these factors on SSRI pharmacokinetics warrants additional discussion. Consider an adolescent girl with generalized anxiety disorder who is treated with the escitalopram (**Figure 1**). Following an initial 10 mg dose of escitalopram, her maximal escitalopram concentration (C_{MAX}) is 9.7 ng/ml, the time to the maximal concentration (T_{MAX}) is 4.1 h, and the trough concentration (C_0) prior to the next dose is 6.6 ng/ml (**Figure 1A**). The area under the curve (AUC) is calculated by summing the area under the concentration-time curve between doses or over a certain time frame (*e.g.*, AUC_{24}) or until infinity (AUC_{∞}). The AUC is dependent on the dose administered and the clearance, and AUC can be calculated by dividing the dose by the clearance. The $t_{½}$ is the time required for a patient to eliminate half the concentration of the drug in the blood. The population average for the $t_{½}$ of most SSRIs is long (*e.g.*, 24 h for escitalopram), so several days are required to reach steady state, and the concentration decreases by half between daily doses.

The patient's "steady state" occurs when the peaks and troughs are consistent across days because the amount of the medication being added each day is equal to the amount being eliminated from the body each day. Importantly, despite the common misconception, steady state does not indicate that the concentration is consistent between doses. As such, for a medication with a $t_{½}$ of 24 h, the concentration still fluctuates by two-fold each day. Along these lines, some clinicians have argued that $t_{½}$ can be used to determine dosing interval; however, given the variation within a $t_{½}$ (**Figure 1**), dosing intervals that are less than the $t_{½}$ may be required to maintain consistent exposure above the therapeutic threshold for some SSRIs in youth (Strawn et al., 2019). Steady state is usually achieved after about 4–5 $t_{½}$s of the drug (**Figure 1B**).

For some SSRIs in youths, CYP activity—which varies across development (Koukouritaki et al., 2004)—substantially impacts exposure (AUC), C_{MAX}, and $t_{½}$. The impact of CYP2C19 activity on exposure (AUC), C_{MAX}, and $t_{½}$ are shown in **Figure 1C**. At steady state, after a 20 mg daily dose, CYP2C19 poor metabolizers are likely above the 80 ng/ml toxicity threshold, while ultrarapid metabolizers are likely to be under the 15 ng/ml therapeutic threshold (Hiemke et al., 2018). CYP2C19 activity is also affected by the variability in its expression during growth (e.g. between 5 months and 10 years of age, 21-fold variability is seen) (Kodidela et al., 2017). Moreover, certain disease conditions, such as inflammation, have an impact on CYP2C19 and other CYPs in children above 12 years of age, but not in children below 12 years of age (Koukouritaki et al., 2004). Such age-related differences in enzyme function shall be taken into consideration along with other factors while dosing titrations are being performed. In clinical trials, C_0 is often determined prior to a dose, but in clinical practice, patients are often seen between 12 and 24 h after the last dose, and this timing affects SSRI concentrations (**Figure 1D**). Similarly, adherence has a significant effect on SSRI concentrations (**Figure 2**). Importantly, failing to account for time since the last dose, the number of previous doses, and adherence introduces substantial variability that obscures the relationship with genotype, metabolizer activity, and response. Yet, many pharmacokinetic models of SSRIs in adults (Shelton et al., 2020) and in youths do not account for many (or all) pertinent covariates (Findling et al., 2006b, 2017; Reinblatt et al., 2009). Failing to account for enzyme ontogeny, allometric scaling or inclusion of the appropriate parameters into these pharmacokinetic models could over or underestimate exposure, which could obscure the relationship between response and exposure or between tolerability and exposure. Inclusion of these covariates in models could help further describe differences in SSRI pharmacokinetics (**Figure 1**) (Cheung et al., 2019). Such interactions of pharmacogenetics and ontogeny of the enzymes, together with auto- or drug-based enzyme inhibition/induction, must be considered in future investigations to develop precision dosing algorithms.

TDM and SSRI Pharmacokinetics/ Pharmacogenetics in Youths

Relationships between pharmacokinetically-relevant genes (e.g., *CYP2D6* and *CYP2C19*) and SSRI exposure have been established over the past 2 decades. Recently, a meta-analysis of 94 unique studies, revealed significant relationships between CYP2D6 and CYP2C19 metabolizer status and escitalopram, fluvoxamine, fluoxetine, paroxetine and sertraline exposure and reciprocal apparent total drug clearance (Milosavljević et al., 2021). In this meta-analysis, the strongest evidence was for escitalopram and sertraline (Milosavljević et al., 2021). However, only recently has the relationship between SSRI exposure and metabolizer phenotype been explored in pediatric patients, despite preliminary evidence that SSRI exposure may relate to response and tolerability in adolescents with anxiety (Birmaher et al., 2003; Reinblatt et al., 2009; Strawn et al., 2020c) and depressive disorders (Sakolsky et al., 2011).

In a modeling-based simulation of CYP2C19 phenotypes in adolescents, CYP2C19 metabolizer phenotype was associated with differences in escitalopram and sertraline C_{MAX} and $AUC_{0\text{-}24}$. C_{MAX} and $AUC_{0\text{-}24}$ were higher in slower metabolizers (*i.e.*, poor and intermediate metabolizers) and lower in patients with increased CYP2C19 activity, although the magnitude of these differences was more pronounced for escitalopram than for sertraline (Strawn et al., 2019). Additionally, these models may have implications for dosing. For escitalopram, poor metabolizers may require 10 mg/day and ultrarapid metabolizers may require 30 mg/day to achieve an exposure that is equivalent to 20 mg/day in a normal metabolizer. For sertraline, to achieve $AUC_{0\text{-}24}$ and C_{MAX} similar to normal metabolizers receiving 150 mg/day, poor metabolizers require 100 mg/day, whereas a dose of 200 mg/day was required in rapid and ultrarapid metabolizers. This raises the possibility that a target concentration could better inform dosing

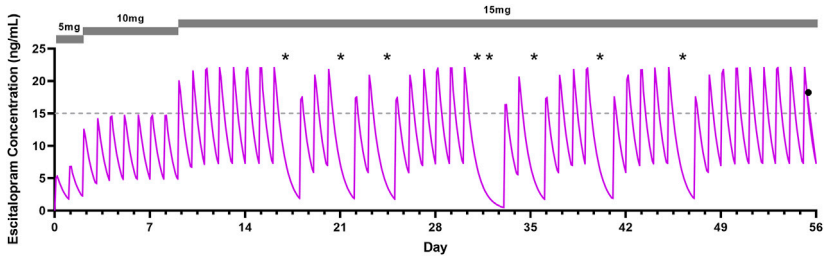

FIGURE 2 | Modeled escitalopram concentration-time profile in a 16-year-old adolescent female CYP2C19 rapid metabolizer with generalized anxiety disorder. Escitalopram dosage is shown in the gray bar (top) and the impact of partial adherence can be seen in the significant decreases in concentration that occurred intermittently beginning in the third week of treatment. The asterisks represent missed doses. The gray dotted-line represents the lower therapeutic threshold for escitalopram (Hiemke et al., 2018). Asterisks represent missed doses, and the black dot reflects the escitalopram determination at the completion of the study.

compared to a target dose (Hiemke et al., 2018). These models lend additional support to previously proposed dosing regimens (Findling et al., 2006a). For example, in younger patients and at lower doses, sertraline has a shorter $t_{½}$, raising the possibility that "twice-daily dosing might be reasonable for youths" (Findling et al., 2006a).

Recently, a prospective trial of adolescents with generalized anxiety disorder demonstrated that patients with faster CYP2C19 metabolism (*i.e.*, rapid and ultrarapid metabolizers) had lower escitalopram $AUC_{0\text{-}24}$ ($p < 0.05$) and lower C_{MAX}. Additionally, two studies have examined CYP2C19 phenotype and sertraline and escitalopram concentrations in large pediatric cohorts. In sertraline-treated youths aged 6–17 years ($N = 107$, mean age: 14.5 ± 2.1 years), our group examined sertraline and desmethylsertraline concentrations. Sertraline dose to concentration ratios were decreased in youths with faster CYP2C19 metabolism relative to those with slower metabolism ($p = 0.002$). Fitting of individual patient data to pharmaokinetic models revealed associations between CYP2C19 phenotype and AUC and C_{MAX} (Poweleit et al., 2021). Also, in escitalopram-treated youths ($N = 104$, mean age: 15 ± 1.8 years) escitalopram concentration to dose ratios were decreased in patients with faster CYP2C19 metabolism relative to those with slower metabolism ($p < 0.001$). Also in this sample, escitalopram $AUC_{0\text{-}24}$ significantly decreased with increased CYP2C19 metabolism and C_{MAX} was higher in slower metabolizers, relative to faster metabolizers (Vaughn et al., 2021b).

One study of single-dose paroxetine pharmacokinetics in youths with depressive disorders ($N = 30$) found "tremendous interindividual variability in paroxetine disposition," but noted clearance and excretion of paroxetine metabolites correlated with CYP2D6 activity (Findling et al., 1999). Similar findings were reported in a larger multiple-dose study of paroxetine in children and adolescents ($N = 62$, 27 children, 35 adolescents). In this sample, oral clearance was "highly dependent" on CYP2D6 activity, although no association was observed between CYP2D6 phenotype or exposure and adverse events (Findling et al., 2006b). However, the relationship between CYP2D6 activity and exposure in paroxetine- and fluoxetine-treated youths is complicated by phenoconversion (Shah and Smith, 2015). As such, treatment with a strong CYP2D6 inhibitor such as paroxetine or fluoxetine reduces CYP2D6 activity to levels seen in poor metabolizers. The product insert for aripiprazole recommends the same 50% dose reduction for patients that are known CYP2D6 poor metabolizers and those that are taking strong inhibitors of CYP2D6 (CDER FDA, 2014). These patients could possibly benefit from TDM.

TDM and Drug-Drug Interactions and SSRIs in Youths

Several studies have used modeling-based approaches and *in vivo* data to examine the impact of drug-drug interactions on SSRIs in youths. The nature of this Perspective precludes an extensive review of these studies, including those with cancer patients, transplant patients and critically ill children and adolescents. As such, we will focus on the interaction between two common drug-drug interactions. These were selected given the frequency of their concurrent use with SSRIs in youths and given the increasing use of cannabis (including tetrahydrocannabinol THC) and cannabidiol (CBD) in adolescents.

Both CBD and THC are moderate to strong inhibitors of CYP enzymes (Bansal et al., 2020; Zendulka et al., 2016) and can interact with SSRIs and increase SSRI plasma concentrations. In a small study of es/citalopram-treated adolescents/young adults, aged 17–24 years, CBD significantly increased citalopram plasma concentrations (Anderson et al., 2021). In pharmacokinetic models of adolescents treated with sertraline or escitalopram, CBD and/or THC increase sertraline and es/citalopram C_{MAX} and $AUC_{0\text{-}24}$ in adolescents (Vaughn et al., 2021a). Additionally, examination of the Food and Drug Administration Adverse Event Reporting System database revealed co-administration of CBD and CYP2C19-metabolized SSRIs increased the risk of some SSRI-related side effects (*e.g.*, diarrhea, dizziness, and fatigue), which may relate to SSRI concentrations (Vaughn et al., 2021a).

Concomitant medications when administered with SSRIs may predispose patients to variation in SSRI plasma concentrations (El Rouby et al., 2018). In adolescents taking some oral contraceptives, steady state plasma citalopram concentrations were significantly affected (Carlsson et al., 2001). This was further confirmed in women taking oral contraceptives and escitalopram in whom metabolite to parent ratios were lower compared to levels in escitalopram-treated women not taking oral contraceptives (Reis et al., 2007). Another study found

co-administration of proton-pump inhibitors and SSRIs increased both escitalopram and es/omeprazole plasma concentrations (Gjestad et al., 2015). Given the potential for drug-drug-gene interactions between proton-pump inhibitors, some oral contraceptives, and SSRIs, TDM could help optimize dosing while mitigating the risk of adverse events and reduced response in children and adolescents.

TDM as a Tool to Assess SSRI Adherence in Youths

TDM has long been used to establish adherence in SSRI-treated adults (Reis et al., 2004, 2010). In fact, in one 6-months sertraline trial using repeated sampling, desmethylsertraline/sertraline ratios were used to identify non-adherence or partial adherence in approximately 10% of the sample (Reis et al., 2004). One pediatric clinical trial has examined concentration-to-dose ratios in youths. In this trial, the Treatment of SSRI-Resistant Depression in Adolescents (TORDIA) study (Brent et al., 2008), the investigators defined a two-fold or greater variation in the dose-adjusted concentrations of the antidepressant medication and metabolite as "non-adherence." Importantly, in this sample, there was a low concordance between clinician pill counts and concentration-dose ratios, and non-adherence was present in just over half of the participants (Woldu et al., 2011). It is difficult to understate the importance of non-adherence in pediatric patients with anxiety and depressive disorders, as well as other chronic health conditions, especially since average non-adherence across most chronic diseases in youths is near 50% (Walders et al., 2005; Modi et al., 2011).

While TDM has been underutilized in individual patients, it represents a useful tool to understand variation in SSRI exposure and non-response. As an example, the patient described in **Figure 2** was a participant in a clinical trial that included measurement of the plasma escitalopram concentrations at the end of treatment. At the 5, 10, and 15 mg daily doses, her C_0 was consistently below the therapeutic threshold of 15 ng/ml (based on adult TDM guidelines) (Hiemke et al., 2018) because she was a CYP2C19 rapid metabolizer and had inconsistent adherence at the 15 mg/day dose. However, her phlebotomy was performed after the C_{MAX}, and was above the lower therapeutic threshold. If her escitalopram concentration had been determined just a few days prior, she would not be at steady state, which would need to be accounted for in the analysis.

Barriers to TDM for SSRIs

In children and adolescents, TDM is frequently restricted to clinical trials and there are significant barriers to its use clinical practice, including a lack of acceptable 'therapeutic targets,' pharmacodynamic confounding of exposure-response relationship, long turnaround times for many assays and lower acceptability of phlebotomy in children. Some of these barriers can be overcome with innovations such as opportunistic sampling and dried blood spot analysis that uses only a finger prick of blood for a liquid chromatography mass spectrometry drug concentration measurement (Frey et al., 2020). However, other challenges will require substantial effort and additional research. In addressing these challenges, we may better understand and measure variation in SSRI metabolism, exposure on response and tolerability and ultimately realize dose personalization.

Limited Evidence of SSRI Concentration-Effect Relationships

The most significant challenge to TDM arises in the clinic where clinicians frequently assert that therapeutic targets for SSRIs are not well established. Indeed, the lack of established pharmacokinetic-pharmacodynamic relationships for SSRIs in pediatric patients encumbers the routine clinical use of TDM in the clinic. However, this view of TDM and therapeutic reference ranges may be somewhat short-sighted. For many clinicians, the therapeutic reference range specifies a population-based, blood concentration below which a "response is relatively unlikely to occur and an upper limit above which tolerability decreases or above which [additional improvement] is relatively unlikely" (Hiemke et al., 2018). Certainly, some patients improve at concentrations below the therapeutic reference range or fail to develop side effects even when concentrations exceed the therapeutic reference range. Thus, it would behoove us to challenge this conceptualization of TDM as a process to evaluate patients with regard to therapeutic reference ranges for a given medication. The utility of TDM for SSRIs in youth may be conceptualized as a continuum of applications—a view consistent with the Consensus Guidelines for Therapeutic Drug Monitoring in Neuropsychopharmacology (Hiemke et al., 2018). Using this approach, the utility of TDM in SSRI-treated youths could be seen as Level 3 (reference ranges are unavailable or based on non-systematic clinical experience) or Level 4 (exposure does not correlate with response or tolerability because of "unique pharmacology of the drug, e.g., irreversible blockade of an enzyme, or dosing can be easily guided by clinical symptoms") (Hiemke et al., 2018).

Pharmacodynamic Confounding of SSRI Concentration-Effect Relationships

Another challenge to establishing therapeutic reference range and the 'lack' of relationships between exposure and response is pharmacodynamic confounding of the exposure-response relationship (**Figure 3**). There is variation in expression of the SSRI target, the serotonin transporter (encoded by *SLC6A4*) that has been associated with genetic variants (Zhu et al., 2017). In one study of adults treated with paroxetine (Tomita et al., 2014), there was no apparent exposure-response relationship until the patients were divided into those predicted to have high expression of the drug target (L allele carriers) and those predicted to have low expression (SS genotype). In the high expression group, the expected positive association was seen between exposure and response. In the low expression group, the opposite was seen, likely due to adequate blockage of the transporter at low exposure and off-target effects at higher exposure. It's difficult to evaluate an exposure-response relationship without accounting for both pharmacokinetic and pharmacodynamic variability (Hertz et al., 2021).

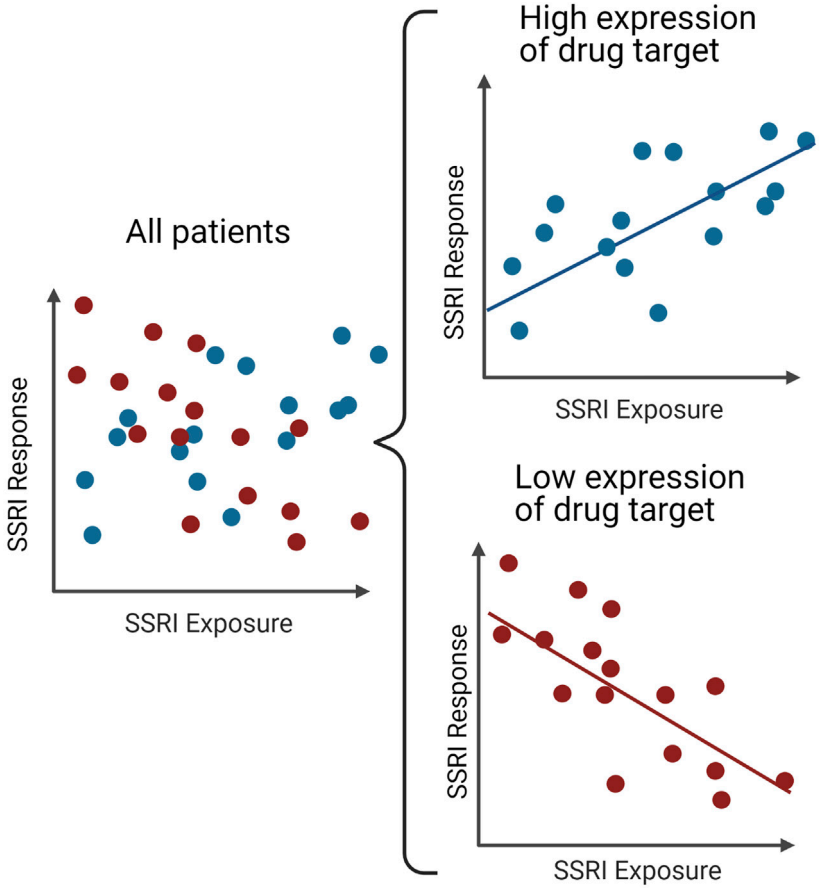

FIGURE 3 | Pharmacodynamic confounding of the SSRI exposure-response relationship. In a combined sample of SSRI treated patients (left), there does not appear to be a relationship between SSRI response and exposure. However, when patients are examined separately, based on a pharmacogenetic variant that impacts pharmacodynamics (e.g., *SLC6A4*), some patients have a positive relationship between response and SSRI exposure whereas other patients—such as those with low expression of the drug target—have a negative correlation between response and SSRI exposure, as per the example in the text of paroxetine and *SLC6A4*.

Developmental and Disease State Influences on SSRI Concentration-Effect Relationships

Therapeutic reference ranges may also vary developmentally and be indication specific (Egberts et al., 2011). Further, therapeutic reference ranges may change based on the phase of the illness, as with other chronic, relapsing-remitting disorders (i.e., higher exposure required during acute exacerbations relative to maintenance phases). How variation in exposure, whether related to intrinsic factors (*e.g.*, metabolism) or extrinsic factors (*e.g.*, adherence), influences multivariate predictive models of response and has received limited attention. Understanding the interaction of family factors, disease state, age, inflammation/acute systemic illness, trauma exposure and co-morbidity is critical to refining and applying TDM-informed predictive models for both efficacy and tolerability.

Traditional SSRI Dosing Approaches as Barriers to TDM

Many presume that exposure can be inferred from a "start low and go slow" approach. However, this approach of standardized initial dosing and titration still places poor metabolizers at risk for side effects given a 3-fold higher exposure (Jukić et al., 2018), and may result in a protracted course for some patients as achieving effective exposure in faster metabolizers requires substantially more time. A second challenge involves the clinical assertion that side effects are unrelated to variation in exposure. Yet, from a tolerability standpoint, variation in pharmacokinetic genes—which produces variation in exposure—has been associated with SSRI tolerability and relationships have been established for escitalopram-related activation and weight gain (Aldrich et al., 2019; Strawn et al., 2020c). Further work is needed to assess this paradigm, especially since retrospective evaluation of SSRI tolerability in pediatric patients has contrasted that of adults (Poweleit et al., 2019; Rossow et al., 2020).

Future Directions

While TDM in SSRI-treated children and adolescents is in its early stages, multiple applications can already be imagined, including evaluating adherence and establishing probabilistic models that identify patients who are at the highest risk of side effects or who require higher doses or alternative dosing regimens (*e.g.*, twice vs. once daily). Another opportunity lies in the advent of big data and machine learning to provide predictions that act as a surrogate or complement to traditional pharmacometrics. Machine learning and

artificial intelligence can serve as a "computational bridge between big data and pharmacometrics," with specific applications towards TDM (*e.g.*, pharmacokinetics/pharmacodynamics and dose optimization) (McComb et al., 2021). Development of tools that allow clinicians to input individual patient characteristics to predict their SSRI concentration comparable to current pharmacokinetic modeling could overcome some barriers of TDM for SSRIs (*e.g.*, the need for phlebotomy, long turnaround times for assays). While further work is needed, machine learning applications have the potential to provide generalizable and autonomous TDM predictions for SSRIs in youths.

DATA AVAILABILITY STATEMENT

The original contributions presented in the study are included in the article, further inquiries can be directed to the corresponding author.

AUTHOR CONTRIBUTIONS

Conceptualization, JS, LR, EP, and UC; methodology, LR, JS, EP; formal analysis, LR and EP; resources, LR and JS; data curation, LR, EP; writing—original draft preparation, JS and LR; writing—review and editing, JS, LR, EP, UC; visualization, EP and LR; supervision, LR and JS; project administration, LR and JS; funding acquisition, LR and JS. All authors have read and agreed to the published version of the manuscript.

FUNDING

This research was funded by Eunice Kennedy Shriver National Institute of Child Health and Human Development, grant numbers R01HD099775 (JS and LR) and R01HD098757 (JS). The funders had no role in the design of the study; in the collection, analyses, or interpretation of data; in the writing of the manuscript, or in the decision to publish the results.

ACKNOWLEDGMENTS

We thank Alexander Vinks, PharmD, PhD for his thoughtful comments and suggestions.

REFERENCES

Aldrich, S. L., Poweleit, E. A., Prows, C. A., Martin, L. J., Strawn, J. R., and Ramsey, L. B. (2019). Influence of CYP2C19 metabolizer status on escitalopram/citalopram tolerability and response in youth with anxiety and depressive disorders. *Front. Pharmacol.*, 10. doi:10.3389/fphar.2019.00099

Anderson, L. L., Doohan, P. T., Oldfield, L., Kevin, R. C., Arnold, J. C., Berger, M., et al. (2021). Citalopram and Cannabidiol. *J. Clin. Psychopharmacol.* 41, 525–533. –9. doi:10.1097/jcp.0000000000001427

Bansal, S., Maharao, N., Paine, M. F., and Unadkat, J. D. (2020). Predicting the Potential for Cannabinoids to Precipitate Pharmacokinetic Drug Interactions via Reversible Inhibition or Inactivation of Major Cytochromes P450. *Drug Metab. Dispos*. 48 (10), 1008–1017. doi:10.1124/dmd.120.000073

Birmaher, B., Axelson, D. A., Monk, K., Kalas, C., Clark, D. B., Ehmann, M., et al. (2003). Fluoxetine for the treatment of childhood anxiety disorders. *J. Am. Acad. Child. Adolesc. Psychiatry* 42, 415–423. doi:10.1097/01.CHI.0000037049.04952.9F

Brent, D., Emslie, G., Clarke, G., Wagner, K. D., Asarnow, J. R., Keller, M., et al. (2008). Switching to another SSRI or to venlafaxine with or without cognitive behavioral therapy for adolescents with SSRI-resistant depression: The TORDIA randomized controlled trial. *JAMA* 299, 901–913. doi:10.1001/jama.299.8.901

Carlsson, B., Olsson, G., Reis, M., Wålinder, J., Nordin, C., Lundmark, J., et al. (2001). Enantioselective analysis of citalopram and metabolites in adolescents. *Ther. Drug Monit.* 23, 658–664. doi:10.1097/00007691-200112000-00011

CDER FDA (2014). *Highlights of Prescribing Information for Abilify*. Tokyo: Otsuka Pharmaceutical Co., Ltd., 101–8535.

Cheung, A. H., Zuckerbrot, R. A., Jensen, P. S., Ghalib, K., Laraque, D., Stein, R. E., et al. (2007). Guidelines for adolescent depression in primary care (GLAD-PC): II. Treatment and ongoing management. *Pediatrics* 120, e1313–26. doi:10.1542/peds.2006-1395

Cheung, K. W. K., Groen, B. D., Burckart, G. J., Zhang, L., Wildt, S. N., and Huang, S. M. (2019). Incorporating Ontogeny in Physiologically Based Pharmacokinetic Modeling to Improve Pediatric Drug Development: What We Know About Developmental Changes in Membrane Transporters. *J. Clin. Pharmacol.*, 59. doi:10.1002/jcph.1489

Dwyer, J. B., Stringaris, A., Brent, D. A., and Bloch, M. H. (2020). Annual Research Review: Defining and treating pediatric treatment-resistant depression. *J. Child. Psychol. Psychiatry* 61, 312–332. doi:10.1111/jcpp.13202

Egberts, K. M., Mehler-Wex, C., and Gerlach, M. (2011). Therapeutic drug monitoring in child and adolescent psychiatry. *Pharmacopsychiatry* 44, 249–253. doi:10.1055/s-0031-1286291

El Rouby, N., Lima, J. J., and Johnson, J. A. (2018). Proton pump inhibitors: from CYP2C19 pharmacogenetics to precision medicine. *Expert Opin. Drug Metab. Toxicol.* 14, 447–460. doi:10.1080/17425255.2018.1461835

Fekete, S., Hiemke, C., and Gerlach, M. (2020). Dose-Related Concentrations of Neuroactive/Psychoactive Drugs Expected in Blood of Children and Adolescents. *Ther. Drug Monit.* 42, 315–324. doi:10.1097/FTD.0000000000000685

Findling, R. L., McNamara, N. K., Stansbrey, R. J., Feeny, N. C., Young, C. M., Peric, F. V., et al. (2006a). The relevance of pharmacokinetic studies in designing efficacy trials in juvenile major depression. *J. Child. Adolesc. Psychopharmacol.* 16, 131–145. doi:10.1089/cap.2006.16.131

Findling, R. L., Nucci, G., Piergies, A. A., Gomeni, R., Bartolic, E. I., Fong, R., et al. (2006b). Multiple dose pharmacokinetics of paroxetine in children and adolescents with major depressive disorder or obsessive-compulsive disorder. *Neuropsychopharmacology* 31, 1274–1285. doi:10.1038/sj.npp.1300960

Findling, R. L., Reed, M. D., Myers, C., O'Riordan, M. A., Fiala, S., Branicky, L., et al. (1999). Paroxetine pharmacokinetics in depressed children and adolescents. *J. Am. Acad. Child. Adolesc. Psychiatry*, 38 952, doi:doi:10.1097/00004583-199908000-00010

Findling, R. L., Robb, A. S., DelBello, M., Huss, M., McNamara, N., Sarkis, E., et al. (2017). Pharmacokinetics and Safety of Vortioxetine in Pediatric Patients. *J. Child. Adolesc. Psychopharmacol.* 27, 526–534. doi:10.1089/cap.2016.0155

Frey, B. S., Damon, D. E., and Badu-Tawiah, A. K. (2020). Emerging trends in paper spray mass spectrometry: Microsampling, storage, direct analysis, and applications. *Mass. Spectrom. Rev.* 39, 336–370. doi:10.1002/MAS.21601

Gjestad, C., Westin, A. A., Skogvoll, E., and Spigset, O. (2015). Effect of proton pump inhibitors on the serum concentrations of the selective serotonin reuptake inhibitors citalopram, escitalopram, and sertraline. *Ther. Drug Monit.* 37, 90–97. doi:10.1097/FTD.0000000000000101

Goodyer, I. M., and Wilkinson, P. O. (2019). Practitioner Review: Therapeutics of unipolar major depressions in adolescents. *J. Child. Psychol. Psychiatry* 60, 232–243. doi:10.1111/jcpp.12940

Hiemke, C., Bergemann, N., Clement, H. W., Conca, A., Deckert, J., Domschke, K., et al. (2018). Consensus Guidelines for Therapeutic Drug Monitoring in Neuropsychopharmacology: Update 2017. *Pharmacopsychiatry* 51, e1–62. doi:10.1055/s-0043-11649210.1055/s-0037-1600991

Hertz, D. L., Ramsey, L. B., Gopalakrishnan, M., Leeder, J. S., and Van Driest, S. L. (2021). Analysis Approaches to Identify Pharmacogenetic Associations With Pharmacodynamics. *Clin. Pharmacol Ther.* 110 (3), 589–594. doi:10.1002/cpt.2312

Jukić, M. M., Haslemo, T., Molden, E., and Ingelman-Sundberg, M. (2018). Impact of CYP2C19 genotype on escitalopram exposure and therapeutic failure: A retrospective study based on 2,087 patients. *Ajp* 175, 463–470. doi:10.1176/appi.ajp.2017.17050550

Koukouritaki, S. B., Manro, J. R., Marsh, S. A., Stevens, J. C., Rettie, A. E., McCarver, D. G., et al. (2004). Developmental Expression of Human Hepatic CYP2C9 and CYP2C19. *J. Pharmacol. Exp. Ther.* 308, 965–974. doi:10.1124/jpet.103.060137

Kodidela, S., Suresh, K., and Uppugunduri, C. R. S. (2017). Developmental Pattern of Hepatic Drug-Metabolizing Enzymes in Pediatric Population and its Role in Optimal Drug Treatment. *Arch. Med. Heal. Sci.* 5, 115–122.

Luft, M. J., Lamy, M., DelBello, M. P., McNamara, R. K., and Strawn, J. R. (2018). Antidepressant-Induced Activation in Children and Adolescents: Risk, Recognition and Management. *Curr. Probl. Pediatr. Adolesc. Health Care* 48, 50–62. doi:10.1016/j.cppeds.2017.12.001

McComb, M., Bies, R., and Ramanathan, M. (2021). Machine learning in pharmacometrics: Opportunities and challenges. *Br. Jnl Clin. Pharma.* doi:10.1111/bcp.14801

Milosavljevic, F., Bukvic, N., Pavlovic, Z., Miljevic, C., Pešic, V., Molden, E., et al. (2021). Association of CYP2C19 and CYP2D6 Poor and Intermediate Metabolizer Status With Antidepressant and Antipsychotic Exposure. *JAMA Psychiatry* 78, 270–280. doi:10.1001/jamapsychiatry.2020.3643

Modi, A. C., Rausch, J. R., and Glauser, T. A. (2011). Patterns of nonadherence to antiepileptic drug therapy in children with newly diagnosed epilepsy. *Jama* 305, 1669. doi:10.1001/jama.2011.506

Poweleit, E. A., Aldrich, S. L., Martin, L. J., Hahn, D., Strawn, J. R., and Ramsey, L. B. (2019). Pharmacogenetics of Sertraline Tolerability and Response in Pediatric Anxiety and Depressive Disorders. *J. Child. Adolesc. Psychopharmacol.* 29, 348–361. doi:10.1089/cap.2019.0017

Poweleit, E. A., Vaughn, S. E., Desta, Z., Strawn, J. R., and Ramsey, L. B. (2019). "Pharmacogenetic Influence of CYP2C19 Variation on Escitalopram Pharmacokinetics in Children and Adolescents [abstract]," in Pharmacogenomics Research Network-American Society for Human Genetics 2021 Symposium, virtual, October 18, 2021. Available at: https://www.pgrn.org/Posters-2021. Abstract B4.

Reinblatt, S. P., DosReis, S., Walkup, J. T., and Riddle, M. A. (2009). Activation adverse events induced by the selective serotonin reuptake inhibitor fluvoxamine in children and adolescents. *J. Child. Adolesc. Psychopharmacol.* 19, 119–126. doi:10.1089/cap.2008.040

Reis, M., Åberg-Wistedt, A., Ågren, H., Åkerblad, A. C., and Bengtsson, F. (2004). Compliance with SSRI medication during 6 months of treatment for major depression: An evaluation by determination of repeated serum drug concentrations. *J. Affect Disord.* 82 (3), 443–6. doi:10.1016/j.jad.2004.02.003

Reis, M., Åkerblad, A.-C., Ekselius, L., and Von Knorring, L. (2010). Partial compliance as determined from plasma levels of sertraline and its metabolite in depressed patients in primary care. *J. Clin. Psychopharmacol.* 30, 746–748. doi:10.1097/JCP.0b013e3181fc2cf1

Reis, M., Chermá, M. D., Carlsson, B., and Bengtsson, F. (2007). Therapeutic drug monitoring of escitalopram in an outpatient setting. *Ther. Drug Monit.* 29, 758–766. doi:10.1097/FTD.0b013e31815b3f62

Rossow, K. M., Aka, I. T., Maxwell-Horn, A. C., Roden, D. M., and Van Driest, S. L. (2020). Pharmacogenetics to Predict Adverse Events Associated With Antidepressants. *Pediatrics* 146, e20200957. doi:10.1542/peds.2020-0957

Ruhé, H. G., Huyser, J., Swinkels, J. A., and Schene, A. H. (2006). Dose escalation for insufficient response to standard-dose selective serotonin reuptake inhibitors in major depressive disorder: Systematic review. *Br. J. Psychiatry* 189, 309–316. doi:10.1192/bjp.bp.105.018325

Sakolsky, D. J., Perel, J. M., Emslie, G. J., Clarke, G. N., Wagner, K. D., Vitiello, B., et al. (2011). Antidepressant exposure as a predictor of clinical outcomes in the Treatment of Resistant Depression in Adolescents (TORDIA) study. *J. Clin. Psychopharmacol.* 31, 92–97. doi:10.1097/JCP.0b013e318204b117

Shah, R. R., and Smith, R. L. (2015). Addressing phenoconversion: the Achilles' heel of personalized medicine. *Br. J. Clin. Pharmacol.* 79, 222–240. doi:10.1111/bcp.12441

Shelton, R. C., Parikh, S. V., Law, R. A., Rothschild, A. J., Thase, M. E., Dunlop, B. W., et al. (2020). Combinatorial Pharmacogenomic Algorithm is Predictive of Citalopram and Escitalopram Metabolism in Patients with Major Depressive Disorder. *Psychiatry Res.* 290, 113017. doi:10.1016/j.psychres.2020.113017

Strawn, J. R., Aaronson, S. T., Elmaadawi, A. Z., Schrodt, G. R., Holbert, R. C., Verdoliva, S., et al. (2020a). Treatment-Resistant Depression in Adolescents: Clinical Features and Measurement of Treatment Resistance. *J. Child. Adolesc. Psychopharmacol.* 30, 261–266. doi:10.1089/cap.2020.0008

Strawn, J. R., Lu, L., Peris, T. S., Levine, A., and Walkup, J. T. (2020b). Research Review: Pediatric anxiety disorders - what have we learnt in the last 10 years. *J. Child. Psychol. Psychiatry* 62, 114–139. doi:10.1111/JCPP.13262

Strawn, J. R., Mills, J. A., Schroeder, H., Mossman, S. A., Varney, S. T., Ramsey, L. B, et al. (2020c). Escitalopram in Adolescents With Generalized Anxiety Disorder: A Double-Blind, Randomized, Placebo-Controlled Study. *J. Clin. Psychiatry* 81, e1–e9. doi:10.4088/JCP.20m13396

Strawn, J. R., Poweleit, E. A., and Ramsey, L. B. (2019). CYP2C19-Guided Escitalopram and Sertraline Dosing in Pediatric Patients: A Pharmacokinetic Modeling Study. *J. Child Adolesc. Psychopharmacol.* 29, 340–347. doi:10.1089/cap.2018.0160

Tomita, T., Yasui-Furukori, N., Nakagami, T., Tsuchimine, S., Ishioka, M., Kaneda, A., et al. (2014). The influence of 5-HTTLPR genotype on the association between the plasma concentration and therapeutic effect of paroxetine in patients with major depressive disorder. *PLoS One* 9, e98099. doi:10.1371/journal.pone.0098099

Vaughn, S. E., Strawn, J. R., Poweleit, E. A., Sarangdhar, M., and Ramsey, L. B. (2021a). The impact of marijuana on antidepressant treatment in adolescents: clinical and pharmacologic considerations. *J. Pers. Med.* 11, 1–14. doi:10.3390/jpm11070615

Vaughn, S. E., Poweleit, E. A., Desta, Z., Strawn, J. R., and Ramsey, L. B. (2021b). CYP2C19 Metabolizer Status Predicts Escitalopram Pharmacokinetics in Children and Adolescents. American Academy of Child and Adolescent Psychiatry 68th Annual Meeting, virtual, October 18–30, 2021. Available at: https://aacap.confex.com/aacap/2021/meetingapp.cgi/Paper/39702. Abstract 32.4.

Walders, N., Kopel, S. J., Koinis-Mitchell, D., and McQuaid, E. L. (2005). Patterns of quick-relief and long-term controller medication use in pediatric asthma. *J. Pediatr.* 146, 177–182. doi:10.1016/j.jpeds.2004.10.014

Walter, H. J., Bukstein, O. G., Abright, A. R., Keable, H., Ramtekkar, U., Ripperger-Suhler, J., et al. (2020). Clinical Practice Guideline for the Assessment and Treatment of Children and Adolescents With Anxiety Disorders. *J. Am. Acad. Child. Adolesc. Psychiatry* 59, 1107–1124. doi:10.1016/j.jaac.2020.05.005

Watson, H. J., and Rees, C. S. (2008). Meta-analysis of randomized, controlled treatment trials for pediatric obsessive-compulsive disorder. *J. Child. Psychol. Psychiatry* 49, 489–498. doi:10.1111/j.1469-7610.2007.01875.x

Wilens, T. E., Biederman, J., Kwon, A., Chase, R., Greenberg, L., Mick, E., et al. (2003). A systematic chart review of the nature of psychiatric adverse events in children and adolescents treated with selective serotonin reuptake inhibitors. *J. Child. Adolesc. Psychopharmacol.* 13, 143–152. doi:10.1089/104454603322163862

Woldu, H., Porta, G., Goldstein, T., Sakolsky, D., Perel, J., Emslie, G., et al. (2011). Pharmacokinetically and clinician-determined adherence to an antidepressant

regimen and clinical outcome in the TORDIA Trial. *J. Am. Acad. Child Adolesc. Psychiatry* 50, 490–498. doi:10.1016/j.jaac.2011.01.018

Zendulka, O., Dovrtělová, G., Nosková, K., Turjap, M., Šulcová, A., Hanuš, L., et al. (2016). Cannabinoids and Cytochrome P450 Interactions. *Curr. Drug Metab.* 17 (3), 206–226. doi:10.2174/1389200217666151210142051

Zhu, J., Klein-Fedyshin, M., and Stevenson, J. M. (2017). Serotonin Transporter Gene Polymorphisms and Selective Serotonin Reuptake Inhibitor Tolerability: Review of Pharmacogenetic Evidence. *Pharmacotherapy* 37, 1089–1104. doi:10.1002/phar.1978

Conflict of Interest: JS has received research support from NIH (National Institute of Mental Health, National Institute of Environmental Health Sciences and the Eunice Kennedy Schriver National Institute of Child Health and Human Development), AbbVie and Otsuka. He has received material support from and provided consultation to Myriad Genetics and has received royalties from the publication of two texts (Springer). He has served as an author for UpToDate, an Associate Editor for Current Psychiatry, and has received honoraria from CMEology, Genomind and Neuroscience Education Institute. He has provided consultation to the Food and Drug Administration. LR has received research support from NIH (Eunice Kennedy Schriver National Institute of Child Health and Human Development). She has received an educational grant and provided consultation to BTG Specialty Pharmaceuticals. UC is supported by CANSEARCH Foundation.

The author declares that the research was conducted in the absence of any commercial or financial relationships that could be construed as a potential conflict of interest.

Publisher's Note: All claims expressed in this article are solely those of the authors and do not necessarily represent those of their affiliated organizations, or those of the publisher, the editors and the reviewers. Any product that may be evaluated in this article, or claim that may be made by its manufacturer, is not guaranteed or endorsed by the publisher.

frontiers in Pharmacology

ORIGINAL RESEARCH
published: 05 November 2021
doi: 10.3389/fphar.2021.750433

Monitoring Tacrolimus Concentrations in Whole Blood and Peripheral Blood Mononuclear Cells: Inter- and Intra-Patient Variability in a Cohort of Pediatric Patients

Amedeo De Nicolò[1†], Michele Pinon[2†], Alice Palermiti[1], Antonello Nonnato[3], Alessandra Manca[1], Jacopo Mula[1], Silvia Catalano[4], Francesco Tandoi[4], Renato Romagnoli[4], Antonio D'Avolio[1*‡] and Pier Luigi Calvo[2‡]*

[1]*Laboratory of Clinical Pharmacology and Pharmacogenetics, Department of Medical Sciences, University of Turin, Turin, Italy,* [2]*Pediatric Gastroenterology Unit, Regina Margherita Children's Hospital, Azienda Ospedaliera-Universitaria Città della Salute e della Scienza, Turin, Italy,* [3]*Clinical Biochemistry Unit, Department of Diagnostic Laboratory, A.O.U. Città della Salute e della Scienza Hospital, Turin, Italy,* [4]*General Surgery, Liver Transplant Center, AOU Città della Salute e della Scienza di Torino, University of Turin, Turin, Italy*

OPEN ACCESS

Edited by:
Alwin Huitema, The Netherlands Cancer Institute (NKI), Netherlands

Reviewed by:
Jiao Zheng, Shanghai Jiaotong University, China
Jonathan Burton Wagner, Children's Mercy Hospital, United States

***Correspondence:**
Alice Palermiti
alice.palermiti@unito.it
Antonio D'Avolio
antonio.davolio@unito.it

†These authors contributed equally to this work and share first authorship
‡These authors share last authorship

Specialty section:
This article was submitted to Obstetric and Pediatric Pharmacology, a section of the journal Frontiers in Pharmacology

Received: *30 July 2021*
Accepted: *15 October 2021*
Published: *05 November 2021*

Citation:
De Nicolò A, Pinon M, Palermiti A, Nonnato A, Manca A, Mula J, Catalano S, Tandoi F, Romagnoli R, D'Avolio A and Calvo PL (2021) Monitoring Tacrolimus Concentrations in Whole Blood and Peripheral Blood Mononuclear Cells: Inter- and Intra-Patient Variability in a Cohort of Pediatric Patients. Front. Pharmacol. 12:750433. doi: 10.3389/fphar.2021.750433

Tacrolimus (TAC) is a first-choice immunosuppressant for solid organ transplantation, characterized by high potential for drug-drug interactions, significant inter- and intra-patient variability, and narrow therapeutic index. Therapeutic drug monitoring (TDM) of TAC concentrations in whole blood (WB) is capable of reducing the incidence of adverse events. Since TAC acts within lymphocytes, its monitoring in peripheral blood mononuclear cells (PBMC) may represent a valid future alternative for TDM. Nevertheless, TAC intracellular concentrations and their variability are poorly described, particularly in the pediatric context. Therefore, our aim was describing TAC concentrations in WB and PBMC and their variability in a cohort of pediatric patients undergoing constant immunosuppressive maintenance therapy, after liver transplantation. TAC intra-PBMCs quantification was performed through a validated UHPLC–MS/MS assay over a period of 2–3 months. There were 27 patients included in this study. No significant TAC changes in intracellular concentrations were observed (p = 0.710), with a median percent change of −0.1% (IQR −22.4%–+46.9%) between timings: this intra-individual variability was similar to the one in WB, −2.9% (IQR −29.4–+42.1; p = 0.902). Among different patients, TAC weight-adjusted dose and age appeared to be significant predictors of TAC concentrations in WB and PBMC. Intra-individual seasonal variation of TAC concentrations in WB, but not in PBMC, have been observed. These data show that the intra-individual variability in TAC intracellular exposure is comparable to the one observed in WB. This opens the way for further studies aiming at the identification of therapeutic ranges for TAC intra-PBMC concentrations.

Keywords: pharmacokinetics, immunosuppressant, pharmacology, pharmacokinetics-pharmacodynamics, transplantation, pharmacokinectics, therapeutic drug monitoring

INTRODUCTION

Currently, tacrolimus (TAC) is among the most used first-line immunosuppressant drug for the prevention of post-transplantation graft rejection (Staatz et al., 2004; Staatz and Tett, 2004). Despite a rather good effectiveness and tolerability, this drug shows a narrow therapeutic range and quite high intra- and inter-patient variability in its concentrations in whole blood (WB) (Bahmany et al., 2018; Kaneko et al., 2018; Álvarez et al., 2020). For these reasons, therapeutic drug monitoring (TDM) is particularly indicated in order to guide therapeutic adjustments during treatment, particularly in the early phase post-transplantation, and then regularly during the maintenance phase. The current standard matrix for TAC TDM is WB, due to the simple withdrawal, higher concentrations compared with plasma and, consequently, a simpler management in terms of sensitivity. However, TAC is characterized by high and variable protein binding and association with red blood cells (RBC) (Takada et al., 1993; Chow et al., 1997; du Souich et al., 1993). Moreover, as a calcineurin inhibitor, TAC exerts its pharmacological activity within T-lymphocytes (particularly on the Th1 subset (Tron et al., 2019)): therefore, the most useful TDM information would derive from intracellular quantification in lymphocytes (Capron et al., 2011; Lemaitre et al., 2013; Lemaitre et al., 2015; Bahmany et al., 2018). In recent years, this topic deserved some interest and several works described methodological approaches to obtain a reliable quantification of TAC within peripheral blood mononuclear cells (PBMCs) (Capron et al., 2009; Pensi et al., 2015; Pensi et al., 2017; Lemaitre et al., 2020a). On the other hand, information about the clinical usefulness, routine applicability, and intra- and inter-patient variability of TAC intra-PBMC concentration is still poorly explored. Intra-patient variability in drug concentrations represents an important challenge for TDM, since it causes the need for a closer monitoring: particularly, a too high intra-individual variability in the absence of significant clinical or therapeutic changes would limit the usefulness of TDM.

TAC has been shown as characterized by significant intra-individual pharmacokinetic (PK) variability in WB, due to clinical and physiopathological changes in patients' conditions (such as liver size, function, and regeneration) (Wallemacq et al., 1998; Wallemacq and Verbeeck, 2001; Pinon et al., 2021) and seasonal variability (Lindh et al., 2011). These physiopathological changes can be particularly marked in the pediatric context. In recent years, high intra-individual variability of TAC concentrations in WB was also described as significantly associated with the risk of graft rejection (Del Bello et al., 2018; Schumacher et al., 2020).

Considering all these issues, the primary endpoint of this study was to evaluate and compare the intra- and inter-patient variability in TAC exposure in WB and PBMC in a cohort of pediatric patients undergoing immunosuppressive maintenance therapy, in the absence of significant adverse events and changes in the therapeutic schedule. The secondary endpoint was to investigate eventual factors associated with intra-individual or inter-individual variability in TAC concentrations in WB and PBMC.

PATIENTS AND METHODS

Patients' Enrolment and Inclusion Criteria

Pediatric patients undergoing maintenance immunosuppressive therapy after liver transplantation with oral TAC in tablet dosage form were prospectively enrolled in this ethically approved study (Città della Salute e della Scienza ethics committe, protocol N° 00107/2019, 25/09/2020). As a clinical policy at the "Regina Margherita Children's Hospital" TDM was used aiming at target maintenance TAC levels in WB in a range between 2 and 5 ng/ml: particularly, the lower part of this range (around 3 ng/ml) was preferred in patients without any history of rejection or with a history of adverse events (renal impairment or lymphoproliferative disorders).

Patients' families, during outpatient visit, were required to fill out a questionnaire in order to assess the therapeutic adherence, concomitant drugs, posology, and quantity of the last dose of TAC. Inclusion criteria comprehended: being in maintenance therapy for at least 1 year; no variations in TAC posology or in the therapeutic schedule (including concomitant drugs) during the study period; no concomitant treatment with everolimus or corticosteroids. The concomitant use of mycophenolate mofetil (MMF) was allowed, considering the absence of significant interaction with TAC. The enrollment was performed using the following exclusion criteria: poor therapeutic adherence; wrong timings for drug intake or assumption with food; vomiting after the last dose intake of TAC; therapeutic changes in TAC posology in the last 2–3 months; rejection episodes or use of steroids in the study period; intake of potentially interfering drugs during the study period. After completing the study questionnaire, healthcare personnel determined the patient's eligibility for blood withdrawal during outpatient visit. The study consisted of at least 2 consecutive visits, with a time lapse comprised between 2 and 3 months, in order to assess intra-patient variability in hematic and intracellular TAC concentrations in the absence of major changes in therapeutic schedules, dose, and clinical episodes. Some patients had more than two PK evaluations. The evaluation of clinical conditions, hematochemical tests including ALT and GGT, total bilirubin, serum creatinine, and hemochrome was performed during each visit.

Peripheral Blood Mononuclear Cells Isolation

Blood samples were withdrawn at the end of dosing interval, before the morning dose intake, in order to obtain trough concentration (C_{trough}) data, at the Pediatric Gastroenterology Unit, Regina Margherita Children's Hospital, Turin, and delivered immediately to the Laboratory of Clinical Pharmacology and Pharmacogenetics of the University of Turin, where PBMCs isolation and intracellular TAC quantification were performed. The whole procedure of PBMCs isolation took less than 1 h. PBMCs isolation was performed with CPT® (Cell Preparation Tube), centrifuged at room temperature for 15 min at 1600 × g for 15 min at 25°C. Cell layers were collected with a Pasteur pipette and transferred into a

falcon tube, brought to a final volume of 50 ml, and then washed twice in sodium chloride 0.9% solution and centrifuged at 2200 × g for 6 min at 4°C, in order to prevent drug loss. Before the second wash, pellet was treated with 2 ml of ammonium salt solution (130 mM ammonium chloride + 7.5 mM ammonium carbonate) for 1 min to obtain red blood cell lysis. After adjusting the volume again to 40 ml with sodium chloride 0.9% solution, 500 µl of cell suspension was diluted, leading to a final volume of 19.5 ml of Isoton and rate in two beakers. The two aliquots were used for cell count and determination of mean cell volume (MCV) through an automated Beckman Coulter Z2 (Instrumentation Laboratory, Milan, Italy). Four counts for each sample (two for each beaker) were performed. Data were processed by Z2 AccuComp software (version 3.01). To obtain blank PBMCs aliquots, the resulting PBMCs pellet was dissolved with an extraction solution (methanol:water, 70:30 [vol:vol]) to a maximum cell concentration for each aliquot of 12 12×10^6 cell/mL. The resulting cell lysates were divided in aliquots, and then stored at −80°C.

Quantification of Tacrolimus Concentrations

TDM of TAC exposure in blood samples was performed through UPLC–MS/MS using Masstrak Immunosuppressants XE kit (CE-IVD marked; "Città della Salute e della Scienza" Hospital, Turin, Italy). Blood sampling in sodium/EDTA vacutainers was performed contextually with sampling for PBMC isolation. Similarly, intraPBMC TAC concentrations were quantified by a UPLC-MS/MS assay coupled with an automated solid phase extraction (SPE), as previously described (Pensi et al., 2015; Pensi et al., 2017). Briefly, the method consisted of cell lysis, sample purification, and TAC concentration by SPE and analysis by positive electrospray ionization. The method was linear in a range between 0.039 and 5 ng, with a lower limit of quantification of 0.019 ng for each PBMC aliquot, with mean accuracy of 100.4% and inter-day coefficient of variation of 6.1%.

The normalization of analytical data obtained from the SPE-UPLC-MS/MS analysis was then performed dividing the obtained absolute TAC amount in each PBMC sample by the number of cells and their MCV, previously determined through the automated cell counter. This normalization allowed to directly compare the intracellular TAC concentrations with the ones in WB.

The observed percent change in TAC concentration in WB and PBMC between the first and second timing was considered as a measure of intra-individual variability, calculated as follows: (TAC concentration at time 2 - TAC concentration at time 1)/ TAC concentration at time 1.

Statistical Analysis

All statistical analyses were performed through Excel and SPSS 27.0 (IBM, Armonk, NY).

Descriptive data have been reported as median and interquartile ranges (IQR). Correlations between continuous data have been evaluated through Pearson or Spearman correlation tests, for normally or not-normally distributed variables, respectively. Differences between categorical groups at the same timing have been tested through the Mann-Whitney or Kruskal-Wallis non-parametric rank tests, while differences between timings in the same patients were tested by Wilcoxon test for coupled samples. Variables which resulted in significantly correlated with TAC concentrations and concentration corrected by dose/weight ratio (C/D/Kg) were tested for their predictive value by univariate and multivariate linear regression model, in the absence of significant co-linearity between the tested independent predictors.

TABLE 1 | Summary of patients' characteristics at the two considered timings. Body mass index (BMI), white blood cells (WBC), aspartate amino-transferase (AST), alanin amino transferase (ALT), gamma glutamil transferase (GGT), C-reactive protein (CRP), calculated glomerular filtration rate (eGFR)

Number of patients: 27
Coupled samples: 43
Sex (Male): 16

	MEDIAN(IQR) T-1	MEDIAN(IQR) T-2
BMI (kg/m^2)	26 (13–39)	-
Age (y.o.)	7 (5–12)	-
WBC (10^9 cells/L)	6.1 (4.2–7.5)	6.0 (4.1–7.8)
Gamma globulins (%)	16.15 (13.95–18.33)	15.6 (14.3–18.1)
Total bilirubin (mg/dl)	0.4 (0.3–0.7)	0.5 (0.3–0.9)
Glucose (mg/dl)	78.0 (73.5–83.3)	78.0 (74.0–81.0)
AST (UI/L)	32.5 (23.0–43.5)	35.0 (29.0–45.8)
ALT (UI/L)	25.0 (17.3–38.3)	26.0 (19.3–64.3)
GGT (UI/L)	12.0 (9.0–23.5)	13.0 (10.0–39.3)
CRP (mg/L)	0.5 (0.2–2.9)	0.4 (0.2–0.8)
Creatinin (mg/dl)	0.4 (0.3–0.5)	0.4 (0.3–0.5)
eGFR (ml/min/1.73 mq)	123.5 (113.0–140.8)	126.5 (111.8–139.5)
Albumin (g/dl)	4.4 (4.2–4.6)	4.4 (4.1–4.5)
Vitamin D (ng/ml)	27.4 (17.5–59.3)	27.6 (21.4–40.1)
Haematocrit (%)	39.8 (36.3–41.4)	40.4 (38.0–41.8)

RESULTS

Patients' Characteristics

Among 56 pediatric patients treated with TAC after liver transplantation who were screened, 27 fit the inclusion criteria and have been enrolled in this study. The overall demographic, anthropometric, and clinical characteristics of these patients are resumed in **Table 1**. Eight patients out of 27 (29.6%) had concomitant MMF treatment.

All the included patients completed at least two consecutive visits without showing adverse events or modifications in their immunosuppressive treatment.

Intra-individual Pharmacokinetic Variability in Whole Blood and Peripheral Blood Mononuclear Cells

The median TAC intracellular concentrations at the first timing and the second timing were 17.5 ng/ml (10.6–27.7) and 16.0 ng/ml (9.8–32.7), respectively. Similarly, median TAC concentrations in WB were 2.8 ng/ml (1.8–3.3) at the first timing and 2.9 ng/ml (1.7–3.8) at the second timing. These differences between timings resulted in not statistically

TABLE 2 | Summary of median (IQR) concentration parameters observed at the first (T1) and second (T2) PK visit.

	MEDIAN (IQR) T-1	MEDIAN (IQR) T-2	% Change	*p* value
WB TAC conc. (ng/ml)	2.8 (1.8–3.3)	2.9 (1.7–3.8)	−2.9 (−29.4–+42.1)	0.870
Intra-PBMC TAC conc. (ng/ml)	17.5 (10.6–27.7)	16.0 (9.8–32.7)	−0.1 (−22.4–+46.9)	0.710
Intra-PBMC/WB ratio	7.0 (5.0–10.0)	6.3 (4.9–8.5)	−0.4(−28.1–+44.5)	0.987
Norm. WB TAC C/D/kg (ng/mg/kg)	48.1 (35.7–67.9)	49.4 (35.4–87.4)	−0.5 (−31.0–+47.0)	0.912
Norm. Intra-PBMC TAC C/D/kg (ng/mg/kg)	372.6 (182.0–480.4)	354.2 (236.5–523.8)	1.9 (−22.3–+42.1)	0.876
Weight-adjusted TAC Dose (mg/kg/day)	0.05 (0.03–0.09)	0.05 (0.03–0.08)	−2.0 (−8.0–+1.0)	0.998

significant ($p = 0.710$ and $p = 0.870$, respectively). Moreover, the intra-individual percent change in TAC concentrations between timings resulted in comparable in WB and PBMC ($p = 0.902$, **Table 2**). Similarly, also the variance in the percent changes between timings in intra-PBMC and whole-blood concentrations was not significantly different ($p = 0.743$ by Levene test, indicating a homogeneous variance) and resulted in mutually correlated ($R = 0.512$, $p = 0.001$). Therefore, intra-individual variations in intra-PBMC concentrations resulted in associated with the variations in WB concentrations. Accordingly, the median percent change in the intra-PBMC/whole-blood TAC concentration ratio between timings was −0.4% (−28.2%–+44.5%; $p = 0.987$).

Factors Associated With Intra-Individual Variability

Once the variability in TAC concentrations in blood and PBMC was described, the correlations between this variability and percent changes in other clinical, hematochemical, and anthropometric characteristics was evaluated. No significant correlations between percent changes in TAC concentrations, neither in whole-blood and PBMC, were observed with changes in BMI, bilirubin, ALT, albumins, hematocrit, and white blood cells count.

The percent change in intra-PBMC concentrations between timings appeared associated with borderline significance ($R = 0.314$; $p = 0.062$) with the minor changes in the weight-adjusted TAC dose (in fact, despite stable TAC dose was administered, patients' growth accounted for this minimal variability). Deepening this issue, we hypothesized a possible role of seasonal variations in the expression of metabolic enzymes, according to previous data (Lindh et al., 2011). For this reason, for each patient we compared TAC concentrations in WB and PBMC monitored during the periods of minimum and maximum sunlight exposure (winter vs autumn/spring or summer vs spring/autumn): this comparison showed significantly lower TAC concentrations in WB during the periods of higher sunlight exposure ($p = 0.040$, **Figure 1**), while this difference was not confirmed as statistically significant for intracellular concentrations ($p = 0.112$).

Inter-individual Variability in Tacrolimus Concentrations

As a secondary endpoint, factors associated with inter-individual variability in TAC concentrations in blood and PBMC among the enrolled patients within the same timing were studied.

A slightly wider inter-individual variability was observed in PBMC, compared with blood, as reported in **Table 2**. Nevertheless, after normalization by mean values, the variance in the intra-PBMC and WB concentrations was not significantly different at both timings ($p = 0.263$ at time 1; $p = 0.522$ at time 2).

First, TAC concentrations in WB and PBMC were tested for correlation with all patients' characteristics, showing strongly significant correlations with serum albumins R values and P values are summarized in **Supplementary Table S1** ($R = -0.384$; $p = 0.012$ and $R = -0.358$; $p = 0.019$, respectively), hematocrit ($R = -0.518$; $p < 0.001$ and $R = -0.467$; $p = 0.002$, respectively), gamma-globulinemia ($R = -0.348$; $p = 0.024$ and $R = -0.404$; $p = 0.007$) and, obviously, the weight-adjusted TAC dose ($R = 0.636$; $p < 0.001$ and $R = 0.583$; $p < 0.001$).

Moreover, the weight-adjusted dose showed a significant negative correlation with albuminemia ($R = -0.398$: $p = 0.044$) and hematocrit ($R = -0.750$; $p < 0.001$). As expected, considering that the patients were in maintenance treatment and the previous use of TDM for dose adjustments in relationship with TAC toxicity and efficacy, no significant correlations were observed neither with eGFR ($R = -0.062$; $p = 0.715$ and $R = 0.017$ $p = 0.922$, respectively) nor with ALT levels ($R = 0.042$; $p = 0.792$ and $R = -0.084$; $p = 0.593$, respectively). No differences were observed in TAC concentrations neither in WB nor in PBMC between patients who had concomitant MMF treatment.

Once the factors correlated with TAC absolute concentration were evidenced, the analysis was refined by testing all the variables for correlation with TAC concentrations adjusted by dose/weight ratio (C/D/Kg), showing a significant correlation with patients' age ($R = 0.301$, $p = 0.056$ and $R = 0.339$, $p = 0.024$ respectively).

Gender Differences in Tacrolimus Concentrations

Interestingly, significant gender differences in TAC concentrations were observed both for regarding WB ($p = 0.003$) and PBMC ($p = 0.002$), with male patients showing higher TAC exposure (**Figure 2**). Conversely, no significant differences between genders were observed in the relative intracellular penetration ($p = 0.435$) and TAC C/D/Kg in blood and PBMC ($p = 0.124$ and $p = 0.152$, respectively). Interestingly, the weight adjusted dose of TAC resulted in significantly higher in male patients ($p = 0.001$), suggesting that the higher TAC exposure in these patients would be due to a previous selection of higher TAC dosage in the male gender.

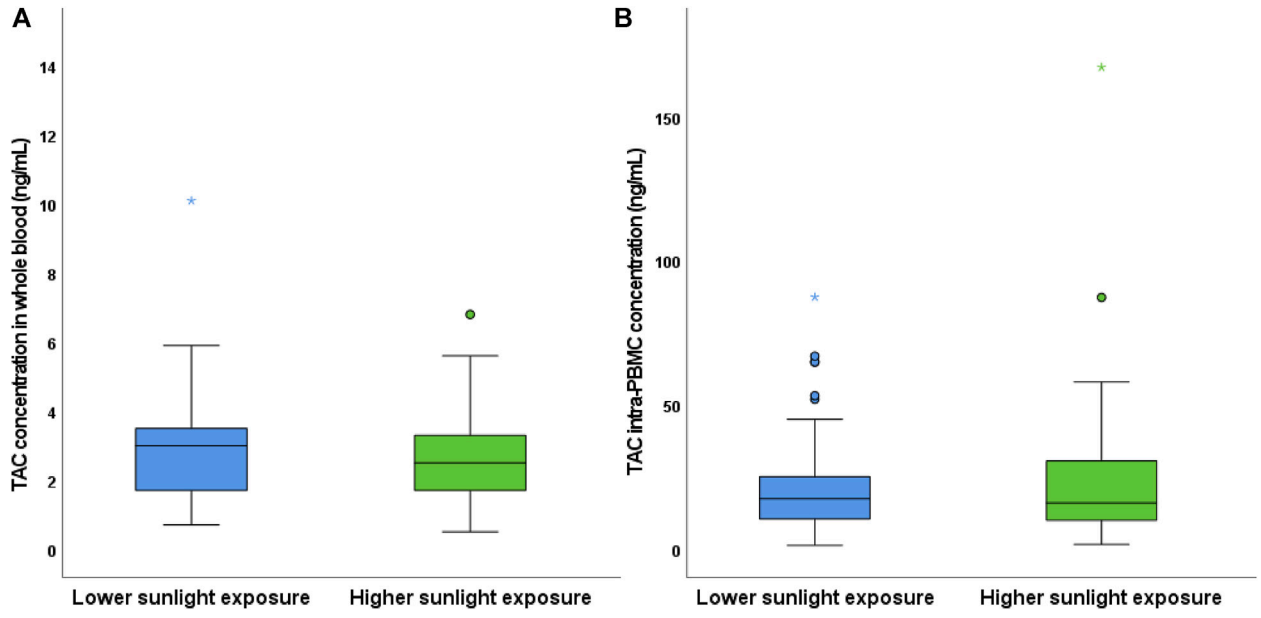

FIGURE 1 | Comparison of TAC concentrations in WB **(A)** and PBMC **(B)** according to seasonal variations. Coupled samples have been assigned to the lower or higher sunlight exposure groups based on the period of the first and second blood sampling (e.g., winter vs autumn/spring or autumn/spring vs summer, respectively).

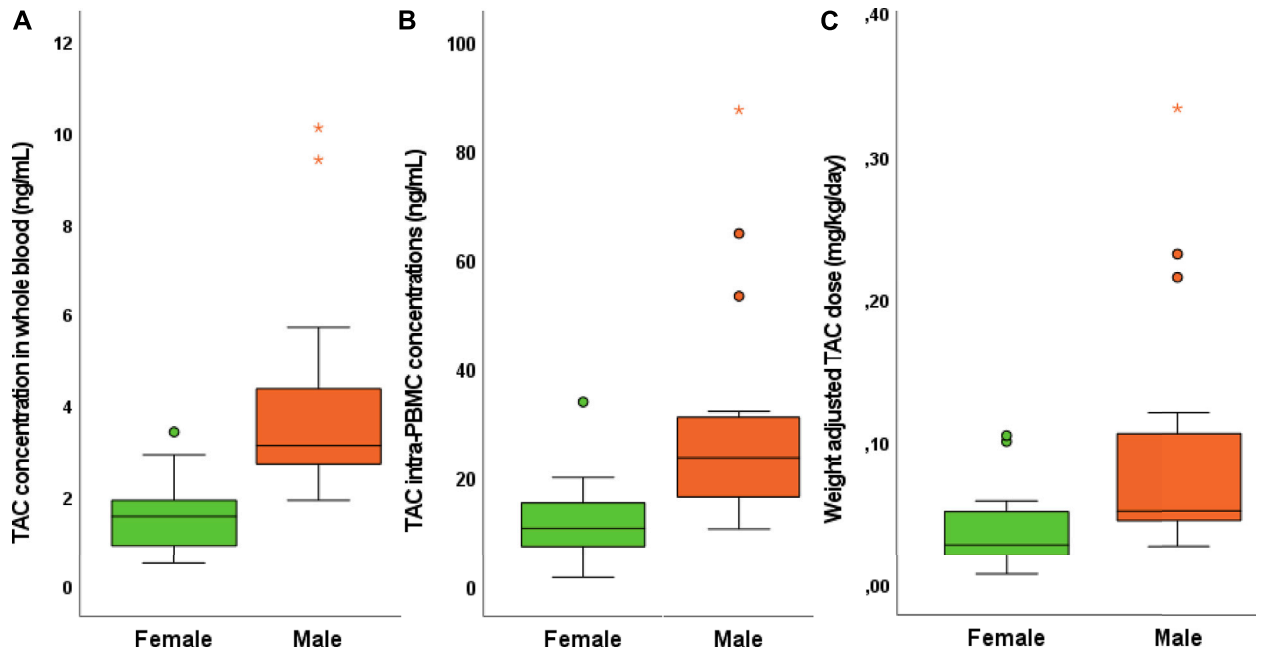

FIGURE 2 | Gender differences in TAC concentrations in WB **(A)**, PBMC **(B)**, and weight adjusted TAC dose **(C)**.

Predictive Factors for Tacrolimus Concentrations in Whole Blood and Peripheral Blood Mononuclear Cells

The factors that showed significant associations/correlations with TAC concentrations in WB and/or PBMC and that did not show any significant co-linearity were tested for their predictive power for TAC concentrations in WB and PBMC. By univariate analysis, the weight-adjusted TAC dose, hematocrit, albumin levels, and gender resulted in significant predictors of TAC concentrations in WB (all regression parameters and p values are reported in **Table 3**). Conversely, patients' age resulted in the only predictor of TAC C/D/kg in WB.

TABLE 3 | Report of the univariate and multivariate regression analysis for the prediction of TAC concentrations in WB. All the statistics have been reported in APA format.

Whole-blood TAC concentration	**Univariate analysis**				
	Age	**Weight-adjusted dose**	**Hematocrit**	**Albumins**	**Gender**
F (d.f.; res.)	-	7.30 (1; 26)	15.80 (1; 26)	5.40 (1; 26)	8.70 (1; 26)
Unstand. B coef.	-	26.30	–0.38	–3.92	2.5
p value	-	<0.001	<0.001	0.029	0.007
Intercept	-	1.20	18.20	20.40	1.64
R^2	-	0.760	0.407	0.190	0.274
Whole-blood TAC concentration adjusted by dose/weight ratio	**Univariate analysis**				
	Age	**Weight-adjusted dose**	**Hematocrit**	**Albumins**	**Gender**
F (d.f.; res.)	6.5 (1; 26)	-	-	-	-
Unstand. B coef.	9.04	-	-	-	-
p value	0.018	-	-	-	-
Intercept	–9.70	-	-	-	-
R^2	0.229	-	-	-	-
Whole-blood TAC concentration	**Multivariate analysis (final model)**				
	Age	**Weight-adjusted dose**			
F (d.f.; res.)		63.4 (2; 25)			
Unstand. B coef.	0.16	28.20			
p value	0.001	<0.001			
Intercept		–0.342			
R^2		0.852			

TABLE 4 | Report of the univariate and multivariate regression analysis for the prediction of TAC concentrations in PBMC. All the statistics have been reported in APA format.

Intra-PBMC TAC concentration	**Univariate analysis**				
	Age	**Weight-adjusted dose**	**Hematocrit**	**Albumins**	**Gender**
F (d.f.; res.)	-	41.5 (1; 26)	18.3 (1; 26)	5.9 (1; 26)	7.1 (1; 26)
Unstand. B coef.	-	201.2	–3.2	–33.3	17.9
p value	-	<0.001	<0.001	0.010	0.013
Intercept	-	8.4	149.3	169.9	12.3
R^2	-	0.624	0.432	0.190	0.274
Intra-PBMC TAC concentration adjusted by dose/weight ratio (C/D/Kg)	**Univariate analysis**				
	Age	**Weight-adjusted dose**	**Hematocrit**	**Albumins**	**Gender**
F (d.f.; res.)	6.8 (1; 26)	-	-	-	-
Unstand. B coef.	38.0	-	-	-	-
p value	0.015	-	-	-	-
Intercept	–109.1	-	-	-	-
R^2	0.215	-	-	-	-
Intra-PBMC TAC concentration	**Multivariate analysis (final model)**				
	Age	**Weight-adjusted dose**			
F (d.f.; res.)	25.7 (2; 25)				
Unstand. B coef.	–1.0	216.0			
p value	0.049	<0.001			
Intercept	–1.65				
R^2	0.681				

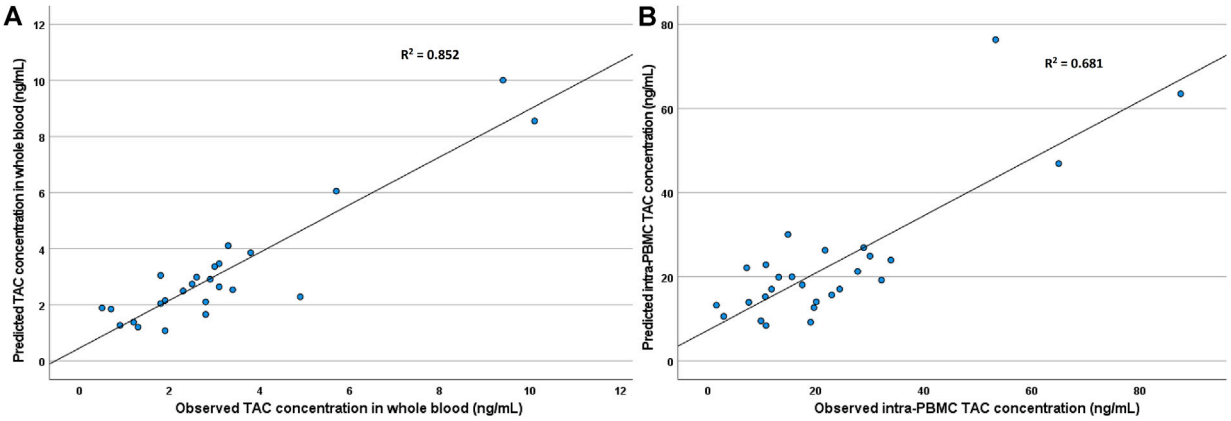

FIGURE 3 | Correlation between the observed TAC concentrations in WB **(A)** and PBMC **(B)** and the predicted concentration obtained by the regression model.

By multivariate analysis, also considering the presence of significant co-linearity between the weight-adjusted dose, serum albumin, hematocrit, and gender, the only significant mutually independent predictors of TAC concentrations in WB resulted in patients' age and the weight-adjusted dose (p = 0.001 and <0.001, respectively; R^2 = 0.852).

Similar results were observed considering both univariate and multivariate analysis regarding intra-PBMC concentrations (regression parameters are reported in **Table 4**). Again, the only significant predictors of TAC concentrations in PBMC were patients' age and the weight-adjusted TAC dose (p = 0.049 and <0.001, respectively; R^2 = 0.681). A graph describing the correlation between the observed TAC concentrations in PBMC and WB and the predicted concentration obtained by the regression model are reported in **Figure 3**.

Association Between Tacrolimus Concentrations and Clinical Parameters

Considering the selection of patients who were in maintenance therapy and no changes in TAC posology during the observation period, no episode of graft rejection in either cases of renal toxicity were observed. A negative significant correlation was observed between TAC concentrations in PBMC and the percentage of gamma-globulins both at the first and second visit (R = 0.393; p = 0.012 and R = −0.482; p = 0.003, respectively): conversely, only a slightly significant correlation was identified between WB TAC concentration at the second visit (R = 0.337; p = 0.049).

No other significant correlations were observed between clinical conditions and TAC concentrations.

DISCUSSION

In the past years, the TDM of TAC concentrations in WB entered in the common clinical practice for the management of the immunosuppressive treatment after solid organ transplantation (Brunet et al., 2019). This is due to the knowledge of therapeutic ranges associated with low probability of graft rejection and toxicity (Brunet et al., 2019; Lemaitre et al., 2020b). Nevertheless, while this practice has been proved effective for therapeutic optimization, some cases of rejection of toxic effects can be observed at TAC concentrations in WB which fall in the therapeutic range. Recently, some reports showed how TAC concentrations within graft or PBMC could be better predictors of its immunosuppressive effect (Capron et al., 2007; Lemaitre et al., 2013; Lemaitre et al., 2020a).

On the other hand, the adoption of TAC concentrations in PBMC for TDM purposes can be considered only if their intra-individual variability in the absence of changes in posology, concomitant drugs, or other physiological changes is rather contained or at least comparable to the one in WB.

This is particularly important in the pediatric context, since these patients have significantly higher probability to experience adverse events and because of continuous physiological changes due to their growth (Wallemacq et al., 1998; Wallemacq and Verbeeck, 2001; Kearns et al., 2003). For these reasons, this work provided useful information regarding the medium-term changes in TAC concentrations in WB and PBMC, showing that their intra-individual variability can be considered comparable. Moreover, this work confirmed a previous report from Lindh et al. (Lindh et al., 2011) showing that TAC concentrations in WB are affected by seasonal variability, with an inverse trend with sunlight exposure. Nevertheless, no increased incidence of graft rejection was previously reported in literature seasons with higher sunlight exposure or related to vitamin D levels (Mosca et al., 2020): conversely, a single work studying seasonal variation in chronic graft rejection reported a slightly higher incidence in winter (Astor et al., 2017). In our work, we observed significant seasonal changes in TAC concentrations in WB, but not in PBMC, possibly explaining this mismatch between TDM data in WB and clinical outcome.

On the other hand, focusing on the inter-individual variability, we observed that several variables were significantly associated with TAC concentrations in WB and PBMC. Among these, the inter-individual differences in the weight-adjusted dose and age were the only emergent significant predictors of TAC concentrations both in WB and PBMC. Nevertheless, considering the values of the

coefficients of determination (R^2 0.852 and 0.681, respectively), further 15 and 32% of this variability remains to be explained. Particularly, the lower fit for the intracellular concentrations the involvement of other factors, such as genetic differences in drug transporters (Capron et al., 2010; Lemaitre et al., 2015; Tron et al., 2019; Tron et al., 2020), in the intracellular disposition of TAC.

The observed inverse correlations between serum albumin levels and TAC concentrations, both in WB and PBMC, could be explained by a higher metabolic activity of the liver, which can be associated with increased drug metabolism. On the other hand, the inverse correlation with hematocrit could be explained by the fact that lower TAC dosages could have been selected in patients with higher hematocrit, since TAC adhesion to erythrocytes can reduce its elimination in the initial phases of therapy (Limsrichamrern et al., 2016; Uchida et al., 2020). In this case, TDM-guided posological adjustments during the first year of therapy would be responsible of these differences, in accordance with the observed negative correlation between the weight-adjusted TAC dose and both albuminemia and hematocrit. This hypothesis seems to be confirmed considering the observed gender differences in TAC dose and concentrations, with higher exposure in male patients. In fact, in previous works from our group focusing on the first days of treatment with TAC, a significantly higher TAC concentration was observed in female patients, guiding a dose reduction in these patients in the following days (Calvo et al., 2017; Pinon et al., 2021). Interesting evidence obtained in this cohort was a significant negative correlation between intra-PBMC concentrations and the percentage of gamma-globulins, which was less marked when considering TAC concentrations in WB. This could be interpreted as a stronger immunosuppressive effect in patients with higher TAC concentrations in PBMC.

This study has several limitations: first, no genetic information was available for these patients; moreover, the evaluation of seasonal variability could be better performed by scheduling PK sampling every 3 months in a year, contextually with vitamin D quantification.

Nevertheless, since the primary endpoint was the intra-individual evaluation, no effect of patients' genetics is expected, while its impact on the inter-individual variability in the absolute TAC concentrations should be contained considering that major dose adjustments guided by TDM, commonly occurring in the first days after liver transplantation, tend to compensate for genetic variability (Pinon et al., 2021). Conversely, regarding the study of seasonal variability in TAC concentrations, this will surely be the subject of future studies.

Concluding, this study shows that the intra-individual variability in TAC concentrations in PBMC and WB are similar, in the absence of significant changes in the therapeutic schedule or in patients' conditions, making the adoption of intracellular TAC quantification for TDM purpose theoretically possible. Further studies focusing on eventual differences in the predictive power between intra-PBMC and WB concentration for adverse events and graft rejection are needed, in order to assess if a real clinical advantage exists.

DATA AVAILABILITY STATEMENT

The raw data supporting the conclusions of this article will be made available by the authors, without undue reservation.

ETHICS STATEMENT

The studies involving human participants were reviewed and approved by the Città della Salute e della Scienza ethics committe. Written informed consent to participate in this study was provided by the participants' legal guardian/next of kin.

AUTHOR CONTRIBUTIONS

ANi: Designed Research, Analyzed data and wrote manuscript; MP: Designed research, Enrolled patients and Wrote manuscript; AP: Wrote manuscript, Analyzed data, Performed research; ANo: Reviewed the manuscript, provided analytical tools; AM: Analyzed data; JM: Reviewed the manuscript; SC: Enrolled patients; FT: Enrolled patients; RR: Enrolled patients; AA: Designed research, Provided analytical tools; PC: Performed enrolment, Designed research.

FUNDING

This study was supported by the "AITF BIMBI ONLUS" non-profit organization

ACKNOWLEDGMENTS

We thank the study participants, their families, and the "AITF BIMBI" non-profit organization for their kind cooperation and support.

SUPPLEMENTARY MATERIAL

The Supplementary Material for this article can be found online at: https://www.frontiersin.org/articles/10.3389/fphar.2021.750433/full#supplementary-material

REFERENCES

Álvarez, M., Hernández, M. C., Macià, P., Jansat, J. M., and Sentellas, S. (2020). Sensitive UHPLC-MS/MS Method for the Determination of Tacrolimus in Minipig Whole Blood. *Bioanalysis* 12 (8), 519–532. doi:10.4155/bio-2020-0039

Astor, B. C., Melamed, M. L., Mandelbrot, D. A., and Djamali, A. (2017). Seasonality of Mortality and Graft Failure Among Kidney Transplant Recipients in the US - a Retrospective Study. *Transpl. Int.* 31 (3), 293–301. doi:10.1111/tri.13047

Bahmany, S., de Wit, L. E. A., Hesselink, D. A., van Gelder, T., Shuker, N. M., Baan, C., et al. (2018). Highly Sensitive and Rapid Determination of Tacrolimus in Peripheral Blood Mononuclear Cells by Liquid Chromatography-Tandem Mass Spectrometry. *Biomed. Chromatogr.* 33 (1), e4416. doi:10.1002/bmc.4416

Brunet, M., van Gelder, T., Åsberg, A., Haufroid, V., Hesselink, D. A., Langman, L., et al. (2019). Therapeutic Drug Monitoring of Tacrolimus-Personalized Therapy: Second Consensus Report. *Ther. Drug Monit.* 41 (3), 261–307. doi:10.1097/FTD.0000000000000640

Calvo, P. L., Serpe, L., Brunati, A., Nonnato, A., Bongioanni, D., Olio, D. D., et al. (2017). Donor CYP3A5 Genotype Influences Tacrolimus Disposition on the First Day after Paediatric Liver Transplantation. *Br. J. Clin. Pharmacol.* 83 (6), 1252–1262. doi:10.1111/bcp.13219

Capron, A., Lerut, J., Latinne, D., Rahier, J., Haufroid, V., and Wallemacq, P. (2011). Correlation of Tacrolimus Levels in Peripheral Blood Mononuclear Cells with Histological Staging of Rejection after Liver Transplantation: Preliminary Results of a Prospective Study. *Transpl. Int.* 25 (1), 41–47. doi:10.1111/j.1432-2277.2011.01365.x

Capron, A., Lerut, J., Verbaandert, C., Mathys, J., Ciccarelli, O., Vanbinst, R., et al. (2007). Validation of a Liquid Chromatography-Mass Spectrometric Assay for Tacrolimus in Liver Biopsies after Hepatic Transplantation: Correlation with Histopathologic Staging of Rejection. *Ther. Drug Monit.* 29 (3), 340–348. doi:10.1097/FTD.0b013e31805c73f100007691-200706000-00012

Capron, A., Mourad, M., De Meyer, M., De Pauw, L., Eddour, D. C., Latinne, D., et al. (2010). CYP3A5 and ABCB1 Polymorphisms Influence Tacrolimus Concentrations in Peripheral Blood Mononuclear Cells after Renal Transplantation. *Pharmacogenomics* 11 (5), 703–714. doi:10.2217/pgs.10.43

Capron, A., Musuamba, F., Latinne, D., Mourad, M., Lerut, J., Haufroid, V., et al. (2009). Validation of a Liquid Chromatography-Mass Spectrometric Assay for Tacrolimus in Peripheral Blood Mononuclear Cells. *Ther. Drug Monit.* 31 (2), 178–186. doi:10.1097/FTD.0b013e3181905aaa

Chow, F. S., Piekoszewski, W., and Jusko, W. J. (1997). Effect of Hematocrit and Albumin Concentration on Hepatic Clearance of Tacrolimus (FK506) during Rabbit Liver Perfusion. *Drug Metab. Dispos* 25 (5), 610–616.

Del Bello, A., Congy-Jolivet, N., Danjoux, M., Muscari, F., Lavayssière, L., Esposito, L., et al. (2018). High Tacrolimus Intra-patient Variability Is Associated with Graft Rejection, and De Novo Donor-specific Antibodies Occurrence after Liver Transplantation. *World J. Gastroenterol.* 24 (16), 1795–1802. doi:10.3748/wjg.v24.i16.1795

du Souich, P., Verges, J., and Erill, S. (1993). Plasma Protein Binding and Pharmacological Response. *Clin. Pharmacokinet.* 24 (6), 435–440. doi:10.2165/00003088-199324060-00001

Kaneko, T., Fujioka, T., Suzuki, Y., Nagano, T., Sato, Y., Asakura, S., et al. (2018). Comparison of Whole-Blood Tacrolimus Concentrations Measured by Different Immunoassay Systems. *J. Clin. Lab. Anal.* 32 (9), e22587. doi:10.1002/jcla.22587

Kearns, G. L., Abdel-Rahman, S. M., Alander, S. W., Blowey, D. L., Leeder, J. S., and Kauffman, R. E. (2003). Developmental Pharmacology-Ddrug Disposition, Action, and Therapy in Infants and Children. *N. Engl. J. Med.* 349 (12), 1157–1167. doi:10.1056/NEJMra035092349/12/1157

Lemaitre, F., Antignac, M., and Fernandez, C. (2013). Monitoring of Tacrolimus Concentrations in Peripheral Blood Mononuclear Cells: Application to Cardiac Transplant Recipients. *Clin. Biochem.* 46 (15), 1538–1541. doi:10.1016/j.clinbiochem.2013.02.011

Lemaitre, F., Blanchet, B., Latournerie, M., Antignac, M., Houssel-Debry, P., Verdier, M. C., et al. (2015). Pharmacokinetics and Pharmacodynamics of Tacrolimus in Liver Transplant Recipients: inside the white Blood Cells. *Clin. Biochem.* 48 (6), 406–411. doi:10.1016/j.clinbiochem.2014.12.018

Lemaitre, F., Tron, C., Renard, T., Jézéquel, C., Houssel-Debry, P., Bergeat, D., et al. (2020). Redefining Therapeutic Drug Monitoring of Tacrolimus in Patients Undergoing Liver Transplantation: A Target Trough Concentration of 4-7 ng/mL during the First Month after Liver Transplantation Is Safe and Improves Graft and Renal Function. *Ther. Drug Monit.* 42 (5), 671–678. doi:10.1097/FTD.0000000000007790000 7691-202010000-00005

Lemaitre, F., Vethe, N. T., D'Avolio, A., Tron, C., Robertsen, I., De Winter, B., et al. (2020). Measuring Intracellular Concentrations of Calcineurin Inhibitors: Expert Consensus from the International Association of Therapeutic Drug Monitoring and Clinical Toxicology Expert Panel. *Ther. Drug Monit.* 42 (5), 665–670. doi:10.1097/FTD.0000000000007800000 7691-202010000-00004

Limsrichamrern, S., Chanapul, C., Mahawithitwong, P., Sirivatanauksorn, Y., Kositamongkol, P., Asavakarn, S., et al. (2016). Correlation of Hematocrit and Tacrolimus Level in Liver Transplant Recipients. *Transpl. Proc* 48 (4), 1176–1178. doi:10.1016/j.transproceed.2015.12.096

Lindh, J. D., Andersson, M. L., Eliasson, E., and Björkhem-Bergman, L. (2011). Seasonal Variation in Blood Drug Concentrations and a Potential Relationship to Vitamin D. *Drug Metab. Dispos* 39 (5), 933–937. doi:10.1124/dmd.111.038125

Mosca, M., Lion-Lambert, M., Bienaimé, F., Berthaud, R., Dorval, G., Garcelon, N., et al. (2020). Association between 25(OH) Vitamin D and Graft Survival in Renal Transplanted Children. *Pediatr. Transpl.* 24 (7), e13809. doi:10.1111/petr.13809

Pensi, D., De Nicolò, A., Pinon, M., Calvo, P. L., Nonnato, A., Brunati, A., et al. (2015). An UPLC-MS/MS Method Coupled with Automated On-Line SPE for Quantification of Tacrolimus in Peripheral Blood Mononuclear Cells. *J. Pharm. Biomed. Anal.* 107, 512–517. doi:10.1016/j.jpba.2015.01.054

Pensi, D., De Nicolò, A., Pinon, M., Pisciotta, C., Calvo, P. L., Nonnato, A., et al. (2017). First UHPLC-MS/MS Method Coupled with Automated Online SPE for Quantification Both of Tacrolimus and Everolimus in Peripheral Blood Mononuclear Cells and its Application on Samples from Co-treated Pediatric Patients. *J. Mass. Spectrom.* 52 (3), 187–195. doi:10.1002/jms.3909

Pinon, M., De Nicolò, A., Pizzol, A., Antonucci, M., D'Avolio, A., Serpe, L., et al. (2021). Early Impact of Donor CYP3A5 Genotype and Graft-To-Recipient Weight Ratio on Tacrolimus Pharmacokinetics in Pediatric Liver Transplant Patients. *Sci. Rep.* 11 (1), 443. doi:10.1038/s41598-020-79574-710.1038/s41598-020-79574-7

Schumacher, L., Leino, A. D., and Park, J. M. (2020). Tacrolimus Intrapatient Variability in Solid Organ Transplantation: A Multiorgan Perspective. *Pharmacotherapy* 41 (1), 103–118. doi:10.1002/phar.2480

Staatz, C. E., Taylor, P. J., Lynch, S. V., and Tett, S. E. (2004). A Pharmacodynamic Investigation of Tacrolimus in Pediatric Liver Transplantation. *Liver Transpl.* 10 (4), 506–512. doi:10.1002/lt.20065

Staatz, C. E., and Tett, S. E. (2004). Clinical Pharmacokinetics and Pharmacodynamics of Tacrolimus in Solid Organ Transplantation. *Clin. Pharmacokinet.* 43 (10), 62343101–62343153. doi:10.2165/00003088-200443100-00001

Takada, K., Katayama, N., Kiriyama, A., and Usuda, H. (1993). Distribution Characteristics of Immunosuppressants FK506 and Cyclosporin A in the Blood Compartment. *Biopharm. Drug Dispos* 14 (8), 659–671. doi:10.1002/bdd.2510140803

Tron, C., Allard, M., Petitcollin, A., Ferrand-Sorre, M. J., Verdier, M. C., Querzerho-Raguideau, J., et al. (2019). Tacrolimus Diffusion across the Peripheral Mononuclear Blood Cell Membrane: Impact of Drug Transporters. *Fundam. Clin. Pharmacol.* 33 (1), 113–121. doi:10.1111/fcp.12412

Tron, C., Woillard, J. B., Houssel-Debry, P., David, V., Jezequel, C., Rayar, M., et al. (2020). Pharmacogenetic-Whole Blood and Intracellular Pharmacokinetic-Pharmacodynamic (PG-PK2-PD) Relationship of Tacrolimus in Liver Transplant Recipients. *PLoS One* 15 (3), e0230195. doi:10.1371/journal.pone.0230195PONE-D-19-21120

Uchida, M., Yamazaki, S., Suzuki, T., Takatsuka, H., and Ishii, I. (2020). Effects of Red Blood Cell Concentrate Transfusion on Blood Tacrolimus Concentration. *Int. J. Clin. Pharm.* 42 (3), 956–964. doi:10.1007/s11096-020-01038-910.1007/s11096-020-01038-9

Wallemacq, P. E., Furlan, V., Möller, A., Schäfer, A., Stadler, P., Firdaous, I., et al. (1998). Pharmacokinetics of Tacrolimus (FK506) in Paediatric Liver Transplant Recipients. *Eur. J. Drug Metab. Pharmacokinet.* 23 (3), 367–370. doi:10.1007/BF03192295

Wallemacq, P. E., and Verbeeck, R. K. (2001). Comparative Clinical Pharmacokinetics of Tacrolimus in Paediatric and Adult Patients. *Clin. Pharmacokinet.* 40 (4), 283–295. doi:10.2165/00003088-200140040-00004

Conflict of Interest: The authors declare that the research was conducted in the absence of any commercial or financial relationships that could be construed as a potential conflict of interest.

Publisher's Note: All claims expressed in this article are solely those of the authors and do not necessarily represent those of their affiliated organizations, or those of the publisher, the editors and the reviewers. Any product that may be evaluated in this article, or claim that may be made by its manufacturer, is not guaranteed or endorsed by the publisher.

frontiers in Pharmacology

ORIGINAL RESEARCH
published: 19 November 2021
doi: 10.3389/fphar.2021.749361

A Novel ELISA-Based Peptide Biosensor Assay for Screening ABL1 Activity *in vitro*: A Challenge for Precision Therapy in BCR-ABL1 and BCR-ABL1 Like Leukemias

Oksana Montecchini[1†], *Stefania Braidotti*[1†], *Raffaella Franca*[1], *Giulia Zudeh*[2], *Christian Boni*[3], *Claudio Sorio*[3], *Eleonora Toffoletti*[4], *Marco Rabusin*[5], *Alberto Tommasini*[1,5], *Giuliana Decorti*[1,5]* *and Gabriele Stocco*[2]

[1]*Department of Medical, Surgical and Health Sciences, University of Trieste, Trieste, Italy,* [2]*Department of Life Sciences, University of Trieste, Trieste, Italy,* [3]*Department of Medicine, University of Verona, Verona, Italy,* [4]*Division of Hematology and Bone Marrow Transplantation, Azienda Ospedaliero-Universitaria, Udine, Italy,* [5]*Institute for Maternal and Child Health (I.R.C.C.S) Burlo Garofolo, Trieste, Italy*

OPEN ACCESS

Edited by:
Raffaele Simeoli,
Bambino Gesù Children's Hospital (IRCCS), Italy

Reviewed by:
Ahmet Emre Eskazan,
Istanbul University-Cerrahpasa, Turkey
Saphy Sharda,
Centre for DNA Fingerprinting and Diagnostics (CDFD), India

***Correspondence:**
Giuliana Decorti
giuliana.decorti@burlo.trieste.it

†These authors have contributed equally to this work and share first authorship

Specialty section:
This article was submitted to Obstetric and Pediatric Pharmacology, a section of the journal Frontiers in Pharmacology

Received: *29 July 2021*
Accepted: *08 October 2021*
Published: *19 November 2021*

Citation:
Montecchini O, Braidotti S, Franca R, Zudeh G, Boni C, Sorio C, Toffoletti E, Rabusin M, Tommasini A, Decorti G and Stocco G (2021) A Novel ELISA-Based Peptide Biosensor Assay for Screening ABL1 Activity in vitro*: A Challenge for Precision Therapy in BCR-ABL1 and BCR-ABL1 Like Leukemias. Front. Pharmacol. 12:749361. doi: 10.3389/fphar.2021.749361*

The pathogenic role of the overactivated ABL1 tyrosine kinase (TK) pathway is well recognized in some forms of *BCR-ABL1* like acute lymphoblastic leukemia (ALL); TK inhibitors represent a useful therapeutic choice in these patients who respond poorly to conventional chemotherapy. Here we report a novel peptide biosensor (P_{ABL})-ELISA assay to investigate ABL1 activity in four immortalized leukemic cell lines with different genetic background. The P_{ABL} sequence comprises an ABL1 tyrosine (Y) phosphorylation site and a targeting sequence that increases the specificity for ABL1; additional peptides (Y-site-mutated ($P_{ABL\text{-}F}$) and fully-phosphorylated ($P_{PHOSPHO\text{-}ABL}$) biosensors) were included in the assay. After incubation with whole cell lysates, average P_{ABL} phosphorylation was significantly increased (basal vs. P_{ABL} phosphorylation: 6.84 ± 1.46% vs. 32.44 ± 3.25%, p-value < 0.0001, two-way ANOVA, Bonferroni post-test, percentages relative to $P_{PHOSPHO\text{-}ABL}$ in each cell line). Cell lines expressing ABL1-chimeric proteins (K562, ALL-SIL) presented the higher TK activity on P_{ABL}; a lower signal was instead observed for NALM6 and REH (p < 0.001 and p < 0.05 vs. K562, respectively). Phosphorylation was ABL1-mediated, as demonstrated by the specific inhibition of imatinib (p < 0.001 for K562, NALM6, ALL-SIL and p < 0.01 for REH) in contrast to ruxolitinib (JAK2-inhibitor), and occurred on the ABL1 Y-site, as demonstrated by $P_{ABL\text{-}F}$ whose phosphorylation was comparable to basal levels. In order to validate this novel P_{ABL}-ELISA assay on leukemic cells isolated from patient's bone marrow aspirates, preliminary analysis on blasts derived from an adult affected by chronic myeloid leukaemia (*BCR-ABL1* positive) and a child affected by ALL (*BCR-ABL1* negative) were performed. Phosphorylation of P_{ABL} was specifically inhibited after the incubation of *BCR-ABL1* positive cell lysates with imatinib, but not with ruxolitinib. While requiring further optimization and validation in leukemic blasts to be of clinical interest, the P_{ABL}-based

ELISA assay provides a novel *in vitro* tool for screening both the aberrant ABL1 activity in *BCR-ABL1* like ALL leukemic cells and their potential response to TK inhibitors.

Keywords: ABL1-class BCR-ABL1 like acute lymphoblastic leukemia, ABL1 peptide biosensor, *in vitro* ELISA assay, ABL1 tyrosin kinase inhibitors, precision therapy

INTRODUCTION

In clinics, a sensitive, quick, convenient and versatile detection method to measure aberrant kinase activity is desirable for many pathologies, including various forms of leukemias, and could be important to improve diagnosis and treatment. The Abelson (ABL)-1 tyrosine kinase (TK) belongs to the non-receptor TK family and is an ubiquitously expressed cytosolic enzyme that plays a role in many key processes linked to cell growth and survival as well as to cell differentiation, cell adhesion and migration (Greuber et al., 2013). Oncogenic forms of ABL1, in particular the *BCR-ABL1* fusion gene with different breakpoints in *BCR* gene, are well-recognized for their pathogenic role in leukemias, including chronic myeloid leukemia (CML), some forms of acute myeloid leukemia (AML), and acute lymphoblastic leukemia (ALL). *BCR-ABL1* results from the chromosomal translocation t (9;22), and encodes for the chimeric BCR-ABL1 protein that leads to an aberrant costitutive activation of the ABL1 proliferation pathway. In the chimeric BCR-ABL1, the N-terminal BCR region interferes with the negative regulation of ABL1 and mediates dimerization of the protein that autophsophorylates the kinase, fully and constitutively activating it (Greuber et al., 2013). Moreover, in ALL, *BCR-ABL1* like forms exist [10–15% of B-ALL pediatric cases, incidence increased with age (Roberts et al., 2014a)], presenting blasts that are transcriptionally related to *BCR-ABL1* expressing cells althought they lack the t(9;22) transloctation. These forms are recognized as a high-risk ALL subtype across all clinical studies, being characterized by an unfavorable prognosis and a higher relapse rate in comparison to other B-ALL subtypes (Roberts et al., 2014a; Boer et al., 2015). *BCR-ABL1* like cells harbour a multitude of other genomic rearrangements that involves either the ABL encoding genes (e.g., *ABL1, ABL2*), the JAK-kinase genes (e.g., *JAK1, JAK2*) or their upstream receptors (e.g., *PDGFRB, CSF1R. CRLF2, EPOR*) (Roberts et al., 2012; Boer et al., 2017), resulting in the presence of chimeric TK costitutively activating either the ABL1 or the JAK-STAT proliferation pathway (Roberts et al., 2014b; Boer and den Boer, 2017). A third, smaller group is characterized by involvement of genetic fusions that lead to altered TK in the RAS pathways (Ofran and Izraeli, 2017).

In reference to the development of a peptide biosensor to detect ABL1 activity, it is important to consider that ABL1 mediates its catalytic function by protein-protein interactions through three SRC homology domains (highly conserved SH3–SH2–SH1 cassette) located at the ABL1 N-terminal. SH1 binds and cleaves ATP, and mediates tyrosine (Y) phosphorylation in target substrate proteins; SH3 and SH2 domains function as interaction modules for targets and as allosteric inhibitors of the catalytic SH1 domain (Corbi-Verge et al., 2013). The consensus motif of an ABL1 substrate is I/V/-**Y**-X-X-P/F (where X is any amino acid, **Y** representing phosphorylation site). This sequence has been considered as the base to develop a peptide biosensor to detect ABL1 activity and was found by screening a library of billion distinct peptides for interaction with purified ABL1 (Songyang et al., 1994; Songyang et al., 1995). Phospho-peptides generated by the incubation with the TK of interest were isolated and sequenced to determine the optimal aminoacid tolerated at each position. The optimized aminoacidic sequence EAI**Y**AAPFAKK (named as "*reporter*" sequence in this manuscript), was designed. This sequence represents an artificial kinase substrate, not a naturally occurring motif of endogenous proteins (Songyang et al., 1994; Songyang et al., 1995) and corresponds to the commercially available Abltide ($P_{ABLTIDE}$), nowadays largely accepted as a reference peptide biosensor for screening ABL1 activity. However, $P_{ABLTIDE}$ is suitable only for biochemical research use (i.e., enzymatic assays on purified ABL1 or pathogenic chimeric ABL1 proteins), and is not intended for use in clinics and diagnostics because of the lack of serum stability, of cell-penetrating properties and of specific ABL1 targeting among other kinases in primary cells (Wu et al., 2010; Henriques et al., 2013). An additional optimized stretch of amino acids (APTYSPPPPP, named as *"targeting"* in this manuscript) has been designed using biocomputing tools on the basis of physicochemical reasoning, and is recognized by the SH3 domain of ABL1 protein (Pisabarro and Serrano, 1996). This sequence could be linked to the *reporter* region, resulting in a novel artificial peptide (named P_{ABL} in this manuscript) with an increased specificity for ABL1. This peptide was further developed to detect intracellular ABL1 kinase activity in live intact cells (Placzek et al., 2010; Tang et al., 2012; Yang et al., 2013), and was applied to the investigation of the activity of the chimeric BCR-ABL1 in whole cell lysates of patients affected by CML (Yang et al., 2013).

The introduction of targeted therapy with imatinib and other small-molecule inhibitors that target BCR–ABL1, competing at the level of the ATP binding site of the kinase, has significantly improved the outcome in patients with *BCR-ABL1* positive leukemias (An et al., 2010; Biondi et al., 2018). It was thus hypothesized that TKIs specific to ABL1 (e.g., imatinib) or JAK (e.g., ruxolitinib) might be valuable options also for *BCR-ABL1* like ALL cases of the ABL-class or JAK-class respectively (Boer et al., 2017; Fazio et al., 2020), and might represent a better therapeutic choice for these patients, who respond poorly to conventional chemotherapy (Den Boer et al., 2009; Roberts et al., 2012; Boer et al., 2015). Nowadays, several ongoing studies are assessing this issue (clinicaltrials.gov identifiers: NCT02883049, NCT02723994, NCT03117751, NCT02420717,

NCT03571321). The heterogeneity in their genetic background makes the identification of *BCR-ABL1* like ALL very challenging. Currently, the molecular analyses carried out on patient's blasts at diagnosis include karyotyping, fluorescence *in situ* hybridization (FISH) or RT-PCR to detect few specific rearrangements. Useful high-throughput genomic approaches such as exome, whole genome and whole transcriptome sequencing are still too expensive to be routinely employed in clinical practice on large patients' cohorts, particularly in low-income countries (Boer et al., 2017). However, none of these genetic methods can give functional information about the aberrant kinase activity or about blasts sensitivity to TKI. This highlights the importance of having functional assays for TKs with key pathogenic role rather than genomic characterization as tools of precision therapy in *BCR-ABL1* like ALL patients (Franca et al., 2018). Functional TK assays would represent an important tool for clinicians also for *BCR-ABL1* CML and ALL: they could be used to guide the choice of TKI for the best target therapy and to identify primary TKI resistance in a timely manner at diagnosis. Indeed, both imatinib and dasatinib pose resistance problems in BCR-ABL1 positive patients: ABL1 kinase domain mutations have been detected in 30–90% patients who failed imatinib and in 20–80% of patients who failed dasatinib (Gunnar Cario et al., 2020). Identifying in a timely manner the best TKI to be used at diagnosis or during treatment would optimize the chances of survival in patients, and would overcome the possible issue of primary and acquired TKI resistance.

The aim of this study was to investigate the role of P_{ABL} ("*reporter*" + "*targeting*" sequence) as a biosensor able to quantify the ABL1 phosphorylation activity in whole lysates of immortalized leukemic cell lines, including *BCR-ABL1* like ALL cells. Kinase activity was monitored *in vitro* by an ELISA assay. Long-term goal is to set up a point-of-care device to improve the diagnosis and clinical management of *BCR-ABL1* and *BCR-ABL1* like leukemias in clinics. Far from overcoming the importance of monitoring the minimal residual disease, these devices could nonetheless boost the therapeutic monitoring by measuring the residual TK activity or the acquired resistance to these drugs in residual blasts.

MATERIALS AND METHODS

Drug and Chemicals

Imatinib (CDS022173, Sigma-Aldrich, Italy) was dissolved in DMSO at a concentration of 1 mg/ml (2 mM) and ruxolitinib (11,609 Cayman Chemical, United States) in ethanol at a concentration of 10 mg/ml (32.6 mM), according to manufacturer instructions.

Cell Cultures

The study was performed on four human leukemia cell lines purchased from the DSMZ GmbH (Germany): NALM6 (ACC 128), ALL-SIL (ACC 511), K562 (ACC 10), REH (ACC 22). Additionally HEL (ACC 11) and SET2 (ACC 608) cell lines, kindly provided by Professor A. Vannucchi (Department of Experimental and Clinical Medicine, University of Florence), were included in MTT cell viability assay.

Cell Lysates Preparation and Western Blot

Cell protein lysates were prepared for both western blot and P_{ABL}-based ELISA assays. The method of extraction has been optimized by Professor Sorio (University of Verona) and requires the use of kinase and phosphatase inhibitors to maintain the integrity of *BCR-ABL1* in the K562 cell line (**Supplementary Material**). Western blots with antibodies against PDGFRB, ABL1, Phospho-ABL1 (Y245) and actin were performed as described in **Supplementary Material**.

Cell Viability Assays

The effect of TKI on NALM6, ALL-SIL, K562, REH, HEL, SET2 cell lines was determined using the 3-(4,5-dimethylthiazol-2-yl)-2,5-diphenyltetrazolium bromide (MTT) assay and trypan blue exclusion assay, as described in **Supplementary Material**.

Peptide Biosensors

Biosensor peptides were synthesized by GenScript (Piscataway, NJ08854, United States) with 98% purity, and are shown in **Table 1**. P_{ABL} comprises two tyrosine, one in the "*target*" and one in the "*reporter*" region. $P_{ABL\text{-}F}$ is a site-mutated biosensor with the tyrosine in the "*reporter*" region replaced by phenylalanine, and was used in order to verify the specificity of the phosphorylation signal on the catalytic site. $P_{PHOSPHO\text{-}ABL}$ is a fully phosphorylated version of P_{ABL}, used for relative quantification of the phosphorylation level obtained.

P_{ABL}-Based ELISA Assay

The P_{ABL}-based ELISA assay procedure is shown in **Figure 1**. All biosensor peptides contain a biotin tag that allows their anchoring to a neutravidin-coated plate (786-766, G-Bioscience, United States), when loaded onto the plate at a concentration 0.5 μM in PBS and shacked for 1 h at room temperature (RT). To avoid non specific signals the plate was first washed with a Quencher Buffer (100 μl/well, PBS +0.1% Tween 20 pH 7.4 + 0.4% BSA) for 20 min while shaking. 4 μg of cell lysates were then loaded into the plate and incubated in Tyrosine Kinase Buffer (4 mM Tris-HCl pH 7.5, 10 mM $MgCl_2$, 0.1 mM EDTA, 0.01% TritonX) with 100 μM ATP, 1x Roche Inhibitors, 2 mM DTT, 0.1 mM Na_3VO_4 and MilliQ-water (final volume 100 μl) for 1 h at RT. To evaluate the effect of TKI, cell lysates were pre-incubated for 15 min at RT with drugs (imatinib 5 μM, ruxolitinib 52 nM e 5 μM, chosen accordingly to plasma steady state concentrations in patients) before adding on the biosensor-coated plate. The phosphorylation of the peptides was measured using an anti phosphorylated tyrosine antibody (05-1050 4G10 Platinum, EDM Millipore Corporation, dilution 1:10,000 in Quencher Buffer, 1 h, RT while shaking) and detected with a secondary antibody ECL Anti Mouse IgG, HRP from goat (5210-0159, Sera-care, United States, dilution of 1:6,000 in Quencher Buffer, 1 h, RT while shaking). Signal was allowed by adding a solution of citrate buffer pH 6.0, 3% H_2O_2, 0.5% Amplex Ultra Reagent Invitrogen (A36006, Thermofischer Scientific, Italy) and measured 25 times every 0.2 s (544 nm excitation, 590 nm emission wavelengths). $P_{PHOSPHO\text{-}ABL}$ was included in each experiment and

TABLE 1 | Biosensor peptides employed in ELISA assay, their sequence and molecular weight. The "*reporter*" sequence is shown in italic, and the "*targeting*" sequence is underlined. In the phosphorylation site of ABL1, tyrosine and peptide modifications are shown in bold.

Peptides	Sequence	Molecular weight
P_{ABL}	*EAI**Y**AAPFAKK*{Lys(biotin)}GGCGGAPTYSPPPPPG	2,956.41 Da
P_{ABL-F}	*EAI**F**AAPFAKK*{Lys(biotin)}GGCGGAPTYSPPPPPG	2,940.41 Da
$P_{PHOSPHO-ABL}$	*EAI**Y**(**P**)AAPFAKK*{Lys(biotin)}GGCGGAPTYSPPPPPG	3,036.39 Da
$P_{ABLTIDE}$	*EAI**Y**AAPFAKK*{Lys(biotin)}	1,562.90 Da

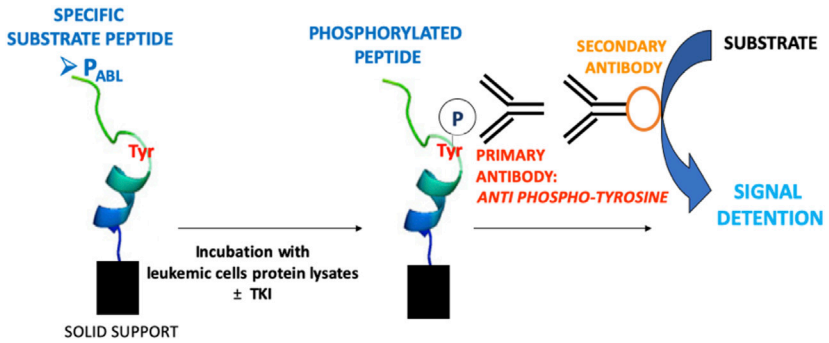

FIGURE 1 | Schematic illustration of P_{ABL}-based ELISA assay principle.

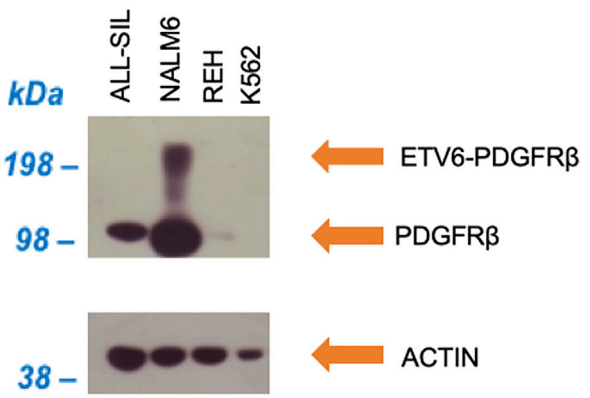

FIGURE 2 | Western blot against human PDGFRB (upper panel) and human actin (lower panel) as loading control.

added to lysates of any cell lines used as an ELISA assay positive control and as a tool to measure the maximal fluorescent signal achievable on the biosensor. P_{ABL} and P_{ABL-F} phosphorylation levels were expressed as a percentage related to $P_{PHOSPHO-ABL}$ phosphorylation in the same cell line, according to the following formula: (mean P_{ABL})/(mean $P_{PHOSPHO-ABL}$) × 100.

Purification of Primary Mononuclear Cells From Patients

Two patients were included in this study. The first was a 40–50 years old male adult affected by chronic myeloid leukaemia (p210 BCR-ABL1 positive), treated at Azienda Ospedaliero-Universitaria in Udine (Italy). The second was a 1–3 years old female child (affected by *BCR-ABL1* negative ALL, data regarding *BCR-ABL1* like translocations not known) treated at IRCCS Burlo Garofolo in Trieste (Italy). Bone marrow aspirates were collected at onset as part of diagnostic procedures, and used for research purpose only when clinical procedures had been completed. Patients' bone marrow aspirates (~3–5 ml) were diluted with PBS to a final volume of 10 ml and loaded on Ficoll-PaqueTM Plus (5 ml); after centrifugation (800 xg, 20 min, 15°C), interphase was recovered and washed twice with PBS (7 ml, 300 xg, 10 min, 15°C); 20×10^6 mononuclear cells were used for cell lysate preparation.

Statistical Analysis

Data obtained from the MTT assay were analyzed using a nonlinear regression on GraphPad Prism8; IC_{50} was determined from the dose-response curve. Statistical analysis was performed using two-way ANOVA and Bonferroni multiple comparison test; statistical significance was set at $p < 0.05$.

RESULTS

Cell Lines Characterization

Four human leukemia cell lines with different genetic background were selected and initially characterized by western blot to confirm the presence of candidate chimeric proteins: NALM6 and ALL-SIL cells were chosen because they harbor the gene fusions *ETV6-PDGFRB* (Matheson and Hall, 2003) and *NUP214-ABL1* respectively, both belonging to the *BCR-ABL1* like

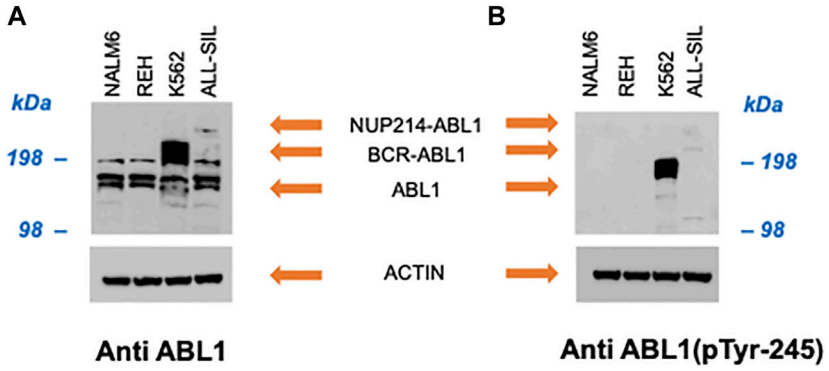

FIGURE 3 | Western blot with **(A)** anti human ABL1 and **(B)** anti human phospho-ABL1. Actin was used as loading control.

aberrations and both leading to ABL1 pathway overactivation (Zhou and Yang, 2014). Because of the t(9;22) rearrangement encoding BCR-ABL1, K562 was used as control model for the P_{ABL}-based ELISA assay. REH cells are carriers of the *ETV6-RUNX1* (*TEL-AML1*) gene fusion.

In NALM6 the presence of ETV6-PDGFRB was investigated using an antibody directed against human PDGFRB. As showed in **Figure 2**, a band with molecular weight of ~100 kDa, corresponding to PDGFRB (predicted molecular weight 125 kDa), was clearly visible in NALM6 and also in ALL-SIL and to a lesser extent in REH cells, while it was lacking in K562. ETV6-PDGFRB has a predicted molecular mass of 76 kDa (Carroll et al., 1996): the monomer should migrate to an apparent molecular weight of 90–100 kDa in SDS-PAGE. In NALM6, a specific band >200 kDa appeared, corresponding to the presence of oligomeric and multimeric complexes of the chimeric protein. Western blots using antibodies against ABL1 and phospho-ABL1 (pTyr-245) were performed as shown in **Figure 3**. In K562 cells the expected band around 210 kDa, corresponding to BCR-ABL1, was visible and in ALL-SIL cells a band around 300 kDa, corresponding to the chimeric protein NUP214-ABL1, was also evident (**Figure 3A**). Wild type ABL1 was visible in NALM6, REH, K562, ALL-SIL in comparable amount (**Supplementary Figure S1**). Western blot with anti phospho-ABL1 showed a band of 210 kDa, corresponding to phosphorylated BCR-ABL1 protein and a band at lower molecular weight (around 125 kDa), corresponding to phosphorylated ABL1, in K562 cells (**Figure 3B**). Phospho-proteins were not detected in other cell lines.

The cytotoxic effect of TKI (imatinib and ruxolitinib) on cell lines was determined using the MTT assay (**Figure 4**). Viability of the 2 cell lines harboring the *ABL1* fusion genes was clearly impaired by imatinib, and differed significantly each other ($p < 0.0001$) with the ALL-SIL being more sensitive (IC_{50} = 46.9 ± 6.99 nM) than K562 [0.38 ± 0.13 μM in accordance to previously reported values (Quintás-Cardama and Cortes, 2009)]. Imatinib affected also NALM6 viability at higher concentration (IC_{50} = 5.56 ± 0.65 μM), whereas a survival of ~70% was observed in REH at 10 μM, the highest concentration tested (**Figure 4A**). As expected, cell lines were resistant to ruxolitinib, a specific JAK1/2 inhibitor (**Figure 4B**), in contrast to what was observed for HEL (IC_{50} = 1.19 ± 0.33 μM) and SET2 cells (IC_{50} = 48.58 ± 0.56 nM), used as positive control (**Supplementary Figure S2**). Cytotoxic effects evaluated by the MTT assay could be confounded by metabolically inactive cells. Therefore, cell viability was also confirmed by trypan blue exclusion assay (**Supplementary Table S1**). Imatinib concentrations were chosen according to MTT results, being 0.38 μM the K562 IC_{50}, 5.5 μM the NALM6 IC_{50} and 10 μM the highest drug concentration tested. Comparable but not perfectly overlapping values in survival rates was observed for K562 at 0.38 μM (37.53 ± 9.11% vs. the expected 50% calculated by MTT results measuring mitochondrial cell activity) and for ALL-SIL (29.30 ± 12.86% at 0.38 μM and 18.58 ± 3.59% at 10 μM vs. the almost 100% mortality reached in MTT assays). A good correspondence was instead observed for NALM6 and REH (survival rates 51.17 ± 9.93% at 5.5 μM and 74.68 ± 31.53% at 10 μM, respectively). In MTT assay, cells were resistant to ruxolitinib at concentration lower than 10 μM, therefore this concentration and a higher one (i.e., 50 μM) were used for trypan blue exclusion assay. As expected, cell viability was only slightly affected at ruxolitinib concentration of 10 μM and required exposure to very high concentration of the drug, well outside the therapeutic range of clinical interest, to be compromised.

Peptide Biosensor *in vitro* Functional Analysis

The P_{ABL}-based ELISA analysis showed a significant phosphorylation of the P_{ABL} biosensor probe after incubation with all four leukemic cell lines tested (two-way ANOVA, Bonferroni post-test, p-value < 0.0001, **Figure 5**). **Supplementary Table S2** reports results of the phosphorylated P_{ABL} as percentages relative to the fully phosphorylated $P_{PHOSPHO-ABL}$, used as positive reference value in each cell line: average basal phosphorylation of lysates was 6.84 ± 1.46% in absence of biosensor vs. 32.44 ± 3.25% in presence of P_{ABL}. As shown in **Figure 5**, K562 cells presented the highest phosphorylation level (mean fluorescence intensity (FI):

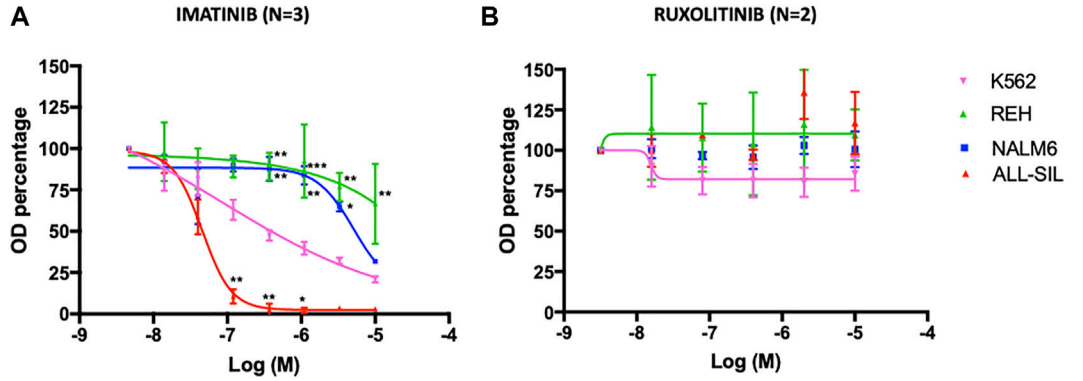

FIGURE 4 | Dose-response curve with **(A)** imatinib and **(B)** ruxolitinib. Leukemia cell lines were seeded at 12,000 cells/well with a range of concentrations of 0.014–10 μM for imatinib and 0.016–10 μM for ruxolitinib. MTT assay was performed after 72 h of incubation. Error bars represent mean ± SEM ($n = 3$ for imatinib, $n = 2$ for ruxolitinib). REH, NALM6 or ALL-SIL versus K562: *$p < 0.05$; **$p < 0.001$, ***$p < 0.0001$ two-way ANOVA, Bonferroni post-test.

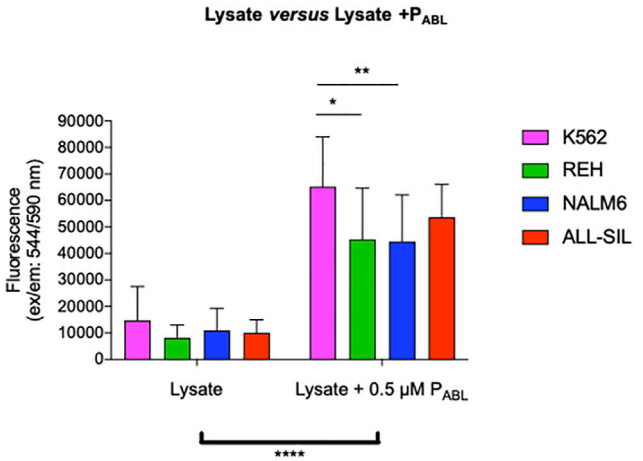

FIGURE 5 | P_{ABL}-based ELISA assay. The graph shows data obtained from 12 independent experiments for K562, REH and NALM6 cell lines and seven experiments for the ALL-SIL cell line. Fluorescence values in ordinate. There is a significant increase in terms of phosphorylation levels for all the lines after incubation with the peptide P_{ABL} (****, p-value ANOVA two-way 0.0001). K562 line showed the highest signal, significantly higher compared to the NALM6 and REH (p-value ANOVA two-way Bonferroni post-test for multiple comparison: *: 0.05; **: 0.001).

65,185.81), similar to the P_{ABL} phosphorylation obtained after incubation with ALL-SIL lysates (mean FI: 53,671.62). A lower signal was instead observed for NALM6 (mean FI: 44,495.64, p-value < 0.01 vs. K562) and REH (mean FI: 45,352.60, p-value < 0.05 vs. K562). To confirm the contribution of ABL1 activity on the probe, cell lysates were pre-incubated with ABL1 specific and non-specific inhibitor (imatinib and ruxolitinib, respectively). Pre-incubation of lysates with 5 μM imatinib lead to a significant decrease of P_{ABL} phosphorylation (two-way ANOVA, Bonferroni post-test, p-value < 0.0001, **Figure 6A**). In contrast, ruxolitinib (a JAK1/2 specific inhibitor) did not affect significantly the P_{ABL} phosphorylation neither at 52 nM nor at 5 μM, although a slight decrease in P_{ABL} signals was observed in NALM6, REH and ALL-SIL at the highest concentration likely due to an aspecific effect (**Figure 6B**).

An ELISA assay was performed on K562 lysates to compare the P_{ABL} ("*target*" + "*reporter*" sequences) to $P_{ABLTIDE}$ ("*reporter*" sequence only). P_{ABL} shows a higher phosphorylation compared to $P_{ABLTIDE}$ (two-way ANOVA, Bonferroni post-test, p-value 0.023), with a significant decrease after imatinib pre-treatment of lysates (p-value 0.0027, **Supplementary Figure S3A**). Interestingly, no significant changes in phosphorylation level of $P_{ABLTIDE}$ was observed increasing both the amount of lysate and the probe concentration (**Supplementary Figure S3B**).

P_{ABL} comprises two tyrosines, one in the "*target*" and one in the "*reporter*" region. In order to verify the specificity of the phosphorylation signal on the catalytic site, a site-mutated biosensor was introduced in the assay (i.e., $P_{ABL\text{-}F}$, with the tyrosine in the "*reporter*" region replaced by phenylalanine). The levels of $P_{ABL\text{-}F}$ phosphorylation were similar among cell lysates, and did not differ from the basal fluorescence signals detectable in all cell lines in the absence of peptide (**Supplementary Figure S4** and **Supplementary Table S3**).

To further validate the novel P_{ABL}-based ELISA assay, lysates of primary leukemic cells derived from two patients, one affected by chronic myeloid leukaemia (p210 *BCR-ABL1* positive, Pt#1) and another by ALL (*BCR-ABL1* negative, Pt#2), were also used. In both cases, the P_{ABL} biosensor probe was phosphorylated after incubation with cell lysates (two-way ANOVA, Bonferroni post-test, Pt#1: p-value < 0.001, Pt#2: p-value < 0.05, **Figure 7**). However, inter-patient differences were observed in the presence of TKI. The pattern of drug inhibition was compatible to the expected ABL1-mediated P_{ABL} phosphorylation in *BCR-ABL1* positive pt#1 (P_{ABL} signal inhibited by imatinib (p-value < 0.001) but not by ruxolitinib), in contrast to what was observed in *BCR-ABL1* negative pt#2 (P_{ABL} signal inhibited by ruxolitinib (p-value < 0.05) but not by imatinib). Cells sensitivity to imatinib and ruxolitinib could not be assessed due to the scanty biological material available.

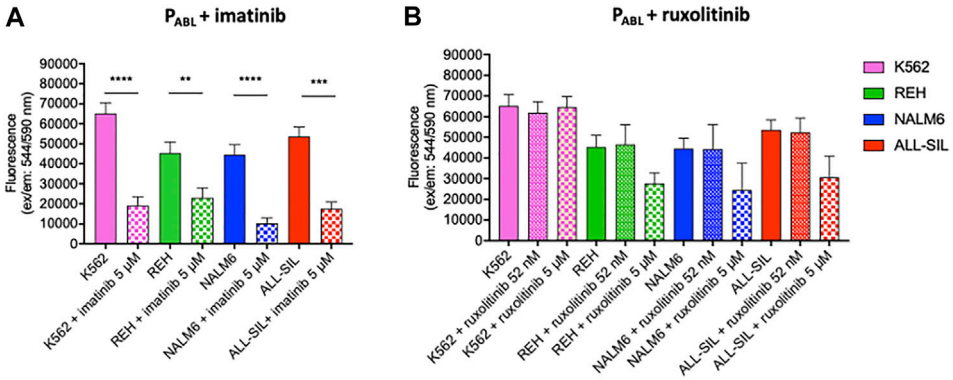

FIGURE 6 | P_{ABL}-based ELISA assay in the presence of **(A)** imatinib and **(B)** ruxolitinib. Fluorescence values in ordinate. Imatinib determines a significant decrease of P_{ABL}-phosphorylation in all cell lines. The reduction is particularly evident for those cell lines with alterations affecting the ABL1-pathway (K562, and ALL-SIL) and is less pronounced in REH. Ruxolitinib treatment does not affect P_{ABL}-phosphorylation. *p*-value according to two-way ANOVA, Bonferroni post-test for multiple comparison: ****, <0.0001; ***, <0.001; **, <0.01.

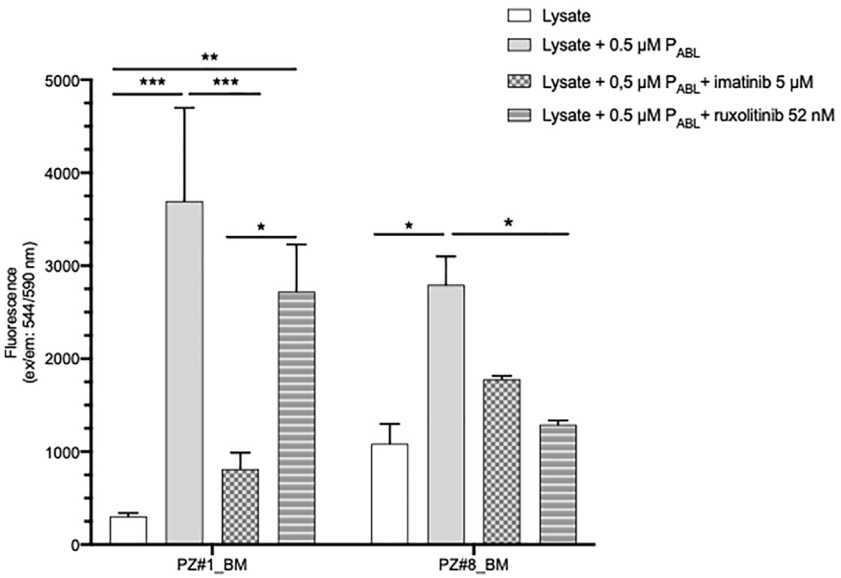

FIGURE 7 | P_{ABL}-based ELISA assay in patients' primary cells lysates. Pt#1 is an adult male patient affected by CML (p210 BCR-ABL1 positive); Pt#2 is a female child affected by *BCR-ABL1* negative ALL (*BCR-ABL1 like* translocations not known). Fluorescence values in ordinate. *p*-value according to two-way ANOVA, Bonferroni post-test for multiple comparison: ***, <0.001; **, <0.01, * <0.05.

DISCUSSION

In recent years, several potential peptides allowing the study of kinases' activity *in vitro* have been developed (Lipchik et al., 2015; Perez et al., 2019). The artificial peptide P_{ABL} resembles the previously published cell-permeable biosensor peptide used to monitor the BCR-ABL1 function in CML (Yang et al., 2013), with "*reporter*" and "*target*" sequences in common. Here, P_{ABL} was employed to validate its use in lysates of ALL cell lines with different genetic background, including those harboring *BCR-ABL1* like ALL translocations of the ABL-class. The phosphorylation of the P_{ABL} probe was detected after the incubation with cell lysates. Interestingly, none of the cell lysates induced an increase of $P_{ABL\text{-}F}$ phosphorylation, indicating a kinase discriminatory action on the tyrosine in the "*reporter*" region. K562 cells showed the highest fluorescence signal on P_{ABL} although comparable to that observed for ALL-SIL. Both these cell lines strongly rely on ABL1 for survival and proliferation, as demonstrated by MTT and trypan blue viability assays, although only BCR-ABL1 and not NUP214-ABL1 could be detected in the phosphorylated form by western blot. It is known that NUP214-ABL1 displays much lower auto-phosphorylation than BCR-ABL1 (Brasher and Van Etten, 2000; De Keersmaecker et al., 2008a; De Keersmaecker et al., 2008b). Because of this lower activation, ALL-SIL cells are more sensitive

than K562 to imatinib, an ABL1 inhibitor that targets specifically the inactive conformation of the ABL1 kinase. Nonetheless, BCR-ABL1 and NUP214-ABL1 largely overlap in their substrate specificity as demonstrated using a peptide array (De Keersmaecker et al., 2008a).

NALM6 cells were chosen because they harbor the gene fusion *ETV6-PDGFRB*. PDRGFB is a cell surface TK receptor that activates the ABL1 pathway (Plattner et al., 2004), and *PDRGFB* rearrangements (*ETV6-PDGRFB* and *EBF1-PDGFRB*) are present in about 1% of *BCR-ABL1* like positive patients (Boer et al., 2017). Recent studies observed a reduction in signalling with imatinib in cases harboring ABL1-class rearrangments (Roberts et al., 2017), and a case-report on a refractory *EBF1-PDGFRB* ALL patient showed the complete remission after the addition of imatinib to the conventional chemiotherapy (Weston et al., 2013). The chimeric protein ETV6-PDGFRB contains the amino-terminal 154 amino acids of ETV6 fused to the transmembrane and cytoplasmic domains of PDGFRB, and has a calculated molecular mass of 76 kDa (Carroll et al., 1996). Western blot using an anti human PDGFRB confirmed the presence of ETV6-PDGFRB in NALM6: the monomer migrated at 90–100 kDa in SDS gel-electrophoresis; however, ETV6-PDGFRB appeared in NALM6 also as oligomeric or multimeric complexes resulting in a band around 200 kDa, as already observed in literature (Sjöblom et al., 1999). The *wild type* PDGFRB was also detectable in all the cell lines (a band around 100 kDa) except for K562. Some investigators report that NALM6 cell line harbors a different translocation, in particular DUX4-rearranged [t (4;14) (q35;q32)]/ERG deletion (Yasuda et al., 2016; Tanaka et al., 2018); however, both our western blotting analysis and cytogenetic information on the t(5;12)(q33.2;p13.2) translocation confirm the presence of the *ETV6-PDGFRB* in the NALM6 cells used in this paper (Wlodarska et al., 1997)[1]. Since PDGRFB is linked to ABL1 activation (Plattner et al., 2003), we expected higher P_{ABL} phosphorylation values also for the *BCR-ABL1* like cell line NALM6, in particular in comparison to REH cells that should not present constitutively active ABL1 based on their genetic profile, but surprisingly, these two cell lines showed similar fluorescence levels. The reason is still unclear, but can be related to the ubiquitous presence of ABL1 in the cell lines (Greuber et al., 2013). Indeed, Western blot analysis with anti-human ABL1 showed the presence of non-phosphorylated ABL1 in both REH and NALM6, without detecting the phosphorylated form.

The specificity of the P_{ABL} phosphorylation signal was also confirmed after treatment with TKI. Indeed, the ABL1-inhibitor imatinib was used at a concentration of 5 μM that, as reported in the literature, represents the steady state plasma concentration after 5–7 days of treatment in adult CML at a dose of 400 mg/day (Druker et al., 2001), and is 20 times higher than the IC_{50} calculated *in vitro* on cellular tyrosine phosphorylation assay (Deininger et al., 2005). At this concentration, a significant decrease in P_{ABL} phosphorylation levels after the incubation with the drug was observed for all cell lines. It is known from the literature that imatinib has an unusually high selectivity to ABL1 because it targets the inactive conformation which is unique to this kinase (Lee and Wang, 2009). Mass spectrometry analysis investigating imatinib-associated proteins in K562 lysates confirmed the direct interaction of the drug with only few targets, including the known interactor BCR-ABL1 and the ABL-releted gene (ARG), Discoidin Domain Receptor Tyrosine Kinase 1 (DDR1) and the proto-oncogene receptor tyrosine kinase (KIT) (Bantscheff et al., 2007; Rix et al., 2007). DDR1 and KIT are receptor tyrosine kinases and their contribution to the ABL1 activation likely depends on extracellular stimuli. Therefore, considering that our *in vitro* system works on cell lysates rather than whole cells in the absence of specific ligands, their confounding contribution to the P_{ABL} phosphorylation, if any, is likely less important. In contrast, contribution of ARG (closely related to ABL1) could be an issue. However, the P_{ABL} *target* region should guarantee an increased specificity for ABL1 compared to ARG. Mass spectrometry studies identified additionally one off-target (non-tyrosine kinase) of imatinib, the NAD(P)H:quinone oxidoreductase NQO2, whose enzymatic function should not influence the peptide phosphorylation (Bantscheff et al., 2007; Rix et al., 2007). In contrast to imatinib, the anti-JAK inhibitor ruxolitinib did not affect the P_{ABL} phosphorylation levels at any of the concentrations selected (52 nM and 5 μM). The concentration of 52 nM was chosen in accordance to pharmacokinetic parameters measured in healthy subjects at steady state following a twice-daily administration of ruxolitinib at 15 mg and is 20 times higher than the IC_{50} of 2.8 ± 1.2 nM calculated *in vitro* for JAK2 by a biochemical enzymatic inhibitory assay (Quintás-Cardama et al., 2010). The second concentration of 5 μM is much higher than the pharmacological range and was included into the P_{ABL}-based ELISA assay in order to verify the absence of inhibition, even at this high concentration.

In our *in vitro* ELISA assay, $P_{ABLTIDE}$ was clearly less performing than P_{ABL}, designed to increase the specificity to ABL1 among other kinases. Besides the increased specificity of P_{ABL} over $P_{ABLTIDE}$, the ELISA assay proposed in this paper presents other advantages over conventional kinase assay. Firstly, the biosensor phosphorylation was quantified on a solid-phase through a neutravidin-coated plate that allows the binding of the biotin in the P_{ABL} sequence. This high specific binding greatly reduces background noise signals. Secondly, whole cell lysates can be used, avoiding tricky ABL1 purification and bypassing the problems related to the peptide penetration into intact cells. Thirdly, a unique primary antibody, i.e., an anti-phosphotyrosine, is required. This advantage is particularly important for *BCR-ABL1* like ALL because the ELISA assay conditions could be optimized regardless of the specific chimeric protein encoded by the genetic abnormalities in *BCR-ABL* like leukemic cells of the ABL-class.

Initial attempts to validate the novel P_{ABL}-based ELISA assay on lysates of patients' leukemic cells were performed. Although results are preliminary and limited to only two samples, they allow some considerations, to be confirmed by further investigations. As observed in immortalized cell lines, P_{ABL} becomes phosphorylated after the incubation with leukemic cell lysates regardless the presence of a BCR-ABL1 chimeric protein; however, in contrast to them, this phosphorylation is ABL-1 mediated only in some patients in which it is specifically

[1]https://www.dsmz.de/collection/catalogue/details/culture/ACC-128.

inhibited by imatinib. A different contribution of ABL1 and other TK on P_{ABL} could be hypothesized among different patients, according to their pathogenetic profile.

Taken together, these observations suggest that the P_{ABL}-based ELISA assay is suitable for measuring the ABL1 kinase activity of cell lysates through the P_{ABL}-Y phosphorylation in the *"reporter"* region. P_{ABL} could be more suitable in detecting aberrant sustained kinase activity of ABL1-chimeric proteins rather than an over-activation of native ABL1 due to upstream signaling; however, a limitation of this study is that the difference between basal and sustained ABL1 activity is still too tiny for the P_{ABL}-based ELISA assay to be of practical clinical interest without any further optimization. To confirm its utility, our system should be improved in sensitivity and accuracy, and results could be strengthened by other TKI, the use of different biosensors (e.g., of downstream signaling components such as STAT5 that is known to be activated by ABL1-class rearrangements), and the test of patient samples of known genotype. Nonetheless, the results here described represents the first step towards the setup of a point-of-care device for diagnosis and therapeutic drug monitoring of pediatric *BCR-ABL1* like patients.

DATA AVAILABILITY STATEMENT

The raw data supporting the conclusion of this article will be made available by the authors, without undue reservation.

ETHICS STATEMENT

The studies involving human participants were reviewed and approved by the Institutional review board IRCCS Burlo Garofolo, Trieste, Italy, Protocol number CE/V 135. Written informed consent to participate in this study was provided by the participants' legal guardian/next of kin.

AUTHOR CONTRIBUTIONS

Conceptualization, RF, CS, GD, and GS; Data curation, OM, RF, SB, and GS; Formal analysis, GS; Funding acquisition, AT, GD, and GS; Investigation, OM, SB, GZ, and CB; Writing–original draft, OM, SB, and RF; Writing–review and editing, ET, CS, MR, AT, GD, and GS.

FUNDING

This research was funded by the grant ROCHE PER LA RICERCA 2016.

SUPPLEMENTARY MATERIAL

The Supplementary Material for this article can be found online at: https://www.frontiersin.org/articles/10.3389/fphar.2021.749361/full#supplementary-material

REFERENCES

An, X., Tiwari, A. K., Sun, Y., Ding, P. R., Ashby, C. R., Jr., and Chen, Z. S. (2010). BCR-ABL Tyrosine Kinase Inhibitors in the Treatment of Philadelphia Chromosome Positive Chronic Myeloid Leukemia: a Review. *Leuk. Res.* 34 (10), 1255–1268. doi:10.1016/j.leukres.2010.04.016

Bantscheff, M., Eberhard, D., Abraham, Y., Bastuck, S., Boesche, M., Hobson, S., et al. (2007). Quantitative Chemical Proteomics Reveals Mechanisms of Action of Clinical ABL Kinase Inhibitors. *Nat. Biotechnol.* 25 (9), 1035–1044. doi:10.1038/nbt1328

Biondi, A., Gandemer, V., De Lorenzo, P., Cario, G., Campbell, M., Castor, A., et al. (2018). Imatinib Treatment of Paediatric Philadelphia Chromosome-Positive Acute Lymphoblastic Leukaemia (EsPhALL2010): a Prospective, Intergroup, Open-Label, Single-Arm Clinical Trial. *Lancet Haematol.* 5 (12), e641–e652. doi:10.1016/s2352-3026(18)30173-x

Boer, J. M., and den Boer, M. L. (2017). BCR-ABL1-like Acute Lymphoblastic Leukaemia: From Bench to Bedside. *Eur. J. Cancer* 82, 203–218. doi:10.1016/j.ejca.2017.06.012

Boer, J. M., Marchante, J. R., Evans, W. E., Horstmann, M. A., Escherich, G., Pieters, R., et al. (2015). BCR-ABL1-like Cases in Pediatric Acute Lymphoblastic Leukemia: a Comparison between DCOG/Erasmus MC and COG/St. Jude Signatures. *Haematologica* 100 (9), e354–7. doi:10.3324/haematol.2015.124941

Boer, J. M., Steeghs, E. M., Marchante, J. R., Boeree, A., Beaudoin, J. J., Beverloo, H. B., et al. (2017). Tyrosine Kinase Fusion Genes in Pediatric BCR-ABL1-like Acute Lymphoblastic Leukemia. *Oncotarget* 8 (3), 4618–4628. doi:10.18632/oncotarget.13492

Brasher, B. B., and Van Etten, R. A. (2000). c-Abl Has High Intrinsic Tyrosine Kinase Activity that Is Stimulated by Mutation of the Src Homology 3 Domain and by Autophosphorylation at Two Distinct Regulatory Tyrosines. *J. Biol. Chem.* 275 (45), 35631–35637. doi:10.1074/jbc.M005401200

Carroll, M., Tomasson, M. H., Barker, G. F., Golub, T. R., and Gilliland, D. G. (1996). The TEL/platelet-derived Growth Factor Beta Receptor (PDGF Beta R) Fusion in Chronic Myelomonocytic Leukemia Is a Transforming Protein that Self-Associates and Activates PDGF Beta R Kinase-dependent Signaling Pathways. *Proc. Natl. Acad. Sci. U S A.* 93 (25), 14845–14850. doi:10.1073/pnas.93.25.14845

Corbi-Verge, C., Marinelli, F., Zafra-Ruano, A., Ruiz-Sanz, J., Luque, I., and Faraldo-Gómez, J. D. (2013). Two-state Dynamics of the SH3-SH2 Tandem of Abl Kinase and the Allosteric Role of the N-Cap. *Proc. Natl. Acad. Sci. USA* 110 (36), E3372–E3380. doi:10.1073/pnas.1303966110

De Keersmaecker, K., Rocnik, J. L., Bernad, R., Lee, B. H., Leeman, D., Gielen, O., et al. (2008). Kinase Activation and Transformation by NUP214-ABL1 Is Dependent on the Context of the Nuclear Pore. *Mol. Cel* 31 (1), 134–142. doi:10.1016/j.molcel.2008.05.005

De Keersmaecker, K., Versele, M., Cools, J., Superti-Furga, G., and Hantschel, O. (2008). Intrinsic Differences between the Catalytic Properties of the Oncogenic NUP214-ABL1 and BCR-ABL1 Fusion Protein Kinases. *Leukemia* 22 (12), 2208–2216. doi:10.1038/leu.2008.242

Deininger, M., Buchdunger, E., and Druker, B. J. (2005). The Development of Imatinib as a Therapeutic Agent for Chronic Myeloid Leukemia. *Blood* 105 (7), 2640–2653. doi:10.1182/blood-2004-08-3097

Den Boer, M. L., van Slegtenhorst, M., De Menezes, R. X., Cheok, M. H., Buijs-Gladdines, J. G., Peters, S. T., et al. (2009). A Subtype of Childhood Acute Lymphoblastic Leukaemia with Poor Treatment Outcome: a Genome-wide Classification Study. *Lancet Oncol.* 10 (2), 125–134. doi:10.1016/s1470-2045(08)70339-5

Druker, B. J., Talpaz, M., Resta, D. J., Peng, B., Buchdunger, E., Ford, J. M., et al. (2001). Efficacy and Safety of a Specific Inhibitor of the BCR-ABL Tyrosine Kinase in Chronic Myeloid Leukemia. *N. Engl. J. Med.* 344 (14), 1031–1037. doi:10.1056/NEJM200104053441401

Fazio, F., Barberi, W., Cazzaniga, G., Fazio, G., Messina, M., Della Starza, I., et al. (2020). Efficacy of Imatinib and Chemotherapy in a Pediatric Patient with Philadelphia-like Acute Lymphoblastic Leukemia with Ebf1-Pdgfrb Fusion Transcript. *Leuk. Lymphoma* 61 (2), 469–472. doi:10.1080/10428194.2019.1668938

Franca, R., Kuzelicki, N. K., Sorio, C., Toffoletti, E., Montecchini, O., Poropat, A., et al. (2018). Targeting Kinase-Activating Genetic Lesions to Improve Therapy of Pediatric Acute Lymphoblastic Leukemia. *Curr. Med. Chem.* 25 (24), 2811–2825. doi:10.2174/0929867324666170727101932

Greuber, E. K., Smith-Pearson, P., Wang, J., and Pendergast, A. M. (2013). Role of ABL Family Kinases in Cancer: from Leukaemia to Solid Tumours. *Nat. Rev. Cancer* 13 (8), 559–571. doi:10.1038/nrc3563

Gunnar Cario, G., Veronica Leoni, V., Valentino Conter, V., André Baruchel, A., Martin Schrappe, M., and Andrea Biondi, A. (2020). BCR-ABL1-like Acute Lymphoblastic Leukemia in Childhood and Targeted Therapy. *Haematologica* 105 (9), 2200–2204. doi:10.3324/haematol.2018.207019

Henriques, S. T., Thorstholm, L., Huang, Y. H., Getz, J. A., Daugherty, P. S., and Craik, D. J. (2013). A Novel Quantitative Kinase Assay Using Bacterial Surface Display and Flow Cytometry. *PLOS ONE* 8 (11), e80474. doi:10.1371/journal.pone.0080474

Lee, S. J., and Wang, J. Y. (2009). Exploiting the Promiscuity of Imatinib. *J. Biol.* 8 (3), 30. doi:10.1186/jbiol134

Lipchik, A. M., Perez, M., Bolton, S., Dumrongprechachan, V., Ouellette, S. B., Cui, W., et al. (2015). KINATEST-ID: a Pipeline to Develop Phosphorylation-dependent Terbium Sensitizing Kinase Assays. *J. Am. Chem. Soc.* 137 (7), 2484–2494. doi:10.1021/ja507164a

Matheson, E. C., and Hall, A. G. (2003). Assessment of Mismatch Repair Function in Leukaemic Cell Lines and Blasts from Children with Acute Lymphoblastic Leukaemia. *Carcinogenesis* 24 (1), 31–38. doi:10.1093/carcin/24.1.31

Ofran, Y., and Izraeli, S. (2017). BCR-ABL (Ph)-like Acute Leukemia-Pathogenesis, Diagnosis and Therapeutic Options. *Blood Rev.* 31 (2), 11–16. doi:10.1016/j.blre.2016.09.001

Perez, M., Blankenhorn, J., Murray, K. J., and Parker, L. L. (2019). High-throughput Identification of FLT3 Wild-type and Mutant Kinase Substrate Preferences and Application to Design of Sensitive *In Vitro* Kinase Assay Substrates. *Mol. Cel Proteomics* 18 (3), 477–489. doi:10.1074/mcp.RA118.001111

Pisabarro, M. T., and Serrano, L. (1996). Rational Design of Specific High-Affinity Peptide Ligands for the Abl-SH3 Domain. *Biochemistry* 35 (33), 10634–10640. doi:10.1021/bi960203t

Placzek, E. A., Plebanek, M. P., Lipchik, A. M., Kidd, S. R., and Parker, L. L. (2010). A Peptide Biosensor for Detecting Intracellular Abl Kinase Activity Using Matrix-Assisted Laser Desorption/ionization Time-Of-Flight Mass Spectrometry. *Anal. Biochem.* 397 (1), 73–78. doi:10.1016/j.ab.2009.09.048

Plattner, R., Irvin, B. J., Guo, S., Blackburn, K., Kazlauskas, A., Abraham, R. T., et al. (2003). A New Link between the C-Abl Tyrosine Kinase and Phosphoinositide Signalling through PLC-Gamma1. *Nat. Cel. Biol.* 5 (4), 309–319. doi:10.1038/ncb949

Plattner, R., Koleske, A. J., Kazlauskas, A., and Pendergast, A. M. (2004). M005401200, Pendergast, A.M Bidirectional Signaling Links the Abelson Kinases to the Platelet-Derived Growth Factor Receptor. *Mol. Cel. Biol.* 24 (6), 2573–2583. doi:10.1128/mcb.24.6.2573-2583.2004

Quintás-Cardama, A., and Cortes, J. (2009). Molecular Biology of Bcr-Abl1-Positive Chronic Myeloid Leukemia. *Blood* 113 (8), 1619–1630. doi:10.1182/blood-2008-03-144790

Quintás-Cardama, A., Vaddi, K., Liu, P., Manshouri, T., Li, J., Scherle, P. A., et al. (2010). Preclinical Characterization of the Selective JAK1/2 Inhibitor INCB018424: Therapeutic Implications for the Treatment of Myeloproliferative Neoplasms. *Blood* 115 (15), 3109–3117. doi:10.1182/blood-2009-04-214957

Rix, U., Hantschel, O., Dürnberger, G., Remsing Rix, L. L., Planyavsky, M., Fernbach, N. V., et al. (2007). Chemical Proteomic Profiles of the BCR-ABL Inhibitors Imatinib, Nilotinib, and Dasatinib Reveal Novel Kinase and Nonkinase Targets. *Blood* 110 (12), 4055–4063. doi:10.1182/blood-2007-07-102061

Roberts, K. G., Li, Y., Payne-Turner, D., Harvey, R. C., Yang, Y. L., Pei, D., et al. (2014). Targetable Kinase-Activating Lesions in Ph-like Acute Lymphoblastic Leukemia. *N. Engl. J. Med.* 371 (11), 1005–1015. doi:10.1056/NEJMoa1403088

Roberts, K. G., Morin, R. D., Zhang, J., Hirst, M., Zhao, Y., Su, X., et al. (2012). Genetic Alterations Activating Kinase and Cytokine Receptor Signaling in High-Risk Acute Lymphoblastic Leukemia. *Cancer Cell.* 22 (2), 153–166. doi:10.1016/j.ccr.2012.06.005

Roberts, K. G., Pei, D., Campana, D., Payne-Turner, D., Li, Y., Cheng, C., et al. (2014). Outcomes of Children with BCR-ABL1–like Acute Lymphoblastic Leukemia Treated with Risk-Directed Therapy Based on the Levels of Minimal Residual Disease. *J. Clin. Oncol.* 32 (27), 3012–3020. doi:10.1200/JCO.2014.55.4105

Roberts, K. G., Yang, Y. L., Payne-Turner, D., Lin, W., Files, J. K., Dickerson, K., et al. (2017). Oncogenic Role and Therapeutic Targeting of ABL-Class and JAK-STAT Activating Kinase Alterations in Ph-like ALL. *Blood Adv.* 1 (20), 1657–1671. doi:10.1182/bloodadvances.2017011296

Sjöblom, T., Boureux, A., Rönnstrand, L., Heldin, C. H., Ghysdael, J., and Ostman, A. (1999). Characterization of the Chronic Myelomonocytic Leukemia Associated TEL-PDGF Beta R Fusion Protein. *Oncogene* 18 (50), 7055–7062. doi:10.1038/sj.onc.1203190

Songyang, Z., Blechner, S., Hoagland, N., Hoekstra, M. F., Piwnica-Worms, H., and Cantley, L. C. (1994). Use of an Oriented Peptide Library to Determine the Optimal Substrates of Protein Kinases. *Curr. Biol.* 4 (11), 973–982. doi:10.1016/S0960-9822(00)00221-9

Songyang, Z., Carraway, K. L., Eck, M. J., Harrison, S. C., Feldman, R. A., Mohammadi, M., et al. (1995). Catalytic Specificity of Protein-Tyrosine Kinases Is Critical for Selective Signalling. *Nature* 373 (6514), 536–539. doi:10.1038/373536a0

Tanaka, Y., Kawazu, M., Yasuda, T., Tamura, M., Hayakawa, F., Kojima, S., et al. (2018). Transcriptional Activities of DUX4 Fusions in B-Cell Acute Lymphoblastic Leukemia. *Haematologica* 103 (11), e522–e526. doi:10.3324/haematol.2017.183152

Tang, J., Wang, J. Y., and Parker, L. L. (2012). Detection of Early Abl Kinase Activation after Ionizing Radiation by Using a Peptide Biosensor. *Chembiochem* 13 (5), 665–673. doi:10.1002/cbic.201100763

Weston, B. W., Hayden, M. A., Roberts, K. G., Bowyer, S., Hsu, J., Fedoriw, G., et al. (2013). Tyrosine Kinase Inhibitor Therapy Induces Remission in a Patient with Refractory EBF1-PDGFRB-Positive Acute Lymphoblastic Leukemia. *J. Clin. Oncol.* 31 (25), e413–6. doi:10.1200/JCO.2012.47.6770

Wlodarska, I., Aventín, A., Inglés-Esteve, J., Falzetti, D., Criel, A., Cassiman, J. J., et al. (1997). A New Subtype of Pre-B Acute Lymphoblastic Leukemia with T(5;12)(q31q33;p12), Molecularly and Cytogenetically Distinct from T(5;12) in Chronic Myelomonocytic Leukemia. *Blood* 89 (5), 1716–1722. doi:10.1182/blood.V89.5.1716

Wu, D., Sylvester, J. E., Parker, L. L., Zhou, G., and Kron, S. J. (2010). Peptide Reporters of Kinase Activity in Whole Cell Lysates. *Biopolymers* 94 (4), 475–486. doi:10.1002/bip.21401

Yang, T. Y., Eissler, C. L., Hall, M. C., and Parker, L. L. (2013). A Multiple Reaction Monitoring (MRM) Method to Detect Bcr-Abl Kinase Activity in CML Using a Peptide Biosensor. *PLOS ONE* 8 (2), e56627. doi:10.1371/journal.pone.0056627

Yasuda, T., Tsuzuki, S., Kawazu, M., Hayakawa, F., Kojima, S., Ueno, T., et al. (2016). Recurrent DUX4 Fusions in B Cell Acute Lymphoblastic Leukemia of Adolescents and Young Adults. *Nat. Genet.* 48 (5), 569–574. doi:10.1038/ng.3535

Zhou, M. H., and Yang, Q. M. (2014). NUP214 Fusion Genes in Acute Leukemia (Review). *Oncol. Lett.* 8 (3), 959–962. doi:10.3892/ol.2014.2263

Conflict of Interest: The authors declare that the research was conducted in the absence of any commercial or financial relationships that could be construed as a potential conflict of interest.

Publisher's Note: All claims expressed in this article are solely those of the authors and do not necessarily represent those of their affiliated organizations, or those of the publisher, the editors and the reviewers. Any product that may be evaluated in this article, or claim that may be made by its manufacturer, is not guaranteed or endorsed by the publisher.

frontiers in Pharmacology

BRIEF RESEARCH REPORT
published: 23 November 2021
doi: 10.3389/fphar.2021.750744

Switching Between LC-ESI-MS/MS and EMIT Methods for Routine TDM of Valproic Acid in Pediatric Patients With Epilepsy: What Clinicians and Researchers Need to Know

Ying Xia[1†], Jia-Yi Long[2†‡], Meng-Yuan Shen[3§], Na Dong[4‡], Hong-Li Guo[1], Ya-Hui Hu[1], Xiao-Peng Lu[5], Xuan-Sheng Ding[2], Feng Chen[1] and Jin-Chun Qiu[1]**

[1]Pharmaceutical Sciences Research Center, Department of Pharmacy, Children's Hospital of Nanjing Medical University, Nanjing, China, [2]School of Basic Medicine and Clinical Pharmacy, China Pharmaceutical University, Nanjing, China, [3]Kangda College of Nanjing Medical University, Lianyungang, China, [4]Institute of Pharmaceutical Science, China Pharmaceutical University, Nanjing, China, [5]Department of Neurology, Children's Hospital of Nanjing Medical University, Nanjing, China

OPEN ACCESS

Edited by:
Raffaele Simeoli,
Bambino Gesù Children's Hospital (IRCCS), Italy

Reviewed by:
Ruichen Guo,
Shandong University, China
Amedeo De Nicolò,
University of Turin, Italy

***Correspondence:**
Feng Chen
cy.chen508@gmail.com
Jin-Chun Qiu
poheqiu@163.com

†These authors have contributed equally to this work and share first authorship

‡Visiting graduate student from China Pharmaceutical University

§Visiting undergraduate from Nanjing Medical University

Specialty section:
This article was submitted to Obstetric and Pediatric Pharmacology, a section of the journal Frontiers in Pharmacology

Received: 31 July 2021
Accepted: 21 October 2021
Published: 23 November 2021

Citation:
Xia Y, Long J-Y, Shen M-Y, Dong N, Guo H-L, Hu Y-H, Lu X-P, Ding X-S, Chen F and Qiu J-C (2021) Switching Between LC-ESI-MS/MS and EMIT Methods for Routine TDM of Valproic Acid in Pediatric Patients With Epilepsy: What Clinicians and Researchers Need to Know. Front. Pharmacol. 12:750744. doi: 10.3389/fphar.2021.750744

Background: Valproic acid (VPA) is a widely used antiseizure medication and its dosing needs to be tailored individually through therapeutic drug monitoring (TDM) to avoid or prevent toxicity. Currently, immune-enzymatic assays such as Enzyme Multiplied Immunoassay Technique (EMIT), and Liquid Chromatography (LC)-based techniques, particularly coupled to Electrospray Ionization Tandem Mass Spectrometry (LC–ESI-MS/MS), resulting a potential lack of concordance between laboratories.

Methods: In this study, plasma VPA concentrations were determined for 711 pediatric patients with epilepsy by a routine EMIT assay and by a validated in-house LC-ESI-MS/MS method on the same group of samples, aimed to address the aforementioned concern. Consistency between two assays was evaluated using linear regression and Bland-Altman analysis.

Results: The calibration curve was linear in the range of 5.00–300 μg/ml for LC-ESI-MS/MS method and 1.00–150 μg/ml for EMIT assay, respectively. The two methods were proven to be accurate with quality control samples. As a result, a significant correlation between two methods was obtained with a regression equation described as [***EMIT***] = 1.214 × [***LC*** – ***ESI*** – ***MS***/***MS***] + 3.054 (r^2 = 0.9281). Bland-Altman plot showed a mean bias of 14.5 μg/ml (95% confidence interval (CI) (–0.2, 29.2) and a mean increase of 27.8% (95% CI (3.3, 52.4) measured by EMIT assay more than that measured by LC-ESI-MS/MS method.

Conclusion: In conclusion, two methods were closely correlated, but EMIT assay overestimate VPA levels in human plasma compared with LC-ESI-MS/MS method.

Abbreviations: CI, Confidence interval; EMIT, Enzyme-multiplied immunoassay; FDA, U.S. Food and Drug Administration; FPIA, Fluorescence polarization immunoassay; GC, Gas chromatography; HQC, High quality control; IS, Internal standard; LC-ESI-MS/MS, Liquid chromatography-electrospray ionization-tandem mass spectrometry; LLOQ, Lowest limit of quantitation; LQC, Low quality control; MQC, Medium quality control; NH_4Ac, Ammonium acetate; PE, Preliminary experiment; QC, Quality control; TDM, Therapeutic drug monitoring; VPA, Valproic acid.

Due to the observed significant discordance between the tested methods, switching from immunoassays to LC-based techniques for TDM of VPA deserves close attention and therapeutic range of 35.0–75.0 μg/ml may be feasible. However, further studies are needed to evaluate the eligibility of this alternative range in the clinical practice. Clinicians should be informed when switching the VPA quantitation methods during the clinical practice.

Keywords: valproic acid, LC-ESI-MS/MS, EMIT, switch, TDM, antiseizure medication

INTRODUCTION

Valproic acid (2-propyl-pentanoic acid, VPA), commercially available in most countries during the 1970s, is one of the first-line option for the treatment of epilepsy, especially prescribed in pediatric epilepsy because of its various mechanisms of action and acceptable safety profiles. Additionally, it is being used with increasing frequency for the management of a range of psychiatric conditions (Fleming and Chetty, 2006; Zighetti et al., 2015; Li et al., 2021). Though VPA represents a useful therapeutic alternative in the treatment of epilepsy, it exhibits high inter-subject variability, remarkably when enzyme-inducing or enzyme-inhibiting drugs are co-administered (Methaneethorn, 2018). Also, some adverse drug reactions have been reported including gastrointestinal symptoms, sedation, increased appetite with weight gain, hair loss, tremor, and ataxia (Methaneethorn, 2018; Guo et al., 2019). In addition, approximately only 5–10% of VPA is free in the plasma, and the association between VPA dose and systemic exposure level is curvilinear (Gu et al., 2021). Moreover, a number of factors can exert influence on the VPA protein binding such as age, accompanying medications, renal and hepatic diseases, and pregnancy status, which result in large differences between patients in the plasma concentration-to-dose relationship (Wallenburg et al., 2017; Patsalos et al., 2018). However, a significant association between the decreased seizure frequency and increased serum VPA level was demonstrated (Patsalos et al., 2008). Thus VPA is a good candidate for therapeutic drug monitoring (TDM) to individualize its therapy. Patients with inadequate response, doubtful compliance, intercurrent illness, significant comorbidity, presence of interacting medications and so on can benefit from TDM (Baumann et al., 2004; Patsalos et al., 2008). The recommended VPA therapeutic range for the epilepsy therapy is 50.0–100 μg/ml and the total concentration is usually measured clinically as a reference for treatment (Gu et al., 2021)' (Cook et al., 2016).

The demands for efficient management of many patients with epilepsy have thus advanced the fast, accurate, and precise assays for the antiseizure drug's monitoring. Gas chromatography (GC)-based methods were the first to be employed for the VPA measurement and played an important role in the clinical studies on VPA (Schobben et al., 1975; Gram et al., 1979). Thereafter, other analytical techniques such as enzyme-multiplied immunoassay technique (EMIT) and fluorescence polarization immunoassay (FPIA), which utilize the same monoclonal antibody against VPA, were widely used (Bowden et al., 1996; Vasudev et al., 2000). They are commercially available, fast, and ease-to-use. However, one potential limitation of EMIT assay for monitoring VPA is fairly low cross-reactivity of certain glucuronide metabolite with antibody used in the immunoassay. In addition, some other disadvantages of the EMIT VPA assay was that the use of EDTA caused a high bias in quantification of VPA (Elyas et al., 1980). High-performance liquid chromatography-tandem mass spectrometry (HPLC-MS/MS) has been used extensively in clinical laboratories over the last 10–15 years (Li et al., 2017). HPLC-MS/MS offers high sensitivity and specificity and is considered to be the gold standard for small-molecule compounds' analysis. Recently, several HPLC-MS/MS methods for the determination of VPA have been demonstrated (Matsuura et al., 2008; Soni et al., 2016; Wen et al., 2018). They all presented great accuracy and were suitable for routine TDM. However, as we know, the most popular assay to therapeutically monitor VPA in clinical laboratories is still EMIT so far. Up to now, no study is available in literature to compare the analytical results derived from EMIT assay and LC–MS/MS method. The aims of this study were: 1) to develop and validate an LC-ESI-MS/MS method for the analysis of VPA; 2) to evaluate the correlation between EMIT and LC-ESI-MS/MS methods in VPA determination using samples from pediatric patients with epilepsy; and 3) to discuss the method switching from EMIT to LC-ESI-MS/MS for routine TDM of VPA in clinical laboratories.

MATERIALS AND METHODS

Samples

For this study, left-over plasma specimens were tested after completing the VPA assay by EMIT method and reporting results to ordering clinicians. These samples are routinely transported to our lab for monitoring plasma VPA levels in pediatric patients with VPA mono- or poly-therapy. Briefly, 782 blood samples were collected from 711 children with epilepsy (males: 444, females: 267; ranging from 1 month to 18 years, median age: 5 years) at the Department of Neurology, Children's Hospital of Nanjing Medical University. All samples were collected between March and May 2021. The blood specimens were centrifuged, and the resulting plasma were analyzed immediately for EMIT assay. The left-over plasma samples were separated and stored at −20°C until further LC-ESI-MS/MS analysis. The study was conducted in accordance with the Helsinki Declaration and the study protocol was approved by the

Children's Hospital of Nanjing Medical University ethics committee (Protocol number 202008095-1). This study aimed to assess the analytical concordance of the plasma VPA levels obtained with an EMIT assay and a LC-ESI-MS/MS method, and no clinical and personal data reported. Therefore, the consent to participate is not applicable.

LC-ESI-MS/MS Method

Materials

The reference standard of sodium valproate (purity: 97%; Lot No. 1-MJJ-83-1; expire date: 2024-03-29) and VPA-d6 as the internal standard (IS, purity: 96%; Lot No. 4-LDO-89-3; expire date: 2024-06-04) were taken from the Toronto Research Chemicals Inc (Toronto, Canada). MeOH (Lot No. I1108707035) of HPLC grade was obtained from Merck KGaA (Darmstadt, Germany). Ammonium acetate (NH_4Ac, ACS Reagent; Lot No. 50Y1905BD) was bought by Sigma-Aldrich, Co. (Wilmington, United States). Ultrapure water was prepared using an in-house Milli-Q water purification system (Millipore, Bedford, MA, United States). Blank human plasma was obtained from the Blood Transfusion Center (Children's Hospital of Nanjing Medical University, Nanjing, China).

HPLC Conditions

Chromatographic separation was performed using a Jasper^{TM} HPLC (AB Sciex Pte. Ltd., Singapore), which is equipped with one SCIEX Dx Controller, SCIEX Dx Sampler, SCIEX Dx Degasser, SCIEX Dx Oven, Jasper HPLC Reservoir, and two SCIEX Dx pumps. A Phenomenex Kinetex^{TM} C18 column (2.1 × 50 mm, 2.6 μm, Torrance, California, United States) and a security Guard-C18 column (4 × 2.0 mm, Phenomenex, Torrance, California, United States) were used for enrichment and separation of VPA and VPA-d6. Gradient elution was designed using a mobile phase consisting of 2 mM NH_4Ac both in water (phase A) and in MeOH (phase B), at a flow rate of 0.300 ml/min. A gradient program ran through as follows: 0–2.5 min, 40% B; 2.6–3.7 min, 40–95% B; 3.8–5.0 min, 40% B. The column and autosampler were kept at 40 and 4°C, respectively.

Mass Spectrometry

The detection was conducted using a Triple Quad™ 4500MD system (AB Sciex Pte. Ltd., Singapore). Quantification was operated with negative ESI multiple reaction monitoring of the following transitions: m/z 143.2→143.1 for VPA and m/z 149.1→149.0 for the IS. Analyst MD software (version 1.6.3, AB Sciex Pte. Ltd., Singapore) was used for the LC-MS/MS system control and data analysis.

Preparation of the Calibration Standards and Quality Control Samples

VPA stock solutions (10.0 mg/ml) were prepared in methanol and were further diluted with MeOH: H_2O (1:1; v/v) to obtain VPA working solutions. All the stock solutions and working solutions were kept at −20°C refrigerator.

Calibration standards and quality control (QC) samples were prepared by spiking appropriate volumes of the working solutions into blank plasma to yield serial concentrations of VPA standard samples. For calibration standards, the concentration levels were 5.00, 10.0, 30.0, 60.0, 120, 200, and 300 μg/ml. The QC samples concentration levels were 5.00 μg/ml (the lower limit of quantification QC, LLOQ QC), 12.0 μg/ml (low QC, LQC), 80.0 μg/ml (medium QC, MQC) and 240 μg/ml (high QC, HQC).

Preliminary Experiments

In the study, the left-over plasma samples were not analyzed immediately by LC-ESI-MS/MS method after routine VPA concentration monitoring by the EMIT assay. The way blood samples are processed may have a certain impact on the accuracy of the real concentration of VPA. So, four possible sample handling methods were tested as the preliminary experiments (PEs) shown below for those routine blood samples submitted to our lab.

(PE-a). The routine blood samples were centrifuged immediately for EMIT assay and the whole left-over supernatants were separated and collected. But the plasma samples were stored at −20°C until further analysis.

(PE-b). The routine blood samples were centrifuged and analyzed immediately for EMIT assay. However, the plasma fractions were not separated after centrifugation. Then the whole centrifuged blood samples were stored at −20°C. Before LC-ESI-MS/MS analysis, the blood samples were thawed, and placed for 30 min at bench-top and a 30 μL aliquot of the upper plasma fraction was used for analysis.

(PE-c). The routine blood specimens were treated and stored as method (PE-b) after the EMIT assay. Before LC-ESI-MS/MS analysis, the blood samples were thawed and centrifuged again, then a 30 μL aliquot of the resulting plasma sample was used for monitoring VPA concentration.

(PE-d). The routine blood samples were treated and stored as method (PE-b) after the EMIT assay. Once thawed and centrifuged, the resulting whole supernatants (plasma fractions) were separated completely and vortexed for 5 min, followed by sample preparation as before for LC-EIS-MS/MS determination.

In addition, in order to assess the possible impact of storage of plasma samples on VPA analysis by LC-ESI-MS/MS, a subgroup of 58 samples were analyzed immediately after EMIT assay and again in different days of 4 days' storage at −20°C.

Sample Clean-Up

After routine VPA concentration monitoring by the EMIT assay, the whole left-over supernatants were performed with procedure (PE-a). Before LC-ESI-MS/MS analysis, the plasma samples were thawed and vortexed sufficiently. Then the plasma sample (30 μL) was added to 570 μL of MeOH containing IS (200 ng/ml). The mixture was vortexed for 10 min and then centrifuged for 10 min (4,285 g, 4°C). The supernatant solution (30 μL) was transferred to another clean 1.5 ml Eppendorf tube containing 870 μL of MeOH: H_2O (1:1; v/v). Then, the resulting mixture was vortexed well for another 3 min and a 5 μL mixture was injected for LC-ESI-MS/MS analysis.

Method Validation

The assay was validated according to the Bioanalytical Method Validation Guideline published by the U.S. Food and Drug

Administration (FDA, 2018). In brief, the method validation involved in selectivity, linearity, lowest limit of quantitation (LLOQ), recovery, matrix effects, intra- and inter-day accuracy and precision, stability and carryover.

EMIT Assay

Reagents

Emit® 2000 Valproic Acid Calibrators (Lot No. N1; expire date: 2021-10-28) and Emit® 2000 Valproic Acid Assay (Lot No. N2; expire date: 2022-01-01) were supplied by Siemens Healthcare Diagnostic Ltd. (Newark, New Jersey, United States). Controls of VPA (Lot No. 57370; expire date: 2022-05-15) were obtained from Bio-Rad Laboratories, Inc. (Irvine, United States).

Assay Performance

The plasma concentration of VPA was assayed using an automated enzyme immunoassay analyzer (SIEMENS, Munich, Germany). The calibration dynamic range of the assay was 1.00–150 μg/mL. A ± 15% deviation of QC samples was accepted to ensure the accuracy and precision of the EMIT method.

Blood samples were centrifuged for 8 min (2,350 g, RT). Afterwards, the resulting supernatant was injected for analysis immediately.

Statistical Analysis

All data were statistically analyzed using GraphPad Prism v5.01 (GraphPad Software, La Jolla, CA, United States) and Medcalc (Medcalc Software, Ostend, Belgium). Linear regression analysis was performed to estimate the association between the two assays by GraphPad Prism software. Medcalc software was used to draw a Bland-Altman difference plot, which is helpful in demonstrating the relationship between the differences and the magnitude of measurements, showing any systematic bias, and in identifying possible outliers (Li et al., 2017).

RESULTS

LC-ESI-MS/MS Method Development and Validation

A sensitive, selective and rapid LC-ESI-MS/MS method was developed and validated for the quantitation of VPA in human plasma. The blank human plasma from six different sources was tested for selectivity and the results proved that no endogenous substances interfered with VPA and IS. The LC-ESI-MS/MS method was linear over the range of 5.00–300 μg/ml and the LLOQ was 5.00 μg/ml for VPA with a signal-to-noise ratio higher than 5. The intra- and inter-day accuracy and precision of the method were all acceptable according to the FDA guidance. No matrix effect or carryover was observed. The full validation data are shown in **Supplemental Material**.

LC-ESI-MS/MS PEs

The four different sample handling procedures used for LC-ESI-MS/MS analysis were described in section "*Preliminary Experiments*". The samples were retested using the four different handing methods, respectively. The deviations of (PE-a) to (PE-d) between initial and repeat measurements are shown in **Table 1**.

TABLE 1 | The deviations (Bias%) of procedure (PE-a) to (PE-d) between initial and repeat measurements.

PE-a (bias%)	PE-b (bias%)	PE-c (bias%)	PE-d (bias%)
0.0 (S1)	−26.0 (S6)	−36.2 (S11)	−0.2 (S16)
2.2 (S2)	−34.4 (S7)	15.0 (S12)	−1.4 (S17)
−5.0 (S3)	−11.2 (S8)	−19.5 (S13)	−6.2 (S18)
−2.7 (S4)	−23.2 (S9)	−71.8 (S14)	−7.6 (S19)
−1.7 (S5)	−38.6 (S10)	−19.0 (S15)	2.4 (S20)

As for the experiment evaluating the effect of storage at −20°C, the VPA concentrations measured by LC-ESI-MS/MS method were within the range of 5.00–300 μg/mL. As a result, the deviations between initial and repeated tests ranged from −11.6 to 6.8% and the mean bias was -3.9% among 58 samples.

EMIT Assay

A calibration curve with a range of 1.00–150 μg/ml was automatically obtained from the Viva-E automatic enzyme immunoassay analyzer. The concentration was calculated by the following formula:

$$\boldsymbol{A} = \boldsymbol{R}_0 + \boldsymbol{K} \times \frac{1}{1 + \boldsymbol{e}^{-\boldsymbol{a}+\boldsymbol{b}\times\ln \boldsymbol{C}}}$$

where $R_0 = 2.21833 \times 10^2$, $K = 2.75793 \times 10^2$, $a = -4.19223$, and $b = 0.870019$.

The accuracy and precision of QC samples based on three concentration levels were all within the acceptable criteria.

Comparison of EMIT and LC-ESI-MS/MS

In total, 782 plasma samples were measured by EMIT assay and then by LC-ESI-MS/MS method. Among those, eight samples were below the LLOQ and were excluded from further statistical analysis. Based on the therapeutic range of 50.0–100 μg/ml, the number of plasma samples measured by two methods is summarized in **Table 2**. VPA concentrations measured by LC-ESI-MS/MS and EMIT were 5.13–126 μg/ml (median 51.8 μg/ml) and 6.00–154 μg/ml (median 66.2 μg/ml), respectively. The median concentration of the plasma VPA determined by EMIT assay was 127.8% of results obtained from LC-ESI-MS/MS method.

Kolmogorov-Smirnov analysis revealed that the distribution style of the concentration data obtained from LC-ESI-MS/MS or EMIT assay was non-normal distribution. Spearman correlation analysis showed that the data from two methods were significantly correlated ($p < 0.0001$). A regression equation was obtained as following:

$$[\boldsymbol{EMIT}] = 1.214 \times [\boldsymbol{LC-ESI-MS/MS}] + 3.054$$

with $r^2 = 0.9281$ (**Figure 1**), which indicated a good correlation between the two methods. Nevertheless, the slope was significantly higher than unity ($p < 0.0001$), which reveals the overestimation of EMIT method. The Bland-Altman difference

TABLE 2 | The distribution of the plasma VPA concentration data (number/percentage; $n = 774$), measured by both EMIT and LC-ESI-MS/MS methods, in sub-therapeutic, therapeutic, and over-therapeutic reference ranges in relation to clinical efficacy of VPA for epilepsy treatment.

Concentration distribution		EMIT		
		<50.0 μg/ml	In range (50.0–100 μg/ml)	>100 μg/ml
LC-ESI-MS/MS	< 50.0 μg/ml	149 (19.3%)	192 (24.8%)	0 (0.0%)
	(50.0–100 μg/ml)	2 (0.3%)	361 (46.6%)	60 (7.8%)
	> 100 μg/ml	0 (0.0%)	0 (0.0%)	10 (1.3%)

This table shows the numbers and percentages of samples which were "concordant under the range" (<50 μg/ml both for EMIT and LC-MS/MS), "concordant within the range" (between 50 and 100 μg/ml for both the methods), "concordant over the range" (>100 μg/ml for both the methods) and the same for the discordant categories.

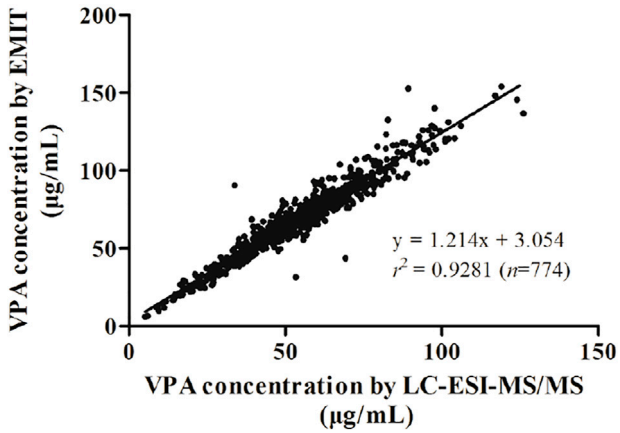

FIGURE 1 | Correlation of the regression curve for LC-ESI-MS/MS and EMIT assay ($n = 774$).

plots of VPA concentration data are presented in **Figures 2**, **3**. **Figure 2** shows the disparities between the VPA levels obtained from EMIT and LC-ESI-MS/MS plotted against the mean concentration measured by two methods. As shown in the plots, the concentrations of VPA determined by EMIT assay were higher than those obtained by LC-ESI-MS/MS method (positive bias: 14.5 μg/ml, 95% confidence interval (CI) (−0.2, 29.2). **Figure 3** shows the relative difference calculated by [(EMIT)—(LC-ESI-MS/MS)]/(LC-ESI-MS/MS), plotted against the LC-ESI-MS/MS data. EMIT assay overestimation caused a mean relative bias of 27.8% compared with the LC-ESI-MS/MS method and the 95% CI was 3.3–52.4%. In general, both plots demonstrate a systematic overestimation of plasma VPA levels by EMIT with respect to LC-ESI-MS/MS values.

DISCUSSION

In this study, the left-over plasma samples analyzed by LC-ESI-MS/MS method were performed with four possible sample handling methods described as "2.2.4 Preliminary experiments (PEs)". Nevertheless, surprisingly, the four different sample handling procedures used for LC-ESI-MS/MS analysis exhibited different accuracy and precision. It was noteworthy that the deviations of method (PE-a) to (PE-d) between initial and repeat measurements were −5.0 to 2.2%, −11.2 to −38.6%, −15.0 to −71.8%, and −7.6 to 2.4%, respectively. Only procedure (PE-a) and (PE-d) could produce repeatable results. It was supposed that the distribution of VPA in the supernatant was not evenly dispersed after freezing, which indicated that the supernatant (plasma fraction) should be vortexed sufficiently once the blood sample had been frozen. Finally, procedure (PE-a) was selected as the standard of practice in this study for LC-ESI-MS/MS analysis.

Moreover, the results of the experiment evaluating the effect of storage shows that LC-ESI-MS/MS method exerted great reproducibility whether the plasma samples were stored at -20°C.

To the best of our knowledge, this is the first study to compare the concentration of VPA measured by LC–ESI-MS/MS and EMIT methods with a large number of samples. The results of this study demonstrated the overestimation by routine EMIT assay compared with LC–ESI-MS/MS, which was in line with previous reports for other medications (Prémaud et al., 2004; Li et al., 2017; Zhou et al., 2020). In the current study, 782 plasma samples from 711 pediatric patients submitted to our lab for routine EMIT assay for VPA monitoring were enrolled. Overall, eight measurements were below the LLOQ and hence were excluded. Finally, 774 concentration data underwent further statistical analysis. A great number of measurements ($n = 774$) enables the reliability of the results. This is one of the major strengths of the current study. As we all know, LC-MS/MS technique has been recognized unanimously to be useful in determination of small molecular chemicals for routine TDM because it is more reliable, selective, and sensitive than EMIT. EMIT technique relies on the reaction between VPA and a biological antibody labeled by glucose-6-phosphate dehydrogenase. The overestimation by EMIT assay could be partly explained by the cross-reactivity of the anti-VPA antibody with other compounds (e.g., glucuronic acid conjugated metabolites, VPA-G). The production insert of Emit® 2000 Valproic Acid Assay shows that "no cross-reactivity" for the EMIT assay based on the testing results for compounds, whose chemical structure would suggest possible cross-reactivity or other therapeutics concurrently used. However, interfering metabolites such as VPAG in the samples were not tested during method validation of the EMIT assay. De Nicolò et al. revealed that the overall comparison between EMIT and LC–MS/MS showing an overestimation by EMIT of 33.5% (De Nicolò et al., 2020). As a result, the disparities between the two methods are noteworthy. In addition, as shown in **Table 2**, the diagnostic mismatch percentage of VPA concentrations was 32.9% between the two methods, indicating that the results from EMIT and LC-ESI-MS/MS cannot be interchangeable easily. Based on our study, differences in the clinical decision making (diagnostic mismatch) when using EMIT or LC-ESI-MS/

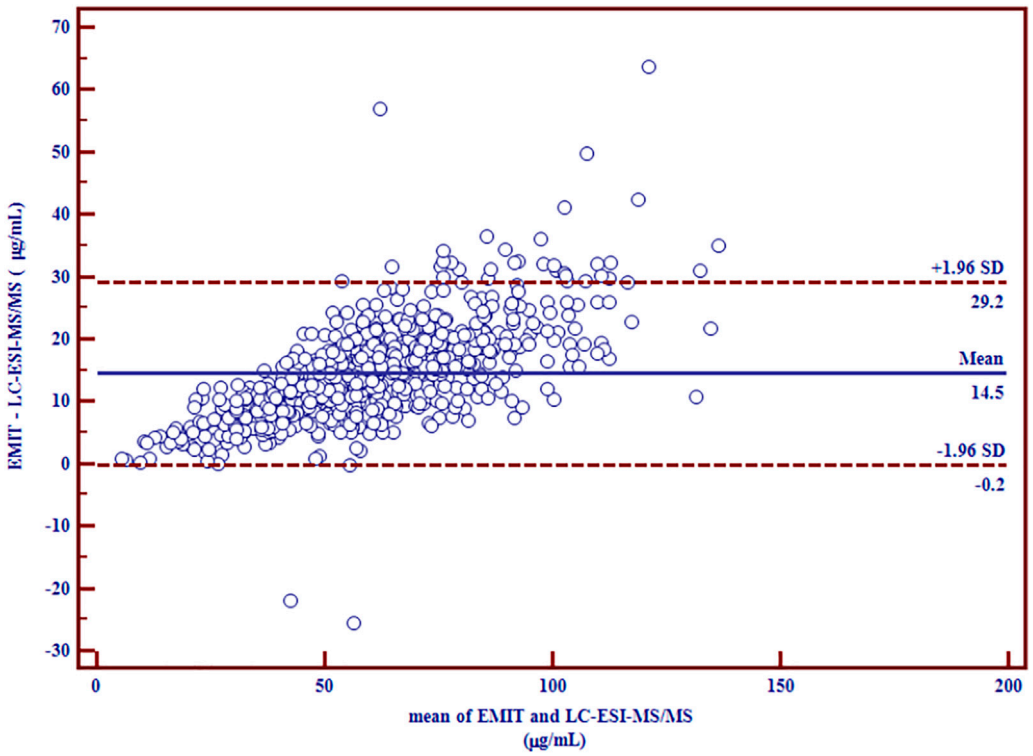

FIGURE 2 | Differences between mean plasma VPA concentrations (μg/ml) measured by LC-ESI-MS/MS and EMIT assay expressed as absolute bias (n = 774).

MS can be evaluated in the big amount samples (n = 774), by comparing results with indication for dose reduction or dose increase by EMIT, but not for LC-ESI-MS/MS. Additionally, clinical laboratory staff should best utilize the same analytical method for routine TDM of VPA, especially for each individual patient. Moreover, clinicians should also be informed when the analytical method has been switched. Timely dose tailoring, if need, should be warranted to avoid drug-related toxicity or loss of antiseizure efficacy.

Potential explanations for the lack of concordance between EMIT assay and LC-ESI-MS/MS for TDM of VPA have been discussed, however, several other factors can also affect TDM activity, such as heterogeneity of each individual sample, drug dosage forms, route of administration, bioavailability, blood sampling time, pathological states, pharmacokinetic interactions, patient compliance and so on. Therefore, standardized operating procedures should be established in clinical practice. Also, consistent detection methods and conditions should be adopted. Furthermore, inter-room quality assessment in clinical laboratories should be conducted regularly to ensure the accuracy and comparability of TDM.

In addition, the early clinical reports published from 1970s to 1990s suggested the therapeutic range of VPA was 50.0–100 μg/ml using GC as the detection method (Schobben et al., 1975; Gram et al., 1979; Henriksen and JOHANNESSEN, 1982; Lundberg et al., 1982). Interestingly, the later literatures used EMIT assay also reported that the therapeutic range of VPA was 50.0–100 μg/ml (Gómez Bellver et al., 1993; Vasudev et al., 2000). In fact, Elyas et al. found that the intercept and higher standard error of the intercept indicated slightly elevated serum concentration of VPA obtained by EMIT in relation to GC, but the concentration difference was acceptable (Elyas et al., 1980). Donniah and Buchanan found that only above or below the therapeutic range (300–700 μM), there was a statistical disparity between the EMIT and GC results (Donniah and Buchanan, 1981), which was line with another report in the same period (Braun et al., 1981). As shown in **Table 2**, if clinical laboratories would switch the quantitative method from EMIT to LC-ESI-MS/MS, our data suggest that aiming for a lower therapeutic range of VPA (35.0–75.0 μg/ml) may be feasible based on the positive bias of 27.8% measured by EMIT assay compared with LC-ESI-MS/MS.

In addition, the study had potential limitations. VPA is a small molecule, the simple chemical structure of VPA posed challenges for the LC-ESI-MS/MS method. In the study, the parent and daughter ions of VPA and the IS were the same, indicating that no fragmentation was performed and the LC-ESI-MS/MS method was run as pseudo MRM method. As other literatures reported previously (Jain et al., 2007; Matsuura et al., 2008; Soni et al., 2016; Linder et al., 2018; Li et al., 2021), VPA did not produce noticeable fragment ions during ionization. On this basis, it seems that the MS/MS method has the same theoretical selectivity and sensitivity of single-MS spectrometry. In summary, we proved that the use of MRM allowed great sensitivity, accuracy and precision even when employing the same precursor and product ions.

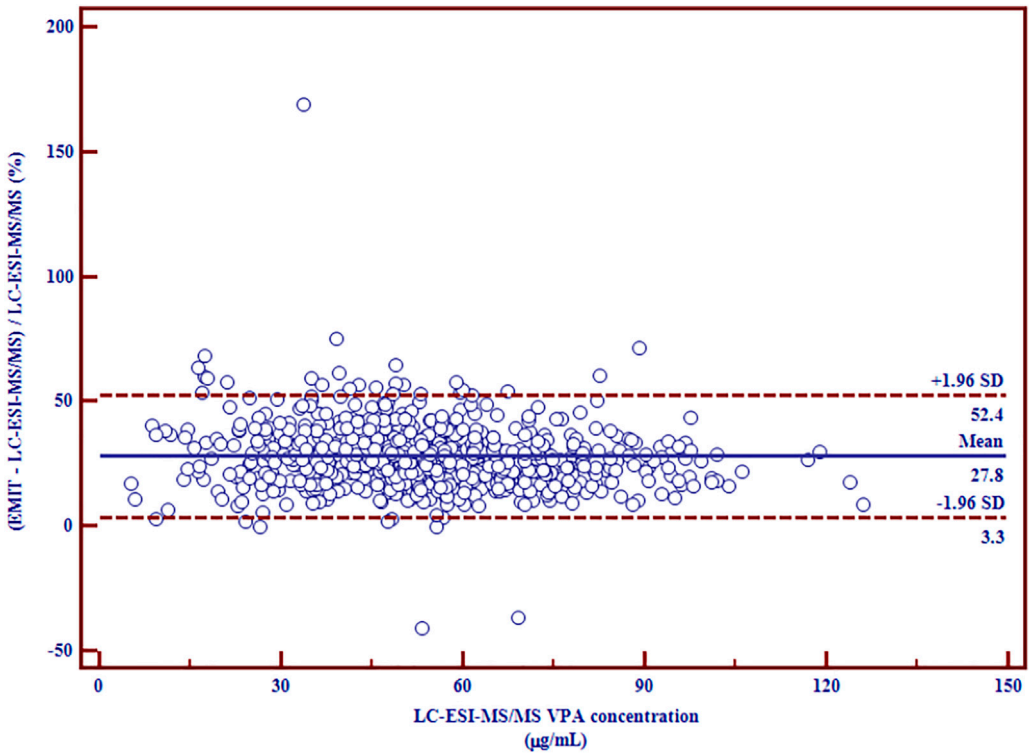

FIGURE 3 | Relative differences between mean plasma VPA concentrations (μg/ml) measured by LC-ESI-MS/MS and EMIT assay expressed in percentage (n = 774).

CONCLUSION

This is the first study to compare the plasma concentration of VPA measured by routine EMIT assay and thereafter by a novel LC–ESI-MS/MS method using a large number of pediatric blood samples (n = 774). In conclusion, EMIT assay overestimated plasma VPA levels by 27.8%, supporting the switch from EMIT to LC–ESI-MS/MS for routine TDM. So far, LC-MS/MS has served as a widespread and efficient technique in many clinical laboratories for monitoring of different medications. Considering the observed significant disparities between EMIT and LC-ESI-MS/MS, switching from immunoassays to LC-based techniques for TDM of VPA deserves close attention and the therapeutic range of 35.0–75.0 μg/ml may be feasible. However, further studies are needed to evaluate the eligibility of this alternative range in the clinical practice.

DATA AVAILABILITY STATEMENT

The original contributions presented in the study are included in the article/**Supplementary Material**, further inquiries can be directed to the corresponding authors.

ETHICS STATEMENT

The studies involving human participants were reviewed and approved by the Children's Hospital of Nanjing Medical University ethics committee. Written informed consent for participation was not required for this study in accordance with the national legislation and the institutional requirements.

AUTHOR CONTRIBUTIONS

YX, J-YL, FC, and J-CQ: Principal investigators for the study, data analysis, primary authors of the paper. H-LG, Y-HH, M-YS, and ND: Performed the data collection and analysis. X-PL and X-SD: Assisted in the design and performance of the study and the writing of the paper. FC: Provided financial support. All the authors reviewed and agreed the final manuscript.

FUNDING

This study was supported by the Specially-Appointed Medical Expert Project of Jiangsu Commission of Health (2019) and the Science and Technology Innovation Project for Overseas Scholars from Nanjing Municipal Bureau of Human Resources and Social Security (2020046).

ACKNOWLEDGMENTS

The authors thank Bei-zi Chen and Chen Hong, visiting undergraduate from Nanjing Medical University (Nanjing, China), for their kind help in the study.

SUPPLEMENTARY MATERIAL

The Supplementary Material for this article can be found online at: https://www.frontiersin.org/articles/10.3389/fphar.2021.750744/full#supplementary-material

REFERENCES

Baumann, P., Hiemke, C., Ulrich, S., Gaertner, I., Rao, M. L., Eckermann, G., et al. (2004). Therapeutic Monitoring of Psychotropic Drugs: an Outline of the AGNP-TDM Expert Group Consensus Guideline. *Ther. Drug Monit.* 26 (2), 167–170. doi:10.1097/00007691-200404000-00014

Bowden, C. L., Janicak, P. G., Orsulak, P., Swann, A. C., Davis, J. M., Calabrese, J. R., et al. (1996). Relation of Serum Valproate Concentration to Response in Mania. *Am. J. Psychiatry* 153 (6), 765–770. doi:10.1176/ajp.153.6.765

Braun, S. L., Tausch, A., Vogt, W., Jacob, K., and Knedel, M. (1981). Evaluation of a New Valproic Acid Enzyme Immunoassay and Comparison with a Capillary Gas-Chromatographic Method. *Clin. Chem.* 27 (1), 169–172. doi:10.1093/clinchem/27.1.169

Cook, A. M., Zafar, M. S., Mathias, S., Stewart, A. M., Albuja, A. C., Bensalem-Owen, M., et al. (2016). Pharmacokinetics and Clinical Utility of Valproic Acid Administered via Continuous Infusion. *CNS Drugs* 30 (1), 71–77. doi:10.1007/s40263-015-0304-5

De Nicolò, A., Ianniello, A., Benagli, C., Della Bruna, R., Keller, F., Antonucci, M., et al. (2020). Lack of Concordance between EMIT Assay and LC-MS/MS for Therapeutic Drug Monitoring of Mycophenolic Acid: Potential Increased Risk for Graft Rejection? *J. Pharm. Biomed. Anal.* 187, 113337. doi:10.1016/j.jpba.2020.113337

Donniah, P., and Buchanan, N. (1981). Serum Sodium Valproate Assays: Comparison between EMIT and GLC Methodologies. *Med. J. Aust.* 1 (4), 192. doi:10.5694/j.1326-5377.1981.tb135452.x

Elyas, A. A., Goldberg, V. D., Ratnaraj, N., and Lascelles, P. T. (1980). Valproic Acid Estimation by Enzyme Immunoassay. *Ann. Clin. Biochem.* 17 (6), 307–310. doi:10.1177/000456328001700605

Fleming, J., and Chetty, M. (2006). Therapeutic Monitoring of Valproate in Psychiatry: How Far Have We Progressed? *Clin. Neuropharmacol.* 29 (6), 350–360. doi:10.1097/01.WNF.0000228209.69524.E8

Gómez Bellver, M. J., García Sánchez, M. J., Alonso González, A. C., Santos Buelga, D., and Domínguez-Gil, A. (1993). Plasma Protein Binding Kinetics of Valproic Acid over a Broad Dosage Range: Therapeutic Implications. *J. Clin. Pharm. Ther.* 18 (3), 191–197. doi:10.1111/j.1365-2710.1993.tb00612.x

Gram, L., Flachs, H., Würtz-Jørgensen, A., Parnas, J., and Andersen, B. (1979). Sodium Valproate, Serum Level and Clinical Effect in Epilepsy: a Controlled Study. *Epilepsia* 20 (3), 303–311. doi:10.1111/j.1528-1157.1979.tb04808.x

Gu, X., Zhu, M., Sheng, C., Yu, S., Peng, Q., Ma, M., et al. (2021). Population Pharmacokinetics of Unbound Valproic Acid in Pediatric Epilepsy Patients in China: a Protein Binding Model. *Eur. J. Clin. Pharmacol.* 77 (7), 999–1009. doi:10.1007/s00228-020-03080-y

Guo, H. L., Jing, X., Sun, J. Y., Hu, Y. H., Xu, Z. J., Ni, M. M., et al. (2019). Valproic Acid and the Liver Injury in Patients with Epilepsy: An Update. *Curr. Pharm. Des.* 25 (3), 343–351. doi:10.2174/1381612825666190329145428

Henriksen, O., and Johannessen, S. I. (1982). Clinical and Pharmacokinetic Observations on Sodium Valproate - a 5-year Follow-Up Study in 100 Children with Epilepsy. *Acta Neurol. Scand.* 65, 504–523. doi:10.1111/j.1600-0404.1982.tb03106.x

Jain, D. S., Subbaiah, G., Sanyal, M., and Shrivastav, P. (2007). A High Throughput and Selective Method for the Estimation of Valproic Acid an Antiepileptic Drug in Human Plasma by Tandem LC-MS/MS. *Talanta* 72 (1), 80–88. doi:10.1016/j.talanta.2006.09.033

Li, W., Li, R., Liu, H., Guo, X., Shaikh, A. S., Li, P., et al. (2017). A Comparison of Liquid Chromatography-Tandem Mass Spectrometry (LC-MS/MS) and Enzyme-Multiplied Immunoassay Technique (EMIT) for the Determination of the Cyclosporin A Concentration in Whole Blood from Chinese Patients. *Biosci. Trends* 11 (4), 475–482. doi:10.5582/bst.2017.01121

Li, Y., Jiang, Y., Cao, H., Lin, H., Ren, W., Huang, J., et al. (2021). Therapeutic Drug Monitoring of Valproic Acid Using a Dried Plasma Spot Sampling Device. *J. Mass. Spectrom.* 56 (4), e4603. doi:10.1002/jms.4603

Linder, C., Hansson, A., Sadek, S., Gustafsson, L. L., and Pohanka, A. (2018). Carbamazepine, Lamotrigine, Levetiracetam and Valproic Acid in Dried Blood Spots with Liquid Chromatography Tandem Mass Spectrometry; Method Development and Validation. *J. Chromatogr. B Analyt. Technol. Biomed. Life Sci.* 1072, 116–122. doi:10.1016/j.jchromb.2017.11.005

Lundberg, B., Nergårdh, A., and Boréus, L. O. (1982). Plasma Concentrations of Valproate during Maintenance Therapy in Epileptic Children. *J. Neurol.* 228 (2), 133–141. doi:10.1007/BF00313758

Matsuura, K., Ohmori, T., Nakamura, M., Itoh, Y., and Hirano, K. (2008). A Simple and Rapid Determination of Valproic Acid in Human Plasma Using a Non-porous Silica Column and Liquid Chromatography with Tandem Mass Spectrometric Detection. *Biomed. Chromatogr.* 22 (4), 387–393. doi:10.1002/bmc.944

Methaneethorn, J. (2018). A Systematic Review of Population Pharmacokinetics of Valproic Acid. *Br. J. Clin. Pharmacol.* 84 (5), 816–834. doi:10.1111/bcp.13510

Patsalos, P. N., Berry, D. J., Bourgeois, B. F., Cloyd, J. C., Glauser, T. A., Johannessen, S. I., et al. (2008). Antiepileptic Drugs-Bbest Practice Guidelines for Therapeutic Drug Monitoring: a Position Paper by the Subcommission on Therapeutic Drug Monitoring, ILAE Commission on Therapeutic Strategies. *Epilepsia* 49 (7), 1239–1276. doi:10.1111/j.1528-1167.2008.01561.x

Patsalos, P. N., Spencer, E. P., and Berry, D. J. (2018). Therapeutic Drug Monitoring of Antiepileptic Drugs in Epilepsy: A 2018 Update. *Ther. Drug Monit.* 40 (5), 526–548. doi:10.1097/FTD.0000000000000546

Prémaud, A., Rousseau, A., Le Meur, Y., Lachâtre, G., and Marquet, P. (2004). Comparison of Liquid Chromatography-Tandem Mass Spectrometry with a Commercial Enzyme-Multiplied Immunoassay for the Determination of Plasma MPA in Renal Transplant Recipients and Consequences for Therapeutic Drug Monitoring. *Ther. Drug Monit.* 26 (6), 609–619. doi:10.1097/00007691-200412000-00005

Schobben, F., van der Kleijn, E., and Gabreëls, F. J. (1975). Pharmacokinetics of Di-n-propylacetate in Epileptic Patients. *Eur. J. Clin. Pharmacol.* 8 (2), 97–105. doi:10.1007/BF00561557

Soni, K., Patel, N., Singh, K., Jha, A., Patel, H., Gupta, R., et al. (2016). A Sensitive Triple Quadrupole Liquid Chromatography Mass Spectrometric Method for the Estimation of Valproic Acid in K2EDTA Human Plasma Using Furosemide as the Internal Standard. *Drug Res. (Stuttg)* 66 (12), 666–672. doi:10.1055/s-0042-114777

Vasudev, K., Goswami, U., and Kohli, K. (2000). Carbamazepine and Valproate Monotherapy: Feasibility, Relative Safety and Efficacy, and Therapeutic Drug Monitoring in Manic Disorder. *Psychopharmacology (Berl)* 150 (1), 15–23. doi:10.1007/s002130000380

Wallenburg, E., Klok, B., de Jong, K., de Maat, M., van Erp, N., Stalpers-Konijnenburg, S., et al. (2017). Monitoring Protein-Unbound Valproic Acid Serum Concentrations in Clinical Practice. *Ther. Drug Monit.* 39 (3), 269–272. doi:10.1097/FTD.0000000000000405

Wen, D., Chen, Z., Yang, C., Liu, H., Li, H., Chen, J., et al. (2018). A Rapid and Simple HPLC-MS/MS Method for the Simultaneous Quantification of Valproic Acid and its Five Metabolites in Human Plasma and Application to Study Pharmacokinetic Interaction in Chinese Epilepsy Patients. *J. Pharm. Biomed. Anal.* 149, 448–456. doi:10.1016/j.jpba.2017.11.042

Zhou, H., Xiang, H., Cai, J., Wang, Y., Zhang, M., Han, Y., et al. (2020). Comparison of a Point-of-Care Testing with EMIT and LC-MS/MS Methods for Therapeutic Drug Monitoring of Mycophenolic Acid: A Preliminary Study. *Ther. Drug Monit.*. Publish Ahead of Print.

Zighetti, M. L., Fontana, G., Lussana, F., Chiesa, V., Vignoli, A., Canevini, M. P., et al. (2015). Effects of Chronic Administration of Valproic Acid to Epileptic

Patients on Coagulation Tests and Primary Hemostasis. *Epilepsia* 56 (5), e49–52. doi:10.1111/epi.12952

Conflict of Interest: The authors declare that the research was conducted in the absence of any commercial or financial relationships that could be construed as a potential conflict of interest.

Publisher's Note: All claims expressed in this article are solely those of the authors and do not necessarily represent those of their affiliated organizations, or those of the publisher, the editors and the reviewers. Any product that may be evaluated in this article, or claim that may be made by its manufacturer, is not guaranteed or endorsed by the publisher.

frontiers in Pharmacology

BRIEF RESEARCH REPORT
published: 06 December 2021
doi: 10.3389/fphar.2021.772873

Pharmacokinetic Evaluation of Eltrombopag in ITP Pediatric Patients

*Marco Dionisi[1†], Sara Cairoli[2†], Raffaele Simeoli[2], Francesca De Gennaro[3], Valeria Paganelli[4], Roberto Carta[4], Francesca Rossi[5], Carlo Dionisi-Vici[2], Giuseppe Palumbo[3,4] and Bianca Maria Goffredo[2]**

[1]National Center for Drug Research and Evaluation, National Institute of Health (ISS), Rome, Italy, [2]Department of Pediatric Specialties and Liver-kidney Transplantation, Division of Metabolic Biochemistry, Bambino Gesù Children's Hospital, IRCCS, Rome, Italy, [3]Department of Systems Medicine, University of Rome "Tor Vergata", Rome, Italy, [4]Department of Pediatric Hemato-Oncology and Cell and Gene Therapy, Scientific Institute for Research and Healthcare, Bambino Gesù Children's Hospital, IRCCS, Rome, Italy, [5]Department of Woman, Child and General and Specialist Surgery, University of Campania "Luigi Vanvitelli", Naples, Italy

OPEN ACCESS

Edited by:
Mohamed A. Yassin,
Hamad Medical Corporation, Qatar

Reviewed by:
Yasser Wali,
Sultan Qaboos University, Oman
Jill Kolesar,
University of Kentucky, United States
Melissa J. Rose,
Nationwide Children's Hospital,
United States

***Correspondence:**
Bianca Maria Goffredo
biancamaria.goffredo@opbg.net

[†]These authors have contributed equally to this work and share first authorship

Specialty section:
This article was submitted to Obstetric and Pediatric Pharmacology, a section of the journal Frontiers in Pharmacology

Received: 08 September 2021
Accepted: 11 November 2021
Published: 06 December 2021

Citation:
Dionisi M, Cairoli S, Simeoli R, De Gennaro F, Paganelli V, Carta R, Rossi F, Dionisi-Vici C, Palumbo G and Goffredo BM (2021) Pharmacokinetic Evaluation of Eltrombopag in ITP Pediatric Patients. Front. Pharmacol. 12:772873. doi: 10.3389/fphar.2021.772873

Background: Eltrombopag (EPAG) is an oral thrombopoietin receptor agonist, approved for refractory primary immune thrombocytopenia (ITP) in pediatric patients. In two pediatric RCTs, EPAG led to an improvement of platelet counts and a reduction in bleeding severity. However, a significant number of pediatric patients did not achieve the primary endpoints. We performed a pharmacokinetic evaluation of EPAG in pediatric patients with refractory ITP.

Methods: Outpatients aged from 1 to 17 y, affected by refractory ITP to first-line treatment, were enrolled for a pharmacokinetic assessment. The analysis of drug plasma concentration was performed by the LC-MS/MS platform. Non-compartmental and statistical subgroup analyses were carried out using the R package ncappc.

Results: Among 36 patients eligible for PK analysis, the median dose of EPAG given once daily was 50 mg. The EPAG peak occurs between 2 and 4 h with a population Cmax and AUC 0–24 geo-mean of 23, 38 µg/ml, and 275, 4 µg*h/mL, respectively. The pharmacokinetic profile of EPAG did not show a dose proportionality. Female patients showed a statistically significant increase of dose-normalized exposure parameters, increasing by 110 and 123% for Cmax and AUC 0–24, respectively, when compared to male patients. Patients aged 1–5 y showed values increased by more than 100% considering both exposure parameters, compared to older children. Furthermore, patients presenting complete response (83%), showed augmented EPAG exposure parameters compared to subjects with partial or no response.

Conclusion: These data highlight the need to further explore the variability of EPAG exposure and its pharmacokinetic/pharmacodynamic profile in pediatric patients also in a real-life setting.

Keywords: eltrombopag, primary immune thrombocytopenia (ITP), pediatric patients, LC-MS/MS, pharmacokinetic (PK) evaluation, area under the concentration–time curve (AUC), gender and age influence, drug exposure

INTRODUCTION

Immune thrombocytopenia (ITP) is a hematological disease characterized by a low platelet count with an annual incidence of 2–5 cases/100,000 people (Marieke Schoonen et al., 2009). Specifically, diagnosis of ITP is established in the presence of a platelet count below 100×10^9/L and in the absence of other possible causes of thrombocytopenia (Rodeghiero et al., 2009). Most patients with ITP are asymptomatic or present episodes of mucocutaneous bleeding at low degree; however, almost 15% of them require hospitalization due to bleeding within 5 y from diagnosis of the disease (Cooper and Ghanima, 2019). Pathogenesis of ITP is not fully understood; it is considered an auto-immune disease due to the formation of antibodies against platelets mediated by auto-reactive B cells; however, in recent years other pathological mechanisms have been proposed including an hyper-activation of the complement system, massive polarization toward a Th1 subtype of T cells, and a prevalence of the M1 pro-inflammatory macrophage phenotype with consequent production of pro-inflammatory cytokines (Johnsen, 2012; Consolini et al., 2016). The result of this immune deregulation is an increased platelet opsonization mediated by the monocyte/macrophage axis, which binds the Fc receptor of auto-reactive IgG and induces the elimination of platelets mainly in the spleen rather than the liver (He et al., 1994).

The spread of ITP within the pediatric population has been summarized by several epidemiological studies that report an ITP incidence comprised between 2.2 and 5.3 cases/10^5 children *per* year (Fogarty and Segal, 2007; Terrell et al., 2010). Compared to adults, pediatric patients with ITP show a higher rate of spontaneous remission and a lower rate of co-morbidities (Schifferli et al., 2018). Moreover, among adult patients, there is a higher prevalence of ITP in female subjects than male subjects with a 2:1 ratio (Vianelli et al., 2001; Schifferli et al., 2018). This gender difference is less evident among pediatric ITP patients; however, in these subjects, a higher rate of severe bleeding has been reported compared to adults (Kühne et al., 2011).

Pharmacological treatment of pediatric patients with a new diagnosis of ITP includes corticosteroids and intra-venous immunoglobulins. This initial therapy, especially with steroids, should be suspended as soon as a safety level of platelet count ($>20 \times 10^9$/L) has been reached. Treatment of pediatric patients with persistent/chronic ITP consists mainly of thrombopoietin receptor (TPO-R) agonists, such as eltrombopag (EPAG) and romiplostim, the anti-CD20 monoclonal antibody rituximab, and mycophenolic acid (MMF). EPAG belongs to the family of biaryl-hydrazones and acts as a TPO-R agonist interacting with the subunit H499 present in the binding site of the TPO receptor. This interaction leads to a conformational change of the TPO-R structure that induces receptor activation and culminates in the final recruitment of the JAK/STAT cascade pathway. The pharmacological effect of EPAG interactions with TPO-R results in an increase of differentiation and proliferation rate of the megakaryocytoblastic cellular line and its precursors. Alongside this effect on platelet count, recent evidence also suggests an immune-modulating and iron chelating property of EPAG (Argenziano et al., 2021; Di Paola et al., 2021).

Safety and efficacy of EPAG have been evaluated in pediatric patients with two registration studies: TRA115450 (PETIT2) and TRA108062 (PETIT) (Bussel et al., 2015; Grainger et al., 2015). In both studies, the primary endpoint was the percentage of patients who reach a platelet count ≥50,000/μl at least once during the randomized therapeutic period. In the same studies, pharmacokinetic (PK) properties of EPAG have been evaluated using a population model on 168 pediatric patients with ITP who were assuming EPAG once a day by oral administration. The results of these studies show that following oral dosage, plasmatic clearance of EPAG proportionally increases with body weight and that female pediatric patients with ITP show a 25% increase of the area under the curve (AUC) of EPAG plasmatic concentrations compared to male pediatric patients (Wire et al., 2018).

EPAG PK data reported in the literature are based on pharmacokinetic population models, reliant on data deriving from randomized clinical trials, where patients are enrolled and strictly monitored throughout the study. Here, however, we present the results of EPAG PK evaluation performed on pediatric patients affected by ITP treated with EPAG, including "real-life" data collected during routine clinical practice.

MATERIALS AND METHODS

Study Design and Procedures

This study was conducted at the Department of Pediatric Hematology and Oncology, Cell and Gene Therapy at Children's Hospital Bambino Gesù in Rome, from December 2019 to March 2021. All procedures were included in a therapeutic drug monitoring application routinely performed in our hospital. Outpatients were included if aged from 1 to 17 y, with a confirmed diagnosis of primary immune thrombocytopenia, had relapsed or refractory disease after one or more previous treatments for immune thrombocytopenia, and were orally treated with EPAG film-coated tablets (Revolade®, Novartis Europharm Limited, Dublin, Ireland) for at least 2 weeks without dose variations. Patients who had other significant non-ITP-related diseases were excluded. Following hospitalization, all patients or legal guardians gave their written informed consent to receive diagnostic procedures and pharmacological treatments. Thereafter, a verbal informed consent was asked to all patients or legal guardians before study procedures. The study was conducted in accordance with the Declaration of Helsinki principles. The ethical committee of our hospital was informed about this therapeutic drug monitoring application.

Enrolled outpatients were present in the clinic from the morning of the visit day for a maximum of 8 h. In addition to routine laboratory analyses and medical exams and procedures, blood samples (3 ml) were obtained through an indwelling peripheral catheter and collected into vacutainer tubes containing EDTA (Becton Dickinson, Rutherford, NJ, United States) immediately before the dose and at 2, 4, and

8 h after the dose. Whenever possible, blood was obtained from central laboratory specimens. Additional or alternative time sampling was allowed in accordance with the ward sampling routine. Blood drawing was performed in accordance with study-related blood loss limits indicated by the EU Commission (European Union, 2008). Routine laboratory blood tests included hematology and chemistry analyses. At the time of the visit, qualified medical staff performed a complete physical exam, also collecting information about ITP duration, response, adverse events, and patients' compliance. Moreover, patients or legal guardians were provided with a diary-like form to fill out the day of the visit. The form contained information such as time of dose administration the day before the visit, concomitant medications, smoking habits (for adolescents), consumption of dairy products, and mineral supplements or caffeinated drinks along with meal times.

A complete response (CR) was defined as at least a single value of PLT >100,000/μl 1 week after starting EPAG therapy, without the need of rescue therapy and no signs of bleeding. A partial response (PR) was characterized by a value of PLT between 30,000/μl and 100,000/μl, and no response (NR) was defined as a number of PLT <30000/μl. A durable response (DR) consists in detection of PLT >50,000/μl for at least 75% of the follow-up period after the initiation of EPAG treatment. Rescue therapy included corticosteroids and/or intravenous immunoglobulins (IVIg). ITP duration was classified according to disease duration since diagnosis: newly diagnosed ITP (<3 months), persistent ITP (6–12 months), and chronic ITP (>12 months) (Rodeghiero et al., 2009).

Drug Assay

Plasma was obtained by centrifuging at 3,500 g for 5 min. 50 μL of plasma was added to 25 μL of IS working solution (50 μg/ml); then, 250 μL of methanol was used to precipitate proteins; samples were vortex-mixed for 30 s and centrifuged at 13,000 rpm for 9 min. The supernatant (10 μl) was then injected into the UHPLC-MS/MS system for analysis. A standard stock solution was prepared dissolving EPAG in methanol and 0.1% of dimethyl sulfoxide (DMSO) at a concentration of 1 mg/ml. The calibration standard solutions were prepared spiking standard stock solutions to drug-free plasma at the following concentrations: 1, 5, 10, 25, 50, 100, and 150 μg/ml. Quality controls were prepared by serial dilution of the stock solution with drug-free plasma at different concentrations: QC low 7.5 μg/ml, QC medium 15 μg/ml, and QC high 75 μg/ml. The stock solution of IS (1 mg/ml) was prepared by dissolving EPAG 13C4 in DMSO. A working solution of the internal standard (50 μg/ml) was prepared in methanol.

Chromatography analysis was performed using a UHPLC Agilent 1290 Infinity II (Agilent Technologies). The separation column was a Kinetex 2.6 μm EVO C18 100 Å 75 × 2.1 mm (Phenomenex, Torrance, CA). Mobile phase A was water with 0.1% formic acid, 31% acetonitrile, and 31% methanol v/v, and mobile phase B was methanol with 0.5% formic acid v/v. The flow rate was 0.3 ml/min according to the following gradient: 0–2.9 min 55% B, 3–3.1 min 95% B, 3.1–4.0 min 95% B, and 4.1–5.0 min 55% B. The injection volume was 10 μl. Samples were analyzed with a 6,470 mass spectrometry system (Agilent Technologies) equipped with an ESI-JET-STREAM source operating in a positive ion (ESI+) mode. The software used for controlling this equipment and analyzing results was MassHunter (Agilent Technologies). Samples were detected in the multiple reaction monitor (MRM) mode. The mass transitions of EPAG were m/z 443.2→ 183 for the quantifier and 443.2 →77 for the qualifier.

All chemicals were of analytical grade and were obtained from Sigma-Aldrich (Saint Louis, MO, United States). EPAG and EPAG-13C4 (employed as an internal standard) were obtained from Toronto Research Chemicals (Toronto, Canada). Drug-free plasma was obtained from healthy volunteers recruited at the Blood Transfusion Center of the Children's Hospital Bambino Gesù after obtaining informed consent and was used as a matrix for standard curve preparation and negative controls. Method validation was performed based on the US Food and Drug Administration (FDA) guidelines for industry bioanalytical method validation. Method validation was carried out including specificity, linearity, inter- and intra-precision and accuracy, extraction recovery, and the matrix effect (data not shown).

Pharmacokinetic Analysis

Analysis of plasma concentration–time data was conducted using the noncompartmental approach using the ncappc package (v0.3.0; Acharya et al., 2016) and Rstudio (RStudio: Integrated Development for R, 2020. RStudio, Inc., Boston, MA URL http://www.rstudio.com/). The estimated pharmacokinetic parameters of EPAG were area under the plasma concentration–time curve from time zero to 24 h (AUC 0-24), maximum observed plasma concentration (Cmax), and time to reach Cmax (Tmax). The area under the concentration–time curve from 0 to 24 h post dose (AUC 0-24) was assessed using the linear-log trapezoidal rule from zero up to the 24 estimated concentration. Dose normalized values (AUC 0-24 DN and Cmax, DN) were derived by dividing AUC 0-24 and Cmax by dose. The concentration at 24 h was estimated using the equation $(C24h) = C8h * e^{-\beta(t24-t8)}$ if the concentration at 8 h post dose was quantifiable (Ruslami et al., 2007).

Statistical Analysis

Demographic data and pharmacokinetic parameters were summarized using descriptive statistics. No formal power calculation was made for the study. Mean with standard deviation or median with ranges was used for normally distributed and non-normally distributed variables, respectively. Number of occurrence and percentage were used to describe categorical data. Cmax, AUC 0-24, and dose-normalized pharmacokinetic parameters were described through the geometric mean and 95% confidence intervals. EPAG dose proportionality over the dose range of 12.5–100 mg was evaluated using a power model, assuming a linear relationship between natural log-transformed exposure parameters (Cmax and AUC 0-24) and natural log-transformed dose values: $ln(PK\ parameter) = \beta 0 + \beta 1\text{-}ln(dose)$.

TABLE 1 | Patients' characteristics at the time of the study visit and estimated pharmacokinetic parameters.

	All	1–5 years	6–11 years	12–17 years
Patients, n (%)	36 (100%)	8 (22.2%)	12 (33.3%)	16 (44.5%)
Age (years), median	10.94	5.08	8.44	15.08
Gender (F) n (%)	22 (61.1%)	6 (27.3%)	5 (22.7%)	11 (50%)
Dose (mg) Mean (SD)	55.9 (24.0)	50.0 (13.3)	47.9 (22.5)	64.8 (27.0)
Body Weight (kg), Median (range)	45.43 (15.5–109)	19.1 (15.5–28.5)	31.5 (20.0–60.0)	60.0 (37.0–109.0)
Platelet count (x 10^9/L), Median (range)	86.5 (10–1,611)	101.5 (10–1,307)	105.5 (17–1,611)	86.5 (24–235)
ITP Duration, n (%)				
Newly Diagnosed	12 (33.3%)	4 (33.3%)	6 (50%)	2 (16.7%)
Persistent	13 (36.1%)	3 (23.1%)	3 (23.1)	7 (53.8%)
Chronic	11 (30.6%)	1 (9.1%)	3 (27.3%)	7 (63.6%)
Response, n (%)				
Complete	30 (83.3%)	6 (20%)	11 (36.7%)	13 (43.3%)
Partial	4 (11.1%)	1 (25%)	-	3 (75%)
Absent	2 (5.6%)	1 (50%)	1 (50%)	-
Durable Response, n (%)	12 (33.3%)	1 (8.3%)	4 (33.3%)	7 (58.4%)
Rescue therapy, n (%)	5 (13.9%)	4 (80%)	-	1 (20%)
T max, h mean (SD)	2.62 (0.90)	2.52 (0.91)	2.37 (0.77)	2.85 (0.94)
Cmax, μg/mL geo-mean (CI 95%)	23.38 (16.20–33.74)	43.00 (26.60–69.66)	18.29 (9.25–36.19)	20.71 (11.63–36.89)
AUC 0–24, μg*h/mL geo-mean (CI 95%)	275.40 (185.87–408.02)	515.48 (278.28–954.88)	200.50 (108.42–970.78)	255.38 (131.19–497.14)
Cmax DN, μg/mL geo-mean (CI 95%)	0.47 (0.34–0.63)	0.89 (0.61–1.31)	0.43 (0.25–0.73)	0.362 (0.23–0.58)
AUC 0–24 DN, μg/mL geo-mean (CI 95%)	5.51 (3.94–7.69)	10.7 (6.17–18.52)	4.68 (2.83–7.72)	4.47 (2.57–7.76)

Furthermore, an equivalence criterion was also used to evaluate the inclusion of the proportional constant β1 and its 90% confidence interval within the acceptance range Food and Drug Administration (FDA) and Center for Drug Evaluation and Research (CDER), (2001). Guidance for Industry: Statistical Approaches to Establishing Bioequivalence. The maximal dose ratio (r) was 8 (100/12.5). The estimated lower limit {$1+ [\ln(0.8)/\ln(r)]$} and the upper limit {$1+ [\ln(1.25)/\ln(r)]$} were 0.892 and 1.107, respectively. The unpaired *t*-test and one-way ANOVA were used to compare log-transformed exposure parameters taking into account the ITP duration and response. Dose-normalized log-transformed pharmacokinetic exposure parameters were considered to compare gender, age groups, and ITP duration. All statistical analyses and graphs were performed using Rstudio (RStudio: Integrated Development for R, 2020. RStudio, Inc., Boston, MA URL http://www.rstudio.com/).

RESULTS

Patients

The study comprised 36 patients, 61 percent of which were females (n = 22). The median age was 10.94 years (range 2.67–17.9 years), and the median body weight was 45.4 kg (range 15.9–109 kg), as shown in **Table 1**. The dose of EPAG given once daily ranged between 12.5 (n = 1) and 100 mg (n = 3). Twelve patients were administered 75 mg of EPAG, and the same number of patients were treated with 50 mg. Eight subjects were treated with 25 mg. The mean dose for all patients was 55.9 mg (standard deviation: 24.0 mg). Mean dose values were similar between the two younger age groups, namely, 1–5 y and 6–11 y. Instead, older children were treated with higher doses (mean = 64.8 mg). The median platelet count was 86.5 PLT x 10^9/L, ranging from 10 to 1611 PLT x 10^9/L. The percentage of patients with a diagnosis of newly diagnosed ITP (ND), persistent ITP (P), or chronic (C) ITP was similar in the study population; nonetheless, the 6–11 y age group showed a higher frequency of ND. Additionally, more than half of the patients affected by P or C ITP were among the 12–17 y age group. Overall, a complete response was found in 30/36 patients (83%). However, only 33% of patients showed a durable response. Rescue therapy during EPAG treatment was required in five patients (13.9%), mainly in the 1–5 y age group.

Concentration–Time Profile of EPAG in Our Pediatric Population

Marked inter-individual variability of the EPAG concentration–time profile was observed in the whole study population (CV% Cmax DN = 130%, CV% AUC 0–24 DN = 157%) (**Figure 1A**), with a high range of variability differences also among patients within the same age group despite the dose normalization of concentrations (CV% Cmax DN 1–5 y = 58%, 6–11 y = 114%, 12–17 y = 183%, CV% AUC 0–24 1–5 y = 80%, 6–11 y = 129%, and 12–17 y = 201%) (**Figure 1B**). Overall, the EPAG peak occurs between 2 and 4 h (mean = 2.62 h) with a Cmax and AUC 0–24 geo-mean of 23, 38 μg/ml (CI95% 16.20–33.74 μg/ml) and 275.4 μg*h/mL (CI95% 185.87–408.02 μg*h/mL), respectively. The dose-normalized Cmax and AUC 0-24 were 0.47 μg/ml and 5.51 μg*h/mL, respectively (**Table 1**).

Evaluation of Dose Proportionality Following EPAG Oral Administration

EPAG did not show a dose proportionality, considering both exposure parameters, with higher values of Cmax and AUC 0–24

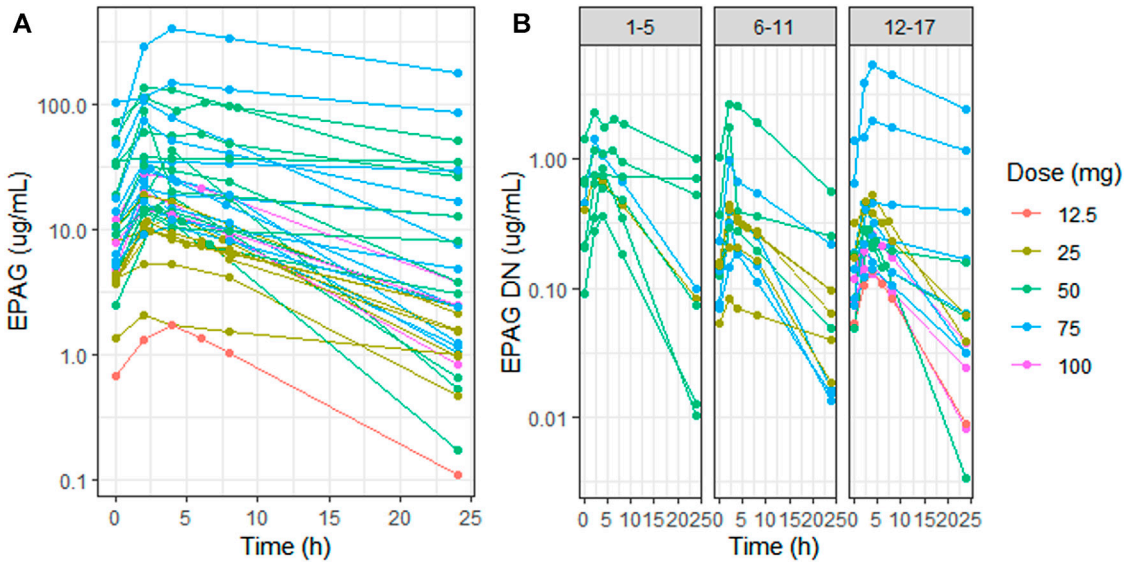

FIGURE 1 | Eltrombopag concentration (log scale) vs. time in all patients **(A)** and dose-normalized eltrombopag concentration (log scale) vs. time in the three different age groups (1–5 y, 6–11 y, and 12–17 y) **(B)**. Patient profiles were stratified by dose: 12.5 mg (red), 25 mg (light-green), 50 mg (green), 75 mg (blue), and 100 mg (purple). EPAG: eltrombopag and DN: dose-normalized.

in patients treated with 50 mg **Figure 2(A,B)**. The estimates of the proportionality constant (90% CI) for Cmax and AUC 0-24 were 0.17 (0.09–0.24) and 0.15 (0.08–0.22), respectively **Figure 2(C,D)**. Hence, according to the equivalence criterion limits, the proportional constant was not included within the prespecified acceptance limits (0.89–1.10) for dose proportionality.

Influence of Gender and Age on EPAG Exposure

Females showed a statistically significant increase of dose-normalized exposure parameters (Cmax DN = 0.619 μg/ml and AUC 0-24 DN = 7.48 μg*h/mL) when compared to males (Cmax DN = 0.301 μg/ml and AUC 0–24 DN = 3.40 μg*h/mL), with a percentage increase of 110 and 123% for Cmax and AUC 0–24, respectively (p = 00,201 and p = 00,198) **Figure 3(A,B)**. No statistically significant differences in dose-normalized Cmax and AUC 0-24 were detected between the distinct age groups. Nevertheless, patients aged 1–5 y showed higher Cmax DN and AUC 0-24 DN (0.89 μg/ml and 10.7 μg*h/mL), compared to the other two groups, undergoing an increase of more than 100% for both exposure parameters **Figure 3(C,D)**. Cmax DN and AUC 0–24 DN were similar between 6–11 y and 12–17 y age groups (**Table 1**).

Differences in Cmax and AUC among Patients with Partial, Complete, and Durable Response to EPAG Therapy

Although not statistically significant, patients presenting a CR during EPAG treatment showed augmented values of Cmax and AUC 0-24 geo-mean (24.16 μg/ml, CI95% 15.6–37.3 μg/ml and 299.84 μg*h/mL, CI95% 188.23–477.63 μg*h/mL, respectively), compared to patients with PR (19.44 μg/ml, CI95% 11.0–34.2 μg/ml and 191.10 μg*h/mL, CI95% 144.08–253.49 μg*h/mL) or no response (20.67 μg/ml and 159.68 μg*h/mL) **Figure 3(E,F)**. No differences in EPAG exposure were found when stratifying patients through evidence of durable response and the need of rescue therapy during EPAG treatment (**Supplementary Figure S1**). Moreover, as concerns adverse reactions during eltrombopag treatment, a higher percentage of patients (52.77%) did not experience side effects, followed by n = 6 (16.66%) patients who reported headaches and n = 4 (11.11%) who showed Grade 3 hypertransaminasemia. Exclusively in this latter situation, EPAG treatment was briefly suspended until clinical parameters were normalized (**Supplementary Table S1**).

DISCUSSION

The use of oral drugs acting on the thrombopoietin receptor has dramatically changed the therapeutic paradigm of first-line refractory and relapsed ITP patients. EPAG is an orally thrombopoietin receptor agonist already approved for ITP treatment in pediatric patients (Burness et al., 2016; Wong et al., 2017; Kim et al., 2018; Fattizzo et al., 2019). EPAG's main mechanism of action is related to the stimulation of platelet production. However, it is also endowed with immune-modulating properties reducing Th1 activation (Bao et al., 2010) and inhibiting macrophage switch toward an inflammatory phenotype (Liu et al., 2016; Di Paola et al.,

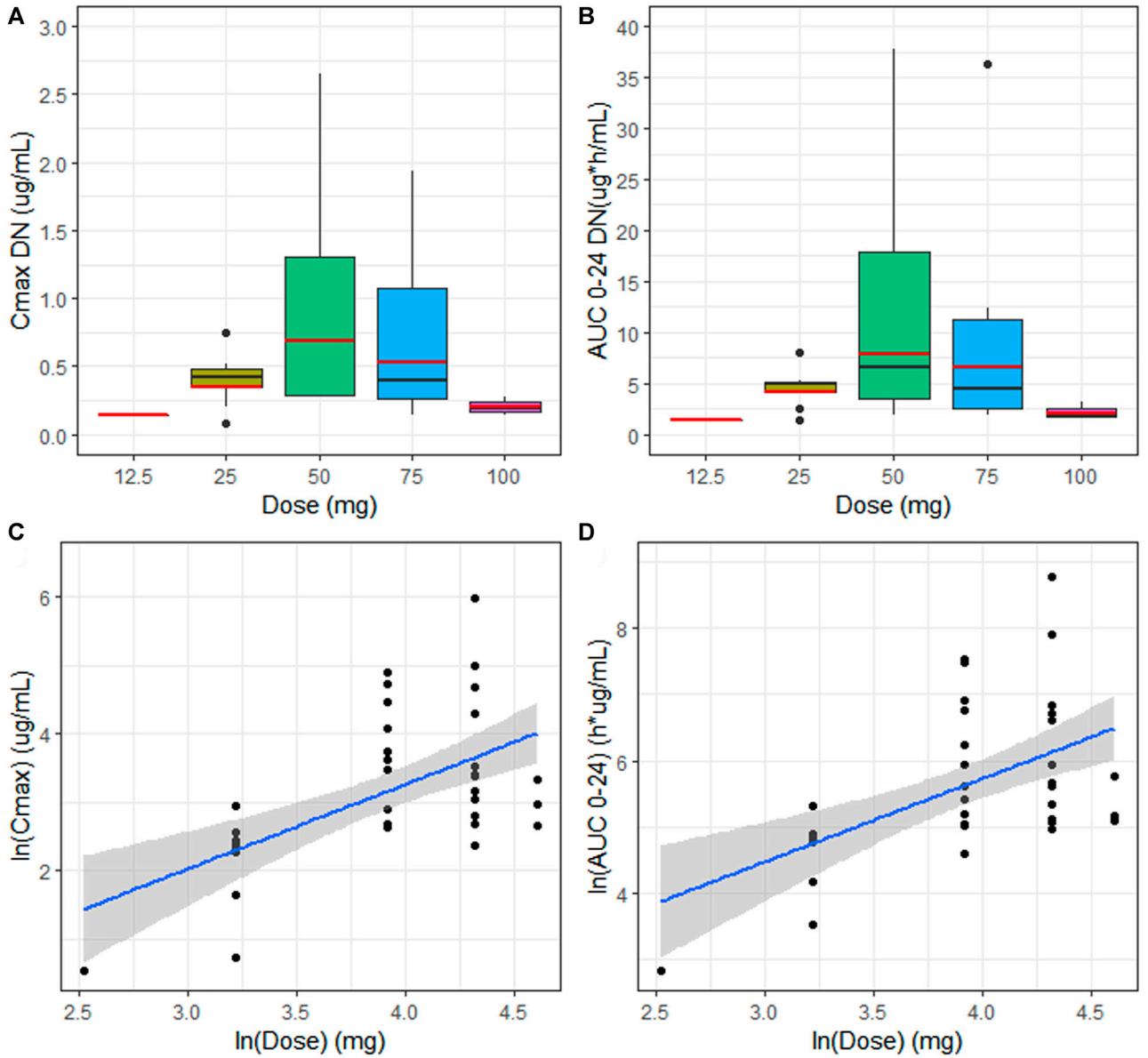

FIGURE 2 | (A, B) Median (black line) and geo-mean (red line) of dose-normalized Cmax (Cmax DN) and dose-normalized AUC 0–24 (AUC 0–24 DN) vs. dose (mg) for the evaluation of dose proportionality. **(C)** Linear regression model with the best fit line (blue) and 90% CI (gray area) describing relationship between the extent of systemic exposure including Cmax and AUC 0–24 **(D)** and dose.

2021). In this study, we propose an exploratory pharmacokinetic evaluation of EPAG exposure in pediatric patients affected by ITP.

In particular, our data show a high degree of inter-variability of EPAG pharmacokinetic within the selected pediatric population. Moreover, our results reveal a lack of EPAG dose proportionality when analyzing the available data according to a power model with the equivalence acceptance criterion. Such evidence represents a novelty if compared to the already published results. In fact, several studies have reported a predictable and dose-proportionate PK behavior of EPAG in ITP patients (Gibiansky et al., 2011; Matthys et al., 2011; Wire et al., 2018). However, this discrepancy could be explained by the fact that our data derive from a "real-life" setting where patients are not hospitalized and, therefore, easily influenced by extrinsic factors such as different dietary habits and poor compliance. As a proof of this, although it was recommended to assume EPAG at least 2 h before or 4 h after meals, at the day of the visit, the overwhelming majority of patients (94%) did not follow the recommendation. For example, almost 17% of patients consumed caffeinated beverages 4 h following EPAG dose. In terms of concomitant medications, around 35% of patients were taking vitamins (Vitamin D, C, and B) and Mg^{2+}/K^{+} saline integrators. Conversely, literature data are based on

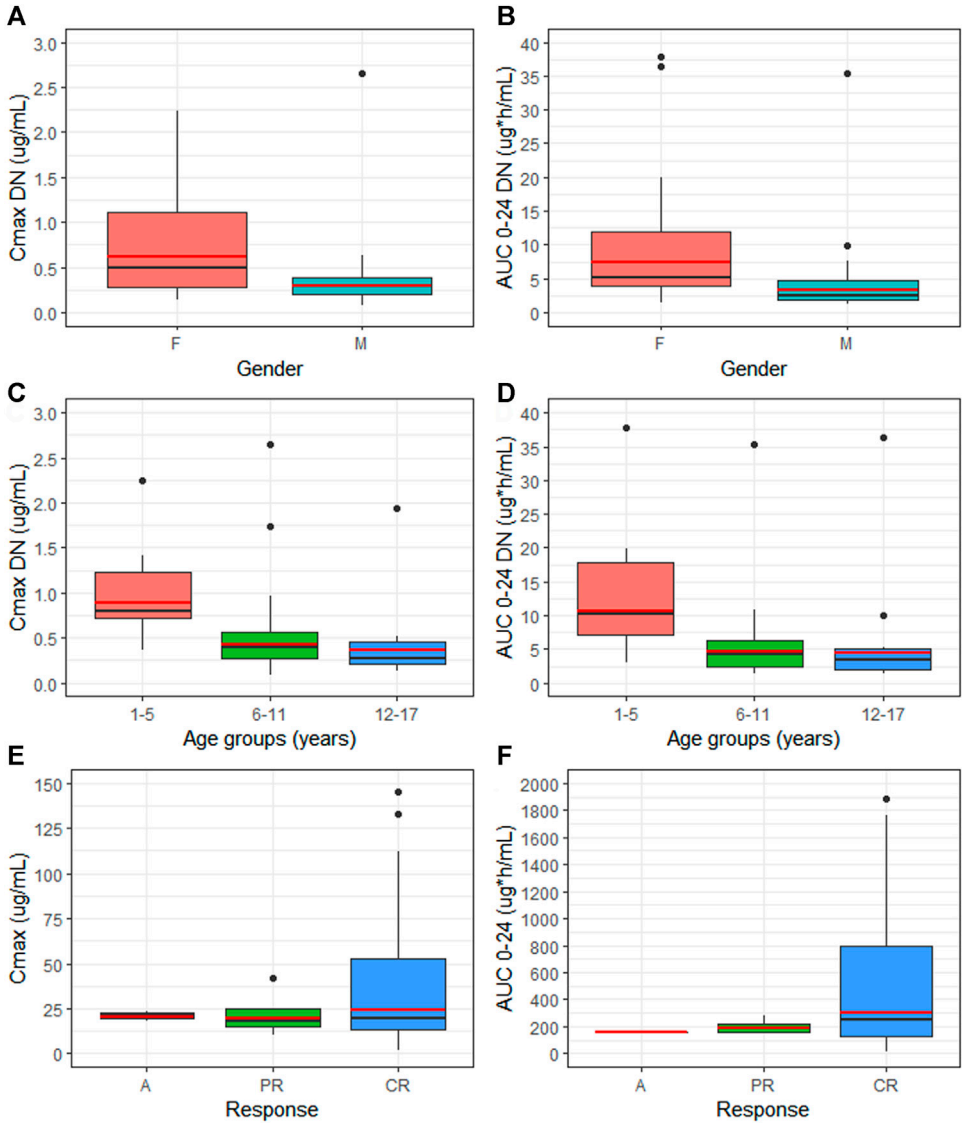

FIGURE 3 | Comparison of median (black line) and geo-mean (red line) of dose-normalized Cmax (Cmax DN) and dose-normalized AUC 0–24 (AUC 0–24 DN) between gender **(A,B)** and different age groups **(C,D)**. Median (black line) and geo-mean (red line) of exposure parameters between patients with distinct EPAG response **(E,F)**. M = male, F = female, C = complete response, PR = partial response, A = no response.

pharmacokinetic population models based on data extracted from randomized clinical trials, where patients are enrolled and strictly monitored throughout the study.

According to the literature, our data confirm that female patients show a higher drug exposure compared to male patients with an increase of 110 and 123% for Cmax DN and AUC 0-24 DN, respectively, compared to males. Conversely, no statistically significant differences in weight between the two genders were found (median body weight F = 43.5 kg, M = 42.95 kg). The gender influence on drug exposure has been well documented by Wire et al. (2018), who included sex as a covariate influencing EPAG clearance in pediatric subjects. These findings could be explained by a reduced metabolic activity of CYP1A2 in females (Relling et al., 1992; Parkinson et al., 2004). This cytochrome isoform is one of the two major enzymes involved in the oxidative hepatic metabolism of EPAG.

Together with gender, we have also analyzed the effect of age on EPAG exposure. Although not statistically significant, younger children (1–5 y age group) displayed increased dose normalized exposure PK values when compared to the children aged more than 6 years, potentially due to a lower body weight and the reduced hepatic EPAG metabolism (Salem et al., 2014; Song et al., 2017; Wire et al., 2018). Furthermore, despite the recommended starting EPAG dose being 25 mg in children aged 1–5 y, only one patient from this age group has been treated with this dose (mean dose 1–5 y age group = 50 mg).

As previously reported, EPAG treatment in pediatric patients reached a response rate between 40 and 81% (Bussel et al., 2015;

Grainger et al., 2015; Neunert et al., 2016). In our study, 30 patients (83%) presented a CR characterized by higher Cmax and AUC 0–24 geo-means compared to PR or non-responder patients. Only 33% of the patients showed durable response. Remarkably, among the six patients with CR in the 1–5 y age group, four of them needed a rescue therapy during treatment. Taking into account the monocentric nature of the study and the incidence of ITP in the pediatric population, a limitation of this study is the relatively contained number of enrolled subjects. This could have impaired the comparison of exposure parameters between the groups. An additional limitation is the extrapolation of the concentration at a 24 h time point since the enrolled subjects were outpatients. However, we decided not to replicate the marketing authorization holder method (the pre-dose sample was duplicated and analyzed as a 24 h sample under the assumption that the PK steady state had been reached) taking into account the variability of the drug administration time the day before the visit in our study population (CHMP, Ema, 2011).

In conclusion, this study showed a marked variability and unpredictability of EPAG concentrations in pediatric outpatients affected by ITP. However, our findings confirmed the gender influence on EPAG exposure. Furthermore, although not statistically significant, children aged 1–5 y had increased dose-normalized PK exposure values compared to older patients. EPAG administration requires dose adjustment according to PLT count throughout treatment. Therefore, a better comprehension of PK behavior of this TPO-RA, particularly in a real-life setting, could shed light on exposure and response gaps in some patient subpopulations and could be a potential tool for dose optimization during EPAG treatment. Nevertheless, 1–5 y old patients resorted more frequently to rescue therapy, despite higher DN exposure EPAG parameters when compared to the other age groups. This suggests that the response to EPAG might not be as strongly linked to PK parameters. To sum up, these results highlight the need to further investigate the lack of complete response persistence and treatment-free ITP remission during and after EPAG treatment in pediatric patients.

DATA AVAILABILITY STATEMENT

The raw data supporting the conclusion of this article will be made available by the authors, without undue reservation.

AUTHOR CONTRIBUTIONS

MD performed data analysis, PK evaluation and elaboration of figures; SC prepared samples and performed HPLC-MS/MS analyses; MD and RS wrote the manuscript; FG, VP, RC, and FR recruited patients, collected samples, and revised the manuscript; CD-V critically revised the manuscript and edited language; GP and BG made substantial contribution to study conception and design.

SUPPLEMENTARY MATERIAL

The Supplementary Material for this article can be found online at: https://www.frontiersin.org/articles/10.3389/fphar.2021.772873/full#supplementary-material

REFERENCES

Acharya, C., Hooker, A. C., Türkyılmaz, G. Y., Jönsson, S., and Karlsson, M. O. (2016). A Diagnostic Tool for Population Models Using Non-compartmental Analysis: The Ncappc Package for R. *Comput. Methods Programs Biomed.* 127, 83–93. doi:10.1016/j.cmpb.2016.01.013

Argenziano, M., Tortora, C., Paola, A. D., Pota, E., Martino, M. D., Pinto, D. D., et al. (2021). Eltrombopag and its Iron Chelating Properties in Pediatric Acute Myeloid Leukemia. *Oncotarget* 12, 1377–1387. doi:10.18632/oncotarget.28000

Bao, W., Bussel, J. B., Heck, S., He, W., Karpof, M., Boulad, N., et al. (2016). Improved Regulatory T-Cell Activity in Patients With Chronic Immune Thrombocytopenia Treated With Thrombopoietic Agents. *Blood* 116 (22), 4639–4645. doi:10.1182/blood-2010-04-281717

Burness, C. B., Keating, G. M., and Garnock-Jones, K. P. (2016). Eltrombopag: A Review in Paediatric Chronic Immune Thrombocytopenia. *Drugs* 76, 869–878. doi:10.1007/s40265-016-0581-4

Bussel, J. B., De Miguel, P. G., Despotovic, J. M., Grainger, J. D., Sevilla, J., Blanchette, V. S., et al. (2015). Eltrombopag for the Treatment of Children with Persistent and Chronic Immune Thrombocytopenia (PETIT): A Randomised, Multicentre, Placebo-Controlled Study. *Lancet Haematol.* 2, e315–25. doi:10.1016/S2352-3026(15)00114-3

Committee For Proprietary Medicinal Products CPMP (2000). *Note for Guidance on the Investigation of Bioavailability and Bioequivalence*.

Consolini, R., Legitimo, A., and Caparello, M. C. (2016). The Centenary of Immune Thrombocytopenia - Part 1: Revising Nomenclature and Pathogenesis. *Front. Pediatr.* 4, 102–112. doi:10.3389/fped.2016.00102

Cooper, N., and Ghanima, W. (2019). Immune Thrombocytopenia. *N. Engl. J. Med.* 381, 945–955. doi:10.1056/NEJMcp1810479

Di Paola, A., Palumbo, G., Merli, P., Argenziano, M., Tortora, C., Strocchio, L., et al. (2021). Effects of Eltrombopag on *In Vitro* Macrophage Polarization in Pediatric Immune Thrombocytopenia. *Ijms* 22, 97–12. doi:10.3390/ijms22010097

Ema, C. (2011). *Assessment Report - Revolade*, 44, 1–6.

European Union (2008). Ethical Considerations for Clinical Trials on Medicinal Products Conducted with the Paediatric Population. *Eur. J. Health L.* 15, 223–250. doi:10.1163/157180908X333228

Fattizzo, B., Levati, G., Cassin, R., and Barcellini, W. (2019). Eltrombopag in Immune Thrombocytopenia, Aplastic Anemia, and Myelodysplastic Syndrome: From Megakaryopoiesis to Immunomodulation. *Drugs* 79, 1305–1319. doi:10.1007/s40265-019-01159-0

Fogarty, P. F., and Segal, J. B. (2007). The Epidemiology of Immune Thrombocytopenic Purpura. *Curr. Opin. Hematol.* 14, 515–519. doi:10.1097/MOH.0b013e3282ab98c7

Gibiansky, E., Zhang, J., Williams, D., Wang, Z., and Ouellet, D. (2011). Population Pharmacokinetics of Eltrombopag in Healthy Subjects and Patients with Chronic Idiopathic Thrombocytopenic Purpura. *J. Clin. Pharmacol.* 51 (6), 842–856. Available at: www.icondevsolutions.com.

Grainger, J. D., Locatelli, F., Chotsampancharoen, T., Donyush, E., Pongtanakul, B., Komvilaisak, P., et al. (2015). Eltrombopag for Children with Chronic Immune Thrombocytopenia (PETIT2): A Randomised, Multicentre, Placebo-Controlled Trial. *Lancet* 386, 1649–1658. doi:10.1016/S0140-6736(15)61107-2

He, R., Reid, D., Jones, C., and Shulman, N. (1994). Spectrum of Ig Classes, Specificities, and Titers of Serum Antiglycoproteins in Chronic Idiopathic Thrombocytopenic Purpura. *Blood* 83, 1024–1032. doi:10.1182/blood.v83.4.1024.bloodjournal8341024

Johnsen, J. (2012). Pathogenesis in Immune Thrombocytopenia: New Insights. *Hematol. Am. Soc. Hematol. Educ. Program* 2012, 306–312. doi:10.1182/asheducation.v2012.1.306.3798320

Kim, T. O., Despotovic, J., and Lambert, M. P. (2018). Eltrombopag for Use in Children with Immune Thrombocytopenia. *Blood Adv.* 2, 454–461. doi:10.1182/bloodadvances.2017010660

Kühne, T., Berchtold, W., Michaels, L. A., Wu, R., Donato, H., Espina, B., et al. (2011). Newly Diagnosed Immune Thrombocytopenia in Children and Adults: A Comparative Prospective Observational Registry of the Intercontinental Cooperative Immune Thrombocytopenia Study Group. *Haematologica* 96, 1831–1837. doi:10.3324/haematol.2011.050799

Liu, X. G., Liu, S., Feng, Q., Liu, X. N., Li, G. S., Sheng, Z., et al. (2016). Thrombopoietin Receptor Agonists Shift the Balance of Fcγ Receptors toward Inhibitory Receptor IIb on Monocytes in ITP. *Blood* 128, 852–861. doi:10.1182/blood-2016-01-690727

Matthys, G., Park, J. W., McGuire, S., Wire, M. B., Bowen, C., Williams, D., et al. (2011). Clinical Pharmacokinetics, Platelet Response, and Safety of Eltrombopag at Supratherapeutic Doses of up to 200 Mg once Daily in Healthy Volunteers. *J. Clin. Pharmacol.* 51, 301–308. doi:10.1177/0091270010368677

Neunert, C., Despotovic, J., Haley, K., Lambert, M. P., Nottage, K., Shimano, K., et al. (2016). Thrombopoietin Receptor Agonist Use in Children: Data from the Pediatric ITP Consortium of North America ICON2 Study. *Pediatr. Blood Cancer* 63, 1407–1413. doi:10.1002/pbc.26003

Parkinson, A., Mudra, D. R., Johnson, C., Dwyer, A., and Carroll, K. M. (2004). The Effects of Gender, Age, Ethnicity, and Liver Cirrhosis on Cytochrome P450 Enzyme Activity in Human Liver Microsomes and Inducibility in Cultured Human Hepatocytes. *Toxicol. Appl. Pharmacol.* 199, 193–209. doi:10.1016/j.taap.2004.01.010

Relling, M. V., Lin, J., and Ayers, G. D. (1992). Racial and Gender Differences in N-Acetyltran"sferase, Xanthine Oxidase, and CYP 1A2* Activities. *Clin. Pharmacol. Ther.* 52 (6), 643–658. doi:10.1038/clpt.1992.203

Rodeghiero, F., Stasi, R., Gernsheimer, T., Michel, M., Provan, D., Arnold, D. M., et al. (2009). Standardization of Terminology, Definitions and Outcome Criteria in Immune Thrombocytopenic Purpura of Adults and Children: Report from an International Working Group. *Blood* 113, 2386–2393. doi:10.1182/blood-2008-07-162503

Ruslami, R., Nijland, H. M., Alisjahbana, B., Parwati, I., Van Crevel, R., and Aarnoutse, R. E. (2007). Pharmacokinetics and Tolerability of a Higher Rifampin Dose versus the Standard Dose in Pulmonary Tuberculosis Patients. *Antimicrob. Agents Chemother.* 51, 2546–2551. doi:10.1128/AAC.01550-06

Salem, F., Johnson, T. N., Abduljalil, K., Tucker, G. T., and Rostami-Hodjegan, A. (2014). A Re-evaluation and Validation of Ontogeny Functions for Cytochrome P450 1A2 and 3A4 Based on *In Vivo* Data. *Clin. Pharmacokinet.* 53, 625–636. doi:10.1007/s40262-014-0140-7

Schifferli, A., Holbro, A., Chitlur, M., Coslovsky, M., Imbach, P., Donato, H., et al. (2018). A Comparative Prospective Observational Study of Children and Adults with Immune Thrombocytopenia: 2-year Follow-Up. *Am. J. Hematol.* 93, 751–759. doi:10.1002/ajh.25086

Schoonen, W. M., Kucera, G., Coalson, J., Li, L., Rutstein, M., Mowat, F., et al. (2009). Epidemiology of Immune Thrombocytopenic Purpura in the General Practice Research Database. *Br. J. Haematol.* 145, 235–244. doi:10.1111/j.1365-2141.2009.07615.x

Food and Drug Administration (FDA) and Center for Drug Evaluation and Research (CDER) (2001). Guidance for Industry: Patient-Reported Outcome Measures: Use in Medical Product Development to Support Labeling Claims: Draft Guidance. *Health Qual. Life Outcomes* 4, 79. doi:10.1186/1477-7525-4-79

Song, G., Sun, X., Hines, R. N., McCarver, D. G., Lake, B. G., Osimitz, T. G., et al. (2017). Determination of Human Hepatic CYP2C8 and CYP1A2 Age-dependent Expression to Support Human Health Risk Assessment for Early Ages. *Drug Metab. Dispos.* 45, 468–475. doi:10.1124/dmd.116.074583

Terrell, D. R., Beebe, L. A., Vesely, S. K., Neas, B. R., Segal, J. B., and George, J. N. (2010). The Incidence of Immune Thrombocytopenic Purpura in Children and Adults: A Critical Review of Published Reports. *Am. J. Hematol.* 85, 174–180. doi:10.1002/ajh.21616

Vianelli, N., Valdrè, L., Fiacchini, M., De Vivo, A., Gugliotta, L., Catani, L., et al. (2001). Long-term Follow-Up of Idiopathic Thrombocytopenic Purpura in 310 Patients. *Haematologica* 86 (5), 504–509.

Wire, M. B., Li, X., Zhang, J., Sallas, W., Aslanis, V., and Ouatas, T. (2018). Modeling and Simulation Support Eltrombopag Dosing in Pediatric Patients with Immune Thrombocytopenia. *Clin. Pharmacol. Ther.* 104, 1199–1207. doi:10.1002/cpt.1066

Wong, R. S. M., Saleh, M. N., Khelif, A., Salama, A., Portella, M. S. O., Burgess, P., et al. (2017). Safety and Efficacy of Long-Term Treatment of Chronic/persistent ITP with Eltrombopag: Final Results of the EXTEND Study. *Blood* 130, 2527–2536. doi:10.1182/blood-2017-04-748707

Conflict of Interest: The authors declare that the research was conducted in the absence of any commercial or financial relationships that could be construed as a potential conflict of interest.

Publisher's Note: All claims expressed in this article are solely those of the authors and do not necessarily represent those of their affiliated organizations or those of the publisher, the editors, and the reviewers. Any product that may be evaluated in this article or claim that may be made by its manufacturer is not guaranteed or endorsed by the publisher.

frontiers in Pharmacology

ORIGINAL RESEARCH
published: 07 December 2021
doi: 10.3389/fphar.2021.750672

Population Pharmacokinetic Model Development of Tacrolimus in Pediatric and Young Adult Patients Undergoing Hematopoietic Cell Transplantation

*Jordan T. Brooks[1], Ron J. Keizer[2], Janel R. Long-Boyle[1,3], Sandhya Kharbanda[3], Christopher C. Dvorak[3] and Brian D. Friend[4]**

[1]Department of Clinical Pharmacy, School of Pharmacy, University of California, San Francisco, San Francisco, CA, United States, [2]Insight RX, Inc, San Francisco, CA, United States, [3]Department of Pediatrics, University of California, San Francisco, San Francisco, CA, United States, [4]Department of Pediatrics, Center for Cell and Gene Therapy, Baylor College of Medicine, Houston, TX, United States

OPEN ACCESS

Edited by:
Alwin Huitema,
The Netherlands Cancer Institute (NKI), Netherlands

Reviewed by:
Georg Hempel,
University of Münster, Germany
Mara Medeiros,
Federico Gómez Children's Hospital, Mexico

***Correspondence:**
Brian D. Friend
bdfriend@texaschildrens.org

Specialty section:
This article was submitted to Obstetric and Pediatric Pharmacology, a section of the journal Frontiers in Pharmacology

Received: 31 July 2021
Accepted: 15 November 2021
Published: 07 December 2021

Citation:
Brooks JT, Keizer RJ, Long-Boyle JR, Kharbanda S, Dvorak CC and Friend BD (2021) Population Pharmacokinetic Model Development of Tacrolimus in Pediatric and Young Adult Patients Undergoing Hematopoietic Cell Transplantation. Front. Pharmacol. 12:750672. doi: 10.3389/fphar.2021.750672

Background: With a notably narrow therapeutic window and wide intra- and interindividual pharmacokinetic (PK) variability, initial weight-based dosing along with routine therapeutic drug monitoring of tacrolimus are employed to optimize its clinical utilization. Both supratherapeutic and subtherapeutic tacrolimus concentrations can result in poor outcomes, thus tacrolimus PK variability is particularly important to consider in the pediatric population given the differences in absorption, distribution, metabolism, and excretion among children of various sizes and at different stages of development. The primary goals of the current study were to develop a population PK (PopPK) model for tacrolimus IV continuous infusion in the pediatric and young adult hematopoietic cell transplant (HCT) population and implement the PopPK model in a clinically available Bayesian forecasting tool.

Methods: A retrospective chart review was conducted of 111 pediatric and young adult patients who received IV tacrolimus by continuous infusion early in the post-transplant period during HCT from February 2016 to July 2020 at our institution. PopPK model building was performed in NONMEM. The PopPK model building process included identifying structural and random effects models that best fit the data and then identifying which patient-specific covariates (if any) further improved model fit.

Results: A total of 1,648 tacrolimus plasma steady-state trough concentrations were included in the PopPK modeling process. A 2-compartment structural model best fit the data. Allometrically-scaled weight was a covariate that improved estimation of both clearance and volume of distribution. Overall, model predictions only showed moderate bias, with minor under-prediction at lower concentrations and minor over-prediction at

Abbreviations: Cl, Clearance; CYP, Cytochrome P450; DDI, Drug-drug interaction; GVHD, Graft-versus-host disease; HCT, Hematopoietic stem cell transplant; Km, Michaelis constant; PK, Pharmacokinetic; PopPK, Population pharmacokinetic; Vd, Volume of distribution.

higher predicted concentrations. The model was implemented in a Bayesian dosing tool and made available at the point-of-care.

Discussion: Novel therapeutic drug monitoring strategies for tacrolimus within the pediatric and young adult HCT population are necessary to reduce toxicity and improve efficacy in clinical practice. The model developed presents clinical utility in optimizing the use of tacrolimus by enabling model-guided, individualized dosing of IV, continuous tacrolimus *via* a Bayesian forecasting platform.

Keywords: population pharmacokinetic model, pediatrics, tacrolimus, hematopoietic stem cell transplantation, therapeutic drug monitoring

INTRODUCTION

Acute graft-versus-host disease (aGVHD) is a major cause of morbidity and mortality in patients who have undergone allogeneic hematopoietic cell transplantation (HCT). In T cell-replete transplants, prevention of acute GVHD using immunosuppressants is necessary to decrease the incidence of GVHD and improve transplant outcomes. Specifically, tacrolimus, a calcineurin inhibitor, is commonly utilized for GVHD prophylaxis (Jacobson et al., 1998; Ram et al., 2009).

With a notably narrow therapeutic window and wide intra- and interindividual pharmacokinetic (PK) variability, initial weight-based dosing along with routine therapeutic drug monitoring of tacrolimus are employed to optimize its safety and efficacy. Both supratherapeutic and subtherapeutic tacrolimus concentrations can result in poor outcomes. Elevated steady-state trough concentrations of tacrolimus are associated with increased risk of adverse effects, including nephrotoxicity, hepatotoxicity, electrolyte abnormalities, and neurotoxicity, while subtherapeutic levels may increase the risk of developing GVHD and graft rejection (Kernan et al., 1986; Kernan et al., 1987; Butts et al., 2016; Andrews et al., 2018). Beyond intrinsically high PK variability, tacrolimus is primarily metabolized hepatically by cytochrome p450 3A4 and 3A5 (CYP3A4/5) and is, therefore, susceptible to many drug-drug interactions. Azole antifungals, used frequently post-HCT to prevent and treat fungal infections, are notorious inhibitors of CYP3A4/5, complicating the goal of reaching a steady, therapeutic concentration of tacrolimus. The clinical experience of the UCSF pediatric HCT center has found that current standard practice commonly results in high initial therapeutic trough levels of tacrolimus in its pediatric and young adult patients.

Tacrolimus PK variability is particularly important to consider in the pediatric population given the differences in absorption, distribution, metabolism and excretion among children of various sizes and at different stages of development (Kearns et al., 2003). Given the known variability in PK of tacrolimus in pediatric patients, several recently published studies have described pediatric-specific population pharmacokinetic (PopPK) models along with their associated dosing guides (Wallin et al., 2009; Andrews et al., 2018; Wang et al., 2020; Zhou et al., 2021). Zhou et al. developed a model within a subpopulation of children undergoing HCT for β-thalassemia (Zhou et al., 2021). Wang et al. and Wallin et al. described similar models where a one-compartment model best described the dataset and allometrically scaled weight improved approximations of clearance (Cl) and volume of distribution (Vd) (Wallin et al., 2009; Wang et al., 2020). Notably, Wang et al. solely examined patients receiving oral tacrolimus and Wallin et al. included a mix of IV and oral tacrolimus patients. While these models were developed in pediatric patients undergoing allogeneic HCT, given the small sample sizes and homogeneous populations of these studies, such approaches are unlikely to be generalizable to a broader population of children and young adults receiving HCT.

The objectives of the current study were to 1) develop a PopPK model for tacrolimus IV continuous infusion in the pediatric and young adult HCT population at UCSF Benioff Children's Hospital and 2) implement model-informed dosing of tacrolimus utilizing the PopPK model in a clinically available Bayesian forecasting tool.

MATERIALS AND METHODS

Patients and Data Collection

A retrospective chart review was conducted of all pediatric and young adult patients age <25 years treated at UCSF Benioff Children's Hospital who received tacrolimus for GVHD prophylaxis during allogeneic HCT from February 2016 to July 2020. Patient characteristics were collected at the time of transplant and included age, gender, ethnicity, total body weight, and height. Transplant-specific characteristics included diagnosis, conditioning regimen, stem cell source, and degree of HLA mismatch. Though found significant in one published model, ursodeoxycholic acid was not evaluated in our model given little variability in its administration, as it is standard practice within the HCT center for nearly all patients to receive this medication (Wang et al., 2020). Transplant outcomes included presence of aGVHD or chronic GVHD (cGVHD), and survival at time of data collection. Tacrolimus-specific information included steady-state trough plasma concentrations for a minimum of 14 days of tacrolimus therapy (if available), time of tacrolimus therapy for which the plasma concentrations corresponded to, dosing rate of tacrolimus, and whether there was concomitant administration of voriconazole or posaconazole during each plasma concentration. In the context of this study, voriconazole or

posaconazole were prescribed for prophylaxis or treatment of fungal infections.

Tacrolimus Administration

The recommended starting dosing rate of tacrolimus for GVHD prophylaxis during HCT was 1.25 mcg/kg/h continuous IV infusion with a goal therapeutic range of 7–10 ng/ml. Steady-state tacrolimus plasma trough concentrations were typically measured every 24–48 h after initiation and every 24 h after a dosing change until the patient was consistently within the therapeutic range. The exact time of concentration measurements was not recorded and, therefore, it was assumed that each concentration was drawn the ideal 15 min before the next continuous infusion was started. Additionally, it was assumed that continuous infusions were given over exactly 24 h.

Population Pharmacokinetic Modeling

The software utilized to build the PopPK model included NONMEM version v7.4 (ICON), PsN v4.8.1, and PiranaJS (beta version). Goodness of fit plots for model evaluation were created in R (v3.6.2) using the ggplot2 and vpc packages. The PopPK model building process included identifying structural and random effects models that best fit the data and then identifying which patient-specific covariates (if any) further improved model fit. Structural model exploration included evaluating fit of data to 1-compartment, 2-compartment, non-linear, and linear models. Both inter-individual and intra-individual variability was evaluated on all parameters and included if it could be estimated from the data and significantly improved fit. Additive, proportional, and combined residual error models were evaluated. Covariates that were available for evaluation were: weight, height, sex, age, co-treatment with CYP3A4/5 inhibitor (voriconazole and/or posaconazole), donor relation, aGVHD, cGVHD, and diagnosis. Weight was implemented allometrically. After implementation of weight, the other covariates were implemented and evaluated consecutively. Covariates were added using a stepwise approach with initial inclusion if covariate account was attributed to significant model fit improvement as quantified by a difference in OFV of -3.58 ($p < 0.05$). After initial covariate inclusion, each covariate was sequentially removed from the model and if any removal resulted in an improvement of fit associated with an alpha = 0.01, it was left out of the final model.

TABLE 1 | Patient demographics and outcomes included in the PopPK tacrolimus continuous, IV infusion model.

Number of patients	111
Females sex number – n (%)	43 (39)
Age (years) – median (range)	7.3 (0.5 - 25)
Actual body weight (kg) – median (range)	23.9 (5.5 - 155.5)
Ancestry - n (%)	
African American	6 (5.4)
American Indian or Alaskan Native	2 (1.8)
Asian/Caucasian/Hispanic	4 (3.6)
Asian	18 (16.2)
Caucasian/Non-Hispanic	38 (34.2)
Caucasian/Hispanic or Latino	38 (34.2)
Multi-ancestry	2 (1.8)
Other/Declined	3 (2.7)
Outcomes - n (%)	
aGVHD	19 (17.1)
cGVHD	16 (14.4)
Deceased	21 (18.9)
Diagnosis - n (%)	
Diagnoses Malignancies	65 (58.6)
Acute lymphoblastic leukemia	34 (30.6)
Acute myeloid leukemia	15 (13.5)
Juvenile myelomonocytic leukemia	8 (7.2)
Chronic myeloid leukemia	2 (1.8)
Myelodysplastic syndrome	3 (2.7)
Lymphoma	2 (1.8)
Natural Killer Cell Leukemia	1 (0.9)
Non-malignancies	46 (41.4)
Primary Immunodeficiencies	19 (17.1)
Aplastic Anemia/Bone Marrow Failure Syndromes	16 (14.4)
Inborn Errors of Metabolism	7 (6.3)
Hemoglobinopathies	4 (3.6)
Conditioning Regimen – n (%)	
Busulfan/Fludarabine/Clofarabine	38 (34.3)
Busulfan/Fludarabine	14 (12.6)
Cyclophosphamide/Fludarabine	14 (12.6)
Cyclophosphamide/Total Body Irradiation	11 (9.9)
Melphalan/Fludarabine	10 (9.0)
Other	24 (21.6)
Serotherapy - n (%)	
Antithymocyte globulin, rabbit	64 (57.7)
alemtuzumab	42 (37.8)
None	5 (4.5)
Donor Source - n (%)	
Bone Marrow	55 (49.5)
Peripheral Blood Stem Cells*	49 (44.1)
Umbilical Cord Blood	7 (6.3)
Degree of HLA mismatch - n (%)	
Fully Matched	62 (55.9)
1 Degree Mismatched	31 (27.9)
≥ 2 Degree Mismatched	18 (16.2)

**1 patient in the peripheral blood stem cell group also received bone marrow cells from the same donor.*

RESULTS

Patient Characteristics

Data from 111 patients were collected and analyzed. The patients included in the dataset were found to be broadly reflective of the population treated at the HCT center, with median age of 7.3 years (range 0.5–25 years) and 66% of patients identified as non-Caucasian. The majority of patients were male (61%). Patients were treated for a variety of malignant and non-malignant diagnoses (**Table 1**). aGVHD was observed in 19 (17.1%) of patients and cGVHD was observed in 16 (14.4%) patients.

A total of 1,648 tacrolimus plasma steady-state trough concentrations were included in the PopPK modeling process. Trough levels were performed for a median of 14 days after starting tacrolimus continuous IV infusion, though not every patient had levels consistently drawn each day for the first

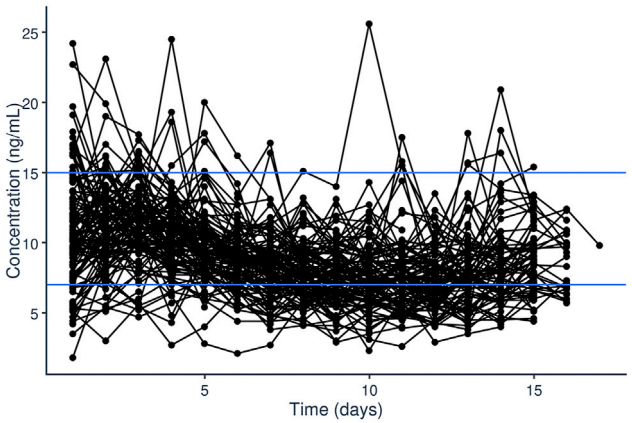

FIGURE 1 | Steady-state trough plasma concentrations of tacrolimus (ng/ml) over time (days) after initiation of tacrolimus IV continuous infusion in pediatric patients undergoing HCT.

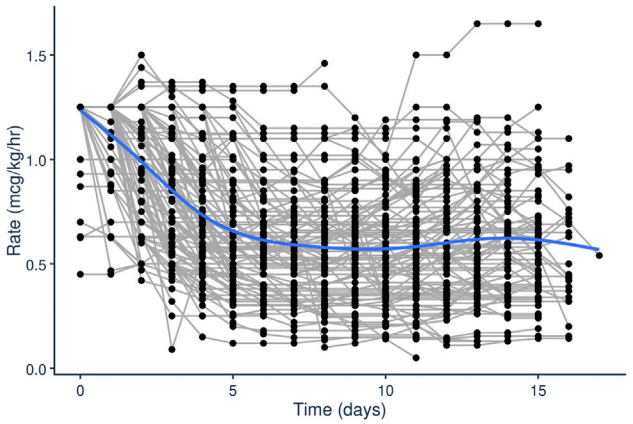

FIGURE 2 | Tacrolimus IV infusion rage (mcg/kg/h) over time (days) after initiation of tacrolimus IV continuous infusion in pediatric patients undergoing HCT.

14 days of treatment. The median tacrolimus dosing rate was 1.25 mcg/kg/h with a range of 0.45 mcg/kg/h to 1.25 mg/kg/h. A total of 929 (56.4%) of the 1,648 samples within the first 14 days were outside of the goal of 7–10 ng/ml (**Figure 1**). For 193 (11.7%) of the 1,648 samples, voriconazole or posaconazole was administered concomitantly. The median first steady-state trough concentration was 10.2 ng/ml (range 1.8–24.2 ng/ml).

Initial dataset investigation informed the PopPK model building process. It became clear that, on average, the fixed initial dosing rate of 1.25 mcg/kg/h generally resulted in initial supratherapeutic tacrolimus trough levels as evident by the median initial trough concentration of 10.2 ng/ml (**Figure 1**). Additionally, looking at the average dosing rate over time showed a distinct decrease in dosing rate over the first few days of treatment which eventually plateaued (**Figure 2**). Specific patient characteristics were then evaluated to probe for potential covariates driving the variation which led to patients being over-dosed at the fixed total body weight institutional practice.

Population Pharmacokinetic Model

A two-compartment model with fixed Q and V2 showed improved model fit ($p < 0.001$) over a one-compartment model. Intercompartmental clearance (Q) and peripheral compartment volume (V2) were fixed to Cl and Vd by a fixed multiplication factor (Fact). Fact was determined based on the average of several published population PK studies, and it was assumed to be the same for both Q and V2 (Xue et al., 2011; Kassir et al., 2014; Moes et al., 2016; Andrews et al., 2018; Andrews et al., 2020). Non-linear clearance was found to lead to significantly better fit, although the improvement in fit was not apparent from any of the goodness of fit plots (plots not included in this report). For the non-linear model iterations, Michaelis constant (Km) was estimated around 10 ng/ml; however, we did not include the non-linear component in the final model. Of note, inclusion of a time-dependent effect on CL did not improve model fit for the 2-compartment model, and only slightly for the 1-compartment model.

In terms of accounting for random effects, between-patient variability was estimated on both CL and V, and improved fit significantly for both parameters and so was included in the final model. Inter-occasion variability was estimated on both CL and V, but only led to significant improvement in fit for CL (and due to fixed implementation of Q, also on Q). A residual error with both proportional and additive components could not be identified from the data. Therefore, only the proportional component was retained, which was estimated to be 17.9%.

Patient-specific covariates were identified which improved model fit upon inclusion. Actual body weight, implemented using allometric principles on all PK parameters, was a significant covariate in the model. Estimation of the allometric parameters only led to moderate improvements in fit and were estimated at close to the theoretic exponents (0.73 vs 0.75 for CL, and 0.83 vs 1.0 for V), so they were fixed at their theoretic values. Use of allometry based on fat-free-mass instead of weight did not improve fit. Co-treatment with a CYP-inhibitor significantly reduced the clearance of tacrolimus ($p = 0.001$, estimate 20%, on clearance 95% CI: 10–33%). No other covariates were found to be predictive factors on either clearance or volume parameters.

As no sensible groupings were identified that would have resulted in relevant group sizes to allow estimation of a covariate effect for diagnosis, it was not attempted to estimate the effect of diagnosis on PK parameters. Likewise, ancestry was evaluated but we did not have large enough group sizes to estimate a covariate effect. None of the transplant-specific characteristics or outcomes (donor, antigen mismatch, aGvHD, cGvHD, alive status) showed significance. Additionally, survival status was not a significant outcome as most recipients were alive (81%) at the time of data collection.

Model Validation

Diagnostic plots and a visual predictive check were utilized to validate the model (**Figures 3**, **4**). Overall, model predictions only

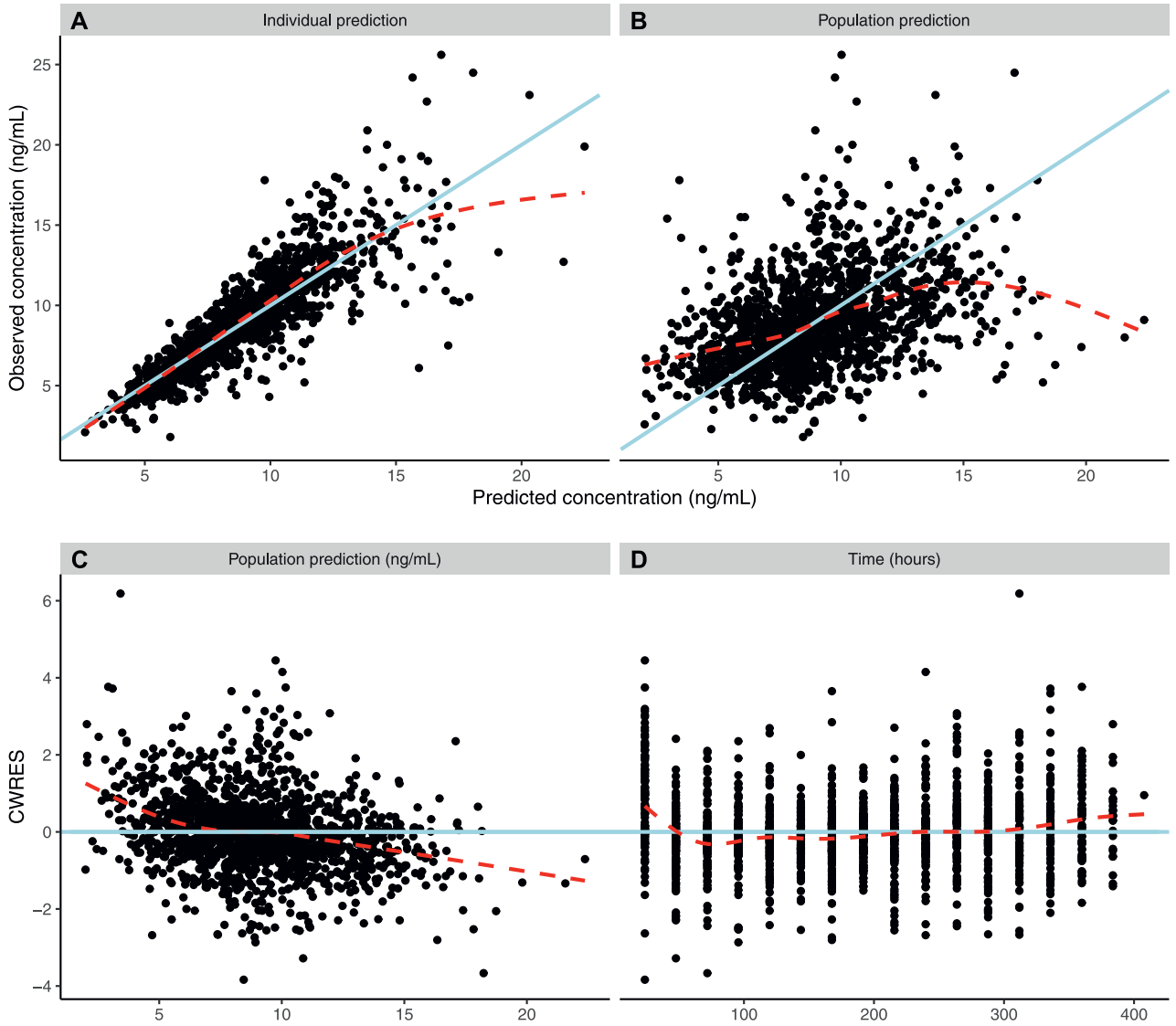

FIGURE 3 | Population pharmacokinetic model diagnostic plots. Dashed lines show a weighted average, while solid lines indicate line of unity (3AB) or line of zero residual (3CD). **(A)** Actual individual tacrolimus steady-state plasma concentrations (ng/ml) versus model-guided individual prediction of tacrolimus steady-state plasma concentrations (ng/ml) taking into account random effects and individual factors. **(B)** Actual individual tacrolimus steady-state plasma concentrations (IPRED) (ng/ml) versus model-guided population predictions of tacrolimus steady-state plasma concentrations (PRED) (ng/ml). **(C)** Conditional weighted residuals (CWRES) (%) over PRED (ng/ml) of tacrolimus. **(D)** CWRES (%) over time (hours).

showed moderate bias, with minor under-prediction at lower concentrations and minor over-prediction at higher predicted concentrations. The VPC plot showed adequate prediction of the median and 5th/95th percentiles over time, with only a slight under-prediction of the median for the concentration at day 1 of treatment (**Figures 3**, **4**). The final model was therefore defined as:

$$CL_i = \theta_{CL} \cdot (WT_i/70)^{0.75} \cdot \theta_{inh}^{INH} \cdot \mathbf{exp}\left(\eta_{CL_i} + \kappa_j\right)$$

$$V_{1,i} = \theta_{V_1} \cdot (WT_i/70)^{1} \cdot \mathbf{exp}\left(\eta_{V_{1,i}}\right)$$

$$Q_{i,j} = CL_{i,j} * Fact$$

$$V_{2,i} = V_{1,i} * Fact$$

The final parameter estimates are reported in **Table 2**.

DISCUSSION

While the standard practice at most transplant centers to therapeutic drug monitoring for tacrolimus is essentially a "guess and check" approach using standard weight-based

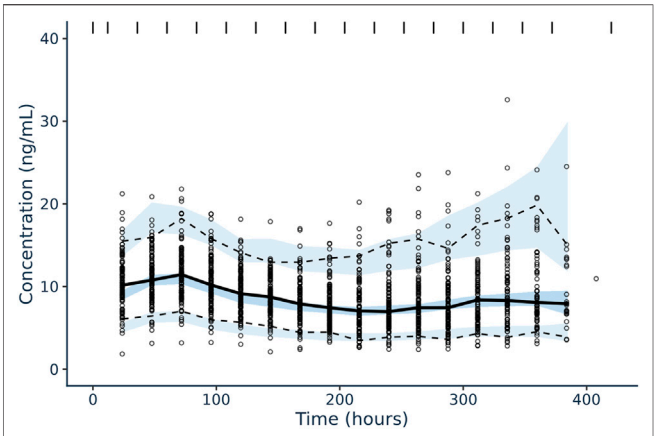

FIGURE 4 | Confidence interval visual predictive check for tacrolimus IV, continuous infusion population pharmacokinetic model in pediatric patients undergoing HCT. Solid black line corresponds to the median plasma concentrations (ng/ml) of tacrolimus over time (hour) and the dotted black lines correspond to the 5% (lower) and 95% plasma concentration (ng/ml) intervals of concentrations included in the dataset utilized for model building. The blue shaded areas correspond to the model-guided predictions of 5%, median, and 95% plasma concentrations (ng/ml) intervals over time.

TABLE 2 | Population pharmacokinetic parameter estimates of final model.

Parameter	Value	RSE	Unit	IIV	IOV
θ_{CL}	4.2	2.95%	L/h	26.1%	28.7%
θ_{V}	61.9	5.98%	L	-	-
θ_{INH}	0.8	6.97%		-	-
Fact	2.0	fixed		-	-

dosing, our center has observed that initial tacrolimus levels are frequently supratherapeutic. This clinical finding led us to hypothesize that a model-informed, precision-based approach to dosing of continuous, IV tacrolimus could enable us to reach our goal therapeutic range more quickly and maintain these levels consistently throughout treatment. Therefore, we developed this PopPK model with the intention of optimizing tacrolimus dosing to improve its safety and effectiveness in clinical practice.

The developed PopPK model has several advantages for our patient population as compared to the current models available in the literature. First, it was developed in a pediatric and young adult population for which it is intended to be used, i.e., continuous infusion for patients undergoing HCT. Furthermore, it was developed from a broad population of patients including diverse age range, ethnicities, and indications for HCT, supporting the generalizability of the model for the population undergoing HCT at the UCSF Benioff Children's Hospital and other large transplant centers. Additionally, the inclusion of voriconazole and posaconazole in covariate analysis was novel from previously published PopPK models of tacrolimus in this population and provides further utility for this approach. Moreover, the PopPK's clinical utility in conjunction with its build into a Bayesian forecasting platform enables smooth translation into improving patient outcomes. Further fine tuning and improvement of the model within the Bayesian forecasting platform is readily attainable, as we have previously demonstrated for other drugs in HCT (Shukla et al., 2020).

Although only concentrations from continuous dosing of tacrolimus were available, we selected a 2-compartment model, as we felt there was significant scientific justification for this decision given that prior publications of tacrolimus PopPK models have demonstrated two-compartment kinetics. Within the pediatric renal transplant setting, Andrews et al. developed a PopPK model of tacrolimus which fit a two-compartment structural model with patient-specific covariates including allometrically scaled weight, CYP3A5 isoform status, hematocrit, estimated glomerular filtration rate, and donor living status factored into tacrolimus clearance (Andrews et al., 2018). While insightful, there are some key disease-state differences that make extrapolation of this model to the HCT setting difficult, including the reliance on IV tacrolimus for extended periods post-HCT, high potential for liver injury secondary to receiving high-dose chemotherapy and radiation in HCT, and difference in intended purpose (preventing both graft rejection and GVHD).

Technically, if the model is only to be used for prediction of steady state levels, which is indeed its intended use, it would not matter if a 1- or 2-compartment model would be selected. However, the more physiologically valid 2-compartment model is expected to be more predictive in clinical situations that deviate from the anticipated use, such as when the tacrolimus continuous infusion would be stopped for some time or given intermittently. For the non-linear PK iterations of the model building process, the Km was estimated to be in the middle of the clinically observed concentration range for continuous IV, lending credibility to the non-linear model. However, as far as we know, no other population PK analyses on tacrolimus have reported non-linear PK in the clinically observed concentration range for common dosage regimens. Given that the current analysis included only sparse data (troughs), obtained only from continuous IV administration, and that the dataset was of relatively limited size (n = 111), we were hesitant to conclude that tacrolimus continuous IV, given at the dosages in this cohort, leads to non-linear PK. Therefore, we did not include the non-linear component in the final model, but we report the Km here for future reference.

While not included in the final two-compartment model, the time effect on clearance, which improved fit of the one-compartment model, is interesting to note. This phenomenon matches clinical experience in which hepatotoxicity secondary to the conditioning regimen progresses on average over the first 2 weeks after transplant and during the time of tacrolimus data collection in our dataset. Since tacrolimus elimination is dependent on the cytochrome P450 system within the liver, hepatocellular toxicity due to high dose chemotherapy prior to HCT resulting in impaired metabolic activity is a logical explanation for such a time-dependent decrease in tacrolimus clearance after HCT. Further studies elucidating the relationship between hepatoxicity secondary to conditioning regimen and tacrolimus clearance are warranted.

In current published PopPK models within the pediatric HCT population, there is some diversity in evaluated and included covariates. Given tacrolimus' hepatic metabolism and the possibility of hepatotoxicity secondary to conditioning in this population, inclusion of liver function tests as covariates and status of veno-occlusive disease/sinusoidal obstruction syndrome as a clinical outcome within the Bayesian forecasting platform may improve the model further. Inclusion of greater numbers of the representative ancestry groups will help to elucidate any potential effect on tacrolimus PK. Likewise, the inclusion of CYP3A4/5 genotyping into the model will likely improve the model significantly given its well documented relationship with tacrolimus PK and pharmacodynamics within the population (Birdwell et al., 2015). While it was not standard clinical practice at the time of data collection for this study, as recent studies support the use of CYP3A5 genotyping in patients undergoing allogeneic HCT (Zhu et al., 2020; Yoshikawa et al., 2021), our group plans to obtain this information for future patients as part of our standard clinical practice, which will further help to guide tacrolimus dosing within the PopPK model. We plan to prospectively evaluate the model-informed dosing of tacrolimus IV continuous infusion in the pediatric HCT population at UCSF Benioff Children's Hospital as well as continue to improve the model over time as more patient data is collected.

CONCLUSION

Prevention of aGVHD after allogeneic HCT is clinically important as this complication is a leading cause of post-HCT morbidity and mortality. Development of a PopPK model of tacrolimus elucidates factors driving variability within this population and accounts for patient-specific covariates to guide initial dosing rate. The described 2-compartment model accounts for relevant patient covariates including allometrically scaled weight and presence of a significant CYP3A4/5 inhibitor. Additionally, implementation of such a model in a Bayesian dosing platform translates this research directly into a clinically impactful application, that has the potential to improve outcomes for pediatric and young adult patients.

DATA AVAILABILITY STATEMENT

The raw data supporting the conclusions of this article will be made available by the authors, without undue reservation.

ETHICS STATEMENT

The studies involving human participants were reviewed and approved by the UCSF Human Research Protection Program IRB # 13-11714. Reference # 197225. Written informed consent from the participants' legal guardian/next of kin was not required to participate in this study in accordance with the national legislation and the institutional requirements.

AUTHOR CONTRIBUTIONS

JB - Contributed to data collection, modeling process, and manuscript preparation. RK - Contributed to modeling process and manuscript preparation. JL - Contributed to data collection and manuscript preparation. SK - Contributed to manuscript preparation. CD - Contributed to data collection and manuscript preparation. BF - Contributed to data collection and manuscript preparation.

ACKNOWLEDGMENTS

All the patients that have contributed to this project. Deborah French, clinical laboratory for assistance of acquiring the data. Inpatient clinical pharmacists in the UCSF Benioff Children's Hospital BMT service – Allyson Thrall, Kimvi Diep, Rebecca Deoras, and Tina Gu.

REFERENCES

Andrews, L. M., de Winter, B. C. M., Cornelissen, E. A. M., de Jong, H., Hesselink, D. A., Schreuder, M. F., et al. (2020). A Population Pharmacokinetic Model Does Not Predict the Optimal Starting Dose of Tacrolimus in Pediatric Renal Transplant Recipients in a Prospective Study: Lessons Learned and Model Improvement. *Clin. Pharmacokinet.* 59 (5), 591–603. doi:10.1007/s40262-019-00831-8

Andrews, L. M., Hesselink, D. A., van Gelder, T., Koch, B. C. P., Cornelissen, E. A. M., Brüggemann, R. J. M., et al. (2018). A Population Pharmacokinetic Model to Predict the Individual Starting Dose of Tacrolimus Following Pediatric Renal Transplantation. *Clin. Pharmacokinet.* 57 (4), 475–489. doi:10.1007/s40262-017-0567-8

Birdwell, K. A., Decker, B., Barbarino, J. M., Peterson, J. F., Stein, C. M., Sadee, W., et al. (2015). Clinical Pharmacogenetics Implementation Consortium (CPIC) Guidelines for CYP3A5 Genotype and Tacrolimus Dosing. *Clin. Pharmacol. Ther.* 98 (1), 19–24. doi:10.1002/cpt.113

Butts, A. R., Brown, V. T., McBride, L. D., Bolaños-Meade, J., and Bryk, A. W. (2016). Factors Associated with Optimized Tacrolimus Dosing in Hematopoietic Stem Cell Transplantation. *J. Oncol. Pharm. Pract.* 22 (2), 275–283. doi:10.1177/1078155215577809

Jacobson, P., Uberti, J., Davis, W., and Ratanatharathorn, V. (1998). Tacrolimus: A New Agent for the Prevention of Graft-Versus-Host Disease in Hematopoietic Stem Cell Transplantation. *Bone Marrow Transpl.* 22 (3), 217–225. doi:10.1038/sj.bmt.1701331

Kassir, N., Labbé, L., Delaloye, J. R., Mouksassi, M. S., Lapeyraque, A. L., Alvarez, F., et al. (2014). Population Pharmacokinetics and Bayesian Estimation of Tacrolimus Exposure in Paediatric Liver Transplant Recipients. *Br. J. Clin. Pharmacol.* 77 (6), 1051–1063. doi:10.1111/bcp.12276

Kearns, G. L., Abdel-Rahman, S. M., Alander, S. W., Blowey, D. L., Leeder, J. S., and Kauffman, R. E. (2003). Developmental Pharmacology-Ddrug Disposition, Action, and Therapy in Infants and Children. *N. Engl. J. Med.* 349 (12), 1157–1167. doi:10.1056/NEJMra035092

Kernan, N. A., Collins, N. H., Juliano, L., Cartagena, T., Dupont, B., and O'Reilly, R. J. (1986). Clonable T Lymphocytes in T Cell-Depleted Bone Marrow

Transplants Correlate with Development of Graft-V-Host Disease. *Blood* 68 (3), 770–773. doi:10.1182/blood.v68.3.770.bloodjournal683770

Kernan, N. A., Flomenberg, N., Dupont, B., and O'Reilly, R. J. (1987). Graft Rejection in Recipients of T-Cell-Depleted HLA-Nonidentical Marrow Transplants for Leukemia. Identification of Host-Derived Antidonor Allocytotoxic T Lymphocytes. *Transplantation* 43 (6), 842–847. doi:10.1097/00007890-198743060-00014

Moes, D. J., van der Bent, S. A., Swen, J. J., van der Straaten, T., Inderson, A., Olofsen, E., et al. (2016). Population Pharmacokinetics and Pharmacogenetics of once Daily Tacrolimus Formulation in Stable Liver Transplant Recipients. *Eur. J. Clin. Pharmacol.* 72 (2), 163–174. doi:10.1007/s00228-015-1963-3

Ram, R., Gafter-Gvili, A., Yeshurun, M., Paul, M., Raanani, P., and Shpilberg, O. (2009). Prophylaxis Regimens for GVHD: Systematic Review and Meta-Analysis. *Bone Marrow Transpl.* 43 (8), 643–653. doi:10.1038/bmt.2008.373

Shukla, P., Goswami, S., Keizer, R. J., Winger, B. A., Kharbanda, S., Dvorak, C. C., et al. (2020). Assessment of a Model-Informed Precision Dosing Platform Use in Routine Clinical Care for Personalized Busulfan Therapy in the Pediatric Hematopoietic Cell Transplantation (HCT) Population. *Front. Pharmacol.* 11, 888. doi:10.3389/fphar.2020.00888

Wallin, J. E., Friberg, L. E., Fasth, A., and Staatz, C. E. (2009). Population Pharmacokinetics of Tacrolimus in Pediatric Hematopoietic Stem Cell Transplant Recipients: New Initial Dosage Suggestions and a Model-Based Dosage Adjustment Tool. *Ther. Drug Monit.* 31 (4), 457–466. doi:10.1097/FTD.0b013e3181aab02b

Wang, D., Chen, X., Xu, H., and Li, Z. (2020). Population Pharmacokinetics and Dosing Regimen Optimization of Tacrolimus in Chinese Pediatric Hematopoietic Stem Cell Transplantation Patients. *Xenobiotica* 50 (2), 178–185. doi:10.1080/00498254.2019.1601791

Xue, L., Zhang, H., Ma, S., Rui, J. Z., and Miao, L. Y. (2011). Population Pharmacokinetics and Pharmacogenetics of Tacrolimus in Healthy Chinese Volunteers. *Pharmacology* 88 (5-6), 288–294. doi:10.1159/000331856

Yoshikawa, N., Takeshima, H., Takeshima, H., Sekine, M., Akizuki, K., Hidaka, T., et al. (2021). Relationship between CYP3A5 Polymorphism and Tacrolimus Blood Concentration Changes in Allogeneic Hematopoietic Stem Cell Transplant Recipients during Continuous Infusion. *Pharmaceuticals (Basel)* 14 (4), 353. doi:10.3390/ph14040353

Zhou, S., Zhang, R., Lv, C., Lu, J., Wei, Y., Li, C., et al. (2021). Initial Dosage Optimization of Tacrolimus in Pediatric Patients with Thalassemia Major Undergoing Hematopoietic Stem Cell Transplantation Based on Population Pharmacokinetics. *Ann. Pharmacother.* 55 (4), 440–451. doi:10.1177/1060028020959039

Zhu, J., Patel, T., Miller, J. A., Torrice, C. D., Aggarwal, M., Sketch, M. R., et al. (2020). Influence of Germline Genetics on Tacrolimus Pharmacokinetics and Pharmacodynamics in Allogeneic Hematopoietic Stem Cell Transplant Patients. *Int. J. Mol. Sci.* 21 (3), 858. doi:10.3390/ijms2103858

Conflict of Interest: RK is an employee and stock owner of InsightRX.

The remaining authors declare that the research was conducted in the absence of any commercial or financial relationships that could be construed as a potential conflict of interest.

Publisher's Note: All claims expressed in this article are solely those of the authors and do not necessarily represent those of their affiliated organizations, or those of the publisher, the editors and the reviewers. Any product that may be evaluated in this article, orclaim that may be made by its manufacturer, is not guaranteed or endorsed by the publisher.

frontiers in Pharmacology

STUDY PROTOCOL
published: 10 December 2021
doi: 10.3389/fphar.2021.750080

The Pharmacokinetics of Beta-Lactam Antibiotics Using Scavenged Samples in Pediatric Intensive Care Patients: The EXPAT Kids Study Protocol

Stef Schouwenburg[1], Enno D. Wildschut[2], M. de Hoog[2], Birgit C.P. Koch[1] and Alan Abdulla[1,2]*

[1]Department of Hospital Pharmacy, Erasmus MC, University Medical Center Rotterdam, Rotterdam, Netherlands, [2]Department of Pediatric Intensive Care, Erasmus MC – Sophia Children's Hospital, University Medical Center Rotterdam, Rotterdam, Netherlands

OPEN ACCESS

Edited by:
Erwin Dreesen, KU Leuven, Belgium

Reviewed by:
Sebastian G. Wicha, University of Hamburg, Germany
Ashwin Karanam, Pfizer, United States

***Correspondence:**
Stef Schouwenburg
s.schouwenburg@erasmusmc.nl

Specialty section:
This article was submitted to Obstetric and Pediatric Pharmacology, a section of the journal Frontiers in Pharmacology

Received: *30 July 2021*
Accepted: *08 November 2021*
Published: *10 December 2021*

Citation:
Schouwenburg S, Wildschut ED, de Hoog M, Koch BCP and Abdulla A (2021) The Pharmacokinetics of Beta-Lactam Antibiotics Using Scavenged Samples in Pediatric Intensive Care Patients: The EXPAT Kids Study Protocol. Front. Pharmacol. 12:750080. doi: 10.3389/fphar.2021.750080

Background: Emerging evidence supports the importance of optimized antibiotic exposure in pediatric intensive care unit (PICU) patients. Traditional antibiotic dosing is not designed for PICU patients, as the extreme pharmacokinetic (PK) behavior of drugs threatens the achievement of optimal antibiotic treatment outcomes. Scavenged sampling is a sampling strategy which may have positive implications for routine TDM and PK research, as well as monitoring other biomarkers. EXPAT Kids study was designed to analyze whether current empiric dosing regimens of frequently used beta-lactam antibiotics achieve defined therapeutic target concentrations in PICU patients.

Methods: A mono-centre, exploratory pharmacokinetic and pharmacodynamic study was designed to assess target attainment of beta-lactam antibiotics. One hundred forty patients will be included within 24 months after start of inclusion. At various time points serum concentration of the study antibiotic (cefotaxime, ceftazidime, ceftriaxone, cefuroxime, flucloxacillin, and meropenem) are determined. In parallel with these sampling moments, residual material is collected to validate the use of blood of scavenged heparinized astrup syringes for the quantification of antibiotic exposure. The primary outcome is the time that the free (unbound) concentration of the study antibiotic remains above one to four the minimal inhibitory concentration during a dosing interval (100%fT > MIC and 100%fT>4xMIC). Other included outcomes are disease severity, safety, length of stay, and inflammatory biomarkers.

Discussion: Potentially, scavenged sampling may enrich the EXPAT Kids dataset, and reduce additional blood sampling and workload for clinical personnel. The findings from the EXPAT Kids study will lead to new insights in the PK parameters of beta-lactams and consecutive effects on target attainment and clinical outcomes. Is there a need for more precision in dosing? *Netherlands Trial Register Number:* Trial NL9326.

Keywords: beta-lactam, antibiotics, criticial illness, children, pharmacokinetics, pharmacodynamics

INTRODUCTION

Infectious disease are among the most prevalent causes of mortality in the pediatric intensive care unit (PICU), with a mortality rate up to 50% depending on the site of infection (Dorofaeff et al., 2012). Early initiation of antibiotic therapy has been demonstrated to be the best intervention for severe infections in this population of critically ill patients (Weiss et al., 2015). Additionally, inappropriate dosing of antibiotics has been associated with increased morbidity and mortality in children, and longer PICU stay (Muszynski et al., 2011; Rosa and Goldani, 2014; Zhang et al., 2015).

Studies have demonstrated that current pediatric dosing strategies for beta-lactams fail to achieve pharmacodynamic endpoints, as approximately 95% of pediatric patients achieve subtherapeutic beta-lactam concentrations (Cies et al., 2018; Hartman et al., 2019a). If indeed exposure is suboptimal, titration of appropriate antibiotic dosing might result in increased treatment efficacy, less development of antibiotic resistance, and less drug-induced toxicity (Abdul-Aziz et al., 2015). To determine whether action is required to adjust existing prescribing practices for beta-lactam antibiotics in critically ill pediatric patients, assessment of the current situation at the PICU is warranted.

Standard of care antibiotic dosing regimens are not designed to treat critically ill children due to the complexity of their physiological state. PICU patients are characterised by altered pharmacokinetic parameters, changes in renal function, and are often infected by less susceptible micro-organisms. Observed extreme pharmacokinetic (PK) behavior of drugs poses a significant threat to achievement of optimal clinical outcomes (Roberts et al., 2010). A larger distribution volume and higher clearance in critically ill children might demand an increased dosage or prolonged infusion (Hartman et al., 2020).

Dosing strategies for beta-lactam antibiotics are based upon the minimum inhibitory concentration (MIC) of micro-organisms. Due to unreliability of techniques to determine the MIC and the fact that often no positive culture is available, the epidemiological cut-off value (ECOFF) for a given species and antibiotic are used (Mouton et al., 2018). The MIC_{ECOFF} describes the highest MIC for organisms devoid of phenotypically-detectable acquired resistance mechanisms and defines the upper end of wild-type distribution (EUCAST, 2018).

For data collection, both scheduled and scavenged sampling will be obtained. Scavenging involves the use of residual material of all biological fluids (e.g. blood, liquor, urine, or saliva) which are left over from standard clinical practice (Cohen-Wolkowiez et al., 2012). Importantly, scavenged sampling does not carry any extra burden or risks for the patient.

Timely initiation and target attainment of antimicrobial treatment in infectious disease such as sepsis is warranted, since acute phase pathophysiological changes alter drug PK (Thakkar et al., 2017; Weiss et al., 2020). In this study we want to analyse whether empirical antibiotic dosing regimens of frequently used beta-lactam antibiotics achieve defined pharmacodynamic target (PDT) concentrations in critically ill pediatric patients. Secondly, the association of target attainment with patient characteristics and clinical outcomes will be examined. Lastly, during this study we aim to validate the use of blood of scavenged heparinized astrup syringes for the quantification of antibiotic exposure.

METHODS

The EXPAT Kids protocol is a prospective, mono-centre, observational study which aims to identify whether critical ill patients treated with beta-lactam antibiotics reach target attainment. The study will include 145 patients over a period of 24 months, recruited at the Sophia Children's Hospital, Erasmus Medical Center, Rotterdam, the Netherlands. See **Table 1** for an overview of the EXPAT Kids study procedures.

Study antibiotics include cefotaxime, ceftazidime, ceftriaxone, cefuroxime, flucloxacillin, and meropenem.

Selection of Subjects

All patients admitted to the PICU and given standard of care intravenous (IV) therapy of the study antibiotics will be screened for inclusion. Eligible patients will be identified on a daily basis. Deferred consent is obtained by research staff at a maximum of 24 h after start of study procedures. Since most participants will be minors, their legal representatives will be inquired. If possible, informed consent from the patient is obtained at day five in case of deferred consent by a legal representative.

In- and Exclusion Criteria

Patients will need to receive IV antibiotic therapy of the study antibiotics which should be aimed for at least 2 days at the time of inclusion. All participants are required to have suitable intra-arterial access to facilitate sample collection, in place through standard of care procedures. Patients will only be included if sampling within 36 h after starts of antibiotic therapy is possible. Patients will be excluded in case of prematurity (<37 weeks old), history of anaphylaxis for study antibiotic, study antibiotic cessation before start of sample collection, and prophylactic use of the study antibiotic.

Sample Size Calculation

Sample size calculation for the primary objective is based on $fT > MIC_{ECOFF}$ PDT attainment prevalence of 60% (95% CI 52–68%), as has been found in the previous EXPAT study on the adult ICU (Abdulla et al., 2020a). For a sample size of 145 patients, an estimated 87 participants are expected to achieve PDT. This amount will be sufficient for the analysis of the primary objective ($fT > MIC_{ECOFF}$ and $fT > 4x\ MIC_{ECOFF}$), for which all antibiotics will be pooled.

Pharmacokinetic Sampling

All collected plasma concentrations of the study antibiotics from which the exact time of blood sampling after administration is known will be used to describe PK profiles. For each patient a trough (t = 0, shortly before dosage) and peak (t = 10–30 min after dosage) blood sample will be drawn during a single IV antibiotic dosage. Additionally, during routine morning (approx. 8:00 h) lab

TABLE 1 | Study procedures timeline. Time path of enrolment, sampling, and assessments in the study.

	Enrolment	Allocation	Post-allocation	Follow-up
Timepoint	t = 0	t = 0–36 h	t = day 1 till day 5	t = day 7
Start target antibiotic	X	—	—	—
Informed consent	—	X	—	—
Eligibility screen	—	X	—	—
Allocation	—	X	—	—
Collection				
Blood sampling	—	A: trough sample B: peak sample	C: sample during routine morning lab	—
Assessments				
Demographics	X	—		—
Lab data	X	—	X	—
Clinical data, admission data	X	—	X	—
Survival	—	—	—	X

TABLE 2 | List of variables captured in the EXPAT Kids study.

Demographic data
Age (in children <1 year also gestational age, postconceptional age)
Gender
Height
Weight
PICU ward
Clinical data
PICU stay (days) OR date of hospital/PICU admission and discharge
Admission diagnosis
Comorbidities
Sickness severity scores (PELOD)
Vasopressors
Body temperature variation
Blood pressure
Heart rate variability – stress/inflammation predictor
Presence/absence of surgery within previous 24 h
Outcome following discharge/transfer from PICU (alive or deceased)
Organ function and clinical chemistry data
Renal function – serum creatinine concentration
Liver function – AST, ALT, conjugated bilirubin
Fluid balance for total length of stay and previous 24 h
Albumin
Urea
Antibiotic dosing data
Antibiotic (also concomitant antibiotics)
Start and end date of the antibiotic treatment
Dose and frequency antibiotic therapy
Time of dosing and sampling
Days of antibiotic therapy
Infection data
White blood cell count
Interleukin-6
Procalcitonin
C-reactive protein
Known or presumed pathogen (positive blood culture and organisms isolated)

sampling an extra blood sample will be drawn for five consecutive days after obtaining trough and peak samples.

Alongside the above described process, scavenged samples will be obtained through collection of residual material from clinical chemistry and blood gas material from heparinized astrup syringes. These samples will vary in time after dosage.

Total and unbound drug concentrations will be measured in serum by means of a validated LC-MS/MS method in the Erasmus University Medical Center (Erasmus MC) (Abdulla et al., 2017). Scavenged samples from blood gas material will be compared with concurrent scheduled samples using Bland-Altman Analysis.

Data Collection

All data collected through study procedures will be stored into an eCRF. Laboratory data will include: albumin, conjugated bilirubin, creatinine, C-reactive protein, interleukin-6, procalcitonin, serum liver enzymes, urea, and white blood cell count. Clinical data involve the Pediatric Logistic Organ Dysfunction (PELOD) score, fluid balance, and presence/absence of surgery in the previous 24 h. Additionally, we will collect admission and discharge dates, admission diagnosis, and outcome following discharge/transfer from PICU. The most prevalent and most severe side effects will also be collected. An overview of variables measured in the EXPAT Kids study is presented in **Table 2**.

DATA ANALYSIS

Baseline Characteristics

Demographic and clinical characteristics will be described using standard statistical analysis methods. Descriptive data will be presented as percentages, means ± SD for normally distributed variables, and medians ± interquartile ranges for non-normally distributed variables. To examine differences between groups in categorical variables, Fisher's exact test will be used. For normally distributed continuous variables, the two-sample Student's t-test will be used. Otherwise the two-sample Mann-Whitney test will be used. Statistical analyses will be conform previously performed research by our research group (Abdulla et al., 2020a).

Primary Outcome

The main objective is to determine the prevalence of target attainment for six beta-lactam antibiotics in the early phase

after start of therapy in PICU patients. Target attainment for beta-lactam antibiotics is set at 100% of time (T) of the dosing interval in which the unbound (free, f) serum antibiotic concentration remains above the epidemiological cut-off (fT > MIC_{ECOFF} and fT > 4x MIC_{ECOFF}). Both fT > MIC_{ECOFF} and fT > 4x MIC_{ECOFF} have been described in literature before as key attainment parameters (Roberts et al., 2014).

Secondary Outcomes

Multiple secondary outcomes were identified, namely: 1) length of PICU stay; 2) concomitant use of other antibiotics; 3) inflammatory biomarkers; 4) serum albumin; and 5) estimated glomerular filtration rate.

We will estimate multivariate binary logistic regression analyses and present the odds ratios (ORs) and 95% confidence intervals (95% CI) for each individual antibiotic. We will include PELOD score at inclusion in the multivariate analysis to control for all our regressions for clinically and relevant baseline characteristics. Multivariate negative binomial regression models examining the association of PDT attainment characteristics with PICU length of stay will be included. For these regressions, we will present the ORs and 95% CI. Statistical significance will be accepted at $p \leq 0.05$.

In addition to our secondary outcomes, we will develop population PK (popPK) models for the study antibiotics using non-linear mixed effect modelling (NONMEM). Potential bias or over- and underestimation of antibiotic exposure introduced by scavenged sampling will be taken into account and investigated.

Data Monitoring

Because of the nature of the trial with a low risk of intermediate complications, an independent monitor will visit once during the study period. A percentage of cases will be randomly selected for verification by the independent monitor. Informed consent, source data, and reported serious adverse events (SAEs) are reviewed for errors. The data will be pseudonymised when stored in the database and then used for analysis.

Ethics and Dissemination

This trial was approved by the Medical Ethics Committee of the Erasmus Medical Centre in Rotterdam, the Netherlands (registration number MEC-2021-0173). For every significant change to the protocol, an amendment will have to be approved by the local medical ethics committee. Written deferred consent will be obtained from the parents or legal representatives and from the patients older than 12 years, within 24 h after start of study procedures.

Findings will be submitted to peer-reviewed journals for publication, and to local and international conferences. As we have multiple secondary outcomes, we expect to submit multiple publications to peer-reviewed journals. Findings will be communicated to the public through media coverage and personal website(s).

DISCUSSION

Previous studies have indicated that beta-lactam antibiotics might not achieve the PDT in critically ill children. The EXPAT Kids study aims to identify the percentage of patients which achieve target attainment and potential risk factors influencing this outcome. Our study has already been conducted in the adult population, in which male patients with higher creatinine clearance, higher serum albumin, higher white blood cell count, higher length, and lower urea and those who received concomitant antibiotics were more likely not to achieve the PDT (Abdulla et al., 2020a).

Several studies have used scavenged samples and concluded that the strategy was suitable for the establishment of popPK models (Leroux et al., 2016; Dong et al., 2018; Hahn et al., 2019; Tang et al., 2019; Shi et al., 2020; Wang et al., 2020; Wu et al., 2020; Zhao et al., 2020). The strategy is feasible when considering the generalizability in context of sampling density, quality, and stability (Leroux et al., 2015). This study will use scavenged sampling to validate the use of residual material from heparinized astrup syringes for antibiotic quantification. If validated, residual material, even in small volumes, may enrich data collection and reduce workload for medical staff.

Based on study results, a randomized controlled trial in which therapeutic drug monitoring with model-based guidelines might be the next step to assure improved clinical outcomes due to beta-lactam pharmacodynamics targets are attained. A similar study, which is finishing the inclusion phase, is currently conducted at the Erasmus Medical Center, namely the DOLPHIN Study (Abdulla et al., 2020b).

More information about the PK parameters of beta-lactam antibiotics in the critical ill pediatric population is warranted. The EXPAT Kids study's findings may lead to new insights to improve clinical outcomes and dosing regimens of beta-lactams.

AUTHOR CONTRIBUTIONS

BK and AA took first responsibility for initiating the trial and admitting the funding application. SS, AA, BK, MH, and EW contributed to the conception of the study protocol and study design. SS and AA wrote the first draft of the manuscript. All authors contributed to subsequent drafts and gave final approval of the version to be published.

FUNDING

This project has received funding from the Erasmus University Medical Center MRace Grant. The funders will have no role in the collection, analysis, and interpretation of data or in writing manuscripts or the decision to publish.

REFERENCES

Abdul-Aziz, M. H., Lipman, J., Mouton, J. W., Hope, W. W., and Roberts, J. A. (2015). Applying Pharmacokinetic/pharmacodynamic Principles in Critically Ill Patients: Optimizing Efficacy and Reducing Resistance Development. *Semin. Respir. Crit. Care Med.* 36 (1), 136–153. doi:10.1055/s-0034-1398490

Abdulla, A., Bahmany, S., Wijma, R. A., van der Nagel, B. C. H., and Koch, B. C. P. (2017). Simultaneous Determination of Nine β-lactam Antibiotics in Human Plasma by an Ultrafast Hydrophilic-Interaction Chromatography-Tandem Mass Spectrometry. *J. Chromatogr. B Analyt Technol. Biomed. Life Sci.* 1060, 138–143. doi:10.1016/j.jchromb.2017.06.014

Abdulla, A., Dijkstra, A., Hunfeld, N. G. M., Endeman, H., Bahmany, S., Ewoldt, T. M. J., et al. (2020). Failure of Target Attainment of Beta-Lactam Antibiotics in Critically Ill Patients and Associated Risk Factors: a Two-center Prospective Study (EXPAT). *Crit. Care* 24 (1), 558. doi:10.1186/s13054-020-03272-z

Abdulla, A., Ewoldt, T. M. J., Hunfeld, N. G. M., Muller, A. E., Rietdijk, W. J. R., Polinder, S., et al. (2020). The Effect of Therapeutic Drug Monitoring of Beta-Lactam and Fluoroquinolones on Clinical Outcome in Critically Ill Patients: the DOLPHIN Trial Protocol of a Multi-centre Randomised Controlled Trial. *BMC Infect. Dis.* 20 (1), 57. doi:10.1186/s12879-020-4781-x

Cies, J. J., Moore, W. S., Enache, A., and Chopra, A.II (2018). β-Lactam Therapeutic Drug Management in the PICU. *Crit. Care Med.* 46 (2), 272–279. doi:10.1097/CCM.0000000000002817

Cohen-Wolkowiez, M., Ouellet, D., Smith, P. B., James, L. P., Ross, A., Sullivan, J. E., et al. (2012). Population Pharmacokinetics of Metronidazole Evaluated Using Scavenged Samples from Preterm Infants. *Antimicrob. Agents Chemother.* 56 (4), 1828–1837. doi:10.1128/aac.06071-11

Dong, Q., Leroux, S., Shi, H. Y., Xu, H. Y., Kou, C., Khan, M. W., et al. (2018). Pilot Study of Model-Based Dosage Individualization of Ganciclovir in Neonates and Young Infants with Congenital Cytomegalovirus Infection. *Antimicrob. Agents Chemother.* 62 (5), e00075. doi:10.1128/aac.00075-18

Dorofaeff, T., Mohseni-Bod, H., and Cox, P. N. (2012). Infections in the PICU. *Textbook Clin. Pediatr.*, 2537–2563. doi:10.1007/978-3-642-02202-9_268

EUCAST (2018). EUCAST General Consultation on "Considerations in the Numerical Estimation of Epidemiological Cutoff (ECOFF) Values". Updated 22-03-2018. Available at: https://eucast.org/fileadmin/src/media/PDFs/EUCAST_files/Consultation/2018/ECOFF_procedure_2018_General_Consultation_20180531.pdf (Accessed 07 07, 2021).

Hahn, D., Emoto, C., Euteneuer, J. C., Mizuno, T., Vinks, A. A., and Fukuda, T. (2019). Influence of OCT1 Ontogeny and Genetic Variation on Morphine Disposition in Critically Ill Neonates: Lessons from PBPK Modeling and Clinical Study. *Clin. Pharmacol. Ther.* 105 (3), 761–768. doi:10.1002/cpt.1249

Hartman, S. J. F., Boeddha, N. P., Ekinci, E., Koch, B. C. P., Donders, R., Hazelzet, J. A., et al. (2019). Target Attainment of Cefotaxime in Critically Ill Children with Meningococcal Septic Shock as a Model for Cefotaxime Dosing in Severe Pediatric Sepsis. *Eur. J. Clin. Microbiol. Infect. Dis.* 38 (7), 1255–1260. doi:10.1007/s10096-019-03535-w

Hartman, S. J. F., Brüggemann, M., Orriëns, L., Dia, N., Schreuder, M. F., and de Wildt, S. N. (2020). Pharmacokinetics and Target Attainment of Antibiotics in Critically Ill Children: A Systematic Review of Current Literature. *Clin. Pharmacokinet.* 59 (2), 173–205. doi:10.1007/s40262-019-00813-w

Leroux, S., Roué, J. M., Gouyon, J. B., Biran, V., Zheng, H., Zhao, W., et al. (2016). A Population and Developmental Pharmacokinetic Analysis to Evaluate and Optimize Cefotaxime Dosing Regimen in Neonates and Young Infants. *Antimicrob. Agents Chemother.* 60 (11), 6626–6634. doi:10.1128/aac.01045-16

Leroux, S., Turner, M. A., Guellec, C. B., Hill, H., van den Anker, J. N., Kearns, G. L., et al. (2015). Pharmacokinetic Studies in Neonates: The Utility of an Opportunistic Sampling Design. *Clin. Pharmacokinet.* 54 (12), 1273–1285. doi:10.1007/s40262-015-0291-1

Mouton, J. W., Muller, A. E., Canton, R., Giske, C. G., Kahlmeter, G., and Turnidge, J. (2018). MIC-based Dose Adjustment: Facts and Fables. *J. Antimicrob. Chemother.* 73 (3), 564–568. doi:10.1093/jac/dkx427

Muszynski, J. A., Knatz, N. L., Sargel, C. L., Fernandez, S. A., Marquardt, D. J., and Hall, M. W. (2011). Timing of Correct Parenteral Antibiotic Initiation and Outcomes from Severe Bacterial Community-Acquired Pneumonia in Children. *Pediatr. Infect. Dis. J.* 30 (4), 295–301. doi:10.1097/INF.0b013e3181ff64ec

Roberts, J. A., Paul, S. K., Akova, M., Bassetti, M., De Waele, J. J., Dimopoulos, G., et al. (2014). DALI: Defining Antibiotic Levels in Intensive Care Unit Patients: Are Current β-lactam Antibiotic Doses Sufficient for Critically Ill Patients? *Clin. Infect. Dis.* 58 (8), 1072–1083. doi:10.1093/cid/ciu027

Roberts, J. A., Ulldemolins, M., Roberts, M. S., McWhinney, B., Ungerer, J., Paterson, D. L., et al. (2010). Therapeutic Drug Monitoring of Beta-Lactams in Critically Ill Patients: Proof of Concept. *Int. J. Antimicrob. Agents* 36 (4), 332–339. doi:10.1016/j.ijantimicag.2010.06.008

Rosa, R. G., and Goldani, L. Z. (2014). Cohort Study of the Impact of Time to Antibiotic Administration on Mortality in Patients with Febrile Neutropenia. *Antimicrob. Agents Chemother.* 58 (7), 3799–3803. doi:10.1128/aac.02561-14

Shi, H. Y., Wang, K., Wang, R. H., Wu, Y. E., Tang, B. H., Li, X., et al. (2020). Developmental Population Pharmacokinetics-Pharmacodynamics and Dosing Optimization of Cefoperazone in Children. *J. Antimicrob. Chemother.* 75 (7), 1917–1924. doi:10.1093/jac/dkaa071

Tang, B.-H., Wu, Y.-E., Kou, C., Qi, Y.-J., Qi, H., Xu, H.-Y., et al. (2019). Population Pharmacokinetics and Dosing Optimization of Amoxicillin in Neonates and Young Infants. *Antimicrob. Agents Chemother.* 63 (2), e02336. doi:10.1128/aac.02336-18

Thakkar, N., Salerno, S., Hornik, C. P., and Gonzalez, D. (2017). Clinical Pharmacology Studies in Critically Ill Children. *Pharm. Res.* 34 (1), 7–24. doi:10.1007/s11095-016-2033-y

Wang, Y. K., Wu, Y. E., Li, X., Tian, L. Y., Khan, M. W., Tang, B. H., et al. (2020). Optimal Dosing of Ceftriaxone in Infants Based on a Developmental Population Pharmacokinetic-Pharmacodynamic Analysis. *Antimicrob. Agents Chemother.* 64 (11), e01412. doi:10.1128/aac.01412-20

Weiss, S. L., Fitzgerald, J. C., Pappachan, J., Wheeler, D., Jaramillo-Bustamante, J. C., Salloo, A., et al. (2015). Global Epidemiology of Pediatric Severe Sepsis: the Sepsis Prevalence, Outcomes, and Therapies Study. *Am. J. Respir. Crit. Care Med.* 191 (10), 1147–1157. doi:10.1164/rccm.201412-2323OC

Weiss, S. L., Peters, M. J., Alhazzani, W., Agus, M. S. D., Flori, H. R., Inwald, D. P., et al. (2020). Executive Summary: Surviving Sepsis Campaign International Guidelines for the Management of Septic Shock and Sepsis-Associated Organ Dysfunction in Children. *Pediatr. Crit. Care Med.* 21 (2), 186–195. doi:10.1097/PCC.0000000000002197

Wu, Y. E., Wang, Y. K., Tang, B. H., Dong, L., Li, X., Zhang, W., et al. (2020). Population Pharmacokinetics and Dosing Optimization of Amoxicillin in Chinese Infants, Article in Press. *J. Clin. Pharmacol.* 61, 538–546. doi:10.1002/jcph.1752

Zhang, D., Micek, S. T., and Kollef, M. H. (2015). Time to Appropriate Antibiotic Therapy Is an Independent Determinant of Postinfection ICU and Hospital Lengths of Stay in Patients with Sepsis. *Crit. Care Med.* 43 (10), 2133–2140. doi:10.1097/ccm.0000000000001140

Zhao, Y., Yao, B. F., Kou, C., Xu, H. Y., Tang, B. H., Wu, Y. E., et al. (2020). Developmental Population Pharmacokinetics and Dosing Optimization of Cefepime in Neonates and Young Infants. *Front. Pharmacol.* 11, 14. doi:10.3389/fphar.2020.00014

Conflict of Interest: The authors declare that the research was conducted in the absence of any commercial or financial relationships that could be construed as a potential conflict of interest.

frontiers in Pediatrics

ORIGINAL RESEARCH
published: 05 January 2022
doi: 10.3389/fped.2021.768438

Ensuring Sufficient Trough Plasma Concentrations for Broad-Spectrum Beta-Lactam Antibiotics in Children With Malignancies: Beware of Augmented Renal Clearance!

Pascal André[1], Léonore Diezi[1], Kim Dao[1], Pierre Alex Crisinel[2], Laura E. Rothuizen[1], Haithem Chtioui[1], Laurent Arthur Decosterd[1], Manuel Diezi[3], Sandra Asner[2] and Thierry Buclin[1]*

[1] Service of Clinical Pharmacology, University Hospital Center, University of Lausanne, Lausanne, Switzerland, [2] Pediatric Infectious Diseases and Vaccinology Unit, Service of Pediatrics, University Hospital Center, University of Lausanne, Lausanne, Switzerland, [3] Pediatric Hemato-Oncology Unit, Service of Pediatrics, University Hospital Center, University of Lausanne, Lausanne, Switzerland

OPEN ACCESS

Edited by:
Raffaele Simeoli, Bambino Gesù Children's Hospital (IRCCS), Italy

Reviewed by:
Georg Hempel, University of Münster, Germany
Raman Venkataramanan, University of Pittsburgh, United States
Abdul Sami Shaikh, Shah Abdul Latif University, Pakistan

***Correspondence:**
Pascal André
Pascal.Andre@chuv.ch

Specialty section:
This article was submitted to Obstetric and Pediatric Pharmacology, a section of the journal Frontiers in Pediatrics

Received: *31 August 2021*
Accepted: *13 December 2021*
Published: *05 January 2022*

Citation:
André P, Diezi L, Dao K, Crisinel PA, Rothuizen LE, Chtioui H, Decosterd LA, Diezi M, Asner S and Buclin T (2022) Ensuring Sufficient Trough Plasma Concentrations for Broad-Spectrum Beta-Lactam Antibiotics in Children With Malignancies: Beware of Augmented Renal Clearance! Front. Pediatr. 9:768438. doi: 10.3389/fped.2021.768438

Introduction: Broad-spectrum beta-lactams are commonly prescribed for empirical or selective treatment of bacterial infections in children with malignancies. In the immunocompromised, appropriate concentration exposure is crucial to ensure antimicrobial efficacy. Augmented renal clearance (ARC) is increasingly recognized in this population, and raises concern for unmet concentration targets. We conducted a retrospective evaluation of meropenem and piperacillin exposure in our hospital's pediatric hematology-oncology patients.

Materials and Methods: We compared trough levels of meropenem and piperacillin in a cohort of unselected pediatric hematology-oncology patients stratified based on their estimated renal function as decreased, normal or with ARC, and on their neutrophil count.

Results: Thirty-two children provided a total of 51 meropenem and 76 piperacillin samples. On standard intermittent intravenous regimen, 67% of all trough plasma concentrations were below targeted concentrations. In neutropenic children with bacterial infection, all meropenem and 60% of piperacillin levels were below target. Nearly two-thirds of total samples came from children with ARC. In these patients, antimicrobial exposure was insufficient in 85% of cases (compared to 36% in the decreased or normal renal function groups), despite a dosage sometimes exceeding the maximum recommended daily dose. Under continuous infusion of piperacillin, only 8% of plasma levels were insufficient.

Discussion: Intermittent administration of meropenem and piperacillin often fails to ensure sufficient concentration exposure in children treated for malignancies, even at maximal recommended daily dosage. This can in part be attributed to ARC. We recommend thorough assessment of renal function, resolute dosage adjustment, continuous infusion whenever possible and systematic therapeutic drug monitoring.

Keywords: meropenem, piperacillin, beta-lactams, child, neoplasms, cancer, kidney function tests, augmented renal clearance

INTRODUCTION

In high-income countries, the survival rate of children affected by malignancies is constantly improving, currently reaching between 80% to nearly 90% 5 years overall survival, primarily thanks to advances in anticancer treatment efficacy and supportive care (1, 2). Yet malignancies remain a leading cause of death during childhood and adolescence in these countries (3, 4). A significant part of this mortality results from their susceptibility to develop bacterial, fungal, and viral systemic infections as a result of secondary neutropenia and immunodeficiency. Mortality due to infections depends on the type of cancer, but it is considered highest for hematological malignancies, mainly acute lymphoblastic leukemia (ALL) and acute myeloid leukemia (AML), which carry a greater burden of disease or treatment-related myelosuppression. In contemporary ALL trials, the frequency of treatment-related mortality is reported to be between 2 and 4%, primarily due to bacterial infections (5–8). In lymphoma, mortality attributed to infection is also significant (9). Thus, bacterial infections are a definite threat for children with malignancies, with leukemia and lymphoma being the most frequent types of cancer occurring between ages 0 to 14 years and 15 to 19 years, respectively (10). Bacterial infections also complicate solid tumors treatments, although to a lesser extent (11, 12).

In neutropenic episodes that follow ALL treatment, infection-related lethality most often occurs within 48 h from first clinical signs of infection, emphasizing the need for prompt diagnosis and effective antibiotic treatment (7). Therefore, the antibiotic should typically be initiated within an hour from any developing sign of sepsis in an immunocompromised patient. The choice is empirical as treatment is initiated before identification of the infectious agent involved, and frequently contains a broad-spectrum beta-lactam. Considering the time-dependent action of beta-lactams, it is widely recommended to maintain free trough blood concentrations above the minimal inhibitory concentration (MIC) of common germs in these patients (13, 14). Indeed the unbound fraction of beta-lactams, which varies between molecules, is sole responsible for the antibacterial effect (15). Because intensive therapy is required, special attention is also to be paid to potential toxicity of beta-lactams, mainly presenting as adverse neurological effects. These antibiotics are predominantly eliminated by renal excretion, through glomerular filtration and active tubular secretion, and recommendations to reduce the unit dose or prolong the dose interval depending on the stages of renal failure is generally acknowledged (16). Accordingly, maximum plasma levels recommended at trough have been formally defined for some beta-lactams (17).

Recently, the concept of augmented renal clearance (ARC), also termed glomerular hyperfiltration, has emerged in clinical medicine. It is defined as a global enhancement of renal function, typically observed in the critically ill, which accelerates clearance of drugs excreted by the kidney (18). It is thought to result from recruiting renal functional reserve in response to inflammation, systemic vasodilation with hyperdynamic circulation, high cardiac output, increased splanchnic blood flow and a global raise in metabolic activity (19). It is characterized by an increase in creatinine clearance above a threshold not clearly agreed upon to date, which varies between 130 mL/min/1.73 m^2 (20) and 170 mL/min/1.73 m^2 (21) according to different authors for adult patients. Overall, ARC is a multiprocess phenomenon comprising enhanced glomerular filtration but presumed to modulate tubular transport as well, notably tubular anionic secretion and reabsorption. This wider term is preferred to glomerular hyperfiltration, which refers only to the enhanced filtration component (22, 23). While initially described in adult patients experiencing acute inflammatory conditions (21), ARC seems no less observed in the pediatric population, with episodes of ARC reported in 30 to 40% of children with malignancies. These episodes are most prevalent before starting and just after the first course of chemotherapy (23), and become less frequent with increasing courses of chemotherapy. Mechanisms hypothesized to contribute to ARC in these observations relate to the hypermetabolic state resulting from the multiplication of malignant cells prior to treatment, and the tumor cells lysis after chemotherapy (23). ARC has been shown to reduce drug exposure, in particular to antibiotics eliminated by glomerular filtration with or without tubular secretion.

The broad-spectrum beta-lactams most frequently used to for the empirical treatment of febrile neutropenia are meropenem (MER) and piperacillin (PIP), which belong to the carbapenem and the ureidopenicillin families, respectively. PIP is combined with the beta-lactamase inhibitor tazobactam. In order to adapt their dosage to a specific clinical state, precision medicine resorts to therapeutic drug monitoring (TDM). This requires to draw and measure plasma concentrations of the drug, and eventually adapt the dosage according to the result, in order to prevent treatment failure due to underexposure, or toxicity. Insufficient exposure to MER and PIP has been observed in adults (24, 25), and to PIP in children (26). Underexposure to antibiotics may lead to therapeutic failure and the emergence of resistant germ strains (21, 27).

We have been developing TDM of large-spectrum antibiotics in our hospital for almost two decades (28). While these efforts initially aimed at a better dosage adjustment in renal failure and renal replacement therapy (29), our attention was drawn to the issue of antibiotic underexposure, particularly in children with cancer, as pediatric oncologists gradually implemented TDM of broad-spectrum antibiotics in situations of febrile neutropenia. In this population, we aim at maintaining plasma concentrations above targets at trough.

This retrospective study evaluates, based on trough levels 1) the frequency of underexposure, 2) its association with ARC, and 3) its relation to prescribed dosages of MER or PIP in children admitted for hematologic or solid malignancies.

Abbreviations: ALL, Acute lymphoblastic leukemia; AML, Acute myeloblastic leukemia; ARC, Augmented renal clearance; ECOFF90, Epidemiological cut-off values covering 90% of germ strains; MER, Meropenem; MIC, Minimal inhibitory concentration; PIP, Piperacillin; TDM, Therapeutic drug monitoring.

MATERIALS AND METHODS

Population

This retrospective study included an unselected cohort of children aged 6 months to 18 years, admitted to the University Hospital Center of Lausanne, Switzerland for hematological or solid malignancies and in whom at least one blood level of MER or PIP was measured. The study period ran from January 2012 to end of June 2018.

Data

Clinical data including age, gender, body weight, height, serum creatinine levels, type of malignancy, clinical indication for antimicrobial therapy, neutrophil count, together with MER and PIP dosage and sampling details were required to perform TDM interpretations and suggest dose adaptations in our routine. Our patients' data were fully anonymized before being transferred to the investigator in charge of their analysis for our research question. As patients could receive several treatment cycles, a new cycle was defined as a beta-lactam prescription initiated earliest 2 weeks after any previous beta-lactam administration. Reference MIC values for common bacteria involved in neutropenia-related infections were deduced from 90% epidemiological cut-off value (ECOFF90) from the EUCAST website (30).

Assessment of Renal Function, Immune Status, and Infection Status

We assessed renal functions using the original Schwartz formula, which estimates creatinine clearance from serum creatinine levels in children (31). We defined ARC as a creatinine clearance value exceeding 160 mL/min/1.73 m^2 (23, 32), and renal insufficiency as a clearance below 80 mL/min/1.73 m^2 (33), and we assumed normal renal function between those limits. These limits are the most conservative ones among various thresholds proposed in the literature to isolate children with a well-established renal insufficiency (low limit) or a well-established ARC (high limit).

Children were classified as neutropenic if their neutrophil count was below 0.5 G/L. A bacterial infection was retained based on clinical diagnosis as listed in the medical chart, with or without an identified bacterial strain, and after having ruled out contamination.

We distinguished plasma samples taken from neutropenic febrile children treated empirically from those taken from neutropenic children with a bacterial infection, and from those sampled from immunocompetent children with bacterial infection.

Therapeutic Drug Monitoring

All MER and PIP plasma concentrations were measured using a validated liquid chromatography assay with mass spectrometry detection (28). Separation was done using a mix of 2 solvents, ammonium formate with formic acid, and acetonitrile. This method is sensitive (limits of quantification 0.05–100 mg/L and 0.08–160 mg/L), accurate (intra/inter-assay bias 3.2/8.6 and 2.8/5.8%) and precise (intra/inter- assay CVs 6.4/3.4 and 11.3/1.9%) for MER and PIP, respectively.

TDM was not practiced systematically according to predefined schedules, but was rather done at the physician's discretion. In intermittent infusions, only blood samples drawn prior to the next dose (troughs) were included in this study, allowing however for an imprecision of ±1 h in sampling time.

In standard intermittent short infusions, the targeted concentration range at trough is between 2 and 8 mg/L for MER, and between 8 and 30 mg/L for PIP. When PIP is given as a continuous infusion, targeted levels are between 30 and 60 mg/L. While the lower limits are the efficacy thresholds given by protein-corrected MIC values of common bacteria, the upper limits are empirical and poorly defined (no established concentration-toxicity relationships). When a bacterial strain was identified in a patient, the lower targeted concentration was defined as its MIC value if available, otherwise as its bacteria-specific ECOFF90 level. These values were corrected for protein binding, although relatively low for these 2 beta-lactams (2% for MER and 15% for PIP), using the formula:

Trough plasma concentration target = (ECOFF90 or MIC) × [100/(100—percent protein binding of the beta-lactam)].

Statistical Analyses

We evaluated the significance of comparisons using two-tailed Student's *t*-tests performed on log-transformed MER and PIP concentration values, and on native biological values otherwise. Associations between study variables were assessed by calculating log-linear or linear correlations, respectively. Imbalance between patient subgroups was evaluated with exact Fisher's test.

RESULTS

Patients' and Treatment Characteristics

Altogether, 32 children provided 51 trough samples for MER and 63 for PIP, administered as intermittent short infusions (0.5 h) three, respectively four times a day during, respectively, 25 and 23 treatment cycles. Two MER and 4 PIP plasma levels were excluded because of sampling at distance from trough, and 1 PIP level as obviously aberrant. All other levels were included, tolerating a slight time deviation for 6 MER (12%) plasma levels (drawn maximum 1 h before through time), and for 15 (24%) and 12 (19%) PIP plasma levels drawn, respectively, slightly before and after trough time (maximum 1 h). In addition, continuous PIP infusions were given in three children previously on intermittent PIP administrations, which provided 13 plasma levels over six treatment cycles. Five children received both MER and PIP in different treatment cycles. The childrens' and plasma levels' characteristics are summarized in **Table 1**.

Febrile neutropenia status was highly represented, accounting for 23 (45%) of MER and 36 (57%) of PIP plasma levels measured under intermittent infusion and 6 (46%) of PIP plasma levels measured under continuous infusion. Immunocompromised children with bacterial infection were in minority, accounting for 7 (14%) of MER and 10 (16%) of PIP samples under intermittent infusion, but they were in majority for PIP samples taken under continuous infusion 7 (54%).

The daily doses given as intermittent infusions were heterogeneous, but mostly consistent with intensive dosage

TABLE 1 | Children and plasma levels characteristics.

Meropenem					**Piperacillin**			
Population								
19 children: 11 females/8 males					18 children: 5 females/13 males			
Cancer								
Hematological: 6 ALL 3 AML 1 Burkitt's lymphoma 1 Diffuse large B-cell lymphoma 1 Mature B-cell lymphoma					Hematological: 6 ALL 4 AML 2 Burkitt's lymphoma 1 Mature B-cell lymphoma			
Solid: 2 Neuroblastoma 1 Adrenocortical carcinoma 1 Medulloblastoma 1 Thoracic neuroblastoma 1 Osteosarcoma 1 Ewing sarcoma					Solid: 2 Neuroblastoma 1 Rhabdomyosarcoma 1 Malignant rhabdoid tumor 1 Atypical teratoid rhabdoid tumor			
Trough plasma levels under intermittent infusions								
51 plasma levels from 25 treatment cycles under mean dosage of 104 ± 42 mg/kg/d (min 40/max 200)					**63 plasma levels from 23 treatment cycles under mean dosage of 336 ± 127 mg/kg/d (min 94/max 625)**			
Immune status	**Infection status**	**Estimated kidney function status**	**Total**		**Immune status**	**Infection status**	**Estimated kidney function status**	**Total**
Neutropenic	Bacterial infection	ARC	7		Neutropenic	Bacterial infection	ARC	10
		Normal	0				Normal	0
		Decreased	0				Decreased	1
	Febrile	ARC	8			Febrile	ARC	25
		Normal	11				Normal	10
		Decreased	4				Decreased	1
Immuno-competent	Bacterial infection	ARC	5		Immuno-competent	Bacterial infection	ARC	7
		Normal	3				Normal	1
		Decreased	0				Decreased	1
	Febrile	ARC	6			Febrile	ARC	3
		Normal	3				Normal	2
		Decreased	4				Decreased	2
Plasma levels under continuous infusions								
		13 plasma levels from 3 treatment cycles under mean dosage 416 ± 104 mg/kg/d (min 132/max 541)						
0 plasma levels	Neutropenic	Bacterial infection	ARC	3				
			Normal	1				
		Febrile	ARC	5				
	Immuno-competent	Bacterial infection	ARC	2				
			Normal	1				
		Febrile	ARC	1				

recommendations, i.e., 120 mg/kg/d for MER and 400 mg/kg/d for PIP (34, 35). For MER, they initially averaged 95 ± 35 mg/kg/d (mean ± SD), and increased to an average of 113 ± 49 mg/kg/d after TDM. Similarly, initial average PIP dosages were 310 ± 97 mg/kg/d with subsequent daily doses averaging 351 ± 140 mg/kg/d. Eleven MER and 17 PIP plasma levels from, respectively, 4 and 5 children were drawn under daily dosages that exceeded intensive dosage, up to 200 and 625 mg/kg/d, respectively. Continuous infusions of PIP used daily dosages of 416 ± 104 mg/kg/d.

Interestingly, initial MER prescriptions were poorly associated with the childrens' renal function (correlation coefficient R^2 of 0.09, $p = 0.15$), with only a slight difference in average dosage between ARC status and children with normal or decreased renal function (102 ± 32 vs. 87 ± 38 mg/kg/d, $p = 0.28$). For all renal functions, the correlation improved slightly with

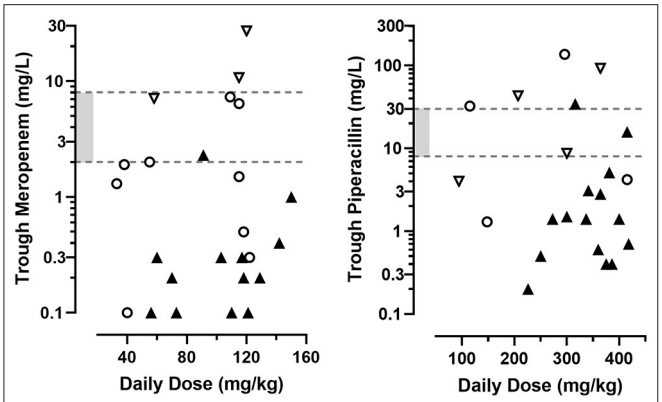

FIGURE 1 | First trough concentration values of MER and PIP obtained during 25, respectively, 23 treatment cycles in a series of hospitalized pediatric hematology-oncology patients, according to the total daily dosage administered as intermittent short infusions. Shaded range is the targeted concentration interval for common bacteria. Symbols represent the patients' creatinine clearance according to the Schwartz formula:
○ normal (80–160 mL/min/1.73 m^2).
▽ decreased (<80 mL/min/1.73 m^2).
▲ augmented (>160 mL/min/1.73 m^2).

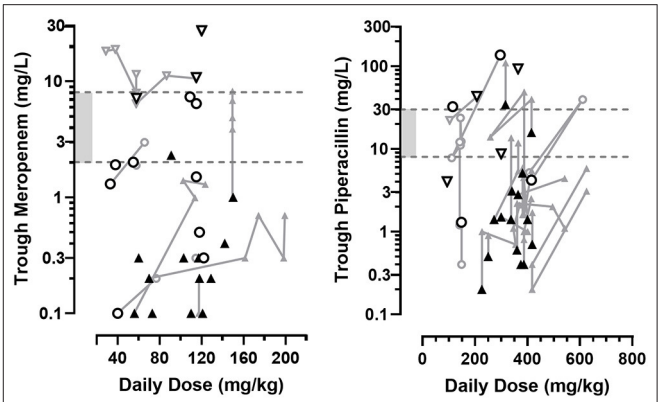

FIGURE 2 | First (black) and subsequent (grey) trough concentration values of MER and PIP obtained during 25, respectively, 23 treatment cycles in a series of hospitalized pediatric hematology-oncology patients, according to the total daily dosage administered as intermittent short infusions. Measurements in individual patients are connected. Shaded range is the targeted concentration interval for common bacteria. Symbols represent the patients' creatinine clearance according to the Schwartz formula:
○ normal (80–160 mL/min/1.73 m^2).
▽ decreased (<80 mL/min/1.73 m^2).
▲ augmented (>160 mL/min/1.73 m^2).

subsequent dosage adjustments (R^2 of 0.16, $p = 0.04$). Renal function was better taken into account in prescribing the initial dose of PIP (R^2 of 0.14, $p = 0.05$), with higher dosages given to ARC patients (343 ± 59 vs. 238 ± 110 mg/kg/d, $p = 0.005$), and, for all renal functions, further improvement of the correlation with subsequent dosages (R^2 of 0.31, $p < 0.001$).

Plasma Concentrations

Intermittent Administration

A majority of trough plasma concentrations from patients receiving MER and PIP as intermittent infusions were below concentrations suitable for the individual situation, both at first monitored level of the treatment cycle (geometric mean ± SD, 0.7 ± 5.8 mg/L for MER and 3.4 ± 33.6 mg/L for PIP, **Figure 1**) as for subsequent measurements during the cycle (1.6 ± 7.1 mg/L for MER and 3.8 ± 19.8 mg/L for PIP, **Figure 2**). This was the case for 32 (63%) of all MER and 44 (70%) of all PIP samples. The plasma levels reached the targeted range only in 11 (21%) MER samples and 10 (16%) PIP samples. They exceeded them in 8 (16%) MER and 9 (14%) PIP samples.

When focusing on febrile neutropenic children, 13/23 (57%) and 27/36 (75%) levels of MER and PIP, respectively, were below concentrations deemed therapeutic. For children in the most critical states (i.e., with both documented bacterial infection and immunocompromised state), observed trough concentrations were below targeted concentrations in 7/7 (100%) of MER and 6/10 (60%) of PIP samples.

When pooling all individual results, trough concentrations of both MER and PIP showed no clear association with the daily doses administered, either on initial or on subsequent TDM results.

Piperacillin Continuous Infusion

Conversely, plasma concentrations obtained from patients receiving PIP as a continuous infusion tended to often be above the targeted concentrations, with 7 (54%) measurements exceeding 60 mg/L. The count of levels within and below the therapeutic range were 5 (38%) and 1 (8%), respectively. Most of these plasma levels were taken from neutropenic children 9 (69%) of which 4 (31%) had, in addition, a documented infection. All plasma levels of the latter patient category reached or exceed targeted concentrations (germ specific MIC or usual therapeutic range). The insufficient plasma level was observed in a neutropenic child without bacterial infection.

Renal Function

Most MER and PIP samples were collected from children presenting ARC, accounting for 26 (51%) of MER and 45 (71%) of PIP trough samples obtained under intermittent administrations. The renal function estimated by the Schwartz formula was deemed normal (i.e. a creatinine clearance between 80 and 160 mL/min/1.73 m^2) for 17 (33%) MER and 13 (21%) PIP plasma levels, and decreased for the remaining 8 (16%) MER and 5 (8%) PIP measurements. Under continuous infusion, 11 (85%) PIP samples were obtained in ARC state and the rest with normal renal clearance. All plasma levels combined, nearly 2/3 of them came from children with ARC.

Trough MER concentrations measured for the first time during a treatment cycle revealed a significant inverse association with the patients' renal function (**Figure 1**, R^2 =0.61, $n = 25$, $p < 0.001$), which persisted on subsequent TDM determinations (**Figure 2**, R^2 =0.53, $n = 26$, $p < 0.001$). Accordingly, the presence of ARC was associated with significantly lower initial

trough MER levels compared to levels sampled in normal and decrease renal function status (geometric mean 0.26 mg/L, $n = 13$, CV = 94% vs. 2.17 mg/L, $n = 12$, CV = 162%, $p < 0.001$), with a difference persisting in subsequent TDM measurements (0.51 mg/L, $n = 13$, CV = 143%, vs. 5.31 mg/L, $n = 13$, CV = 133%, $p < 0.001$). Similarly, higher through PIP concentrations correlated with lower renal function initially ($R^2 = 0.50$, $n = 23$, $p < 0.001$), but less so for subsequent measures ($R^2 = 0.16$, $n = 40$, $p = 0.001$), with ARC being associated with very low levels initially (1.5 mg/L, $n = 15$, CV = 141% vs. 15.5 mg/L, $n = 8$, CV = 167%). The difference in measured levels between ARC and pooled other renal functions slightly lessened in subsequent PIP TDM measurements (2.9 mg/L, $n = 31$, CV = 134% vs. 8.9 mg/L, $n = 8$, CV = 166%, $p = 0.04$).

Consequently, trough MER and PIP concentrations observed in the first TDM samples of each treatment cycles were below the recommended range in 71% of the cases. Such below target exposures were more frequent in the presence of ARC compared to normal or decreased renal function status (90% vs. 45%, $p = 0.003$). This imbalance persisted in TDM samples measured subsequently, which remained below target levels in 64% of the measurements, and most frequently observed in ARC (83% vs. 26%, $p < 0.001$). All combined, underexposure was observed much more often in samples taken from children with ARC compared to samples taken under normal or decreased renal function status (85% vs. 36%, $p < 0.001$).

DISCUSSION

This retrospective study emphasizes the high frequency of underexposure to broad-spectrum beta-lactam antibiotics administered as intermittent infusions in children admitted for cancer treatment, with roughly two-thirds of trough MER and PIP plasma levels found below targeted concentrations. We observed similar frequencies of low antibiotic levels in febrile neutropenic children. Underexposure was highest in the most at-risk children, i.e., those with neutropenic state and bacterial infection combined (100 and 60% for MER and PIP, respectively). This underexposure appears clearly related to the high prevalence of ARC among the young cancer patients included in this study. Acute malignancies such as leukemia or lymphoma affect children usually devoid of previous kidney impairment, allowing for significant functional reserve to be made available to recruitment in case of superimposed infection. It is only recently that this phenomenon has drawn attention as a potential source of antibiotic underexposure and therapeutic failure. Our study confirms the sizeable importance of this problem.

Our observations suggest that the dosages prescribed in our cohort were inadequate, despite most often nearing the maximum recommended daily doses (i.e., 120 mg/kg/d for MER and 400 mg/kg/d for PIP (34, 35). This "single size" daily dose led to overexposure in three children with renal insufficiency, but much more often to underexposure in relation with ARC, as observed in 26 children. Another interesting finding was that the current practice of TDM and dosage adjustment failed to correct the problem of antibiotic underexposure in most cases. Prescribers remain understandably shy on exceeding maximum recommended dosages, as iatrogenic complications may become difficult to defend. Only in a few patients did the worrisome clinical course lead the physician to prescribe MER or PIP in doses beyond those recommended, reaching 200 and 625 mg/kg/d, respectively. Use of such dosages in children have not yet been reported in the literature and no dose-dependent toxicity has been described to date for MER, while use of PIP above 600 mg/kg/d has been associated with side effects such as bone marrow toxicity (36). Still, we infer that daily doses exceeding the maximum recommendations would have little chance of causing toxicity in patients with ARC, as systemic concentrations are not expected to exceed the targeted range. We would highly encourage a change in usual practice aimed at adapting MER and PIP infusion modalities to reach the suitable therapeutic targets. As beta-lactams are time-dependent antibiotics, increased administration frequency and infusion duration will increase trough levels while foreseeably respecting the manufacturer's maximum dose. In addition, the physicochemical stability of PIP allows administration as continuous infusion. Our observations confirm that continuous infusions maintain circulating concentrations in and above the target range in most cases (92%). In contrast, MER demonstrates less stability, making multiple sequential infusions necessary for safe and effective exposure (37). Yet extended-time infusions may not be sufficient to guarantee appropriate exposure in all cases (38). An advantage of TDM in continuous infusions is that samples can be drawn at any time after reaching steady state.

Our results also raise concern that underexposure will occur with other drugs eliminated by renal filtration in young cancer patients observed to frequently present ARC. Among these is probably vancomycin (39), as shown in a study conducted in neutropenic children (32). This is of particular concern as most documented bacterial infections in cancer children are due to Gram-positive bacteria, notably *Staphylococcus aureus*.

The impact of antibiotic underexposure on clinical outcomes was difficult to assess and beyond the scope of this study. Febrile state or infection will usually delay further anticancer treatments, and recovery from chemotherapy-induced neutropenia or agranulocytosis will vary and likely contribute in helping to eradicate an infection differently in each child. In addition, data on concomitant anti-infectious agents (e.g., vancomycin, antifungals, antiviral agents) were not systematically gathered in this study.

The limitations of our study are its retrospective nature and a rather limited number of samples. Yet we did not identify any previous study having assessed MER and PIP exposures in cancer children clearly taking the impact of ARC into account (26, 40). This could be explained by the restricted hematology-oncology patient population and the still restricted availability or adopted practice of TDM for beta-lactams.

Applying TDM in this clinical setting was not standardized, as only a prospective design could have guaranteed systematic measurements in children receiving MER or PIP following cancer therapy. A selection bias may thus in part explain the very high frequency of ARC among our patients, exceeding the 30%

to 40% reported in previous publications for this population (22, 23). TDM may have been preferably performed in patients with unsatisfactory outcome, and children with ARC resulting in underexposure could be overrepresented. Even if ARC is rather common in children experiencing various pathological states, it seems to occur with a highly variable frequency (41, 42).

Another limitation is some weakness in estimating the renal function, inherent to the Schwartz's formula (43). Serum creatinine values may not always appropriately reflect muscle mass, especially after prolonged hospitalization or in neurological diseases. Moreover, this formula was developed using measurements from children with impaired or normal renal function. Its performance may be questioned in the higher range of clearance values that characterize ARC (31). Therefore, we opted for a high cut-off at 160 mL/min/1.73 m^2 to define ARC and minimize the risk of misclassifying patients.

The reliability of blood sampling information or its transcription could also be a limitation. In intermittent infusions, included samples were presumably drawn at time of trough $\pm$1 h. Nonetheless, the very short half-lives of MER and PIP ($\sim$1 and 0.7 h, respectively) easily makes sampling inaccuracy translate into a significant imprecision in concentration result. As more samples were taken rather slightly earlier than later to the trough time, blood levels would more often have been overestimated.

Our definition of target ranges for MER and PIP trough concentrations might be disputed. While most authors agree on recommending to maintain a protein-corrected MIC coverage throughout the entire dosing interval in neutropenic and critically ill patients (44, 45), lower targets may be sufficient in immunocompetent children. A minimum of 40 to 50% of the dosing interval time above MIC is usually tolerated to ensure a bactericidal effect of MER or PIP in immunocompetent patients (46, 47).

In conclusion, the administration of MER and PIP as intermittent infusions often fails to ensure sufficient concentration exposure in children admitted for cancer treatment developing febrile neutropenia. This mainly results from a state of ARC, frequently observed during acute malignancies and episodes of febrile neutropenia. First steps to ensure proper antibiotic coverage in these patients will probably require modifying treatment modalities (prolonged infusion time, continuous infusion for PIP) and eventually increasing daily dosages beyond those currently recommended. Thorough assessment of renal function, possibly with improved diagnostic tests, and systematic TDM seem clearly advisable in such conditions. Prospective clinical trial remain warranted to validate the benefits and the safety of such suggested practice changes.

DATA AVAILABILITY STATEMENT

The raw data supporting the conclusions of this article will be made available by the authors, without undue reservation.

ETHICS STATEMENT

Ethical review and approval was not required for the study on human participants in accordance with the local legislation and institutional requirements. Written informed consent from the participants' legal guardian/next of kin was not required to participate in this study in accordance with the national legislation and the institutional requirements.

AUTHOR CONTRIBUTIONS

PA, LD, and KD contributed to conception and design of the study. PA organized the database. TB analyzed data and performed the statistical analysis. PA and LR wrote the first draft of the manuscript. PC, HC, LD, MD, and SA wrote sections of the manuscript. All authors contributed to manuscript revision, read, and approved the submitted version.

REFERENCES

1. Lam CG, Howard SC, Bouffet E, Pritchard-Jones K. Science and health for all children with cancer. *Science.* (2019) 363:1182–6. doi: 10.1126/science.aaw4892
2. Erdmann F, Frederiksen LE, Bonaventure A, Mader L, Hasle H, Robison LL, et al. Childhood cancer: survival, treatment modalities, late effects and improvements over time. *Cancer Epidemiol.* (2021) 71(Pt. B):101733. doi: 10.1016/j.canep.2020.101733
3. Centers for Disease Control and Prevention, National Center for Health Statistics. *Underlying Cause of Death 1999-2019 on CDC WONDER Online Database, Released in 2020. Data Are From the Multiple Cause of Death Files, 1999-2019, as Compiled From Data Provided by the 57 Vital Statistics Jurisdictions Through the Vital Statistics Cooperative Program.* (2020). Available online at: http://wonder.cdc.gov/ucd-icd10.html (accessed October 27, 2021).
4. Institut National de la Statistique et des Etudes Economiques (INSEE). *i. Données Annuelles de 2000 à 2016.* ed (2019). Available online at: https://www.insee.fr/fr/statistiques/2386052 (accessed October 27, 2021).
5. Inaba H, Pei D, Wolf J, Howard SC, Hayden RT, Go M, et al. Infection-related complications during treatment for childhood acute lymphoblastic leukemia. *Ann Oncol.* (2017) 28:386–92. doi: 10.1093/annonc/mdw557
6. Christensen MS, Heyman M, Mottonen M, Zeller B, Jonmundsson G, Hasle H, et al. Treatment-related death in childhood acute lymphoblastic leukaemia in the Nordic countries: 1992-2001. *Br J Haematol.* (2005) 131:50–8. doi: 10.1111/j.1365-2141.2005.05736.x
7. O'Connor D, Bate J, Wade R, Clack R, Dhir S, Hough R, et al. Infection-related mortality in children with acute lymphoblastic leukemia: an analysis of infectious deaths on UKALL2003. *Blood.* (2014) 124:1056–61. doi: 10.1182/blood-2014-03-560847
8. Creutzig U, Zimmermann M, Reinhardt D, Dworzak M, Stary J, Lehrnbecher T. Early deaths and treatment-related mortality in children undergoing therapy for acute myeloid leukemia: analysis of the multicenter clinical trials AML-BFM 93 and AML-BFM 98. *J Clin Oncol.* (2004) 22:4384–93. doi: 10.1200/JCO.2004.01.191
9. Zajac-Spychala O, Wachowiak J, Szmydki-Baran A, Hutnik L, Salamonowicz M, Matysiak M, et al. Infectious complications in children treated for hodgkin and non-hodgkin lymphomas in polish pediatric leukemia/lymphoma study group: incidence, epidemiology and etiology.

Leuk Lymphoma. (2019) 60:124–32. doi: 10.1080/10428194.2018.1466293
10. Steliarova-Foucher E, Colombet M, Ries LAG, Moreno F, Dolya A, Bray F, et al. International incidence of childhood cancer, 2001-10: a population-based registry study. *Lancet Oncol.* (2017) 18:719–31.
11. Auletta JJ, O'Riordan MA, Nieder ML. Infections in children with cancer: a continued need for the comprehensive physical examination. *J Pediatr Hematol Oncol.* (1999) 21:501–8. doi: 10.1097/00043426-199911000-00010
12. Celkan T, Ozkan A, Apak H, Diren S, Can G, Yuksel L, et al. Bacteremia in childhood cancer. *J Trop Pediatr.* (2002) 48:373–7. doi: 10.1093/tropej/48.6.373
13. Cojutti PG, Candoni A, Lazzarotto D, Fili C, Zannier M, Fanin R, et al. Population pharmacokinetics of continuous-infusion meropenem in febrile neutropenic patients with hematologic malignancies: dosing strategies for optimizing empirical treatment against *Enterobacterales* and *P. aeruginosa*. *Pharmaceutics.* (2020) 12:785. doi: 10.3390/pharmaceutics12090785
14. Sime FB, Roberts MS, Tiong IS, Gardner JH, Lehman S, Peake SL, et al. Can therapeutic drug monitoring optimize exposure to piperacillin in febrile neutropenic patients with haematological malignancies? A randomized controlled trial. *J Antimicrob Chemother.* (2015) 70:2369–75. doi: 10.1093/jac/dkv123
15. Wong G, Briscoe S, Adnan S, McWhinney B, Ungerer J, Lipman J, et al. Protein binding of beta-lactam antibiotics in critically ill patients: can we successfully predict unbound concentrations? *Antimicrob Agents Chemother.* (2013) 57:6165–70. doi: 10.1128/AAC.00951-13
16. Deshayes S, Coquerel A, Verdon R. Neurological adverse effects attributable to beta-lactam antibiotics: a literature review. *Drug Saf.* (2017) 40:1171–98. doi: 10.1007/s40264-017-0578-2
17. Roger C, Louart B. Beta-lactams toxicity in the intensive care unit: an underestimated collateral damage? *Microorganisms.* (2021) 9:1505. doi: 10.3390/microorganisms9071505
18. Dhont E, Van Der Heggen T, De Jaeger A, Vande Walle J, De Paepe P, De Cock PA. Augmented renal clearance in pediatric intensive care: are we undertreating our sickest patients? *Pediatr Nephrol.* (2020) 35:25–39. doi: 10.1007/s00467-018-4120-2
19. Udy AA, Jarrett P, Stuart J, Lassig-Smith M, Starr T, Dunlop R, et al. Determining the mechanisms underlying augmented renal drug clearance in the critically ill: use of exogenous marker compounds. *Crit Care.* (2014) 18:657. doi: 10.1186/s13054-014-0657-z
20. Mahmoud SH, Shen C. Augmented renal clearance in critical illness: an important consideration in drug dosing. *Pharmaceutics.* (2017) 9:36. doi: 10.3390/pharmaceutics9030036
21. Cook AM, Hatton-Kolpek J. Augmented renal clearance. *Pharmacotherapy.* (2019) 39:346–54. doi: 10.1002/phar.2231
22. Hjorth L, Wiebe T, Karpman D. Hyperfiltration evaluated by glomerular filtration rate at diagnosis in children with cancer. *Pediatr Blood Cancer.* (2011) 56:762–6. doi: 10.1002/pbc.22971
23. Kwatra NS, Meany HJ, Ghelani SJ, Zahavi D, Pandya N, Majd M. Glomerular hyperfiltration in children with cancer: prevalence and a hypothesis. *Pediatr Radiol.* (2017) 47:221–6. doi: 10.1007/s00247-016-3733-5
24. Udy AA, De Waele JJ, Lipman J. Augmented renal clearance and therapeutic monitoring of beta-lactams. *Int J Antimicrob Agents.* (2015) 45:331–3. doi: 10.1016/j.ijantimicag.2014.12.020
25. Udy AA, Varghese JM, Altukroni M, Briscoe S, McWhinney BC, Ungerer JP, et al. Subtherapeutic initial beta-lactam concentrations in select critically ill patients: association between augmented renal clearance and low trough drug concentrations. *Chest.* (2012) 142:30–9. doi: 10.1378/chest.11-1671
26. Saffioti C, Mesini A, Barco S, Cangemi G, Bandettini R, Castagnola E. Piperacillin-tazobactam concentration target attainment in children with cancer. *Pediatr Blood Cancer.* (2019) 66:e27882. doi: 10.1002/pbc.27882
27. Carrie C, Petit L, d'Houdain N, Sauvage N, Cottenceau V, Lafitte M, et al. Association between augmented renal clearance, antibiotic exposure and clinical outcome in critically ill septic patients receiving high doses of beta-lactams administered by continuous infusion: a prospective observational study. *Int J Antimicrob Agents.* (2018) 51:443–9. doi: 10.1016/j.ijantimicag.2017.11.013
28. Decosterd LA, Mercier T, Ternon B, Cruchon S, Guignard N, Lahrichi S, et al. Validation and clinical application of a multiplex high performance liquid chromatography - tandem mass spectrometry assay for the monitoring of plasma concentrations of 12 antibiotics in patients with severe bacterial infections. *J Chromatogr B Analyt Technol Biomed Life Sci.* (2020) 1157:122160. doi: 10.1016/j.jchromb.2020.122160
29. Robatel C, Decosterd LA, Biollaz J, Eckert P, Schaller MD, Buclin T. Pharmacokinetics and dosage adaptation of meropenem during continuous venovenous hemodiafiltration in critically ill patients. *J Clin Pharmacol.* (2003) 43:1329–40. doi: 10.1177/0091270003260286
30. EUCAST. *Data From the EUCAST MIC Distribution Website.* (2021). Available online at: http://www.eucast.org (accessed October 27, 2021).
31. Schwartz GJ, Haycock GB, Edelmann CM Jr., Spitzer A. A simple estimate of glomerular filtration rate in children derived from body length and plasma creatinine. *Pediatrics.* (1976) 58:259–63. doi: 10.1542/peds.58.2.259
32. Hirai K, Ihara S, Kinae A, Ikegaya K, Suzuki M, Hirano K, et al. Augmented renal clearance in pediatric patients with febrile neutropenia associated with vancomycin clearance. *Ther Drug Monit.* (2016) 38:393–7. doi: 10.1097/FTD.0000000000000270
33. Group ET, Wuhl E, Trivelli A, Picca S, Litwin M, Peco-Antic A, et al. Strict blood-pressure control and progression of renal failure in children. *N Engl J Med.* (2009) 361:1639–50. doi: 10.1056/NEJMoa0902066
34. Taketomo CK, Hodding JH, Kraus DM. *Pediatric & Neonatal Dosage Handbook: A Universal Resource for Clinicians Treating Pediatric and Neonatal Patients*. 21st ed. Hudson, OH: Lexi-Comp (2014-2015).
35. SwissPedDose T. *Database of Harmonized Dosage Recommendations for Pediatric Pharmacotherapy.* (2021). Available online at: https://swisspeddose.ch/ (accessed October 27, 2021).
36. Zobell JT, Waters CD, Young DC, Stockmann C, Ampofo K, Sherwin CM, et al. Optimization of anti-pseudomonal antibiotics for cystic fibrosis pulmonary exacerbations: II. Cephalosporins and penicillins. *Pediatr Pulmonol.* (2013) 48:107–22. doi: 10.1002/ppul.22669
37. Cielecka-Piontek J, Michalska K, Zalewski P, Jelinska A. Recent advances in stability studies of carbapenems. *Curr Pharmaceut Anal.* (2011) 7:213–27. doi: 10.2174/157341211797457989
38. Carlier M, Carrette S, Roberts JA, Stove V, Verstraete A, Hoste E, et al. Meropenem and piperacillin/tazobactam prescribing in critically ill patients: does augmented renal clearance affect pharmacokinetic/pharmacodynamic target attainment when extended infusions are used? *Crit Care.* (2013) 17:R84. doi: 10.1186/cc12705
39. Curth HM, Pelc A, Kutting F, Steffen HM. Augmented renal vancomycin clearance in cancer patients: a case report and review of the literature. *Oncol Res Treat.* (2015) 38:182–4. doi: 10.1159/000377652
40. Maarbjerg SF, Thorsted A, Kristoffersson A, Friberg LE, Nielsen EI, Wang M, et al. Piperacillin pharmacokinetics and target attainment in children with cancer and fever: can we optimize our dosing strategy? *Pediatr Blood Cancer.* (2019) 66:e27654. doi: 10.1002/pbc.27654
41. Sridharan K, Al-Daylami A, Ajjawi R, Ajooz HAA. Vancomycin use in a paediatric intensive care unit of a tertiary care hospital. *Paediatr Drugs.* (2019) 21:303–12. doi: 10.1007/s40272-019-00343-9
42. Van Der Heggen T, Dhont E, Peperstraete H, Delanghe JR, Vande Walle J, De Paepe P, et al. Augmented renal clearance: a common condition in critically ill children. *Pediatr Nephrol.* (2019) 34:1099–106. doi: 10.1007/s00467-019-04205-x
43. Skinner R, Cole M, Pearson AD, Keir MJ, Price L, Wyllie RA, et al. Inaccuracy of glomerular filtration rate estimation from height/plasma creatinine ratio. *Arch Dis Child.* (1994) 70:387–90. doi: 10.1136/adc.70.5.387
44. Turnidge JD. The pharmacodynamics of beta-lactams. *Clin Infect Dis.* (1998) 27:10–22. doi: 10.1086/514622
45. Huttner A, Harbarth S, Hope WW, Lipman J, Roberts JA. Therapeutic drug monitoring of the beta-lactam antibiotics: what is the evidence and which patients should we be using it for? *J Antimicrob Chemother.* (2015) 70:3178–83. doi: 10.1093/jac/dkv201
46. Nicolau DP. Pharmacokinetic and pharmacodynamic properties of meropenem. *Clin Infect Dis.* (2008) 47(Suppl. 1):S32–40. doi: 10.1086/590064
47. Frei CR, Burgess DS. Pharmacokinetic/pharmacodynamic modeling to predict *in vivo* effectiveness of various dosing regimens of piperacillin/tazobactam and piperacillin monotherapy against gram-negative

pulmonary isolates from patients managed in intensive care units in 2002. *Clin Ther.* (2008) 30:2335–41. doi: 10.1016/j.clinthera.2008.12.009

Conflict of Interest: The authors declare that the research was conducted in the absence of any commercial or financial relationships that could be construed as a potential conflict of interest.

Publisher's Note: All claims expressed in this article are solely those of the authors and do not necessarily represent those of their affiliated organizations, or those of the publisher, the editors and the reviewers. Any product that may be evaluated in this article, or claim that may be made by its manufacturer, is not guaranteed or endorsed by the publisher.

frontiers in Pharmacology

REVIEW
published: 07 March 2022
doi: 10.3389/fphar.2022.826004

Therapeutic Drug Monitoring of Conditioning Agents in Pediatric Allogeneic Stem Cell Transplantation; Where do We Stand?

M. Y. Eileen C. van der Stoep[1], Lisa V. E. Oostenbrink[2], Robbert G. M. Bredius[2], Dirk Jan A. R. Moes[1], Henk-Jan Guchelaar[1], Juliette Zwaveling[1] and Arjan C. Lankester[2]*

[1]Department of Clinical Pharmacy and Toxicology, Leiden University Medical Center, Leiden, Netherlands, [2]Willem-Alexander Children's Hospital, Department of Pediatrics, Leiden University Medical Center, Leiden, Netherlands

Allogeneic hematopoietic stem cell transplantation (HSCT) is an established curative treatment that has significantly improved clinical outcome of pediatric patients with malignant and non-malignant disorders. This is partly because of the use of safer and more effective combinations of chemo- and serotherapy prior to HSCT. Still, complications due to the toxicity of these conditioning regimens remains a major cause of transplant-related mortality (TRM). One of the most difficult challenges to further improve HSCT outcome is reducing toxicity while maintaining efficacy. The use of personalized dosing of the various components of the conditioning regimen by means of therapeutic drug monitoring (TDM) has been the topic of interest in the last decade. TDM could play an important role, especially in children who tend to show greater pharmacokinetic variability. However, TDM should only be performed when it has clear added value to improve clinical outcome or reduce toxicity. In this review, we provide an overview of the available evidence for the relationship between pharmacokinetic parameters and clinical outcome or toxicities of the most commonly used conditioning agents in pediatric HSCT.

Keywords: conditioning regimen, TDM, pediatrics, HSCT, pharmacokinetics

OPEN ACCESS

Edited by:
Raffaele Simeoli, Bambino Gesù Children's Hospital (IRCCS), Italy

Reviewed by:
Salvador F. Aliño, University of Valencia, Spain
Jeannine S. McCune, Beckman Research Institute, City of Hope, United States

****Correspondence:***
M. Y. Eileen C. van der Stoep
e.vanderstoep@lumc.nl

Specialty section:
This article was submitted to Obstetric and Pediatric Pharmacology, a section of the journal Frontiers in Pharmacology

Received: *30 November 2021*
Accepted: *18 February 2022*
Published: *07 March 2022*

Citation:
van der Stoep MYEC, Oostenbrink LVE, Bredius RGM, Moes DJAR, Guchelaar H-J, Zwaveling J and Lankester AC (2022) Therapeutic Drug Monitoring of Conditioning Agents in Pediatric Allogeneic Stem Cell Transplantation; Where do We Stand? Front. Pharmacol. 13:826004. doi: 10.3389/fphar.2022.826004

INTRODUCTION

Allogeneic hematopoietic stem cell transplantation (HSCT) is an established curative treatment for malignant and non-malignant disorders in both adult and pediatric patients. In HSCT, the hematopoiesis of the host (i.e., the patient) is eliminated by a conditioning regimen in order to allow donor (i.e., healthy individual) stem/progenitor cell engraftment in the bone marrow and thymic niches. Furthermore, prevention of immune-mediated rejection is an important goal of conditioning regimens that should facilitate a successful HSCT outcome (Copelan 2006). Depending on the underlying disease, the conditioning regimen usually consists of agents that have myeloablative (MA) properties to create "space" in the bone marrow of the patient and eradicate the primary disease (Shaw et al., 2019). Immunoablative/-suppressive agents are applied to prevent rejection (host-versus-graft) as well as graft-versus-host disease (GvHD). After the infusion of the donor stem cells containing graft, immunosuppressive agents are usually used as prophylaxis to ensure engraftment and prevent the development of GvHD (McCune and Bemer 2016).

The choice for the optimal conditioning regimen is dependent on different factors. The required intensity of the conditioning regimen, particularly the immunosuppressive component, is usually greater when an unrelated or mismatched family donor is used. Myeloablative regimens are associated with a high likelihood to result in full donor chimerism, a situation where the newly developed hematopoietic system is of donor origin only (Bader et al., 2005). For malignant diseases, MA regimens are often required to eradicate all malignant cells, whereas in patients with non-malignant diseases less intense protocols can also be sufficient, depending on the specific disease and required level of chimerism. These less intense, non-MA protocols are often referred to as reduced intensity (RIC) regimens, in which the use of reduced doses of myeloablative drugs (or radiotherapy) is more likely to result in mixed chimerism, a state where donor and recipient hematopoiesis coexist within the recipient (Bader et al., 2005; Shaw et al., 2019). In addition, patient specific factors, such as age, immune status, DNA repair disorders, tumor load, disease activity and comorbidities, play a role in requirement for and tolerability to the various conditioning agents and therefore the choice for the preferred regimen (Nagler and Shimoni 2019). Nowadays, more emphasis is placed on the immunosuppressive aspect of the regimen to prevent rejection and GvHD in the case of unrelated or mismatched donors (Baron et al., 2017). While an effective conditioning regimen is necessary prior to the infusion of the HSCs, it may also be accompanied with acute toxicity which can even be life-threatening. Complications related to toxicity of the conditioning regimen are still a major cause of transplant-related mortality (TRM). Besides the risk of acute toxicity, late toxicities, such as infertility, are also a major problem (Diesch-Furlanetto et al., 2021). One of the main challenges to improve HSCT outcome is reducing toxicity caused by the conditioning regimen while maintaining efficacy.

In the last decade, significant improvements have been made to optimize efficacy and safety of conditioning regimens. These include the use of less toxic agents, less toxic combinations and dose optimization. Personalized dosing of several components of the conditioning regimen by means of therapeutic drug monitoring (TDM) has contributed to more favorable HSCT outcome. Therapeutic Drug Monitoring is the clinical practice of individualization of dosage by measuring plasma or blood drug concentrations and maintaining it within a therapeutic range or window. TDM is considered useful when the following criteria are met (Saha 2018): 1) There should be a clear relationship between concentration and effect (either efficacy or toxicity or both), 2) drug concentrations cannot be predicted from a given dose, because of high interindividual variability in pharmacokinetic (PK) parameters, 3) the drug has a narrow therapeutic index, 4) the dose cannot be easily optimized by clinical observation and 5) a bioanalytical assay should be available. TDM in combination with the use of mathematical models (such as population PK models), and other patient and disease characteristics, such as genotype, organ function, and age, is now increasingly being used to personalize dosing right at the start of treatment; a dosing paradigm that is now often referred to as 'model-informed precision dosing (MIPD)' (Darwich et al., 2021).

Especially in children, TDM/MIPD can be of value. Because of the development and maturation of organ systems, in general children have greater pharmacokinetic variability than adults due to age-related differences in drug metabolism (Kearns et al., 2003). Also, the developing organ systems may lead to different susceptibility to toxicity. Moreover, pharmacokinetic studies in children are sparse which makes it challenging to establish evidence based TDM recommendations. In this review, the focus lies on providing an overview of the available evidence for the relationship between pharmacokinetic parameters and clinical outcome or toxicities of the most commonly used conditioning agents given prior to pediatric HSCT and discuss whether TDM could be a useful tool to improve outcome.

LITERATURE SEARCH METHODS

Literature searches in PubMed were conducted using the generic names of the conditioning agents and the terms "pharmacokinetics" and "pediatric" (e.g., treosulfan AND pharmacokinetics AND pediatric). The results were screened and studies were included if the majority of patients were ≤18 years of age and if PK parameters of the drug were studied in relationship to toxicities and/or outcome. For busulfan, only the studies that report either a hazard ratio (HR), odds ratio (OR) or relative risk (RR) were selected to limit results and keep the review concise. For a detailed overview of busulfan PK studies we refer to two recent reviews (Ben Hassine et al., 2021; Lawson et al., 2021). Studies were described in chronological order.

CHEMOTHERAPY

Busulfan

Busulfan (Bu) is a widely used and established chemotherapeutic agent in conditioning regimens prior to HSCT. It is a bifunctional alkylating agent that diffuses into cells, where it is hydrolyzed to produce highly reactive carbonium ions that alkylate and damage DNA (Pierre Fabre Médicament, 2017). Its metabolism is complex and not yet completely understood. It is primarily metabolized by the liver through conjugation with glutathione, mainly by glutathione-S-transferase A1 (GSTA1). The glutathione conjugate is then further oxidized before it is excreted into the urine. Intravenous (i.v.) Bu has widely replaced oral Bu when this formulation became available, which was expected to reduce pharmacokinetic variability (Ciurea and Andersson 2009). However, interpatient variability in clearance of i.v. Bu is still reported to be up to 30% (McCune and Holmberg 2009; Lee et al., 2012). Factors explaining this interpatient variability in children are age, body weight and GSTA1 genotype, among others (Lawson et al., 2021). In the past decades, many studies have shown that Bu exposure is related to clinical outcome. In **Table 1**, the studies that report

TABLE 1 | Reported associations of pharmacokinetic parameters of busulfan and clinical outcomes.

First author, year	*n*	Age, median (range)	Diagnosis	Regimen	Dose interval	Major findings
Bartelink et al. (2009)	102	3.1 (0.2–21.0)	Malignant: 46 (45%) Non-malignant: 56 (55%)	BuCyMel: 43 (42%) Other: 59 (58%)	Once daily: 64 (63%) 4 times daily: 38 (37%)	Bu exposure of 72–80 mg*h/L was associated with the highest OS and EFS (p = 0.021 and p = 0.028). Increased AUC was associated with less graft failure and relapse (HR 0.047; p = 0.004), but more aGVHD (HR 1.56; p = 0.019).
Ansari et al. (2014)	75	6.2 (0.1–20.0)	Malignant (ALL/AML/MDS): 48 (64%) Non-malignant: 27 (36%)	BuCy: 67 (89%) BuCyVP16: 6 (8%) BuMel: 2 (3%)	4 times daily	$C_{ss,day1}$ > 600 ng/ml (daily AUC of 14.4 mg*h/L or cumulative AUC of 57.6 mg*h/L) was associated with lower EFS (HR 5.14; 95%CI 2.19–12.07; p < 0.001) and lower OS (HR 7.55; 95%CI 2.20–25.99; p = 0.001).
Bartelink et al. (2016)	674	4.5 (0.1–30.4)	Malignant: 274 (41%) Non-malignant: 400 (59%)	BuCy: 352 (52%) BuFlu: 252 (37%) BuCyMel: 70 (10%)	Once daily: 267 (40%) 4 times daily: 324 (48%) Other: 83 (12%)	Optimum cAUC of 78–101 mg*h/L decreased the probability of graft failure or relapse (HR 0.57; 95%CI 0.39–0.84, p = 0.0041). High cAUC increased the risk of TRM (HR 2.99; 95%CI 1.82–4.92, p < 0.0001) and toxicities (HR 1.69; 95%CI 1.12–2.57; p = 0.013).
Benadiba et al. (2018)	36	5.9 (0.6–19.3)	AML: 23 (63.9%) MDS: 13 (36.1%)	BuCy: 33 (91.7%) BuMel: 2 (6%) BuCyVP16: 1 (2.3%)	4 times daily	$C_{ss,day1}$ > 600 ng/ml (daily AUC of 14.4 mg*h/L or cumulative AUC of 57.6 mg*h/L) was a significant risk factor for OS (HR 5.2; 95%CI 1.26–21.5, p = 0.02) and EFS (HR 3.83; 95%CI 1.33–11.05, p = 0.01).
Philippe et al. (2019)	293	6.2 (0.2–21.0)	Malignant: 170 (58%) Non-malignant: 123 (42%)	Not clearly specified	4 times daily: 282 (96%) Once daily: 10 (3.4%0 Twice daily: 1 (0.6%)	The incidence of VOD was 25.6%. Patients with C_{max} of ≥1.88 ng/ml were 6 times more likely to develop VOD (63.3 vs. 21.3%, RR 6.0 p < 0.001).

ALL, acute lymphoblastic anemia; AML, acute myeloid leukemia; MDS, myelodysplastic syndrome; Mel, melphalan; Cy, cyclophosphamide; VP16, etoposide.

either a hazard ratio (HR), odds ratio (OR) or relative risk (RR) are shown.

Bartelink et al. reported the results of a retrospective study of 102 pediatric patients (median age 3.1 years [range 0.2–21.0)] undergoing allogeneic HSCT for malignant (45%) and non-malignant (55%) indications. Patients received conditioning with busulfan, cyclophosphamide and melphalan (BuCyMel) (43%) or in other combinations. A once daily regimen was given in 63% of the patients, the rest received Bu 4 times daily. OS, EFS and toxicity were associated with Bu exposure. In multivariate analysis, a cumulative Bu exposure between 72 and 80 mg*h/L was associated with the most favorable EFS and OS. Higher AUC was associated with a lower incidence of graft failure and relapse. Higher Bu exposure was also a significant predictor for aGVHD, but not for veno-occlusive disease (VOD) or mucositis (Bartelink et al., 2009).

Ansari et al. performed a prospective study to examine the association between i. v. Bu exposure and clinical outcome in a pediatric cohort of 75 patients [median age 3.2 years (range 0.1–20.0)]. Patients were included with malignant (64%) and non-malignant diseases (36%). The majority of patients received a conditioning regimen consisting of BuCy (89%) and Bu was given 4 times daily over 4 days. They found that an average Bu concentration of the first dose ($C_{ss,day1}$) > 600 ng/ml (corresponding with a daily AUC of 14.4 mg*h/L or cumulative AUC of 57.6 mg*h/L) was associated with higher incidence of aGvHD and higher risk of non-relapse mortality (NRM). In multivariate analysis, $C_{ss,day1}$ > 600 ng/ml was associated with lower EFS and lower OS (Ansari et al., 2014).

A landmark study done by *Bartelink* and others in 2016 included 674 patients [median age 4.5 years (range 0.1–30.4)] from 15 different pediatric transplantation centers. Malignant (41%) and non-malignant (59%) indications were included and the majority received a conditioning regimen with BuCy (52%), followed by BuFlu (37%) and BuCyMel (10%). The main outcome of interest was EFS; secondary outcomes were graft failure, relapse, TRM, acute toxicity, cGvHD, OS and cGvHD free survival. They defined that a target of 90 mg*h/L (range 78–101 mg*h/L) gave the highest probability of EFS. Compared with the low AUC group (<78 mg*h/L), the optimal AUC decreased the probability of graft failure or disease relapse and a high AUC (>101 mg*h/L) increased the risk of TRM and acute toxicities (Bartelink et al., 2016).

Benadiba et al. conducted a study with 36 pediatric patients [median age 5.9 years (range 0.6–19.3)] receiving a umbilical cord blood (UCB) transplantation for a myeloid malignancy. All patients received Bu in a regime of 4 times daily in combination with Cy (91.7%), Mel (6%) or Cy plus etoposide (2.3%). In multivariate analysis, $C_{ss,day1}$ > 600 ng/ml (daily AUC of 14.4 mg*h/L or cumulative AUC of 57.6 mg*h/L) was a significant risk factor for OS and EFS. Furthermore, neutrophil and platelet recovery and non-relapse mortality were significantly

TABLE 2 | Reported associations of pharmacokinetic parameters of treosulfan and clinical outcomes.

First author, year	*n*	Age, median (range)	Diagnosis	Regimen	Dose	Major findings
van der Stoep et al. (2017)	77	4.8 (0.2–18.3)	HBP: 31 (40.3%) Hem. malig: 12 (15.6%) IEI: 22 (28.5%) BMF: 11 (14.3%) Other: 1 (1.3%)	TreoFlu: 25 (35.5%) TreoFluThio: 52 (67.5%)	3 × 10 g/m^2: 12 (15.6%) 3 × 14 g/m^2: 65 (84.4%)	High Treo $AUC_{0-\infty}$ (>1,650 mg*h/L per day) was associated with a higher risk of ≥ grade 2 mucositis (OR 7.03; 95%CI 1.60–30.86, $p = 0.01$). There is also an increased risk of skin toxicity (OR 9.96; 95%CI 1.85–53.46, $p = 0.007$).
Mohanan et al. (2018)	87	9.0 (1.5–25)	TM: 87	TreoFluThio	3 × 14 g/m^2: 87 (100%)	In a *post-hoc* analysis, lower Treo clearance (<7.97 L/h/m^2) was associated with poor overall survival (HR 2.7; 95%CI 1.09–6.76, $p = 0.03$) and event free survival (HR 2.4; 95%CI 0.98–5.73, $p = 0.055$). No association with toxicity.
Chiesa et al. (2020)	87	1.6 (0.2–16.7)	IEI: 79 (91%) IBD: 5 (5%) JMML: 2 (2%) IEM: 1 (1%)	TreoFlu	3 × 10 g/m^2: 4 (5%) 3 × 12 g/m^2: 23 (26%) 3 × 14 g/m^2: 60 (69%)	Higher cumulative Treo $AUC_{0-\infty}$ showed higher risk of mortality in multivariable analysis (HR 1.32; 95%CI 1.07–1.64, $p = 0.0093$), a trend was seen for low $AUC_{0-\infty}$ associated with poor engraftment (HR 0.61; 95%CI 0.36–1.04, $p = 0.072$) in univariable analysis. TRM was higher in patients with AUC>6,000 mg*h/L than <6,000 mg*h/L (39% vs. 3%, $p = 0.00001$). A cumulative $AUC_{0-\infty}$ of 4,800 mg*h/L is proposed as target.
van der Stoep et al. (2021)	110	5.2 (0.2–18.8)	IEI: 38 (35%) HBP: 55 (50%) BMF: 17 (15%)	TreoFlu: 37 (32%) TreoFluThio: 77 (68%)	3 × 10 g/m^2: 18 (16%) 3 × 14 g/m^2: 92 (84%)	All grade mucositis was associated with high Treo $AUC_{0-\infty}$ (OR 4.43; 95%CI 1.43–15.50, $p = 0.01$), but not mucositis ≥2 or higher (OR 1.51; 95%CI 0.52–4.58, $p = 0.46$). Skin toxicity ≥ grade 2 was associated with high $AUC_{0-\infty}$ (OR 3.97; 95%CI 1.26–13.67, $p = 0.02$). No association with 1-year donor chimerism, 2-years OS and EFS.

HPB, hemoglobinopathies; hem. malig, hematological malignancies; IEI, inborn errors of immunity; BMF, bone marrow failure; TM, thalassemia major; IBD, inflammatory bowel disorder; JMML, juvenile myelomonocytic leukemia; IEM, inborn errors of metabolism.

higher in patients with $C_{ss,day1}$ < 600 ng/ml than $C_{ss,day1}$ > 600 ng/ml (Benadiba et al., 2018).

Philippe et al. specifically looked at the occurrence of VOD in relationship with Bu exposure. In this retrospective study, 293 pediatric patients with a median age of 6.2 years (0.2–21) were included of whom 75 (25.6%) developed VOD. There was a 6-fold increased risk of VOD in patients with a maximum drug concentration level (C_{max}) of ≥1.88 ng/ml. Also, weight <9 kg and age <3 years were independent predictors of VOD (Philippe et al., 2019).

Together, these data suggest that overexposure to Bu (either on day one, or overall AUC) has a negative effect on OS and EFS. A cumulative AUC of 78–101 mg*h/L or $C_{ss,day1}$ < 600 ng/ml are suggested as possible targets. A target value for the first dose below 600 ng/ml (= 14.4 mg*h/L per day and 57.6 mg*h/L in total) seems rather low, but adequate overall exposure over the course of the treatment could still be achieved because of decreased clearance of Bu over time (Gaziev et al., 2010; Bartelink et al., 2012; Kawazoe et al., 2018). On the other hand, the target suggested by Bartelink et al. is higher than the historical target of 56–86 mg*h/L (Css 600–900 ng/ml), which seems to be in contrast with the results of Ansari et al. Also, the study done by Bartelink et al. shows that low cAUC (<78 mg*h/L) gave a higher risk of graft failure or disease relapse. However, the considerable variability in Bu dosing (once, twice or four times daily), difference in exposure targets (C_{ss}, cAUC, AUC_{dose}), difference of exposure units (mg*h/L, μM*min), the method of exposure estimation and co-medication (cyclophosphamide versus fludarabine) makes comparison of all these results difficult and complex. Also, optimal exposure may differ between groups based on factors, such as underlying disease, age and comorbidities (McCune et al., 2000). A proposal of harmonizing Bu exposure unit to mg*h/L has been done and will hopefully lead to more accurate assessment of exposure and thereby evaluation of outcomes in multicenter studies (McCune et al., 2019).

Treosulfan

In the last decade, treosulfan (Treo) has gained popularity as a chemotherapeutic agent in conditioning regimens prior to HSCT for malignant and non-malignant disorders. It is a water-soluble bifunctional alkylating agent and a structural analogue of busulfan. Although Treo has structural similarities with Bu, its mechanism of alkylation is different. As a pro-drug, it undergoes non-enzymatic and pH-dependent conversion into active mono- and diepoxide derivatives under physiological conditions. These derivatives cause DNA alkylation and interstrand DNA crosslinking, leading to DNA fragmentation and apoptosis (Hartley et al., 1999). Approximately 25–40% of Treo is excreted renally in unchanged form (Hilger et al., 1998). Interpatient variability of clearance in children is high; between 30 and 68% have been reported in population pharmacokinetic studies (Mohanan et al., 2018; van der Stoep et al., 2019; Chiesa et al., 2020). Age, bodyweight and renal clearance are covariates that were found to (partially) explain the large interindividual variability. More recently, the

relationship between Treo exposure and clinical outcome has been explored in several studies with pediatric patients undergoing HSCT. **Table 2** summarizes the reports of Treo PK associated with outcome in pediatric patients.

Van der Stoep et al. described a pediatric cohort of 77 patients transplanted for non-malignant (84.4%) and malignant (15.6%) diseases [median age 4.8 years (range 0.2–18.3)]. Patients received Treo with fludarabine only (35.5%) or with additional thiotepa (67.5%). Twelve patients <1 year of age received a total dose of 30 g/m^2 and 65 patients ≥1 year of age received 42 g/m^2. Patients were divided into three exposure groups (on day 1); low (<1,350 mg*h/L, medium (1,350–1,650 mg*h/L) and high (>1,650 mg*h/L). Patients in the high exposure group had an higher risk for mucosal and skin toxicity compared to the low exposure group. The risk of experiencing two or more toxicities was also higher in the high exposure group compared with the low exposure group. No relationship was found between exposure and aGvHD, engraftment, chimerism and survival (van der Stoep et al., 2017).

In a study done by Mohanan et al., 87 patients with thalassemia major undergoing HSCT were included to study the PK of Treo in relationship with outcome. The majority of included patients were children, although some adults up to 25 years of age were also included [median age 9.0 years (range 1.5–25)]. Treo was given in combination with fludarabine and thiotepa in a total dose of 42 g/m^2. The influence of Treo PK on rejection, toxicities, OS, EFS and TRM was evaluated and no association was found with these outcome parameters. A trend was seen towards better OS with high Treo clearance (>7.97 L/h/m2) and low day 1 AUC (<1828 mg*h/L). In a *post-hoc* analysis they found that lower Treo clearance (<7.97 L/h/m^2) was significantly associated with poor OS and EFS (Mohanan et al., 2018).

Chiesa et al. investigated the relationship between Treo PK and OS and donor engraftment in 87 children [median age 1.6 years (range 0.2–16.7)], transplanted mainly for an inborn error of immunity (91%). All patients received Treo with fludarabine with a total dose of 42 g/m^2 in children aged >12 months, 36 g/m^2 in children aged 3–12 months and 30 g/m^2 in children ≤3 months. A higher Treo cumulative AUC (the sum of Treo AUC on 3 days, cAUC) showed a higher risk of mortality in multivariable analysis. Also, children with cAUC >6,000 mg*h/L had higher TRM than children with cAUC <6,000 mg*h/L (39% vs. 3%). A trend was seen for low AUC to be associated with poor donor engraftment (≤20%), but this was observed only in univariable analysis. The authors propose a therapeutic target of cAUC 4,800 mg*h/L, corresponding with 1,600 mg*h/L daily (Chiesa et al., 2020).

Very recently, *Van der Stoep* et al. published results on Treo PK in a cohort of 110 pediatric patients with non-malignant diseases [median age 5.2 years (range 0.2–18.8)]. The influence of Treo PK on early and long-term clinical outcome was evaluated. The main outcome of interest was 2-years EFS and secondary outcomes were 2-years OS, toxicities, engraftment, donor chimerism and GvHD. No association was found between Treo PK and 2-years EFS, nor with 2-years OS, engraftment, donor chimerism and GvHD. High Treo exposure (>1750 mg*h/L) on day 1 was associated with all grade mucositis, but not with mucositis ≥ grade 2. High Treo exposure was also associated with ≥ grade 2 skin toxicity (van der Stoep et al., 2021).

While there seems to be a relationship with Treo PK and mucositis in the first study of *Van der Stoep* et al., this was not confirmed by *Mohanan* and *Chiesa* et al. Furthermore, in a more recent study of *Van der Stoep* et al., only a relationship between exposure and all grade mucositis was seen, but not with grade 2 or higher, which is clinically more relevant. However, in both studies of *Van der Stoep* et al. as well as the study of *Chiesa* et al., high Treo exposure was related to the risk of ≥ grade 2 skin toxicity. In terms of survival, *Chiesa* et al. showed a relationship between exposure and OS, while *Mohanan* et al. hinted towards a trend and *Van der Stoep* et al. did not observe a relationship. These differences could possibly be explained by interindividual variability in exposure between the studies, which was higher in the studies of *Chiesa* et al. and *Mohanan* et al. Also, no relationship with EFS was found (Mohanan et al., 2018; van der Stoep et al., 2021) and overall, it is noticed that Treo is well tolerated, with limited regimen-related toxicities, while still achieving good results when it comes to clinical outcome. Together, these results indicate a moderate exposure-toxicity relationship, but a relationship with survival is not evident and consistent. The clinical value of TDM could be investigated to prevent skin toxicity, although implementation of preventive care guidelines could possibly reduce the incidence of cutaneous complications as well. The current evidence do not justify the use of TDM in routine patient care, but can be useful in specific cases and subgroups and warrants further investigation.

Fludarabine

The purine analogue fludarabine (Flu) has become an alternative for cyclophosphamide (Cy) in the classical myeloablative conditioning regimen Bu-Cy, because of the lower risk NRM without compromising efficacy (Ben-Barouch et al., 2016). Flu is currently being used as part of various different conditioning regimens, whether it be myeloablative, reduced-intensity or non-myeloablative. Fludarabine phosphate is a prodrug that is rapidly converted into F-ara-A in the systemic circulation. Subsequently, F-ara-A is phosphorylated in the cell into the active metabolite fludarabine triphosphate, F-ara-ATP, which is responsible for the inhibition of DNA synthesis and RNA production, leading to apoptosis (Gandhi and Plunkett 2002). Flu is predominantly excreted renally. Interpatient variability in clearance is high and bodyweight and renal clearance were found to be contributing factors to this variability (Ivaturi et al., 2017; Chung et al., 2018; Langenhorst et al., 2018). **Table 3** summarizes the reports of Flu PK associated with outcome in pediatric patients.

Ivaturi et al. reported a prospective PK study of 133 pediatric patients transplanted for malignant (44%) and non-malignant (56%) indications [median age 5.0 years (range 0.2–17.9)]. Patients received Flu in various different conditioning regimens and in different dosages. No association was found between Flu exposure and the primary endpoint TRM. The highest 1-year OS rate was seen in patients with a cumulative AUC (cAUC) between 15 and 19 mg*h/L, however this was not

TABLE 3 | Reported associations of pharmacokinetic parameters of fludarabine and clinical outcomes.

First author, year	*n*	Age, median (range)	Diagnosis	Regimen	Dose	Major findings
Ivaturi et al. (2017)	133	5.0 (0.2–17.9)	Hem. malig: 59 (44%) IEI: 18 (14%) HBP: 8 (6%) Metabolic: 22 (16%) BMF: 22 (16%) Epidermolysis bullosa: 4 (4%)	BuFlu: 40 (30%) FluCy: 45 (34%) BuFluClo: 18 (14%) FluThioMel: 15 (11%) Other: 15 (11%)	3–5 x 40 mg/m^2: 55 (41%) 3–5 x 12.5–35 mg/m^2: 40 (30%) 3–5 x 0.9–1.22 mg/m^2: 38 (29%)	No association with Flu and TRM (p = 0.35). In the malignancy group DFS was highest at 1 year post HSCT in patients with a cumulative AUC >15 mg*h/L compared to <15 mg*h/L (82.6 vs. 52.8%, p = 0.04). A cumulative AUC of >15 mg*h/L is considered as a minimum exposure threshold.
Mohanan et al. (2017)	53 (no. of children not specified)	17 (3–57)	AA: 40 (75%) FA: 13 (25%)	FluCy: 29 (55%) FluCyTBI: 20 (38%) FluCyATG: 4 (7%)	6 × 30 mg/m^2	AUC >29.4 μM*h was a significant factor associated with aGVHD in multivariate analysis (p = 0.02) None of the PK parameters showed any association with engraftment, mixed chimerism, rejection, overall survival or TRM.
Chung et al. (2018)	43	11.8 (1.3–18.5)	Acute leukemia: 29 (67.4%) Other malig: 2 (4.7%) Non-malignant: 12 (28%)	BuFluVP16: 24 (55.8%) BluFlu: 12 (27.9%) BuFluMel: 4 (9.3%) FluCy: 2 (4.7%) BuFluCy: 1 (2.3%)	6 × 40 mg/m^2: 40 (93%) 5 × 40 mg/m^2: 3 (7%)	No significant association was found between AUC and toxicities, GvHD, relapse and survival.
Langenhorst et al. (2019)	192 (119 adults, 73 children	36.2 (0.23–74)	Benign: 68 (35%) Leukemia/ lymphoma: 71 (37%) MDS: 30 (16%) Plasma cell disorder: 23 (12%)	BuFlu	4 × 40 mg/m^2	Flu exposure is a predictor for EFS. NRM was increased with high Flu exposure (p < 0.001) and more graft failure was seen with low exposure (p = 0.04). An optimal cumulative AUC of 20 mg*h/L (±5) is suggested. The optimal exposure group had a significantly higher EFS compared with the above-optimal exposure group (HR 2.0; 95%CI 1.1–3.5, p = 0.01) and (non-significantly) higher than the below-optimal group (HR 1.8; 95%CI 0.72–4.5, p = 0.21).

AA, aplastic anemia; FA, fanconi anemia; TBI, total body irradiation.

statistically significant. In the malignant subgroup, 1- year disease free survival (DFS) was higher in patients with a cAUC between 15 and 19 mg*h/L than <15 mg*h/L (82.6% vs. 52.8%). Based on the data in their study, the authors propose a minimum exposure threshold of 15 mg*h/L to achieve the best possible outcome (Ivaturi et al., 2017).

Mohanan et al. studied the pharmacokinetics of Flu in 53 patients with aplastic anemia (75%) and Fanconi anemia (25%). They included both children and adults, however the number of children was not specified [median age 17 years (range 3–57)]. The majority of patients received a regimen with Flu and Cy (55%), others received Flu and Cy in combination with TBI (38%) or anti-thymocyte globulin (ATG) (7%). All patients received a dose of 30 mg/m^2 daily for 6 days. There was no association between the PK parameters of Flu and engraftment, mixed chimerism, rejection, OS or TRM. In multivariate analysis, a cAUC of >29.4 μM*h was associated with a higher risk of aGVHD (Mohanan et al., 2017).

Chung et al. described the pharmacokinetics of Flu in 43 Korean pediatric patients [median age 11.8 years (range 1.3–18.5)]. The majority of patients received a transplantation for a malignant disease (72.1%). Flu was given in combination with various different agents, but the majority received a regimen with Bu and etoposide (55.8%) with a daily dose of 40 mg/m^2 for 6 days. In their exploratory analyses, they did not find any relationship between Flu cAUC and toxicities, GVHD, relapse, EFS and survival (Chung et al., 2018).

The most recent study is from *Langenhorst* and others, who conducted a retrospective cohort analysis in 192 patients [119 adults and 73 children, median age 36.2 years (range 0.23–74)]. All patients received a conditioning regimen of BuFlu (4 × 40 mg/m^2), mostly for malignant diseases (65%). They found an increased incidence of NRM with higher Flu cAUC and more graft failures were observed with lower Flu cAUC. No influence on relapse was seen. Based on these results, they calculated that a cAUC of 15–25 mg*h/L was the optimal target window for Flu to

minimize the chance of an event. When considering three exposure groups (below-optimal, optimal and above-optimal), the optimal exposure group had a significantly higher EFS compared with the above-optimal exposure group and (non-significantly) higher than the below-optimal group. NRM was the main cause of an event in the above-optimal group and immune reconstitution was significantly lower, whereas the risk of graft failure and NRM was increased in the below-optimal group (Langenhorst et al., 2019).

The abovementioned studies show variable results. *Langenhorst* et al. showed that Flu exposure within the optimal target (cumulative AUC of 15–25 mg*h/L) had significant higher EFS than the above-optimal group and *Ivaturi* et al. showed better DFS with a cumulative Flu exposure >15 mg*h/L in a subgroup of 59 children with malignancy. However, Mohanan et al. and Chung et al. failed to show associations with EFS and OS. Patient cohorts in the last two studies were small (53 and 43, respectively), so it is possible that a statistically significant relationship could not be detected. Also, in all studies except *Langenhorst* et al. various different conditioning regimens were included with various Flu dosage schemes, which makes comparison of the results difficult. Currently, a randomized phase II study is ongoing to study the influence of individualized fludarabine conditioning on the incidence of severe viral infections and other transplant-related outcomes in adult patients with hematological malignancies (Clinicaltrialsregister.eu: TARGET study 2018-000356-18)). Whether these results can be extrapolated to children remains to be determined. Ideally, a randomized study in children is done to address whether individualized dosing improves clinical outcome. For now, the evidence for TDM for Flu is growing, but more studies are needed to explore whether a single optimal target can be defined. In the meantime, the use of TDM in routine patient care remains limited.

Clofarabine

The addition of clofarabine (Clo) to the conditioning regimen with Bu and Flu prior to HSCT in pediatric hematological malignancies has proven to be a safe and promising strategy (Alatrash et al., 2016; Versluys et al., 2021). Similar as fludarabine, clofarabine is a purine analogue and a prodrug that is converted intracellularly to its active metabolite clofarabine-5'-triphosphate. This metabolite inhibits DNA polymerase-α, resulting in inhibition of DNA synthesis and repair. Furthermore, it disrupts mitochondrial membrane integrity, leading to apoptosis (Bonate et al., 2006). Excretion is predominantly through the kidneys. Very recently, the pharmacokinetics of Clo in pediatric HSCT recipients have been characterized by two groups (Wang et al., 2019; Nijstad et al., 2021). Bodyweight, age and renal function were covariates influencing clofarabine variability in clearance. Exposure-response relationships between clofarabine and clinical outcome have not been published so far.

Thiotepa

Thiotepa is an alkylating drug that is often combined with Treo and Flu or Bu and Flu in a myeloablative regimen. It is given in a dose of 8–10 mg/kg, (usually 8 mg/kg once or 5 mg/kg for 2 days). Because of its highly lipophilic nature and therefore its ability to cross the blood brain barrier, the addition of thiotepa not only adds myeloablative ability, but may also be beneficial in diseases with central nervous system involvement (Naik et al., 2020). Thiotepa is quickly metabolized in the liver into the active metabolite triethylene phophoramide (TEPA), which has a comparable alkylating activity as thiotepa. By cross-linking of DNA strands, these compounds inhibit DNA, RNA and protein synthesis. Thiotepa and TEPA are eliminated in urine, but also dermally via sweat (Horn et al., 1989). The pharmacokinetics of thiotepa has been studied in adults and children, but not in the allogeneic HSCT setting (Heideman et al., 1989; Huitema et al., 2001; Kondo et al., 2019).

SEROTHERAPY

ATG

Serotherapy with rabbit anti-thymocyte globulin (ATG) or anti-T lymphocyte globulin (ATLG) is often added to the conditioning regimen in pediatric allogeneic HSCT for prophylaxis against GvHD and graft rejection. ATG is a rabbit polyclonal IgG that is produced by the immunization of rabbits with human thymocytes (Thymoglobulin®, Sanofi Genzyme), whereas ATLG is generated upon immunization with the Jurkat T-cell line (Grafalon®, Neovii Pharmaceuticals AG). Both ATG and ATLG contain antibodies recognizing antigens expressed on the surface of many immune and non-immune cells, and several mechanisms by which ATG/ATLG eliminates these targeted cells are described, including inducing apoptosis, complement-dependent lysis or NK-cell mediated lysis (Mohty 2007). Due to the differences in the manufacturing of both products, the lymphodepleting capacity of both brands is not the same. This is reflected in the total dosage given, which varies in the pediatric setting for ATG between 4.5 and 10 mg/kg while for ATLG it is much higher (15–45 mg/kg). The fraction that is capable of lymphocyte binding is also described as active ATG/ATLG and is only a minor part of the total rabbit IgG (total ATG/ATLG) dosage. The lympholytic level of active ATG/ATLG is 1 AU/mL (Waller et al., 2003). ATG/ATLG is given i.v. and the total dosage is often divided over 3–4 days. As for all antibodies, target binding is besides the main mechanism of action also one of the main clearance mechanisms of ATG/ATLG together with non-specific degradation. A third clearance method, leading to rapid elimination of ATG/ATLG, may occur when anti-drug-antibodies (anti-ATG/ATLG) are developed (Jol-van der Zijde et al., 2012). The pharmacokinetics and–dynamics (PD) of ATG in the pediatric HSCT setting have been described, however only in a limited number of studies (Call et al., 2009; Admiraal et al., 2015a; Admiraal et al., 2015b; Admiraal et al., 2016). Interindividual variability for linear clearance is reported to be between 50% and 86%, with body weight and absolute lymphocytes number pre-ATG as important covariates (Call et al., 2009; Admiraal et al., 2015b). For ATLG, no population PK models have been published so far, and knowledge about its PK and PD is only obtained from a few studies investigating concentration-time curves (Oostenbrink et al., 2019; Vogelsang

TABLE 4 | Reported associations of pharmacokinetic parameters of ATG and clinical outcomes.

First author, year	*n*	Age, median (range)	Diagnosis	Regimen	Dose ATG	Major findings
Call et al. (2009)	13	10 (2–16)	AML: 4 (31%) ALL: 3 (23%) CML: 3 (23%) JCML: 2 (15%) MDS: 1 (8%)	TBI/Thio/CY	Thymoglobulin 10 mg/kg, administered as 1 mg/kg on day -4 and 3 mg/kg/day on days -3 to −1	Weight-based dosing regimen (total dose 10 mg/kg) of Thymoglobulin was effective and well tolerated by all patients. None of the patients developed grade III-IV aGvHD.
Admiraal et al. (2015a)	251	6.2 (0.2–22.7)	Malignancy: 116 (46%) IEI: 51 (20%) BMF:15 (6%) Non-malignant: 69 (27%)	RIC MAC – chemo MAC - TBI	Thymoglobulin <9 mg/kg 4% 9–11 mg/kg 94% >11 mg/kg 2% Day start ATG -5, dose divided over 4 days	Individualized dosing of ATG could result in improved outcomes. For the CB group, AUC ≥20 AU × day/mL decreased immune reconstitution in CB, but decreased immune reconstitution was noted only if AUC ≥100 AU × day/mL in BM and PB. Successful immune reconstitution by day 100 was associated with increased OS. An AUC before HSCT of ≥40 AU × day/mL resulted in a lower incidence of aGvHD, cGvHD and graft failure compared with an AUC <40 AU × day/mL.
Admiraal et al. (2016)[a]	137	7.4 (0.2–22.7)	ALL: 22 (16%) AML: 30 (22%) Lymphoma: 4 (3%) IEI: 33 (24%) BMF: 7 (5%) Benign non-IEI (41 (30%)	Bu-Flu Bu-Flu-Clo TBI based Cy-Flu	Thymoglobulin Before 2010 10 mg/kg Day start ATG -5, dose divided over 4 days After 2010 <40 kg: 10 mg/kg >40 kg: 7.5 mg/kg Day start ATG -9, dose divided over 4 days	Low ATG exposure (AUC <16 AU[a]day/mL) was the best predictor for CD + T cell recovery in CB transplant. Patients with a high AUC had a significantly lower EFS compared to low exposure or without ATG. Every 10-point increase in ATG exposure resulted in 5% lower survival probability. Patients receiving ATG had a significantly lower incidence of aGvHD (III-IV) compared with those not receiving ATG (HR, 0.27; 95% CI, 0.08–0.86; $p = 0.027$).
Oostenbrink et al. (2019)	58 42 Thymoglobulin 16 Grafalon	9 (1–18) 6 (1–17)	ALL: 33 (57%) AML: 25 (43%)	Chemo + TBI Chemo	Thymoglobulin 8.7 (6.0–10.5) mg/kg Grafalon 53 (45–60) mg/kg	Active ATG of both ATG products was cleared at different rates, more variability in the Thymoglobulin treated group. Patients treated with Grafalon had a median level of 27.9 AU/mL and with Thymoglobulin 10.6 AU/mL at day 0. Three weeks after HSCT, 15/16 Grafalon patients had an active ATG level <1 AU/mL while 17/42 Thymoglobulin patients had still active ATG levels above this threshold. For Thymoglobulin, exposure to ATG was significantly higher with 10 mg/kg compared to 6–8 mg/kg and was associated with delayed immune recovery. Occurrence of aGvHD (grade III–IV) was highest in the Thymoglobulin low dosage group.
Vogelsang et al. (2020)	32 22 Thymoglobulin 10 Grafalon	5.3 (0.1–17.3) 13.7 (1.5–17.2)	Non-malignant: 22 (69%) Malignant: 10 (31%)	TreoFluThio NMA TBI/VP-16	Thymoglobulin 4.5–10 mg/kg Grafalon 30–60 mg/kg	Grafalon and Thymoglobulin show different pharmacological and immunological impact in children. Active plasma levels for Grafalon were less variable compared to Thymoglobulin. Median active peak plasma levels were 77.9 µg/ml for Grafalon and 8.11 µg/ml for Thymoglobulin. Incidence of GvHD was similar for patients with high (above the median) or low (below the median) exposure. Immune recovery of total leucocytes and T cells was delayed in patients with high ATG exposure. No significant difference was found for overall survival.

[a]*66 patients (48%) were included in the previous analysis of 2015. (J)CML: (juvenile) chronic myeloid leukemia, RIC, reduced intensity conditioning; MAC, myeloablative conditioning.*

et al., 2020). **Table 4** summarizes the reports of ATG PK associated with outcome in pediatric patients.

Call et al. evaluated the pharmacokinetics of total and active ATG Thymoglobulin in a prospective trial with 13 children [median age 10 years (range 2–16)] who underwent an unrelated donor HSCT with non-T-cell–depleted bone marrow grafts for hematologic malignancies. There were no occurrences of grade III–IV acute GvHD and none of the patients had serious infections following transplantation. Call et al. concluded that the use of a 10 mg/kg dose of ATG in children with hematologic malignancies can be administered without increasing the risk of rejection, or serious infection in pediatric patients with a low rate of GvHD (Call et al., 2009).

Admiraal et al. described in 2015 the pharmacokinetics of ATG in a much larger patient cohort, including 267 HSCT patients from two study centers (Admiraal et al., 2015b). With the use of a population PK model, pharmacokinetic endpoints (i.e., AUC) were calculated and studied in relation to the clinical outcome measures of the patients, to determine the therapeutic window and the optimal active Thymoglobulin exposure. The results of this analysis were published in a separate publication. Successful immune reconstitution, defined as $CD4^+$ T cells $>0.05 \times 10^9$ cells/L within 100 days, was lower in patients with a higher AUC post-HSCT (for patients receiving a cord blood graft ≥20 AU x day/mL, and for patients with a bone marrow or peripheral blood stem cell graft ≥100 AU x day/mL) and correlated with TRM and viral reactivations. A lower risk for graft failure and acute GvHD was seen in patients with an AUC pre-HSCT of ≥40 AU x day/mL compared to patients with an AUC less than 40 AU x day/mL (Admiraal et al., 2015a).

Based on these two publications, *Admiraal* et al. developed an individualized dosing regimen taken body weight, baseline lymphocytes pre-ATG and stem cell source for each patient into account. The effectiveness of this individualized dosing regimen was assessed in a cohort of 137 children receiving a cord blood graft and in a prospective, open-label, phase II clinical trial including 58 patients and 112 historical controls. Chance of successful immune recovery was significantly increased in the individualized dosing group in both studies, but no differences were seen between patients with low or high ATG exposure for severe acute GvHD (grade III-IV) and failure of the graft (Admiraal et al., 2016; Admiraal et al., 2022).

Concluding from the above-mentioned publications, using an individualized dosing regimen for ATG could improve patient outcome. Both ATG population PK models described so far showed large interpatient variability, which could be minimized by applying TDM. However, TDM for ATG at this moment is time-consuming, expensive and the assays to measure active ATG are to our knowledge performed only at a few centers worldwide. For ATLG, both studies assessing the PK/PD mentioned differences in the pharmacological and immunological impact between ATLG and ATG (Oostenbrink et al., 2019; Vogelsang et al., 2020). The next step would be to assess whether there is a relationship between ATLG drug concentrations and clinical and immunological outcome in order to determine if TDM could be useful.

Alemtuzumab

Besides ATG/ATLG, an alternative lymphodepleting drug that is often used as serotherapy is Alemtuzumab (Campath®). Alemtuzumab is a humanized monoclonal antibody targeting CD52, which is expressed on the surface of various hematopoietic cells. Alemtuzumab can be given subcutaneously or intravenously for *in vivo* depletion of immune cells, but the use of alemtuzumab for *in vitro* T-cell depletion, by adding alemtuzumab to the graft before infusion, has also been described (Barge et al., 2006; von dem Borne et al., 2006). The total dose given in children usually varies between 0.5 and 1.5 mg/kg, however for some diseases (such as hemophagocytic lymphohistiocytosis (HLH)) much higher dosages are being used. The lytic level of alemtuzumab in humans is presumed to be near 0.1–0.16 μg/ml (Marsh et al., 2016; Riechmann et al., 1988). Based on the few studies analyzing alemtuzumab PK and PD in the pediatric HSCT setting (see for an overview **Table 5**), a difference between ATG and alemtuzumab PK is clearance, both linear and saturable, which is lower for alemtuzumab. Furthermore, the interindividual variability for alemtuzumab clearance is described to be much higher than for ATG (Admiraal et al., 2019).

In 2016 *Marsh* et al. reported their recommended therapeutic range of alemtuzumab at the day of transplantation of 0.2–0.4 μg/ml. They investigated the relation between alemtuzumab concentrations at day HSCT with several clinical outcome parameters in 105 (mainly) pediatric patients [median age 4.7 years (range 0.3–27.2)]. A level ≤0.15 μg/ml at the day of transplantation was associated with a lower incidence of mixed chimerism, however also led to a higher probability of acute GvHD. For T-cell recovery at day 100 after transplantation, day 0 alemtuzumab levels ≥0.57 μg/ml were correlated with lower T-cell counts (Marsh et al., 2016).

Bhoopalan et al. described the pharmacokinetics of alemtuzumab in 13 patients [median age 15.5 years (range 3–21)] with haploidentical HSCT. Alemtuzumab was given subcutaneous from days -14 to -11 using a BSA-based dosing, except for five patients who received intravenous dosing for their last two doses. Patients received a test dose of 2 mg on day -4 followed by a total dose of 45 mg/m^2 in escalating doses of 10, 15 and 20 mg/m^2 on days -13, -12 and -11. Ten of 13 patients had detectable alemtuzumab levels at week 4 after HSCT. Median AUC was 117.1 (range 28.1–165.4) μg*day/mL. No significant correlation was found between AUC and clinical outcome parameters such as overall survival, engraftment, lymphocyte counts and GvHD (Bhoopalan et al., 2020).

The publication of *Dong* et al. described the results of a patient cohort of 29 patients with non-malignant disease undergoing HSCT [median age 6.4 years (range 0.28–21.4)], who were enrolled in two different studies (Marsh et al., 2017; Arnold et al., 2021). Alemtuzumab was given as a total dose of 1 mg/kg divided over days -14 to -10 in study 1 ($n = 17$) and in study 2 as a total dose of 0.5–0.6 mg/kg. For patients in study two who were expected to clear alemtuzumab by day of HSCT to ≤0.15 μg/ml, a top up dose was calculated and given either on day -3 or day -1. The authors concluded that the currently used dosing per kilogram strategy causes uneven exposure of alemtuzumab across different weight and age cohorts. They propose an

TABLE 5 | Reported associations of pharmacokinetic parameters of alemtuzumab and clinical outcomes.

First author, year	*n*	Age, median (range)	Diagnosis	Regimen	Dose alemtuzumab	Major findings
Marsh et al. (2016)	105	4.7 (0.3–27.2)	HLH: 54 (51%) BMF: 13 (12%) (S)CID: 17 (17%) CGD: 5 (5%) Metabolic: 4 (4%) SCD: 2 (2%) Other: 10 (10%)	FluMel	Distal dosing 3/10/15/20 mg over days -22 to −19 <10 kg: 3/10/10/10 mg Intermediate dosing 1 mg/kg over days -14 to −10 Proximal dosing 3/10/15/20 mg or 1 mg/kg starting at day -12 or closer to HSCT	Peritransplant alemtuzumab levels have impact on the incidence of aGvHD, mixed chimerism and lymphocyte recovery. 18% developed GvHD with alemtuzumab levels ≥0.16 μg/ml, 68% in patients with levels ≤0.15 μg/ml. Mixed chimerism occurred in 21% of the patients with ≤0.15 μg/ml, in 42% with levels between 0.16 and 4.35 μg/ml and in 100% if levels were above 4.35 μg/ml. Patients with levels ≥0.57 μg/ml had lower T-cell counts at day 100. A therapeutic range at day 0 of 0.2–0.4 μg/ml is recommended.
Bhoopalan et al. (2020)	13	15.5 (3–21)	ALL: 8 (61.5%) AML: 3 (23.1%) CML: 1 (7.7%) Therapy-related MDS: 1 (7.7%)	FluThioMelRitux	Subcutaneous n = 8 Subcutaneous and intravenous n = 5 Test dose of 2 mg/m^2 plus total dose of 45 mg/m^2 Dose given from days -14 to -11	BSA-based dosing of alemtuzumab is feasible in pediatric haplo-transplantation patients. AUC of alemtuzumab did not have a significant relation with OS, engraftment, IR and GvHD.
Dong et al. (2021)	29	6.4 (0.28–21.4)	HLH: 13 (45%) CGD: 2 (7%) IPEX: 2 (7%) SAA: 5 (17%) (S)CID: 3 (10%) Other: 4 (14%)	FluMel	Subcutaneous 0.5–0.6 mg/kg 1 mg/kg Dose given days -14 to −10 or -14 – -12 Top-up dose was given either on day -3 or -1	Proposed therapeutic range of 0.15–0.6 μg/ml on the day of transplantation is associated with better HSCT outcomes (less aGVHD and improved lymphocyte recovery). To achieve this optimal level allometric or BSA-based dosing is advised. Top-up dose on day -3 for patients who, based on individualized PK estimation, will have a concentration <0.15 μg/ml on the day of transplantation is recommended.

HLH, hemophagocytic lymphohistiocytosis; (S)CID, (severe) combined immune deficiency; CGD, chronic granulomatous disease; SCD, sickle cell disease; IPEX, immunodysregulation polyendocrinopathy enteropathy X-linked syndrome; SAA, severe aplastic anemia; Ritux, rituximab.

allometric- or body surface area- based starting dosing regimen in combination with TDM to achieve a recommended therapeutic range of 0.15–0.6 μg/ml on the day of transplantation, which is associated with better HSCT outcomes (less aGVHD and improved lymphocyte recovery) (Dong et al., 2021).

Altogether, based on the above-mentioned publications, it can be concluded that, as for ATG, a more individualized dosing strategy of alemtuzumab could improve HSCT outcomes of patients. Since there are only a few studies published about alemtuzumab PK and PD in pediatric patients, the need for further PK&PD analyses is urgent. Currently, an international multicenter observational trial (ARTIC study) is open for patient inclusion. The aim of this study is to evaluate current clinical practice and develop a population PK model and explore the exposure response for alemtuzumab in children with non-malignant diseases. This model will be used to provide important additional information on alemtuzumab treatments and might support the need for therapeutic drug monitoring.

DISCUSSION

There is a certain set of criteria to determine which drugs are suitable for TDM. The drug should have a narrow therapeutic index and considerable pharmacokinetic variability between patients. Importantly, there should be a reasonable relationship between plasma concentrations and clinical effects, e.g., efficacy or toxicity. The dose cannot be easily optimized by clinical observation and last, but certainly not less important, a bioanalytical assay should be available. The main focus of this review was to assess whether there is a reasonable relationship between plasma concentrations of the most commonly used conditioning agents prior to pediatric HSCT and clinical effects. Taken all the available evidence into account, Bu fulfills all criteria for TDM at the moment which is also reflected in various study protocols and guidelines (Lankester et al., 2021; Peters et al., 2021). Refinement of exposure targets could further improve results for specific subgroups. For Treo, there seems to be some relationship with clinical outcome, however contrasting results are reported. High exposure increases the risk of skin toxicity and, in one study, an association with mortality is seen (van der Stoep et al., 2017; Chiesa et al., 2020; van der Stoep et al., 2021). A cumulative target concentration of 4,800 mg*h/L is suggested in this particular study. In two other studies, no relationship was seen with EFS and OS. For now, the evidence is not convincingly enough to implement Treo TDM for all pediatric patients undergoing HSCT. For Flu, the same arguments can be made. Although a large retrospective study showed a relationship of Flu exposure and EFS, and suggested an optimal target of 15–25 mg*h/L, other studies did not find a clear relationship (Ivaturi et al., 2017; Mohanan et al., 2017; Chung et al., 2018; Langenhorst et al.,

2019). More research on Flu PK/PD may provide further evidence whether Flu TDM is of added value in routine clinical practice. For ATG, almost all studies that studied clinical outcome in relation to exposure (pre- and post HSCT) are done with Thymoglobulin. Delayed immune reconstitution was seen in patients with high (post-HSCT) exposure in several studies, which means that patients could potentially benefit from individualized dosing of ATG (Admiraal et al., 2015a; Admiraal et al., 2016). For ATLG, this still needs to be determined, but a correlation between exposure and outcome seems most likely. High alemtuzumab levels also seem to be correlated with delayed immune reconstitution, but data is still scarce, and more research is needed in order to define a therapeutic target and an optimal dosing regimen (Marsh et al., 2016; Bhoopalan et al., 2020; Arnold et al., 2021; Dong et al., 2021).

While most of the transplant community is convinced that Bu TDM is necessary, it is still not implemented in every transplantation center, since not every center has a bioanalytical assay available, and logistics of shipping samples is challenging or costly. The available population PK models with identified covariates could help centers define individual Bu doses to achieve exposure within the target range without using TDM. However, given the narrow therapeutic index of Bu and the fact that there is still considerable unexplained variability in Bu PK, the use of population PK models in combination with TDM would be the best option. For ATG, the evidence is suggesting that individualized, PK-guided dosing of ATG improves patient outcome, but due to the time-consuming and expensive assays that are currently available, TDM will probably not be an option for most centers at short notice (Keogh et al., 2022). Easy to operate and less expensive bioanalytical assays are warranted to overcome this hurdle. Because the therapeutic index of ATG is likely to be much wider, using population PK models to estimate individual ATG doses would be a feasible option for most transplant centers.

When interpreting the data of all these studies, there are some limitations that must be kept in mind. Some studies only report small patient numbers, which makes it difficult to assess the possible influence of transplantation related covariates on outcome. Also, different combinations of conditioning agents and the addition of serotherapy to the regimen are major factors that influence outcome. Furthermore, due to the constantly evolving field and improvement of the transplant procedures over time, some of the regimens and procedures in the reported studies are already amended or revised/renewed.

As much as we can limit the toxicities of chemo-based conditioning, not all side effects are avoidable. Serious concerns about the long-term effects have driven the search for alternative conditioning regimens. Leukocytolytic monoclonal antibodies can provide a potential alternative to achieve myelosuppression and immunosuppression without the concomitant non-hematological toxicity of chemotherapy. Anti-CD45 monoclonal antibodies target CD45 that are selectively expressed on all leukocytes and hematopoietic progenitors. In a study with high-risk pediatric patients with different inborn errors of immunity (IEI), conditioning with anti-CD45 antibodies in combinations with alemtuzumab, fludarabine and cyclophosphamide resulted in myeloid and lymphoid engraftment (Straathof et al., 2009). Antibodies conjugated with radionuclides, known as radioimmunotherapy, can deliver radiotherapy directly to the surface of the targeted cells. Normal tissue gets spared, making this kind of conditioning a potentially less toxic alternative (Schulz et al., 2011). Promising results with anti-CD117 monoclonal antibody as an alternative for traditional conditioning can possibly change the way we prepare patients for HSCT in the future (Kwon et al., 2019). For an increasing number of pediatric diseases, alternative treatment strategies have become available, such as gene therapy. However, while these therapies are very promising, allogeneic HSCT with the use of "regular" conditioning regimens will still be the first (and sometimes only) option in many diseases. More research regarding the late effects of conditioning is therefore crucial to further optimize combinations and dosing of conditioning regimens.

AUTHOR CONTRIBUTIONS

MS and LO prepared the manuscript; all authors reviewed and approved the final version of the manuscript.

REFERENCES

Admiraal, R., Jol-van der Zijde, C. M., Furtado Silva, J. M., Knibbe, C. A. J., Lankester, A. C., Boelens, J. J., et al. (2019). Population Pharmacokinetics of Alemtuzumab (Campath) in Pediatric Hematopoietic Cell Transplantation: Towards Individualized Dosing to Improve Outcome. *Clin. Pharmacokinet.* 58, 1609–1620. doi:10.1007/s40262-019-00782-0

Admiraal, R., Lindemans, C. A., van Kesteren, C., Bierings, M. B., Versluijs, A. B., Nierkens, S., et al. (2016). Excellent T-Cell Reconstitution and Survival Depend on Low ATG Exposure after Pediatric Cord Blood Transplantation. *Blood* 128, 2734–2741. doi:10.1182/blood-2016-06-721936

Admiraal, R., van Kesteren, C., Jol-van der Zijde, C. M., Lankester, A. C., Bierings, M. B., Egberts, T. C., et al. (2015a). Association between Anti-thymocyte Globulin Exposure and CD4+ Immune Reconstitution in Paediatric Haemopoietic Cell Transplantation: a Multicentre, Retrospective Pharmacodynamic Cohort Analysis. *Lancet Haematol.* 2, e194–203. doi:10.1016/S2352-3026(15)00045-9

Admiraal, R., van Kesteren, C., Jol-van der Zijde, C. M., van Tol, M. J., Bartelink, I. H., Bredius, R. G., et al. (2015b). Population Pharmacokinetic Modeling of Thymoglobulin(®) in Children Receiving Allogeneic-Hematopoietic Cell Transplantation: towards Improved Survival through Individualized Dosing. *Clin. Pharmacokinet.* 54, 435–446. doi:10.1007/s40262-014-0214-6

Admiraal, R., Nierkens, S., Bierings, M. B., Bredius, R. G. M., van Vliet, I., Jiang, Y., et al. (2022). Individualised Dosing of Anti-Thymocyte Globulin in Paediatric Unrelated Allogeneic Haematopoietic Stem-Cell Transplantation (PARACHUTE): A Single-Arm, Phase 2 Clinical Trial. *Lancet Haematology* 9, e111–e120. doi:10.1016/S2352-3026(21)00375-6

Alatrash, G., Thall, P. F., Valdez, B. C., Fox, P. S., Ning, J., Garber, H. R., et al. (2016). Long-Term Outcomes after Treatment with Clofarabine ± Fludarabine with Once-Daily Intravenous Busulfan as Pretransplant Conditioning Therapy for Advanced Myeloid Leukemia and Myelodysplastic Syndrome. *Biol. Blood Marrow Transpl.* 22, 1792–1800. doi:10.1016/j.bbmt.2016.06.023

Ansari, M., Théoret, Y., Rezgui, M. A., Peters, C., Mezziani, S., Desjean, C., et al. (2014). Association between Busulfan Exposure and Outcome in Children Receiving Intravenous Busulfan before Hematopoietic Stem Cell

Transplantation. *Ther. Drug Monit.* 36, 93–99. doi:10.1097/FTD.0b013e3182a04fc7

Arnold, D. E., Emoto, C., Fukuda, T., Dong, M., Vinks, A. A., Lane, A., et al. (2021). A Prospective Pilot Study of a Novel Alemtuzumab Target Concentration Intervention Strategy. *Bone Marrow Transplant.* 56, 3029. doi:10.1038/s41409-021-01460-1

Bader, P., Niethammer, D., Willasch, A., Kreyenberg, H., and Klingebiel, T. (2005). How and when Should We Monitor Chimerism after Allogeneic Stem Cell Transplantation? *Bone Marrow Transpl.* 35, 107–119. doi:10.1038/sj.bmt.1704715

Barge, R. M., Starrenburg, C. W., Falkenburg, J. H., Fibbe, W. E., Marijt, E. W., and Willemze, R. (2006). Long-term Follow-Up of Myeloablative Allogeneic Stem Cell Transplantation Using Campath "in the Bag" as T-Cell Depletion: the Leiden Experience. *Bone Marrow Transpl.* 37, 1129–1134. doi:10.1038/sj.bmt.1705385

Baron, F., Mohty, M., Blaise, D., Socié, G., Labopin, M., Esteve, J., et al. (2017). Anti-thymocyte Globulin as Graft-Versus-Host Disease Prevention in the Setting of Allogeneic Peripheral Blood Stem Cell Transplantation: a Review from the Acute Leukemia Working Party of the European Society for Blood and Marrow Transplantation. *Haematologica* 102, 224–234. doi:10.3324/haematol.2016.148510

Bartelink, I. H., Boelens, J. J., Bredius, R. G., Egberts, A. C., Wang, C., Bierings, M. B., et al. (2012). Body Weight-dependent Pharmacokinetics of Busulfan in Paediatric Haematopoietic Stem Cell Transplantation Patients: towards Individualized Dosing. *Clin. Pharmacokinet.* 51, 331–345. doi:10.2165/11598180-000000000-00000

Bartelink, I. H., Bredius, R. G., Belitser, S. V., Suttorp, M. M., Bierings, M., Knibbe, C. A., et al. (2009). Association between Busulfan Exposure and Outcome in Children Receiving Intravenous Busulfan before Hematologic Stem Cell Transplantation. *Biol. Blood Marrow Transpl.* 15, 231–241. doi:10.1016/j.bbmt.2008.11.022

Bartelink, I. H., Lalmohamed, A., van Reij, E. M., Dvorak, C. C., Savic, R. M., Zwaveling, J., et al. (2016). Association of Busulfan Exposure with Survival and Toxicity after Haemopoietic Cell Transplantation in Children and Young Adults: a Multicentre, Retrospective Cohort Analysis. *Lancet Haematol.* 3, e526–e536. doi:10.1016/S2352-3026(16)30114-4

Ben Hassine, K., Powys, M., Svec, P., Pozdechova, M., Versluys, B., Ansari, M., et al. (2021). Total Body Irradiation Forever? Optimising Chemotherapeutic Options for Irradiation-free Conditioning for Paediatric Acute Lymphoblastic Leukaemia. *Front. Pediatr.* 9, 775485. doi:10.3389/fped.2021.775485

Ben-Barouch, S., Cohen, O., Vidal, L., Avivi, I., and Ram, R. (2016). Busulfan Fludarabine vs Busulfan Cyclophosphamide as a Preparative Regimen before Allogeneic Hematopoietic Cell Transplantation: Systematic Review and Meta-Analysis. *Bone Marrow Transpl.* 51, 232–240. doi:10.1038/bmt.2015.238

Benadiba, J., Ansari, M., Krajinovic, M., Vachon, M. F., Duval, M., Teira, P., et al. (2018). Pharmacokinetics-adapted Busulfan-Based Myeloablative Conditioning before Unrelated Umbilical Cord Blood Transplantation for Myeloid Malignancies in Children. *PLoS One* 13, e0193862. doi:10.1371/journal.pone.0193862

Bhoopalan, S. V., Cross, S. J., Panetta, J. C., and Triplett, B. M. (2020). Pharmacokinetics of Alemtuzumab in Pediatric Patients Undergoing *Ex Vivo* T-Cell-Depleted Haploidentical Hematopoietic Cell Transplantation. *Cancer Chemother. Pharmacol.* 86, 711–717. doi:10.1007/s00280-020-04160-7

Bonate, P. L., Arthaud, L., Cantrell, W. R., Jr., Stephenson, K., Secrist, J. A., 3rd, and Weitman, S. (2006). Discovery and Development of Clofarabine: a Nucleoside Analogue for Treating Cancer. *Nat. Rev. Drug Discov.* 5, 855–863. doi:10.1038/nrd2055

Call, S. K., Kasow, K. A., Barfield, R., Madden, R., Leung, W., Horwitz, E., et al. (2009). Total and Active Rabbit Antithymocyte Globulin (rATG; Thymoglobulin) Pharmacokinetics in Pediatric Patients Undergoing Unrelated Donor Bone Marrow Transplantation. *Biol. Blood Marrow Transpl.* 15, 274–278. doi:10.1016/j.bbmt.2008.11.027

Chiesa, R., Standing, J. F., Winter, R., Nademi, Z., Chu, J., Pinner, D., et al. (2020). Proposed Therapeutic Range of Treosulfan in Reduced Toxicity Pediatric Allogeneic Hematopoietic Stem Cell Transplant Conditioning: Results from a Prospective Trial. *Clin. Pharmacol. Ther.* 108, 264–273. doi:10.1002/cpt.1715

Chung, H., Hong, K. T., Lee, J. W., Rhee, S. J., Kim, S., Yoon, S. H., et al. (2018). Pharmacokinetics of Fludarabine and its Association with Clinical Outcomes in Paediatric Haematopoietic Stem Cell Transplantation Patients. *Bone Marrow Transplant.* 54, 284. doi:10.1038/s41409-018-0260-z

Ciurea, S. O., and Andersson, B. S. (2009). Busulfan in Hematopoietic Stem Cell Transplantation. *Biol. Blood Marrow Transpl.* 15, 523–536. doi:10.1016/j.bbmt.2008.12.489

Copelan, E. A. (2006). Hematopoietic Stem-Cell Transplantation. *N. Engl. J. Med.* 354, 1813–1826. doi:10.1056/nejmra052638

Darwich, A. S., Polasek, T. M., Aronson, J. K., Ogungbenro, K., Wright, D. F. B., Achour, B., et al. (2021). Model-Informed Precision Dosing: Background, Requirements, Validation, Implementation, and Forward Trajectory of Individualizing Drug Therapy. *Annu. Rev. Pharmacol. Toxicol.* 61, 225–245. doi:10.1146/annurev-pharmtox-033020-113257

Diesch-Furlanetto, T., Gabriel, M., Zajac-Spychala, O., Cattoni, A., Hoeben, B. A. W., and Balduzzi, A. (2021). Late Effects after Haematopoietic Stem Cell Transplantation in ALL, Long-Term Follow-Up and Transition: A Step into Adult Life. *Front. Pediatr.* 9, 773895. doi:10.3389/fped.2021.773895

Dong, M., Emoto, C., Fukuda, T., Arnold, D. E., Mehta, P. A., Marsh, R. A., et al. (2021). Model-informed Precision Dosing for Alemtuzumab in Paediatric and Young Adult Patients Undergoing Allogeneic Haematopoietic Cell Transplantation. *Br. J. Clin. Pharmacol.* 88, 248. doi:10.1111/bcp.14955

Gandhi, V., and Plunkett, W. (2002). Cellular and Clinical Pharmacology of Fludarabine. *Clin. Pharmacokinet.* 41, 93–103. doi:10.2165/00003088-200241020-00002

Gaziev, J., Nguyen, L., Puozzo, C., Mozzi, A. F., Casella, M., Perrone Donnorso, M., et al. (2010). Novel Pharmacokinetic Behavior of Intravenous Busulfan in Children with Thalassemia Undergoing Hematopoietic Stem Cell Transplantation: a Prospective Evaluation of Pharmacokinetic and Pharmacodynamic Profile with Therapeutic Drug Monitoring. *Blood* 115, 4597–4604. doi:10.1182/blood-2010-01-265405

Hartley, J. A., O'Hare, C. C., and Baumgart, J. (1999). DNA Alkylation and Interstrand Cross-Linking by Treosulfan. *Br. J. Cancer* 79, 264–266. doi:10.1038/sj.bjc.6690043

Heideman, R. L., Cole, D. E., Balis, F., Sato, J., Reaman, G. H., Packer, R. J., et al. (1989). Phase I and Pharmacokinetic Evaluation of Thiotepa in the Cerebrospinal Fluid and Plasma of Pediatric Patients: Evidence for Dose-dependent Plasma Clearance of Thiotepa. *Cancer Res.* 49, 736–741.

Hilger, R. A., Harstrick, A., Eberhardt, W., Oberhoff, C., Skorzec, M., Baumgart, J., et al. (1998). Clinical Pharmacokinetics of Intravenous Treosulfan in Patients with Advanced Solid Tumors. *Cancer Chemother. Pharmacol.* 42, 99–104. doi:10.1007/s002800050791

Horn, T. D., Beveridge, R. A., Egorin, M. J., Abeloff, M. D., and Hood, A. F. (1989). Observations and Proposed Mechanism of N,N',N''-triethylenethiophosphoramide (Thiotepa)-induced Hyperpigmentation. *Arch. Dermatol.* 125, 524–527. doi:10.1001/archderm.125.4.524

Huitema, A. D., Mathôt, R. A., Tibben, M. M., Schellens, J. H., Rodenhuis, S., and Beijnen, J. H. (2001). Population Pharmacokinetics of thioTEPA and its Active Metabolite TEPA in Patients Undergoing High-Dose Chemotherapy. *Br. J. Clin. Pharmacol.* 51, 61–70. doi:10.1046/j.1365-2125.2001.01301.x

Ivaturi, V., Dvorak, C. C., Chan, D., Liu, T., Cowan, M. J., Wahlstrom, J., et al. (2017). Pharmacokinetics and Model-Based Dosing to Optimize Fludarabine Therapy in Pediatric Hematopoietic Cell Transplant Recipients. *Biol. Blood Marrow Transpl.* 23, 1701–1713. doi:10.1016/j.bbmt.2017.06.021

Jol-van der Zijde, C. M., Bredius, R. G., Jansen-Hoogendijk, A. M., Raaijmakers, S., Egeler, R. M., Lankester, A. C., et al. (2012). IgG Antibodies to ATG Early after Pediatric Hematopoietic SCT Increase the Risk of Acute GVHD. *Bone Marrow Transpl.* 47, 360–368. doi:10.1038/bmt.2011.166

Kawazoe, A., Funaki, T., and Kim, S. (2018). Population Pharmacokinetic Analysis of Busulfan in Japanese Pediatric and Adult HCT Patients. *J. Clin. Pharmacol.* 58, 1196–1204. doi:10.1002/jcph.1120

Kearns, G. L., Abdel-Rahman, S. M., Alander, S. W., Blowey, D. L., Leeder, J. S., and Kauffman, R. E. (2003). Developmental Pharmacology-Ddrug Disposition, Action, and Therapy in Infants and Children. *N. Engl. J. Med.* 349, 1157–1167. doi:10.1056/NEJMra035092

Keogh, S. J., Dalle, J. H., Admiraal, R., and Pulsipher, M. A. (2022). Serotherapy as Graft-Versus-Host Disease Prophylaxis in Haematopoietic Stem Cell Transplantation for Acute Lymphoblastic Leukemia. *Front. Ped.* 9, 805189. doi:10.3389/fped.2021.805189

Kondo, E., Ikeda, T., Goto, H., Nishikori, M., Maeda, N., Matsumoto, K., et al. (2019). Pharmacokinetics of Thiotepa in High-Dose Regimens for Autologous Hematopoietic Stem Cell Transplant in Japanese Patients with Pediatric Tumors or Adult Lymphoma. *Cancer Chemother. Pharmacol.* 84, 849–860. doi:10.1007/s00280-019-03914-2

Kwon, H. S., Logan, A. C., Chhabra, A., Pang, W. W., Czechowicz, A., Tate, K., et al. (2019). Anti-human CD117 Antibody-Mediated Bone Marrow Niche Clearance in Nonhuman Primates and Humanized NSG Mice. *Blood* 133, 2104–2108. doi:10.1182/blood-2018-06-853879

Langenhorst, J. B., van Kesteren, C., van Maarseveen, E. M., Dorlo, T. P. C., Nierkens, S., Lindemans, C. A., et al. (2019). Fludarabine Exposure in the Conditioning Prior to Allogeneic Hematopoietic Cell Transplantation Predicts Outcomes. *Blood Adv.* 3, 2179–2187. doi:10.1182/bloodadvances.2018029421

Langenhorst, J. B., Dorlo, T. P. C., van Maarseveen, E. M., Nierkens, S., Kuball, J., Boelens, J. J., et al. (2018). Population Pharmacokinetics of Fludarabine in Children and Adults during Conditioning Prior to Allogeneic Hematopoietic Cell Transplantation. *Clin. Pharmacokinet.* 58, 627. doi:10.1007/s40262-018-0715-9

Lankester, A. C., Albert, M. H., Booth, C., Gennery, A. R., Güngör, T., Hönig, M., et al. (2021). EBMT/ESID Inborn Errors Working Party Guidelines for Hematopoietic Stem Cell Transplantation for Inborn Errors of Immunity. *Bone Marrow Transpl.* 56, 2052–2062. doi:10.1038/s41409-021-01378-8

Lawson, R., Staatz, C. E., Fraser, C. J., and Hennig, S. (2021). Review of the Pharmacokinetics and Pharmacodynamics of Intravenous Busulfan in Paediatric Patients. *Clin. Pharmacokinet.* 60, 17–51. doi:10.1007/s40262-020-00947-2

Lee, J. W., Kang, H. J., Lee, S. H., Yu, K. S., Kim, N. H., Yuk, Y. J., et al. (2012). Highly Variable Pharmacokinetics of Once-Daily Intravenous Busulfan when Combined with Fludarabine in Pediatric Patients: Phase I Clinical Study for Determination of Optimal Once-Daily Busulfan Dose Using Pharmacokinetic Modeling. *Biol. Blood Marrow Transpl.* 18, 944–950. doi:10.1016/j.bbmt.2011.11.025

Marsh, R. A., Fukuda, T., Emoto, C., Neumeier, L., Khandelwal, P., Chandra, S., et al. (2017). Pretransplant Absolute Lymphocyte Counts Impact the Pharmacokinetics of Alemtuzumab. *Biol. Blood Marrow Transpl.* 23, 635–641. doi:10.1016/j.bbmt.2017.01.071

Marsh, R. A., Lane, A., Mehta, P. A., Neumeier, L., Jodele, S., Davies, S. M., et al. (2016). Alemtuzumab Levels Impact Acute GVHD, Mixed Chimerism, and Lymphocyte Recovery Following Alemtuzumab, Fludarabine, and Melphalan RIC HCT. *Blood* 127, 503–512. doi:10.1182/blood-2015-07-659672

McCune, J. S., and Bemer, M. J. (2016). Pharmacokinetics, Pharmacodynamics and Pharmacogenomics of Immunosuppressants in Allogeneic Haematopoietic Cell Transplantation: Part I. *Clin. Pharmacokinet.* 55, 525–550. doi:10.1007/s40262-015-0339-2

McCune, J. S., Gibbs, J. P., and Slattery, J. T. (2000). Plasma Concentration Monitoring of Busulfan: Does it Improve Clinical Outcome? *Clin. Pharmacokinet.* 39, 155–165. doi:10.2165/00003088-200039020-00005

McCune, J. S., and Holmberg, L. A. (2009). Busulfan in Hematopoietic Stem Cell Transplant Setting. *Expert Opin. Drug Metab. Toxicol.* 5, 957–969. doi:10.1517/17425250903107764

McCune, J. S., Quinones, C. M., Ritchie, J., Carpenter, P. A., van Maarseveen, E., Yeh, R. F., et al. (2019). Harmonization of Busulfan Plasma Exposure Unit (BPEU): A Community-Initiated Consensus Statement. *Biol. Blood Marrow Transpl.* 25, 1890–1897. doi:10.1016/j.bbmt.2019.05.021

Mohanan, E., Panetta, J. C., Lakshmi, K. M., Edison, E. S., Korula, A., Na, F., et al. (2018). Pharmacokinetics and Pharmacodynamics of Treosulfan in Patients with Thalassemia Major Undergoing Allogeneic Hematopoietic Stem Cell Transplantation. *Clin. Pharmacol. Ther.* 104, 575–583. doi:10.1002/cpt.988

Mohanan, E., Panetta, J. C., Lakshmi, K. M., Edison, E. S., Korula, A., Fouzia, N. A., et al. (2017). Population Pharmacokinetics of Fludarabine in Patients with Aplastic Anemia and Fanconi Anemia Undergoing Allogeneic Hematopoietic Stem Cell Transplantation. *Bone Marrow Transplant.* 52, 977. doi:10.1038/bmt.2017.79

Mohty, M. (2007). Mechanisms of Action of Antithymocyte Globulin: T-Cell Depletion and beyond. *Leukemia* 21, 1387–1394. doi:10.1038/sj.leu.2404683

Nagler, A., and Shimoni, A. (2019) Conditioning. In: *The EBMT Handbook* (ed. by E. Carreras, C. Dufour, M. Mohty, and N. Kroger).

Naik, S., Eckstein, O., Sasa, G., Heslop, H. E., Krance, R. A., Allen, C., et al. (2020). Incorporation of Thiotepa in a Reduced Intensity Conditioning Regimen May Improve Engraftment after Transplant for HLH. *Br. J. Haematol.* 188, e84–e87. doi:10.1111/bjh.16370

Nijstad, A. L., Nierkens, S., Lindemans, C. A., Boelens, J. J., Bierings, M., Versluys, A. B., et al. (2021). Population Pharmacokinetics of Clofarabine for Allogeneic Hematopoietic Cell Transplantation in Paediatric Patients. *Br. J. Clin. Pharmacol.* 87, 3218–3226. doi:10.1111/bcp.14738

Oostenbrink, L. V. E., Jol-van der Zijde, C. M., Kielsen, K., Jansen-Hoogendijk, A. M., Ifversen, M., Müller, K. G., et al. (2019). Differential Elimination of Antithymocyte Globulin of Fresenius and Genzyme Impacts T-Cell Reconstitution after Hematopoietic Stem Cell Transplantation. *Front. Immunol.* 10, 315. doi:10.3389/fimmu.2019.00315

Peters, C., Dalle, J. H., Locatelli, F., Poetschger, U., Sedlacek, P., Buechner, J., et al. (2021). Total Body Irradiation or Chemotherapy Conditioning in Childhood ALL: A Multinational, Randomized, Noninferiority Phase III Study. *J. Clin. Oncol.* 39, 295–307. doi:10.1200/JCO.20.02529

Philippe, M., Neely, M., Rushing, T., Bertrand, Y., Bleyzac, N., and Goutelle, S. (2019). Maximal Concentration of Intravenous Busulfan as a Determinant of Veno-Occlusive Disease: a Pharmacokinetic-Pharmacodynamic Analysis in 293 Hematopoietic Stem Cell Transplanted Children. *Bone Marrow Transpl.* 54, 448–457. doi:10.1038/s41409-018-0281-7

Pierre Fabre Médicament (2017). Busilvex (Busulfan) [Summary of Product Characteristics]. European Medicines Agency. Available at: : https://www.ema.europa.eu/en/documents/product-information/busilvex-epar-product-information_en.pdf Revised (Accessed November 2021.

Riechmann, L., Clark, M., Waldmann, H., and Winter, G. (1988). Reshaping Human Antibodies for Therapy. *Nature* 332, 323–327. doi:10.1038/332323a0

Saha, N. (2018) Clinical Pharmacokinetics and Drug Interactions. *Pharmaceutical Medicine and Translational Clinical Research*. (ed. by D. Vohora and G Singh), pp. 81–106.

Schulz, A. S., Glatting, G., Hoenig, M., Schuetz, C., Gatz, S. A., Grewendorf, S., et al. (2011). Radioimmunotherapy-based Conditioning for Hematopoietic Cell Transplantation in Children with Malignant and Nonmalignant Diseases. *Blood* 117, 4642–4650. doi:10.1182/blood-2010-06-284349

Shaw, P., Shizuru, J., Hoenig, M., and Veys, P. (2019). Conditioning Perspectives for Primary Immunodeficiency Stem Cell Transplants. *Front. Pediatr.* 7, 434. doi:10.3389/fped.2019.00434

Straathof, K. C., Rao, K., Eyrich, M., Hale, G., Bird, P., Berrie, E., et al. (2009). Haemopoietic Stem-Cell Transplantation with Antibody-Based Minimal-Intensity Conditioning: a Phase 1/2 Study. *Lancet* 374, 912–920. doi:10.1016/S0140-6736(09)60945-4

van der Stoep, M., Bertaina, A., Moes, D., Algeri, M., Bredius, R. G. M., Smiers, F. J. W., et al. (2021). Impact of Treosulfan Exposure on Early and Long-Term Clinical Outcome in Pediatric Allogeneic HSCT Recipients: a Prospective Multicenter Study. *Transpl. Cel Ther* 99, e1. doi:10.1016/j.jtct.2021.09.018

van der Stoep, M. Y. E. C., Bertaina, A., Ten Brink, M. H., Bredius, R. G., Smiers, F. J., Wanders, D. C. M., et al. (2017). High Interpatient Variability of Treosulfan Exposure Is Associated with Early Toxicity in Paediatric HSCT: a Prospective Multicentre Study. *Br. J. Haematol.* 179, 772–780. doi:10.1111/bjh.14960

van der Stoep, M. Y. E. C., Zwaveling, J., Bertaina, A., Locatelli, F., Guchelaar, H. J., Lankester, A. C., et al. (2019). Population Pharmacokinetics of Treosulfan in Paediatric Patients Undergoing Hematopoietic Stem Cell Transplantation. *Br. J. Clin. Pharmacol.* 85, 2033–2044. doi:10.1111/bcp.13995

Versluys, A. B., Boelens, J. J., Pronk, C., Lankester, A., Bordon, V., Buechner, J., et al. (2021). Hematopoietic Cell Transplant in Pediatric Acute Myeloid Leukemia after Similar Upfront Therapy; a Comparison of Conditioning Regimens. *Bone Marrow Transpl.* 56, 1426–1432. doi:10.1038/s41409-020-01201-w

Vogelsang, V., Kruchen, A., Wustrau, K., Spohn, M., and Müller, I. (2020). Influence of Anti-thymocyte Globulin Plasma Levels on Outcome Parameters in Stem Cell Transplanted Children. *Int. Immunopharmacol* 83, 106371. doi:10.1016/j.intimp.2020.106371

von dem Borne, P. A., Beaumont, F., Starrenburg, C. W., Oudshoorn, M., Hale, G., Falkenburg, J. H., et al. (2006). Outcomes after Myeloablative Unrelated Donor Stem Cell Transplantation Using Both *In Vitro* and *In Vivo* T-Cell Depletion with Alemtuzumab. *Haematologica* 91, 1559–1562. doi:10.3324/%25x

Waller, E. K., Langston, A. A., Lonial, S., Cherry, J., Somani, J., Allen, A. J., et al. (2003). Pharmacokinetics and Pharmacodynamics of Anti-thymocyte Globulin in Recipients of Partially HLA-Matched Blood Hematopoietic Progenitor Cell Transplantation. *Biol. Blood Marrow Transpl.* 9, 460–471. doi:10.1016/s1083-8791(03)00127-7

Wang, H., Jones, A. K., Dvorak, C. C., Huang, L., Orchard, P., Ivaturi, V., et al. (2019). Population Pharmacokinetics of Clofarabine as Part of Pretransplantation Conditioning in Pediatric Subjects before Hematopoietic Cell Transplantation. *Biol. Blood Marrow Transpl.* 25, 1603–1610. doi:10.1016/j.bbmt.2019.04.017

Conflict of Interest: AL has received research support from Neovii Pharmaceutical AG.

The remaining authors declare that the research was conducted in the absence of any commercial or financial relationships that could be construed as a potential conflict of interest.

Publisher's Note: All claims expressed in this article are solely those of the authors and do not necessarily represent those of their affiliated organizations, or those of the publisher, the editors, and the reviewers. Any product that may be evaluated in this article, or claim that may be made by its manufacturer, is not guaranteed or endorsed by the publisher.

frontiers in Pharmacology

BRIEF RESEARCH REPORT
published: 18 March 2022
doi: 10.3389/fphar.2022.828094

Therapeutic Drug Monitoring of Anti-Thymocyte Globulin in Allogeneic Stem Cell Transplantation: Proof of Concept

J.I. Meesters-Ensing[1†], R. Admiraal[1,2†], L. Ebskamp[3], A. Lacna[3], J. J. Boelens[4], C. A. Lindemans[1,2] and S. Nierkens[1,3]*

[1]Princess Máxima Center for Pediatric Oncology, Utrecht, Netherlands, [2]Department of Pediatrics, University Medical Center Utrecht, Utrecht, Netherlands, [3]Center for Translational Immunology, University Medical Center Utrecht, Utrecht, Netherlands, [4]Stem Cell Transplantation and Cellular Therapies, Memorial Sloan Kettering Cancer Center, New York, NY, United States

Anti-thymocyte globulin (ATG), a polyclonal antibody, is used in allogeneic hematopoietic cell transplantation (HCT) to prevent graft-vs.-host-disease (GvHD) and graft failure (GF). Overexposure to ATG leads to poor early T-cell recovery, which is associated with viral infections and poor survival. Patients with severe inflammation are at high risk for GF and GvHD, and may have active infections warranting swift T-cell recovery. As ATG exposure may be critical in these patients, individualized dosing combined with therapeutic drug monitoring (TDM) may improve outcomes. We describe the individualized dosing approach, an optimal sampling scheme, the assay to measure the active fraction of ATG, and the workflow to perform TDM. Using a previously published population pharmacokinetic (PK) model, we determine the dose to reach optimal exposures associated with low GvHD and rejection, and at the same time promote T-cell recovery. Based on an optimal sampling scheme, peak and trough samples are taken during the first 3 days of once-daily dosing. The fraction of ATG able to bind to T-cells (active ATG) is analyzed using a bio-assay in which Jurkat cells are co-cultured with patient's plasma and the binding is quantified using flow cytometry. TDM is performed based on these ATG concentrations on the third day of dosing; subsequent doses can be adjusted based on the expected area under the curve. We show that individualized ATG dosing with TDM is feasible. This approach is unique in the setting of antibody treatment and may result in better immune reconstitution post-HCT and subsequently better survival chances.

Keywords: anti-thymocyte globulin (ATG), TDM (therapeutic drug monitoring), stem cell transplant (SCT), antibody, pediatrics–children

OPEN ACCESS

Edited by:
Erwin Dreesen, KU Leuven, Belgium

Reviewed by:
Salvador F. Aliño, University of Valencia, Spain
John Carl Panetta, St. Jude Children's Research Hospital, United States

***Correspondence:**
R. Admiraal
r.admiraal-4@prinsesmaximacentrum.nl

[†]These authors have contributed equally to this work

Specialty section:
This article was submitted to Obstetric and Pediatric Pharmacology, a section of the journal Frontiers in Pharmacology

Received: *02 December 2021*
Accepted: *25 February 2022*
Published: *18 March 2022*

Citation:
Meesters-Ensing JI, Admiraal R, Ebskamp L, Lacna A, Boelens JJ, Lindemans CA and Nierkens S (2022) Therapeutic Drug Monitoring of Anti-Thymocyte Globulin in Allogeneic Stem Cell Transplantation: Proof of Concept. Front. Pharmacol. 13:828094. doi: 10.3389/fphar.2022.828094

INTRODUCTION

Allogeneic hematopoietic cell transplantation (HCT) is a potentially curative treatment option for a plethora of hematological and non-hematological diseases. While the vast majority of adult patients receive an HCT for malignant underlying conditions, approximately 50% of pediatric patients have a non-malignant disease as transplant indication. This group includes immune deficiencies, of which part lack (part of) cellular immunity (e.g., severe combined immunodeficiency), while other patients

with immune deficiencies present with immune dysregulation and hyperinflammation (e.g., hemophagocytic lymphohistiocytosis, chronic granulomatous disease, combined variable immune deficiency).

The main limitations of HCT in these patient groups include graft failure (GF), infections, and graft-versus-host-disease (GvHD). Without rigorous recipient T-cell depletion, the T-cell compartment is prone to activation causing a high risk of GF. On the other hand, patients with active inflammation and activation of antigen-presenting cells are susceptible to development of GvHD. As such, an allogeneic HCT in these patients is a relatively high-risk procedure.

Anti-thymocyte globulin (ATG) was introduced to prevent GvHD and GF after allogeneic HCT (Storek et al., 2015). It mainly depletes T-lymphocytes of the recipient and graft, which are important mediator cells in GvHD and rejection (Mohty, 2007). However, in line with the mode of action, too rigorous T-cell depletion of the graft may result in delayed or absent T-cell reconstitution after HCT, leading to an increased risk for viral reactivations (Admiraal et al., 2017). ATG therefore has a central role in outcome after HCT, and appears to have a delicate balance between its efficacy and toxicity (Admiraal et al., 2015a; Admiraal et al., 2016).

ATG is a remarkable drug from a pharmacological perspective. The drug infused is a rabbit-derived polyclonal IgG with antibodies against a variety of epitopes found on human cells. Main manufacturing methods include inoculating rabbits with either whole human thymus tissue (Thymoglobulin, Sanofi, France) or Jurkat cells (human T-cell lymphoblasts; Grafalon [previously known as ATG-Fresenius], Neovii, Switzerland). Horse-derived ATG, enriched after inoculation with human leukocytes (Atgam, Pfizer, NY, United States), is not frequently used for the indication of allogeneic HCT. The different brands are not bio-equivalent due to their different production processes. The fraction of infused IgG varies between brands and is reported to be ~9% for Thymoglobulin (Regan et al., 2001). Moreover, the specificity and capacity to bind to certain surface molecules on both lymphocytes and myeloid cells is different between the two brands (Bourdage and Hamlin, 1995; Oostenbrink et al., 2019). Since the PK, the PD and possibly also the assay to quantify exposure may be brand-specific, we only focus on Thymoglobulin in the current paper. Any mentioning of ATG should be therefore read as "Thymoglobulin". Moreover, as the pharmacodynamics of the active fraction of ATG predict clinical outcome, we only focus on this active fraction.

Using a fixed dose of ATG, the exposures are highly variable and unpredictable (Admiraal et al., 2015b). However, the population pharmacokinetics (popPK) of ATG have been elucidated in recent years (Admiraal et al., 2015b). Body weight and absolute lymphocyte counts (ALC) before the first dose of ATG have been identified as drivers of its pharmacokinetics. The popPK model can be used to calculate expected ATG exposures given the patient characteristics. Moreover, with blood samples, the model can be used to perform therapeutic drug monitoring (TDM) to gain optimal control over the ATG exposure in an individual patient.

The exposure of ATG in the setting of an allogenic HCT can be divided in the exposure before and after infusion of the stem cell product. The exposure before graft infusion is suggested to be pivotal for the pharmacological effects (i.e., prevention of GvHD and GF), while the exposure to ATG after graft infusion is associated with T-cell reconstitution (Admiraal et al., 2015a; Admiraal et al., 2016). As such, in the setting of hyperinflammation with high risk for GvHD and GF, the exposure to ATG before graft infusion is of importance. On the other hand, the most optimal exposure to ATG after graft infusion still allowing immune reconstitution, is suggested to depend mainly on the stem cell source (Admiraal et al., 2015a). Using individualized dosing of ATG based on body weight and ALC, we aim to achieve maximal protection against GvHD and GF, while still promoting early T-cell recovery. However, for patients suffering from immune deficiencies and/or hyperinflammation the exposure prediction may be less accurate due to a potential large variation in dysregulated ALC in blood vs. inflamed tissue.

The aim of this paper is to describe the process of individualized dosing and TDM of ATG in the setting of immune deficiencies with hyperinflammation. We describe steps involved, including the individualized dosing, the optimal sampling scheme, the assay for the active fraction of ATG, the therapeutic drug monitoring and the workflow to perform the aforementioned steps.

NEED FOR INDIVIDUALIZED DOSING AND TDM

This protocol was designed for patients to reach optimal exposures to ATG both before HCT (associated with graft failure and GvHD) and after HCT (associated with T-cell recovery and survival) (Admiraal et al., 2015a; Admiraal et al., 2016). As a first step, we evaluated the performance of standard pediatric dosing of ATG (Thymoglobulin, Genzyme) in most protocols, being a cumulative dose of 10 mg/kg given in 4 consecutive days starting day-5. We simulated four representative patients with the indication of hyperinflammation: a body weight of 25 and 50 kg with an absolute lymphocyte counts before the first dose of 2×10 (Admiraal et al., 2015b)/L and 4×10 (Admiraal et al., 2015b)/L. We performed a total of 1,000 simulations per scenario, with full interindividual variability and residual error. The percentage of virtual patients reaching optimal exposure is shown in **Table 1**. The attainment of optimal exposure is relatively low, especially for the pre-HCT AUC <20% for all scenario's), while over 50% of cord blood recipients in each scenario are over-exposed. As such, there was a clear indication to develop an individualized dosing regimen. As the dosages needed were higher than those used in most protocols, we also performed TDM, both to have more control over the exposures and to have more safety measures in place.

TABLE 1 | Attainment of desired pre- and post-HCT Area Under the Curve.

Body weight	ALC	Pre-HCT AUC (all sources)	Post-HCT AUC (cordblood)	Post-HCT AUC (bone marrow/peripheral blood)
25	2	9.4	30.2	80.7
25	4	6.3	48.9	90.5
50	2	19.3	21.1	68
50	4	13	38.7	83.3

*Percentage of simulated patients reaching desired pre- and post-HCT AUC, for the indication of hyperinflammation (pre-HCT AUC, 60–120 AU*day/L; post-HCT AUC, cordblood <10 AU*day/L; post-HCT AUC, bone marrow/peripheral blood <50 AU*day/L) using a standard dosing regimen of ATG: 10 mg/kg over four consecutive days, starting day-5. ALC: Absolute lymphocyte count before first dose of ATG.*

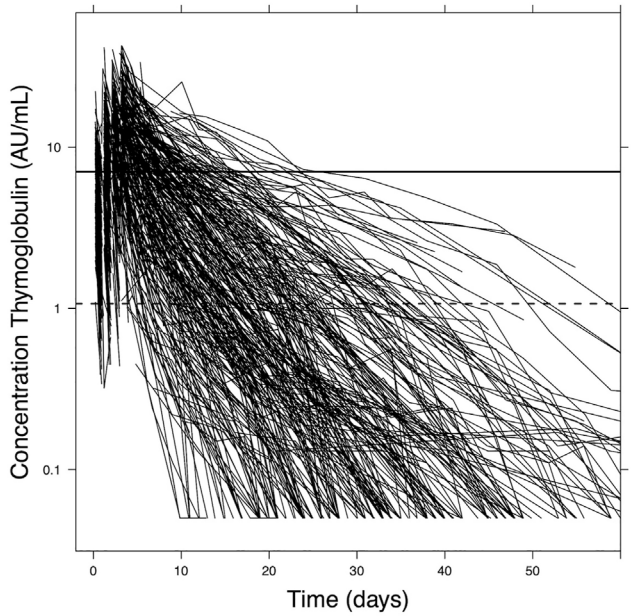

FIGURE 1 | Active ATG plasma concentration data. The graph shows aATG concentrations over time in pediatric patients ($n = 267$) during the whole course of ATG treatment up to 60 days after first dosing. ATG clearance varies extensively between patients. Adapted from Admiraal et al., Lancet Haematology 2017.

PATIENTS ELIGIBLE FOR TDM AND SIMULATION FOR THE CALCULATED OPTIMAL DOSE

The patients for whom this protocol is developed include those with immune deficiencies with hyperinflammation, who are at a high risk for graft failure and/or GvHD and are dependent on fast immune reconstitution to prevent infection. This includes but is not limited to patients with hemophagocytic lymphohistiocytosis (HLH), chronic granulomatous disease (CGD) and common variable immunodeficiency (CVID). The decision to include a patient in this protocol is at the treating physician's discretion.

Simulation studies are performed to find the optimal individualized dose based on the patient characteristics. We use the previously published popPK model for all exercises regarding the ATG dosing and TDM (Admiraal et al., 2015b). This model was developed in a pediatric population treated with ATG in the setting of allogeneic hematopoietic cell transplantation. Historically, the maximum dose of ATG given was 10 mg/kg, which led to a wide range of exposures due to the variable pharmacokinetics (**Figure 1**) (Admiraal et al., 2015a; Admiraal et al., 2015b). The popPK-model was made based on this population. Covariates included in the model were actual body weight and ALC before the first dose of ATG. The desired exposures were derived from previously published data (Admiraal et al., 2015a; Admiraal et al., 2016). We use NONMEM 7.5.0 (Icon, Hanover, MD, United States) with data visualization in R version 4.0.5 for all pharmacological analyses. For simulations, a total of 1,000 virtual patients were analyzed given the patient characteristics with full inter-individual variability to evaluate expected exposures to ATG.

In general, patients included in the protocol have a relatively high ALC, leading to a relatively high ATG clearance. Thus, the cumulative starting dose is usually higher than the accustomed 10 mg/kg. Patients with an ALC above $4 * 10^9$/L are capped at $4 * 10^9$/L, as this was the maximum ALC in the population the PK-model was built on. The optimal exposures were set at 60–120 AU*day/L before graft infusion; after graft infusion the target was <10 AU*day/L for cord blood recipients and <50 AU*day/L for bone marrow grafts. These target exposures were derived from previous observations, where an ATG exposure before graft infusion >40 AU*day/L was associated with lower GvHD and GF (Admiraal et al., 2015a). Under the assumption of increased (tissue) ALC in the hyperinflammatory patient, we determined the dose with the model to a desired exposure of ATG before graft infusion of 60–120 AU*day/L. Exposures after HCT are set to those found in previous reports (Admiraal et al., 2015a; Admiraal et al., 2016). A cumulative dose of ATG is chosen so that median simulated exposures are well within the desired ranges. In order to maximize the safety of the procedure, the daily dose in the protocol was 5 mg/kg/day, this was capped to twice the daily dose in regular regimens, i.e., 2.5 mg/kg/day. Given the relatively high dose needed in most dosing scenarios (given the high ALC and thus high clearance), dosing of ATG is usually spread over six consecutive days. This also gives more time to perform the elaborate assay to measure active ATG concentrations and to adjust the dose for the last days. To ensure maximum exposure to ATG before graft infusion and minimize exposure after graft infusion, upfront ATG starting day-15 was chosen.

TABLE 2 | RMSE of evaluated dosing regimens.

Scenario	Description	Clearance	Volume 1	Tm	Vmax	Km
Scenario 0	Hourly samples	0.28	0.26	7.55	1.73	17.88
Scenario 1	1 sample 1 day	2.43	1.23	16.61	1.80	17.88
Scenario 2	2 samples 1 day	2.25	1.20	13.53	1.79	17.89
Scenario 3	4 samples 2 days	1.34	0.92	13.29	1.79	17.89
Scenario 4	5 samples 2 days	1.04	0.92	11.93	1.79	17.89
Scenario 5	5 samples 3 days	1.36	0.80	13.29	1.79	17.89
Scenario 6	6 samples 3 days	0.59	0.82	12.72	1.79	17.89
Scenario 7	8 samples 3 days	0.58	0.81	11.32	1.79	17.89

Root mean square error (RMSE) after stochastic simulation and estimation for optimal sampling. A lower RMSE (range 0–∞) means less error in estimation of the parameter at hand. No interindividual variability is included on K21 and Tmax, therefore the RMSE, is 0 in all scenarios.

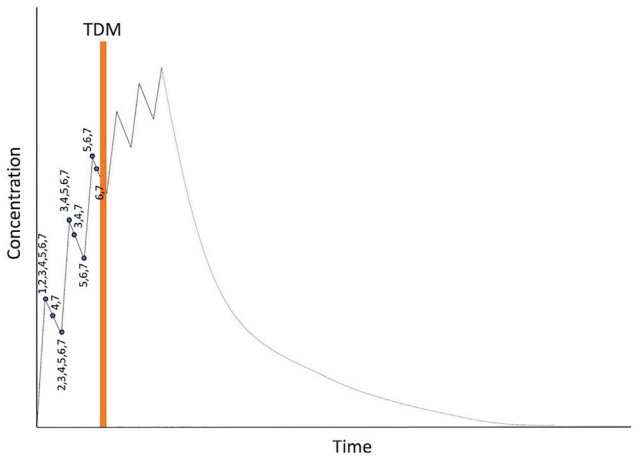

FIGURE 2 | Overview of evaluated dosing regimens. Numbers represent the different dosing scenarios in **Table 2**.

DEFINITION OF THE OPTIMAL SAMPLING SCHEME FOR TDM

The optimal sampling scheme was developed using stochastic simulations and estimations (SSE). The SSE was performed by comparing the selected dosing regimens to a full PK-profile with hourly simulated concentrations samples. In the first step, concentration-time profiles of a 1,000 patients were simulated with hourly sampling incorporating full inter-individual variability. Covariate values (body weight, baseline lymphocyte counts) were chosen from at random from the distribution that was observed in the patients based on whom the population PK-model was developed. Next, out of these simulated 1,000 patients, for each of the scenarios only the indicated times were selected. In the next step, we estimated all of the PK-parameters for each individual patient given their available samples in the scenario and their covariate values. In a last step, the root mean square error (RMSE) was calculated between the PK-parameter estimations of the full PK-profile and that of different dosing scenarios.

Given that the maximum daily dose of ATG was set at 5 mg/kg from a safety perspective, patients received their total dose of ATG divided over up to six consecutive days. We evaluated dosing regimens where the assay for ATG will be performed during the 3rd or the 4th day of ATG, in both cases starting early in the morning. With this approach, the 4th (in case of day 3 TDM), 5th and 6th dose of ATG can be amended if necessary. This leaves the maximum window for potential sampling schemes from the start of the first dose up until the early morning of the day of assay (+68 h). We decided not to take any samples during infusion of ATG given the relatively slow distribution and clearance, combined with the potential inaccuracy in noting the times, and sampling a mixture of blood and infusion of drugs. The evaluated samplings schemes can be found in **Table 2**, with a graphical representation in **Figure 2**. RMSE's showed that the scenario's that take samples during 3 days of dosing with a sample on the early morning of the ATG assay (scenario 6 and 7) perform better in terms of clearance prediction compared to sampling during 1 or 2 days of dosing. Balancing the number of samples and amount of blood needed with the accuracy for all PK-parameters, the decision was made to sample according to scenario 6. As such, we draw blood at peak and trough during the first 3 ATG infusions, and one sample early in the morning of the 4th day of ATG for a total of six samples.

We tried to translate the inaccuracy of the different sampling schemes to the percentage of desired target attainment. The differences between actual and estimated AUC can be divided into two factors: a discrepancy between actual and estimated PK parameters, and the within-subject variability that may change the PK from dose to dose.

There is no contribution of within-subject variability in a potential inaccurate estimation, as this was explored but not identified in the modelling exercise. When trying to estimate the imprecision of the different sampling schemes, we tried developing a script that could automate the adjustment of the dose based on the TDM. Due to the non-linear elimination found in ATG, and the two separate desired optimal exposures (before and after HCT), we could not calculate the dose by multiplying AUC with clearance. We therefore are unable to present the percentage of desired target attainment in the presented sampling schemes.

THERAPEUTIC DRUG MONITORING

During the days the patient is treated with ATG, the nurses register the exact times of starting and ending the ATG infusion,

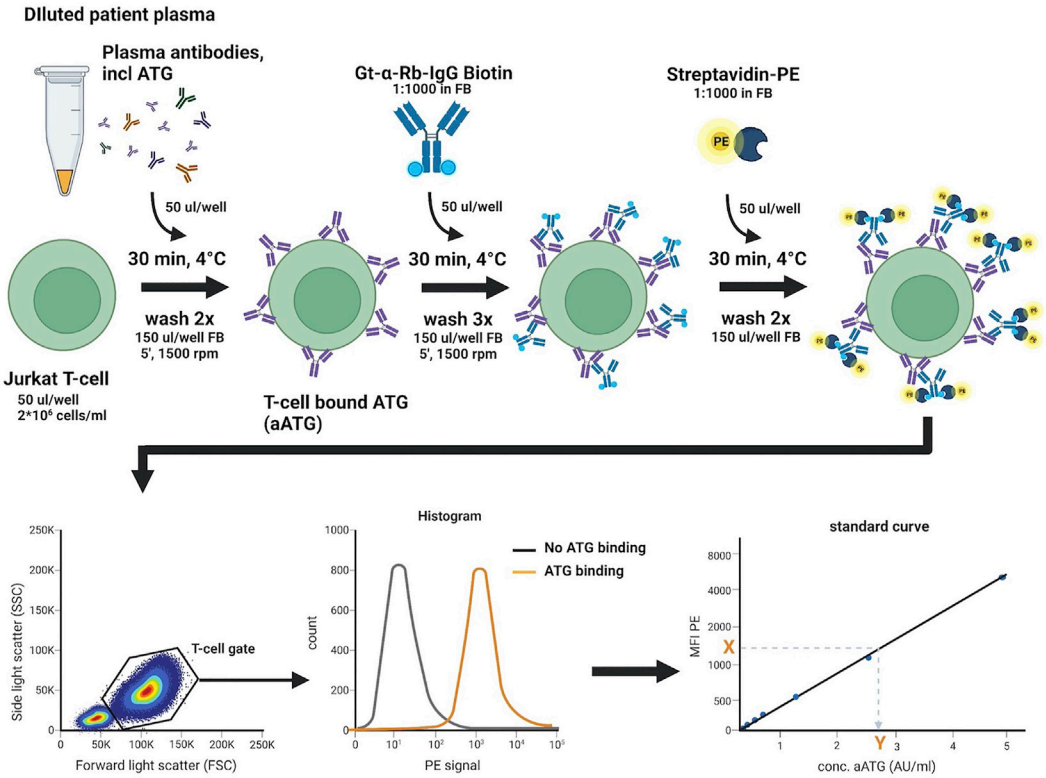

FIGURE 3 | Active ATG binding assay. Standard curve, QC, negative control, and 4- and 8-fold diluted patient plasma samples are incubated in a 96-well U-bottom plate with target Jurkat T-cells, to allow for binding of aATG. Detection of bound aATG is done by subsequent incubation with a Gt-α-Rb-Ig-biotin antibody and streptavidin-PE. Cells are then analyzed on a FACS Canto II flow cytometer by acquiring 70 µl sample at a flow rate of 3 µl/s and intermittent mixing, measuring 10.000 events within the live T-cell gate. The median fluorescence intensity (MFI) of PE measured is then used to extrapolate the concentration of aATG (in AU/ml) in the patient sample from the standard curve. FB, FACS buffer (PBS/1%HSA). This figure was created with Biorender.com.

and the exact times on which the blood is drawn. At the set times, the samples are drawn from the central line and are sent to the lab where these are and frozen at −20 or −80°C until further use. The form with dosing and sampling times is sent to the clinical pharmacologists/pharmacist after completion. After performing the assay as described in the following paragraphs, the measured concentrations along with the patient characteristics, dosing details and actual dosing/sampling times are entered into a command-line based script. Based on these dosing- and sampling records and the patient characteristics, a NONMEM-ready database is compiled holding only the information for the individual patient using R version 4.0.5. Next, the data is run in NONMEM 7.5.0 ((Icon Devel-opment Solutions LLC, Hanover, MD, United States) using a previously developed population PK model (Admiraal et al., 2015b). Here, the population means are fixed to those found in the reported analysis with interindividual variability and residual error as was found in the report. Empirical Bayes estimates were calculated using the POSTHOC option with MAXEVAL = 0. AUC was calculated as a virtual third compartment in the PK-model.

The exposure to ATG before and after graft infusion is outputted by NONMEM, and along with a full concentration-time curve visualized in a time graph based on the measured and calculated concentrations and individual PK. The same script allows for adjustments to the dose and the number of dosages, as well as number of days between first dose of ATG and the time of graft infusion. Based on the individual pharmacokinetic parameters and the measured concentrations, the AUC before and after graft infusion is calculated when implementing dose adjustments. The target AUC did not differ between individualized dosing and TDM: 60–120 AU*day/L before graft infusion and after graft infusion <10 AU*day/L for cord blood recipients and <50 AU*day/L for bone marrow grafts (Admiraal et al., 2015a; Admiraal et al., 2016). In case of ±25% adjustment in cumulative dosing, another session of TDM is advised on the 5th day.

DEVELOPMENT AND PERFORMANCE OF A QUANTITATIVE METHOD FOR MEASURING ACTIVE ATG

Assay Protocol

The assay to measure active ATG is based on an assay previously described by Rebello *et al.* (Rebello and Hale, 2002), where the concentration of an active compound in serum was quantified by measuring binding of this compound to a specific T-cell line using flow cytometry. **Figure 3** shows a detailed description of the assay we developed.

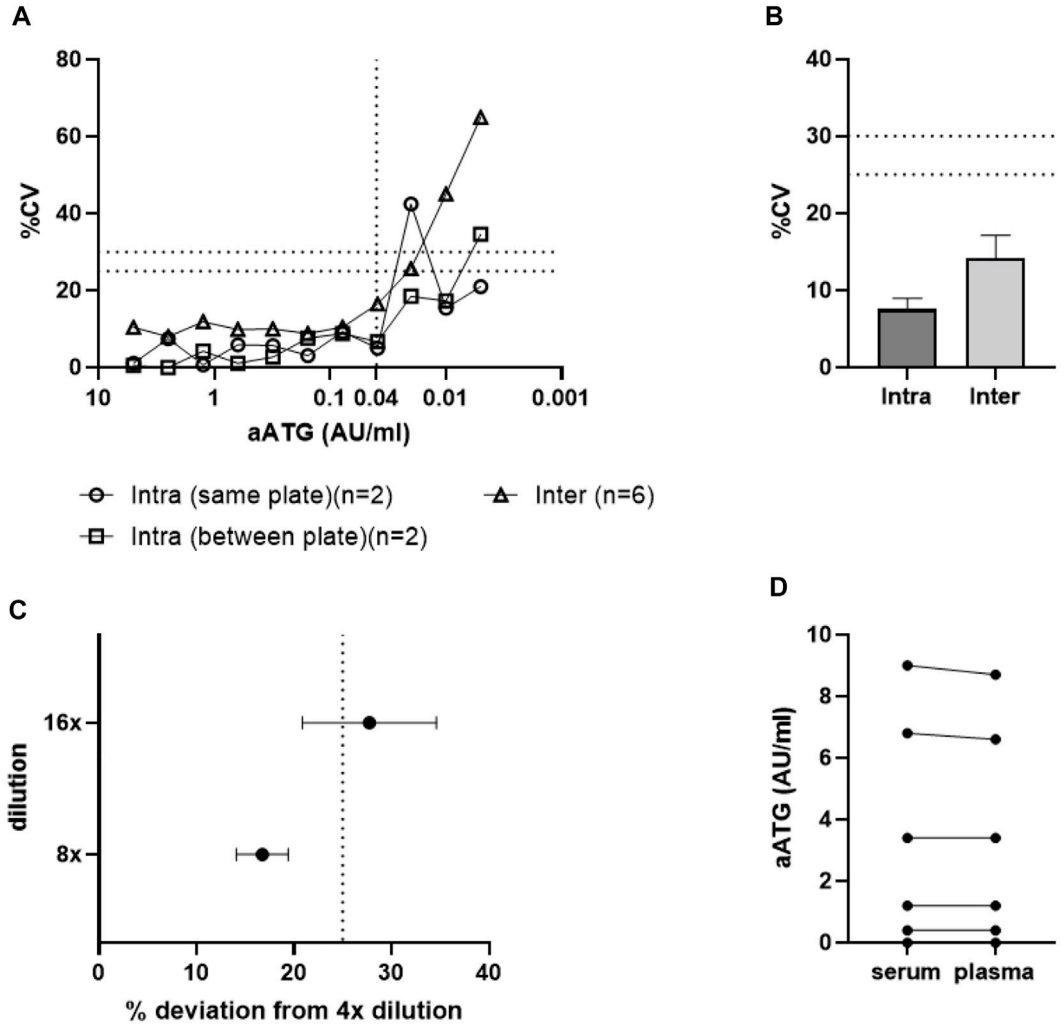

FIGURE 4 | Active ATG binding assay validation. Graph A and B show results for assay accuracy and precision expressed in %CV. Results are shown for Intra- and inter-assay variability results of **(A)** standard curve samples and **(B)** patient samples (data shown as mean +SEM). The LLoQ was set at 0.04 AU/ml **(A)**. Graph **(C)** demonstrates that high patient sample dilutions (16-fold) show increased deviation above the threshold of 25% and should therefore be excluded from analysis (data shown as mean ± SEM). Dashed lines in graphs **(A–C)** represent maximal acceptable assay/sample variability expressed in %CV. Graph **(D)** demonstrates that both plasma and serum samples from the same patient show similar results in the aATG binding assay and can therefore both be used for analysis.

We selected the Jurkat T-cell line as target for active ATG. Jurkat cells are maintained in RPMI 1640 medium (Fisher scientific, #11594506), supplemented with 10% (v/v) human serum albumin (HSA, Sanquin, #15522598), 1% (v/v) L-Glutamine (200 mM, Fisher scientific, #11500626), and 1% (v/v) penicillin/streptomycin (100x, Fisher scientific, #15140122) and cultured at 37°C and 5% CO_2. Cells are expanded for a maximum of 10 passages, passaging cells every 2-3 days. On the day of measurement, the cells are harvested and diluted in PBS.

Binding of active ATG is detected by incubating $1*10^5$ cells with thawed patient samples that are filtered (0.45 μM filter plate, Millipore, #MSHVN4510) and diluted 4- and 8-fold in PBS to ensure active ATG levels detection within a quantification range for all samples. After incubation with samples, the cells are subsequently incubated with a Goat-anti-Rabbit IgG-Biotin antibody (Bio-connect, #111-065-045), followed by streptavidin-PE (BD, #554061) substrate to measure fluorescence on a FACS Canto II flow cytometer.

Active ATG concentrations present in patient samples are extrapolated from a standard curve using Thymoglobulin® (Genzyme, #726816). A stock solution of 5000 AU/ml is prepared by dissolving the lyophilized product in PBS to a concentration of 5 mg/ml, which is aliquoted and stored at −80°C and diluted in PBS to create standards ranging from 5—0.005 AU/ml on the day of measurement.

Assay Validation

Assay accuracy and precision: intra- and inter-assay variability, including intra- and inter-plate variability were determined using spiked QC samples that were created by preparing ATG stock solutions in PBS, which were then mixed 1:1 with ATG-naïve human plasma. ATG-naive human plasma also served as a

negative control. An acceptable coefficient of variation (CV) for the bio-assay was defined to be below 25% or 30% for intra- and inter assay variability, respectively. Average CV values of the intra-assay variability was 10.7% for intra-plate and 9.3% for inter-plate samples, measured in at least 2 independent experiments. For the inter-plate variability this was 21.1%, measured over six independent experiments.

Based on individual CV values per standard concentration, the lower limit of quantification (LLoQ) was determined at 0.04 AU/ml (**Figure 4A**), as multiple samples with active ATG concentrations below 0.04 AU/ml exceeded the 25% CV limit. In addition to spiked standards, assay variability was also assessed using patient samples. For intra-assay variability the average CV was 7.6% with only 1 out of 29 samples not reaching the criterium of 25%. For the inter-assay this variability was 14.2%, with 2 out of 14 samples not reaching the criterium of 30% (**Figure 4B**).

As a final assessment of assay accuracy and precision, the influence of patient sample dilutions on assay outcome was investigated as patient samples taken both at peak and trough time points should be within the range of quantification. Patient plasma samples were diluted 4-, 8-, and 16-fold in PBS and deviations in concentration measured in the 8- and 16-fold dilutions compared to the 4-fold dilution were acceptable up to a bias of 25% (**Figure 4C**). We noticed that dilution did not show an exact linear relation with calculated ATG levels and that the 16-fold dilutions showed increased sample variation and should therefore not be included in the assay.

Overall, these results indicate that the assay is very robust with sample dilutions up to 8x and active ATG concentrations within the range of the standard curve and above the LLoQ.

Analytical Specificity and Selectivity

To demonstrate assay specificity for the identification of active ATG in plasma, the assay was performed using spiked plasma samples of ATG-naive controls. Recovery of active ATG in these spiked plasma samples was 100%, compared to 0% in non-spiked plasma controls (data not shown). Sample variation was high in the 1.5 AU/ml samples, however overall, these data demonstrate that the assay can correctly quantify active ATG in plasma and that there was no non-specific detection of active ATG in control samples. It is of note that in patients receiving specific medication the measurements might potentially be interfered, but we could not find a compound-specific effect.

In addition to analytical specificity, selectivity of the assay was assessed by measuring active ATG levels in both plasma and serum samples of patients, taken at the same timepoint during ATG treatment. **Figure 4E** demonstrates that these different matrices do not influence assay outcome and that both patient materials can be used in this assay.

Ethical Considerations

We used patient samples for the assay accuracy, which were collected after giving informed consent. We also used sera from healthy controls that were taken from volunteers. Institutional ethical committee approval for sample collection was given through trial numbers 11/063-k (patients) and 07/125 (healthy donors).

CONCLUSION

This paper gives an overview of the pharmacology and the bio-assay needed to perform TDM on the polyclonal antibody ATG. We describe the processes of individualized dosing, the optimal sampling scheme, the actual TDM of active ATG, and present the optimized assay for measuring the active fraction of ATG. This protocol can be applied for difficult-to-treat patients, such as those with immunodeficiencies with hyperinflammation who are at a high risk for GF and GvHD, to check whether the prediction of exposure related to the given dose was accurate, and, if needed, to adjust the dose for the last administration(s). While this protocol may improve the control over the exposure to ATG, and thereby potentially clinical outcome, the assay and the need for pharmacokinetic analysis represent a limit in its application.

The main hurdles for setting up a protocol for TDM of active ATG include the complexity of the assay and the experience on using popPK for TDM. This elaborate description of the validated assay for quantifying ATG, using readily available reagents and cell lines, will support centers to implement this locally or a central lab should be defined that is able to perform the assay on the day of the day 3 sample (day 3 of ATG administration). As the described assay requires biological materials, results will be subject to a certain margin of error. To minimize assay variability, standardized batches of critical materials should be used (e.g., cells, buffers, ATG, and QC stock solutions) when implementing the assay for clinical use.

Another limitation may be the software and expertise on popPK that are used in the current protocol. In order to reduce the complexity of database building and running TDM using NONMEM, the popPK model was recently implemented in the software package InsightRx (InsightRx, CA, United States). This will make the simulation and modelling easier and more accessible.

The need for serotherapy in patients with hyperinflammation in the context of HCT for immune deficiencies is quite clear. Currently, rabbit ATG (Thymoglobulin, Grafalon) and alemtuzumab, an anti-CD52 monoclonal antibody, are available for this indication (Fox et al., 2018; Slatter et al., 2018; Chandra et al., 2021). Alemtuzumab is more potent, as reflected in a lower lympholytic level (Lane et al., 2014; Marsh et al., 2016), with a longer half-life compared to ATG (Admiraal et al., 2019). Therefore, when given in normal dosages at the same day relative to graft infusion, alemtuzumab may yield in more potent suppression of GvHD and GF, but potentially also leads to poor T-cell recovery. Still, alemtuzumab is currently used for the indication of hyperinflammation, with subcutaneous low dosing implemented to overcome slow or absent T-cell recovery (Bhatt et al., 2020). TDM of alemtuzumab is mainly focused on preventing underdosing (Arnold et al., 2021). From a pharmacokinetic perspective, exposure of ATG is easier to control given the higher clearance compared to alemtuzumab. A formal study comparing ATG and alemtuzumab, both with therapeutic drug monitoring, with endpoint PK-target attainment or clinical outcomes, would be needed to demonstrate which approach is superior.

In conclusion, we describe the assay to accurately measure active ATG concentrations, and the framework for TDM of ATG

in an allogeneic HCT setting. This approach is unique in the setting of antibody treatment and may result in less complications, better immune reconstitution post-HCT and subsequently better survival chances.

DATA AVAILABILITY STATEMENT

The original contributions presented in the study are included in the article/**Supplementary Material**, further inquiries can be directed to the corresponding author.

AUTHOR CONTRIBUTIONS

JM-E and RA wrote the paper, all authors reviewed the manuscript.

SUPPLEMENTARY MATERIAL

The Supplementary Material for this article can be found online at: https://www.frontiersin.org/articles/10.3389/fphar.2022.828094/full#supplementary-material

REFERENCES

Admiraal, R., de Koning, C. C. H., Lindemans, C. A., Bierings, M. B., Wensing, A. M. J., Versluys, A. B., et al. (2017). Viral Reactivations and Associated Outcomes in the Context of Immune Reconstitution after Pediatric Hematopoietic Cell Transplantation. *J. Allergy Clin. Immunol.* 140, 1643–1650.e9. doi:10.1016/j.jaci.2016.12.992

Admiraal, R., Jol-van der Zijde, C., Furtado Silva, J., Knibbe, C. A. J., Lankester, A. C., Boelens, J. J., et al. (2019). Population Pharmacokinetics of Alemtuzumab (Campath) in Pediatric Hematopoietic Cell Transplantation: towards Individualized Dosing to Improve Outcome. *Popul. Pharmacokinet.* 58, 1609–1620. **ePub**. doi:10.1007/s40262-019-00782-0

Admiraal, R., Lindemans, C. A., van Kesteren, C., Bierings, M. B., Versluijs, A. B., Nierkens, S., et al. (2016). Excellent T-Cell Reconstitution and Survival Depend on Low ATG Exposure after Pediatric Cord Blood Transplantation. *Blood* 128, 2734–2741. doi:10.1182/blood-2016-06-721936

Admiraal, R., van Kesteren, C., Jol-van Der Zijde, C. M., Lankester, A. C., Bierings, M. B., Egberts, T. C., et al. (2015). Association between Anti-Thymocyte Globulin Exposure and CD4+ Immune Reconstitution in Paediatric Haemopoietic Cell Transplantation: a Multicentre, Retrospective Pharmacodynamic Cohort Analysis. *Lancet Haematol.* 2, e194–203. doi:10.1016/S2352-3026(15)00045-9

Admiraal, R., van Kesteren, C., Jol-van der Zijde, C. M., van Tol, M. J., Bartelink, I. H., Bredius, R. G., et al. (2015). Population Pharmacokinetic Modeling of Thymoglobulin® in Children Receiving Allogeneic-Hematopoietic Cell Transplantation: towards Improved Survival through Individualized Dosing. *Clin. Pharmacokinet.* 54, 435–446. doi:10.1007/s40262-014-0214-6

Arnold, D. E., Emoto, C., Fukuda, T., Dong, M., Vinks, A. A., Lane, A., et al. (2021). A Prospective Pilot Study of a Novel Alemtuzumab Target Concentration Intervention Strategy. *Bone Marrow Transpl.* 56, 3029–3031. doi:10.1038/s41409-021-01460-1

Bhatt, S. T., Schulz, G., Hente, M., Slater, A., Murray, L., Shenoy, S., et al. (2020). A Single-center Experience Using Alemtuzumab, Fludarabine, Melphalan, and Thiotepa as Conditioning for Transplantation in Pediatric Patients with Chronic Granulomatous Disease. *Pediatr. Blood Cancer* 67, e28030–5. doi:10.1002/pbc.28030

Bourdage, J. S., and Hamlin, D. M. (1995). Comparative Polyclonal Antithymocyte Globulin and Antilymphocyte/antilymphoblast Globulin Anti-CD Antigen Analysis by Flow Cytometry. *Transplantation* 59, 1194–1200. doi:10.1097/00007890-199504270-00020

Chandra, S., Chandrakasan, S., Dávila Saldaña, B. J., Bleesing, J. J., Jordan, M. B., Kumar, A. R., et al. (2021). Experience with a Reduced Toxicity Allogeneic Transplant Regimen for Non-CGD Primary Immune Deficiencies Requiring Myeloablation. *J. Clin. Immunol.* 41, 89–98. doi:10.1007/s10875-020-00888-2

Fox, T. A., Chakraverty, R., Burns, S., Carpenter, B., Thomson, K., Lowe, D., et al. (2018). Successful Outcome Following Allogeneic Hematopoietic Stem Cell Transplantation in Adults with Primary Immunodeficiency. *Blood* 131, 917–931. doi:10.1182/blood-2017-09-807487

Lane, J. P., Evans, P. T., Nademi, Z., Barge, D., Jackson, A., Hambleton, S., et al. (2014). Low-dose Serotherapy Improves Early Immune Reconstitution after Cord Blood Transplantation for Primary Immunodeficiencies. *Biol. Blood Marrow Transpl.* 20, 243–249. doi:10.1016/j.bbmt.2013.11.005

Marsh, R. A., Lane, A., Mehta, P. A., Neumeier, L., Jodele, S., Davies, S. M., et al. (2016). Alemtuzumab Levels Impact Acute GVHD, Mixed Chimerism, and Lymphocyte Recovery Following Alemtuzumab, Fludarabine, and Melphalan RIC HCT. *Blood* 127, 503–512. doi:10.1182/blood-2015-07-659672

Mohty, M. (2007). Mechanisms of Action of Antithymocyte Globulin: T-Cell Depletion and beyond. *Leukemia* 21, 1387–1394. doi:10.1038/sj.leu.2404683

Oostenbrink, L. V. E., Jol-Van Der Zijde, C. M., Kielsen, K., Jansen-Hoogendijk, A. M., Ifversen, M., Müller, K. G., et al. (2019). Differential Elimination of Antithymocyte Globulin of Fresenius and Genzyme Impacts T-Cell Reconstitution after Hematopoietic Stem Cell Transplantation. *Front. Immunol.* 10, 1–11. doi:10.3389/fimmu.2019.00315

Rebello, P., and Hale, G. (2002). Pharmacokinetics of CAMPATH-1H: Assay Development and Validation. *J. Immunol. Methods* 260, 285–302. doi:10.1016/s0022-1759(01)00556-7

Regan, J. F., Lyonnais, C., Campbell, K., Smith, L. V., and Buelow, R. (2001). Total and Active Thymoglobulin Levels: Effects of Dose and Sensitization on Serum Concentrations. *Transpl. Immunol.* 9, 29–36. doi:10.1016/s0966-3274(01)00048-x

Slatter, M. A., Rao, K., Abd Hamid, I. J., Nademi, Z., Chiesa, R., Elfeky, R., et al. (2018). Treosulfan and Fludarabine Conditioning for Hematopoietic Stem Cell Transplantation in Children with Primary Immunodeficiency: UK Experience. *Biol. Blood Marrow Transpl.* 24, 529–536. doi:10.1016/j.bbmt.2017.11.009

Storek, J., Mohty, M., and Boelens, J. J. (2015). Rabbit Anti-T Cell Globulin in Allogeneic Hematopoietic Cell Transplantation. *Biol. Blood Marrow Transpl.* 21, 959–970. doi:10.1016/j.bbmt.2014.11.676

Conflict of Interest: RA, JJB, CAL, and SN received an unrestricted research grant from Sanofi.

The remaining authors declare that the research was conducted in the absence of any commercial or financial relationships that could be construed as a potential conflict of interest.

frontiers in Pharmacology

CASE REPORT
published: 24 March 2022
doi: 10.3389/fphar.2022.822981

Case Report: Therapeutic Drug Monitoring of Polymyxin B During Continuous Renal Replacement Therapy in Two Pediatric Patients: Do Not Underestimate Extracorporeal Clearance

Caifang Xu[1†], Xiaofen Liu[2,3†], Yun Cui[1], Xiaolan Huang[2,3], Yu Wang[2,3], Yaxin Fan[2,3], Hailan Wu[2,3], Xin Li[2,3], Beining Guo[2,3], Jing Zhang[2,3,4] and Yucai Zhang[1*‡]*

[1]Department of Critical Care Medicine, Shanghai Children's Hospital, Shanghai Jiao Tong University School of Medicine, Shanghai, China, [2]Institute of Antibiotics, Huashan Hospital, Fudan University, Shanghai, China, [3]Key Laboratory of Clinical Pharmacology of Antibiotics, National Health Commission of the People's Republic of China, Shanghai, China, [4]Phase I Clinical Trial Center, Huashan Hospital, Fudan University, Shanghai, China

Background: Polymyxin B has become the last choice for patient with carbapenem-resistant bacterial infection. However, the optimal dosing of polymyxin B in critically ill children receiving continuous renal replacement therapy (CRRT) remains unclear.

Case Presentation: Two cases of critically ill pediatric patients (7 years old) with acute kidney injury requiring continuous renal replacement (CRRT) received polymyxin B treatment due to carbapenem-resistant organism bloodstream infections. Therapeutic drug monitoring (TDM) of polymyxin B was carried out by liquid chromatography tandem mass spectrometry (LC-MS/MS). The average steady-state plasma concentration ($C_{ss,avg}$) of 2–4 mg/L was set as the target level. Initial polymyxin B dose was 1 mg/kg every 12 h, and the $C_{ss,avg}$ at 4–5th dosing were 1.76 and 1.06 mg/L for patient 1 and patient 2, respectively. TDM-guided polymyxin B dose was escalated to 2 mg/kg every 12 h for both patients, resulting in the $C_{ss,avg}$ of 2.60 and 1.73 mg/L, and the infection was controlled subsequently. $C_{ss,avg}$ of polymyxin B with the same dosing regimens and infusion length were different during CRRT and after termination of CRRT for both patients (2.60 mg/L vs. 4.94 mg/L with 2 mg/kg every 12 h in 2 h infusion for patient 1; and 1.73 mg/L vs. 3.53 mg/L with 2 mg/kg every 12 h in 2 h infusion for patient 2). The estimation of drug exposure (estimated by $AUC_{ss,12h}$ at the same dose) during CRRT and cessation of CRRT showed that 45% and 51% of polymyxin B was cleared during CRRT.

Conclusion: Our study showed high clearance of polymyxin B through CRRT, and supplanted dosing of polymyxin B is necessary in pediatric patients undergoing CRRT.

Keywords: polymyxin B, CRRT, children, therapeutic drug monitoring, pharmacokinetic

OPEN ACCESS

Edited by:
Raffaele Simeoli, Bambino Gesù Children's Hospital (IRCCS), Italy

Reviewed by:
Abdul Sami Shaikh, Shah Abdul Latif University, Pakistan
Kamilia Abdelraouf, Hartford Hospital, United States

****Correspondence:***
Yucai Zhang
zyucai2018@163.com
Jing Zhang
zhangj_fudan@aliyun.com

†These authors have contributed equally to this work

‡ORCID:
Yucai Zhang
orcid.org/0000-0002-4905-3600

Specialty section:
This article was submitted to Obstetric and Pediatric Pharmacology, a section of the journal Frontiers in Pharmacology

Received: *26 November 2021*
Accepted: *03 March 2022*
Published: *24 March 2022*

Citation:
Xu C, Liu X, Cui Y, Huang X, Wang Y, Fan Y, Wu H, Li X, Guo B, Zhang J and Zhang Y (2022) Case Report: Therapeutic Drug Monitoring of Polymyxin B During Continuous Renal Replacement Therapy in Two Pediatric Patients: Do Not Underestimate Extracorporeal Clearance. Front. Pharmacol. 13:822981. doi: 10.3389/fphar.2022.822981

INTRODUCTION

Carbapenem-resistant organisms (CROs) are global public health threat due to limited options of antimicrobials. Polymyxins are considered as a last option against CROs (Satlin et al., 2020). The two forms of polymyxins, polymyxin B and colistin, are clinically available. Notwithstanding the similar structures and antimicrobial activity, polymyxin B has some advantages such as direct administration in the active form and lower risk of nephrotoxicity (Tsuji et al., 2019). Furthermore, polymyxin B is the only available form of polymyxins in some countries, although colistin has been more broadly used than polymyxin B internationally (Satlin et al., 2020).

Pharmacokinetic (PK) studies are of paramount importance for suitable dosage of drugs, and to date, research on PK of polymyxin B is conducted mainly with adults (Sandri et al., 2013; Liu et al., 2021). International consensus guidelines recommended a target average steady-state plasma concentration ($C_{ss,avg}$) of 2–4 mg/L for the optimal use of polymyxin B. However, the guidelines have not provided the recommend dosage regimens in children (Tsuji et al., 2019). There are only a few studies that reported polymyxin B used in pediatric patients, with a dose of 1~4 mg/kg per day (Shih and Gaik, 2014; Gothwal et al., 2016). The huge diversity of doses provided in these studies has made it hard to establish the optimal dose for pediatrics. Furthermore, continuous renal replacement therapy (CRRT) has been increasingly used in critically ill patients with fluid overload or acute kidney injury (AKI). Antibiotics dosage in patients with normal renal function cannot be directly applied to patients under CRRT because of the different pharmacokinetics (Willems et al., 2021). Clinical data also suggested that dose in patients undergoing CRRT could potentially lead to drug underexposure, resulting poor outcomes (Li et al., 2020). Nevertheless, there was a lack of comprehensive guidelines providing antibiotics strategies of polymyxin B for patients undergoing CRRT (Pistolesi et al., 2019). Two reports including three cases of adult patients receiving polymyxin B while CRRT was being operated suggested both continuous venovenous hemodialysis (CVVHD) and continuous venovenous hemofiltration (CVVHF) had a limited impact (no more than 12% clearance) on the removal of polymyxin B (Teng et al., 2008; Sandri et al., 2012). Contrarily, another study with three critical ill adults reported that 45% of colistin was removed during CRRT under the CVVHDF mode (Liu et al., 2020). Whether continuous venovenous hemodiafiltration (CVVHDF) would affect the clearance of polymyxin B in pediatric patients has not been reported. This report evaluates the extent of polymyxin B clearance by continuous hemodiafiltration in two critically ill pediatric patients.

CASE DESCRIPTION

Patients

Case 1 was a 7-year-old female with a previous history of nephrotic syndrome. She was admitted to the nephrology department due to repeated puffiness for nearly 3 months, on January 23rd, 2021. Two weeks later, she was transferred to the pediatric intensive unit (PICU) for severe pneumocystis pneumonia, respiratory failure, sepsis, and AKI. She was received mechanical ventilation, sulfamethoxazole–trimethoprim, caspofungin, and CRRT. After 3 weeks, carbapenem-resistant *K. Pneumoniae* was isolated from both her urinary catheter and blood. Minimum inhibitory concentrations (MICs) and disk diffusion tests (DISK) of *K. pneumoniae* showed it was only susceptible to polymyxin B (15 mm of DISK and 0.5 mg/L of MIC) and tigecycline (2 mg/L of MIC). Tigecycline combined with fosfomycin was applied, but the efficacy was very limited. Therefore, tigecycline and fosfomycin were replaced by polymyxin B from March 5th 2021 (1 mg/kg every 12 h). On March 18th, due to the recovery of kidney function, CRRT ceased and polymyxin B therapy continued until April 5th.

Case 2 was a 7-year-old female with fulminant myocarditis. She was admitted to the PICU and given venoarterial extracorporeal membrane oxygenation (VA-ECMO) on June 30th 2021. The duration of extracorporeal cardiopulmonary resuscitation (ECPR) was about 70 min, leading to multiple organ dysfunction syndrome (MODS). In addition, CRRT was required (from June 30th to July 25th) for AKI. After 8 days, ECMO was weaned. However, the body temperature elevated between 38 and 40°C, accompanied by an increase in C-reactive protein (123 mg/L) and procalcitonin (16.95 ng/mL). *Stenotrophomonas maltophilia* (multidrug-resistant bacteria, susceptible to cefoperazone–sulbactam and polymyxin B) was identified by blood culture, abdominal fluid and in ECMO catheters. Meanwhile, *Aspergillus fumigatus* was cultured using bronchoalveolar lavage fluid. With cefoperazone–sulbactam combined with linezolid and voriconazole treatment, the clinical symptoms did not ameliorate. Therefore, polymyxin B (17 mm of DISK) was added from July 10th 2021 to August 4th 2021.

Continuous Renal Replacement Therapy Mode and Parameters

Two patients received CRRT with the CVVHDF mode (GAMBRO, Prismaflex, hemofilter M60). As the coagulation dysfunction, citric acid was used for anticoagulation for both the patients. For patient 1, 25 kg, the settings of CRRT were 30 mL/min for blood flow, 60 mL/h for citric acid, 100 mL/h for replacement fluid, 300 mL/h for dialysate fluid, and 60 mL/h for effluent. For patient 2, 20 kg, 40 mL/min for blood flow, 64 mL/h for citric acid, 300 mL/h for replacement fluid, 150 mL/h for dialysate fluid, and 80 mL/h for effluent was set.

Samples and Therapeutic Drug Monitoring

For both patients, trough and peak blood samples at steady state (about 0.5 h before and after the infusion of 4–5th dosing) were collected for TDM of polymyxin B. If the dosage regimens needed to be adjusted according to TDM, trough and peak blood samples after the third post-adjustment dose were collected. In the meantime, post-filtration blood samples were collected at the same time to evaluate the drug elimination during CRRT.

Polymyxins B1 and B2 were determined following a validated liquid chromatography tandem with mass spectrometry (LC-MS/MS) method (Liu et al., 2020). In brief, plasma samples were

TABLE 1 | Concentrations at different dosing regimens.

Patient No.	Polymyxin B dosing regimens (q12 h)	CRRT	eGFR* (mL/min)	Peak (mg/L)	Trough (mg/L)	Average (mg/L)
1	1 mg/kg with 1 h infusion	Yes	69.7	3.31	0.20	1.76
	2 mg/kg with 2 h infusion	Yes	111.3	4.79	0.41	2.60
	2 mg/kg with 2 h infusion	No	108.7	7.67	2.21	4.94
	1.5 mg/kg with 2 h infusion and 0.5 mg/kg inhalation	No	101.6	6.95	3.39	5.17
	1 mg/kg with 2 h infusion	No	116.8	6.45	0.80	2.63
2	1 mg/kg with 2 h infusion	Yes	40.2	1.87	0.23	1.06
	1.5 mg/kg with 2 h infusion	Yes	71.8	1.70	0.22	0.96
	2 mg/kg with 2 h infusion	Yes	60.8	3.19	0.26	1.73
	2 mg/kg with 2 h infusion	No	128.9	5.24	1.82	3.53

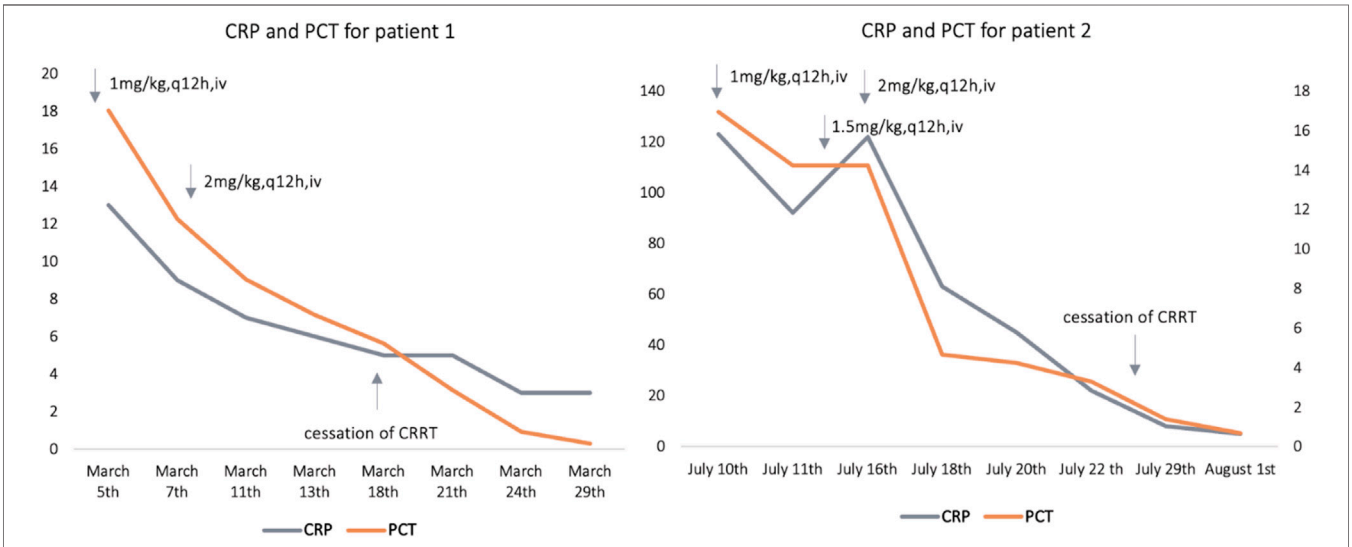

FIGURE 1 | Polymyxin B dose regimens with the concomitant drugs and estimated C-reactive protein (CRP), and procalcitonin (PCT) levels at different time points; for patient 1, cessation of CRRT (continuous renal replacement) was on 18th March; for patient 2, cessation of CRRT was on 25th July. CRP: C-reactive protein (mg/L), PCT: procalcitonin (ng/mL).

mixed with internal standard (polymyxin E2) and 30% ammonia and then loaded on a preconditioned (conditioned by methanol and water as per product instruction) 96-well Oasis WCX plate (30 mg, Waters Corporation, Milford, MA, United States). The WCX plate was washed and eluted by 30% acetonitrile in water (containing 6% formic acid, v/v). The elute was injected into LC-MS/MS (Shimadzu 30A series coupled with AB Sciex Triple Quad 5500 mass spectrometry platform) for analysis. Concentrations of polymyxin B were calculated by the sum of polymyxins B1 and B2 by the molar terms and molecular weight. The $C_{ss,avg}$ of 2–4 mg/L (estimated by the average of peak and trough concentration) of polymyxin B was set as the target concentration.

AUC Estimates

Compartmental modeling using WinNonlin 8.0 was applied for PK parameters estimation and AUC calculation. Due to the limited data with C_{max} and C_{trough} for the second patient, an alternative equation-based approach for two PK samples methods was used for the AUC_{24h} estimates (Pai et al., 2014) under similar eGFR. The equations are given as follows:

$$K_e = \frac{LnC_{max} - Ln\,C_{trough}}{t_2 - t_{infusion}},$$

$$AUC_{24h} = \left(\frac{t_{infusion} \times (C_{max} + C_{trough})}{2} + \frac{C_{max} - C_{trough}}{k_e}\right) \times n,$$

where K_e is the elimination rate constant, t_2 is the drug administration interval, $t_{infusion}$ is the infusion length, and n is the administration times during 24 h.

RESULTS

Polymyxin B and Plasma Concentrations

After treatment with polymyxin B (1 mg/kg, every 12 h, $C_{ss,avg}$ = 1.76 mg/L), C-reactive protein (CRP) of patient 1 decreased from 13 mg/L to 5 mg/L, and procalcitonin (PCT) fell from 18.04 ng/mL

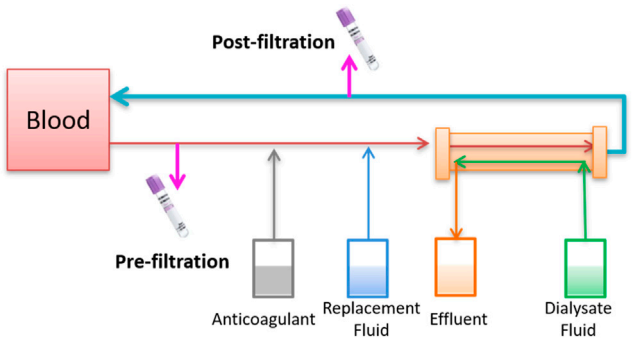

FIGURE 2 | Schematic diagram of blood collection in the extracorporeal catheter prefilter and postfilter of CRRT.

to 5.62 ng/mL. Nonetheless, the body temperature of patient 1 fluctuated around 38.0°C. When $C_{ss,avg}$ ascended to 2.60 mg/L, CRP and PCT decreased to the normal range (CRP ≤ 5 mg/L, PCT 0.02 ng/ml) and the body temperature to normal. For patient 2, the levels of CRP and PCT did not decline until the $C_{ss,avg}$ of polymyxin B reached 1.73 mg/L. The concentrations of polymyxin B at corresponding dosing regimens for the two patients and estimated glomerular filtration rate (eGFR, calculated by Schwartz formula) levels are presented in **Table 1**. In addition, the polymyxin B dose regimens with the concomitant drugs and C-reactive protein (CRP) and procalcitonin (PCT) levels at different times are shown in **Figure 1**.

Comparing $C_{ss,avg}$ of polymyxin B with the same dosing regimens and infusion length, it showed significantly lower concentrations during CRRT than that after termination of CRRT for both patients (2.60 mg/L vs. 4.94 mg/L with 2 mg/kg every 12 h in 2 h infusion for patient 1; and 1.73 mg/L vs. 3.53 mg/L with 2 mg/kg every 12 h in 2 h infusion for patient 2).

Drug Removal by the Hemofilter Membrane

To assess whether CRRT could remove polymyxin B, blood samples from prefilter and postfilter were measured (**Figure 2**). The same type of hemofilter membrane was used for both patients. The concentrations of post-filtration and pre-filtration blood samples were 0.23 and 3.31 mg/L, respectively, which indicated 93.1% of polymyxin B was removed during the CVVHDF mode for patient 1. Two more pairs of pre- and post-filtration blood samples were evaluated for the drug removal during CRRT, and plasma concentrations showed 90.9–95.3% of polymyxin B was cleared. Similarly, 86.6% of polymyxin B was cleared for patient 2, with the concentrations of 0.43 and 3.19 mg/L (**Table 2**).

Compartmental modeling was conducted using WinNonlin 8.0 for patient 1 whose samples were collected during and recess of CRRT. Drug exposure (estimated by $AUC_{ss,12h}$ at the same dose) during CRRT and recess of CRRT through a preliminary pharmacokinetic modeling for patient 1 was estimated. The results showed that 45% of polymyxin B was removed during CRRT (**Figure 3**). By applying the equation-based method for calculating AUC_{24h} for the first patient, 57% of polymyxin B was removed during CRRT, which was similar to that obtained using the compartmental modeling method. The same equation-based method was applied for the AUC_{24h} estimation of the second patient. It was calculated that AUC_{24h} was 30.2 mg•h/L and 60.6 mg•h/L for the 2 g and 2 h infusion of polymyxin B during CRRT and without CRRT, respectively, indicating 51% of polymyxin B lost during CRRT.

DISCUSSION

The incidence of carbapenem-resistant organism infection is increasing globally, mainly carbapenem-resistant Enterobacteriaceae and *Acinetobacter baumannii*. Polymyxin is considered as the salvage therapy for aforementioned infections. The international consensus guideline recommended a polymyxin B dose of 1.25–1.5 mg/kg every 12 h for patients with severe infection patients. With doses of 2.5 and 3.0 mg/kg/day, 90% of adults would be expected to achieve a $C_{ss,avg}$ of 1.8 and 2.2 mg/L, respectively (Tsuji et al., 2019). In addition, the consensus guideline suggested that polymyxin B dose need not be adjusted during CRRT. However, the guideline has not provided the recommended dosage regimens for children. In our study, to achieve the target $C_{ss,avg}$, a polymyxin B dose of 4.0 mg/kg/d was needed, which was far from the recommended doses in adults.

Young children show changes in drug absorption, disposition, metabolism, and excretion of drugs (Kearns et al., 2003; Downes et al., 2014). For example, in absorptive surfaces such as the gastrointestinal tract, skin, and pulmonary tree, it can influence the rate and extent of the bioavailability of drugs. Age-related changes in body composition alter the volume of distribution of antibiotics. Delayed maturation of drug-metabolizing enzyme activity and developmental changes in renal function account

TABLE 2 | Concentration of polymyxin B of prefilter and postfilter at 0.5 h after infusion during CRRT.

Patient No.	Pre-filtration plasma concentration (mg/L)	Post-filtration plasma concentration (mg/L)	Ratio of drug loss (%)
1	3.31	0.23	93.1
	4.02	0.19	95.3
	5.55	0.50	90.9
2	3.19	0.43	86.6

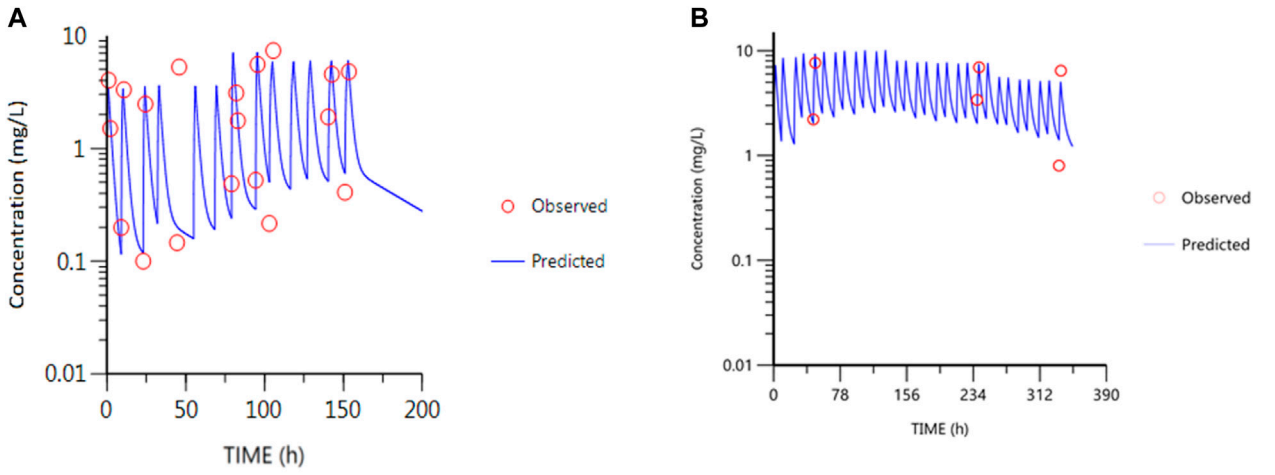

C

Parameters	Unit	CRRT	No CRRT
$AUC_{ss,12h}$	mg•h/L	27.1	49.4
V	L	8.1	5.6
Cl	L/h	1.3	0.5
$T_{1/2}$	h	4.2	7.1

FIGURE 3 | PK parameters of polymyxin B and the simulations for patient 1. **(A)** Observed concentrations vs. predicted concentrations during CRRT. **(B)** Observed concentrations vs. predicted concentrations after recess of CRRT. The last two samples in **(B)** were deviated from the blue line due to the dose adjustments from 1.5 mg/kg (with 0.5 mg/kg inhalation) to 1.0 mg/kg infusion. Red circles represent observed concentrations; blue line represents the predicted concentrations according to the two-compartmental PK model. **(C)** Table for the PK parameters during CRRT and without CRRT.

for the difference in drug clearance. Additionally, in critically ill patients, the hemodynamic alterations or renal dysfunction during critical illness pathophysiologically change the volume of distribution, protein binding, and drug clearance. In PICU patients, antibiotic concentrations are outside of the therapeutic window up to 95%, while these non-target concentrations in adult critically ill patients are up to 41% (Hartman et al., 2019). In our study, the clearance of polymyxin B (Cl) was 1.3 L/h (correspondingly 0.05 L/h/kg) during CRRT and 0.5 L/h (correspondingly 0.02 L/h/kg) without CRRT, which was in the range of Cl reported previously (0.02–0.07 L/h/kg in critically ill patients) (Sandri et al., 2013; Liu et al., 2021). The half-life ($t_{1/2}$) of polymyxin B was different from that during CRRT and without CRRT (4.2 vs. 7.1 h), but in line with previous reports (healthy subjects (~5 h) and critically ill patients (~11.9 h) (Sandri et al., 2013; Liu et al., 2021). These suggested that changes in the dose of polymyxin B in these two patients had little to do with the special population of children themselves.

On the other hand, antibiotics with large molecular weight and high protein binding rate forming drug–protein complexes are not easily removed by CRRT (Pistolesi et al., 2019). Therefore, in theory, polymyxin B is difficult to be removed during CRRT because of its large molecular weight of more than 1,000 Da (e.g., 1,203, 1,189, and 1,203 for polymyxins B1, B2, and B1-Ile, respectively) and protein binding rate of 58% (Sandri et al., 2013). Two reports with three cases of adult patients suggested that only 5.6% and 12.2% of polymyxin B were removed by CVVHD and 5.0% was removed by CVVHF (Teng et al., 2008; Sandri et al., 2012). Conversely, another study with three critically ill adults reported that 45% of colistin was removed during CRRT under the CVVHDF mode (Nikolaos et al., 2012). In this study, both cases showed significant drug clearance of polymyxin B during CRRT with the CVVHDF mode. Comparing $C_{ss,avg}$ of polymyxin B with the same dosing regimens and infusion length, it showed significantly lower concentrations during CRRT than that after termination of CRRT for both patients (2.60 mg/L vs. 4.94 mg/L with 2 mg/kg every 12 h in 2 h infusion for patient 1; and 1.73 mg/L vs. 3.53 mg/L with 2 mg/kg every 12 h in 2 h infusion for patient 2). This was also confirmed by the estimation of drug exposure (estimated by $AUC_{ss,12h}$ at the same dose) during CRRT and recess of CRRT through a preliminary pharmacokinetic. Results showed that 45% and 51% of polymyxin B was

clearance during CRRT which was much higher than that in the reported studies (no more than 12%) (Teng et al., 2008; Sandri et al., 2012). In addition, the plasma concentrations in prefilter and postfilter membranes showed 86.6–95.3% drug removal during filtration, suggesting the remarkable extracorporeal clearance. A previous study reported colistin absorption by the hemofilter, and the removal of dialysis contributed to its extracorporeal clearance (Nikolaos et al., 2012). In our study, we measured the concentration of the effluent fluid of CRRT, but due to the dilution effect and the large volume of the effluent (more than 5 L for 12 h), the concentration of polymyxin B was lower than the detection limit of the LC-MS/MS assay. Further studies are needed to evaluate the drug removal by adsorption of the hemofilter. Since this study only provided two cases, the exact clearance of polymyxin B through CRRT indicating supplanted dosing is necessary for pediatric patients undergoing CRRT.

CONCLUSION

CRRT (CVVHDF mode) significantly affects the drug concentrations and exposure of polymyxin B in the present two cases, indicating supplantation of polymyxin B is necessary in pediatrics undergoing CRRT. The TDM of polymyxin B is critically important for the dosing regimen optimization for patients undergoing CRRT. Larger PK studies are urgently needed to further refine dosing recommendations of polymyxin B in pediatric population receiving CRRT.

DATA AVAILABILITY STATEMENT

The original contributions presented in the study are included in the article/**Supplementary Material**, further inquiries can be directed to the corresponding authors.

ETHICS STATEMENT

This study was reviewed and approved by the Huashan Hospital Institutional Review Board and Clinical Research Ethics Committee of Shanghai Children's Hospital affiliated to Shanghai Jiao Tong University School of Medicine. The patients' legal guardian provided their written informed consent to participate in this study. Written informed consent was obtained from the patients' legal guardian for the publication of any potentially identifiable images or data included in this article.

AUTHOR CONTRIBUTIONS

CX and XoL drafted the manuscript and collected data; YZ, YC, and JZ provided insights and edited the manuscript; and XH, YW, YF, HW, XnL, and BG helped collecting data and worked on the figures and tables.

FUNDING

This research was supported by the Shanghai Municipal Science and Technology Commission (Grant Number: 19411964900).

REFERENCES

Downes, K. J., Hahn, A., Wiles, J., Courter, J. D., and Vinks, A. A. (2014). Dose Optimisation of Antibiotics in Children: Application of Pharmacokinetics/pharmacodynamics in Paediatrics. *Int. J. Antimicrob. Agents* 43 (3), 223–230. doi:10.1016/j.ijantimicag.2013.11.006

Gothwal, S., Meena, K., and Sharma, S. D. (2016). Polymyxin B Induced Generalized Hyperpigmentation in Neonates. *Indian J. Pediatr.* 83, 179–180. doi:10.1007/s12098-015-1798-z

Hartman, S. J. F., Brüggemann, R. J., Orriëns, L., Dia, N., Schreuder, M. F., and de Wildt, S. N. (2019). Pharmacokinetics and Target Attainment of Antibiotics in Critically Ill Children: A Systematic Review of Current Literature. *Clin. Pharmacokinet.* 59 (2), 173–205. doi:10.1007/s40262-019-00813-w

Kearns, G. L., Abdel-Rahman, S. M., Alander, S. W., Blowey, D. L., Leeder, J. S., and Kauffman, R. E. (2003). Developmental Pharmacology-Ddrug Disposition, Action, and Therapy in Infants and Children. *N. Engl. J. Med.* 349, 1157–1167. doi:10.1056/NEJMra035092

Li, L., Li, X., Xia, Y., Chu, Y., Zhong, H., Li, J., et al. (2020). Recommendation of Antimicrobial Dosing Optimization during Continuous Renal Replacement Therapy. *Front. Pharmacol.* 11, 786. doi:10.3389/fphar.2020.00786

Liu, X., Yu, Z., Wang, Y., Wu, H., Bian, X., Li, X., et al. (2020). Therapeutic Drug Monitoring of Polymyxin B by LC-MS/MS in Plasma and Urine. *Bioanalysis* 12, 845–855. doi:10.4155/bio-2020-0051

Liu, X., Chen, Y., Yang, H., Li, J., Yu, J., Yu, Z., et al. (2021). Acute Toxicity Is a Dose-Limiting Factor for Intravenous Polymyxin B: A Safety and Pharmacokinetic Study in Healthy Chinese Subjects. *J. Infect.* 82, 207–215. doi:10.1016/j.jinf.2021.01.006

Nikolaos, M., Marizoza, F., Markantonis, S. L., Zidianakis, B., Hroni, D., Boutzouka, E., et al. (2012). Colistin Pharmacokinetics in Intensive Care Unit Patients on Continuous Venovenous Haemodiafiltration: an Observational Study[J]. *J. Antimicrob. Chemother.* 67 (10), 2459–2462. doi:10.1093/jac/dks257

Pai, M. P., Neely, M., Rodvold, K. A., and Lodise, T. P. (2014). Innovative Approaches to Optimizing the Delivery of Vancomycin in Individual Patients. *Adv. Drug Deliv. Rev.* 77, 50–57. doi:10.1016/j.addr.2014.05.016

Pistolesi, V., Morabito, S., Di Mario, F., Regolisti, G., Cantarelli, C., and Fiaccadori, E. (2019). A Guide to Understanding Antimicrobial Drug Dosing in Critically Ill Patients on Renal Replacement Therapy. *Antimicrob. Agents Chemother.* 63, e00583-19. doi:10.1128/AAC.00583-19

Sandri, A. M., Landersdorfer, C. B., Jacob, J., Boniatti, M. M., Dalarosa, M. G., Falci, D. R., et al. (2013). Population Pharmacokinetics of Intravenous Polymyxin B in Critically Ill Patients: Implications for Selection of Dosage Regimens. *Clin. Infect. Dis.* 57, 524–531. doi:10.1093/cid/cit334

Sandri, A. M., Landersdorfer, C. B., Jacob, J., Boniatti, M. M., Dalarosa, M. G., Falci, D. R., et al. (2012). Pharmacokinetics of Polymyxin B in Patients on Continuous Venovenous Haemodialysis. *J. Antimicrob. Chemother.* 68, 674–677. doi:10.1093/jac/dks437

Satlin, M. J., Lewis, J. S., II, Weinstein, M. P., Patel, J., Humphries, R. M., Kahlmeter, G., et al. (2020). Clinical and Laboratory Standards Institute and European Committee on Antimicrobial Susceptibility Testing Position Statements on Polymyxin B and Colistin Clinical Breakpoints. *Clin. Infect. Dis.* 71, e523–e9. doi:10.1093/cid/ciaa121

Shih, L. K., and Gaik, C. L. (2014). Polymyxin B Induced Generalized Skin Hyperpigmentation in Infants. *J. Pediatr. Neurosciences* 6, e215. doi:10.17334/jps.10375

Teng, C. B., Koh, P. T., Lye, D. C., and Ang, B. S. (2008). Continuous versus Intermittent Infusion of Polymyxin B in the Treatment of Infections Caused by Multidrug-Resistant Gram-Negative Bacteria. *Int. J. Antimicrob. Agents* 31, 80–82. doi:10.1016/j.ijantimicag.2007.08.004

Tsuji, B. T., Pogue, J. M., Zavascki, A. P., Paul, M., Daikos, G. L., Forrest, A., et al. (2019). International Consensus Guidelines for the Optimal Use of the

Polymyxins: Endorsed by the American College of Clinical Pharmacy (ACCP), European Society of Clinical Microbiology and Infectious Diseases (ESCMID), Infectious Diseases Society of America (IDSA), International Society for Anti-infective Pharmacology (ISAP), Society of Critical Care Medicine (SCCM), and Society of Infectious Diseases Pharmacists (SIDP). *Pharmacotherapy* 39, 10–39. doi:10.1002/phar.2209

Willems, J., Hermans, E., Schelstraete, P., Depuydt, P., and De Cock, P. (2021). Optimizing the Use of Antibiotic Agents in the Pediatric Intensive Care Unit: A Narrative Review. *Paediatr. Drugs* 23, 39–53. doi:10.1007/s40272-020-00426-y

Conflict of Interest: The authors declare that the research was conducted in the absence of any commercial or financial relationships that could be construed as a potential conflict of interest.

Publisher's Note: All claims expressed in this article are solely those of the authors and do not necessarily represent those of their affiliated organizations, or those of the publisher, the editors, and the reviewers. Any product that may be evaluated in this article, or claim that may be made by its manufacturer, is not guaranteed or endorsed by the publisher.

Advantages of publishing in Frontiers

OPEN ACCESS
Articles are free to read for greatest visibility and readership

FAST PUBLICATION
Around 90 days from submission to decision

HIGH QUALITY PEER-REVIEW
Rigorous, collaborative, and constructive peer-review

TRANSPARENT PEER-REVIEW
Editors and reviewers acknowledged by name on published articles

Frontiers
Avenue du Tribunal-Fédéral 34
1005 Lausanne | Switzerland

Visit us: www.frontiersin.org
Contact us: frontiersin.org/about/contact

REPRODUCIBILITY OF RESEARCH
Support open data and methods to enhance research reproducibility

DIGITAL PUBLISHING
Articles designed for optimal readership across devices

FOLLOW US
@frontiersin

IMPACT METRICS
Advanced article metrics track visibility across digital media

EXTENSIVE PROMOTION
Marketing and promotion of impactful research

LOOP RESEARCH NETWORK
Our network increases your article's readership